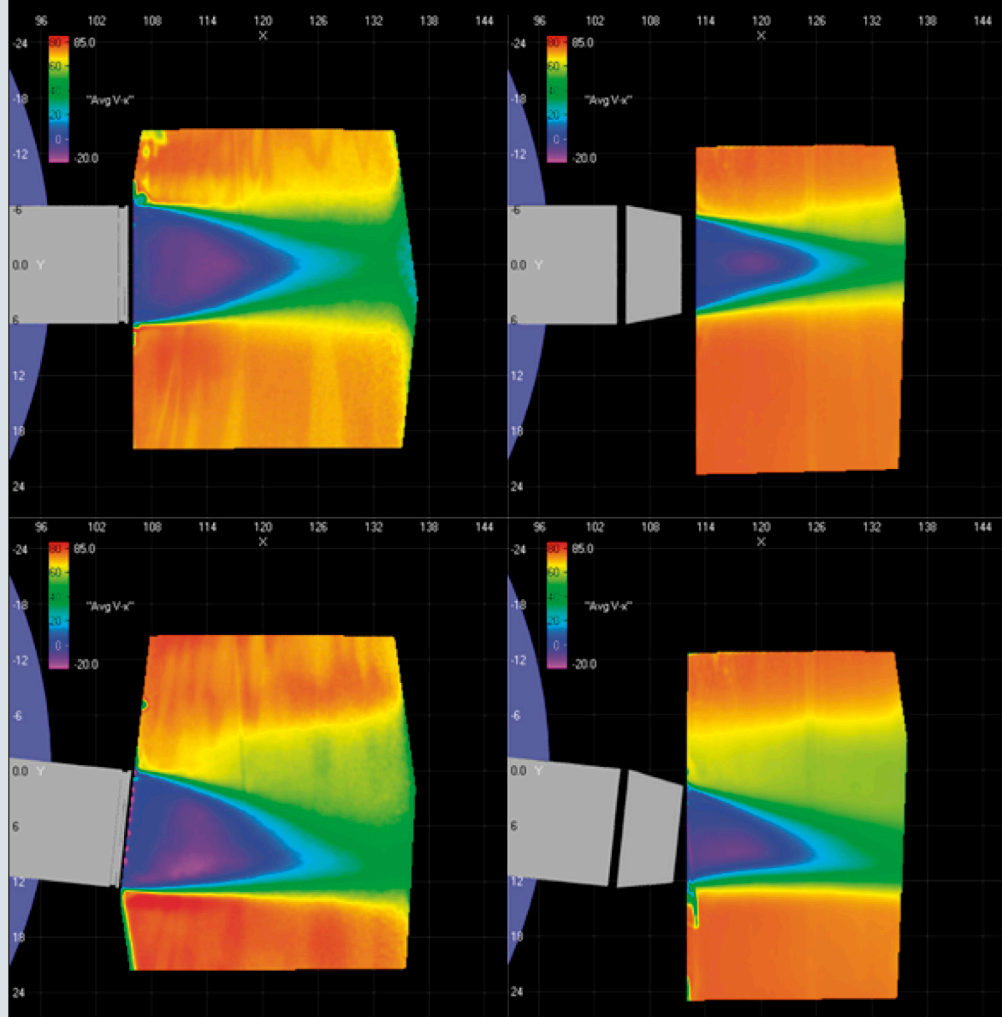


Vehicle Systems

2016 Annual Report

Vehicle Technologies Office



Front Cover Picture: The picture shows wind-tunnel air flow diagnostic plots that were used to gain a deeper understanding of the flow features in the heavy vehicle wake (for baseline (left) and boattail & skirt (right) cases, at 0 degree (top) and 6 degree (bottom) yaw angles). The high-resolution 3D particle image velocimetry (PIV) datasets were obtained for the baseline heavy vehicle with and without a trailer boattail. PIV analysis was an important step in validating models that were used to design the second generation of highly aerodynamic heavy duty tractor trailers. Compared to the baseline, the GSF2 design lowered the coefficient of drag (C_d) by 80% at 0 degree yaw angle and exhibits negative C_d at yaw angles greater than 17 degrees.

Credit: Lawrence Livermore National Laboratory

Disclaimer

This report was prepared as an account of work sponsored by an agency of the United States government. Neither the United States government nor any agency thereof, nor any of their employees, makes any warranty, express or implied, or assumes any legal liability or responsibility for the accuracy, completeness, or usefulness of any information, apparatus, product, or process disclosed or represents that its use would not infringe privately owned rights. Reference herein to any specific commercial product, process, or service by trade name, trademark, manufacturer, or otherwise does not necessarily constitute or imply its endorsement, recommendation, or favoring by the United States government or any agency thereof. The views and opinions of authors expressed herein do not necessarily state or reflect those of the United States government or any agency thereof.

Table of Contents

Acronyms and Abbreviations	xvii
I. Introduction	1
I.1. Mission and Objectives.....	1
I.2. Accomplishments	3
I.3. Approach and Organization of Activities	9
I.4. Future Directions for Vehicle Systems.....	16
II. Industry Awards.....	19
II.1. Integrated Boosting and Hybridization for Extreme Fuel Economy and Downsizing	19
II.2. Multi-Speed Transmission for Commercial Delivery Medium Duty PEDVs [DE-EE0006843]	25
II.3. Advanced Vehicle Testing & Evaluation (AVTE) [DE-EE0005501]	39
II.4. Energy Impact of Connected and Automated Vehicles [DE-FOA-0001213]	47
II.5. Methods to Measure, Predict and Relate Friction, Wear and Fuel Economy	57
THERMAL LOAD REDUCTION.....	79
II.6. Advanced Climate Control and Vehicle Preconditioning [DE-EE0006445].....	79
II.7. Design and Implementation of a Thermal Load Reduction System for a Hyundai Sonata PHEV for Improved Range	89
II.8. Unitary Thermal Energy Management for Propulsion Range Augmentation [DE-EE0006840]	101
II.9. Electric Phase Change Material Assisted Thermal Heating System (ePATHS) [DE-EE0006444]	109
SUPERTRUCK.....	117
II.10. Volvo SuperTruck [DE-EE0004232]	117
TIRES 121	
II.11. A System for Automatically Maintaining Pressure in a Commercial Truck Tire DE-EE0005447.....	121
II.12. Improved Tire Efficiency through Elastomeric Polymers Enhanced with Carbon-Based Nanostructured Materials.....	129
WIRELESS POWER TRANSFER	135
II.13. High Efficiency, Low EMI and Positioning Tolerant Wireless Charging of EVs [DE EE0005963]	135
II.14. Wireless Charging of Electric Vehicles [FOA #667]	141
ZERO EMISSION CARGO TRANSPORT 1.....	156
II.15. Zero Emission Drayage Trucks Demonstration [EE-0005961].....	156
II.16. Hydrogen Fuel-Cell Electric Hybrid Truck Demonstration [EE0005978] & Houston Zero Emission Delivery Vehicle Deployment [EE0005979].....	165
ZERO EMISSION CARGO TRANSPORT 2.....	172
II.17. San Pedro Bay Ports Hybrid & Fuel Cell Electric Vehicle Project [DE-EE0006874]	172

III. Vehicle Technology Evaluations	177
III.1. Advanced Vehicle Testing Activity.....	177
III.2. Medium- and Heavy-Duty Field Testing.....	184
III.3. Zero Emissions Cargo Transport Data Collection and Analysis	239
III.4. Analysis Process for Thermal Load Reduction Off-Cycle Credit Technologies.....	245
III.5. Advanced Technology Vehicle Lab Benchmarking (Level 1 & Level 2)	255
III.6. Road and Lab Coordinated Assessment of Active Transmission Warm-up.....	275
IV. Modeling and Simulation.....	283
IV.1. Evaluation of Dynamic Wireless Charging Demand.....	283
IV.2. Autonomie for Model Based System Engineering	293
IV.3. Connected and Automated Vehicle	300
IV.4. Vehicle Technologies Benefits on Real-World Drive Cycles Using POLARIS Regional Transportation System Model.....	316
IV.5. Long-Haul Truck Idle Climate Control Load Reduction & VTCab, Rapid Vehicle HVAC Load Estimation Tool	324
IV.6. Vehicle Thermal System Model Development in Simulink	339
IV.7. Real World Effectiveness of Engine Start-Stop Systems	352
V. Codes and Standards	358
V.1. Codes and Standards and Technical Team Activities.....	358
V.2. SAE J2907 Performance Characterization of Electrified Powertrain Motor-drive Subsystem.....	365
V.3. PEV-Grid Connectivity	373
VI. Vehicle Systems Efficiency Improvements.....	390
AERODYNAMIC DRAG REDUCTION.....	390
VI.1. DOE’s Effort to Improve Heavy Vehicle Fuel Efficiency through Improved Aerodynamics.....	390
VI.2. Line Haul Truck Platooning	400
THERMAL.....	409
VI.3. Thermal Control of Power Electronics of Electric Vehicles with Small Channel Coolant Boiling	409
VI.4. Underhood Thermal Analysis of Tractor-Trailer.....	430
HYBRIDIZATION	442
VI.5. Cummins MD&HD Accessory Hybridization CRADA.....	442
WIRELESS POWER TRANSER	452
VI.6. Wireless and Conductive Charger Evaluation	452
GRID MODERNIZATION.....	460
VI.7. Vehicle to Building Integration Pathway [GM0062].....	460
VI.8. Systems Research for Standards and Interoperability [GM0085]	465
VI.9. Modeling and Control Software Tools to Support Vehicle to Grid Integration [GM0086]	471
VI.10. Diagnostic Security Modules for Electric Vehicle to Building Integration [GM0163].....	481

List of Figures

Figure I-1: VS outcome objectives and mission	1
Figure I-2: VS primary processes, project objectives, and outcome objectives.....	2
Figure I-3: Projected cumulative freight transportation fuel savings from trailer skirt and box-tail technologies	3
Figure I-4: VS activities integration – Arrows represent information flow between activity focus areas that enhances effectiveness of individual activities.	9
Figure I-5: VS activities providing estimates of national benefits and impacts of advanced technologies.	10
Figure II-1: Baseline Model Results Compared to Experimental Data	21
Figure II-2. Fuel Economy Results with Different EAVS/WHR features.....	22
Figure II-3: Expander Operation at 700C	22
Figure II-4: Expander Repeatability Results.....	23
Figure II-5: Finalized Roots Expander Design	23
Figure II-6: EAVS/WHR System Packaged into Engine Compartment.....	24
Figure II-7: Proterra BE35 electric bus field test based on the Altoona ADB drive cycle is used to validate the baseline vehicle model with 2 speed transmission.	29
Figure II-8: Simulation results of Proterra BE35 electric bus for various drive cycles: The graphs show the energy efficiency improvement (%) with the new 4-speed transmission with 3 & 4 Gear setups over the baseline 2-speed transmission.	32
Figure II-9: Total wheel torque versus vehicle speed simulation results for 4 speed (options 4 & 5 with 4-Gear setup) Transmission using full throttle drive cycle testing.....	32
Figure II-10: External views of 3 and 4-speed automated mechanical transmission layout.	34
Figure II-11: Equivalent stress contours in the front (left) and rear (right) housings under 1300 Nm input torque.	35
Figure II-12: 4-speed transmission bearing reliability analysis results.....	36
Figure II-13: Average Sound Pressure Level (SPL) as function of motor output speed.....	37
Figure II-14: The display unit of the new 4-speed EV Transmission.	38
Figure II-15: AVTE fleet vehicles at Intertek for a review with the DOE team in January 2016.	42
Figure II-16: 2016 Chevrolet Volt that completed baseline testing.....	44
Figure II-17: EZ Messenger Phoenix fleet location charging infrastructure with AVTE vehicles and Storage-Assisted Vehicle Recharging (StAR) Unit in red climate-controlled chamber.	45
Figure II-18: Vehicle temperature chamber with Advanced Charging Technologies DCFC configured with both CHAdeMO and combined charging system connectors located at Intertek in Phoenix, Arizona.....	45
Figure II-19: VLI-EV DCFC unit installed at the EZ Messenger fleet location with both CHAdeMO and combined charging system connectors (the CHAdeMO connector is shown).	46
Figure II-20: CAV Human Display Under Development	53
Figure II-21: Example time-space trajectory extracted from the Safety Pilot Model Deployment Database	54
Figure II-22: A new microscopic simulation model under development, to enhance the ability of the POLARIS model to simulate CAV functions	55
Figure II-23: HIL simulation platform for adaptive traffic signal control development.....	55
Figure II-24: Selected 6-intersection corridor for future adaptive traffic signal control study.....	56
Figure II-25: Axial variation of cylinder temperature at three speeds.	59
Figure II-26: Stribeck number as a function of crank angle for 15W/40 oil under motored and fired conditions assuming axial temperature profile in Figure II-25.	60

Figure II-27: Stribeck number as a function of crank angle for 15W/40 oil for benchtop conditions. 61

Figure II-28: Range of Stribeck numbers expected for benchtop and engine tests that simulate ring-on-liner conditions..... 62

Figure II-29: Summary of boundary friction coefficients for ring-on-liner and skirt-on-liner tests with the baseline Isuzu components. 63

Figure II-30: A cast-iron liner segment coated with a DLC coating from C2D showing delamination. 64

Figure II-31: Micrograph showing coating delamination. 64

Figure II-32: Profilometric measurement and corresponding line scan across delaminated area. 65

Figure II-33: Photo of the three rings (top ring, 2nd ring, and OCR) after C2D attempted coating with a DLC..... 65

Figure II-34: Comparison of friction coefficient as a function of time for two coated piston skirt segments..... 65

Figure II-35: Profilometric line scans for a liner surface as-is and "cut" at certain heights..... 66

Figure II-36: Bearing area curves for an original liner profile mathematically processed such that features above a certain height are "cut" at zero, -500 nm, and +500 nm. 66

Figure II-37: Friction traces over a range of conditions for the 3 variants provided by ZYNP..... 67

Figure II-38: Friction waveforms for 2 variants. 68

Figure II-39: Optical micrographs of all ZYNP liners post-test. 68

Figure II-40: Examination of ZYNP ring post-test and after application of EDTA on the same location for the original (uncoated) liner and the C2D coated liner..... 69

Figure II-41: Summary of EMA measured friction coefficient for Isuzu baseline ring-on-liner test. 69

Figure II-42: Summary of EMA measured friction coefficient for Isuzu baseline piston skirt-on-liner test. 70

Figure II-43: Illustration of unstable coefficient of friction measured during skirt-on-liner tests at ANL. 71

Figure II-44: Illustration of the AART benchtop rig. 71

Figure II-45: Friction as a function of time for a segment of time during test # 150707a (100°C). 72

Figure II-46: Friction as a function of time during a nominal room temperature run at 5 Hz (test # 150707c)..... 72

Figure II-47: RINGPAK model setup to replicate AART benchtop tests..... 73

Figure II-48: AART RINGPAK predicted and measured friction behavior for 150707C..... 73

Figure II-49: Illustration of full engine RINGPAK model results under fired conditions: 2500 rpm and 141 bar cylinder pressure. 75

Figure II-50: Illustration of full engine PISDYN model results under fired conditions: 2500 rpm and 141 bar cylinder pressure. 76

Figure II-51: Instrumented block with thermocouples (top) and piston with templogs (bottom)..... 77

Figure II-52: Block interbore temperatures at the full load speed at various fueling and coolant temperature conditions. 77

Figure II-53: Liquid (left) and Solid (right) Phase Change Material 81

Figure II-54: Effect of thermal storage on total HVAC energy consumed at -5°C..... 82

Figure II-55: Effect of Cold Thermal Storage in Water Cooled Condenser (WCC) 83

Figure II-56: Full refrigerant system modifications as evaluated 84

Figure II-57: Power required with and without "cold" thermal storage (TS) 85

Figure II-58: Vehicle Test Showing Need for Charge Management 86

Figure II-59: Refrigerant system schematic..... 87

Figure II-60: Glycol loop schematic 87

Figure II-61: Phase I candidate thermal load reduction technologies. Photo Credits: A - PGW, B - Gentherm..... 92

Figure II-62: Phase I vehicles at NREL's Vehicle Testing and Integration Facility	93
Figure II-63: Warm weather (upper) and cold weather (lower) testing methodologies used for Phase I testing of candidate technologies	94
Figure II-64: Summary of Phase I warm weather baseline testing	95
Figure II-65: Transient and steady-state cooling energy used compared to baseline for glass packages A, B, and C.....	96
Figure II-66: Transient and steady-state cooling energy use for vehicle modified with solar reflective paint compared to baseline.....	96
Figure II-67: Transient and steady-state cooling tests using ventilated/cooled seats compared to baseline. Results are specific to each occupant that performed the test.....	97
Figure II-68: Summary of Phase I cold weather baseline testing	97
Figure II-69: Transient and steady-state heating tests using heated surfaces compared to baseline. Results are specific to each occupant that performed the test.	98
Figure II-70: Cold weather defogging performance of heated windshield and door demisters compared to baseline	98
Figure II-71: Go/No-Go decision matrix for selection of technologies for Phase II thermal load reduction package	99
Figure II-72: Schematic of a sample configuration of the UTEMPRA refrigerant loop	103
Figure II-73: Thermal management of the Fiat 500e.....	104
Figure II-74: UTEMPRA Coolant loop architecture	105
Figure II-75: Controlled atmosphere braze furnace installed in MAHLE Lockport facility	106
Figure II-76: MAHLE Benchtop glass furnace (left) and T-sample braze outcomes.....	106
Figure II-77: Comparison of the tunnel test data (Baseline) and CoolSim cabin simulation results: Left - warm-up; Right - cool-down cases.....	107
Figure II-78: Effect of leakage (numerical values are coolant leakage mass flow rates – kg/sec) level on heater air discharge temperature	107
Figure II-79: Improved ePATHS System Design	112
Figure II-80: GEN-1 Radiator-Type PCM Thermal Storage Module.....	113
Figure II-81: Plate-Type PCM Thermal Storage Module	113
Figure II-82: PCM Thermal Storage with Four GEN-2 Modules with Parallel-Serial Plumbing.....	114
Figure II-83: Photos of the ePATHS Bench Prototype Hardware in ORNL's BTRIC Test Chamber	114
Figure II-84: Volvo's SuperTruck concept vehicle	120
Figure II-85: SEM image of exfoliated rGO. Summarized Raman spectra of the exfoliated platelets. The spectrum of the CVD synthesized graphene is also included.	132
Figure II-86: SEM images at different magnifications of the synthesized silica nanofibers.	132
Figure II-87: Wireless Charging System Topology	136
Figure II-88: Coil Placement Under Kia Soul EV	137
Figure II-89: Coil Design.....	137
Figure II-90: Transmitter & Receiver Assemblies.....	138
Figure II-91: EMF Measurement Location.....	139
Figure II-92: Electric and Magnetic Field Levels around the Vehicle.....	139
Figure II-93: Temperature Rise of Vehicle Receiver Assembly.....	140
Figure II-94: Operational block diagram of the direct battery or CHAdeMO connection of vehicle side WPT equipment.	143
Figure II-95: Toyota RAV4 EV test results: Power flow and efficiency across 5 power conversion stages.....	144
Figure II-96: Test results across all power conversion stages as well as the primary coil and tuning capacitor voltages.....	145

Figure II-97: Operational waveforms for high frequency elements (inverter, transformer, coupling coils)..... 145

Figure II-98: Operational waveforms for low frequency elements (AC grid input, DC link, vehicle battery). 146

Figure II-99: Unmatched (interoperable) coils on the left and matched coils on the right. 146

Figure II-100: Laboratory test setup with RAV4 with matched coils..... 147

Figure II-101: Updated test results with matched coils and SS tuning with improved efficiencies. 147

Figure II-102: High power (20kW) transfer efficiency test results by power conversion stage for Toyota RAV4..... 148

Figure II-103: End to End Efficiency versus Power for Toyota RAV4..... 149

Figure II-104: Efficiency of power stages vs. power when the system is optimized for 20kW power transfer. 149

Figure II-105: Track layout for the dynamic wireless charging setup with two coils (green squares). 150

Figure II-106: In-motion wireless charging test results: Power vs. position and comparison of SS and SP tuning configurations. 151

Figure II-107: In-motion wireless charging test results: Efficiency vs. position comparisons for SS and SP tuning configurations. 151

Figure II-108: TransPower BEV System..... 158

Figure II-109: US Hybrid BEV System..... 159

Figure II-110: TransPower PHEV System..... 159

Figure II-111: US Hybrid PHEV System 160

Figure II-112: TransPower EDD Trucks 161

Figure II-113: TransPower EDD1 with new battery cells and BMS 162

Figure II-114: US Hybrid BET 162

Figure II-115: US Hybrid PHET..... 163

Figure II-116: Block diagram of BAE Systems battery electric truck with hydrogen fuel cell range extender..... 174

Figure II-117: Changes to baseline TransPower battery electric truck for fuel cell range extender variants 174

Figure II-118: U.S. Hybrid battery electric truck with on-board fuel cell generator 175

Figure II-119: Block diagram of BAE Systems and Kenworth hybrid electric truck with CNG range extender..... 175

Figure III-1: Battery capacity data shown for a 2013 Ford Focus Electric. The data shown are from tests performed at 4,000; 14,000; and 60,000 miles. Two additional tests will be performed prior to completion of testing to characterize battery performance through the life of the battery. 181

Figure III-2: A 2014 BMW i3 electric vehicle fitted with testing and measurement equipment for track testing..... 181

Figure III-3: Electrical energy consumption data are shown for a 2015 Chevrolet Spark electric vehicle. The data shown are from on-road operations logged over several thousand miles. 182

Figure III-4: The range and mean of EVSE port use is shown by region. 182

Figure III-5: Comparison of diesel (blue) and EV (red) routes..... 189

Figure III-6: Federal Way Smith Newton EV and conventional diesel daily driving distance distribution 189

Figure III-7: Federal Way Vehicle Daily Performance Metrics Shown with Standard Deviations (σ) 190

Figure III-8: Federal Way Smith Newton EV DC energy consumption per mile, data collected 4/14--5/14..... 190

Figure III-9: Fuel economy vs. average speed for Federal Way depot diesels and EVs..... 191

Figure III-10: Energy efficiency vs. kinetic intensity for Federal Way depot diesels and EVs..... 192

Figure III-11: Energy consumption as a function of daily distance traveled 192

Figure III-12: Distribution of daily EV energy consumption 193

Figure III-13: Cost savings of EVs over conventional diesels based on average annual mileage and fuel price, assuming an electricity cost of \$0.102/kWh 193

Figure III-14: 2014 PSE total electricity (kWh) by generation source and CO2 emissions (metric ton) 194

Figure III-15: Average CO2e emissions by energy source and distance travelled based on Federal Way delivery vehicle operation 195

Figure III-16: Opportunity charging, delayed charging, and managed charging 195

Figure III-17: Average hourly output of 100-kW AC system based on array orientation at Federal Way facility 196

Figure III-18: Campus net load with simulated 100-kW PV array and managed EV charging..... 197

Figure III-19: Solar energy potential. National map shows low solar resource potential near Federal Way 198

Figure III-20: Campus net load with simulated 100-kW PV array using Casa Grande solar resource profile and managed EV charging..... 198

Figure III-21: Campus net load with managed EV charging and simulated 100-kW PV array using a 6-hour time shifted Casa Grande solar resource profile..... 199

Figure III-22: Miami-Dade County’s first generation (MY13) hydraulic hybrid refuse trucks at the 58th St. PWWMD facility 201

Figure III-23: MY15 Parker Hannifin RunWise hybrid system shown out of vehicle chassis 202

Figure III-24: Parker Hannifin RunWise hybrid system schematic 202

Figure III-25: Overview of the Miami-Dade PWW 58th St location 203

Figure III-26: High level project timeline 204

Figure III-27: Three configurations of refuse trucks from which data were collected 204

Figure III-28: Installation location of on-board Isaac data logger 205

Figure III-29: Neighborhood detail showing global positioning system vehicle routes 205

Figure III-30: Kinetic intensity vs. average driving speed..... 206

Figure III-31: Multiple scatter plots and a histogram demonstrating the similarities between the operation of the HHVs and the conventional diesel automated side loader refuse trucks 206

Figure III-32: Fuel economy vs. kinetic intensity shown with standard deviation ranges..... 207

Figure III-33: MY15 HHV Cummins ISL 9, 380-hp, 8.9-L diesel engine operating heat map. Color indicates frequency of data points..... 208

Figure III-34: MY07 Caterpillar C11 ACERT, 335-hp 11.1-L conventional diesel engine operating heat map. Color indicates frequency of data points. 208

Figure III-35: MY15 HHV engine fuel rate as a function of engine speed and wheel-based vehicle speed 209

Figure III-36: Conventional vehicle diesel engine fuel rate as a function of engine speed and wheel-based vehicle speed 210

Figure III-37: Field data from MY13 HHVs, MY15 HHVs, and Conventional diesels shown with select chassis 211

Figure III-38: City of Denver 2015 Peterbilt with ISX 12..... 212

Figure III-39: 2013 AutoCar E3 MY15 HHV refuse truck with Cummins ISL-G engine at NREL’s ReFUEL laboratory 213

Figure III-40: Data collection periods shaded according to daily mileage accumulation for all 12 BEBs..... 214

Figure III-41: Vehicle speed, battery pack SOC, and distance for one typical “loop” on Line 291 with three charge events shown 215

Figure III-42: Kinetic intensity vs. average driving speed for all Proterra BEBs with $\pm 3\sigma$ reference box. Standard test cycles are also shown. 215

Figure III-43: Average daily acceleration rates vs. stops per mile..... 216

Figure III-44: Typical day of operation showing average battery pack SOC and cumulative distance travelled..... 216

Figure III-45: Vehicle-reported SOC for all BEBs over the entire data reporting period..... 217

Figure III-46: BEB energy efficiency vs. mean, mean maximum, and mean minimum temperatures 218

Figure III-47: Distribution of driving time where speed is greater than zero vs. amount of time when system is “ON” for BEBs and CNG vehicles 218

Figure III-48: BEB and CNG daily distance vs. stops per day 219

Figure III-49: School bus distance driven daily 221

Figure III-50: School bus average speed driven 222

Figure III-51: OCTA Dynamometer Test Cycle 222

Figure III-52: RUCSBC Dynamometer Test Cycle 222

Figure III-53: CARB HHDDT Dynamometer Test Cycle 222

Figure III-54: NREL Custom School Bus Dynamometer Test Cycle 222

Figure III-55: Daily average driving speed vs. kinetic intensity for school buses field data and dynamometer cycles 223

Figure III-56: (a and b) EV2G bus at the ReFUEL laboratory 224

Figure III-57: EV2G bus at ESIF 225

Figure III-58: Odyne parallel hybrid architecture schematic 226

Figure III-59: Duke Energy service territory 227

Figure III-60: Odyne Hybrid Systems aerial bucket truck 228

Figure III-61: Odyne Hybrid Systems underground utility vehicle 228

Figure III-62: BYD 40-ft BEB at Long Beach Transit 229

Figure III-63: Zion NPS propane-powered bus connected to a non-powered passenger trailer 230

Figure III-64: Median fit road grade profile from GLONASS-enabled global positioning system over 63 trips. 231

Figure III-65: Multiple scatter plots demonstrating the highly repetitive driving behavior of the propane-powered buses..... 232

Figure III-66: FASTSim vehicle simulator results showing impact of different component sizes..... 233

Figure III-67: Probability distribution of traction and regeneration power output from electric transit buses..... 235

Figure III-68: Peak power duration for traction and regeneration power from electric transit buses 236

Figure III-69: Screen shot from NREL’s DriveCAT website 238

Figure III-70: Geographic regions for trip-level origin and destination analysis..... 240

Figure III-71: Trip results from the top categories identified in the origin and destination analysis 241

Figure III-72: Trip level maximum speed vs. average driving speed 242

Figure III-73: Constant kinetic intensity curves shown with characteristic acceleration and aerodynamic speed 243

Figure III-74: Four component LA/LB drayage composite drive cycle 244

Figure III-75: Analysis process used for solar/thermal off-cycle credit calculations 247

Figure III-76: CoolCalc geometric rendering of a mid-size sedan..... 247

Figure III-77: Initial (A) and final (B) TMY3 locations used in the thermal model..... 249

Figure III-78: Actual versus requested evaporator capacity (A), and COP versus capacity and engine rpm (B)..... 251

Figure III-79: Real-world vehicle speed profile for the 18.4-minute drive (A), and vehicle fuel economy as a function of A/C load for three vehicles over the 18.4-minute drive (B)..... 252

Figure III-80: Advanced Vehicle Testing Activity process. 256

Figure III-81: Illustration of the chassis dynamometer in thermal chamber long with facility capabilities 258

Figure III-82: Data dissemination and project partners 259

Figure III-83: Map of Downloadable Dynamometer Database content..... 259

Figure III-84: eGolf electric energy consumption for different drive cycles across different temperatures 260

Figure III-85: eGolf battery polarization curves across different temperatures 261

Figure III-86: B-class electric energy consumption for different drive cycles across different temperatures 262

Figure III-87: B-class battery system resistance as a function of battery temperature 262

Figure III-88: Fuel Economy of the 2015 Impala Bi-fuel at varying ambient temperatures 264

Figure III-89: Full charge test on the UDDS cycle at 72F and 20F for the 2016 Volt 266

Figure III-90: Engine operation of the international combustion engine from the testing shown in Figure III-89 266

Figure III-91: 2014 BMW i3 REx mounted in APRF for evaluation. 268

Figure III-92: Full charge test at 72F on the UDDS, the highway and the US06 cycles 269

Figure III-93: Overview of charge sustaining operation..... 270

Figure III-94: Range extended engine operation and efficiency 270

Figure III-95: Overview of Battery Electric Vehicles Range 271

Figure III-96: Example of the APRF single cycle report 272

Figure III-97: Example of a Full Charge Test (FCT) summaries for PHEV's 273

Figure III-98: Example sheets from an APRF Recharge Report 274

Figure III-99: Diagram of 2011 Ford Fusion drivetrain and sensors installed on the vehicle. 277

Figure III-100: Engine coolant routing from the engine block to the transmission heater. The red fluid line clamp in the photo is used to stop coolant flow and disable the active transmission warm-up operation. 278

Figure III-101: Sample fuel economy variation by road type and ambient temperature. 278

Figure III-102: The simulated operation of the thermally sensitive vehicle model over two consecutive UDDS cycles. The magenta lines show the difference between no transmission warming, solid line, and active warming, dashed line..... 279

Figure III-103: 2016 Ram 1500 component temperatures during dynamometer testing over three consecutive UDDS cycles with active transmission warm-up on and disabled. Transmission temperature is shown in magenta, with the solid line representing active warm-up on, and the dotted line representing warm-up disabled. 280

Figure III-104: Results of on-road testing from two tests at approximately the same ambient temperature. The thick red and blue lines show transmission oil temperature with active warm-up on and disabled, respectively. 281

Figure IV-1: Voltage curve versus battery capacity [9]..... 285

Figure IV-2: The traffic-based power demand (TBPD) framework 286

Figure IV-3: Geometry of the simulated corridor 287

Figure IV-4: LA92 speed and energy profiles 289

Figure IV-5: Speed and energy profiles of a simulated car charged at idling..... 289

Figure IV-6: Spatial distribution of power demand 290

Figure IV-7: Speed and energy profiles of a simulated car charged along its route 290

Figure IV-8: Autonomie Available and Future Workflows 295

Figure IV-9: Autonomie Single Vehicle Run Titled View 296

Figure IV-10: Autonomie Single Vehicle Run Tabbed View..... 296

Figure IV-11: Autonomie Multi-Vehicle Run 297

Figure IV-12: Autonomie Data Analysis Workflow..... 298

Figure IV-13: Highlighted ACC Project System Components (vehicle on-dyno, MITM computer and connections, data)..... 303

Figure IV-14: On-road ACC data collection of lead/following vehicle speeds and relative distance 303

Figure IV-15: Fuel consumption (or equivalent for BEV) for various CAV scenarios: absolute values (left), relative savings to reference case (right) 304

Figure IV-16: Multi-vehicle simulation framework in Simulink..... 305

Figure IV-17: Capacity change vs. market penetration of CACC 307

Figure IV-18: Merging Roads with connected and automated vehicles coordinated by a centralized controller 308

Figure IV-19: (a) Initial vehicle positions on each road for the scenario 1 and (b) position trajectories of the four vehicles for the scenario 1 308

Figure IV-20: Position trajectories of the four vehicles for the scenario 2 309

Figure IV-21: (a) Control input and (b) speed profile of the vehicles for the scenario 2..... 309

Figure IV-22: (a) Cumulative fuel consumption and (b) travel time. 310

Figure IV-23: Fuel Consumption Impact..... 311

Figure IV-24: Polynomial MetaModel 312

Figure IV-25: Analysis of Platoonable Miles for a Targeted Truck Application 313

Figure IV-26: Impact on fuel/electricity consumption of alternative CAV designs 314

Figure IV-27: Influence of Road Segment Free Flow Speed (FFS) and Average Speed at Time of Travel for an Example Conventional Vehicle Design..... 314

Figure IV-28: Utilization of multiple efforts funded by DOE is necessary for this study. 317

Figure IV-29: Overview of the process to estimate gasoline and electricity demand for vehicles by combining energy consumption, driving behavior, and market share predictions..... 318

Figure IV-30: Overview of the process to generate real-world cycles from POLARIS. 318

Figure IV-31: Overview of the simulation process involving vehicles from multiple time frames and synthetic drive cycles. 319

Figure IV-32: Fuel economy improvement on standard and POLARIS Chicago cycles for a conventional vehicle in lab years 2010 and 2020..... 320

Figure IV-33: Fuel economy improvement on standard and POLARIS Chicago cycles for a HEV in lab years 2010 and 2020..... 320

Figure IV-34: Fuel economy improvement on standard and POLARIS Chicago cycles for EREV-40 vehicle in lab years 2010 and 2020. 321

Figure IV-35: Fuel economy estimates for all vehicle types considered in MA3T. Values are truncated at 200 mpgge..... 321

Figure IV-36: The market share predicted for every vehicle class in MA3T. 322

Figure IV-37: Gasoline and electricity needed for automotive applications in years 2015 and 2025. 322

Figure IV-38: Reduction in transportation energy consumption in the next 10 years as vehicles become more efficient..... 323

Figure IV-39: Relationship between the rest-period climate control fuel use estimation process and energy conversion 327

Figure IV-40: Map of weather station locations for A, all stations and B, remaining top 200 stations..... 328

Figure IV-41: Auxiliary A/C system battery pack recharge process sequence for fuel use estimation. A (left), beginning of a recharge event; B (right), end of a recharge event. 330

Figure IV-42: VTCab interface: A, convection GUI, B, construction pallet, and C, zone assignment painter 332

Figure IV-43: A (left), daily peak cooling power for combined cooling loads of 200 US locations and B (right), daily maximum 10-hour window A/C electric loads..... 333

Figure IV-44: A (left), daily peak cooling power for combined cooling loads of 200 U.S. locations and B (right), daily maximum 10-hour window A/C electric loads..... 335

Figure IV-45: A (left), savings for the battery-electric A/C with TLRP and B (right), savings for the fuel fired heater with TLRP 337

Figure IV-46: Schematic of NREL's CFL system. ESS not shown. 343

Figure IV-47: NREL's CFL test bench 343

Figure IV-48: HWFET2X - cycle velocity profile..... 346

Figure IV-49: HWFET2X - cycle cabin heat delivered by the full system CFL 346

Figure IV-50: HWFET2X – Energy balance and mode selection at +5°C 347

Figure IV-51: HWFET2X – Energy balance at all temperatures 347

Figure IV-52: HWFET2X – PTC power..... 347

Figure IV-53: HWFET2X – Blower flow rate 347

Figure IV-54: HWFET2X compressor rpm 348

Figure IV-55: HWFET2X – Compressor power..... 348

Figure IV-56: HWFET2X – Cabin air temperature 348

Figure IV-57: HWFET2X – Heater air discharge temperature..... 348

Figure IV-58: HWFET2X – Energy consumed by different system variants..... 349

Figure IV-59: HWFET2X – Energy savings relative to PTC heating 349

Figure IV-60: UDDS drive-cycle vehicle velocity 349

Figure IV-61: UDDS energy consumed by the system at various ambient temperatures..... 349

Figure IV-62: Weighted range 45% UDDS 55% HWFET2X 350

Figure IV-63: Weighted range impact 45% UDDS 55% HWFET2X 350

Figure IV-64: Fuel consumption reduction attributable to start-stop systems in four different vehicles..... 353

Figure IV-65: Sample sets that conform to the NHTS drive pattern are taken from the pool of real world driving cycles (RWDC) 354

Figure IV-66: Distribution of fuel economy values for four vehicles over 100 sample sets 354

Figure IV-67: FC reductions observed in real world cycles due to various micro/mild hybrid technologies on a generic midsize passenger car 355

Figure IV-68: Real world benefits compared against the improvements observed in regulatory cycles..... 355

Figure IV-69: Driving distance has a good correlation to many other drive cycle properties. 356

Figure IV-70: Driving distance has a good correlation to many other drive cycle properties. 356

Figure V-1: Bench testing conducted on eight wireless charging systems to support SAE J2954 codes and standards development. 360

Figure V-2: User interface of the INL developed test HC/DAS that is based in LabVIEW..... 361

Figure V-3: Steady-state tests at different voltage levels and charge rates..... 363

Figure V-4: Types of Electric Traction Motors 368

Figure V-5: Torque-speed and power characteristics of selected traction motor types 368

Figure V-6: Basic architectures of electric traction motors 369

Figure V-7: Functional diagram for bench dynamometer test 370

Figure V-8 Objectives..... 373

Figure V-9: Common Integration Platform/IoT System Architecture 378

Figure V-10: Architecture for local control and monitoring of subsystems 379

Figure V-11: Proof of Concept Smart Charge Adaptor	380
Figure V-12: Submeter	381
Figure V-13: Communications gateways.....	381
Figure V-14: EUMD Rev 5 metrology IC board	382
Figure V-15: Submeter data and power connectors.....	382
Figure V-16: HB44-3.41 Test Fixture	383
Figure V-17: PEV-EVSE interoperability testbed.....	383
Figure V-18: PEV SOC and drive cycle profile	385
Figure V-19: Research center test equipment.....	387
Figure VI-1: Baseline heavy vehicle model (1/8th scale) in the NASA Ames 7x10 wind tunnel.....	392
Figure VI-2: Drag coefficient as a function of yaw angle for the 1/8th scale models tested in the NASA Ames 7x10 wind tunnel	392
Figure VI-3: One-eighth scale models of the a) GSF1 and b) GSF2 in the NASA Ames 7x10 wind tunnel.....	393
Figure VI-4: Force vector plot of the "sailing effect" exhibited by the GSF2 for large yaw angles.....	393
Figure VI-5: a) GSF2 heavy vehicle geometry with boattails b) 1 and c) 2	394
Figure VI-6: Experimental setup for the PIV system in the NASA Ames 7x10 wind tunnel.....	394
Figure VI-7: Time-averaged velocity magnitude at the mid-height of the trailer at 0 deg (top) and 6 deg (bottom) yaw	395
Figure VI-8: Time-averaged velocity streamlines in the trailer wake at 6° yaw	395
Figure VI-9: Thermal images of the GSF2. The arrows indicate fingering patterns on the model nose at two different yaw angles	396
Figure VI-10: Model heavy vehicle platoon (1/50th scale) and splitter plate design	396
Figure VI-11: Internal details of the 1/50th scale platoon model.	397
Figure VI-12: Pressure probe installed on the engine grill of the platooning heavy vehicle models.....	397
Figure VI-13: Wind-averaged a) drag and b) pressure coefficient as a function of vehicle spacing for the two-vehicle platoon.	398
Figure VI-14: Wind-averaged a) drag and b) pressure coefficient as a function of vehicle spacing for the three-vehicle platoon with a lead and middle vehicle spacing of 20'	398
Figure VI-15: Wind-averaged a) drag and b) pressure coefficient as a function of vehicle spacing for the three-vehicle platoon with a lead and middle vehicle spacing of 30'	399
Figure VI-16: Truck platooning air flow	401
Figure VI-17: Trucks in platoon formation during testing.....	402
Figure VI-18: Platooning evaluations comparison	403
Figure VI-19: Platooning evaluations comparison of savings decrease for rear vehicle from 50' to 30' - Image: NREL	404
Figure VI-20: Platooning evaluations comparison - Image: NREL.....	405
Figure VI-21: Selective Catalytic Reduction (SCR) inlet total NOx comparison	406
Figure VI-22: SCR inlet brake-specific NOx comparison.....	406
Figure VI-23: Dither rate comparison.....	406
Figure VI-24: Naturalistic "background platooning" - Image: NREL.....	407
Figure VI-25: Concept of Subcooled Flow Boiling System	411
Figure VI-26: Vehicle Power Electronic Package	412
Figure VI-27: Side View of Vehicle Power Electronic Package	412
Figure VI-28: Fin Structure	413
Figure VI-29: Mesh Structure (All Units in Meter).....	413
Figure VI-30: TIM Thermal Conductivity Effects	415

Figure VI-31: Junction Temperatures 415

Figure VI-32: Coolant Flow Velocity Effects..... 416

Figure VI-33: Fluid Inlet Temperature Effects 417

Figure VI-34: Heat Flux Effects 417

Figure VI-35: High Heat Flux Applications 418

Figure VI-36: Experimental Test Module..... 420

Figure VI-37: Experimental Test Module Overview 420

Figure VI-38: Convective Heat Transfer Simulation Results 421

Figure VI-39: Subcooled Boiling Heat Transfer Simulation Results 421

Figure VI-40: Heat Loss Calibration Results..... 422

Figure VI-41: Fin Effect on Subcooled Boiling..... 422

Figure VI-42: Wall Temperature as a Function of Subcooled Boiling Length..... 423

Figure VI-43: Heat Flux and Heat Transfer Coefficient as Functions of Wall Superheat under Top Heating Condition 425

Figure VI-44: Heat Flux and Heat Transfer Coefficient as Functions of Wall Superheat under Bottom Heating Condition 427

Figure VI-45: Heat Transfer Coefficient Comparison 428

Figure VI-46: Vehicle underhood components; (i) top view and (ii) cooling package 434

Figure VI-47: Fan-shroud; (i) control points and (ii) Adjoint position sensitivity vectors 435

Figure VI-48: Leading Vehicle (LV) and Trailing Vehicle (TV) configuration in single-lane traffic 435

Figure VI-49: Comparison of cooling package temperature in single-lane traffic vehicles at different vehicle separation distances [averaged values of three different yaw angles 0°, -6°, and 6°]; (i) Constant heat rejection rate and (ii) variable heat rejection rate. 436

Figure VI-50: Temperature distribution in 0° yaw angle at 30ft vehicle separation distance (constant heat rejection rate)..... 436

Figure VI-51: Leading Vehicle (LV) and Trailing Vehicle (TV) configuration in two-lane traffic 437

Figure VI-52: Comparison of cooling package temperature in one-way two-lane traffic vehicles at different vehicle separation distances [averaged values of three different yaw angles 0°, -6°, and 6°].; (i) Constant heat rejection rate and (ii) variable heat rejection rate. 437

Figure VI-53: Temperature distribution in 0° yaw angle at 30ft vehicle separation distance (constant heat rejection rate)..... 438

Figure VI-54: Geometry (i) vehicle underhood compartment (ii) computational domain, and (iii) mesh side view 438

Figure VI-55: Comparison of (i) original and (ii) optimized fan-shroud..... 439

Figure VI-56: Position sensitivity magnitudes at 2nd and 6th iteration [surface optimizes @ higher position sensitivities]..... 439

Figure VI-57: Original Autonomie “lumped” mechanical accessory model. 445

Figure VI-58: Separated accessory models. (cooling fan, air compressor, power steering, air conditioning, and electrical accessories)..... 445

Figure VI-59: HD class 8 line haul sleeper cab based on a chassis tested Kenworth T700..... 446

Figure VI-60: First component test cell setup. Conventional sleeper cab setup with electrified condenser fan. 447

Figure VI-61: Second component test cell setup. Electrified compressor with electrified condenser fan..... 448

Figure VI-62: ORNL's VSI Component test cell. Open configuration. 449

Figure VI-63: ORNL's VSI Component test cell with insulated environmental box..... 450

Figure VI-64: NREL's CoolSim model and the structure it will take inside our Autonomie model when validated. 450

Figure VI-65: Testing conducted on the wireless charging system from the ORNL/Toyota/Evatran wireless charger for FOA-667..... 455

Figure VI-66: Efficiency test results from the ORNL/Toyota/Evatran wireless charger for FOA-667, with respect to coil misalignment and coil gap. 455

Figure VI-67: System efficiency test results from ORNL/Toyota/Evatran wireless charger for FOA-667 over a wide range of coil misalignment. 456

Figure VI-68: Magnetic field results at the rear of the vehicle: ORNL/Toyota/Evatran wireless charger for FOA-667..... 457

Figure VI-69: ABB Terra CJ 53 DCFC ready to commence testing. 457

Figure VI-70: Testing and evaluation of the ABB Terra CJ 53 DCFC, showing a constant current and constant voltage mode of operation. 458

Figure VI-71: Efficiency of the ABB Terra CJ 53 DCFC across a wide range of charge powers..... 458

Figure VI-72: Vehicle to Building Integration Pathway (GM0062) Project 461

Figure VI-73: Vehicle to Building Integration Pathway Use Case Review Responses 463

Figure VI-74: Difference in scope of this project with GM0062 Vehicle to Building Integration Pathway..... 468

Figure VI-75: Overview of the phenomena considered by each toolkit within VGISoft 473

Figure VI-76: Schematic overview of intended functionality and information flow within VGISoft toolkits..... 474

Figure VI-77: The whole framework of quantifying EV battery degradation 476

Figure VI-78: Average capacity losses of 100 EVs by performing different V2G services for ten years. In the extreme cases, all EVs provide the chosen grid service every day. The ten-year capacity losses from peak load shaving, frequency regulation and net load shaping increase by 3.62%, 5.6% and 22.6% compared to the base case, respectively. In the more realistic cases, EVs provide V2G services for 20 times per year. The ten-year capacity losses increase by 0.38%, 0.21% and 1.18%, respectively..... 477

Figure VI-79: Trends of the four parameters of the net load with uncontrolled charging demand on the extreme days: (a) minimum load; (b) maximum load; (c) maximum ramping down; (d) maximum ramping up..... 478

Figure VI-80: The contributions of EVs on (a) filling the load valley and (b) shaving the load peak, on the most extreme days from Year 2015 - 2025. 479

Figure VI-81: The contributions of EVs on mitigating (a) ramping down and (b) ramping up, on the most extreme days from Year 2015 - 2025. 479

Figure VI-82: DSM Framework and Data Exchange Overview 483

Figure VI-83: The DSM Prototype Hardware and Software - Showing 2 EVSE DSM Nodes (Blue) and a PEV Node (Green) Connected to EVSE #2. The BEMS Displaying the Status of the DSM Framework..... 484

Figure VI-84: The Initial DSM Development Lab Space..... 485

List of Tables

Table I-1 FY 2016 Accomplishment Highlights..... 4

Table I-2 Projects assigned to Grid and Infrastructure Program in FY 2017..... 16

Table I-3 Projects assigned to Energy Efficient Mobility Systems Program in FY 2017..... 17

Table I-4 Projects assigned to Advanced Combustion Systems in FY 2017 18

Table II-1: The baseline performance of Proterra EV Model BE35 baseline vehicle with 2-speed transmission and the target performance with the new 4-speed automated mechanical transmission (AMT)..... 26

Table II-2: Baseline model validation results for Proterra EV Model BE35 Bus based on vehicle acceleration time. 28

Table II-3: Baseline model validation results of the energy efficiency of Proterra BE35 electric bus 29

Table II-4: Trade off analysis of medium duty electric vehicle transmission concepts. 30

Table II-5: Gear ratio options with the headset ratios of 1.55 and 1.88.for the 4-speed transmission. 31

Table II-6: Proterra BE35 electric transit bus performance comparisons with the baseline 2-speed and the new 4-speed transmissions. 33

Table II-7: AVTE Vehicles Tested During FY 2016..... 43

Table II-8: Subtasks of Task 1: Instrumentation and data acquisition of energy related information 48

Table II-9: Description of Oil + FM Evaluated. 63

Table II-10: Summary of friction coefficient for 3 variants provided by ZNP..... 67

Table II-11: Comparison of EMA to ANL ring-on-liner measurements. 70

Table II-12: Comparison of EMA to ANL skirt-on-liner measurements..... 70

Table II-13: Sample and Exposure Time for DPT-68 Material Compatibility Study..... 112

Table II-14: PCM Charging Capacity Validation 115

Table II-15: Thermal Loss Evaluation during Cold Soak (Cooling from 100°C to 72.6°C) 115

Table II-16: Milestones..... 124

Table II-17: Deliverables or Milestones 133

Table II-18: Impact of High Frequency Transformer Turns Ratio on System Limits and Maximum Power 148

Table II-19: Impact of Higher Magnetic Airgap on System Limits..... 150

Table II-20: 2012 Zero Emission Drayage Truck Demonstration Portfolio 157

Table II-21: TransPower EDD Trucks Average Daily Use 161

Table III-1: Federal Way vehicles monitored..... 188

Table III-2: Hybrid Propulsion-Related System Specifications..... 201

Table III-3: Vehicle specifications for chassis dynamometer testing 210

Table III-4: EV2G School Bus Specifications 220

Table III-5: EVG2 Dynamometer Results 223

Table III-6: EV2G School Bus DC KWH/mile 223

Table III-7: EV2G Dynamometer Results with Charging Efficiency Considered..... 224

Table III-8: Spring schedule high-level summary statistics from propane powered buses..... 231

Table III-9: Solar/Thermal Control Technology Off-Cycle Credits 246

Table III-10: Baseline and Solar Control Glazing Direct Solar Transmittance (Tds, %) 248

Table III-11: Time of Day of Travel..... 249

Table III-12: Time Spent Between Trips 249

Table III-13: Trip Duration..... 250

Table III-14: 2015 VW E-Golf specifications 260

Table III-15: 2015 Mercedes Benz B-Class Electric specifications 261

Table III-16: 2015 Chevrolet Impala Bi-Fuel Specifications 263

Table III-17: Fuel Economy and Emissions of 2015 Chevrolet Impala Bi-Fuel at 72F ambient 264

Table III-18: 2016 Chevrolet Volt specifications 265

Table III-19: 2014 BMW i3 Rex Specifications..... 267

Table III-20: Results of dynamometer testing and model simulation of 2011 Ford Fusion with pre-warmed transmission and hypothetical active warm-up system, respectively. A positive fuel economy benefit corresponds to a decrease in fuel use. 279

Table III-21: Results of 2016 Ram 1500 dynamometer testing at various temperatures to determine the fuel economy benefit of active transmission warm-up. A positive fuel economy benefit corresponds to a decrease in fuel use due to active transmission warm-up. 281

Table IV-1: Parameters of vehicle for road load power estimation 287

Table IV-2: Statistics from the Monte Carlo Simulations 288

Table IV-3: Scenario Setup and Analysis Results 311

Table IV-4: Battery sizing impacts of TLRP 334

Table IV-5: A/C national-level fuel use simulation result summary 334

Table IV-6: Heating national-level fuel use simulation results summary 336

Table V-1: Instrumentation Tolerance 370

Table V-2: VOLTTRON and CIP.io Comparison 380

Table VI-1: Materials and Dimensions of Each Layer 412

Table VI-2: Comparison of Convection and Subcooled Boiling 418

Table VI-3: Operating conditions for aerodynamic drag simulations 433

Table VI-4: Heat exchanger porous body modeling 434

Table VI-5: Heat exchanger porous body modeling 438

Table VI-6: Operating Conditions 438

Table VI-7: Heat exchanger cooling air mass outflow rates 439

Table VI-8: Accessory Fuel Consumption Entitlements for the Cummins Proprietary Cycle (HD class 8 line haul sleeper cabin) 448

Table VI-9: GM0062 Use Cases 462

Table VI-10: Production PEVs being characterized 470

Acronyms and Abbreviations

A

AC	Alternating Current
ACC	Adaptive Cruise Control
accel	Acceleration
ACS	Advanced Combustion Systems
ACSforEVER	Advanced Climate Systems for EV Extended Range
AER	All-electric range
AFV	Alternative Fuel Vehicle
AMI	Advanced Metering Infrastructure
AMT	Automated Mechanical Transmission
ANL	Argonne National Laboratory
ANN	Artificial Neural Network
AOI	Areas of Interest
APEC	Asia Pacific Economic Council
APRF	Advanced Powertrain Research Facility
APT	Pressure Sensor
ASD	Aftermarket Safety Device
AVTA	Advanced Vehicle Testing Activity
AVTE	Advanced Vehicle Testing and Evaluation

B

BaScce	Baseline and Scenario
Batt	Battery
BEB	Battery Next-Generation Electric Transit Bus
BEC	Bussed Electrical Center
BEMS	Building Energy Management System
BET	Battery Electric Truck
BEV	Battery Electric Vehicle
BMW	Bayerische Motoren Werke AG
BSFC	Brake Specific Fuel Consumption
BTE	Brake Thermal Efficiency

C

CAC	Charge Air Cooler
CACC	Cooperative Adaptive Cruise Control
CAE	Computer-Aided Engineering
CAFE	Corporate Average Fuel Economy
CAN	Controller Area Network
CAV	Connected and automated vehicles
CARB	California Air Resources Board

CBD	Central Business District
CCS	Combined Charging System
CW, CCW	Clockwise, Counter Clockwise
CD	Charge-Depleting
CERV	Conference on Electric Roads and Vehicles
CFD	Computational Fluid Dynamics
CFDC	Commercial Fleet Data Center
CFL	Combined Fluid Loop
CH4	Methane
CHTS	California Household Travel Survey
CIP	Common Integration Platform
Cm ³	Cubic
CNG	Compressed Natural Gas
CO	Carbon monoxide
CO ₂	Carbon Dioxide
COMM	Commuter
Conv	Conventional Vehicle
COP	Coefficient of Performance
CRADA	Cooperative Research and Development Agreement
CS	Charge Sustaining
Cs	Cold start
CV	Conventional vehicle

D

D3	Downloadable Dynamometer Database
DC	Direct current
DCFC	Direct Current Fast Charge
DCT	Dual-clutch transmission
decel	Deceleration
DER	Distributed energy resource
DFGM	Digital Flux Gate Magnetometer
DFMEA	Design of Failure Modes Analysis
DOE	U.S. Department of Energy
DOHC	Dual overhead cam
DS	Down speeding
DSM	Distributed Security Module
DSM	Diagnostic Security Module
DSP	Digital Signal Processor
DSRC	Dedicated Short Range Communications
dt	Change in time
dv	Change in velocity
Dyno	Dynamometer

E

EAVS	Electrically Assisted Variable Speed Supercharger
EC	European Commission
EDV	Electric Drive Vehicle
EDX	Energy dispersive x-ray spectroscopy
EERE	Energy Efficiency and Renewable Energy
EGR	Exhaust Gas Recirculation
EG/W	Ethylene glycol/water
EOL	End of life
EPA	Environmental Protection Agency
ePATHS	Electrical PCM Assisted Thermal Heating System
EREV	Extended-Range Electric Vehicles
ESIF	Energy Systems Integration Facility
ESS	Energy Storage System
ETT	Electric Transportation Technologies
E-TREE	Electric Truck with Range Extending Engine
EUMD	End-Use Measurement Device
EV	Electric Vehicle
EV2G	Electric Vehicle-to-Grid
EVSE	Electric Vehicle Service Equipment
EXV	Electronic Expansion Valve

F

F	Force
FASTSim	Future Automotive Systems Technology Simulator
FC	Fuel cell
FC	Fast charge
FCons	Fuel consumption
FCTO	Fuel Cell Technologies Office
FE	Fuel Economy
FEA	Finite Element Analysis
FEX	Front-end Heat Exchanger
FHWA	Federal Highway Administration
FLNA	Frito-Lay North America
FM	Friction Modifier
FMEP	Friction Mean Effective Pressure
FOA	Funding Opportunity Announcement
FTIR	Fourier transform infrared spectroscopy
FTP	Federal Test Procedure
FWD	Four wheel drive
FY	Fiscal year

G

g	gram
GB	Gigabyte
GCEDV	Grid Connected Electrical Drive Vehicles
GEM	Gas Emissions Model
GHG	Greenhouse Gas
GITT	Grid Interaction Tech Team
GMLC	Grid Modernization Lab Consortium
GnPs	graphene nanoplatelets
GO	Graphene Oxide
GPRA	Government Performance and Results Act
GPS	Global Positioning System
GREET	Greenhouse gases, Regulated Emissions, and Energy use in Transportation
GSF1	Generic Speed Form 1
GSU	Grid side unit
GUI	Graphic User Interface
GVW	Gross Vehicle Weight

H

h-APU	hybrid Auxiliary Power Unit
HATCI	Hyundai America Technical Center, Inc.
HC	Unburned hydrocarbons
HD	Heavy Duty
HEV	Hybrid-Electric Vehicle
H-GAC	Houston-Galveston Area Council
HHDDT	Heavy Heavy-Duty Diesel Truck
HHV	Hydraulic Hybrid Vehicle
HIL	Hardware-In-the-Loop
HP	Heat Pump
Hp	Horsepower
HTML	HyperText Markup Language
HV	High Voltage
HVAC	Heating Ventilating and Air Conditioning
HWFET	Highway Fuel Economy Test
HPMS	Highway Performance Monitoring System
HVTB	High Voltage Traction Battery
HWY	Highway Program or Highway Fuel Economy Test Cycle
HPC	High Performance Computing
HTR	Heater
Hz	Hertz

I

I	Inertia
IC	Internal Combustion
ICD	Iterim Component Durability
ICDV	Internal Combustion Drive Vehicles
ICE	Internal Combustion Engine
ICTF	Intermodal Container Transfer Facility
ICU	Inverter-Charger Unit
IEB	Information Exchange Bus
IEC	International Electrotechnical Commission
IGBT	Insulated Gate Bipolar Transistors
IHX	Internal Heat Exchanger
INL	Idaho National Laboratory
INTEGRATE	Integrated Network Testbed for Energy Grid Research and Technology
IOT	Internet of Things
IR	Infrared Radiation
ISO	International Organization for Standardization
ITS	Intelligent Transportation Systems

J

JIT	Just-in-Time
-----	--------------

K

kg	Kilogram
km	Kilometer
kW	Kilowatt
kWh	Kilowatt hour

L

L	litre
L1	Level 1 benchmark
L2	Level 2 benchmark
Lbf	Pounds force
LCC	Liquid-Cooled Condenser
LD	Light-duty
LH	line haul
Li	Lithium
LIB	Lithium ion battery
LLNL	Lawrence Livermore National Laboratory
LTC	Lockport Technical Center
LV	Leading Vehicle

M

M	Mass
MBSE	Model Based System Engineering
MD	Medium Duty
mpg	Miles per gallon
MMTCE	Million Metric Tons of Carbon Equivalent
MIIT	Ministry of Industry and Information Technology
mi	Mile
MJ	Megajoules
MOSFET	Metal-Oxide Semiconductor Field-Effect Transistor
mph	Miles per hour
MPGe, MPGe	Miles per gallon equivalent, Miles per gallon gasoline equivalent
MTDC	Medium Truck Duty Cycle
MOVES	Motor Vehicle Emission Simulator
MRF	Moving Reference Frame
MURECP	Medium-Duty Urban Range Extended Connected Powertrain
MY	Model year
M ²	Meters squared

N

NACFE	North American Council for Freight Efficiency
NDA	Non-Disclosure Agreement
NETL	National Energy Technology Laboratory
NHTS	National Household Travel Survey
NHTSA	National Highway Transportation Safety Administration
NM	Newton meters
NO _x	Nitrogen oxides
NR	Natural Rubber
NRE	Non Recurring Engineering
NREL	National Renewable Energy Laboratory
NRT	National Retail Trucking
NVH	Noise, vibration, and harshness
NVUSD	Napa Valley Unified School District
NYSERDA	New York State Energy Research Development Authority

O

OBC	On-board charger
OCBC	Orange County Bus Cycle
OEM	Original Equipment Manufacturer
OneSAF	One Semi-Automated Forces
ORNL	Oak Ridge National Laboratories

P

P	Active Power
PC	Polycarbonate
PCM	Phase-Change Material
PCU	Power Control Unit
PCU	Powertrain Control Unit
PEEM	Power Electronics and Electric Motor
PFC	Power factor correction
PFI	Port fuel injection
PGW	Pittsburgh Glass Works
PHEV	Plug-in Hybrid Electric Vehicle
PHEV##	Plug-in hybrid electric vehicle with ## miles of all-electric range
PI	Principal Investigator
PM	Permanent Magnet
PM	Particulate Matter
ppm	Parts per Million
PTC	Positive Temperature Coefficient (Electric Heater)
PTO	Power Take-Off
PVP	Polyvinylpyrrolidone
PWWMD	Public Works and Waste Management Department
λ	Power Factor
φ	Power Angle

Q

Q	Reactive power
QA	Quality assurance
QC	Quality control

R

R2	Coefficient of Determination
R/D	Receiver / Dryer
REV	New York State's Reforming the Energy Vision Initiative
REx	Range Extending Engine
rGO	reduced graphene oxide
RH	Relative Humidity
RMS	Root Mean Square
ROL	Ring-On-Liner
rpm	Revolutions Per Minute
RSU	Road Side Unit
RWDC	Real-World Drive-Cycle

S

S	Apparent power
SAE	Society of Automotive Engineers
SBR	Styrene-Butadiene Rubber
SC03	SC03 Supplemental Federal Test Procedure
SCAG	Southern California Association of Governments
SCAQMD	South Coast Air Quality Management District
SCIG	Southern California International Gateway
SCR	Silicon Controlled Rectifier
SCR	Selective Catalytic Reduction
SDO	Standards Definition Organizations
SI	Système International d'Unités
SI	Gasoline Spark Ignition
SNR	Sensor
SOC	State of Charge
SPL	Sound Pressure Level
SR	Speed Ratio
SS	Steady State
S/S	Start/Stop
SPaT	Signal Phase and Timing
StAR	Storage-Assisted Recharging

T

T	Torque
TA	Technical Area
TA	Torque Assist
TC	Thermocouple
TE	Thermoelectric
TE	Transmission Error
TES	Thermal Energy Storage
TGA	thermogravimetric analysis
THC	Total hydrocarbon emissions
TIM	Thermal Interface Materials
TLRP	Thermal Load Reduction Package
TN	Testing Network
TOU	Time-Of-Use
TSDC	Transportation Secure Data Center
TSI	Turbocharged stratified injection
TUSD	Torrance Unified School District
TV	Trailing Vehicle
TXVs	Thermal Expansion Valves

U

U.S. DRIVE	U.S. Driving Research and Innovation for Vehicle Efficiency and Energy Sustainability
UA	Transfer Coefficient
UC	Ultra-capacitor
UCR	University of California, Riverside
UDDS	Urban Dynamometer Driving Schedule
UM	University of Michigan
UN ECE	United Nations Economic Council for Europe
UPS	United Parcel Service
URL	Uniform Resource Locator
US06	Environmental Protection Agency US06 or Supplemental Federal Test Procedure
USABC	United States Advanced Battery Consortium
USCAR	U.S. Council for Automotive Research
Util	Battery capacity utilization

V

V	Voltage
V2G	Vehicle-to-Grid
VAr	Volt-Amp-reactive
VGI	Vehicle-Grid Integration
VGT	Variable Geometry Turbocharger
VIP	Vacuum Insulated Panels
VMT	Vehicle Miles Traveled
VS	Vehicle Systems
VSATT	Vehicle Systems Analysis Technical Team
VSI	Vehicle Systems Integration
VSST	Vehicle Systems Simulation and Testing
VTCab	Vehicle Thermal Cab Simulator
VTIF	Vehicle Testing and Integration Facility
VTO	Vehicle Technologies Office

W

dw	Change in Angle W
WCC	Water Cooled Condenser
WEC	World Endurance Championship
WEG	Water/Ethylene Glycol
Wh	Watt hour
WHR	Waste Heat Recovery
WPT	Wireless Power Transfer

WTW	Well-to-Wheels
-----	----------------

X

XPS	x-ray photoelectron spectroscopy
-----	----------------------------------

Y

Z

ZECT	Zero-emissions cargo transport
------	--------------------------------

I. Introduction

On behalf of the Vehicle Technologies Office (VTO) of the U.S. Department of Energy (DOE), we are pleased to submit the Annual Progress Report for Fiscal Year (FY) 2016 for the Vehicle Systems (VS) program activities.

I.1. Mission and Objectives

VS is concerned with advancing light-, medium-, and heavy-duty (HD) vehicle systems to support DOE’s goals of developing technologies for the U.S. transportation sector that enhance national energy security, increase U.S. competitiveness in the global economy, and support improvement of U.S. transportation and energy infrastructure. To help reach those goals, VTO conducts research and development (R&D) programs implementing strategies to help maximize the number of electric vehicle miles driven, increase the energy efficiency of transportation vehicles, and modernize the U.S. electric grid.

VS’s mission is to accelerate the market introduction and penetration of advanced vehicles and systems with R&D that have a significant impact on DOE’s petroleum displacement and electrification goals. Figure I-1 below outlines the outcome objectives that VS has identified as important to fulfilling its mission. Figure I-2 lists the primary processes and examples of tangible R&D project objectives that contribute to one or more VS outcome objectives.

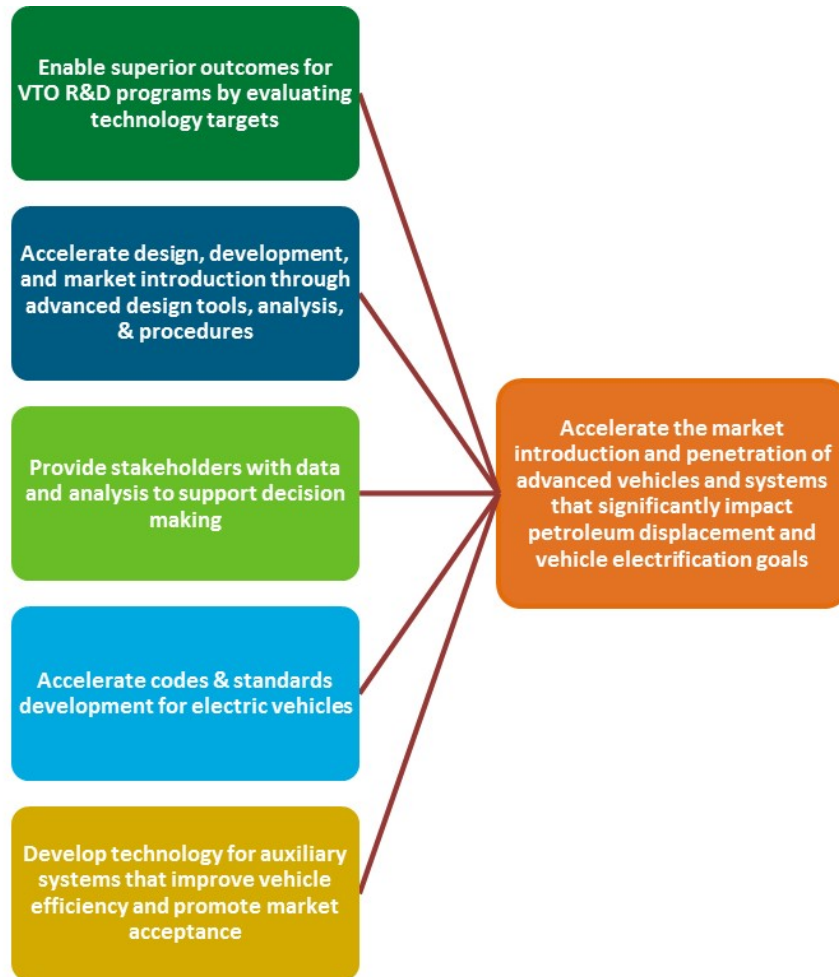


Figure I-1: VS outcome objectives and mission

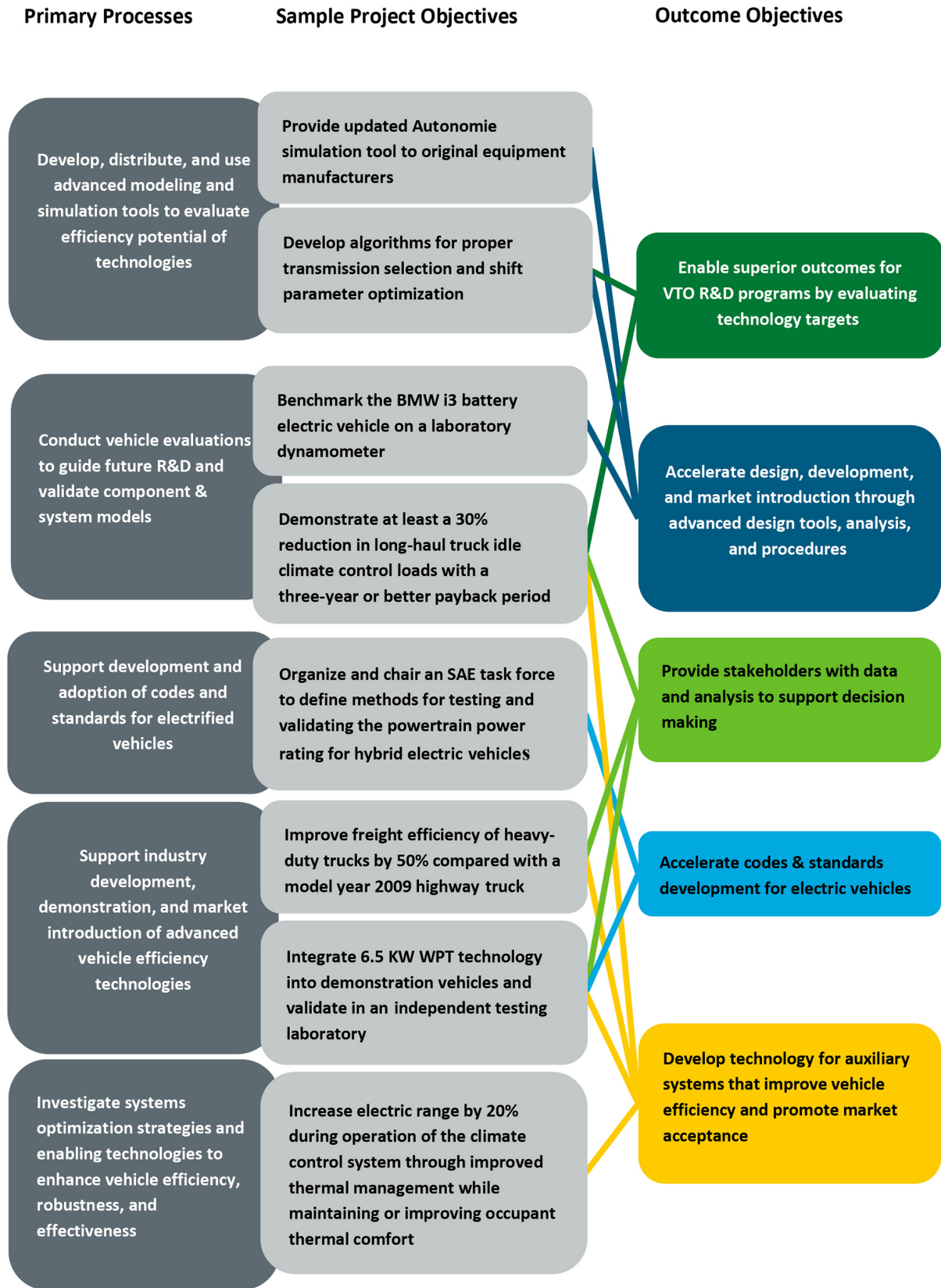


Figure I-2: VS primary processes, project objectives, and outcome objectives

I.2. Accomplishments

A snapshot of VS project highlight accomplishments for FY 2016 are provided in Table I-1. These accomplishments are intermediate steps to realizing the potential real world benefits of advanced vehicle systems technologies. As an example of end-goal real world benefits that VS is working toward, the section below describes the benefits accruing from market adoption of aero-reduction retro-fit technologies. The retro-fit technologies were developed from 2001-2013 as part of VS’s project on Heavy Vehicle Aerodynamic Drag.

Class 8 Aero Drag Reduction Project Real World Fuel Savings

Real world petroleum reduction benefits are accruing from commercial fleet adoption of trailer skirt and box-tail technologies developed by phase one of DOE’s Project on Heavy Vehicle Aerodynamic Drag. The on-going real world benefits to the U.S. economy given below are the successful outcome of the VS sustained R&D project from 2001-2013. The project was led by Dr. Kambiz Salari at Lawrence Livermore National Laboratory (LLNL) and featured collaborative technology development with component manufacturers and commercial fleet managers. A 2014 study by the North American Council for Freight Efficiency (NACFE) documented commercial fleet adoption of Class 8 trailer skirts and box-tail drag reduction devices. Rapid adoption has been accomplished in the absence of additional regulatory mandates because commercial fleet operators receive an attractive return on their investment in these fuel saving devices. Using NACFE’s fleet adoption numbers we conservatively estimate the following benefits from trailer skirt and box-tail retrofits:

- The devices reduced diesel fuel consumption by U.S commercial truck fleets by 1.1 billion gallons annually in 2014, 2015, and 2016. The 1.1 billion gallon reduction of diesel consumption also reduced air pollution by more than 11 million metric tons annually.
- U.S. commercial fleet adoption of the project’s trailer skirt and box-tail retro-fit technologies are on track to deliver the following cumulative real world benefits by 2035¹
 - 27 billion gallon reduction in diesel fuel consumption 270 million metric tons reduction in CO₂ production
 - \$81 billion in freight transportation fuel savings.

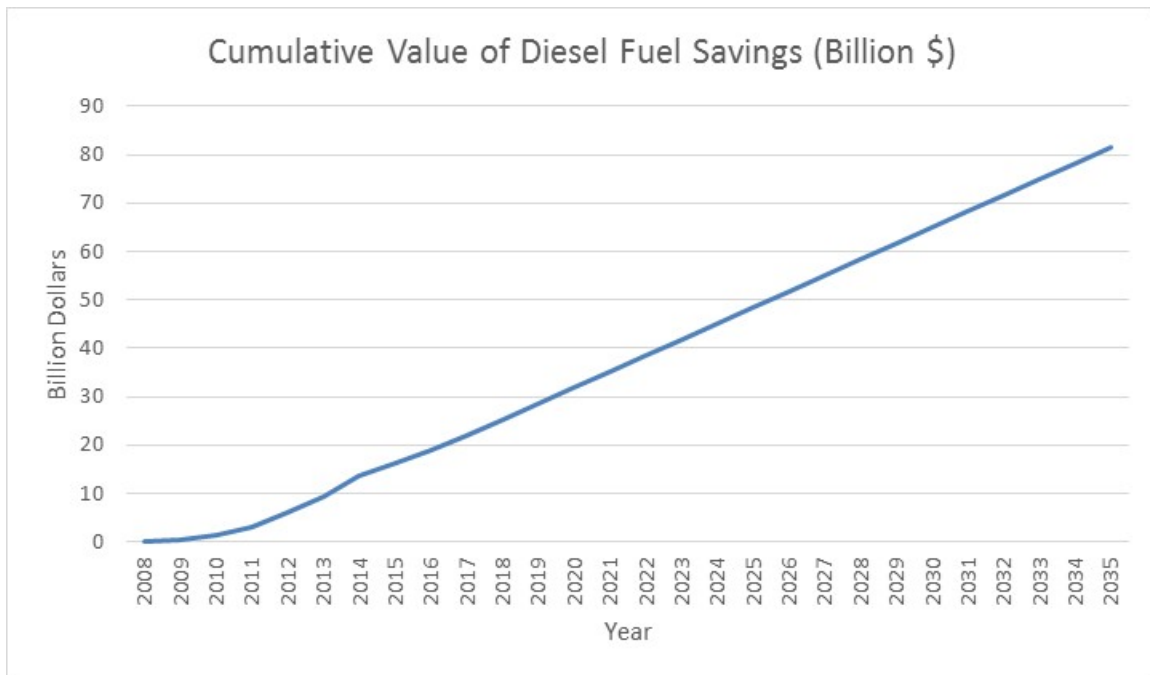


Figure I-3: Projected cumulative freight transportation fuel savings from trailer skirt and box-tail technologies

¹ Assumes number of retrofitted trucks remains constant at 2014 levels and diesel price of \$3.00 per gallon from 2018-2035

Table I-1 FY 2016 Accomplishment Highlights

Accomplishment	Significance	R&D Organization	Links to Details
<p>Researchers prototyped and evaluated a Thermal Energy Storage (TES) unit and the ePATHS phase change material (PCM) heat exchanger</p>	<p>The prototype’s PCM thermal storage capacity met a design target capable of improving the electric drive range by 20% in cold ambient conditions.</p>	<p>MAHLE Behr Troy Inc.</p>	<p>Electric Phase Change Material Assisted Thermal Heating System (ePATHS) DE-EE0006444</p>
<p>Researchers prototyped an analysis process for thermal load reduction of Off-Cycle Credit technologies</p>	<p>The analysis informed the assignment of off-cycle credits for thermal load reduction technologies. This offers vehicle manufacturers the possibility of receiving the maximum credit for technologies that improve vehicle efficiency.</p>	<p>NREL</p>	<p>Analysis Process for Thermal Load Reduction Off-Cycle Credit Technologies (112)</p>
<p>Researchers completed an assessment of active transmission warm-up based on data from coordinated on-road and laboratory tests</p>	<p>The assessment informed the assignment of off-cycle credits for an active transmission warm-up. This offers vehicle manufacturers the possibility of receiving the maximum credit for technologies that improve vehicle efficiency.</p>	<p>ANL, INL</p>	<p>Road and Lab Coordinated Assessment of Active Transmission Warm-up, Advanced Technology Vehicle Lab Benchmarking (Level 1 & Level 2)</p>
<p>Researchers quantified the real world effectiveness of engine start-stop systems</p>	<p>The analysis informed the assignment of off-cycle credits for engine start-stop technology. This offers vehicle manufacturers the possibility of receiving the maximum credit for technologies that improve vehicle efficiency.</p>	<p>INL,ANL,NREL</p>	<p>Real World Effectiveness of Engine Start-Stop Systems</p>
<p>Researchers prototyped five battery electric trucks (BETs) and demonstrated four of the BETs with fleet partners at the Ports of Los Angeles and Long Beach. Researchers also prototyped a plug-in hybrid electric truck (PHET) and began validation testing of the vehicle.</p>	<p>Real world demonstration of BETs and PHET are critical steps for transitioning advanced HD technologies to the marketplace.</p>	<p>SCAQMD</p>	<p>The Zero Emission Drayage Trucks Demonstration (ZECT 1, SCAQMD)</p>
<p>Researchers completed end-of-vehicle life testing on five vehicles and</p>	<p>Published test reports benefit industry, regulators, researchers, and consumers by quantifying vehicle performance, energy</p>	<p>Intertek, INL</p>	<p>Advanced Vehicle Testing & Evaluation</p>

Accomplishment	Significance	R&D Organization	Links to Details
implemented a storage-assisted recharging unit at a fleet test location to facilitate opportunity charging of fast charge-capable vehicles.	efficiency, battery performance degradation, maintenance and repairs, and overall cost of ownership for the vehicles.		(AVTE) [DE-EE0005501]
Researchers designed the second generation of an integrated tractor-trailer geometry that radically decreases aerodynamic drag and improves the fuel economy (GSF2)	GSF2 represents a breakthrough in aerodynamic performance that was validated by wind tunnel testing.	LLNL	DOE's Effort to Improve Heavy Vehicle Fuel Efficiency through Improved Aerodynamics
Researchers completed preliminary analysis of the in-field Hydraulic Hybrid Vehicle (HHV) test data that indicates an average fuel economy improvement of 52% with the second-generation HHVs over the 2007 conventional diesels when operated on similar routes.	Typical fuel efficiency for a 2007 conventional refuse truck is 3 mpg. The 2 nd generation HHV technology would significantly reduce diesel consumption, pollution, and brake wear as compared to 2007 conventional diesel refuse trucks.	National Renewable Energy Laboratory (NREL)	Medium- and Heavy-Duty Field Testing
Researchers showed that a fuel fired heater with thermal load reduction package (TLRP) could save 973 gallons of fuel per truck annually	These results complement the previous electric air conditioning (A/C) battery idle-off savings of 774 gallons per truck per year. The combined battery-electric A/C idle-off system, fuel-fired heater, and TLRP system has potential to reduce U.S. long-haul truck consumption of diesel by 213 million gallons annually. Cost estimates for the installed combined system show that the payback period of this system is 2 years or less.	NREL	Long-Haul Truck Idle Climate Control Load Reduction & VTCab, Rapid Vehicle HVAC Load Estimation Tool
Researchers achieved 20 kW wireless power transfer (WPT) at 162 mm airgap, with 95% DC-to-DC efficiency (from inverter DC input to vehicle battery). The results were measured on a WPT system where the secondary coil was integrated into a Toyota RAV4.	The WPT power level demonstrated was three times that of an AC L2 (wired) EVSE. This demonstration of high power WPT at high efficiency and relatively large airgap demonstrates that WPT technology increased charging convenience while fulfilling the upper bound power transfer rate requirements of today's AC L2 corded technology standard.	ORNL	Wireless Charging of Electric Vehicles [FOA #667]
Researchers completed Phase I candidate thermal load reduction technology evaluations to improve Hyundai Sonata range.	The analyses of the experimental results identified several technologies with potential to extend EV range by reducing thermal loads consumption. A package of these technologies will be integrated into the PHEV and evaluated during Phase II (FY 2017).	NREL	Design and Implementation of a Thermal Load Reduction System for a Hyundai Sonata

Accomplishment	Significance	R&D Organization	Links to Details
<p>Researchers evaluated the performance of three solar control glazing packages, solar reflective paint, and cooled/ventilated seating in warm weather conditions Evaluated the performance of heated surfaces, and a combined heated windshield and door demisters in cold weather conditions.</p>			<p>PHEV for Improved Range</p>
<p>Researchers completed technology assessment of five advanced technology vehicles of multiple classes and fuel types.</p>	<p>The data from laboratory assessments are used as inputs to models and analyses that inform stakeholders on the fuel and energy consumption characteristics of vehicles that employ advanced technologies.</p>	<p>Argonne National Laboratory (ANL)</p>	<p>Advanced Technology Vehicle Lab Benchmarking (Level 1 & Level 2)</p>
<p>Researchers quantified the energy saving potential of vehicle trip profiles resulting from Connected and Autonomous Vehicles (CAV) technologies on multiple powertrain technologies.</p>	<p>The study assessed a 13% fuel savings potential for "green routing" (drivers' following the most fuel efficient route) in comparison to actual routes taken for thousands of real-world trips. Initial analysis for conventional powertrain vehicles indicated that 35% of trips (representing 45% of fuel consumption) showed potential for green routing benefit.</p>	<p>ANL</p>	<p>Connected and Automated Vehicle</p>
<p>Researchers demonstrated 88% increase in freight efficiency [ton-mi/gal] compared with a 'best in class' MY 2009 highway truck, measured on-road over a variety of road profiles, surpassing the 50% goal</p>	<p>The experimental Class 8 truck demonstrated a 188 ton-mi/gal freight efficiency. The Volvo truck's package of new technologies has potential to significantly reduce diesel consumption and improve long-haul transportation freight efficiency by 88%. The design featured a powertrain with 50% brake thermal efficiency capability. The project's simulations predict that the technology can be modified to achieve 56% BTE capability.</p>	<p>Volvo</p>	<p>Volvo SuperTruck [DE-EE0004232]</p>
<p>Researchers demonstrated enabling technologies for EV grid integration. The technologies included a Common Integration Platform (CIP), a prototype Smart Charge Adaptor (SCA), and a refined submeter.</p>	<p>The demonstration of enabling technologies and publication of open source interface code accelerates the evolution of EV grid integration codes and standards. Evolution of industry standards is critical for market introduction of new technologies and services that enhance the environmental benefits, convenience, and economic viability of EVs.</p>	<p>ANL</p>	<p>PEV-Grid Connectivity [2.4.0.7]</p>
<p>Researchers released new versions of Autonomie (R15 and R15SP1) with large number of new features</p>	<p>Car manufacturer researchers and engineers rely on system simulation to introduce new technologies in the market and government agencies use Autonomie to assess the energy impact of a large number of technologies and scenarios as part of their R&D portfolio. Autonomie is licensed to more than 175</p>	<p>ANL</p>	<p>Autonomie for Model Based System Engineering</p>

Accomplishment	Significance	R&D Organization	Links to Details
	companies and research organizations worldwide.		
Researchers quantified the impact of new technologies on real-world driving cycles (RWDC) and compared the impact to the benefits observed in regulatory cycles.	The study informed VTO component R&D activities by evaluating the energy consumption impacts of advanced technologies in the context of both real world and regulatory drive cycles. The energy requirement of various types of vehicles, ranging from conventional gasoline vehicles to battery electric vehicles, including various hybrids and alternate fuel vehicles, were considered.	ANL	Vehicle Technologies Benefits on Real-World Drive Cycles Using POLARIS Regional Transportation System Model
Researchers extended the CoolSim modeling framework and used it in projects with several industry partners.	The CoolSim modeling framework was used to collaborate with industry to model and develop energy-saving advanced thermal management systems and their required control strategies.	NREL	Vehicle Thermal System Model Development in Simulink
Researchers completed development of out-of-vehicle maximum power procedure and laboratory requirements in support of SAE J2907. This is a major step in establishing a consistent and repeatable mechanism for the assessment of motor net power and maximum 30 minute power	Prior to this study, there was no widely accepted standard for specifying the performance of a traction motor designed for use in electrified vehicles whether hybrid, battery electric, fuel cell, or range extended. J2907 was introduced as a TIR - technical information report to establish a uniform set of test procedures for users and independent testing facilities to validate manufacturer claims in an out-of-vehicle, laboratory environment.	ORNL	SAE J2907 Performance Characterization of Electrified Powertrain Motor-drive Subsystem
Researchers successfully implemented Wireless Power Transfer (WPT) charger-to-vehicle communications with closed loop current control, and charged electric vehicle from 0 to 100% state-of-charge using wireless charging system at ~6.8 kW output. Total system (grid to DC output) efficiency was 91% at 6.6kW output.	The implementation of vehicle integrated WPT system is a critical milestone in developing and demonstrating the project objectives. The WPT system efficiency was measured as 91% and exceeded the project's goal of 85% grid to DC efficiency with minimum 20 cm coil-to-coil gap at 6.6KW output.	Hyundai North America Technical Center	High Efficiency, Low EMI and Positioning Tolerant Wireless Charging of EVs

Accomplishment	Significance	R&D Organization	Links to Details
<p>Designed and tested a hybrid Auxiliary Power Unit (h-APU) architecture that would allow for hybridization for the air conditioning, electrification of the condenser fans, and energy storage for other electrical hotel loads of MD/HD trucks. This allows for the truck to eliminate or greatly reduce all over night idling by providing hotel loads from a battery pack that uses regenerative braking for charging.</p>	<p>The tested architecture allows for the truck to eliminate or greatly reduce all over night idling by providing hotel loads from a battery pack that uses regenerative braking for charging. The project uses a two-part approach for developing fuel saving auxiliary load components that includes selecting the best component technology, and/or architecture, and optimized controls that are vehicle focused. The approach addresses idle reduction and optimized component strategies.</p>	<p>ORNL</p>	<p>Cummins MD&HD Accessory Hybridization CRADA</p>

I.3. Approach and Organization of Activities

VS groups its projects into focus area activity categories that implement its primary processes (see Figure I-2). In FY 2016, these focus areas were Vehicle Modeling and Simulation (M&S), Vehicle Technology Evaluations (VTE), Codes and Standards (C&S), Industry Projects, and Vehicle Systems Efficiency Improvements (VSEI).

Projects within each focus area typically produce outputs in one or more of the following forms: data, analysis, reports, tools, specifications, and procedures. The outputs from one project are often used as the inputs for one or more projects in other focus areas. The integration of computer modeling and simulation, laboratory and field vehicle evaluations, and codes and standards development and validation for vehicle classes from LD to HD is critical to the success of the VS program. Information exchange between focus area activities enhances the effectiveness of each activity (illustrated in Figure I-3).



Figure I-4: VS activities integration – Arrows represent information flow between activity focus areas that enhances effectiveness of individual activities.

An example of beneficial data exchange is the increased accuracy of predictive simulation models for advanced technology vehicles made possible by empirical test data that characterize a vehicle's real-world performance. (In the example case, VTE activities feed information to the M&S activity). Laboratory and field technology evaluation studies provides data that informs support of Codes and Standards. Test data from VTE activities are also used to identify requirements for new more efficient technologies and validate those technologies that are developed under VSEI.

VS provides an overarching vehicle systems perspective in support of the technology R&D activities of DOE's VTO and Fuel Cells Technology Office (FCTO). VS uses analytical and empirical tools to model and simulate potential vehicle systems, validate component performance in a systems context, verify and benchmark emerging technologies, and validate computer models. HIL testing allows components to be controlled in an emulated vehicle environment. Laboratory testing then provides measurement of progress toward VTO technical goals and eventual validation of DOE-sponsored technologies at ANL's Advanced Powertrain Research Facility (APRF) for light- and medium-duty vehicles and at NREL's Renewable Fuels and Lubricants (ReFUEL) facility for HD vehicles. For this program to be successful, extensive collaboration with the technology development activities within the VTO and FCTO is required for both analysis and testing. Analytical results of this sub-program are used to estimate national benefits and/or impacts of DOE-sponsored technology development (illustrated in Figure I-4).

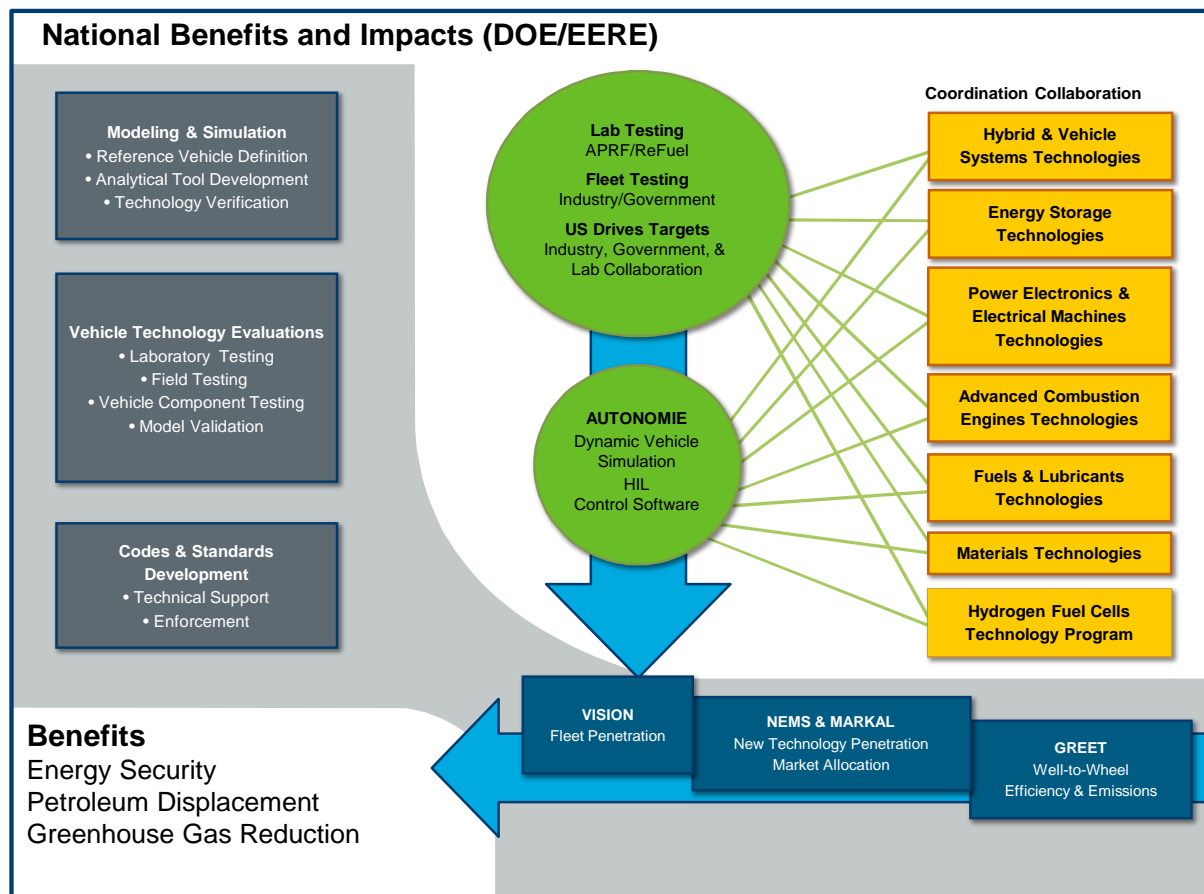


Figure I-5: VS activities providing estimates of national benefits and impacts of advanced technologies.

VS R&D activities are performed by the national laboratories and industry. National laboratory R&D activities are organized into the four focus areas. A brief description of each focus area and its major accomplishments for FY 2016 are outlined below.

Modeling and Simulation

DOE has developed and maintains software tools that support VTO research. VISION, NEMS, MARKAL, and GREET are used to forecast national-level energy, environmental, and economic parameters, including oil use, market impacts, and GHG contributions of new technologies. These forecasts are based on VTO vehicle-level simulations that predict fuel economy and emissions using VS’s Autonomie modeling tool. Autonomie’s simulation capabilities allow for accelerated development and introduction of advanced technologies through computer modeling rather than through expensive and time-consuming hardware building. Modeling and laboratory and field testing are closely coordinated to enhance and validate models as well as ensure that laboratory and field test procedures and protocols comprehend the needs of new technologies that may eventually be commercialized.

Autonomie is a MATLAB-based software environment and framework for automotive control system design, simulation, and analysis. This platform enables dynamic analysis of vehicle performance and efficiency to support detailed design, hardware development, and validation. Autonomie was developed under a cooperative research and development agreement (CRADA) with General Motors and included substantial input from other original equipment manufacturers (OEMs), and replaces its predecessor, the Powertrain Systems Analysis Toolkit (PSAT). One of the primary benefits of Autonomie is its plug-and-play foundation, which allows integration of models of various degrees of fidelity and abstraction from multiple engineering software environments. This single powerful tool can be used throughout all the phases of model-based design of the vehicle development process (VDP).

HIL simulation provides a novel and cost-effective approach to isolate and evaluate advanced automotive component and subsystem technologies while maintaining the rest of the system as a control. HIL allows actual hardware components to be tested in the laboratory at a full vehicle level without the extensive cost and lead time of building a complete prototype vehicle. This approach integrates modeling and simulation with hardware in the laboratory to develop and evaluate propulsion subsystems in a full vehicle-level context. The propulsion system hardware components—batteries, inverters, electric motors, and controllers—are further validated in simulated vehicle environments to ensure that they meet the vehicle performance targets established by the government–industry technical teams.

Vehicle Technology Evaluations

This section describes the activities related to laboratory validation and fleet testing of advanced propulsion subsystem technologies and advanced vehicles. In laboratory benchmarking, the objective is to extensively test production vehicle and component technology to ensure that VTO-developed technologies represent significant advances over technologies that have been developed by industry. Technology validation involves the testing of DOE-developed components or subsystems in the proper systems context. Validation helps to guide future VTO research and facilitates the setting of performance targets.

The facilities that perform laboratory and field testing activities include the APRF, INL’s transportation testing facilities, NREL’s ReFUEL and thermal test facilities, and ORNL’s Vehicle Systems Integration (VSI) laboratory.

The APRF is equipped with dynamometers (for testing integrated components such as engines, electric motors, and powertrains), and a thermal chamber (for testing battery electric vehicles, hybrid electric vehicles, and plug-in hybrids in temperatures from as low as 20°F to as high as 95°F).

INL’s transportation testing facilities encompass the Advanced Vehicle Test and Evaluation Activity (AVTE) facility for LD vehicles, the Heavy Duty Transportation Test Facility, and the Energy Storage Technologies Laboratory. AVTE’s capability to securely collect, analyze, and disseminate data from multiple field tests located throughout the United States is critical to VS laboratory and field activities.

NREL’s ReFUEL facility is equipped with dynamometers for testing medium-duty vehicles and components. NREL’s thermal test facilities have capabilities for LD vehicle cabin thermal studies and outdoor HD vehicle cabin studies. NREL also has facilities for testing subsystems (such as energy storage systems and EVSE) and functions as the VS data collection and evaluation hub for medium-duty and HD vehicle fleet tests.

ORNL’s facilities for integrated testing include advanced engine technologies (e.g., advanced combustion modes, fuels, thermal energy recovery, and emissions after-treatment), advanced power electronics and electric machines (e.g., motor drives, components, power electronics devices, and advanced converter topologies), and vehicle testing and evaluation (e.g., chassis and component dynamometers, integrated powertrain stands, test track evaluations, and field operational testing).

The AVTE, working with industry partners, conducts field and fleet testing to accurately measure real-world performance of advanced technology vehicles. The AVTE testing regime uses test procedures developed with input from industry and other stakeholders. The performance and capabilities of advanced technologies are benchmarked to support the development of industry and DOE technology targets. The testing results provide data for validating component, subsystem, and vehicle simulation models and hardware-in-the-loop testing. Fleet managers and the public use the test results for advanced technology vehicle acquisition decisions. INL conducts LD testing activities. In FY 2016, INL continued its partnership with an industry group led by Intertek. Accelerated reliability testing provides reliable benchmark data of the fuel economy, operations and maintenance requirements, general vehicle performance, engine and component (such as energy storage system) life, and life cycle costs. These tests are described below.

Baseline Performance Testing

The objective of baseline performance testing is to provide a highly accurate snapshot of a vehicle’s performance in a controlled testing environment. The testing is designed to be highly repeatable. Hence it is conducted on closed tracks and dynamometers, providing comparative testing results that allow “apples-to-

apples” comparisons within respective vehicle technology classes. The APRF at ANL is used for the dynamometer testing of the vehicles.

Fleet Testing

Fleet testing provides a real-world balance to highly controlled baseline performance testing. Some fleet managers prefer fleet testing results to the more controlled baseline performance or the accelerated reliability testing.

During fleet testing, a vehicle or group of vehicles is operated in normal fleet (field) applications. Operating parameters such as fuel use, operations and maintenance, costs/expenses, and all vehicle problems are documented. Fleet testing usually lasts one to three years and, depending on the vehicle and energy storage technology, between 5,000 and 12,000 miles are accumulated on each vehicle.

For some vehicle technologies, fleet testing may be the only viable test method. Neighborhood electric vehicles are a good example. Their manufacturer-recommended charging practices often require up to 10 hours per charge cycle, while they operate at low speeds (<26 mph). This makes it impractical to perform accelerated reliability testing on such vehicles.

Accelerated Reliability Testing

The objective of accelerated reliability testing is to quickly accumulate several years or an entire vehicle-life’s worth of mileage on each test vehicle. The tests are generally conducted on public roads and highways, and testing usually lasts for up to 36 months per vehicle. The miles to be accumulated and time required depend heavily on the vehicle technology being tested. For instance, the accelerated reliability testing goal for plug-in hybrid electric vehicles and battery electric vehicles is to accumulate 12,000 miles per vehicle in one year, while the testing goal for hybrid electric vehicles is to accumulate 160,000 miles per vehicle within three years. This is several times greater than most hybrids will be driven in three years, but it is required to provide meaningful vehicle-life data within a useful time frame. Generally, two vehicles of each model are tested to ensure accuracy. Ideally, a larger sample size would be tested, but funding tradeoffs necessitate testing only two of each model.

Depending on the vehicle technology, a vehicle report is completed for each vehicle model for both fleet and accelerated reliability testing. However, because of the significant volume of data collected for hybrid electric vehicles, the test results are published in the form of summary fleet testing fact sheets (including accelerated reliability testing) and maintenance sheets.

Codes and Standards Development

A comprehensive and consistent set of codes and standards addressing grid-connected vehicles and infrastructure is essential for the successful market introduction of electric drive vehicles. The VTO is active in driving the development of these standards through committee involvement and technical support by the national laboratories. Codes and Standards work performed by the national laboratories emphasized grid modernization during FY 2016. These activities also supported the United States Driving Research and Innovation for Vehicle Efficiency and Energy sustainability(U.S. DRIVE) partnership’s Grid Interaction Tech Team (GITT), a government/industry partnership aimed at ensuring a smooth transition for vehicle electrification by closing technology gaps that exist in connecting vehicles to the electric grid.

The consumer markets for electric vehicles transcend national boundaries. ANL was employed in international cooperative initiatives to adopt international electric drive vehicle standards and promote market penetration of grid-connected vehicles. Many new technologies require adaptations and more careful attention to specific procedures. ANL supported development of interoperability validation procedures and operated the SmartGrid Joint Interoperability Center as the U.S. base for international cooperative work between the European Union and U.S. energy R&D laboratories.

Vehicle Systems Efficiency Improvements

This focus area involves R&D on a variety of mechanisms to improve the energy efficiency of LD, medium-duty, and HD vehicles. Projects in this focus area involve reducing the aerodynamic drag of vehicles, thermal management approaches to increase the engine thermal efficiency and reduce parasitic energy losses. Projects also address the development of advanced technologies to improve the fuel efficiency of critical engine and driveline components by characterizing the fundamental friction and wear mechanisms. Another set of projects address fast and wireless charging technology development.

Aerodynamic Drag Reduction

The primary goal of this focus area is improving the freight efficiency of vehicles. Aerodynamic drag reduction, thermal management, and friction and wear are the main focuses of this area. Reduction of aerodynamic drag in Class 8 tractor-trailers can result in a significant improvement on fuel economy while satisfying regulatory and industry operational constraints. An important part of this effort is to expand and coordinate industry collaborations with DOE. Industry collaboration CRADAs establish buy-in through and accelerate the introduction of proven aerodynamic drag reduction devices into new vehicle offerings.

The project's approach seeks to reduce drag through design features that control the flow of air around the vehicle. These 'flow field control' design features include geometry modifications, integration, and flow conditioning. Phase 1 of this project focused on development and design of retrofit devices from 2001-2013. Phase 2 of this project began in 2014 and focuses on developing and designing the next generation of aerodynamically integrated tractor-trailers.

Thermal Management

Thermal management of vehicle engines and support systems is a technology area that addresses reduction in energy usage through improvements in engine thermal efficiency and reductions in parasitic energy uses and losses. Fuel consumption is directly related to the thermal efficiency of engines and support systems. New methods to reduce heat-related losses are investigated and developed under this program.

FY 2016 thermal management R&D focused on exploring:

- The possibilities of repositioning the Class 8 tractor radiator and modifying the frontal area of the tractor to reduce aerodynamic drag
- The possibilities of using evaporative cooling under extreme conditions of temperature and engine load
- Engine coolant subcooled boiling heat transfer phenomena in heavy-duty vehicles
- Small channel coolant boiling for thermal control for power electronics
- Under hood thermal analysis of truck platooning

Friction and Wear

Parasitic engine and driveline energy losses arising from boundary friction and viscous losses consume 10% to 15% of fuel used in transportation. Thus engines and driveline components are being redesigned to incorporate low-friction technologies to increase fuel efficiency of passenger and HD vehicles. Research to improve the fuel efficiency and reliability of critical engine and driveline components included developing a web-based tool kit based on friction mean effective pressure (FMEP) maps to predict the impact of key tribological engine parameters on vehicle fuel economy.

On the highway, heavy trucks spend 32% of their usable propulsion energy to overcome rolling resistance. Research to improve the fuel efficiency by reducing rolling resistance of heavy trucks included:

- Goodyear Tire and Rubber Company's project to develop a system for automatically maintaining pressure in a commercial truck tire

- ORNL's project to improve tire efficiency through elastomeric polymers enhanced with carbon-based nanostructured materials

Fast and Wireless Charging

Electrification of the transportation sector will be enabled by adoption of vehicle charging technologies that minimize costs in terms of time and money while maximizing energy throughput, battery life, safety, and convenience.

Grid Modernization

The Grid Modernization projects listed below were added to the VS portfolio in FY 2016. The project performers are members of the Grid Modernization Laboratory Consortium (GMLC):

- Vehicle to Building Integration Pathway (GM0062)- The Vehicle to Building Integration Pathway project will develop and demonstrate methods needed to develop a standardized and interoperable communication pathway and control system architecture between plug-in electric vehicles (PEVs), electric vehicle support equipment (EVSE) and building/campus energy management systems (BEMSs) to enable the integration of clean variable renewable sources with workplace PEV charging infrastructure to promote greater PEV adoption.
- Systems Research Supporting Standards and Interoperability (GM0085) - The objective of the project is to address the uncertainty regarding the degree to which PEVs can provide grid services and mutually benefit the electric utilities, PEV owners, and auto manufacturers. The project seeks to answer the question, "How can the potential benefits be unlocked without negative unintended consequences?". The project will perform hardware-in-the-loop (HIL) studies to explore how to effectively incorporate PEVs into the grid as controllable loads.
- Modeling and Control Software Tools to Support V2G Integration (GM0086) - The project will determine the feasibility of vehicle to grid integration (VGI) by quantifying the potential value, cost, complexity, and risks in different implementations of VGI. The project's approach will be to allocate value among stakeholders and determine pathways for electrification of transportation to enable beneficial grid services such as mitigating renewables intermittency.
- Diagnostic Security Modules for Electric Vehicle to Building Integration (GM0163) - The project will develop a Distributed Security Module (DSM) framework that will allow a micro-grid to deploy several inexpensive sensors (hardware and/or software) that operate independent of the core grid infrastructure, and monitor the micro-grid for anomalous events.
- Establishment of Grid Modernization Laboratory Consortium (GMLC Foundational Technical Area (TA) 1.2.3) – Testing Network (GMLC–TN) The principal goal of this activity is to accelerate grid modernization by (a) enabling access to a comprehensive testing infrastructure, and (b) creating a repository of models and simulation tools.
- Technical Support to the New York State Reforming the Energy Vision (REV) Initiative (GMLC-Foundational TA 1.3.22) - This project's goal is to provide objective technical assistance by a team of experts from the national laboratories to NYS agencies and policy makers to enable the REV vision. Another goal of the project is to gain knowledge that can be leveraged for DOE's national grid modernization initiative.
- Definitions, Standards and Test Procedures for Grid Services from Devices (GMLC-Foundational TA 1.4.2) The project's goal is to enable and spur the deployment of a broad range of distributed energy resource (DER) devices with the proven ability to provide the flexibility required for operating a clean and reliable power grid at reasonable cost. The project's objectives address the primary barriers that will limit the ability of devices to provide grid services at scale in the future.
- Control Theory (GMLC-Foundational TA 1.4.10) This project will develop new control solutions including control topologies, control algorithms, and control deployment strategies for the US power grid. The major focus will be on distribution systems to support the vision for transitioning the power grid to a state where a huge number of distributed energy resources (DER) are participating in grid

control. The enhanced grid will operate with lean reserve margins and to enable resilient distribution feeders with a high percentage of low carbon DER.

Industry Awards

Industry projects for FY 2016 include the categories of transportation electrification, SuperTruck, wireless charging, zero-emissions cargo transport (ZECT), and energy load reduction and management. In FY 2016, the following new projects were added to the VS portfolio:

- Commercial Delivery PHEV – Class 6, [Awardee: McLaren]. The project objective is to develop and test a MD grid connected EV using an Electric axle. The design will integrate two electric motors (EM) into the vehicles rear axle to improve efficiency and performance.
- Electric Truck with Range Extending Engine (E-TREE) [Awardee: Cummins-PACCAR]. The objective of the project is to develop a MD grid connected Hybrid EV with range extender engine that reduces fuel consumption by 50% when compared to a conventional MD vehicle.
- Medium-Duty Urban Range Extended Connected Powertrain (MURECP), [Awardee: Robert Bosch]. The project will develop a powertrain to improve class 4 delivery vans. The powertrain features two planetary gear sets and optimized electric motors.

The new technology development and demonstration projects listed above were awarded through DOE's competitive solicitation process and involve resource matching by DOE and industry.

This report describes major projects conducted by the national laboratories and industry partners in support of these areas in FY 2016. The reports describe the approaches, accomplishments and future directions for the projects. For further information on an individual project, please contact the DOE project leader.

I.4. Future Directions for Vehicle Systems

A re-organization of the VTO in January 2017 ended the Vehicle Systems program. The projects of the former VS organization were reassigned to the Energy Efficient Mobility Systems (EEMS), Grid and Infrastructure (G&I), and Advanced Combustion Systems (ACS) programs as listed in the tables below. The projects will continue to support DOE's goals of developing technologies for the U.S. transportation sector that enhance national energy security by reducing reliance on imported petroleum, improve U.S. competitiveness in the global economy, and support improvement of U.S. transportation and energy infrastructure.

VTO competitively awards funding through funding opportunity announcement (FOA) selections, and projects are fully funded through the duration of the project in the year that the funding is awarded. The future direction for direct-funded work at the national laboratories is subject to change based on annual appropriations.

Table I-2 Projects assigned to Grid and Infrastructure Program in FY 2017

Project Title	PI	Organization
Vehicle to Building Integration Pathway (GM0062)	Richard Pratt (PNNL)	GMLC
Systems Research Supporting Standards and Interoperability (GM0085)	John Smart (INL)	GMLC
Modeling and Control Software Tools to Support V2G Integration (GM0086)	Samveg Saxena (LBNL)	GMLC
Diagnostic Security Modules for Electric Vehicle to Building Integration (GM0163)	Kenneth Rohde (INL)	GMLC
Establishment of Grid Modernization Laboratory Consortium (GMLC Foundational TA 1.2.3) – Testing Network (GMLC–TN)	Abraham Ellis (SNL)	GMLC
Technical Support to the New York State Reforming the Energy Vision (REV) Initiative (GMLC-Foundational TA 1.3.22)	J. Patrick Looney (Brookhaven National Laboratory)	GMLC
Definitions, Standards and Test Procedures for Grid Services from Devices (GMLC-Foundational TA 1.4.2)	Rob Pratt (PNNL)	GMLC
Control Theory (GMLC-Foundational TA 1.4.10)	Scott Backhaus (LANL) and Jakob Stoustrup (PNNL)	GMLC
Advanced Vehicle Testing & Evaluation	Jeremy Diez	Intertek
Advanced Technology Vehicle Lab Benchmarking (L1&L2)	Kevin Stutenberg	ANL
Medium and Heavy-Duty Vehicle Field Evaluations	Kenneth Kelly	NREL
Comprehensive Assessment of On-and Off-Board Vehicle-to-Grid Technology Performance And Impacts on Battery and the Grid	Sunil Chhaya	EPRI
CALSTART/UPS	Mike Ippoliti	CALSTART/UPS
EV-Smart Grid Research & Interoperability Activities	Keith Hardy	ANL

Project Title	PI	Organization
Wireless & Conductive Charging Testing to Support Code & Standards	Barney Carlson	INL
Advanced Climate Systems for EV Extended Range (ACSforEVER)	Nicos Agathocleous	Hanon Systems
Electrical PCM Assisted Thermal Heating System (EPATHS)	Mingyu Wang	Mahle Behr USA, LLC
Unitary Thermal Energy Management for Propulsion Range Augmentation (UTEMPRA)	Sourav Chowdhury	Mahle Behr USA, LLC
Design and Implementation of a Thermal Load Reduction System in a Hyundai PHEV	John Rugh	NREL
Multi-Speed Transmission for Commercial Delivery Medium Duty Plug-In Electric Drive Vehicles	Bulent Chavdar	Eaton
Electric Truck with Range Extending Engine (E-TREE)	John Kresse	Cummins - PACCAR
Medium-Duty Urban Range Extended Connected Powertrain (MURECP)	Alexander Freitag	Robert Bosch
Zero Emission Drayage Truck Demonstration (ZECT I)	Brian Choe	SCAQMD
Zero Emission Cargo Transport II: San Pedro Bay Ports Hybrid & Fuel Cell Electric Vehicle Project	Joseph Impullitti	SCAQMD
Hydrogen Fuel-Cell Electric Hybrid Truck & Zero Emission Delivery Vehicle Deployment	Andrew DeCandis	Houston-Galveston Area Council
Commercial Delivery PHEV – Class 6	Kevin Ledford	McLaren
Hybridization of Class 8 Line Haul and Regional Refrigeration Trucks CRADA	Dean Deter	ORNL

Table I-3 Projects assigned to Energy Efficient Mobility Systems Program in FY 2017

Project Title	PI	Organization
Energy Impact of Connected and Automated Vehicles,	Huei Peng	University of Michigan
SMART Mobility - Connected & Automated Vehicles	Eric Rask	ANL
SMART Mobility - Advanced Fueling Infrastructure	John Smart	INL
SMART Mobility - Multi-Modal	Diane Davidson	ORNL

SMART Mobility - Mobility Decision Science	Anand Gopal	LBNL
SMART Mobility - Urban Science	Stan Young	NREL

Table I-4 Projects assigned to Advanced Combustion Systems in FY 2017

Project Title	PI	Organization
DOE's Effort to Improve Heavy Vehicle Fuel Efficiency through Improved Aerodynamics	Kambiz Salari	LLNL
Improved Tire Efficiency through Elastomeric Polymers Enhanced with Carbon-Based Nanostructured Materials	Geogios Polyzos	ORNL
Advanced Bus and Truck Radial Materials for Fuel Efficiency	Lucas Dos Santos Freire	PPG
Advanced Non-Tread Materials for Fuel-Efficient Tires	Tim Okel	PPG
HD Powertrain Optimization	Paul Chambon	ORNL

Inquiries regarding the VS FY 2016 activities may be directed to the undersigned.



David L. Anderson and Lee Slezak
Technology Managers

II. Industry Awards

II.1. Integrated Boosting and Hybridization for Extreme Fuel Economy and Downsizing

Vasilios Tsourapas, Principal Investigator

Eaton Corporation
 W126N7250 Flint Drive
 Menomonee Falls, WI 53051-4404
 Phone: (248) 226-7114
 E-mail: VasiliosTsourapas@Eaton.com

Jason Conley, DOE Program Manager

U.S. Department of Energy's (DOE)
 National Energy Technology Laboratory (NETL)
 Phone: (304) 285-2023
 E-mail: John.Conley@NETL.doe.gov

Start Date: October 1, 2014
 End Date: December 31, 2017

II.1.A. Abstract

Objectives

The objective of this project is to develop, demonstrate, and evaluate commercialization of a highly efficient downsized engine by electrification of the air delivery and waste heat recovery system and optimizing energy usage to achieve a 20% fuel economy improvement at a commercially viable cost.

Accomplishments

- Roots expander development and functional testing for selected engine
 - Thermal and stress analysis completed
 - CFD for porting, rotor geometry and exhaust manifold to maximize power generation completed
 - Displacement selection completed
 - Generator specification established and supplier selected
 - Functional durability testing completed
- Integration of EAVS/WHR system onto selected engine and vehicle packaging completed
- Model based analysis of the EAVS/WHR system completed for selected engine and vehicle
 - GT power vehicle level model established
 - Initial control strategy established
 - Preliminary fuel economy improvement predictions completed
- Engine dyno upgrades to receive and test selected engine
 - Instrumentation and software installed
 - Control and system calibration completed
 - Repeatability assessment of measurement system completed

Future Achievements

Next steps include:

- Setting up target diesel engine on dyno

- Baseline vehicle testing
- Determination of EGR strategy through simulation and hardware implementation
- Model based system level optimization to maximize fuel economy
- Integration and testing of EAVS/WHR hardware on engine

II.1.B. Technical Discussion

Background

Improvement in fuel economy in the automotive market is driven both by regulations (EPA, CAFÉ, EURO etc.) as well as the increasing gas prices. Consumers demand cost effective solutions that can reduce vehicle fuel consumption and which, at the same time, meet their performance (vehicle acceleration) requirements. A primary solution to reduced fuel consumption is engine downsizing and downspeeding; a smaller and slower engine will exhibit fewer friction losses and higher operating efficiency since it will be forced, for the same vehicle mass, to operate at a relative higher percentage of load.

Introduction

The project will develop, build and test a highly efficient and fully controllable technology for optimizing engine energy usage. Through energy usage and breathing optimization of a downsized and downsped engine a fuel economy (FE) improvement of more than 20% will be targeted over an already turbocharged and downsized engine while maintaining or improving performance, at an industry accepted cost point. Recovering both brake and exhaust energy and using it in a variable ratio boosting system (rather than a traction system) offers cost-effective, high impact hybridization independent of the drive cycle.

Delays getting the subcontract in place with Isuzu will result in a timing change for BP2 regarding when Eaton's EAVS/WHR system will be evaluated on engine.

Approach

The project is being conducted in three budget periods:

Budget Period 1: Model-based System Analysis and Individual Technology Risk Mitigation

The activities focused on evaluating integration of the two technologies in a model-based environment where the architecture and the component sizes were optimized. Multiple integration schemes were examined that combined Electrically Assisted Variable Speed (EAVS) supercharger and Waste Heat Recovery (WHR) in different ways in a model environment. The sizes of the motor, generator, and battery were optimized. The component risks were addressed, such as WHR high temperature durability, by designing and testing WHR hardware on an engine.

Budget Period 2: Design and Engine Dynamometer Testing of System and Optimize Controls

The second budget period will focus on designing and integrating the two technologies on a full engine dynamometer. The engine with EAVS and WHR will be designed and tested in preparation for transferring and installing the system in a demonstration vehicle. The engine with the EAVS/WHR system will be calibrated on the dynamometer for emissions, performance and fuel economy. In parallel, the vehicle-level supervisory controls will be optimized and ready for transfer to the demonstration vehicle.

Budget Period 3: Vehicle Demonstration and Testing; Commercialization Analysis

The third budget period will focus on integrating and testing the demonstration vehicle against the fuel economy, emissions, performance, and cost targets. The engine developed in budget period 2 will be

transferred to the demonstration vehicle. The vehicle will be finalized and calibrated on a chassis dynamometer and tested. The cost estimate, commercialization, and manufacturing readiness will be analyzed and the next steps to production will be finalized.

Results

Tasks 1.1

Based on testing and model based analysis the EAVS and WHR technologies show promising results for light and medium duty diesel engine applications. Isuzu Motors has agreed to be a project partner to demonstrate the EAVS/WHR system on a 1.9L diesel engine which is utilized in a light duty truck application.

Task 1.2

Using the 1.9 VGT engine model that was provided to Eaton by Isuzu, Eaton developed a vehicle model with two different engines. The two engines that were used are a) the baseline 1.9lt turbo production engine and b) the 1.9lt EAVS/WHR engine. The baseline vehicle model was validated against experimental data provided by Isuzu in order to verify the prediction of fuel economy and performance. The model predicted fuel economy of the baseline engine correlated to actual measured data within a +/- 3% error band. In terms of performance validation with the experimental data, Eaton showed good matching of the 0-100kph performance with measured data as illustrated in Figure II-1.

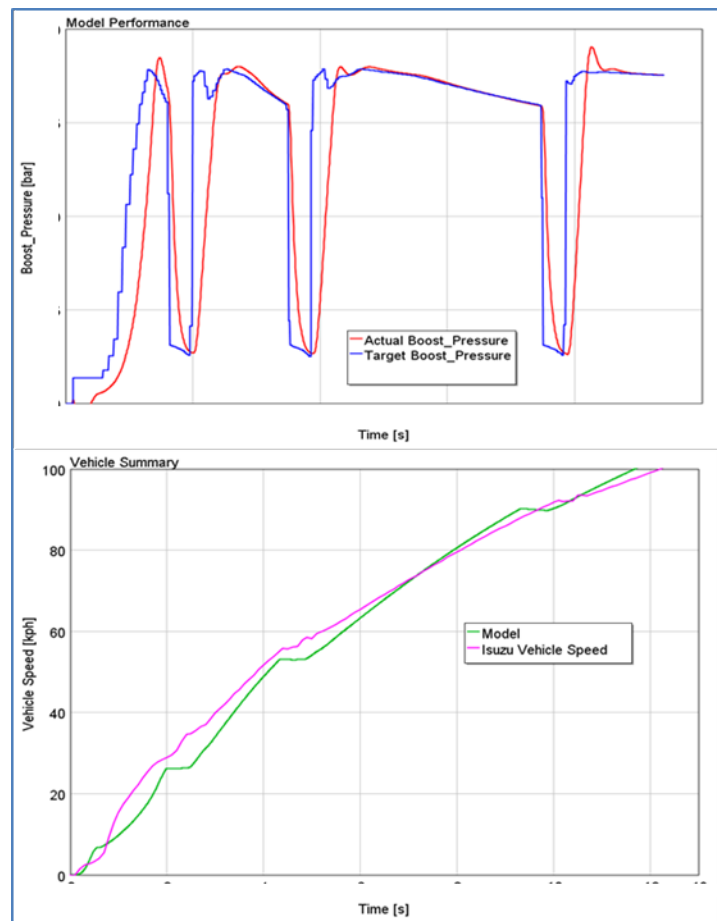


Figure II-1: Baseline Model Results Compared to Experimental Data

The EAVS/WHR vehicle model was developed after removing the VGT from the baseline engine and adding the EAVS and WHR component models as well as preliminary control algorithms to operate those

components. Several EAVS/WHR features were evaluated and compared to the baseline VGT vehicle to assess the fuel economy improvement potential. The different features included:

1. Boost: EAVS matches desired intake boost pressure with motor speed control.
2. Torque Assist (TA): EAVS applies torque to supplement engine torque when no boost is required.
3. Start/Stop (S/S): Engine turns off when vehicle is stopped to save fuel.
4. Downspeeding (DS): Reduced final drive ratio in order to reduce engine speed for a given vehicle speed and thus reduce engine friction losses
5. Waste Heat Recovery (WHR): Exhaust energy is recovered via the roots expander unit and converted to electrical energy via a generator to charge the battery

A detailed system level optimization and tradeoff assessment is in progress to maximize fuel economy but preliminary simulation results show over a 20% improvement as outlined in Figure II-2.

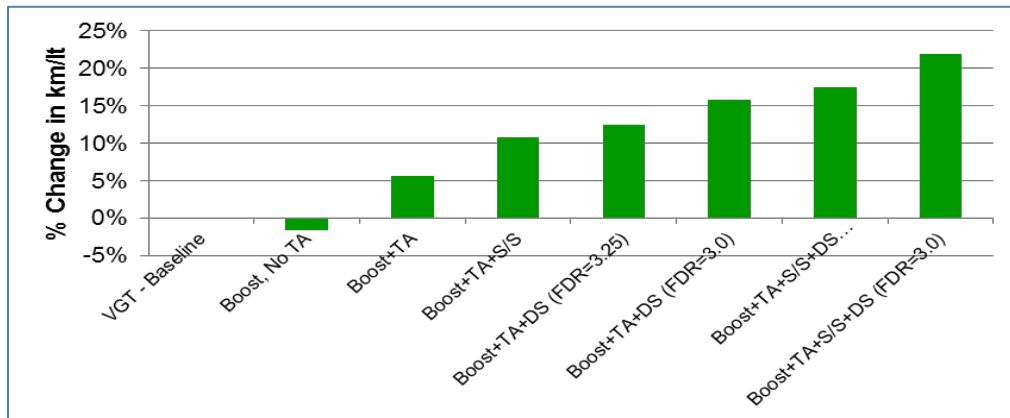


Figure II-2. Fuel Economy Results with Different EAVS/WHR features

Task 1.3

Functional and proof of concept durability testing of the Roots expander has been completed on a 2.4L diesel off road engine with a R410 electrically driven supercharger. The Roots expander successfully operated at 700C as depicted in Figure II-3 and completed 70 hours of testing at various operating conditions with no functional issues.

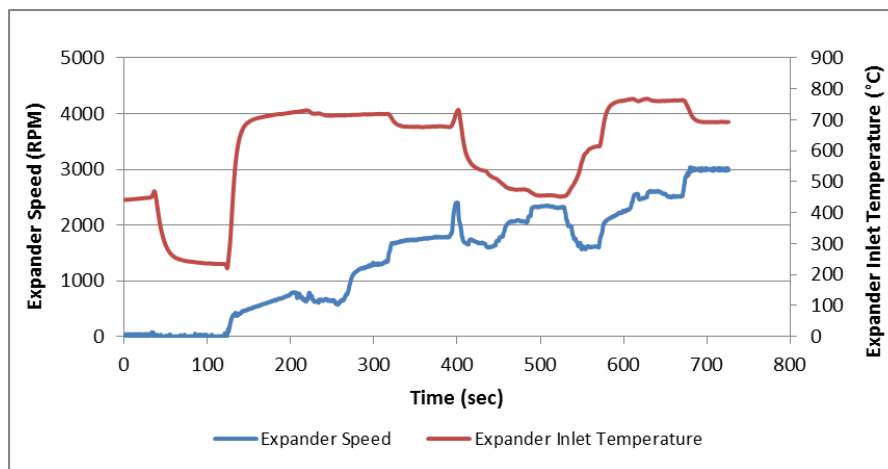


Figure II-3: Expander Operation at 700C

The repeatability of the WHR power generation was assessed and showed greater than a 96% repeatability rate indicating that the design is robust. Results are shown in Figure II-4.

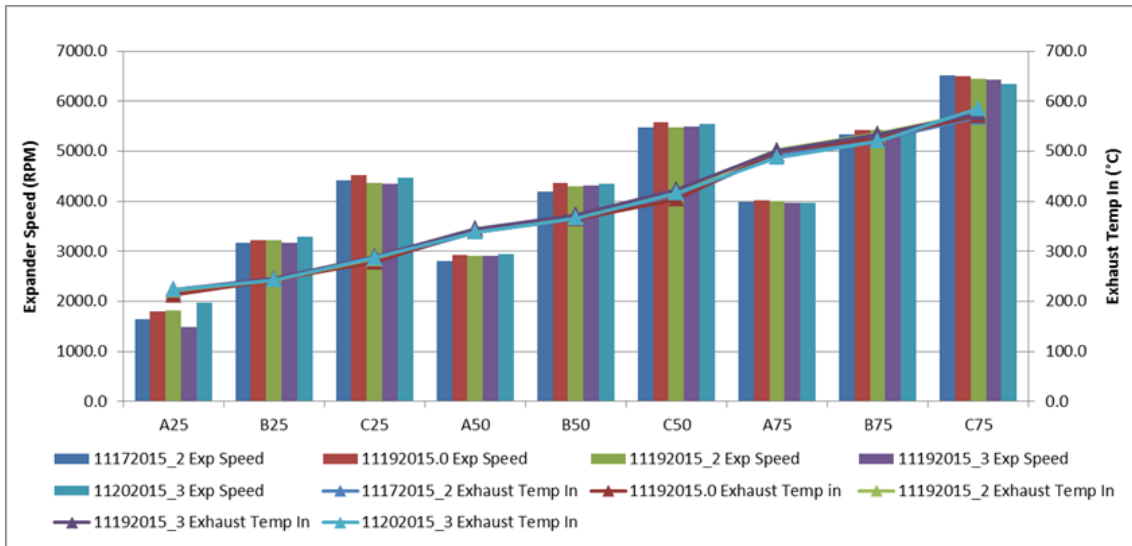


Figure II-4: Expander Repeatability Results

Based on the results from the GT Power simulations, expander analytical development studies and testing the expander design was finalized. To maximize device efficiency extensive thermal and structural analysis was conducted on the expander housing to minimize bore deflection across the broad range of operating conditions that the expander will be subjected to. The final displacement is 0.21 L/revolution and all aspects of the design have been finalized including the generator as depicted in Figure II-5.

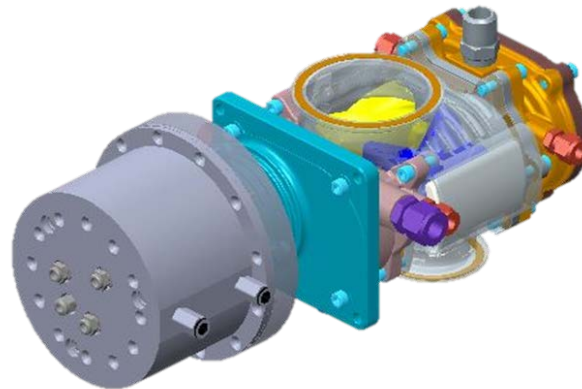


Figure II-5: Finalized Roots Expander Design

Task 1.4

The EAVS and WHR were adapted and packaged within the Isuzu engine bay as shown in Figure II-6. The EAVS was packaged on the cold side of the engine while the WHR unit is on the hot side of the engine replacing the turbocharger. Packaging and ducting to accommodate the selected EGR strategy is pending the simulation results.

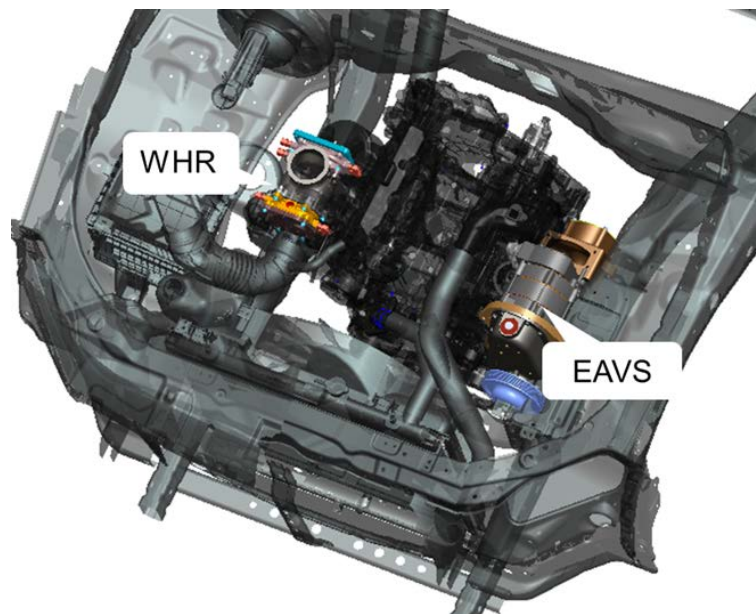


Figure II-6: EAVS/WHR System Packaged into Engine Compartment

Conclusions

Based on testing and model based analysis to date the EAVS and WHR technologies show promising results for diesel engine applications. The team will continue to optimize the system to maximize fuel economy in BP2 and work with the team members to ensure that the target engine is ready to be installed in the demonstration vehicle in BP3.

II.1.C. Products

Presentations/Publications/Patents

1. 2016-DOE-AMR PowerPoint Presentation at Arlington, Washington
2. IAA conference in Hanover, Germany

II.1.D. References

1. No References

II.2. Multi-Speed Transmission for Commercial Delivery Medium Duty PEDVs [DE-EE0006843]

Bulent Chavdar, Principal Investigator

Eaton Corporation
 W126N7250 Flint Drive
 Menomonee Falls, WI 53051-4404
 Phone: (248) 226-6219; Fax: (248) 226-7166
 E-mail: bulentchavdar@eaton.com

Jason Conley, DOE Program Manager

The National Energy Technology Laboratory (NETL)
 Phone: (304) 285-2023
 E-mail: John.Conley@netl.doe.gov

Start Date: October 1, 2014
 End Date: October 31, 2017

II.2.A. Abstract

Objectives

- The objective of this project is to develop a multi-speed transmission for medium duty electric vehicles (EVs) to expand the vehicle's operating performance and range. The project addresses the following technical barriers:
 - Reduced performance gap between EVs and Internal Combustion Drive Vehicles (ICDVs), Reliability, affordability, scalability, and lower weight, and
 - Increased public acceptance of electric vehicles.
- Following the departure of Smith Electric from the project team, Eaton partnered with Proterra as the EV-OEM vehicle integrator in Budget Period 2. Proterra's EV Model BE35 Electric Transit Bus was selected as the baseline vehicle for the integration of a new multi speed transmission. The proposed 4-speed transmission will narrow motor operation to the peak efficiency region thereby increasing the electric powertrain efficiency. The baseline vehicle currently uses a 2-speed transmission made by Eaton. The performance improvements targeted by replacing the current 2-speed transmission with the new 4-speed transmission are listed in Table II-1. The new 4-speed transmission will enhance customer satisfaction by improving range, vehicle acceleration, top speed and gradeability over the baseline.

Table II-1: The baseline performance of Proterra EV Model BE35 baseline vehicle with 2-speed transmission and the target performance with the new 4-speed automated mechanical transmission (AMT).

Metric	Current 2-speed AMT (Baseline)	New 4-speed AMT (Target)
Top vehicle speed @ GVW	53 mph	> 65 mph
Vehicle Efficiency @ SLW		
On -UDDS	20.4 mpg,de	24.8 mpg,de
On Orange County - OCC	19.9 mpg,de	23.9 mpg,de
On Manhattan - NYC	17.7 mpg,de	21.2 mpg,de
On Altoona-ADB	20.2 mpg,de	25 mpg,de
Acceleration time @ SLW		
0 to 30 mph	15.5 s	< 13 s
30 to 50 mph	27.5 s	< 19 s
Gradeability @ GVW		
10 mph	15%	>20%
20 mph	7%	> 10%

Accomplishments (BP2, Q1-Q4)

- Extended electric vehicle modeling and simulations on electric transit bus, school bus, refuse and drayage trucks were completed.
- Preliminary design layout of the 4-speed AMT completed.
- Modeling and simulations of both the baseline electric transit bus with 2-speed transmission and the improved electric bus with 4-speed transmission were completed. Top speed, efficiency, acceleration and gradeability of the electric transit bus are predicted to be improved by 50%, 15%, 40% and 30% respectively.
- Initial transmission system design completed.
 - Gear ratios were selected for the Proterra BE35 electric transit bus.
 - Finite Element Analysis (FEA) of the transmission housings, rotating components analysis of the shafts, gears and bearings, and the noise, vibration and harshness (NVH) analysis of 4-speed transmission completed.
 - The new 4-speed transmission design meets the 500,000 miles reliability requirements of the BE35 electric transit bus.
- Prototyping of the new 4-speed transmission has started.
- One display unit of the new 4-speed transmission was completed.

Future Achievements (BP3)

- Complete procurement of the prototyping parts.
- Complete prototype transmission build.
- Complete transmission and controller initial shakedown testing at Eaton.
- Complete the integration of new 4-speed transmission on BE35 electric transit bus at Proterra facility.
- Complete the integrated powertrain hardware-in-the-loop (HIL) testing at Oak Ridge National Laboratory (ORNL).
 - Complete steady-state and transient HIL tests.
 - Validate the energy efficiency achievements.

- Complete transmission controls fine tuning and the shift strategy on the integrated vehicle at Eaton
- Complete vehicle performance testing and verification on the track and on the chassis dynamometer at National Renewable Energy Laboratory (NREL).

II.2.B. Technical Discussion

Background

The EV Everywhere Grand Challenge aims at realizing plug-in electric drive vehicles (PEDVs) that meet or exceed the performance of ICDVs on the basis of cost, convenience, and consumer satisfaction. The average range of a PEDV is approximately one-third the range of an ICDV. The Eaton team proposed to develop a multi-speed transmission that will help close the range gap by increasing the electric powertrain efficiency. Customer satisfaction will also improve when vehicle acceleration, top speed, and gradeability improve significantly over the baseline vehicle.

Successful completion of the project will set a course for improving the quality of life in three areas by overcoming key challenges in the gearbox for commercial-delivery, medium-duty, PEDVs. It will reduce US dependency on foreign oil through the use of electric driven propulsion instead of fuel driven. It will reduce health risks by replacing tailpipe emissions in densely populated city centers. Finally, it will improve the performance-cost basis to meet or exceed the expectations of the targeted medium duty vehicle fleet owners and the independent customers.

Introduction

The project will develop a new multi-speed gearbox to match the performance characteristics of an electric motor. The gear ratios, shift strategy, cost, and weight will be optimized to provide a commercially feasible solution to meet medium duty EV requirements for starting torque, top speed, acceleration, and efficiency.

Eaton has assembled the appropriate team to develop a multi-speed transmission for medium duty PEDVs. The team includes a leading transmission developer for medium and heavy duty vehicles (Eaton), the leader in Electric Transit Busses (Proterra) and two critical testing laboratories (ORNL and NREL). Eaton will design the transmission hardware and controller, integrate the transmission with power electronics, conduct a motor drive optimization study, prepare a manufacturing plan and provide a prototype transmission. Proterra will provide the vehicle integration of the new multi-speed transmission. ORNL will perform vehicle level simulations, powertrain loop integration, component testing and HIL testing. NREL will conduct duty cycle analysis, and vehicle integration and testing.

Approach

The project is conducted over three budget periods:

Budget Period 1: Technology Development – The high-level vehicle powertrain models will be used to optimize candidate transmission architectures and ratios along with a variety of traction motor characteristics for concept selection. The detailed driveline design and component dynamics will be chosen to meet medium duty EV requirements. The optimized solution will include a multi-speed transmission, a permanent magnet motor, and an integrated bidirectional shift strategy.

Budget Period 2: Technology Development and Prototype Demonstration – The modeling and simulations with multi-speed transmissions will be extended to other medium and heavy duty EV platforms. Clean sheet design of a compact, lightweight, flexible, and modular, 3 and 4-speed transmission will be completed. The procurement of the prototype transmission and the controller will be started and 80% completed.

Budget Period 3: Technology Integration, Testing, and Demonstration – The prototyping will be completed. The transmission will be fully integrated into a demonstration vehicle. The vehicle will be tested and compared with the baseline vehicle performance. Transmission development will continue with the vehicle testing to further refine the transmission.

Results

Baseline Vehicle and Drive Cycle Information

In Budget Period 2, Proterra provided the simulation parameter requirements document to Eaton. The full information set included: weight parameters, driveline parameters, wheel parameters, vehicle drag parameters, motor parameters, battery parameters, drive system overview and powertrain interface schematic, drive controller power limiting description, baseline vehicle acceleration test data at various gross vehicle weights, and a sample high resolution drive cycle with a mix of urban and highway driving to serve as source for model calibration.

Proterra also provided the field test results for the EV Model BE35 Bus in order to validate our Matlab/Simulink model and evaluate all vehicle acceleration performance. The field tests consist of three runs in both the clockwise and counterclockwise directions on the test track.

Velocity versus time data obtained for each run and results are averaged together to minimize any test variability which might be introduced by wind or other external factors. The test was performed up to a maximum speed of 50 mph. From these tests, gradeability and the average acceleration time from 0 to 50 mph are calculated.

Baseline Model Validation

The vehicle acceleration performance results obtained from the simulation are compared to the Proterra field test results for the baseline vehicle are listed in Table II-2.

Table II-2: Baseline model validation results for Proterra EV Model BE35 Bus based on vehicle acceleration time.

Vehicle Speed (mph)	Field Test Results Average Acceleration Time (s)			Simulation Results
	CCW Direction	CW Direction	Average	
10	3.2	3.0	3.1	2.6
20	9.2	7.4	8.3	8.3
30	15.9	15.0	15.5	15.8
40	26.9	25.1	26.0	26.5
50	46.1	39.8	43.0	43.9

From the above results, the baseline simulated model equipped with a 2-speed transmission correlated very well with the actual vehicle acceleration time obtained from the field tests and it is deemed to be very close to represent the real vehicle. However, there is a slight error for the first 10mph acceleration which could be due to the restriction of motor torque at low speed that was not implemented in our baseline model.

The Altoona ADB field test results of Proterra BE35 electric transit bus was used to validate the energy efficiency and the power losses predicted by the baseline model. The Altoona ADB field test run is comprised of 3 Central Business District (CBD) phases, 2 Arterial phases, and 1 Commuter phase. The Altoona ADB field test is structured as a set of cycles with a number of miles in a fixed time in the following order: CBD, Arterial, CBD, Arterial, CBD, and Commuter (COMM). This test includes: a CBD phase of approximately two miles with seven stops per mile and a top speed of 20 mph; an Arterial phase of approximately two miles with two stops per mile and a top speed of 40 mph; and a COMM phase of approximately four miles with one stop and a maximum speed of 40 mph as shown in Figure II-7.

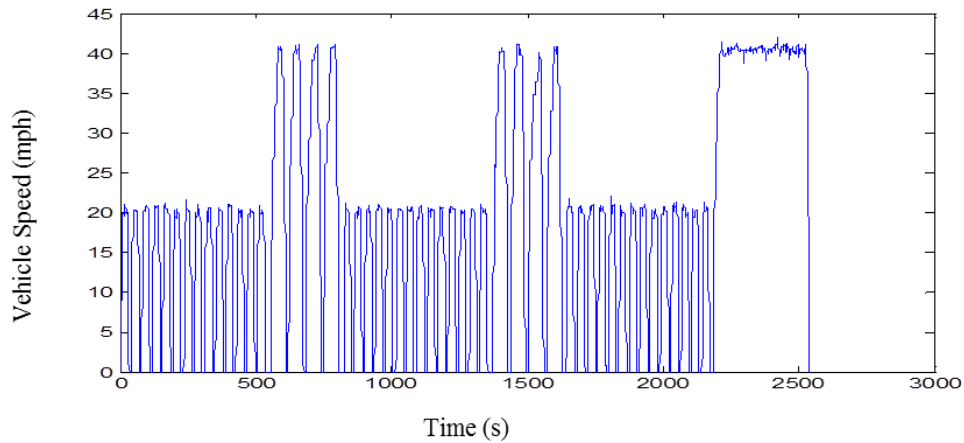


Figure II-7: Proterra BE35 electric bus field test based on the Altoona ADB drive cycle is used to validate the baseline vehicle model with 2 speed transmission.

The energy efficiency simulation results are compared to Proterra BE35 electric bus field test results in Table II-3.

Table II-3: Baseline model validation results of the energy efficiency of Proterra BE35 electric bus

	Altoona ADB Field Test	Model Prediction	Errors (%)
Energy efficiency (kwh/mile)	1.81	1.87	3.0
Overall Energy Consumption (kwh)	48.5	49.5	1.8
Regenerated Energy (kwh)	13.6	13.9	2.7

The energy efficiency simulation results correlated very well with the Proterra, BE35 electric bus field test results. Therefore, the baseline vehicle model is deemed to be very close to and representative of the real vehicle.

Selection of a multi speed transmission concept for medium duty EVs

The leading transmission concepts were identified as follows:

- Automated mechanical transmission (AMT) with 3 or 4-speed layshaft gears
- Wet dual clutch transmission (DCT) with a 4-speed layshaft gear architecture
- Dry DCT with a 4-speed layshaft gear architecture
- AMT with a 3-speed planetary gear architecture
- Automatic powershift transmission with a 3-speed planetary gear architecture

These concepts were subjected to a trade-off analysis based on leading performance and business criteria. The importance of each criterion was ranked and the specification and margin limits of each criterion were determined. A trade-off analysis matrix shown in Table II-4 was used to rank each transmission concept for the leading criteria. An AMT with a 3 or 4-speed layshaft gear architecture scored the highest points. The biggest advantages of an AMT layshaft concept are low non-recurring engineering (NRE) cost, low capital costs, high reliability, high efficiency and better application commonality across the market segments and vehicle classes. The first runner up concept was a dry DCT with 4-speed layshaft gear architecture. The dry DCT has better comfort and NVH performance than an AMT concept does. However, the importance of comfort and NVH is much lower than the importance of unit cost, NRE cost, capital spending and reliability where AMT layshaft concept has clear advantage over the DCT concepts.

Table II-4: Trade off analysis of medium duty electric vehicle transmission concepts.

MD-EV Transmission Concepts	Status Legend		NRE Costs	Application Commonality	Acceleration	Gradeability	Startability	Efficiency	Top speed	Comfort/NVH	Reliability	Use Current Tooling	Packaging and Weight
	Pass = 1.0												
	Marginal = 0.5												
	Fail = 0.0												
Score													
AMT-Layshaft (3 or 4-speed)	14.3												
DryDCT-Layshaft (4-speed)	11.8												
3-spd AMT-Planetary	8.4												
3-spd Wet-Powershift-Planetary	7.6												
WetDCT-Layshaft (4-speed)	11.4												

Gearbox Model Development

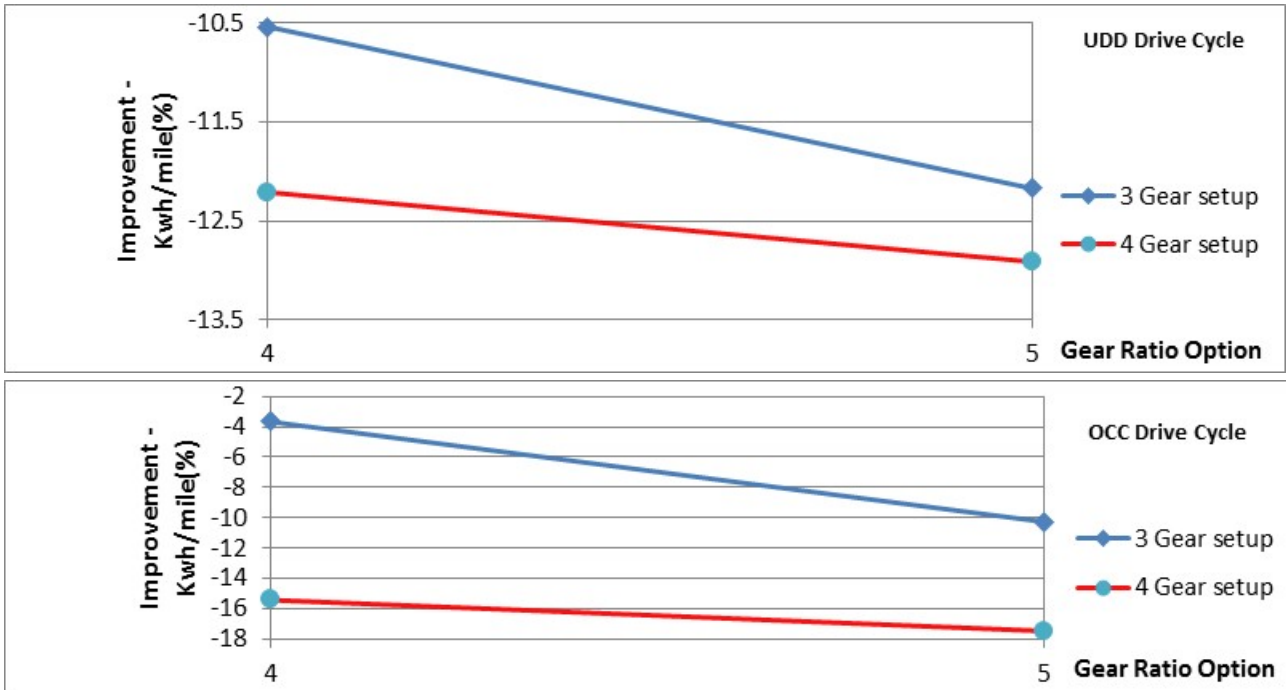
The Eaton team worked with Proterra to determine the approximate Gear Ratios for a 4-speed AMT to enable drivability and efficiency that meet the performance targets. Combinations of existing production gears were used to create 6 potential Gear Ratio Options, two headset gear ratios and three final drive ratios that offered 36 potential solutions. Production gears were chosen to reduce production time (no additional castings needed) and use the material selection and wear analysis already performed by previous design teams in Eaton’s transmission group.

The flexible and modular design concept of the Eaton 4-speed ATM offers 6 potential input gearset ratios with the headset ratio choices of 1.55 or 1.88 as listed in Table II-5. The availability of three choices of final drive ratio 6.2, 7.38 and 9.2 increases the number of potential solutions to 36. However, the final drive ratio of 9.2 was eliminated quickly due to the low drive axle efficiency at this ratio. Furthermore, the headset ratio of 1.55 was selected in order to get a high enough torque rating that mimics maximum motor torque and also achieves our target gradeability requirements for the BE35 electric bus. Hence 6 viable input gearset ratios and two final drive ratio combinations were evaluated for Proterra EV Model BE35 bus application that will be equipped with the new 4-speed AMT transmission.

Table II-5: Gear ratio options with the headset ratios of 1.55 and 1.88 for the 4-speed transmission.

	1.55	Gear Ratio	Step		1.88	Gear Ratio	Step	
	4.00	2.58			4.00	2.13		
	2.50	1.61	1.60		2.50	1.33	1.60	<i>Option #1</i>
	1.60	1.03	1.56		1.60	0.85	1.56	
	1.00	0.65	1.60		1.00	0.53	1.60	
	4.26	2.75			5.17	2.75		
	2.76	1.78	1.54		3.16	1.68	1.64	<i>Option #2</i>
	1.64	1.06	1.68		1.79	0.95	1.77	
	1.00	0.65	1.64		1.00	0.53	1.79	
Headset								
Gear Ratio	1.55	Gear Ratio	Step		1.88	Gear Ratio	Step	
Existing Gear	4.45	2.87			5.40	2.87		
New Gear	2.76	1.78	1.61		3.16	1.68	1.71	<i>Option #3</i>
Direct Drive	1.64	1.06	1.68		1.75	0.93	1.81	
	1.00	0.65	1.64		1.00	0.53	1.75	
	4.82	3.11			5.85	3.11		
	2.76	1.78	1.75		3.16	1.68	1.85	<i>Option #4</i>
	1.64	1.06	1.68		1.79	0.95	1.77	
	1.00	0.65	1.64		1.00	0.53	1.79	
	6.76	4.36			8.20	4.36		
	3.57	2.30	1.90		4.08	2.17	2.01	<i>Option #5</i>
	1.94	1.25	1.84		1.99	1.06	2.05	
	1.00	0.65	1.94		1.00	0.53	1.99	
	7.29	4.70			8.84	4.70		
	3.80	2.45	1.92		4.32	2.30	2.04	<i>Option #6</i>
	1.94	1.25	1.96		2.07	1.10	2.09	
	1.00	0.65	1.94		1.00	0.53	2.07	

The simulation results for the energy consumption improvement using different drive cycles with the new 4-speed transmission (options 4 & 5 with final drive ratio 6.2) using either 3 & 4-Gear setup over the baseline 2-speed transmission (3.53/1 and final drive ratio 9.2) are presented in Figure II-8.



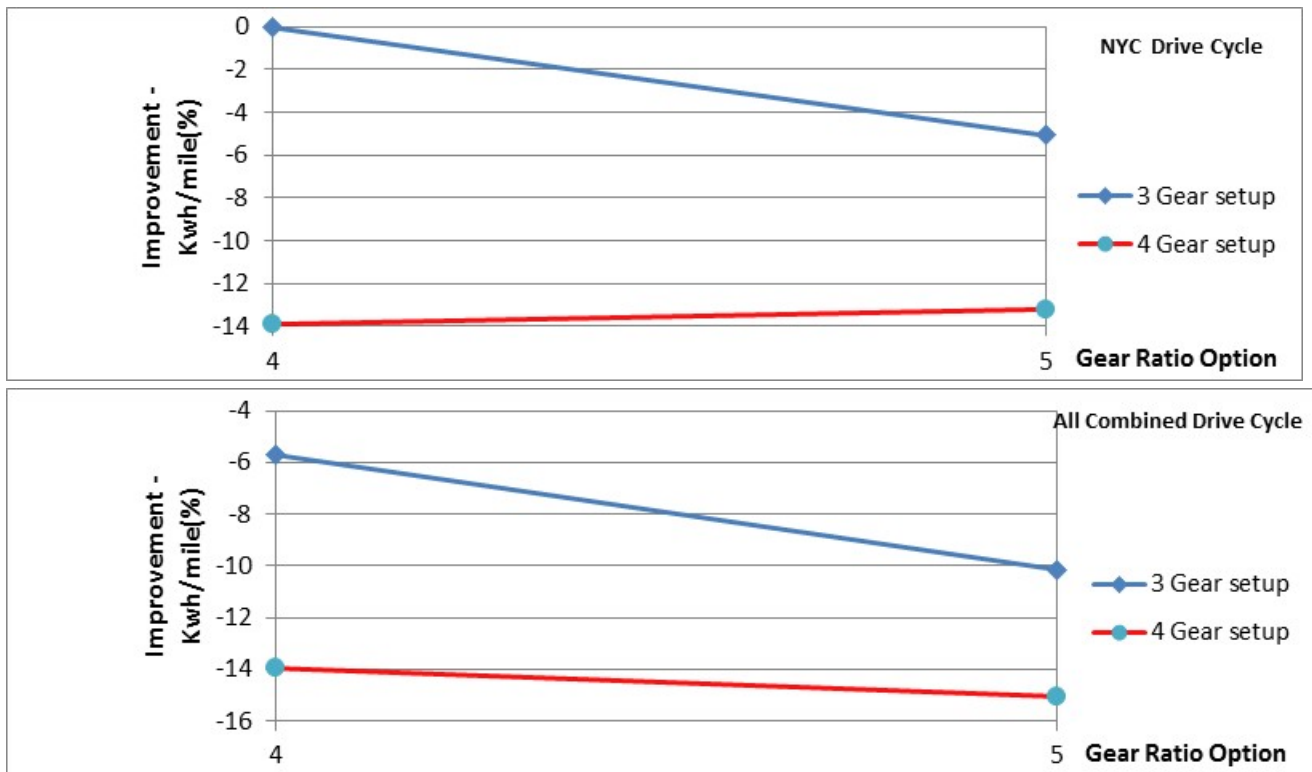


Figure II-8: Simulation results of Proterra BE35 electric bus for various drive cycles: The graphs show the energy efficiency improvement (%) with the new 4-speed transmission with 3 & 4 Gear setups over the baseline 2-speed transmission.

From the results illustrated in Figure II-8, Option-5 with 4-Gear setup shows slightly better efficiency over Option-4 with 4-Gear setup except the NYC drive cycle testing. In order to finalize the gear ratios selection with either options 4 or 5 using the 4-Gear setup, the total wheel torque values need to be evaluated during the vehicle acceleration and gear shifting by using the full throttle drive cycle testing as shown in Figure II-9.

It was clear from Figure II-9 that the overall reduction in the total wheel torque during shifting gears from 1st to 2nd is larger with Option-5 as compared to Option-4. The large reduction in the torque with Option-5 may

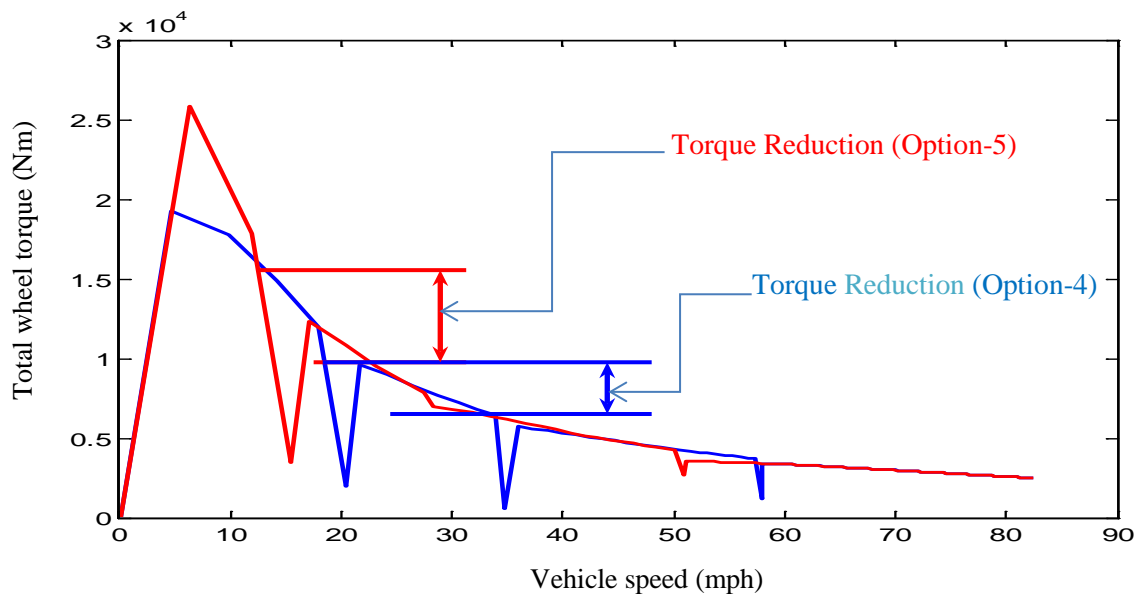


Figure II-9: Total wheel torque versus vehicle speed simulation results for 4 speed (options 4 & 5 with 4-Gear setup) Transmission using full throttle drive cycle testing.

cause the wheels to spin and would feel a little rough driving; in this case the motor torque needs to be limited for the sake of driver comfort. However, limiting the motor torque lowers the re-generator power efficiency. Therefore, Option-4 will be our final selection for integration in the new 4-speed ATM with a 4-Gear setup and also to be integrated on the Proterra EV BE35 electric transit bus. This configuration will be used for the test plan. Finally, Table II-6 illustrates the performance metrics based on the simulation results and the benefits of using the new 4-speed transmission (Option-4 with 4-Gear setup) as compared to the current 2-speed transmission for the Proterra BE35 electric transit bus application.

Table II-6: Proterra BE35 electric transit bus performance comparisons with the baseline 2-speed and the new 4-speed transmissions.

Metric	Current 2 speed AMT	New 4 speed AMT	Benefits 4 Speed vs 2 Speed AMT	
	(Baseline)	(Simulation Results)	(%)	
1	Top vehicle speed @ GVW	53 mph	81 mph > 65 mph	52.8%
	Vehicle Efficiency @ SLW			
2	On -UDDS	20.4 mpg,de	23.2 mpg,de	15.7%
	On Orange County - OCC	19.9 mpg,de	23.5 mpg,de	18.3%
	On Manhattan - NYC	17.7 mpg,de	20.5 mpg,de	16.1%
	On Altoona-ADB	20.2 mpg,de	24.4 mpg,de	20.8%
3	Acceleration time @ SLW			
	0 to 30 mph	15.5 s	9.7 s < 13 s	41.2%
	30 to 50 mph	27.5 s	16.6 s < 19 s	65.4%
4	Motor & Generator Efficiency	Motor Generator	Motor Generator	Motor Generator
	On -UDDS	92.0% 87.6%	92.2% 89.6%	0.2% 2.2%
	On Orange County-OCC	90.2% 83.9%	90.9% 89.0%	0.7% 6.0%
	On Manhattan- NYC	89.4% 83.7%	90.2% 89.3%	0.9% 6.7%
	On Altoona -ADB	91.1% 82.3%	91.1% 89.6%	0.0% 11.6%
5	Gradeability @ GVW			
	- 10 MPH	15%	20%	33.3%
	- 20 MPH	7.0%	10%	42.9%

Transmission Design

The transmission assembly was conceived and laid out in a model - with the goal of leveraging current product design while preserving an optimum EV transmission platform. After a series of layout design reviews, the components were then individually designed, detailed, and were ready for prototyping. The design team completed the initial 3D design layout of the transmission, maximizing reuse of current production components for speed-to-market and minimizing risk to reliability and durability. Two different views of the result are shown in Figure II-10.

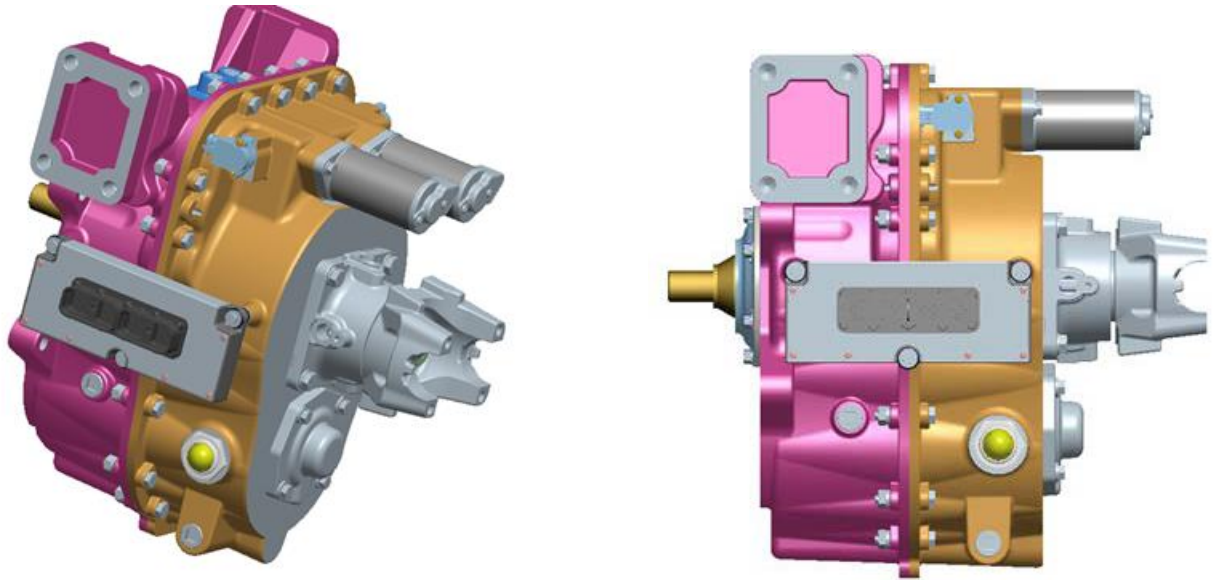


Figure II-10: External views of 3 and 4-speed automated mechanical transmission layout.

The design layout was reviewed with a cross-functional Eaton team, including several Eaton colleagues who are very experienced with the transmission platform of which components, sub-assemblies, and general design strategy is being leveraged from for this product. Several very good suggestions and observations were made and implemented.

Dry Sump versus Wet Sump Churning Loss Study

A study was conducted to evaluate the cost benefit of designing the proposed transmission with a dry sump versus a wet sump lubrication system. A dry sump system utilizes an internal pump and piping system in which oil is distributed throughout the transmission by means of oil pressurization. This method is advantageous as it reduces the oil level thereby decreasing oil churning (drag losses) and weight (oil volume). However, the internal pump and piping system add anywhere between \$200 to \$400 in supplementary material and design cost. A wet sump design simply fills the transmission to a predetermined level and allocates the oil via gear churning; as the gears spin through the oil they create an oil mist which spreads throughout the entire transmission. A wet sump is typically associated with higher parasitic losses thus producing an overall lower efficiency.

A simulation was conducted using an internal Eaton program to evaluate the benefits of a dry vs wet sump for this particular design. The churning losses are based on the following parameters:

- Transmission input speed: 1000-5000 RPM
- Oil Type: Eaton PS-386 Synthetic Transmission fluid
- Oil characteristics based on operating temperature (Density, viscosity)
- Oil Volume: 3.5-6 L
- Oil Level: 217.5-0 mm from the centerline of the main shaft

The oil characteristics were evaluated at 100°C. The churning losses were studied at speeds ranging between 1000-5000 RPM and at an oil level 119 mm from the main shaft centerline (wet sump) and 187.5 mm from centerline (dry sump). A nominal operation point of the electric motor was used to compare the churning power losses:

- 3500 RPM
- Electric Motor Power – 100 kW

Results indicate that at nominal operation, only a 0.55% efficiency savings is gained by using a dry sump over a wet sump design. The absolute efficiency losses due to churning were observed to be 0.34% (0.3 kW) and 0.99% (~1 kW) for dry and wet sumps, respectively. Since only half a kilowatt of power is gained by going with a dry sump design at nominal operation it was determined that the added cost of the pump and complexity of the design is not justified for this application. Please note that any speeds lower than 3500 RPM produce even smaller efficiency gains. Also, since the motor will likely be operating at more than 100kW the 0.3-1 kW of power loss due to churning will be an even smaller percentage of the total power.

Finite Element Analysis of Housings, Analysis of Rotating Components, NVH Analysis

Front and rear housings of the 4-speed transmission were designed and two iterations of finite element analysis were completed. The design improvements on the front and rear housings have been implemented to eliminate the deficiencies indicated by the FEA. Figure II-11 shows the equivalent stresses under the maximum input torque (1300 Nm) conditions in the front (left) and rear (right) housings.

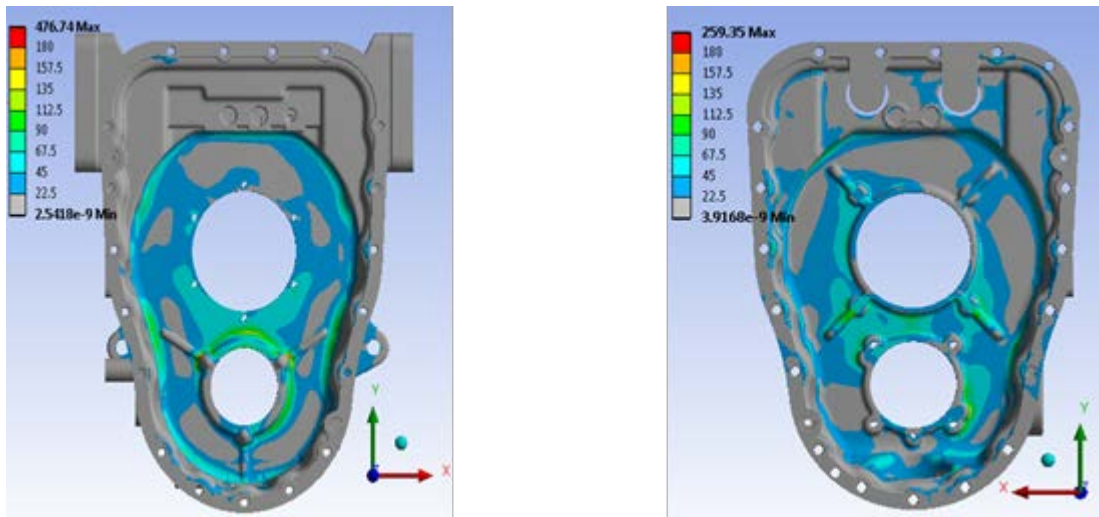


Figure II-11: Equivalent stress contours in the front (left) and rear (right) housings under 1300 Nm input torque.

After the design of the front and rear main gearbox enclosures were completed, the aluminum cast housings underwent three full cycles of FEA and resulting design revisions before the finished 3D CAD models and 2D details could be completed. Since these are long-lead items, an order for six sets of housings were placed with a selected fabrication vendor after getting several quotes to make the parts.

However, the vendor was requested to only cast and machine one set of housings, and to hold back on the other five sets, so that we may inspect and install mating components to the housings to ensure the design is correct – as these are very complicated components that mate with nearly all of the major bearings, covers, housings, shift bars, shift motors, sensors, and many other key components. Once the designs are checked and all fits verified, the other five sets of housings will be released for fabrication.

The design of the rotating components were completed. The gears and bearings stress and initial reliability analysis were completed – of which results are used for the FEA input using MASTA software. Analysis of the gearset life was completed (number of hours of life available at a peak torque and speed), and checked against the requirements of the vehicle duty cycles based on the combined duty cycle received from Proterra. Gears and bearings meet the reliability requirements for 500,000 miles of design life for the BE35 electric transit bus application. Bearing reliability analysis results are shown in Figure II-12.

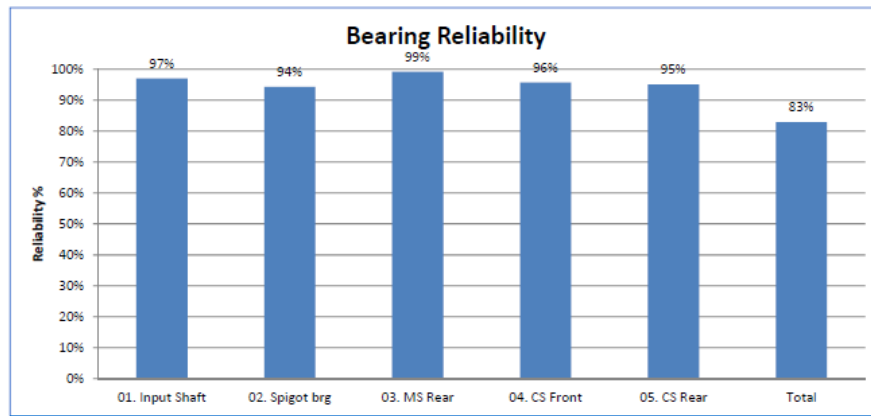


Figure II-12: 4-speed transmission bearing reliability analysis results

The gear whine noise performance of Eaton’s 4 speed EV transmission was evaluated. The simulation was based on the latest transmission design. The CAD models of the housing and internal gear sets have been imported into rotation system dynamic models to accurately predict the gear whine noise due to transmission error (TE).

- The TE analysis and gear tooth micro-geometry optimization was performed using the LDP program.
- The bearing stiffness analysis was performed using the MASTA program.
- The system dynamic analysis was performed with the Ansys program.
- The vibro-acoustics of the transmission was performed using the LMS program.

It was found that the gear tooth profile crown and lead crown have significant impacts to the TE values. An optimized gearset can reduce the TE values by 25% to 50%, which helps to reduce noise generation by 3 to 6 decibel (dB). For example, a lead crown of 10 micron and tip relief of 18 micron were proposed for the headset gear. The TE value is reduced by half as compared to the baseline. The proposed micro-geometry modifications shall not impact the contact and bending stress during the optimization and have the least impact to the manufacturing processes. Further investigations will be carried out with more emphasis on practical design and manufacturing considerations. The dynamic models of the gear, shaft, bearing, and housing are used to identify major vibration modes of the system and potential design changes. Major structure vibration modes and natural frequencies are obtained from the simulations. The overall noise radiation of the transmission is shown in Figure II-13.

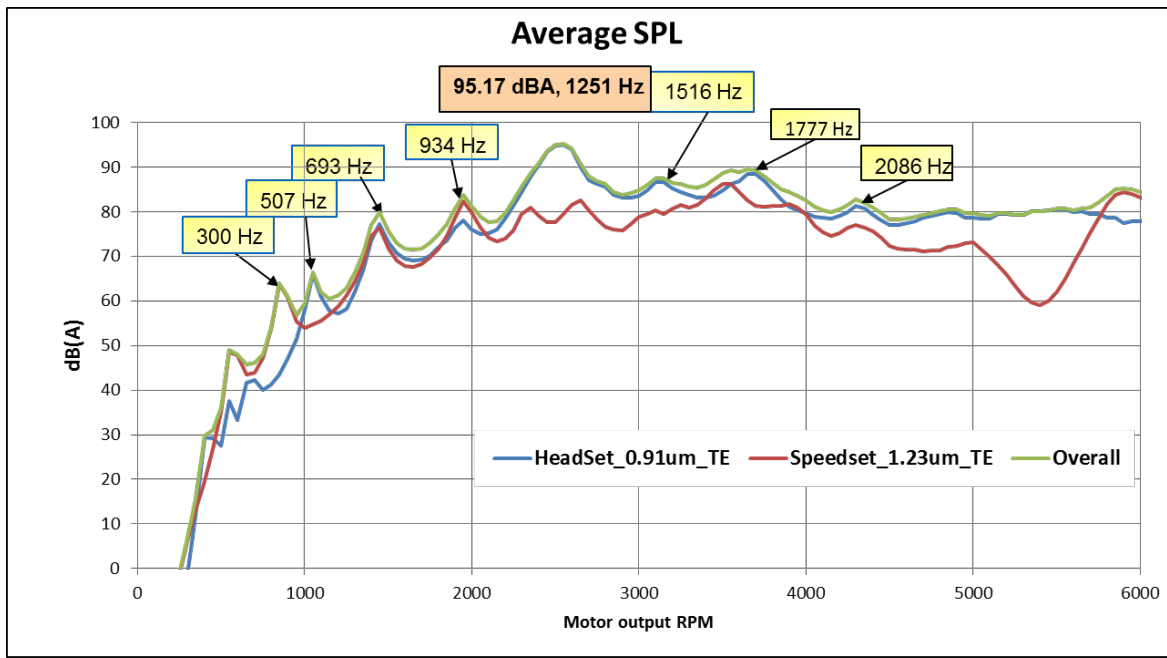


Figure II-13: Average Sound Pressure Level (SPL) as function of motor output speed.

The NVH modeling and simulation helped the engineering team to understand potential noise and vibration issues and their root causes. These simulations also help to evaluate the effectiveness of various design and manufacturing changes without prototyping, thus significantly reducing development time and cost.

Design of Shift Actuation Components

Design of the shift bars, shift forks, shift actuation blocks, and related hardware were completed and readied for fabrication. The FEA on the shift forks is also complete – showing acceptable deflection and stress characteristics. There are several actuation components and sub-assemblies being taken directly from Eaton’s production X-Y shifter assembly, and have been designed into the new transmission. These production components include electric motors, ball-screw assemblies, position sensors and related linkage, bearings, and bushings. The new transmission is employing these production components in a manner very similar to Eaton’s production transmissions – therefore minimizing risk and development time.

Stackup Tolerance Analysis

This analysis is ongoing with the final design assembly and will be finalized before fabrication of the critical internal components are ordered. However, since much of the design philosophy was adopted from Eaton’s current 6-speed transmission product family, the need for extensive stackup analysis is minimal as the transmission architecture is setup to be very tolerant of part dimension variations.

Prototype Fabrication

The 1st stage of prototyping is in progress. One set of prototype front and rear housings were made by using rapid-prototyped castings. These housings were made to check for fit of existing production shafts and bearings that will be used for this program, as well as, to have a mockup housing to check overall size and fit. Additional housings can be cast from these castings. One display unit was prepared as shown in Figure II-14. The display unit has all the exterior components but not all the interior components. The unit was displayed at the IAA Commercial Vehicles Trade Fair in Hannover in September 22-29, 2017.

Fabrication quotes on long lead items (housings, gears, shafts, shift forks, motor adaptor plate etc.) and the procurement of standard Eaton hardware are in progress.



Figure II-14: The display unit of the new 4-speed EV Transmission.

Conclusions

- Project is on schedule. All required project milestones have been met to date.
- Transmission concepts were developed and a 4-speed AMT was selected as the winning concept.
- Baseline vehicle model development was completed for the Proterra BE35 electric transit bus.
- Model was validated with on-route data of the BE35 electric transit bus.
- Optimum transmission and driveline gear ratios were simulated from the validated models.
- Initial transmission layout design and detailed transmission system design were completed.
- Initial engineering analysis of the subsystems and components were completed.
- Prototyping process has started. One display unit was prepared. The procurement and prototyping process is in progress.

II.2.C. Products

Presentations/Publications/Patents

1. Chavdar, B., 2015-DOE-AMR PowerPoint Presentation at Arlington, Washington, on June 11, 2015. Project ID-vss161, Multi-Speed Transmission for Commercial Delivery Medium Duty Plug-In Electric Drive Vehicles.
2. Chavdar, B., 2016-DOE-AMR PowerPoint Presentation at Arlington, Washington, on June 9, 2016. Project ID-vss161, Multi-Speed Transmission for Commercial Delivery Medium Duty Plug-In Electric Drive Vehicles
3. Chavdar, B., Deng, Y., Naghshtabrizi, P., Genise, T., “Modular Multi-Speed Transmission for MD EV”, CTI Symposium China, Automotive Transmissions, HEV and EV Drives, 5th International Congress and Expo, 21-23 September, 2016, Shanghai, China.
4. One display unit of the new 4-speed EV Transmission was displayed at the IAA Commercial Vehicles Trade Fair in Hannover on September 22-29, 2017.

II.2.D. References

1. No references.

II.3. Advanced Vehicle Testing & Evaluation (AVTE) [DE-EE0005501]

Jeremy Diez, Principal Investigator

Intertek Testing Services NA, Inc.
430 S. 2nd Avenue
Phoenix, AZ 85003
Phone: (480) 525-5873
E-mail: Jeremy.Diez@intertek.com

Lee Slezak, DOE Program Manager

U.S. Department of Energy
Phone: (208) 586-2335
E-mail: Lee.Slezak@ee.doe.gov

Start Date: October 1, 2011
End Date: September 30, 2018

II.3.A. Abstract

Objectives

- Test and evaluate advanced vehicle technologies that reduce petroleum consumption.
- Produce lifecycle cost data for vehicles that are utilizing these advanced technologies.
- Provide fleet operations data to the Idaho National Laboratory database in order to disseminate the results of vehicle and infrastructure testing and analysis.
- Provide benchmark data for advanced technology vehicles and their associated fueling infrastructure.

Accomplishments

- Acquired four new advanced technology vehicles during Fiscal Year 2016 for a total of 97 vehicles tested throughout the year.
- Completed baseline testing information on four vehicles of four separate makes and models.
- A total of 71 vehicle component durability tests were completed on 68 different vehicles.
- Five vehicles met their final mileage target and completed end-of-life testing.
- Implemented a storage-assisted recharging unit at a fleet test location to facilitate opportunity charging of Advanced Vehicle Testing and Evaluation fast charge-capable vehicles.
- Continued collaboration between Intertek and U.S. Department of Energy national laboratories for baseline vehicle and interim component durability report creation.

Future Achievements

- Collaborate with Idaho National Laboratory, Argonne National Laboratory, and the National Renewable Energy Laboratory to engage original equipment manufacturers and suppliers for future Advanced Vehicle Testing and Evaluation vehicle testing.
- Continue testing and rapid mileage accumulation of fuel-efficient vehicles based on their advanced technologies and market availability.
- Accelerated reliability testing of a fuel cell vehicle.

II.3.B. Technical Discussion

Background

The Advanced Vehicle Testing and Evaluation (AVTE) Project incorporates the conduct of advanced technology vehicle and infrastructure testing in the U.S. Department of Energy (DOE) Advanced Vehicle Testing Activity (AVTA). It is the only activity tasked by DOE to conduct field evaluations of vehicle technologies that use advanced technology systems and subsystems in vehicles to reduce petroleum consumption. The results are available through reports published on the AVTA website at <http://avt.inl.gov/>. The website provides insight into advanced vehicle technology's long-term performance, durability, maintenance, and lifecycle costs that cannot be found through media outlets. The site is a resource for DOE stakeholders and the public to gain knowledge on advanced technology vehicle progress and innovation.

Idaho National Laboratory (INL) has responsibility for technical direction of the overall project, along with data collection, analysis, and test reporting of light-duty vehicles in coordination with Intertek Testing Services NA, Inc. (Intertek). Medium and heavy-duty truck data collection, analysis, and test reporting is coordinated between Intertek and the National Renewable Energy Laboratory. The project is administered by the National Energy Technology Laboratory for DOE. All participating DOE laboratories coordinate with Intertek to determine project scope and direction within AVTA.

The objective of the AVTE Project is to conduct unbiased laboratory and field evaluations of advanced technology vehicles and their associated fueling infrastructure, as well as development of new test procedures and/or modifications of existing test procedures necessary to accomplish these performance evaluations. The scope of work included baseline performance, accelerated reliability, and fleet testing of state-of-the-art light, medium, and heavy-duty advanced technology vehicles and the vehicle-to-infrastructure interface required for fueling/charging the vehicles.

Introduction

The AVTE Project focuses on testing and evaluating commercially available, early production, and pre-production light, medium, and heavy-duty advanced technology vehicles using internal combustion engines (ICEs) burning advanced fuels (such as hydrogen and compressed natural gas [CNG] fuels); electric, extended range electric, hybrid electric (HEV), plug-in hybrid electric (PHEV), or fuel cell powertrains; advanced energy storage technologies (such as batteries, ultra-capacitors, and hydrogen storage tanks); advanced drivetrains; and the necessary infrastructure required to fuel and/or charge advanced technology vehicles (i.e., electric vehicles and PHEVs), including the interaction between infrastructure, vehicles, and the electric grid. Onboard engines may include, but are not limited to, fuel cells, advanced ICE, and other energy-enabling engines and motors. Evaluation data collected through the AVTE Project are used to validate the results of research, modeling, and simulation activities using laboratory and field tests.

Approach

The AVTE Project is managed in separate tasks to accomplish testing of advanced technology vehicles and their respective infrastructure. The tasks are as follows:

Project Management

This task includes activities necessary to provide management of AVTE activities, including budget and schedule control, fleet coordination, procurement, status reporting, presentations of activity results and status to DOE and industry, preparation of the project management plan, and quarterly updates of the project management plan. Work under this task also includes management of test results reports and/or data sheets for each task.

Vehicle Specification and Test Procedure Development

Specifications for vehicles, components, and infrastructure are prepared to define specific design and performance requirements. Test procedures are developed that will evaluate requirements stated in the specification.

New testing procedures incorporate industry standard test procedures as applicable. Vehicle tests typically include closed track testing of performance and operating characteristics and DOE laboratory chassis dynamometer testing. Special tests for components and infrastructure are developed, with unique test facilities to validate specification requirements.

Existing procedures for accelerated and fleet testing are revised, as necessary, to include specific aspects of each class of the anticipated subject vehicles and to keep them current with new industry standards and requirements. Procedures incorporate mission-based requirements (i.e., simulating actual fleet operating practices). Data collection techniques are developed to measure and record the data necessary to provide information required for each class of vehicle.

Baseline Performance Testing

Baseline test procedures include, but are not limited to, testing of acceleration, speed at distance, gradeability, deceleration due to regenerative braking, braking distance, time to recharge and charging efficiency (for grid-connected vehicles), energy storage capacity, and fuel efficiency on various dynamometer test cycles and in various operating modes. Additional baseline test procedures are developed, as required, for vehicles with unique operational characteristics.

Baseline vehicle performance testing is performed at a limited access test track. Chassis dynamometer testing is conducted at Argonne National Laboratory's Advanced Powertrain Research Facility. Dynamometer testing of vehicle technologies with unique operational characteristics (e.g., transit, agricultural, and military) will be provided as required. As part of baseline testing, beginning-of-test battery testing is performed on all vehicles with battery energy storage. Vehicles will be purchased, leased, or rented unless provided by DOE or manufacturers and suppliers. All vehicles will be insured, operated, and maintained in accordance with manufacturer's recommendations.

Accelerated Vehicle Testing

During accelerated testing, at least one vehicle is tested under supervised and semi-controlled conditions in order to evaluate one or more characteristics of the vehicle's performance or operational characteristics and to obtain data in an accelerated timeframe, evaluating vehicle reliability, maintenance requirements, long-term performance, energy efficiency, and lifecycle costs. The assumption with accelerated testing is that the vehicle is unlikely or too expensive to operate in a long-term fleet application due to technical and manufacturing robustness.

The accelerated testing duration is based on the objectives of testing for the particular subject vehicle. Testing typically achieves a minimum of 6,000 miles on a subject vehicle, but may reach higher mileage as documented in the project management plan. Vehicles are purchased, leased, or rented unless provided by another program. All vehicles are insured, operated, and maintained in accordance with manufacturer's recommendations. Fueling infrastructure is provided, as required, to conduct testing and evaluation.

Fleet Testing

Fleet testing includes high-mileage testing of two or four production vehicles of the same make and model in an operating fleet to determine vehicle reliability, maintenance requirements, long-term performance, lifecycle costs, and user acceptance. Vehicles are driven on road to achieve a target mileage suitable for the advanced technology that is being studied during a 3-year minimum exposure to fleet operation. HEV and ICE vehicles are targeted to achieve 195,000 miles in fleet testing. PHEVs are targeted to achieve 160,000 miles in fleet testing due to the requirement to start the day in charge-depleting mode. BEVs are targeted to achieve 36,000 miles in fleet testing due to the limited range achievable per charge. Vehicles are purchased, leased, or rented unless provided by another organization. All vehicles are insured and maintained in accordance with the manufacturer's recommendations. Fueling infrastructure is provided, as required, to conduct testing and evaluation.

Data collection systems necessary for collecting operating data as required per test procedures are installed on all fleet vehicles. Repair and maintenance costs are collected manually. The fleet operator maintains logs of fuel dispensed (including electricity on plug-in electric vehicles) and mileage. Operating data and repair and maintenance costs are maintained current on a monthly basis. Quality checks and trend analysis are performed to ensure data are accurate and vehicles are performing properly.

Interim Component Testing

This task includes testing of vehicle components during accelerated or fleet testing. Interim component durability (ICD) tests for traction-battery-equipped vehicles are capacity and performance related between baseline and end-of-testing. For vehicles using CNG as a fuel, compression testing is conducted for engine performance over the life of the vehicle. Other advanced vehicle technology component testing specifications and procedures will be developed as other technologies and components are tested. Raw data from the testing are provided to AVTA at INL for analysis and verification.

End-of-Test Vehicle and Component Testing

This task consists of vehicle and component testing at completion of fleet or accelerated testing and includes, but is not limited to, vehicle performance, mechanical components, batteries, and other energy storage devices. Tests are performed as required by the project management plan and are conducted in accordance with procedures developed under test procedure development. Raw data from the testing is provided to AVTA at INL for analysis and verification.

Infrastructure Test and Evaluation

This task consists of testing vehicle and infrastructure interface, operations, and reliability. For grid-connected electric-drive vehicles, the testing will include charger efficiency, vehicle-to-grid communication, and bi-directional power flow (if applicable). The evaluation will collect data on installation, operation, energy, and maintenance costs of the infrastructure and track user feedback related to overall interface and operation of the infrastructure. Deliverables include test result data sheets and a report on the cost, safety, operation, maintenance, and reliability of the infrastructure.

Additional Procedure Development, Testing, or Test Support

This task consists of various additional procedure development, testing, and test support activities that may be determined necessary by DOE and Intertek. The activities will be detailed in the project management plan and the work will be reviewed and approved by DOE.

Results

Vehicle Testing

A total of 97 vehicles were tested during Fiscal Year (FY) 2016, which accumulated 2,727,726 miles in fleet testing. There were four 2016 Chevrolet Volt vehicles acquired during the fiscal year. Vehicles under test during the fiscal year are summarized in Table II-7.

Two vehicles were transferred from AVTA (DE-FC26-05NT42486) to AVTE on March 22, 2013, to continue mileage accumulation and component testing. The remaining two 2011 Chevrolet Volts continue to accumulate mileage and perform component testing to reach their goal of 160,000 miles.

Prior to the start of FY 2016, there were 93 vehicles that were underway with mileage accumulation and advanced component testing. A selection of current fleet vehicles is pictured in Figure II-15.



Figure II-15: AVTE fleet vehicles at Intertek for a review with the DOE team in January 2016.

Intertek

Table II-7: AVTE Vehicles Tested During FY 2016.

Quantity	Year	Make	Model	Type	Vehicle Testing Focus	FY 2016 Mileage
2	2011	Chevrolet	Volt	PHEV	Energy storage system (ESS)	43,890
4	2013	Volkswagen	Jetta TDI	ICE	12-V accessory loads	76,259
4	2012	Honda	Civic CNG	ICE	Compression testing/12-V accessory loads	135,684
4	2013	Chevrolet	Malibu ECO	HEV	ESS	110,145
4	2013	Chevrolet	Volt	PHEV	ESS	169,505
3	2013	Honda	Civic Hybrid	HEV	ESS	136,881
4	2013	Toyota	Prius Plug-In	PHEV	ESS	149,331
4	2013	Volkswagen	Jetta Hybrid	HEV	ESS	177,755
2	2012	Mitsubishi	i-MiEV	BEV	ESS	11,720
4	2013	Nissan	Leaf	BEV	ESS	24,717
3	2013	Ford	C-Max Energi	PHEV	ESS	196,023
4	2013	Ford	C-Max Hybrid	HEV	ESS	134,849
4	2013	Ford	Fusion Energi	PHEV	ESS	217,957
4	2013	Ford	Focus Electric	BEV	ESS	22,999
4	2014	Smart	ED	BEV	ESS	15,906
3	2014	Mazda	Mazda3 i-ELOOP	ICE	Capacitor	149,323
4	2014	Chevrolet	Cruze Turbo Diesel	ICE	12-V accessory loads	167,814
4	2014	BMW	i3 Range Extender	PHEV	ESS	50,272
4	2014	BMW	i3	BEV	ESS	35,101
4	2015	Kia	Soul	BEV	ESS	35,968
4	2015	Chevrolet	Spark EV	BEV	ESS	28,801
4	2015	Honda	Accord Hybrid	HEV	ESS	241,650
4	2015	Volkswagen	e-Golf	BEV	ESS	39,950
4	2015	Mercedes	B-Class Electric	BEV	ESS	41,796
4	2015	Chevrolet	Impala Bi-Fuel	ICE	Compression testing/12-V accessory loads	208,212
4	2016	Chevrolet	Volt	PHEV	ESS	105,217
97	Total	Tested	Vehicles		FY 2016 Total Miles	2,727,726

New vehicles for FY 2016 were vetted with DOE during annual reviews and project management plan updates. An additional four advanced technology vehicles (i.e., 2016 Chevrolet Volts) were acquired for testing during FY 2016. The testing of four similar make and model vehicles not only provides statistical accuracy to the data recorded, but also ensures that advanced vehicle technologies can be evaluated during their final target mileage.

One 2015 Volkswagen (VW) e-Golf, one 2015 Mercedes B-Class, one 2015 Chevrolet Impala Bi-Fuel, and one 2016 Chevrolet Volt completed baseline testing, including testing at the Argonne National Laboratory's Advanced Powertrain Research Facility and at INL for power quality testing of the plug-in vehicles. A total of 71 vehicle component durability tests were completed on 68 different vehicles in FY 2016. At the end of FY 2016, 83 vehicles were in fleet operation. The remaining vehicles that did not continue from the 97 vehicles



that were tested during FY 2016 include five end-of-test vehicles (three 2013 Honda Civic Hybrids and two 2013 Toyota Prius Plug-Ins), two removed from fleet for battery failures (one 2014 Smart ED and one 2014 BMW i3 with Range Extender), three totaled vehicles (two 2013 Ford C-Max Hybrids, and one 2013 Ford Fusion Energi), and four 2013 VW Jetta TDIs due to the VW 2.0 Liter TDI Diesel Emissions Settlement. On September 21, 2016, at a DOE review, approval was granted by DOE to move forward with the process for VW to buy back these four vehicles. The vehicles were removed from fleet testing prior to the end of FY 2016.

Figure II-16: 2016 Chevrolet Volt that completed baseline testing.
Intertek

Vehicle Testing Intervals

All fleet test vehicles must meet a minimum of 3 years in fleet use for each vehicle and a minimum mileage target. The fleet and interim component durability testing results of these vehicles have historical AVTA test results for comparison.

The mileage target for ICE vehicles and HEVs is a minimum of 3 years and 195,000 miles of fleet testing. For PHEVs, the minimum is 3 years and 160,000 miles of fleet testing. For BEVs, the minimum is 3 years and 36,000 miles of fleet testing.

Component testing for each vehicle is adjusted based on the new mileage targets. For ICE vehicles and HEVs, baseline testing occurs at approximately 4,000 miles and ICD testing occurs at approximately 50,000, 105,000, and 160,000 miles, with a final test at approximately 195,000 miles. For BEVs, initial baseline component testing occurs at approximately 400 miles and ICD testing occurs at approximately 4,000, 12,000, and 24,000 miles, with a final test at approximately 36,000 miles. For PHEVs, due to their capability to drive in charge-sustaining mode after the energy storage device is depleted in charge-depleting mode from an overnight charge, their testing is based on time intervals in the fleet after the initial baseline testing at 4,000 miles. ICD testing occurs at approximately 6 months, 1 year and 6 months, and 2 years and 6 months of fleet testing, with a final test at approximately 3 years of fleet testing with a minimum of 160,000 miles obtained during this period.

Collaboration between Intertek and DOE National Laboratories

Deliverables for the AVTE Project consist of vehicle baseline reports, interim component durability reports, and end-of life component reports that are posted to the INL AVTA website. INL provides technical direction for the project and direction on data required from the vehicles, infrastructure projects, and analysis of the data collected. When putting together the initial vehicle baseline report, data are compiled from literature review, closed track testing at a proving ground, vehicle inspection, and fuel economy results from chassis dynamometer testing at the Argonne National Laboratory's Advanced Powertrain Research Facility. Highway, city, and air-conditioning cycle results at multiple ambient temperatures are included in the baseline report. The multiple ambient temperatures provide background on functioning of the propulsion systems, the secondary heating and cooling systems, and their effects on fuel economy, which are not evident in the Environmental Protection Agency fuel economy ratings for the vehicle. Argonne National Laboratory also conducts additional testing that is requested for Autonomie simulations with the AVTE vehicles and provides

public access to all obtained data through their Downloadable Dynamometer Database website at <http://www.anl.gov/d3>.

Fleet Locations

EZ Messenger, a courier and legal document delivery service, and Specialized Delivery Services operate AVTE fleet vehicles in multiple fleet locations. With installation of 24 EVSE units at the EZ Messenger location in Phoenix, a majority of the AVTE plug-in vehicles recharge here. Figure II-17 shows the charging infrastructure in place at this location. EZ Messenger also operates vehicles out of their Tucson, Houston, Dallas, Austin, and Oklahoma City locations, with plans to expand to other locations in cooler climates. Based on the need for obtaining vehicle data in cooler climates, the vehicles can be moved as needed, but fueling infrastructure will need to be in place to allow AVTE vehicles to obtain their target mileages. For example, the 2012 Honda Civic CNG vehicles are based out of Oklahoma City and Texas due to the large network of CNG filling stations in the area. The Chevrolet Impala bi-fuel vehicles that can operate on both gasoline and CNG are also planned for fleet operation in this area.

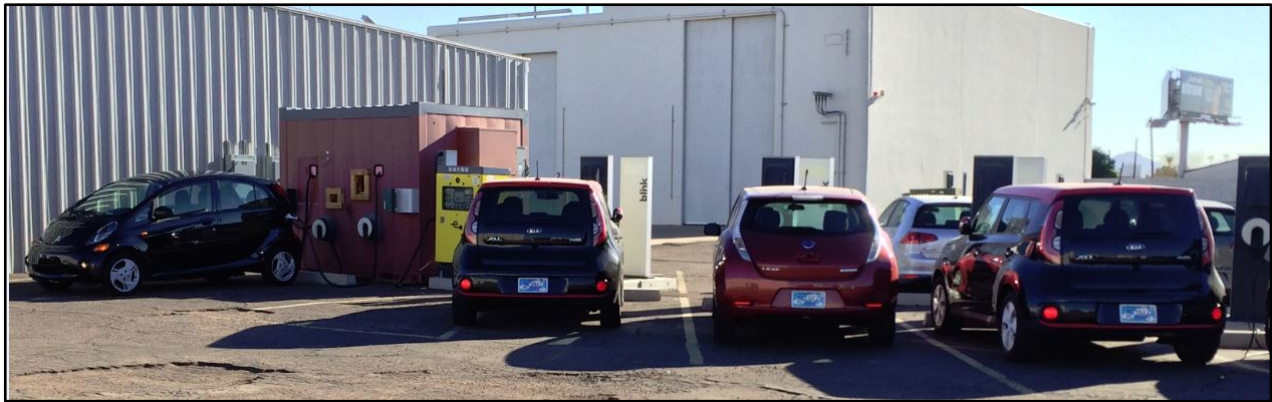


Figure II-17: EZ Messenger Phoenix fleet location charging infrastructure with AVTE vehicles and Storage-Assisted Vehicle Recharging (StAR) Unit in red climate-controlled chamber.

Intertek

Direct Current Fast Charging at Temperature

All direct current fast charge (DCFC)-capable BEVs perform testing at 0, 25, and 50°C while DCFC to



provide analysis about the effects of ambient temperature on charge times and energy delivered. Figure II-18 for provides a picture of the vehicle temperature chamber and Advanced Charging Technologies DCFC unit. DCFC baseline testing is conducted at 4,000 miles, 24,000 miles, and 36,000 miles, which coincide with baseline and component testing intervals for BEVs. Progress reports are posted on the AVTA website and summarize testing completed for the 2013 Nissan Leaf, 2012 Mitsubishi i-MiEV, 2014 BMW i3 BEV, 2015 Chevrolet Spark EV, 2015 Kia Soul EV, and the 2015 VW e-Golf EV.

Figure II-18: Vehicle temperature chamber with Advanced Charging Technologies DCFC configured with both CHAdeMO and combined charging system connectors located at Intertek in Phoenix, Arizona.

Intertek

Storage-Assisted Vehicle Recharging



A StAR unit was installed at the Phoenix, Arizona EZ Messenger fleet location during May 2016. Figure II-19 provides a picture of the StAR unit. The entire unit is housed in a temperature-controlled chamber due to the maximum 40°C ambient limitation from the manufacturer, which can be exceeded in Phoenix, Arizona. The unit is under evaluation with DCFC-capable AVTE fleet vehicles. The StAR unit, sourced from VLI-EV, is the only one that met all project requirements, which included having both the CHAdeMO and the Combined Charging System (CCS) connectors and an onboard energy storage system. A 12-kWh onboard ESS is designed into the unit and will be evaluated for its overall capability to avoid electric utility demand charges that would have been present with a standard DCFC that does not have an ESS onboard.

Figure II-19: VLI-EV DCFC unit installed at the EZ Messenger fleet location with both CHAdeMO and combined charging system connectors (the CHAdeMO connector is shown).

Intertek

Conclusions

The AVTE Project provides real-world testing of production vehicles, their energy storage systems, and their associated infrastructure that is not publically available. The selection of advanced technology vehicles has grown in FY 2016 with the addition of four 2016 Chevrolet Volts. Future AVTE vehicles will be sourced through collaboration between DOE and manufacturers and suppliers. A large majority of affordable advanced technology vehicles are included within AVTE to provide a full dataset for those considering advanced technology vehicles and understanding their technologies and benefits.

Data and reports from vehicle testing are available for further study by DOE national laboratories and dissemination to the public. This valuable unbiased information provides performance data that cannot be found in media outlets, such as performance of ESS over the life of the vehicle, maintenance cost/mile, fuel economy over the life of the vehicle, and charging economy, which are all available through the AVTA website.

II.3.C. Products

Presentations/Publications/Patents

1. "Vehicle Specifications and Testing Results, Series of Reports," Idaho National Laboratory, Intertek Testing Services NA, 2015-2016.
2. "Battery Pack Laboratory Testing Results, Series of Reports," Idaho National Laboratory, 2015-2016.
3. "DC Fast Charging at Different Temperatures, Series of Reports," Idaho National Laboratory, Intertek Testing Services NA, 2015-2016.
4. All listed reports can be found on the AVTA website. Vehicle-specific reports are organized by vehicle make and model. Access <http://avt.inl.gov/> for more information on vehicle testing.

II.4. Energy Impact of Connected and Automated Vehicles [DE-FOA-0001213]

Huei Peng, Principal Investigator

University of Michigan
2350 Hayward Street
Ann Arbor, MI 48109-2125
Phone: (734) 936-0352; Fax: (734) 764-4256
E-mail: hpeng@umich.edu

John Jason Conley, DOE Program Manager

U.S. Department of Energy
National Energy Technology Laboratory
Phone: (304) 285-2023
E-mail: John.Conley@NETL.DOE.gov

Start Date: October 1, 2015
End Date: December 31, 2018

II.4.A. Abstract

Objectives

The objective of the project is to study the energy impacts of connected and automated vehicle technologies for a wide range of use cases and technology scenarios using both test data and high fidelity models. The project will evaluate the impact of a fast emerging technology on the energy benefit of current and future vehicle technologies through test data currently not available and by providing guidance for future R&D directions (i.e., component requirements, operating conditions) through the use of simulation tools.

Accomplishments

This project consists of five inter-connected tasks. The accomplishments are reported for these five tasks separately below.

- Task 1 Instrumentation and data acquisition of energy related information
 - Task 1 creates the data collection and data fusion capabilities to support the experimental and analysis portions of the project. Elements of this overall capability set are also developed in other tasks, but Task 1 is responsible to enable those data to be fused together. A major accomplishment was the selection of the dongle vendor to be Fleetcarma.
 - The table shows the proposed subtasks and delivery times for the six subtasks of Task 1.

Table II-8: Subtasks of Task 1: Instrumentation and data acquisition of energy related information

Subtask	Subtask	Schedule	Schedule end date	Status
1.1	Coordinate and prioritize vehicle signals	M1	12/5/2015	Complete
1.2	Main data acquisition/ storage/ transmission hardware development and OBD port logger	M2-M12	11/5/2016	Ahead of schedule
1.3	Decode and translate vehicle energy usage information for logging	M5-M7	6/5/2016	Complete
1.4	Integrate safety and other DAQ systems into main aggregation equipment	M5-M10	9/5/2016	On time
1.5	Integrate driver choice/behavioral model (routing) information	M13-M18	5/5/2017	On time
1.6	Data collection, instrumentation refinement, and QC	M8-M36	7/5/2016	Started 8/15/16

- Task 2 Display energy related information to study its influence on the driver
 - Task 2 is to develop a flexible driver information module capable of displaying information relevant to energy savings applications to the driver, and to keep a record of the information displayed that this can be used for later analysis. Through a display screen, we will display information (i.e. countdown to traffic signal change from red to green) to allow for a range of potential energy-saving applications. The type and nature of the information displayed to the driver will be adjusted to aid in the assessment of various driver messaging related to different energy saving applications. The table below shows the status of the four subtasks of Task 2.

Table II-2: Subtasks of Task 2: Display energy related information to study its influence on the driver

Subtask	Subtask	Schedule	Schedule end date	Status
2.1	Identify CAV user applications, co-design and prioritize signals	M1	12/5/2015	Complete
2.2	Develop driver information display hardware and communication	M2-M7	6/6/2016	On time – early phases
2.3	Design vehicle information display screen(s) and experimental cases	M8-M12	12/7/2016	On time
2.4	Review of the finished human test results. Review the field performance of the designed user interface	M13-M24	12/6/2017	On time

- Task 3 Travel Behavior Modeling
 - Task 3 will model travelers’ driving and travel behavior in the context of controlling and reacting to connected and automated vehicles (CAV). It provides input to Task 4 of modeling the CAV system for the City of Ann Arbor in POLARIS. As Task 3 is the core modeling piece of this project, at this stage, we are analyzing existing dataset to model the impact of CAV on activity choice and conduct literature review. The table below shows the status of the five subtasks of Task 3.

Table II-3: Subtasks of Task 3: Travel behavior modeling

Subtask	Subtask	Schedule	Schedule end date	Status
3.1	Experiment and survey design	M1	11/5/2015	Complete
3.2	Model departure-time choice behavior	M2-M6	5/5/2016	Delayed
3.3	Model route choice behavior	M7-M12	7/5/2016	On time
3.4	Model travel activity pattern change	M13-M20	11/5/2016	On time
3.5	Calibration of POLARIS traveler behavior model	M21-M24	11/5/2017	Not started yet

- Task 4 System model development and validation
 - The objective of Task 4 is the development and validation of the transportation system model of the Ann Arbor region, both for baseline analysis as well as CAV scenario analysis. Task 4 will incorporate data collected as a part of Task 1 and Task 2, as well as behavioral models developed in Task 3 into an integrated travel behavior and transportation system simulation model using the POLARIS software. The updated POLARIS model will then be used to simulate various connected vehicle technologies and quantify changes in energy consumption resulting from those scenarios. The table shows the proposed subtasks and delivery times for the seven subtasks of Task 4.

Table II-4: Subtasks of Task 4: System model development and validation

Subtask	Subtask	Schedule	Schedule end date	Status
4.1	Implement baseline POLARIS model	M1-M12	9/16	On time
4.2	Determine data needs for further model development	M1-M12	9/16	On time
4.3	Query, collect and process data from the connected vehicle fleet	M13-M24	9/17	Started early
4.4	Implement traveler and CAV agent behavior rules	M25-26	11/17	Not yet started
4.5	Implement and calibrate the POLARIS-Autonomie model	M27-M30	3/18	Not yet started
4.6	Model validation with new data from field tests	M31-M32	5/18	Not yet started
4.7	Vehicle energy consumption quantification	M31-M36	8/18	Not yet started

- Task 5 Adaptive Signal Control
 - In this task, we study the energy savings achievable through adaptive traffic signal control systems with varying penetration percentage of connected and automated vehicles (CAV). We selected that the Plymouth road between Green and Barton roads to be the area for the study. The intersections are equipped with road side units (RSU), i.e., they can communicate with vehicles through Dedicated Short Range Communications (DSRC). We are building a model in the VISSIM environment. Adaptive signal control algorithms will then be developed and simulated. The following table shows the status of the subtasks of Task 5.

Table II-5: Subtasks of Task 5: Adaptive Signal Control

Subtask	Content	Schedule	End Date	Status
5.1	Build and calibrate the traffic simulation environment	M1-M6	5/5/2016	On time
5.2	Develop the adaptive signal control algorithm	M7-M18	5/5/2017	Not yet started
5.3	Deploy and conduct field experiment at M city and Plymouth Rd	M19-M30	5/5/2018	Not yet started
5.4	Evaluate the energy saving of adaptive signal control	M31-M36	11/5/2018	Not yet started

Future Achievements

- The final envisioned achievements of the project include: (i) Collected 400-500 vehicles with high quality DSRC, GPS and CAN bus data, which can be used as the basis to calibrate simulation models and understand the behavior of CAVs; (ii) Developed human driver models to simulate human drivers' reaction to advise from CAV functions as well as travel behavior; (iii) Use these data and models developed to calibrate/validate the POLARIS model as well as to implement adaptive traffic signal control algorithms.
- In the near-term, we will focus on the following
 - Volunteer driver recruiting
 - Design of a thoughtful human interface and experiment plan
 - Concept design of a large-scale modeling of household travel activity optimization
 - Analyze and incorporate travel demand from SE Michigan in the Ann Arbor model
 - Assessment of behavioral implications of select CAV technologies leading into the data needs assessment for POLARIS
 - Use software to convert connected vehicle safety pilot data into synthetic travel survey for model estimation/calibration of baseline POLARIS model
 - Estimation and calibration of base and CAV behavioral models
 - Develop adaptive signal control models and algorithms to reduce energy use and congestion
 - Acquire data logger and integrated into the existing UM connected vehicle fleet.
- After finishing all the future research tasks, the UM/ANL/INL team will have the following research tools available: leveraging the world's largest CAV test fleet (now at 1600 vehicles), 400-500 of them will have detailed energy related data collected, a test-data calibrated model that can simulate the energy impacts of CAV, and a corridor of six intersections with adaptive traffic signal control algorithms reacting to real-time traffic information collected from the connected vehicle fleet.

II.4.B. Technical Discussion

Background

Connected and automated vehicles are being actively developed by companies, and pilot deployment by industry-government collaborative projects around the world. The initial focus of these projects are safety and robust performance. Their possible impacts (positive or negative) have not been adequately studied. The objective of this project is to study the energy impacts of connected and automated vehicle technologies for a wide range of use cases and technology scenarios using both test data and high fidelity models. We plan to achieve this goal through the carefully planned and coordinated effort by the proposing team: (1) we will start by leveraging the existing fleet already operational at the University of Michigan and expand it to include energy related data acquisition and analysis to (2) leverage existing expertise within the DOE National Laboratories to enhance and validate system simulation models, so that (3) these tools can be used to evaluate the energy impact of CAVs using current and future vehicle technologies. This project is led by the University of Michigan (UM) in collaboration with two DOE labs—the Argonne National Lab (ANL) and Idaho National Lab (INL). The three organizations bring together complementary expertise and facilities critical to the success of this project.

Introduction

Modern vehicles today can generate tens to hundreds of GB of data every hour. Much of the utility of connected vehicle technologies lies in the potential value of this vast amount of data, including vehicle internal states, geographic road features, traffic flow and density, and individual vehicle movements, some of which are now available in separated repositories. The confluence of connected mobility data and emerging big data analytics presents both a challenge and an opportunity. The available data can be used to better understand driver behavior, energy and carbon emission, and traffic dynamics. For this project, data are being collected to (1) develop behavioral models representing how drivers react to information they are provided, (2) validate the traffic flow simulation model of Ann Arbor developed in POLARIS and (3) develop new driver model for Autonomie (e.g., how do drivers react to traffic signal information projected on a screen).

Another current trend in the industry is the rapid development of automated vehicle technologies. Recent breakthroughs in sensors, perception, and control technologies make vehicle automation much closer to reality. Almost all major OEMs and first tier suppliers have active programs for Connected and Automated Vehicles (CAVs). Many of them have aggressively target dates to bring the concept to the market. While numerous research activities have occurred in the US over the past couple of years, the vast majority of projects have been focused on safety rather than on energy and mobility.

In the US, the University of Michigan was selected to lead a project named Safety Pilot Model Deployment in 2012. In Europe, more than 15 projects have been supported to develop and demonstrate the potential of CAV technologies to improve safety, ease congestion, and reduce energy consumption and emissions. This incubator project is among the first CAV research projects sponsored by the U.S. Department of Energy, and will focus on the energy impacts.

The experimental data will be analyzed and used to develop and calibrate an open-source transportation network models POLARIS, which can be linked to and used in coordination with more detailed energy simulation tools such as Autonomie to simulate the City of Ann Arbor traffic and the accumulative performance indices in energy/mobility. The calibrated transportation model will also become the backbone for developing and implementing new mobility concepts such as adaptive traffic signal control for congestion reduction or energy saving, and many other new concepts and applications.

Approach

This project consists of five inter-connected tasks. The approach of these five tasks are described below

- Task 1 Instrumentation and data acquisition of energy related information

- A list of candidate vehicle signals for energy purposes was constructed in the first quarter of the project by Idaho National Lab (INL) and the Argonne National Lab (ANL). This list included a basic set as well as an “ideal set.” Based on conversations with the project task leads, a prioritization of the signals was finalized in the Task 1 Workshop.
- We compared data loggers from four different vendors, and tested the two leading devices on vehicles. We selected FleetCarma loggers and did additional test for 30 days on a Chevy Volt and on a Ford Fusion Hybrid with excellent data logging results.
- The purchase order for the data has been placed and the first batch has been received. Installation on volunteers' vehicles have started.
- When the data are collected, we plan to fuse data from multiple sources into a comprehensive data set to support analyses for the project.
- We plan to outfit the 500 vehicles with the ODB-II logger, validation of the system – including the backhaul – and maintaining operations.
-
- Task 2 Display energy related information to study its influence on the driver
 - Identify CAV user functions, co-design and prioritize signals.
 - Develop driver information display hardware and communication.
 - Design vehicle information display screen(s) and experimental cases.
 - Review human test results. Review the field performance of the designed user interface.
 -
- Task 3 Travel Behavior Modeling
 - Experiment and survey design for travel behavior model.
 - Model departure-time choice behavior.
 - Model route choice behavior.
 - Model travel activity pattern change.
 - Calibration of POLARIS traveler behavior model.
- Task 4 System Model Development and Validation
 - Develop the Ann Arbor and Ypsilanti region baseline POLARIS model.
 - Determine data needs for further model development.
 - Query, collect and process data from the connected vehicle fleet.
 - Implement traveler and CAV agent behavior rules.
 -
- Task 5 Adaptive Signal Control
 - Build and calibrate the traffic simulation environment for the adaptive traffic signal control.
 - Develop the adaptive signal control algorithm.
 - Deploy and conduct field experiment at MCity and the Plymouth Road corridor.
 - Evaluate the energy saving of adaptive signal control.

Results

This project consists of five inter-connected tasks. The results of these five tasks are described below

- Task 1 Instrumentation and data acquisition of energy related information
 - After deciding that Fleetcarma’s C2 device was the best option for this project we needed to optimize cellular data costs. With that in mind we would be installing these logging devices into 100 PEVs and 400 ICE vehicles and determined the following data logging parameters and rates would be optimal:
 - VIN, Odometer, OBD time since previous trip and Auxiliary power in summary
 - Timestamp at every data point
 - Vehicle and engine speed, Accel pedal, brake pedal every 2 seconds
 - Fuel consumption, battery current and voltage every 5 seconds
 - GPS latitude and longitude every 5 seconds

- Battery SOC, HVAC and ambient temperature every 60 seconds
- Pilot testing began the first week of August and the data transmission and storage has been worked out after a few weeks of pilot testing. Installation procedures has been drafted, used, adjusted and completed.
- We are currently working on the data quality control and fusion plan.
- Task 2 Display energy related information to study its influence on the driver
 - Two key CAV functions were identified that both show significant potential, and had not been implemented in large-scale experiments: eco approach and departure, and green wave (speed recommendation).
 - We worked with Savari Inc. to develop hardware, software, and communication solutions for the in-vehicle SPaT (Signal Phase and Timing) visualization and speed recommendation near intersections. The hardware include ASD (Aftermarket Safety Device), antennas, DVI display (tablet), WIFI dongle, and USB drive.
 - Several forms of presenting speed advice and SPaT information have been designed and evaluated visually, will selected to a subset for further testing.
 - Four potential issues related to presenting the recommended speed in real-world driving environment were analyzed.

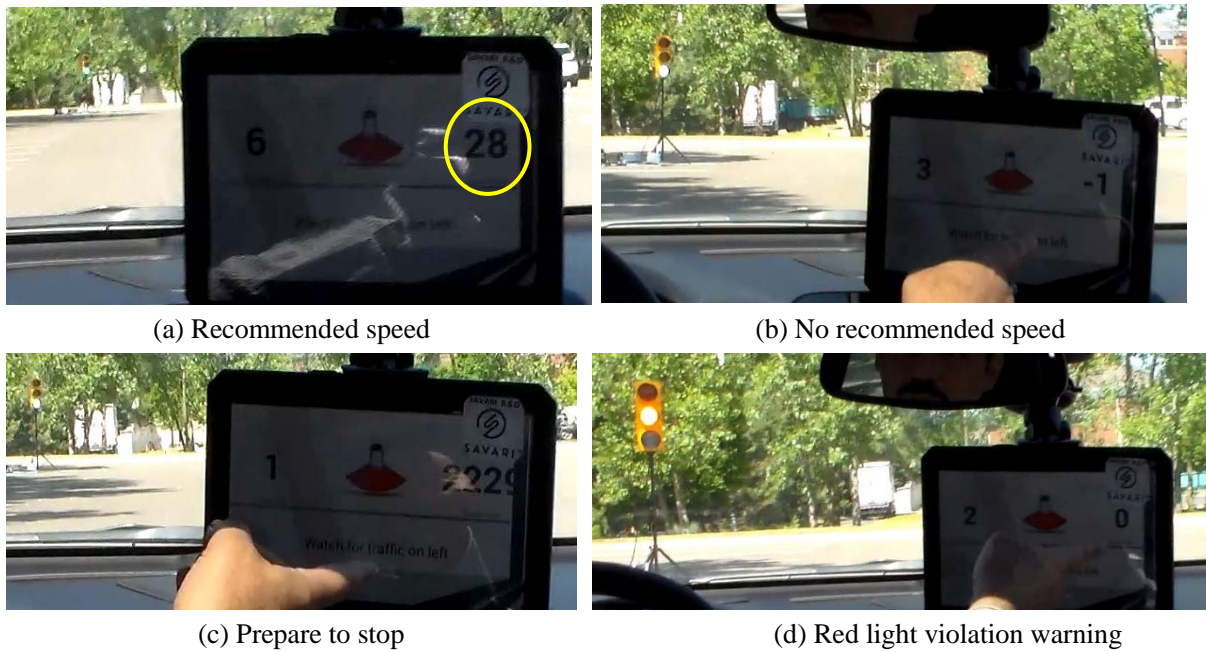


Figure II-20: CAV Human Display Under Development

- Task 3 Travel Behavior Modeling
 - We have extracted travel patterns (including departure-time, route choice, activities, and destinations) from the Safety Pilot Model Deployment (SPMD) database and conducting statistical analysis. For the drivers in the SPMD study, we have extracted their travel patterns over a period of 7-month (the personal identifiable index has been scrubbed for privacy protection).
 - “Stay points” along a GPS trace (i.e., a static point with a staying duration of more than a certain threshold) contains importation travel “semantic” information and have been analyzed.
 - The identified stay points are then imported to ArcGIS (www.arcgis.com) to map points to land use. There are 13 land use types, including On road, Single-family/ Multiple-family residential, Commercial, Industrial, Governmental/Institutional, Parks/Recreation/Open Space, etc.
 - An example time-space trajectory is shown in Figure II-21.



Figure II-21: Example time-space trajectory extracted from the Safety Pilot Model Deployment Database

- Task 4 System Model Development and Validation
 - Estimated the internal behavioral models for the local context using existing survey data from the local MPO as well as activity-travel data reconstructed from the previous connected vehicle safety pilot deployment data.
 - The assessment of data needs for added POLARIS model functionality is underway concurrently with the assessment of behavioral implications of CAV technologies. These data needs are classified into five groups: Population, Network/Physical systems, Travel, Vehicle, and Connected vehicle.
 - The data processing algorithms were expanded to incorporate the activity-travel and socio-demographic estimation processes documented in NCHRP Report 775 into the base map matching routines. This will then serve as input to the characterization process where the activity episodes are appended with purpose, timing, and other characteristics based on the above referenced algorithms.
 - The implementation of traveler and CAV agent behavior rules has started independently of the data collection and model estimation tasks.
 - The ANL and UM team have collaborated on enhancing the POLARIS model to have the capability to simulate Eco-Routing.
 - A preliminary model for simulating CAV vehicles along the links of the POLARIS model was developed.
 - Graduate students from University of Michigan spent the summer of 2016 at the Argonne National Laboratory to work on POLARIS to improve its usability for simulating CAV technologies.
 - A new microscopic model was developed to enable more accurate simulation of energy consumption of individual vehicles (see Figure II-22).

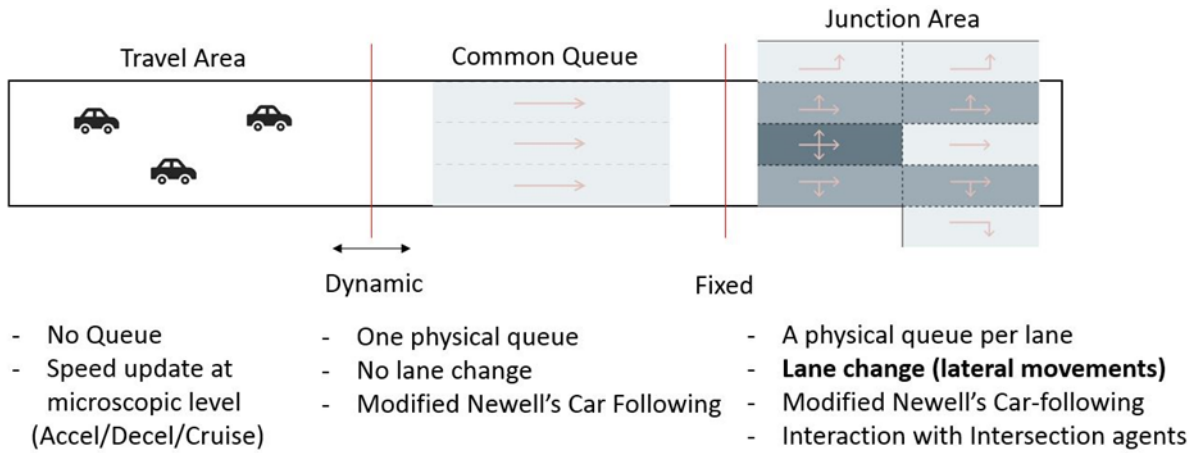


Figure II-22: A new microscopic simulation model under development, to enhance the ability of the POLARIS model to simulate CAV functions

● Task 5 Adaptive Signal Control

- A hardware-in-the-loop (HIL) simulation platform was designed to test and evaluate the models in a microscopic simulation environment. The simulation platform replicates the real-world situation so that control algorithms can be calibrated efficiently. The structure of the simulation platform is shown in Figure II-23.
- A VISSIM simulation model was built for a six-intersection corridor at Plymouth Rd, Ann Arbor (see Figure II-24).
- A data hub device was designed to interface with roadside unit (RSU) and traffic signal controller to simultaneously collect DSRC messages from connected vehicles, as well as high resolution detector and signal status data from traffic signal controller.
- A central server was designed to process and visualize data from different intersections (data hubs) as well as generate optimal adaptive signal timing plans regarding energy efficiency.
- A framework for joint control of traffic signals and vehicle trajectories and considers both efficiency and energy impact was designed.

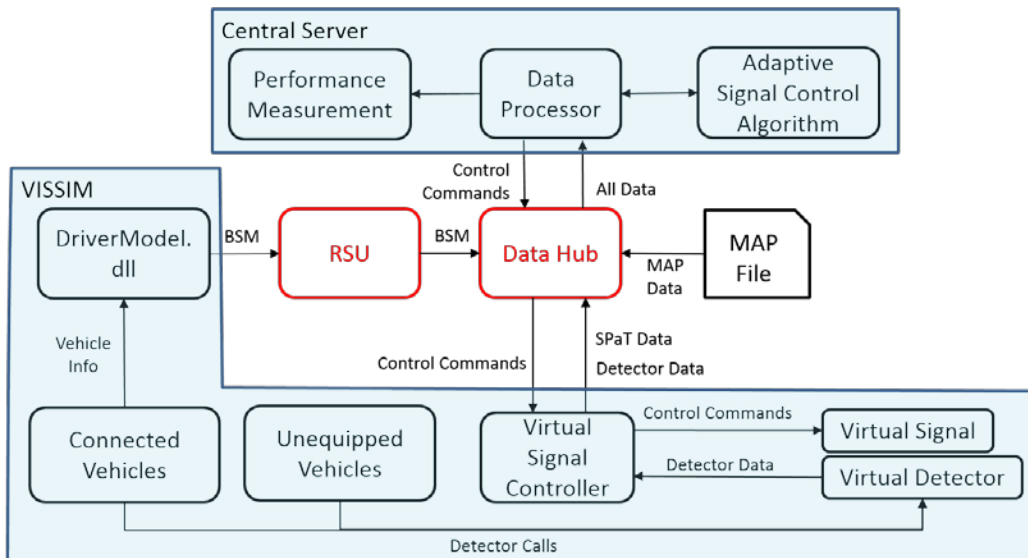


Figure II-23: HIL simulation platform for adaptive traffic signal control development

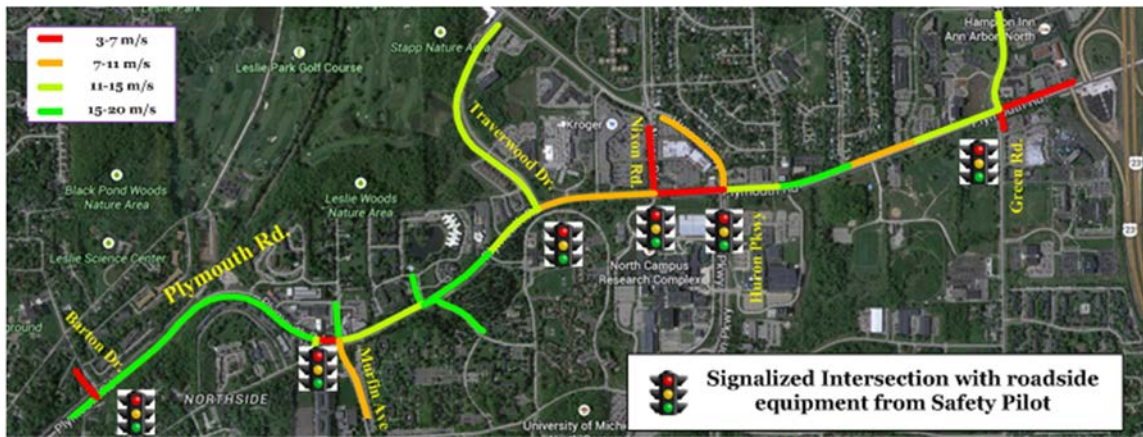


Figure II-24: Selected 6-intersection corridor for future adaptive traffic signal control study

Conclusions

This project is one of the first research projects sponsored by the Department of Energy focusing on the study of energy impacts of connected and automated vehicles (CAV). The three partnering units (University of Michigan, Argonne National Laboratory, and Idaho National Laboratory) work closely on five tasks. Two Ph.D. students spent about 2 months each at the Argonne National Laboratory to work on modification of the POLARIS software to enable simulation of CAVs, with special focus on their energy consumptions.

Significant progress has been made during the first year of this project. Some data loggers have been installed on volunteers' vehicles, the user interface has been designed and prototyped by an industrial partner, the human driver behaviors are being developed using the Safety Pilot Model Deployment data, a POLARIS model for the Ann Arbor region has been developed, and a simulation model was developed and some equipment has been deployed in the Plymouth Road corridor. The team has laid a strong foundation for the future work of this project.

This team is very proud to have been selected for this highly visible project and will look forward to the next two years when we expect to produce even more results!

II.4.C. Products

Presentations/Publications/Patents

1. Feng, Y., Yu, C., and Liu, H., Spatiotemporal Intersection Control in a Connected and Automated Vehicle Environment, Submitted to 2017 TRB Annual Meeting for Presentation and Transportation Research Part B for publication.
2. Zheng, J. and Liu, H., Estimating Traffic Volumes at Signal Intersections Using Connected Vehicle Data, Submitted to 2017 TRB Annual Meeting for Presentation and Transportation Research Part C for publication.
3. Di, X., Zhao, Y., Zhang, Z., and Liu, H., Data-Driven Similarity Analysis for Activity-based Travel Demand Modeling, Submitted to 2017 TRB Annual Meeting for Presentation.
4. Huang, X. and Peng, H., Eco-Driving at Signalized Intersections Using Sequential Convex Optimization, submitted to the 2017 American Control Conference.

II.5. Methods to Measure, Predict and Relate Friction, Wear and Fuel Economy

Steve P. Gravante, Principal Investigator

Ricardo, Inc.
40000 Ricardo Drive
VanBuren Township, MI 48111
Phone: (630) 468-8712; Fax: (630) 789-0127
E-mail: Steve.Gravante@ricardo.com

Nick D'Amico, DOE Program Manager

U.S. Department of Energy/NETL
P.O. Box 10940
626 Cochrans Mill Road
Pittsburgh, PA 15236-0940
Phone: (412) 386-7301; Fax: (412) 386-5835
E-mail: Nicholas.Damico@netl.doe.gov

Start Date: December 15, 2014

End Date: December 15, 2017

II.5.A. Abstract

Objectives

To develop characterizations of friction and wear mechanisms in internal combustion engines and methods to predict the impact of such mechanisms on engine fuel consumption or vehicle fuel economy respectively. The methods of prediction will be both empirically and analytically based.

- Fundamental tribological parameters will be measured using lab-scale tests.
- Changes in engine friction will be calculated using CAE methods based on input provided from the lab-scale tests.
- Empirical correlations will be established that allows for estimating changes in brake specific fuel consumption (BSFC) based on engine power and speed and changes in friction power computed from the CAE methods.
- Empirical models will be integrated to derive vehicle fuel economy benefits.
- In a similar way, component wear will be analyzed and predicted.

Accomplishments

- Successful presentation at the Annual Merit Review (AMR).
- Successful determination of the oil+FM to be used in engine testing.
- Completed benchtop measurements of the baseline Isuzu components at Argonne National Lab (ANL) and Electromechanical Associates (EMA).
- Completed creation and validation of the RINGPAK model of ANL benchtop tests.
- Completed benchtop measurements of the ZYNP components at ANL.
- Completed benchtop measurements of the coated Isuzu components at ANL.
- Created preliminary RINGPAK and PISDYN models of the Isuzu engine.

Future Achievements

- Complete thermal survey of the Isuzu engine.
- Complete setup of RINGPAK and PISDYN models for the motored and fired engine configurations.
- Complete CFD/FEA simulation of the engine block and piston for calculation of distortion.
- Start friction testing.
- Start long term wear testing.

II.5.B. Technical Discussion

Background

A Funding Opportunity Announcement (FOA) was issued on January 24th, 2014 (DE-FOE-0000991). This FOA is supported by the Vehicle Technologies Office (VTO) in the Department of Energy (DOE) with the following objectives:

- Reduce the usage of highway petroleum by 1.4 million barrels per day by 2020.
- Develop cost-effective technologies to improve vehicle fuel efficiency and achieve or exceed corporate average fuel economy (CAFE) standards of 144 gCO₂/mile (61.6 miles per gallon) for cars and 203 gCO₂/mile (43.7 miles per gallon) for light trucks by 2025.

Fourteen (14) Areas of Interest (AOI) that focus on advanced light-weighting, advanced battery development, power electronics, advanced heating, ventilation, air conditions systems and fuels and lubricants make up the scope of the FOA. Ricardo along with Argonne National Lab requested funding under AOI 11B.

Introduction

AOI 11 is concerned with powertrain friction and wear reduction. According to the FOA, parasitic losses within vehicle powertrains (engine and transmission) account for approximately two million barrels of oil consumption per day in the US.

Under topic 11 there are two subtopics: 11A and 11B. Subtopic 11A is concerned with the development and demonstration of friction and wear reduction technologies for light-, medium- and heavy-duty vehicles.

Subtopic 11B, for which this grant has been issued, is concerned with the identification and quantification of friction losses along with methods to measure and predict fuel economy gains in full engines and/or vehicles.

- Ricardo's objective is to develop empirical characterizations of friction and wear mechanisms in internal combustion engines and methods to predict the impact of such mechanisms of engine fuel consumption and/or vehicle fuel economy. This work will include advanced analytical methods as well.
- The value of such predictive schemes is that if one knows how a particular friction reduction technology changes oil viscosity and/or friction coefficient then the fuel consumption or economy impacts can be estimated without the excessive cost of motored or fired engine tests realizing that it is more cost effective to measure oil properties and friction coefficients in a lab-scale test.

Approach

Ricardo's technical approach begins with acquiring a detailed and high fidelity dataset of the friction and wear characteristics of typical power cylinder components, e.g., piston ring, liner and piston skirt. The friction and wear characteristics will be measured for different ring-on-liner and piston-skirt-on-liner configurations in combination with typical friction and/or wear reduction technologies such as a low viscosity oil, friction modifying oil additives and coatings.

The dataset will be obtained by using the same components and friction/wear reduction technologies through a progression of control tests each with its own pros and cons for quantifying friction and wear. These include lab-scale bench tests using a reciprocating test rig (Adjustable Angle Reciprocating Tester or AART), motored dyno tests and fired engine tests.

The data obtained will be used as follows:

- To provide necessary inputs to CAE simulations of the engine power cylinder for friction and wear prediction.
- To provide data for validation of CAE methods used for the prediction friction and wear.
- To establish wear rate coefficients for the prediction of wear.

Calculated changes in friction and wear will be used to develop scaling factors for estimating drive cycle specific fuel consumption and component wear.

Results

Subtask 1.1.2 – Develop Engine Stribeck Map

This task entails the mapping of the Stribeck parameter as a function of engine speed and load for a typical diesel engine. It will be used to identify the friction regime in which the engine is operating as a function of speed and load to guide the development of an appropriate test matrix for the lab-scale bench tests and engine dyno tests.

Previous reports highlighted efforts to calculate and map the range of Stribeck numbers ($\eta S/L$) that are present in motored, fired, and benchtop tests. Prior assessments assumed a constant oil film temperature as a function of position along the bore. While this is a good assumption for the benchtop tests, the temperature from the top to the bottom of the liner is not constant and the constant temperature assumption over predicts the Stribeck number near TDC. Taking this into consideration, the Stribeck data was reanalyzed to account for the liner temperature as a function of position.

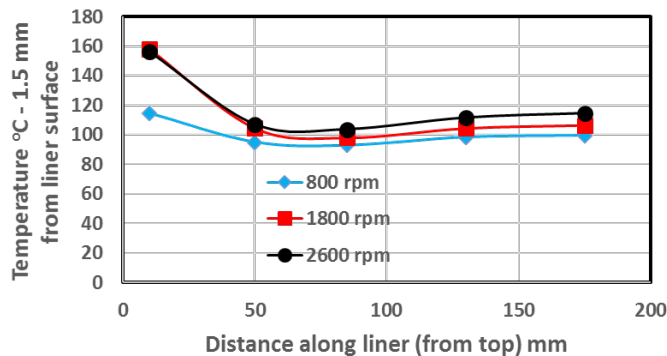


Figure II-25: Axial variation of cylinder temperature at three speeds.

Figure II-25 (above) shows the measured liner temperature (measured 1.5 mm from the inner surface of the cylinder) as a function of distance from the top of the bore. The data at each location are averages obtained from four separate cylinders at different circumferential locations (a total of 7 measurements). The temperature data at 1800 rpm (30 Hz) was used to calculate the Stribeck number as a function of crank angle where the Stribeck number is defined as:

$$Str. \# = \frac{\eta S}{L}$$

Where: η = viscosity (Pa-s)

S = speed (m/s)

L = load (N/m)

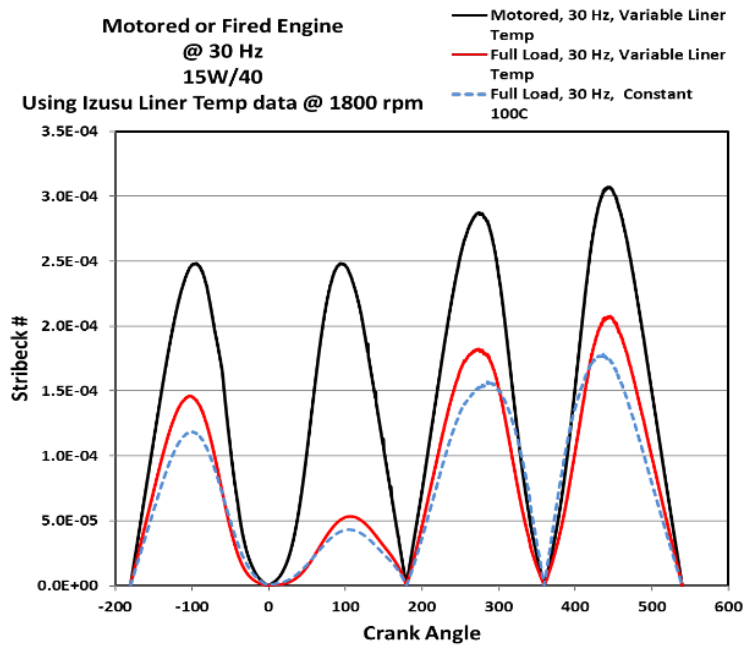


Figure II-26: Stribeck number as a function of crank angle for 15W/40 oil under motored and fired conditions assuming axial temperature profile in Figure II-25.

Figure II-26 shows the results of the calculations of the Stribeck number as a function of crank-angle for a motored and fired (@ full load) engine running @ 1800 rpm (30 Hz). The solid black curve shows calculations under motored (low loads) conditions, while the solid red curve shows calculated Stribeck numbers under full load (high loads). The dashed blue line shows calculations assuming a constant liner temperature of 99.8°C. Note that the peak Stribeck number for the data in Figure II-26 is approximately 3×10^{-4} .

For comparison, Figure II-27 shows Stribeck numbers for benchtop simulations at 20 and 100°C at 5 N/mm and 25 N/mm ring loading. Temperature has a larger impact on the Stribeck number through viscosity changes (236 mPa-s @ 20°C vs. 11.2 mPa-s at 100°C – a factor of 20) than does load (25 to 5 N/mm – a factor of 5). Together the peak Stribeck numbers differ by a factor of 100 just between the different benchtop conditions. Note the peak Stribeck number for the benchtop simulations is approximately 1.5×10^{-5} .

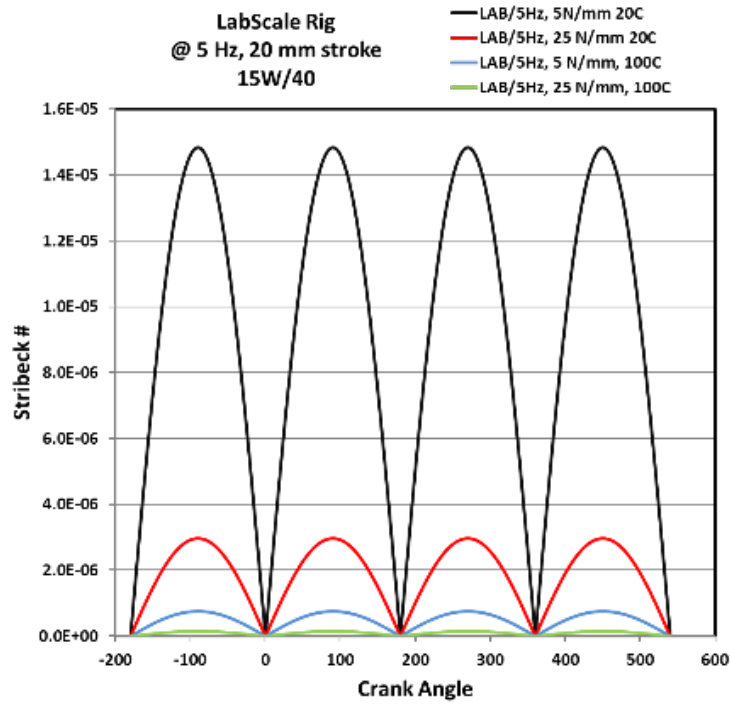


Figure II-27: Stribeck number as a function of crank angle for 15W/40 oil for benchtop conditions.

Figure II-28 summarizes the ranges of Stribeck numbers one can expect to encounter with benchtop and engine rigs for different conditions. The Stribeck numbers range from the low 10^{-9} s for a benchtop test at 100°C at high load to the mid 10^{-3} s for high speed motored engine run at room temperature.

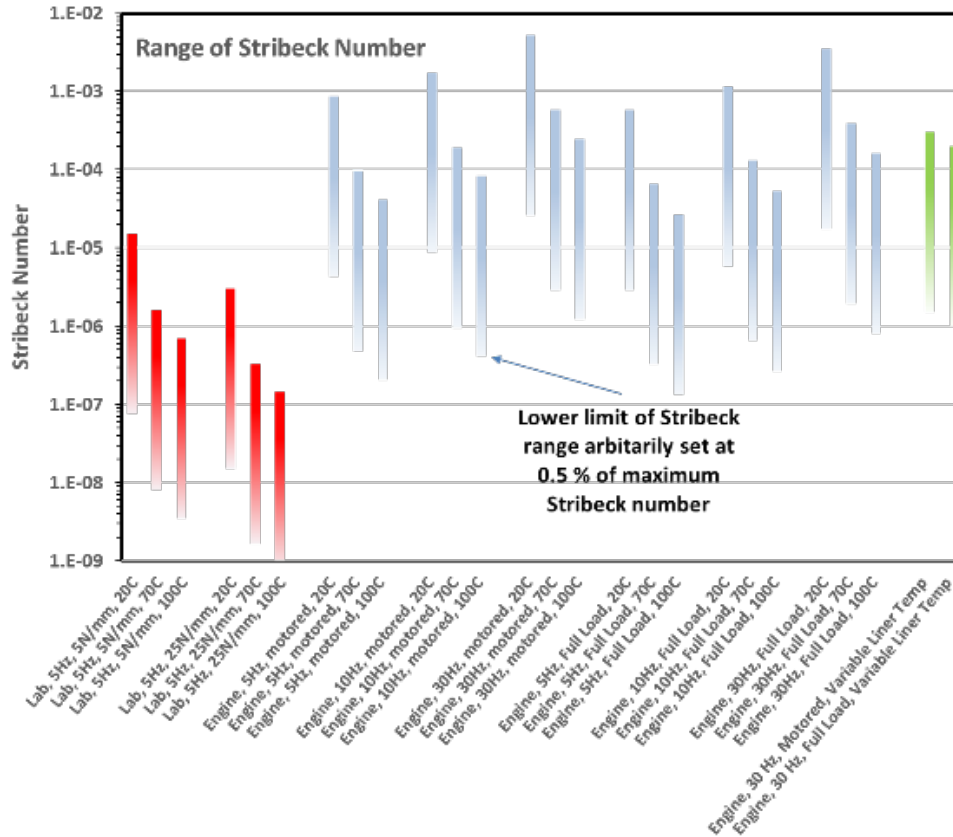


Figure II-28: Range of Stribeck numbers expected for benchtop and engine tests that simulate ring-on-liner conditions.

The results suggest poor overall replication of the Stribeck conditions between the benchtop tests and an actual fired, or, motored engine rig due in large part to the differences in the maximum speeds typically available in benchtop simulations.

However, the low load, room temperature benchtop operation provides the best overlap of conditions (Lab, 5 Hz, 5 N/mm, 20°C with either Motored, 5Hz, 100°C, or, Full Load, 30 Hz, 100°C).

Subtask 1.1.3 – Lab-Scale Component Testing at ANL

A test matrix which identifies the number of hardware combinations and the range of contact loads, relative velocities and oil viscosities to be tested will be developed. The test matrix will be executed using samples cut from actual components, e.g., rings, liners, pistons. This testing will provide the needed data for subsequent tasks as well as facilitate comparison to full component lab-scale test results at EMA (subtask 1.1.4).

One of the primary deliverables of this task is to identify the appropriate friction modifier (FM) to be used in subsequent testing, e.g., full component lab-scale tests, engine tests, etc.

Table II-9 shows all of the oil combinations tested since the beginning of this project. A large number of iterations were necessary to determine the two final candidate oils which will be used in subsequent testing.

Batch 1 consisted of blends of a low- and high viscosity oil with and without a FM. Batch 1 testing showed that the FM treat rate used had minimal impact on friction. It was then decided to re-blend the oils using a PCMO additive package to achieve additional friction reduction which became Batch 2. Batch 2 testing showed a measurable difference between 15W/40 HDDO and 5W/20 PCMO for oil 3. An attempt was made to gain further friction reduction by optimizing the treat rate for oil 3, i.e., oils 3a and 3b in Batch 3. However,

oils 3a and 3b showed very little improvement in friction reduction. At this point it was realized that a blending error had occurred in Batches 2 and 3 that necessitated the re-blend of all of the oils: 1, 2, 3, 3a, 3b, 4, 5, 6, 7, 8.

The re-blending led to Batch 4. Batch 4 testing showed significant differentiation in the friction response between HDDO high-vis (15W/40) No FM oil (baseline) and HDDO (5W/20) High FM oil 7. From this testing, the final two engine oil candidates for subsequent testing was determined, which from now on will be referred to as the HDDO high-vis (15W/40) No FM and 5W20 High FM. This meets the requirements of the first GO/NO GO point.

Table II-9: Description of Oil + FM Evaluated.

Oil	Description	Test Performed	Naming
Batch 1 Oils	2 high vis HDDO oils (15W/40) - one with no FM, one with a high FM treat	Ring-on-Liner and Ball-on-Flat	IM15023-2
	2 low-vis HDDO oils (5W/20) - one with, one without FM	Ring-on-Liner and Ball-on-Flat	
Batch 2 Oils	4 PCMO 5W/20 oils (1-4) with different FMs	Ball-on-Flat	E01031-074
	4 HDDO 5W/20 oils (5-8) with different FM	Ball-on-Flat	
Batch 3 Oils	2 PCMO variants of PCMO oil 3 (3a and 3b) with different FM chemistry and treat rate	Ball-on-Flat	E00365-698
Batch 4 Oils	6 PCMO 5W/20 oils (1, 2, 3, 3a, 3b, 4) - confirmation blends	Ball-on-Flat	E00365-708
	5 HDDO 5W/20 oils (5-8) - confirmation blends	Ball-on-Flat	

Figure II-29 shows a summary table of the boundary friction measurements for both ring-on-liner and skirt-on-liner configurations of the baseline Isuzu engine components. Note that the low viscosity high FM oil reduced the asperity friction by roughly 25% for the ring-on-liner and 48% for skirt-on-liner tests. The values of asperity friction coefficient (μ_{asp}) summarized in the figure will be used as a direct input into the RINGPAK model. In addition to μ_{asp} , crank angle resolved coefficient of friction measurements were also obtained. The crank angle resolved data will be used to facilitate the calibration and validation of the RINGPAK model. See subtask 1.1.6 for an example of the crank angle resolved coefficient of friction and the status of the modeling efforts.

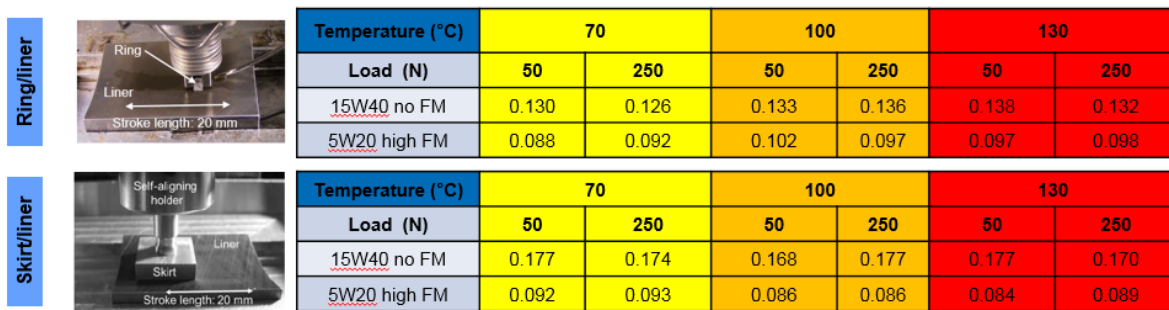


Figure II-29: Summary of boundary friction coefficients for ring-on-liner and skirt-on-liner tests with the baseline Isuzu components.

The remaining deliverables for this task include the following:

- Reciprocating tribometer tests with the coated Isuzu pistons and rings.
- Accelerated wear testing.
- Reciprocating tribometer tests with the ZYNP components.

Reciprocating tribometer tests with the coated Isuzu pistons and rings

Uncoated Isuzu liner test coupons were sent out to C2D to be coated with a DLC coating. When the coated liner coupons were received, segments were extracted and tests were performed to evaluate the friction behavior of the coating against uncoated rings. Unfortunately, only a limited amount of tests was performed using the coated liners because an adhesion issue with the coating was discovered during testing. As shown in the image in Figure II-30, evidence of coating delamination can be seen. The other samples looked similar. The sliding direction in these images is left-to-right. The bright area corresponds to the substrate (cast iron liner).



Figure II-30: A cast-iron liner segment coated with a DLC coating from C2D showing delamination.

Further examination using optical microscopy and profilometry confirmed delamination is shown in Figure II-31. The dark areas correspond to the coating.

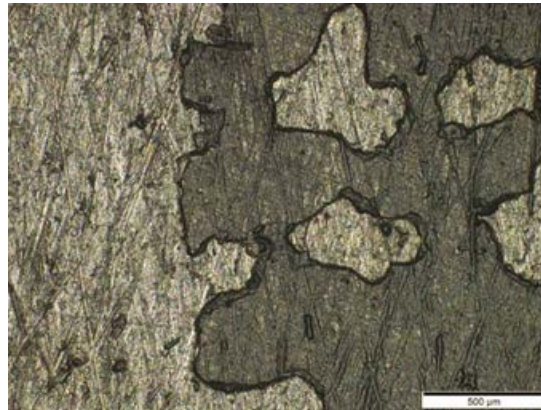


Figure II-31: Micrograph showing coating delamination.

The thickness of the coating which was approximately 10 microns was measured at the same area using optical profilometry (see Figure II-32).

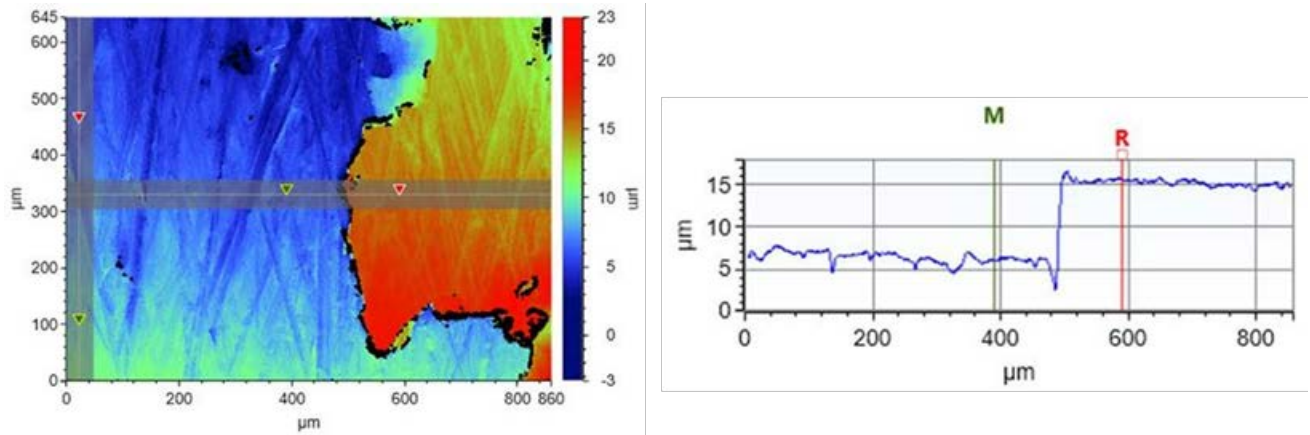


Figure II-32: Profilometric measurement and corresponding line scan across delaminated area.

Rings were also sent to C2D for coating. The rings were examined upon receipt before testing using optical microscopy which showed that the coating did not adhere uniformly. The photo in Figure II-33 shows that the rubbing edge of the top compression ring (i.e., the edge subject to contact in the reciprocating tests) is coated irregularly. The 2nd ring could not be coated at all due to adhesion issues, while the oil control ring (OCR) was coated irregularly.

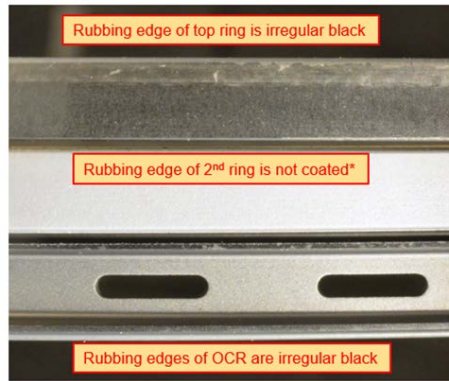


Figure II-33: Photo of the three rings (top ring, 2nd ring, and OCR) after C2D attempted coating with a DLC.

Uncoated pistons were received by Isuzu in two sizes. These were nominal-sized and under-sized; twenty-two (undersized) pistons were sent out to be coated with a MoS₂ coating. Ten pistons were sent to Ricardo for engine testing and 6 were sent to EMA for evaluation. The rest were kept by ANL for tribological testing. One of the coated pistons was sectioned and segments were extracted for testing. Results show a high wear rate for this coating while the friction is comparable to the baseline Isuzu pistons which are coated with Grafal, even though this was supposed to be a low friction coating (see Figure II-34).

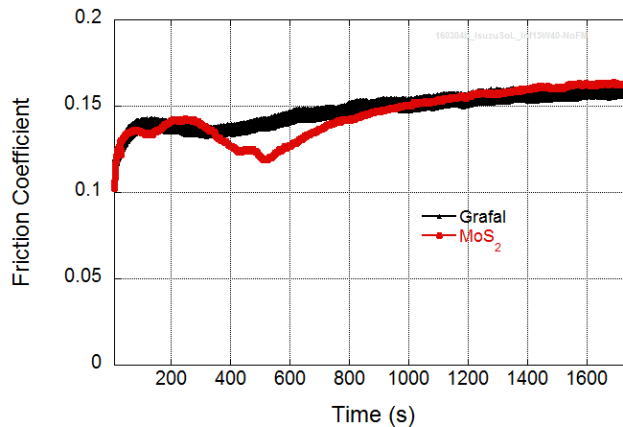


Figure II-34: Comparison of friction coefficient as a function of time for two coated piston skirt segments.

Accelerated wear testing

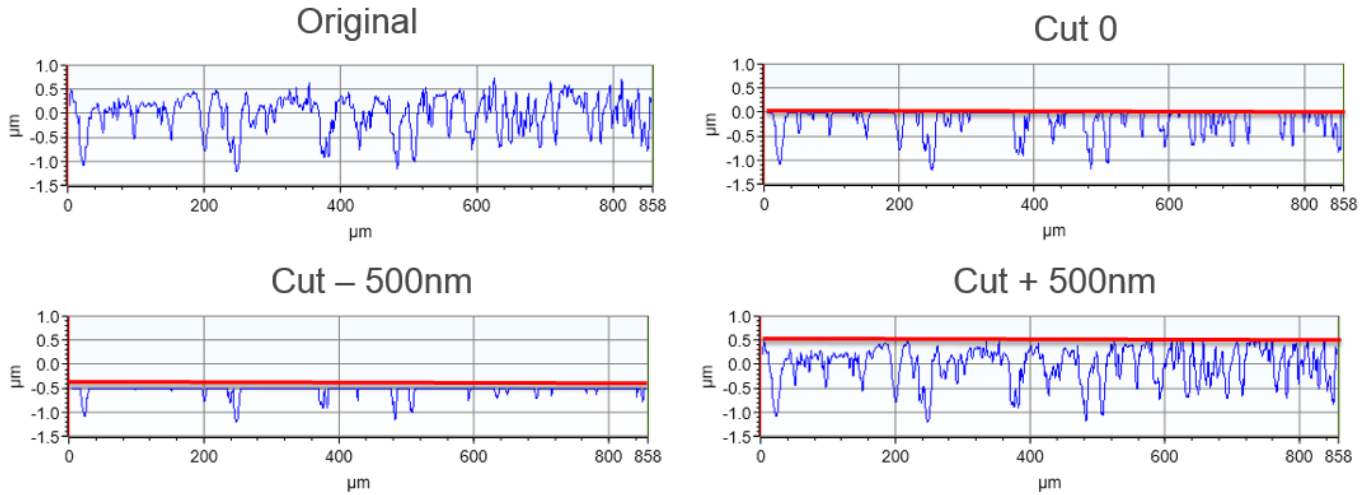


Figure II-35: Profilometric line scans for a liner surface as-is and "cut" at certain heights.

The literature does not provide any information on how to measure liner wear. For this work, a new method to measure liner wear is proposed. To illustrate the method, a liner profile was mathematically processed such that features above a certain height were “cut” from the profile. This process is depicted in Figure II-35.

If the "cut" and "uncut" profiles are subtracted from one another, a volume can be calculated which exactly corresponds to the volume of the material that has been removed. In a similar way, for a real surface that has been worn, the profile before and after testing can be used to determine wear provided that the amount of wear remains low enough that the deepest honing grooves remain largely unaffected.

If a surface profile before testing is not available or cannot be measured, as in the case of a cylinder liner that has been already used in an actual engine, the same method can be applied successfully in a statistical manner based on a region of the liner outside the area of wear. Several profilometric measurements must be performed, and the deepest grooves (>85%) will have to be matched on the basis of the bearing area curve. For the surface profiles shown above, the corresponding bearing area curves (BAC) are shown in Figure II-36 below. Processing of BAC curves the yields the percentage of material removal can be determined. This process needs to be validated on actual components.

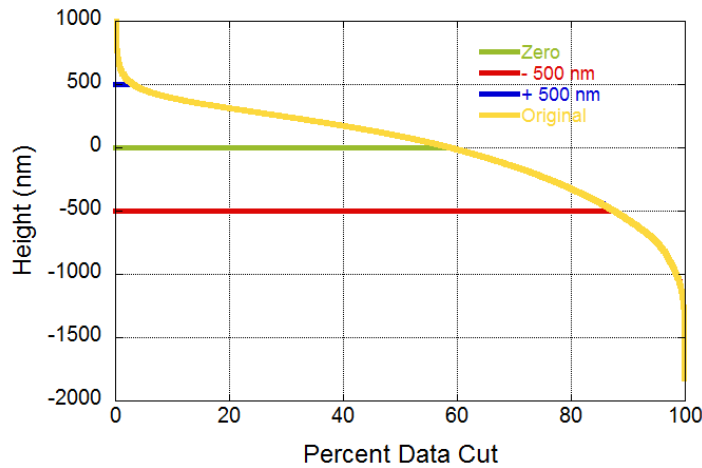


Figure II-36: Bearing area curves for an original liner profile mathematically processed such that features above a certain height are "cut" at zero, -500 nm, and +500 nm.

Reciprocating tribometer tests with the ZYNP components

Liners and rings to be tribologically evaluated were received from ZYNP. There were three liner variants:

- Original/Normal honing.
- Z-fine - honing.
- Z-fine – honing coated with C2D DLC.

The ZYNP provided ceramic chromium coated rings were used for all of the tests. The ring and liners were tested under a wide range of conditions using Infineum’s 5W20 High FM formulation. The friction coefficient was evaluated and the results are summarized in Table II-10 for all conditions.

Table II-10: Summary of friction coefficient for 3 variants provided by ZNP.

Temperature (°C)	70		100		130	
Load	50	250	50	250	50	250
Original	0.10	0.10	0.11	0.11	0.12	0.11
Z-fine	0.10	0.10	0.10	0.10	0.12	0.11
C2D	0.11 No SS	0.12 No SS	0.12 No SS	0.12 No SS	0.11 No SS	0.12 No SS

The friction data was plotted as a function of time for 1 hr long tests at 70°C, 100°C and 130°C, as well as 50 N and 250 N for the 5W20 High FM oil. The friction traces are shown in Figure II-37.

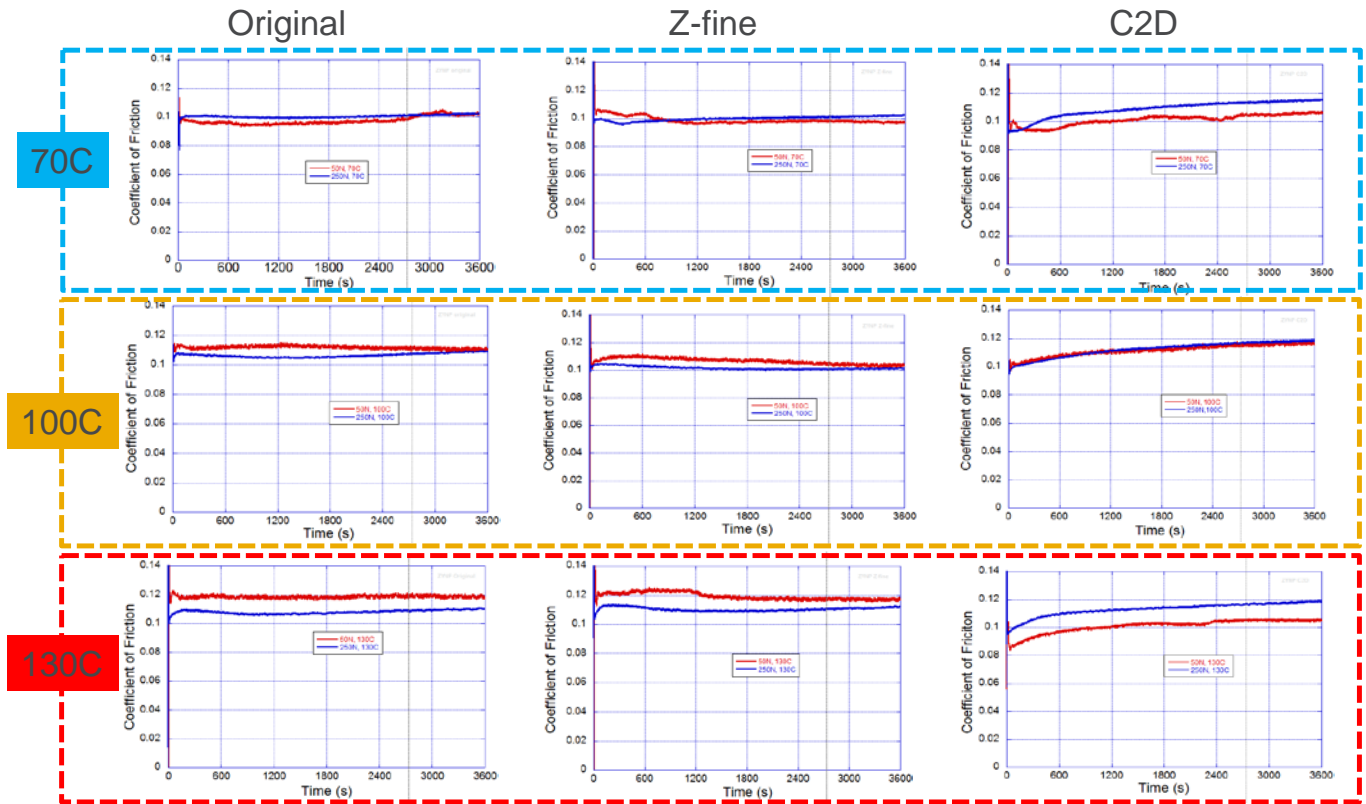


Figure II-37: Friction traces over a range of conditions for the 3 variants provided by ZYNP.

Examining the results of Figure II-37 it can be seen that temperature has a noticeable effect. More specifically, as temperature increases, so does the friction coefficient. That is the case for all three variants. On the other hand, the load has a less pronounced effect on friction coefficient, especially at 70°C and 100°C. Furthermore, there is no significant difference between the baseline/original honed surface and the fine-honed surface for all data points in the matrix. However, differences between baseline and Z-fine-honed surfaces will be prominent in the mixed and hydrodynamic regimes. This can be demonstrated by maintaining a high viscosity, high speed, and low load using a benchtop tribometer. Using a 15W40 at room temperature (to maintain a high viscosity), friction waveforms were acquired at 120 rpm and 50 N. This condition has been plotted in Figure II-38. The graph shows that the Z-fine honing enables faster transition from boundary to mixed or hydrodynamic.

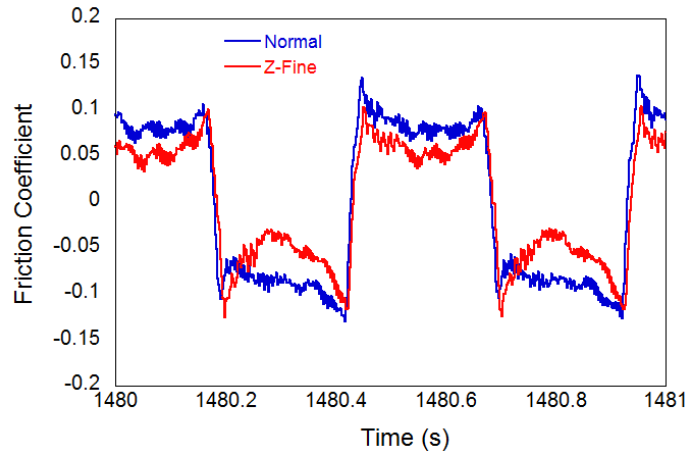


Figure II-38: Friction waveforms for 2 variants.

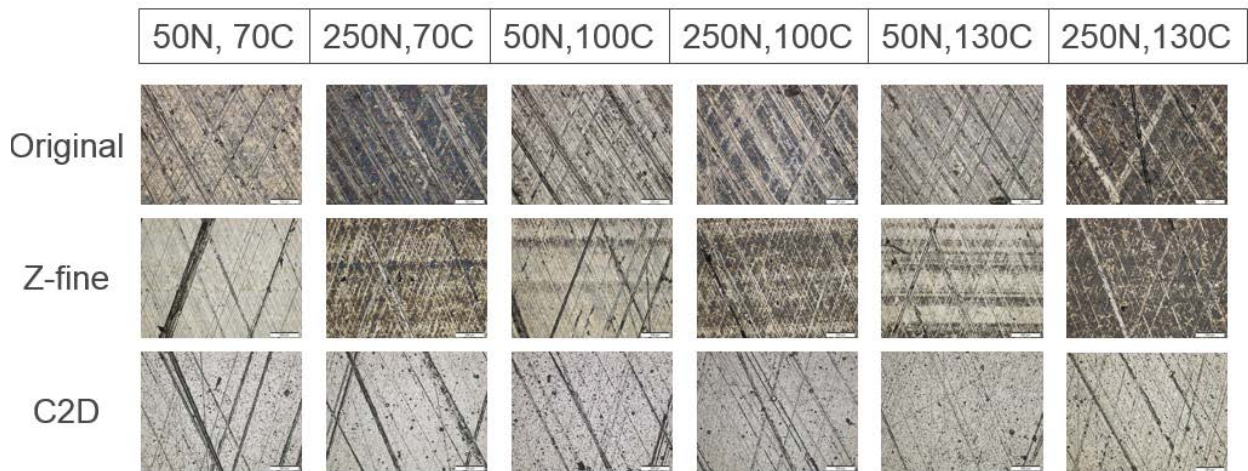


Figure II-39: Optical micrographs of all ZYNP liners post-test.

Furthermore, it can be seen in Figure II-37 that the friction coefficient value of the C2D coating never reached a steady-state. The inertness of the surface coating may not allow for tribochemical film formation (on the liner) which might limit wear performance. This is evident in Figure II-39. However, it is interesting to note that the coating survived against delamination in contrast to the first application on the Isuzu liner.

Examination of the ZYNP ring revealed that the rings look intact after testing against the original liner. However, in the case when the ring was rubbed against the C2D DLC coated liner, features along the sliding direction were evident indicating that the coating might have an abrasive nature, though, quantification is very difficult and observation at the moment can only be qualitative in nature. Please see Figure II-40.

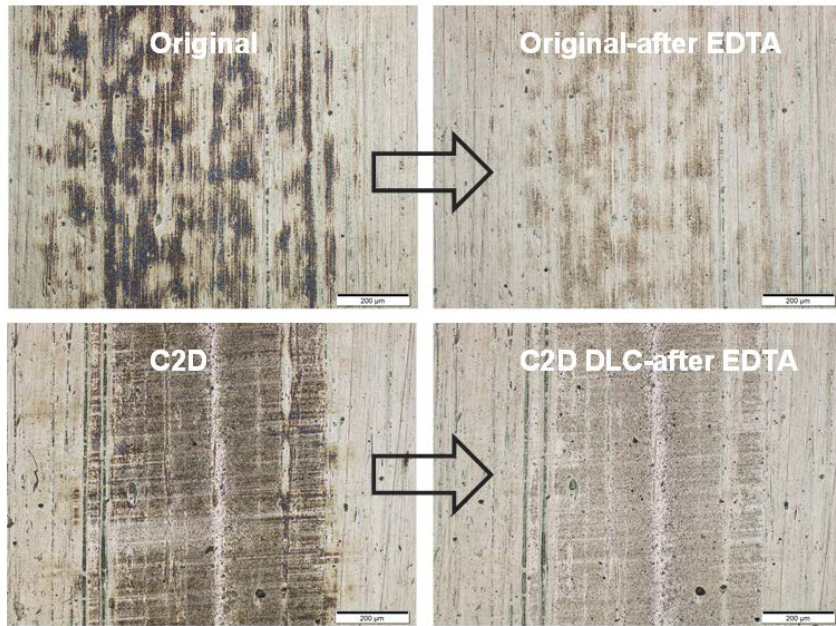


Figure II-40: Examination of ZYNP ring post-test and after application of EDTA on the same location for the original (uncoated) liner and the C2D coated liner.

Subtask 1.1.4 – Full-Scale Component Testing at EMA

This task entails friction testing of Isuzu and ZYNP components using full-scale components instead of test coupons like the lab-scale testing at ANL. The data will be compared to friction coefficients obtained at ANL to understand any limitations or differences due to the measurement method.

Full scale testing of the baseline Isuzu ring, cylinder bore and piston skirt has been completed but with minor exceptions which will be described shortly. The ring-on-liner data for the baseline Isuzu components is summarized in Figure II-41 as function of Stribeck #. Please note the Stribeck # has been multiplied by 10^8 for convenience in plotting. The data was obtained for the two oils of interest (the high viscosity 10W40 and the low viscosity 5W20 with friction modifier (FM)), at two loads (15 and 100 N) and three speeds (100, 500 and 600 rpm).

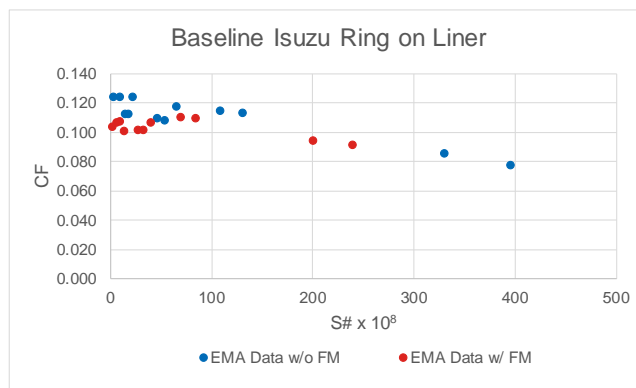


Figure II-41: Summary of EMA measured friction coefficient for Isuzu baseline ring-on-liner test.

By design, EMA’s data covers a larger range of Stribeck # which should include both boundary and mixed friction regimes. As Stribeck # increases a reduction of the coefficient of friction (CF) is seen indicating that the friction regime has moved into the mixed regime.

Table II-11: Comparison of EMA to ANL ring-on-liner measurements.

	EMA	ANL	% Diff
15W40	0.12	0.13	8%
5W20	0.11	0.1	9%

Conversely, ANL’s data covers a much smaller range of Stribeck # to mainly capture the boundary friction regime. Extrapolating CF to a Stribeck # of zero by using only the EMA and ANL data at a Stribeck # $\times 10^8 \leq 20$ shows that EMA’s measurements are within about 10% of Argonne’s (see Table II-11 above).

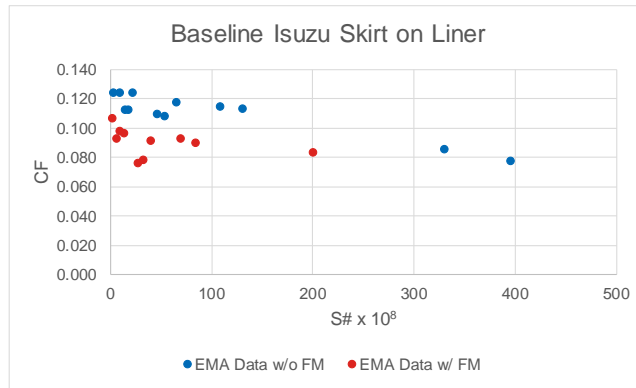


Figure II-42: Summary of EMA measured friction coefficient for Isuzu baseline piston skirt-on-liner test.

Figure II-42 summarizes EMA full scale data from their skirt-on-liner tests plotted against Stribeck #. Behavior similar to the ring-on-liner tests is observed. Making a similar comparison to Argonne’s measurements by extrapolating CF to a Stribeck # of zero by using only the EMA and ANL data at a Stribeck # $\times 10^8 \leq 20$ yields the following:

Table II-12: Comparison of EMA to ANL skirt-on-liner measurements.

	EMA	ANL	% Diff
15W40	0.12	0.17	42%
5W20	0.1	0.09	10%

Table II-12 indicates close agreement between EMA’s measurement and ANL’s for the low viscosity oil with FM. However, for the high viscosity oil there is a large discrepancy. This can be attributed to the transitory behavior of the coefficient of friction observed by ANL and reported in the Q1 BY2 progress report. The figure illustrating this behavior has been reproduced here (see Figure II-43). The duration of EMA’s tests are 1200 minutes and steady-state values are reported from the end of the test. This implies that they are reporting a CF value from a different part of the curve than does ANL. In other words, steady-state is defined differently by EMA and ANL.

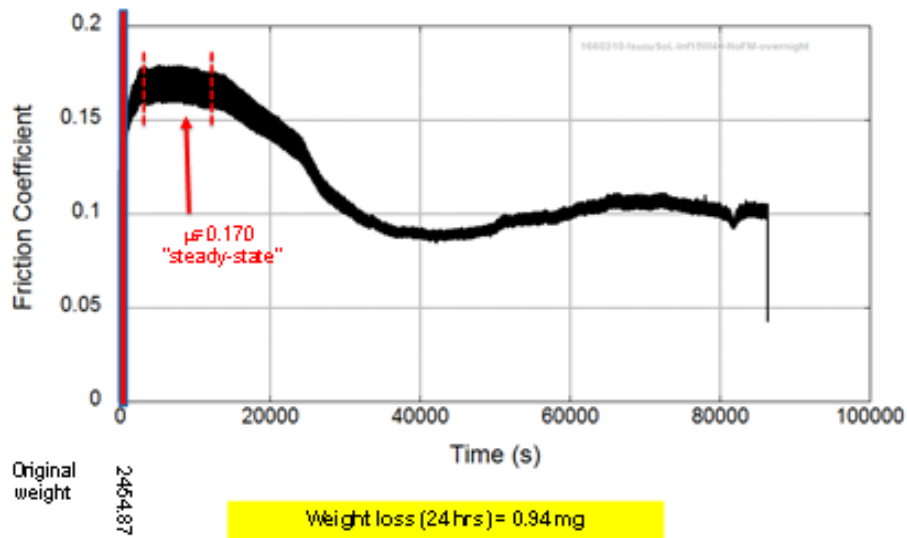


Figure II-43: Illustration of unstable coefficient of friction measured during skirt-on-liner tests at ANL.

Please note the ANL doesn't see as much variation in the coefficient of friction for the skirt-on-liner tests when using the low viscosity oil. Steady state is reached within the first 15 minutes of testing. This explains why EMA's value correlates better to the ANL measurement for the low viscosity oil than it does for the high viscosity oil.

EMA is reviewing whether or not they can extract steady state values from an earlier point in time in the skirt-on-liner test with the high viscosity oil.

Subtask 1.1.6 – Development and Validation of RINGPAK Modeling Best Practice of a Lab-Scale Test

The purpose of this task is to develop a RINGPAK simulation best practice capable of achieving a high degree of correlation between simulation predictions and lab-scale measurements. The appropriate inputs, model parameters, assumptions, physics, boundary conditions, solver settings, etc. will be defined so that a high fidelity simulation is achieved.

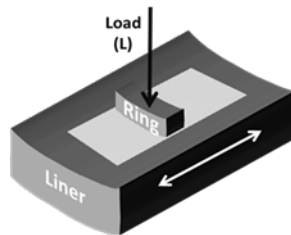


Figure II-44: Illustration of the AART benchtop rig.

The configuration of the AART benchtop test is illustrated in Figure II-44. It consists of segments of the top compression ring (from the Isuzu engine) that is "rubbed" back and forth against a segment of the cylinder bore. Tests have been performed at a range of loads (50, 250, and 500 N), at different temperatures (70, 100, and 130°C, and a few at nominal room temperature), and at speeds ranging from 1 Hz up to 5 Hz (20 mm stroke).

One series in particular (test # 150707) consisted of:

- A 1 hour run @ 250 N, 100°C, 2 Hz, 15W/40 NO FM oil to break-in the surface and establish a tribofilm on the surface (test # 150707a).

- An 8-10 minute run at nominal room temperature at different loads (25, 50, 100, 250 N) at speeds ranging from 10 rpm to 300 rpm (test # 150707b).
- A second (repeat) 8-10 minute run at nominal room temperature at different loads (25, 50, 100, 250 N) at speeds ranging from 10 rpm to 300 rpm (test # 150707c).

The runs at 100°C exhibited nearly ‘square-wave’ behavior indicating that at 100°C, the friction is predominantly boundary friction – little or no mixed or hydrodynamic friction (see Figure II-45).

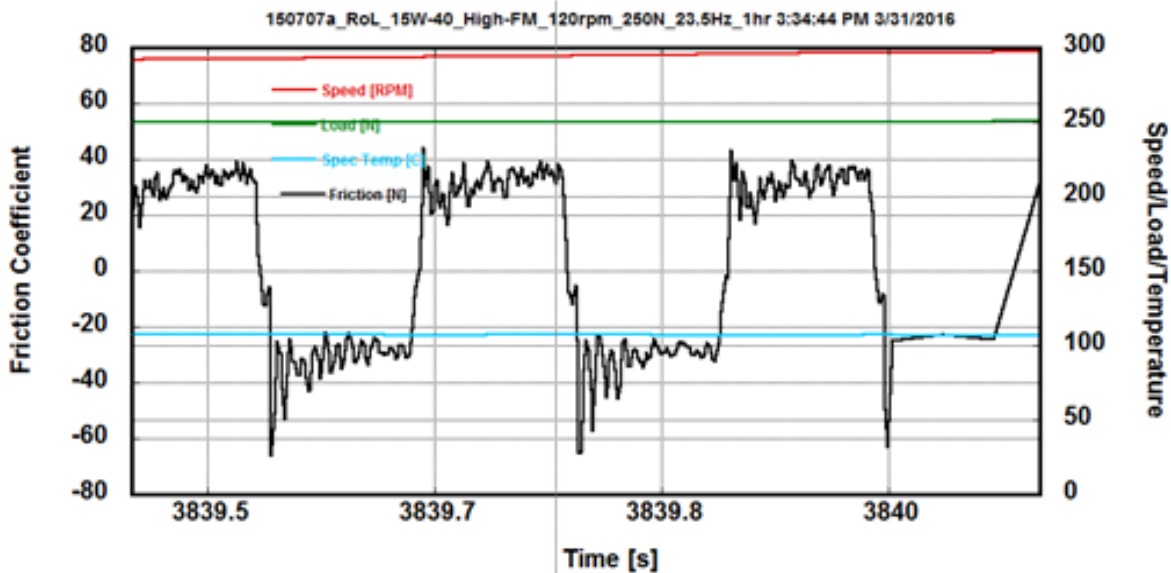


Figure II-45: Friction as a function of time for a segment of time during test # 150707a (100°C).

At room temperature however, the friction trace was ‘scalloped’ (see Figure II-46), indicating that friction was a mixture of boundary and mixed – boundary at the end/reversal points where the speeds were low, and mixed at the mid-stroke where the speed and viscosity were such that partial film formation was occurring.

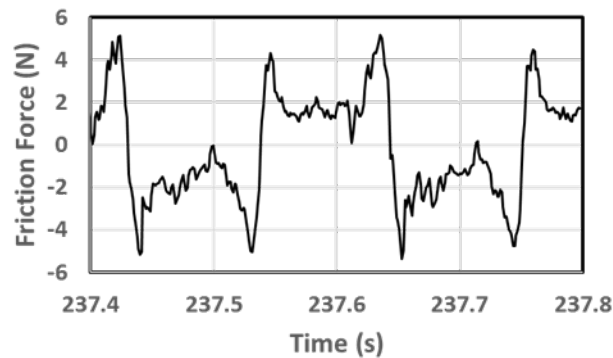


Figure II-46: Friction as a function of time during a nominal room temperature run at 5 Hz (test # 150707c).

A model of the AART benchtop configuration was created in Ricardo's RINGPAK software. The model configuration is shown in Figure II-47 – it consists of a piston inside of a cylinder bore with a single piston ring. The AART RINGPAK model uses an exceptionally long connecting rod (10 m) coupled with a short crank offset to simulate the short stroke of the ARRT rig. The normal force between the ring and the cylinder bore is mimicked by controlling the ring tension. A number of AART RINGPAK simulation runs were performed to understand the sensitivity of the frictional behavior of the configuration shown in Figure II-47 (nominal room temperature, 5 Hz, 50 N). The 50 N normal loading (spread over an assumed track of 10 mm) corresponds to a ring tension of approximately 600 N.

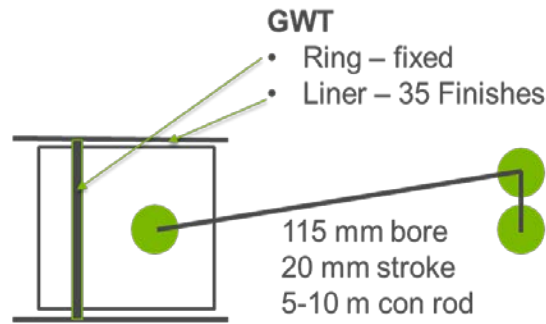


Figure II-47: RINGPAK model setup to replicate AART benchtop tests.

The variables that were considered in the simulation study included the following:

- Temperature: 20, 25, 30, 35, 40, 70 and 100°C; the runs at 25, 30, and 35°C were included to mimic the effect of frictional heating at a nominal room temperature run.
- Oil: currently set at 15W/40 oil; will include 5W/20 oil later.
- Speed: 150 and 300 rpm (2.5 and 5 Hz).
- Load (Fd): 300, 600, 900, 1200, and 1500 N (2.5 to 12 N/mm).
- Inlet oil film thickness (partial film lubrication): 0.2, 1, 5, 10, and 20 μm .
- Material Dependent Parameters:
 - Asperity friction coefficient: 0.1, 0.13, and 0.15.
 - Surface finish/texture: 35 surface finishes (GWT parameters).
 - Honing parameters – honing angle.

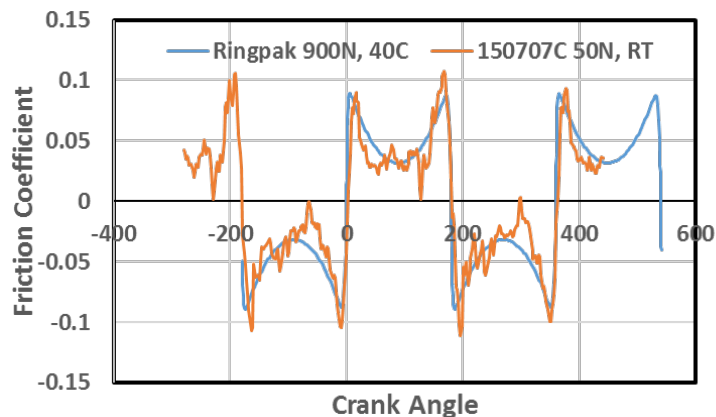


Figure II-48: AART RINGPAK predicted and measured friction behavior for 150707C.

After considerable analysis, a set of parameters were established that when used with the AART RINGPAK model would accurately predict the friction forces and traces. The data in Figure II-48 shows a comparison of the experimental friction coefficient with the predicted frictional trace assuming the following conditions: 40°C oil film temperature, 0.1 asperity friction, GWT parameters consistent with an as-received liner (MATUTIL), and inlet oil film thickness of 10 μm .

Conclusions drawn from the model-experiment simulation study indicate:

- The results are sensitive to the inlet oil film thickness, especially for values below 1 μm . Values below 1 μm result in significant asperity friction and are unrealistic to the flooded condition used in the experiment. Above 1 μm , the results are not sensitive to this parameter.

- Ring tension has a significant effect and caution must be taken to use the correct value. Initial analysis assumed the 50 N load was distributed over a contact length of 10 mm. In reality, the contact width is dependent on a number of factors including load and radius of curvatures of the ring and bore coupons. More detailed analysis suggests that a contact width of 6-8 mm corresponding to a unit loading of 7 N/mm (900 N Fd) is more appropriate.
- Temperature plays an important role. In particular, the role of frictional heating and surface heating needs to be considered. While frictional power at the interface may be low (less than 1 watt), a simple estimate using simple conductive heat flow ($-kAdT/dx = q$) suggests an oil film temperature of 40°C is reasonable.
- The surface finish plays a significant role in the simulation. The agreement with the experiment in Figure II-48 was achieved using GWT parameters (as derived with the MATUTIL package) for an as-received/unworn surface. When GWT parameters for the worn surface were used, the friction trace was dominated by hydrodynamic lubrication – the asperity-to-asperity friction was significantly reduced. ANL are currently investigating the procedures used by MATUTIL used to calculate the GWT parameters to determine how they compare with other methods to calculate GWT parameters.

At this point, this task has been completed, an AART RINGPAK model has been developed and validated by comparing predicted frictional behavior with observed experimental results. ANL is currently ‘mining’ the AART RINGPAK data to determine if data/trends on asperity/hydrodynamic loads can be extracted that can be used to develop wear relationships that can eventually be used to predict liner/ring wear in a fired engine.

Subtask 2.1.3 – Motored Engine RINGPAK and PISDYN Modeling

This task entails the creation of detailed 3D RINGPAK and PISDYN models of the motored engine setup as well as correlation to motored engine tests. The task may also include modifying the simulation best practice in order to improve model accuracy.

A baseline RINGPAK and PISDYN model of the ISUZU 4H engine has been created based on the information available from Isuzu: general engine data such as bore and stroke, dimensional input data for piston, liner, connecting rod, and rings, mechanical and thermal properties for piston, liner, and rings, and surface properties for piston groove, liner, and rings provided by ANL.

To simulate the motored engine configuration, the following information is still needed:

- Assembly deformation of cylinder bore
- Block and piston temperature

To simulate the fired engine configuration, the following information is still needed:

- Cylinder pressure
- In-cylinder gas temperature
- Block and piston temperature
- Thermal deformation of cylinder
- Thermal deformation of piston

The deformation of the cylinder bore under assembly loads will be obtained from a FEA (subtask 3.1.3). The block/piston temperature will be obtained during motored friction testing (subtask 2.1.2). The cylinder pressure will be obtained during dyno testing measurements (subtask 3.1.2). The in-cylinder gas temperature will be estimated as part subtask 3.1.3 as well. The thermal deformation of the cylinder and piston will be obtained when the thermal-structural FEA work is completed (subtask 3.1.3).

To test the model setup, assumptions were made for the "missing" data for fired engine configuration. The results from this test run are shown below in Figure II-49 and are an illustration of typical results that will be obtained from RINGPAK. The top graph shows a breakdown of frictional losses by mechanism. The bottom graph shows a breakdown of losses by individual rings. The figure also indicates that the model is working properly.

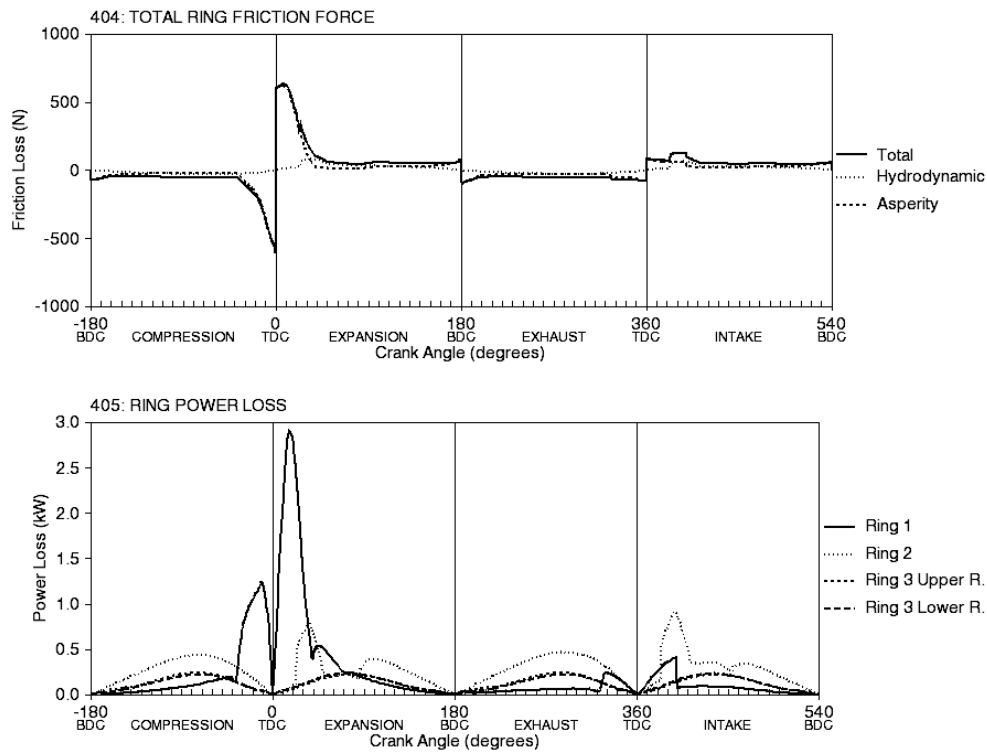


Figure II-49: Illustration of full engine RINGPAK model results under fired conditions: 2500 rpm and 141 bar cylinder pressure.

Creation of the PISDYN model of the Isuzu 4H hasn't completed due to lack of information. Specifically, to complete the PISDYN model, following data are required: clearance data between the wrist pin and wrist-pin bushing and pin, piston and conrod masses.

However, to test the model's functionality, assumptions were made for the clearance and component masses and the model was simulated using the same boundary conditions assumed for the RINGPAK model. The results from this test run are shown below in Figure II-50 and are an illustration of typical results that will be obtained from the PISDYN. The top picture shows a spatial distribution of contact loads indicating where on the skirt where there are significant friction losses. The bottom graph is a chart of friction power loss through the skirt as a function of crank angle. The figure also indicates that the model is working properly.

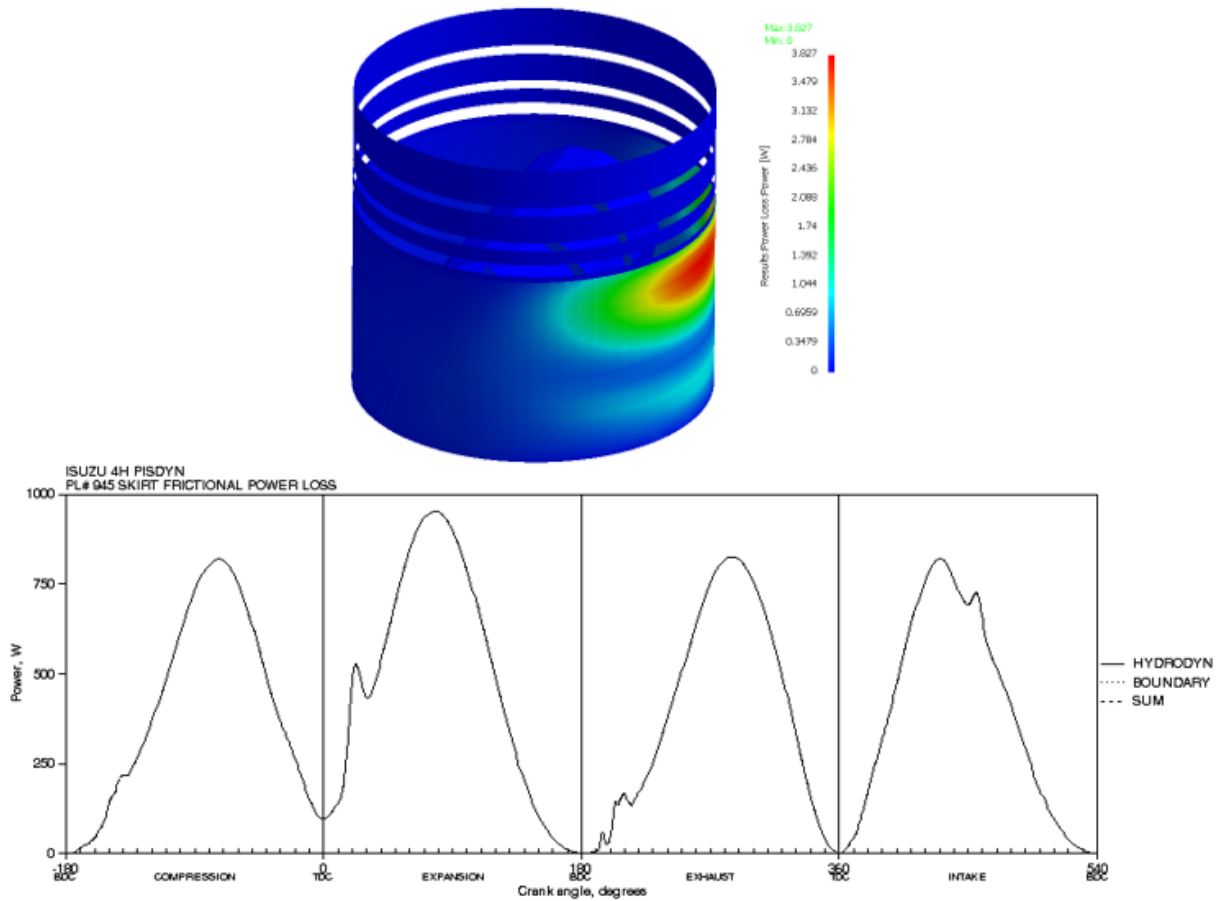


Figure II-50: Illustration of full engine PISDYN model results under fired conditions: 2500 rpm and 141 bar cylinder pressure.

Subtask 3.1.1 – Thermal Survey of Fired Engine

This task will provide a map of the engine bore and piston temperature profile which will be used for the subsequent calibration and validation of a thermal FEA simulation (subtask 3.1.3).

The engine block and piston have been machined and thermocouples (TCs) and templugs have been installed. Figure II-51 shows how the engine block has been instrumented with TCs and how the piston has been instrumented with templugs.

The engine has been rebuilt and block temperature measurements have been made at various engine speed and load conditions. Piston templug measurements are currently in progress.



Figure II-51: Instrumented block with thermocouples (top) and piston with templugs (bottom).

Cylinder block temperatures were recorded along the full load curve of the engine, at engine idle, and at the peak torque and full load speed for various fueling conditions. Measurements at these operating points were repeated for different coolant temperatures: 75, 85 and 95°C. A sample of the measurements made in the interbore region between cylinders 1 and 2 at the full load engine speed and various coolant temperatures and fueling conditions is shown for illustration purposes in Figure II-52.

This data will be used to develop empirical correlations that will allow for the interpolation of block temperatures at conditions not actually measured during the thermal survey testing. This data, whether measured or interpolated, will be used to adjust FEA boundary conditions in order to achieve a high fidelity prediction of bore temperature and distortion.

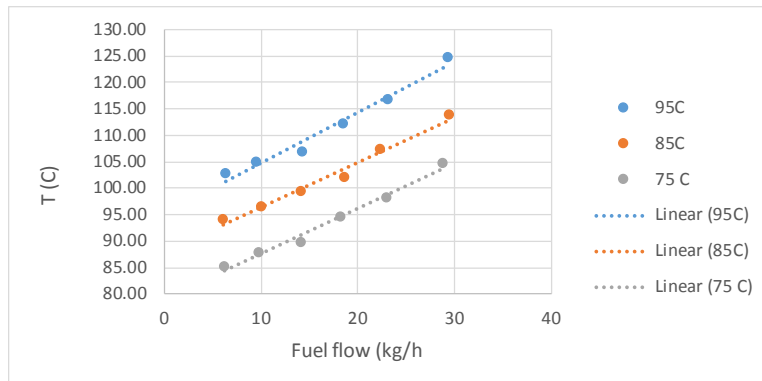


Figure II-52: Block interbore temperatures at the full load speed at various fueling and coolant temperature conditions.

Conclusions

Adequate progress continues to be made in achieving the goals set forth for this project but delays in receiving information from OEM partners still plagues the project. In addition, the poor quality of the coated Isuzu rings and the underperforming friction coating on the Isuzu piston skirt has resulted in a significant setback for the project. The project team is currently evaluating alternatives and next steps as it is still hoped to validate the method for predicting friction and wear can be validated against changes in both oil viscosity and surface characteristics.

II.5.C. Products

Presentations/Publications/Patents

1. NA

II.5.D. References

1. NA

THERMAL LOAD REDUCTION

II.6. Advanced Climate Control and Vehicle Preconditioning [DE-EE0006445]

John Meyer, Principal Investigator

Hanon Systems
 One Village Center Drive
 Van Buren Twp., MI 48111
 Phone: (734) 710-5420
 E-mail: jmeyer8@hanonsystems.com

David Anderson, DOE Program Manager

Phone: (202) 287-5688
 E-mail: David.Anderson@ee.doe.gov

Start Date: October 2013

End Date: January 2017

II.6.A. Abstract

Objectives

- Increase the range of light duty electric drive vehicles through climate system load-reducing technologies
- Maintain occupant comfort
- Validate energy efficient technologies through the use of computer aided engineering (CAE) models
- Develop a commercial pathway toward utilizing the load-reducing technologies in light duty electric vehicles
- Integrate and validate technologies in a vehicle.

Accomplishments (FY 2016)

- Evaluation of phase-change material to aid heating and cooling
- Comfort model evaluation
- Evaluation of water cooled condenser
- Wind tunnel test fully-modified vehicle to assess range-extending technologies
- Developed refrigerant charge management procedure
- Final system configuration recommendation
- Baseline testing of final demonstration vehicle

Future Achievements

- Make final modifications to demonstration vehicle
- Wind tunnel test demonstration vehicle to allow calculation of range extension
- Demonstrate vehicle with final range extending technologies
- Prepare and present final report

II.6.B. Technical Discussion

Background

The transportation sector is an industry segment that must contribute to reducing petroleum dependence in the United States, as well as greenhouse gas emissions. One area with a high potential to decrease oil consumption and emissions is the electric drive vehicle. However, a barrier to its widespread acceptance is consumer “driving range anxiety.” Can an electric vehicle take me the distance I need to go? Increasing the range of electric vehicles is a key factor in achieving its mass market adoption. Since the climate system is the largest auxiliary load on electric drive vehicles, it is a prime candidate for onboard load reduction, which in turn increases vehicle range and, positively impacts consumer acceptance of electric vehicles. This is especially true in extreme hot and cold climates where range is significantly diminished by the climate system load.

Introduction

This project is exploring a technical approach to reducing the power required to operate the climate control system on a grid-connected electric drive vehicle, while still maintaining occupant comfort. It focuses on three main technology areas for climate system load reduction in an electric drive vehicle: thermal energy storage with preconditioning, refrigerant system performance and zonal cabin comfort.

Providing occupant thermal comfort can consume as much as 40 percent of the energy stored in GCEDV batteries, and thus improving the way comfort is achieved will result in extending the range of these vehicles. Achievements in electric vehicle climate load reduction has the opportunity to improve the current electric vehicle market, as well as open the market to climate zones previously unable to utilize these vehicles.

Approach

A three phase approach is being taken to define, design and demonstrate climate power reduction technologies. This method ensures positive progress and results of shorter term objectives, which are vital to overall project success, before moving between phases. During phase 1, the major project metrics were defined. These metrics will be used throughout the project to guide and measure the success of the technologies introduced. In addition, the computer aided engineering (CAE) models were built and correlated to data from baseline vehicle and system level testing. These validated models were then used to support trade studies that assess various technology alternatives. This phase ended with a decision on the most favorable technologies to be applied to the baseline vehicle architecture to improve range. In phase 2, the componentry necessary for each of the technology areas were designed, fabricated and verified through vehicle testing. Finally the new vehicle will be integrated with the new technology in phase 3 and the vehicle level impacts confirmed. The project is currently in phase 3.

Results

Highlights of FY 2016 accomplishments include fabricating hardware for and evaluating phase-change material, sensible thermal storage, a water-cooled condenser, and an EXV. Also, at the vehicle-level, the comfort model was evaluated, the fully-modified vehicle was wind tunnel tested, the final system configuration was developed, and a new Kia Soul EV was purchased and baseline tested so the final technologies can be installed and the performance quantified.

Phase Change Material

Although the original premise was to solely utilize existing mass for thermal storage, testing and CAE analysis led to the conclusion that this would be insufficient to meet the cooling targets. An examination of using PCMs to increase the benefit of thermal storage, primarily while cooling was undertaken.

Because the vehicle was scheduled to begin undergoing modifications in early 2016, only a quick evaluation of PCM was completed. For the evaluation, a shell-and-tube heat exchanger was obtained. The shell-side of this heat exchanger was filled with PCM with a freezing temperature of 9°C and a latent heat of fusion of

178 kJ/kg. The heat exchanger was instrumented with thermocouples to monitor glycol in and out temperatures as well as the temperature of the PCM near the inlet and outlet ports.

The PCM-filled and instrumented heat exchanger was then integrated into the latest level glycol loop architecture. A separate reservoir was filled with ice water, which was used to cool the glycol and thus the PCM. Once the PCM was solid the ice water bath was valved out of the circuit and the solid PCM was ready to cool the cabin. The status of the PCM was monitored visually and constantly with direct temperature measurement. Examples of what the PCM looks like in a liquid state and a solid state can be seen in Figure II-53. Under the liquid PCM surface the tubes that carry the glycol through the PCM are clearly visible. The PCM was evaluated in our onsite soak room, and the experimental results were favorable.

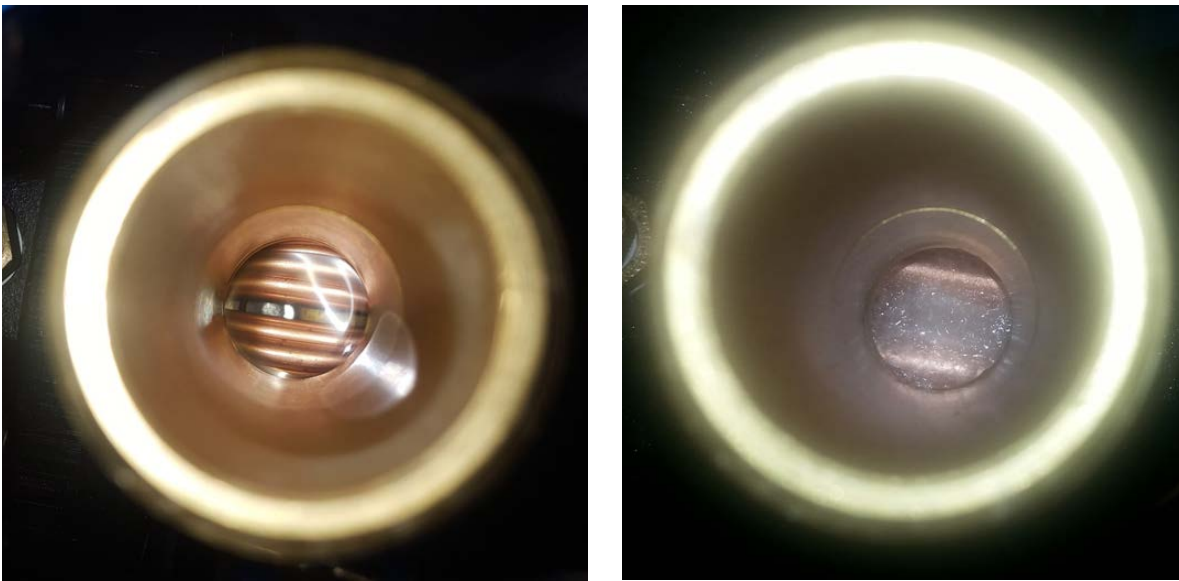


Figure II-53: Liquid (left) and Solid (right) Phase Change Material

Sensible Thermal Storage

To evaluate sensible thermal storage, the test vehicle was run in the baseline configuration and with thermal storage. As is shown in Figure II-54, the addition of thermal storage reduced the battery energy required to maintain comfort by 40% at -5°C . Although the percent savings is bigger at $+5^{\circ}\text{C}$, the magnitude of the savings is lower. The converse is true at -18°C .

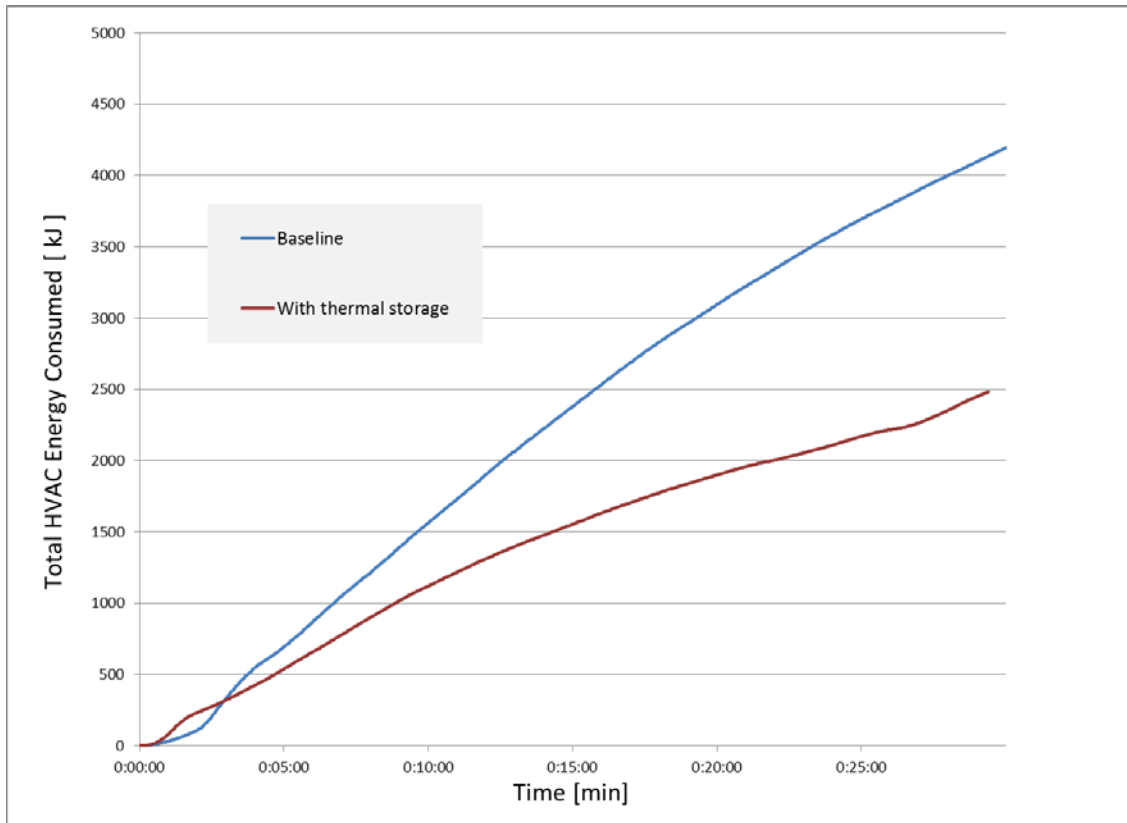


Figure II-54: Effect of thermal storage on total HVAC energy consumed at -5°C

Water Cooled Condenser

A Water Cooled Condenser (WCC) was integrated into the vehicle just downstream of the air cooled condenser. When cool thermal storage is available, glycol is pumped through the thermal storage and then through the WCC. Having cool glycol aid in the condensing process reduces the compressor power significantly. Results from a WCC test are shown in Figure II-55. The cabin controls were set to 72°F-Auto on a sunny, 32°C day. At approximately 14-16 minutes the system was at steady-state operation with the compressor working at 2000RPM (red line) and consuming nearly 600W of power (green line). When the glycol pump was activated the glycol temperature was 20°C (blue line). It slowly warmed to 34°C as the thermal mass absorbed heat from the refrigerant system. As a result of having this additional heat sink, the compressor RPM reduced to 1000 and the power consumption dropped to less than 200W.

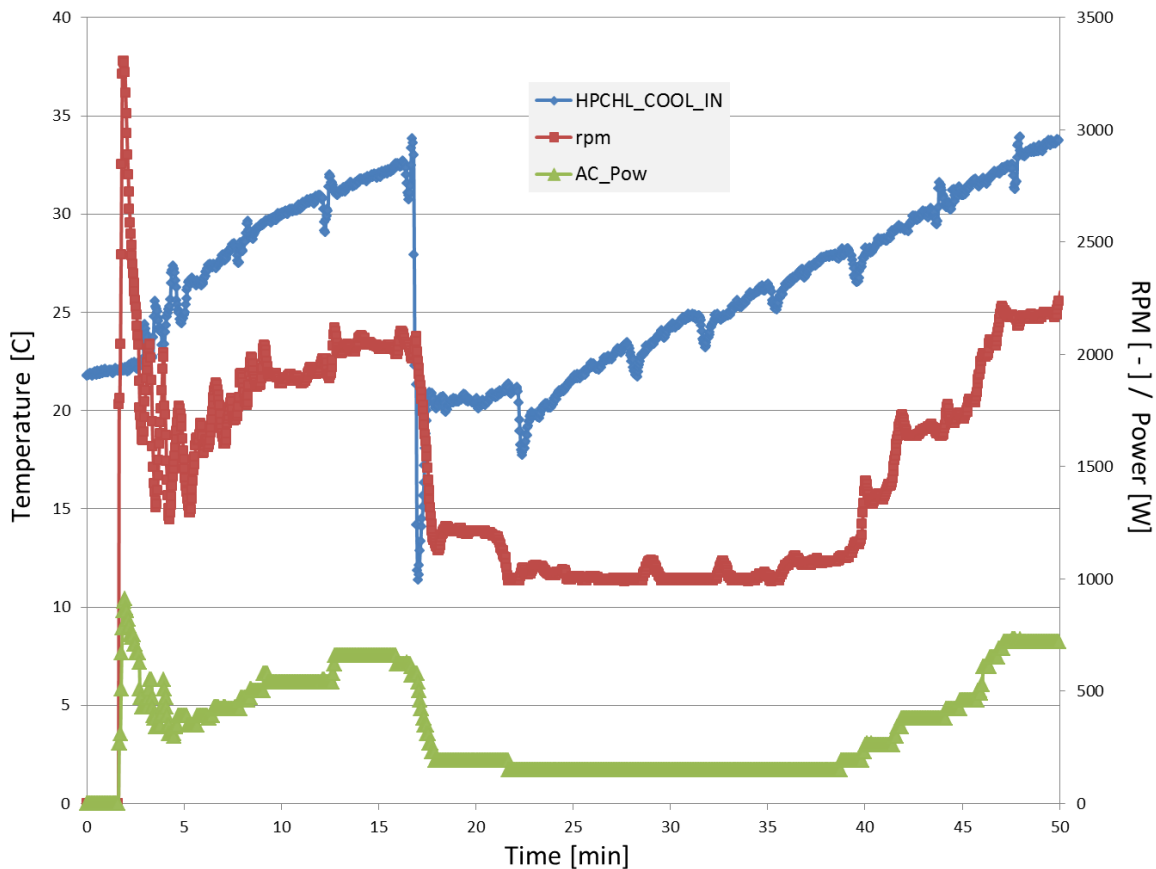


Figure II-55: Effect of Cold Thermal Storage in Water Cooled Condenser (WCC)

Comfort Model Investigation

To better understand the comfort model and specifically its use to predict the response to small transients, soak room testing was run and the subjective responses were compared to model predictions. The soak room was set to 28°C with a solar load of 750 W/m². Subjects entered the chamber five minutes before getting into the car. At Time = 0 the car was started with the climate controls set to 22°C AUTO. Although there was some discomfort initially, after approximately twelve minutes the highest comfort value of 1.25 “votes” was reached. The value stayed at 1.25 until twenty minutes into the test, when the set-point for the climate control system was increased to 23°C. Ten minutes later the set-point was increased to 24°C, and then ten minutes later it was increased to 25°C. During this gradual 3°C warming the average comfort of four subjects decreased by 2.0 “votes” but the Berkeley model predicted a decrease of approximately 0.5 “votes”.

Although time and effort were spent trying to improve the model, it was decided that the comfort model lacked the resolution needed to accurately predict the impact of several competing technologies. For this reason the comfort model is little use to us.

Vehicle-Level Evaluation

The vehicle was modified to include various range extending technologies that have been developed during this project. The refrigerant system was modified as shown in Figure II-56 with green indicating new or modified components. The condenser and evaporator were not been replaced for this round of testing, as it was decided that predictions of effectiveness of the improvements were well understood. Although the condenser core remained in place, the integrated receiver-dryer was removed. It was relocated downstream of the water cooled condenser. The evaporator core, however, was completely un-touched.

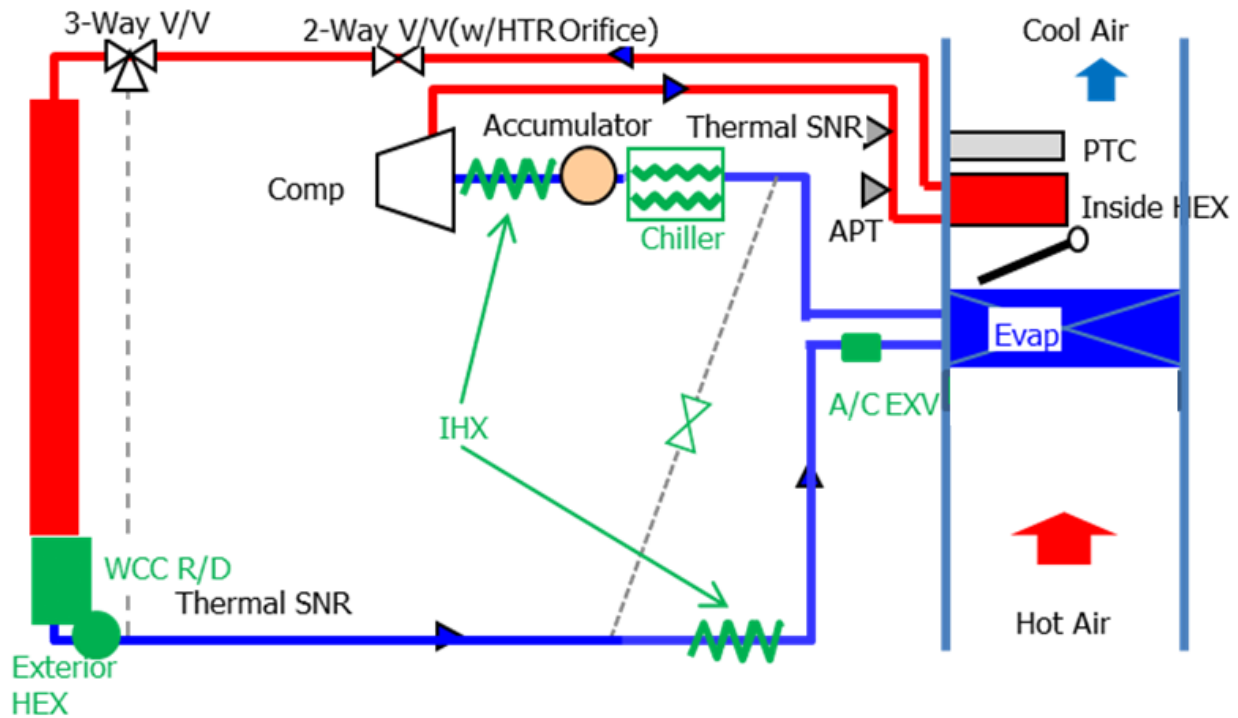


Figure II-56: Full refrigerant system modifications as evaluated

The production IHX has a necessarily low effectiveness, as a higher value would result in the compressor overheating. However, by introducing an EXV with proper controls, the compressor can be protected from getting too hot. The EXV can also be used as the “dehumidification” valve by opening and allowing cold refrigerant to circulate through the evaporator when heating. The chiller was re-located such that it was in series with the evaporator, allowing it to be used when storing “cold” by acting as the refrigerant system evaporator, cooling glycol.

The glycol loop has also undergone significant modification. The production glycol loop is fairly simple, with one pump and one three-way valve. By adding the functionality required for all of the range-extending technologies the glycol loop must add a pump, two three-way valves, a four-way valve, and a heater.

Wind tunnel tests were run at warm/hot conditions to evaluate the air conditioning concepts. Whereas heat was added via an electric heater for the cold tests, the vehicle’s AC was used to build “cold” thermal storage for the warm tests. During precondition for the cold tests the PTC heater warmed the cabin while a separate heater built thermal storage. During preconditioning for the hot tests, however, the air conditioning system had to do “double duty,” as it was the sole source to both cool the cabin and build thermal storage. The result was disappointing, as the system had difficulty doing both, especially at high temperatures.

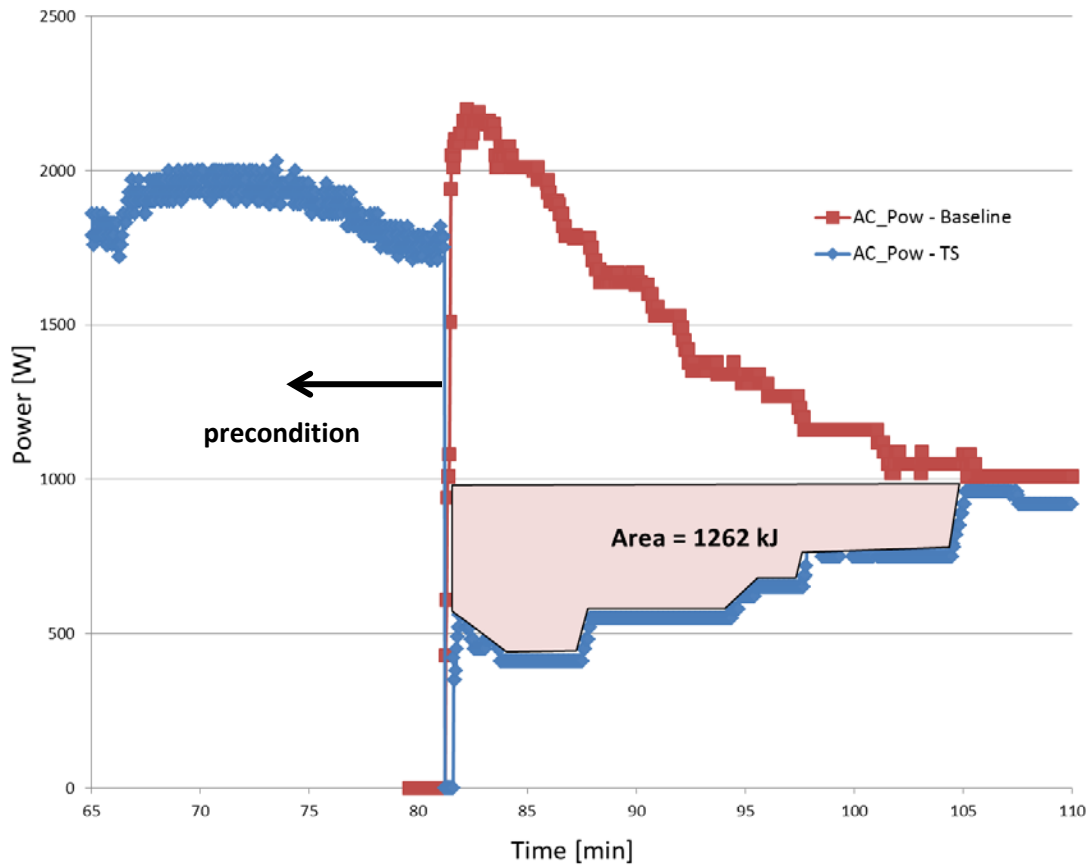


Figure II-57: Power required with and without "cold" thermal storage (TS)

Data were obtained for the cases of warm cabin and warm motor and cool cabin and cool motor at 28°C, 32°C, and 43°C. The results for the 32°C runs are shown in Figure II-57. The blue line shows the compressor power consumption for the test with thermal storage, the red line compressor power without thermal storage. The compressor power is approximately 2,000W during preconditioning, as the system tried to cool the cabin and the thermal storage simultaneously. After the test started, however, the power consumption dropped to approximately 400 Watts, but the non-preconditioned vehicle required over 2,000 Watts to cool the hot cabin.

After the beginning of the test the preconditioned car benefits from both the cooled cabin and thermal storage. While appropriate, glycol is routed through the thermal storage, where it cools, and then through the water-cooled-condenser (WCC) to aid in the condensing process. By reducing the amount of heat the refrigerant must reject in the condenser, the discharge pressure is lowered, reducing compressor power. The baseline consumption, the steady-state power needed to maintain comfort, for this trial is a constant 960 Watts. That's what the compressor would draw for a completely pre-conditioned cabin with no thermal storage. Both the no preconditioning and cool cabin with thermal storage runs require approximately 1000 Watts at the end of the test, indicating this is indeed the steady state power requirement for this system at these conditions. The pink area in Figure II-57 represents the amount of battery energy saved, versus a pre-conditioned production vehicle, as a result of thermal storage. This test indicates that 1262 kJ of battery energy were saved, which equates to approximately 3 km range extension.

During cold testing we measured the energy savings and thus range extension at +5°C, -5°C, and -18°C. Understood performance problems prevented us from taking full advantage of thermal storage opportunities. At -18°C our heater (1.5kW) was under-powered, resulting in significantly less thermal storage than our model assumed. For the final build we will employ two 1.5kW heaters. At +5°C the problem was not being able to remove the stored heat fast enough. We undertook a charge management study to increase the heat transfer from thermal storage to refrigerant, and are optimistic that this will alleviate the problem.

Charge Management

During heat pump testing we noticed less heat transfer than expected in the chiller. This acts as the heat source for the heat pump, so performance is critical. In practice, what seems to be happening is that when we are bypassing the outside condenser and providing warm glycol to the chiller the outside condenser fills with liquid refrigerant. When this happens the rest of the system can become grossly under-charged, resulting in poor heat transfer in the evaporator (or chiller, for heat pump operation). A symptom of this behavior is the refrigerant exiting the chiller extremely super-heated, close to the inlet glycol temperature. This is due to too small of a refrigerant mass in the evaporator, and thus very little energy is required to boil and heat the refrigerant.

In an attempt to solve this refrigerant management issue, a check-valve was installed at the condenser outlet to prevent refrigerant from accumulating in the outside condenser. A production 3-way valve is located immediately upstream of the condenser, and in bypass mode prevents refrigerant from entering the core through the inlet. Although we can now isolate the core, there is no way to identify how much refrigerant is in the core initially. A procedure to “flush” the core with two-phase refrigerant has been developed and will be incorporated into the final test.

Figure II-58 shows the importance of refrigerant management. Initially, with the outside condenser full of liquid refrigerant, the system was under charged and the refrigerant temperature exiting the chiller (red line) is nearly equal to the inlet glycol temperature (light blue line). The refrigerant superheat, which should be zero if charged properly, is the vertical distance between the red and dark blue lines. At the 64-minute mark we briefly switched the three-way valve upstream of the condenser, flowing two-phase refrigerant through the outside condenser, flushing any stored liquid out of it. After flushing, the bypass valve and the check valve prevented additional refrigerant from entering the condenser. The result is the performance after minute 64. The refrigerant inlet and outlet temperatures (red and dark blue lines) are nearly the same, indicating the heat added from the glycol is evaporating liquid refrigerant rather than heating refrigerant vapor. For the system to operate with maximum evaporator (chiller) capacity the entire refrigerant side should contain some liquid.

At the 83-minute mark the thermal storage became cool enough to allow refrigerant flow through the outside condenser continuously. After this the refrigerant in and out of the chiller overlapped, and they both became colder than ambient (green line), indicating the refrigerant is now absorbing heat through the outside condenser.

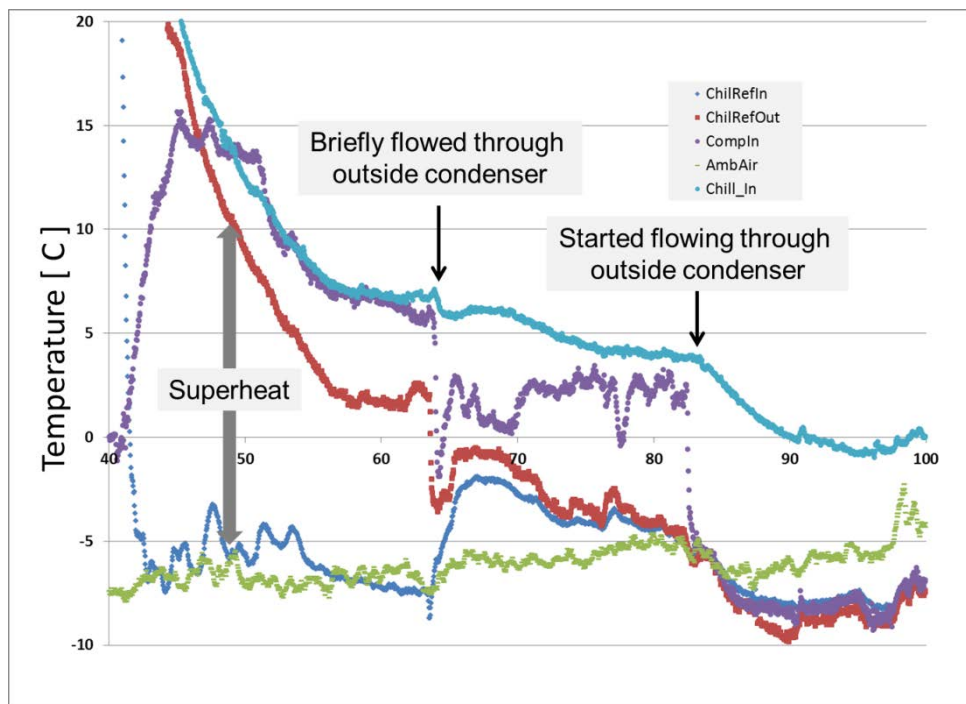


Figure II-58: Vehicle Test Showing Need for Charge Management

Final Architectures

For the final demonstration vehicle we plan to proceed with technologies that extend the range during heat pump operation but not those for AC operation. In general, the enhancements for the cooling mode were not technologies that could be successfully commercialized. Figure II-59 shows a schematic of the proposed refrigerant system. It is unchanged from production with the exception of a check valve downstream of the condenser, as the value in investing in improved AC hardware is poor.

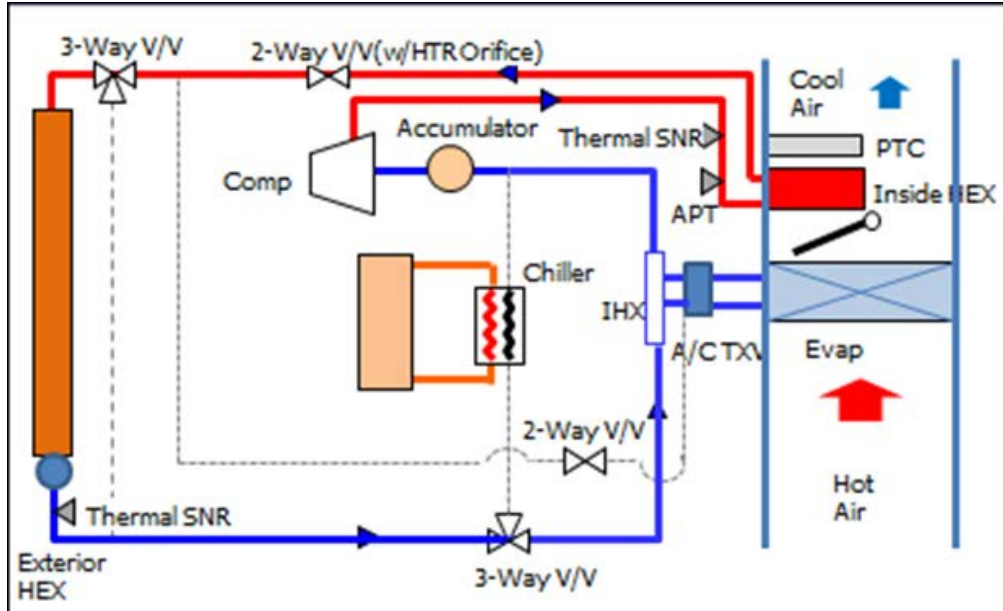


Figure II-59: Refrigerant system schematic

Figure II-60 shows the proposed glycol loop for heat pump enhancement. The main change here is the addition of thermal storage and supporting hardware/software to enable heat transfer to the cabin. The method of transferring this heat is the subject of a submitted patent, and so remains proprietary. In addition to the glycol loop modifications, a check valve will be added to the refrigerant circuit to aid in refrigerant management during heat pump operation.

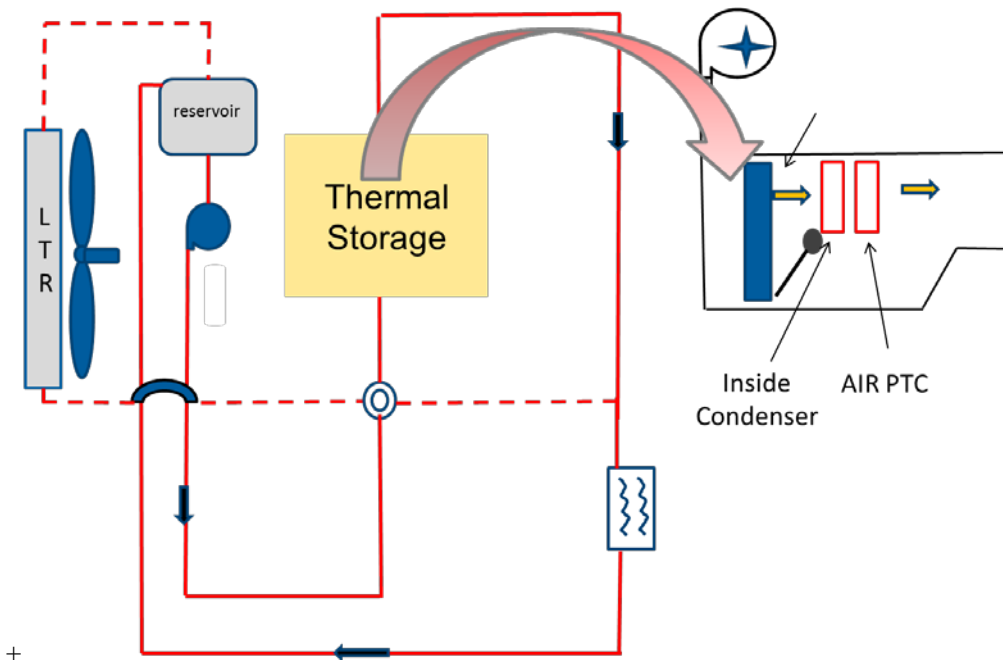


Figure II-60: Glycol loop schematic

Conclusions

During FY 2016 we fabricated and tested many concepts. After evaluating the results, the final technologies were recommended at a go/no-go presentation at the conclusion of BP2. Although we showed it is possible to extend the range while cooling the vehicle, the overall efficacy of these technologies is quite low. Because it was felt these technologies could not be developed into something marketable it was recommended to stop development on this half of the project.

The benefit while heating, however, is substantial. The final demonstration vehicle will have the production AC system (with the inclusion of a check valve for refrigerant management during heat pump operation) but range extending technologies for cold weather.

II.6.C. Products

Presentations/Publications/Patents

1. J. Meyer & N. Agathocleous, "Advanced Climate Systems for EV Extended Range." 2016 Department of Energy Annual Merit Review Conference, Washington DC, June 8, 2016.
2. J. Meyer, N. Agathocleous, SH Kang, T. Vespa, "Extending the Range of a BEV - Early Progress" 2015 SAE Thermal Management Systems Symposium, Troy, MI, September 30, 2015.

II.7. Design and Implementation of a Thermal Load Reduction System for a Hyundai Sonata PHEV for Improved Range

Cory Kreutzer, Principal Investigator; John P. Rugh, Task Leader

National Renewable Energy Laboratory (NREL)

Transportation and Hydrogen Systems Center

15013 Denver West Parkway, MS 1633

Golden, CO 80401

Phone: (303) 275-3772, (303) 275-4413

E-mail: Cory.Kreutzer@nrel.gov, John.Rugh@nrel.gov

David Anderson, Lee Slezak, DOE Program Managers

Vehicle Technologies Office

Phone: (202) 287-5688, (202) 586-2335

E-mail: David.Anderson@ee.doe.gov, Lee.Slezak@ee.doe.gov

Start Date: October 1, 2015

End Date: September 30, 2017

II.7.A. Abstract

Objectives

- Increase grid-connected electric-drive vehicle (EDV) range by 20% during operation of the climate control system by reducing thermal loads
- Implement a thermal load reduction system on a production vehicle and quantify performance of the system over the combined city/highway drive cycle at peak heating and cooling conditions
- Maintain occupant thermal comfort, verified through experimental evaluations

Accomplishments

- Completed Phase I candidate thermal load reduction technology evaluations
 - Evaluated the performance of three solar control glazing packages, solar reflective paint, and cooled/ventilated seating in warm weather conditions
 - Evaluated the performance of heated surfaces, and a combined heated windshield and door demisters in cold weather conditions
- Transitioned from *Phase I: Technology Design and Development* to *Phase II: Technology Integration and Validation with the completion of the Phase I candidate technology Go/No-Go decision matrix and initiation of Phase II technology integration*
- Completed baseline heating, ventilating, and air conditioning (HVAC) system performance evaluation for the 2016 Hyundai Sonata plug-in hybrid vehicle by Hanon Systems; vehicle cabin and HVAC system analysis models were developed to support Phase II national-level analysis tasks

Future Achievements

- Integrate technologies into Phase II vehicle platform and quantify the vehicle's performance during operation of the climate control system
 - Evaluate the Phase II vehicle with integrated technologies using Hyundai America Technical Center, Inc. (HATCI) standard cold and hot weather field evaluations
 - Evaluate the Phase II vehicle in an environmental chamber over the combined city/highway drive cycle with peak heating and cooling conditions
- Calculate the national-level impact of the Phase II thermal load reduction system on EV range
- Provide DOE an on-site Phase II vehicle demonstration and project summary presentation

II.7.B. Technical Discussion

Background

The EV Everywhere Grand Challenge identified major opportunity areas to increase the adoption of plug-in hybrid vehicles and EVs that address the hurdles associated with vehicle market penetration. These opportunity areas are vehicle lightweighting, reducing battery cost per unit of energy delivered, reducing the cost of electric drive systems, improved charging infrastructure, and improved climate control efficiency [1]. Operation of the climate control system has been shown to significantly impact the range of EDVs due to the need to power not only the air conditioning (A/C) system, but also the heating system since significant waste heat is not available, unlike the conventional vehicle platform. As an example, a Ford Focus Electric vehicle tested at Argonne National Laboratory's Advanced Powertrain Research Facility measured a degradation in vehicle range of 53.7% due to operation of the A/C system and a 59.3% degradation in range due to operation of the cabin heating system [2]. By minimizing the amount of energy needed for vehicle climate control, more energy is available for vehicle propulsion, thereby increasing the range of the vehicle.

Climate control energy use is determined by the efficiency of the HVAC components, the effectiveness of conditioned air being delivered to the occupant, control strategy, and the thermal energy exchange between the surroundings and the occupied space. Reduction of thermal energy exchange between the surroundings and the occupied space is commonly referred to as thermal load reduction. Placing emphasis on thermal load reduction for plug-in hybrid and electric vehicles is expected to lead to battery sizing and cost reductions, reduced climate control equipment capacities, as well as enabling advanced HVAC system components and control strategies. In addition, thermal load reduction and advanced climate control design can positively impact occupant comfort. The quantification of a number of individual thermal load reduction strategies have been performed for both heating and cooling at the proof-of-concept level. For instance, an infrared reflective windshield combined with pre-ventilation demonstrated on a pre-production electric vehicle reduced the transient 20-minute A/C cool-down energy consumption in summer conditions by 44.2% [3]. Similarly, a combination of driver-only panel air ventilation in combination with heated seating, steering wheel, and floor mat demonstrated on the pre-production electric vehicle reduced the 20-minute transient heating energy consumption in winter conditions by 28.5% [4]. In addition, the potential impact of improved vehicle cabin on steady-state heating performance was quantified on the pre-production electric vehicle, with a 3.3% reduction in energy consumption [5]. Finally, the potential impact of solar reflective coatings on the exterior opaque surfaces of the vehicle was measured by applying a solar-reflective film on the roof of a light-duty vehicle during summer daytime conditions, obtaining a 6.7°C reduction in exterior surface temperature of the vehicle roof, demonstrating its ability to positively impact vehicle thermal performance [6].

While the impact of thermal load reduction strategies has been demonstrated under various conditions, their performance is dependent on manufacturing constraints, and the need remains to quantify individual technologies at a production-ready stage rather than the proof-of-concept stage. In addition, it is expected that the performance of some thermal load reduction technologies are dependent on one another. Therefore, a need exists to implement and quantify an entire thermal load reduction system as a whole.

Introduction

NREL, in partnership with HATCI, Pittsburgh Glass Works (PGW), PPG Industries, Hanon Systems, Sekisui S-LEC America, and Gentherm, is focusing on development and subsequent integration of a complete thermal load reduction system for a light-duty EV. The project scope was developed in response to the FY14 Vehicle Technologies Office-wide funding opportunity announcement solicitation for the Advanced Climate Control Auxiliary Load Reduction area of interest. The overall goal of the project is to provide technology solutions that improve customer acceptance of EDVs and increase the penetration of these vehicles into the national fleet. To achieve the project goals, the project objective is to increase grid-connected EDV range by 20% at peak heating and cooling conditions over the combined city/highway drive cycle. The objective is expected to be met by decreasing thermal loads during all modes of vehicle operation, including thermal soak, cool-down and warm-up transients, steady-state operation, and thermal preconditioning while connected to the grid. The project duration is three years, divided into an individual technology development and assessment phase (Phase I) followed by a technology integration and performance evaluation phase (Phase II). The project will

be completed by providing vehicle performance results of the thermal load reduction system obtained through standardized experimental testing performed at HATCI's test facilities as well as estimation of national-level range improvements based on validated models.

Approach

To evaluate thermal load reduction technologies both independently and as an entire system, the project was divided into two phases. During Phase I, the project team focused on identification of candidate thermal load reduction technologies, determination of the design specifications for the technologies, implementation on a pre-production vehicle, and individual evaluation of the technologies. In addition, analysis tools were constructed during Phase I, including a vehicle cabin thermal model, HVAC system model, overall vehicle model, and national-level analysis process tools. Analysis tools were validated with Phase I experimental results and will be leveraged in Phase II to provide an estimation of the impact of the thermal load reduction system on vehicle range on the national scale. Phase I concluded with a Go/No-Go decision point for the integration of the candidate thermal load reduction technologies into the Phase II vehicle. Phase II was recently initiated and began with the integration of the successful individual technologies into a drivable vehicle. Once the thermal load reduction system is fully integrated into the vehicle, its performance will be evaluated experimentally through outdoor cold and hot weather testing in addition to environmental chamber testing. Phase II will conclude with a demonstration and summary presentation of the vehicle to key U.S. Department of Energy personnel.

The project relies heavily on collaboration between NREL and project partners to complete all components of the project work plan. HATCI provided the vehicle platform, modeling data, and technology interfacing requirements for Phase I evaluation of technologies. HATCI also leads Phase II of the project, with integration of technologies into the Hyundai vehicle platform and manufacturer testing at HATCI facilities to characterize the performance of the vehicle. In addition to HATCI's contributions, the project relies heavily on select tier one and tier two supplier research teams to develop, manufacture, aid in testing and analysis tasks, and provide general direction for the project. PGW provided automotive glass manufacturing capabilities for the project in addition to advanced glass technologies for evaluation. Sekisui provided advanced materials and integration expertise for candidate thermal load reducing glass technologies, collaborating with PGW for manufacturing. PPG Industries developed and provided baseline and solar reflective paint formulations for the Phase I and Phase II vehicles in addition to their thermal property characterization. Gentherm interfaced directly with both NREL and HATCI to develop and provide active seating, door glass defogging, and individual heated surface technologies. Finally, Hanon Systems performed experimental characterization of the vehicle HVAC system and model inputs for the construction and validation of the HVAC system model, in addition to expertise in HVAC system control.

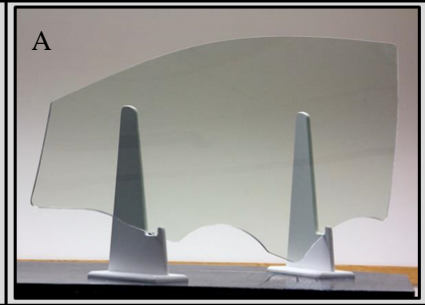
Description of Phase I Candidate Technologies

A description of both the cold weather and warm weather Phase I candidate technologies and the corresponding project partner is provided in Figure II-61. Technologies in red represent candidates for warm weather load reduction while those in blue represent candidates for cold weather load reduction.

Solar Control Glazings: PGW & Sekisui

	Package A	Package B	Package C
Outer Glass	2.1 mm Clear	2.1 mm Clear with Double Silver IR Reflective Coating	2.0 mm Ultraclear with Triple Silver IR Reflective Coating
Interlayer	Sekisui IR Reflecting & Absorbing	Sekisui IR Absorbing	0.76 mm Polyvinyl Butyral
Inner Glass	2.1 mm Green	1.8 mm Solex	2.1 mm Clear

Laminated solar control automotive glass for windshield, front door, and rear door locations.



Solar Reflective Paint: PPG Industries

	Total Solar Reflectivity [%]
Conventional Vehicle Paint	6.62%
NIR Reflective Vehicle Paint	38.11%
Difference	31.49%

Automotive paint with an elevated reflectivity in the near infrared spectrum.



Ventilated/Cooled Seats: Gentherm

Power Requirements	Standard 12VDC System
Seat Cooling Levels	High, Medium, Low, Off
Test Procedure Used	Transient and steady-state with occupant thermal sensation evaluation

Modified climate control seat ventilated cushion and back with thermoelectric device enabled cooling.



Heated Surfaces: Gentherm

Driver Side Surfaces	Door arm rest and bolster, crash pad, console wall, console top, advanced heated seat
Passenger Side Surfaces	Console wall, glove box, door arm rest and bolster
Test Procedure Used	Transient and steady-state with occupant thermal sensation evaluation

Temperature regulated electrical resistance heaters embedded in select interior body panels.



Heated Windshield & Door Demisters: PGW & Gentherm

Power Requirements, Windshield	42VDC
Power Requirements, Door Demister	Standard 12VDC System
Door Demister Heater Type	PTC Heater
Test Procedure Used	Cold Weather Defogging

Electrical resistance heated windshield (PGW) combined with PTC heater based demister and integrated blower assembly (Gentherm)

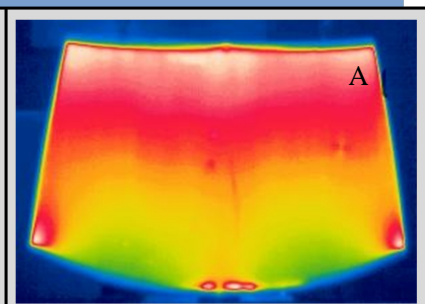


Figure II-61: Phase I candidate thermal load reduction technologies. Photo Credits: A - PGW, B - Gentherm.

Phase I Experimental Setup

For Phase I summer testing, two pre-production 2016 Hyundai Sonata plug-in hybrid electric vehicles (PHEVs) were provided by HATCI and instrumented at NREL's Vehicle Integration and Testing Facility, as shown in Figure II-62. The facility is located in Golden, Colorado, at an elevation of 5,997 feet, latitude 39.7 N, and longitude 105.1 W. The two vehicles were oriented to face south for maximum solar irradiation into the air volume surrounding the driver. The vehicles were separated to minimize shadowing effects. Each vehicle was instrumented with a total of 48 k-type thermocouples installed on the exterior glass and opaque surfaces, interior glass and trim surfaces, and front occupant seating, as well as a range of internal air temperature measurements, including driver's breath and foot well locations and HVAC vent outlet locations. Air temperature sensors were equipped with a double concentric cylindrical radiation shield to prevent errors due to direct solar radiation exposure. A National Instruments cDAQ-9188 equipped with multiple NI-9214 thermocouple cards was used for data acquisition. All thermocouples were calibrated using a five-point calibration protocol, achieving a U95 uncertainty of less than 0.11°C for each measurement in accordance with American Society of Mechanical Engineers standards [7]. For warm weather testing, a Load Controls Universal Power Cell was used to measure traction battery power with an accuracy of $\pm 75\text{ W}$ and because the vehicles were kept in EV mode, only electric power was recorded. For cold weather testing, thermocouples were installed in the coolant flow both upstream and downstream of the heater core. In addition, a Flow Technology turbine flow meter was installed to measure coolant flow rate and the coolant composition measured by its refractive index. Thermal power entering the vehicle from the heater core was calculated from the flow, temperature differential, and coolant composition data. Finally, the vehicle positive temperature coefficient (PTC) heater electrical power was recorded and assumed to convert 100% of its electrical energy into thermal energy going into the vehicle. The heater core and PTC heater powers were combined for cold weather testing data analysis.



Figure II-62: Phase I vehicles at NREL's Vehicle Testing and Integration Facility

Phase I Experimental Test Process

A three-step method was used to experimentally quantify the performance of individual candidate technologies and collect data for analysis tool validation. For both cold and warm weather testing, the three-step method consisted of a vehicle soak period in outdoor conditions, followed by a transient period, and finally a steady-state period. A schematic representation of the test process is provided in Figure II-63 for both warm and cold weather testing. For warm weather testing, baseline and modified vehicles were preconditioned by soaking in the morning outdoor environment. Next, the transient cool-down step was performed with maximum A/C settings and the power delivered to the HVAC system was integrated until the cabin mean air temperature attained a target value. Finally, the A/C settings were changed to fully automatic temperature control with a set point of 72°F and power delivered was once again integrated for a specified time interval. Cold weather testing was similar although testing was completed starting at 3:00 a.m. to remove variations caused by the sun.

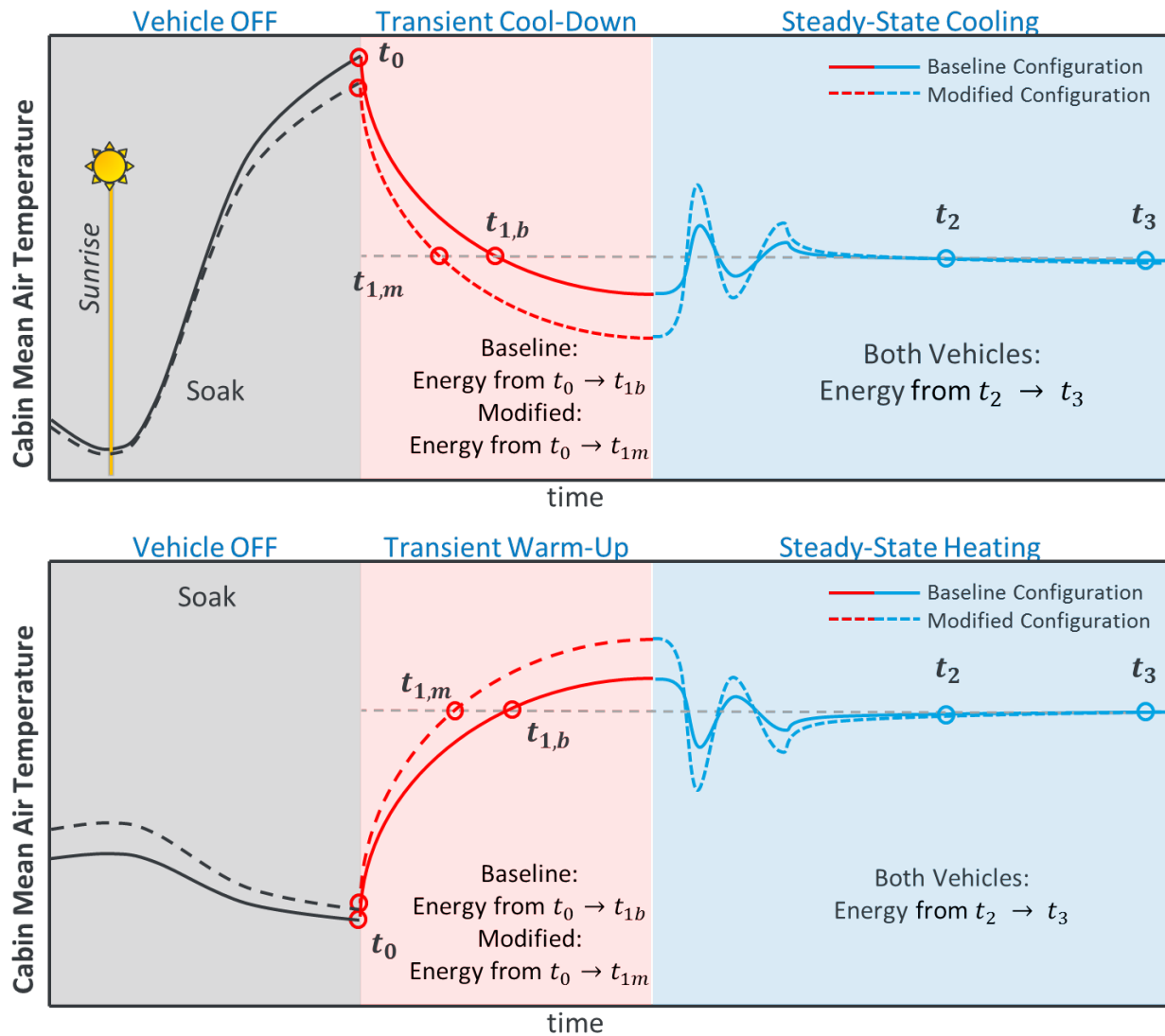


Figure II-63: Warm weather (upper) and cold weather (lower) testing methodologies used for Phase I testing of candidate technologies

The three-step testing methodology was adapted for candidate technologies that more directly targeted occupant climate conditioning rather than the boundary between the vehicle and outdoor environment. For summer testing of these technologies, human occupants were included and provided real-time evaluation of their thermal sensation throughout the test. The preconditioning phase included a 30-minute occupant precondition in an office environment. The transient cool-down endpoint was determined by the occupant achieving a target thermal sensation rather than a target cabin air temperature. For steady-state cooling, the occupant in the modified vehicle adjusted the cabin air temperature set point such that the combined effect of the candidate technology and the modified air temperature provided a body sensation equivalent to that obtained in the baseline vehicle. Analogous adaptations were made for cold weather testing.

Cold Weather Defogging Test Description

For evaluation of the heated windshield and door demister compared to the baseline vehicle, each vehicle was equipped with humidifiers in the vehicle cabin. The defogging test procedure consisted of four parts: preconditioning, transient defogging, steady-state defogging, and steady-state defogging with moderate heating. Electrical power for the heated windshield was measured using a digital power supply and door demister power was measured using a voltage reference and current shunt. For preconditioning, the vehicles were soaked in cold weather conditions and the humidifiers were operated for 20 minutes in order to provide

saturated conditions for the vehicle interior. Thereafter, transient defogging was initiated by setting the baseline vehicle to maximum heat and defrost while only the windshield and door demisters were activated for the modified vehicle. Windshield clearing was visually monitored, and the time was recorded when the windshield area was fully cleared as defined by the swept area of the windshield wipers. After both windshields were clear, the test was continued undisturbed to collect steady-state defogging energy use. Because the heated windshield and door demisters do not directly contribute to vehicle interior heating, a final comparison was made by setting the modified vehicle to include moderate heating with medium blower, maximum temperature, and panel and floor ventilation, while the baseline vehicle was kept in defrost mode.

Results

Phase I Summer Technology Evaluation Results

Prior to the evaluation of the technologies, baseline testing of the two vehicles was completed to characterize the vehicle-to-vehicle differences and sensitivity to changes in the outdoor environment. A summary of the baseline testing is provided in Figure II-64, including the vehicle HVAC settings used for both portions of the test and the correlation between the test and control vehicles. A strong correlation between the vehicles was obtained for both the transient cool-down and steady-state cooling portions of the test, with least-squares coefficients of determination (R^2) of 0.99 and 0.91, respectively. Baseline test correlations between vehicles were used to provide a correction factor to the control vehicle to represent an unmodified test vehicle performance during technology evaluations.

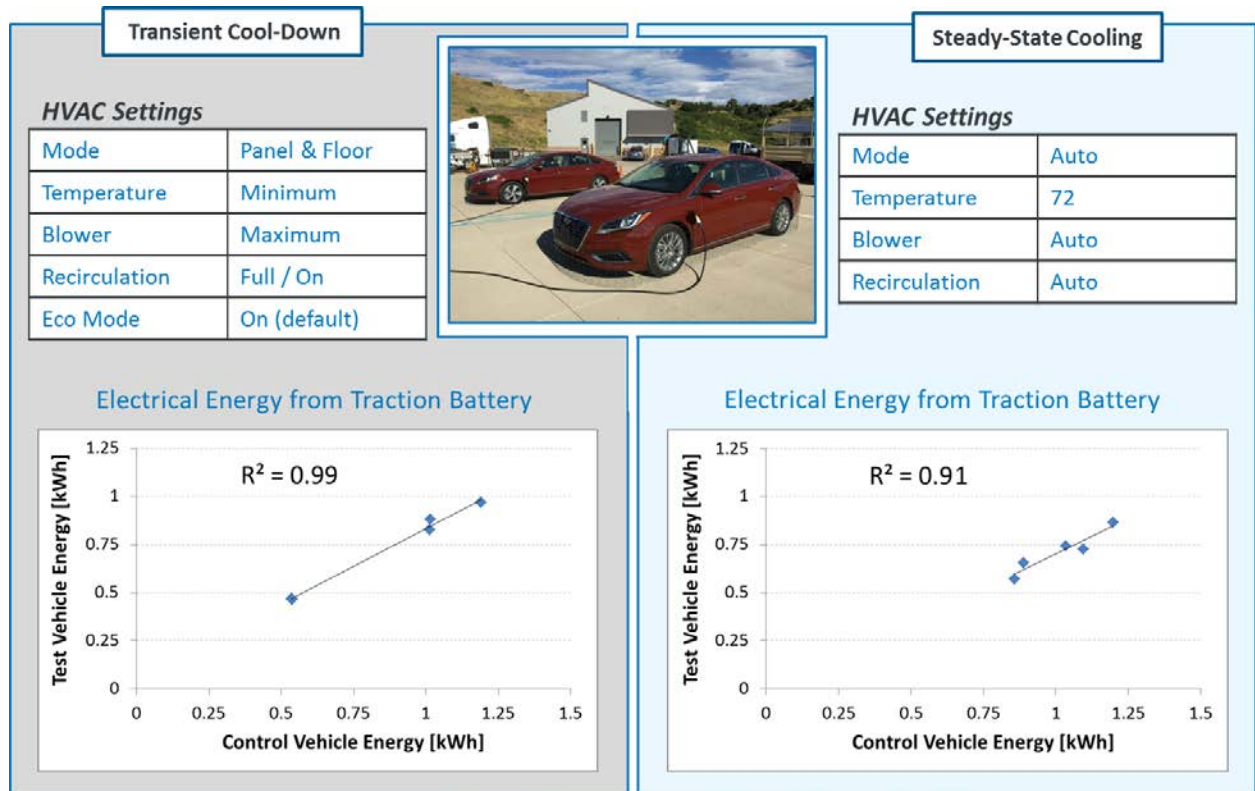


Figure II-64: Summary of Phase I warm weather baseline testing

The first summer technologies evaluated were three solar control glazing configurations, each of which provides a trade-off of properties while maintaining visible light transmission standards. The glass packages were provided by project partners PGW and Sekisui and all packages consisted of the windshield and front and rear door glass. Plots of the transient and steady-state cooling energy use compared to the baseline are provided in Figure II-65. The results are the average of a minimum of three test days collected in good weather conditions. Vehicle energy delivered for climate control was normalized to the peak test day for the entire test

season in order to remove seasonal and daily fluctuations. While normalizing results to the peak test day represents a maximum condition for Golden, Colorado, the climate is moderate in comparison to many regions of the United States. All glass packages provided benefits to both transient and steady-state cooling energy use, with particularly large benefits in the transient cool-down portion of the test. Package C provided the largest benefit, obtaining a 42.5% reduction in the transient phase and 12.8% reduction in the steady-state phase. For this reason, Package C will be included as part of the Phase II thermal load reduction system.

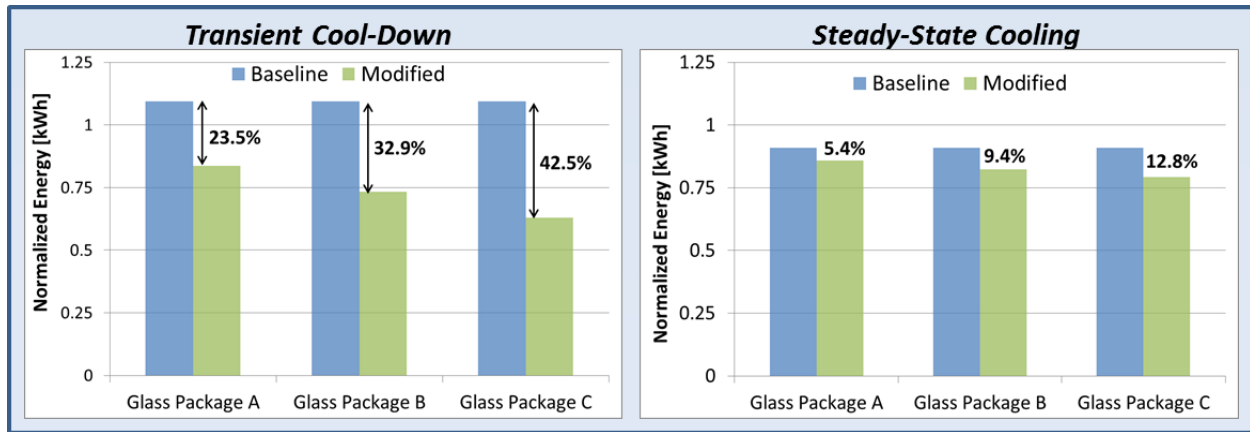


Figure II-65: Transient and steady-state cooling energy used compared to baseline for glass packages A, B, and C

In addition to solar control glazings, the impact of solar reflective paint on warm weather cooling energy use was also quantified. Dark red solar reflective paint provided by PPG Industries was used for the tests and compared against the baseline color-matched standard version of the paint. A photo of the painted vehicles is provided in Figure II-61. Four tests were completed for the solar reflective paint configuration and the normalized average results compared to the baseline for both transient and steady-state cooling are provided in Figure II-66. The solar reflective paint reduced transient cooling energy use by 5.3% and steady-state cooling energy use by 16.1%. Due to the energy savings achieved for solar reflective paint, it will be included in the Phase II thermal load reduction package.

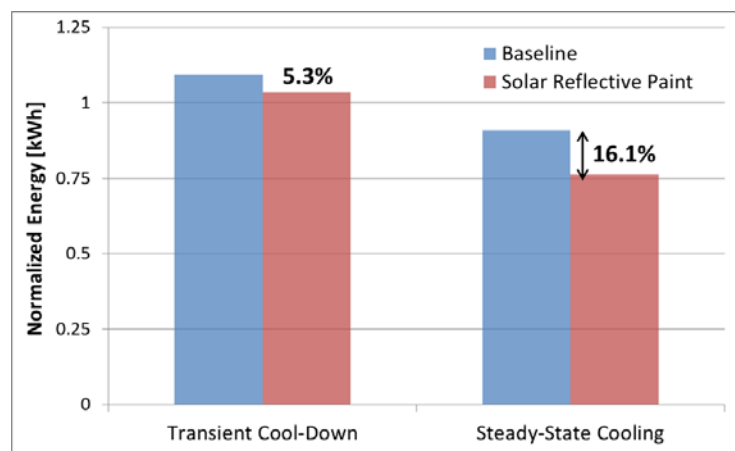


Figure II-66: Transient and steady-state cooling energy use for vehicle modified with solar reflective paint compared to baseline

Ventilated/cooled seats were evaluated in warm weather conditions using the test method adapted to include occupants. The transient and steady-state results of warm weather testing using the ventilated/cooled seats in comparison to baseline is provided in Figure II-67. The ventilated/cooled seat had a significant impact on the energy required for the transient cool-down for two occupants, saving 25.2% with occupant C and 45.5% with occupant D. Due to poor weather conditions, occupants A and B transient test data were omitted from the results. The energy savings during the transient cool-down period were due to the reduced time necessary to achieve a target whole body sensation for the occupant. In addition to the savings for transient cool-down, the ventilated/cooled seats provided an energy savings during the steady-state portion of the test, ranging from a 10.3% to 17.2% reduction for cooling. During the steady-state portion of the test, energy savings were obtained by reducing the cooling for cabin air because the occupant was partially cooled with the ventilated/cooled seat. Due to the energy savings obtained using the ventilated/cooled seats for both the transient and steady-state cooling, the seats will be included in the Phase II thermal load reduction system.

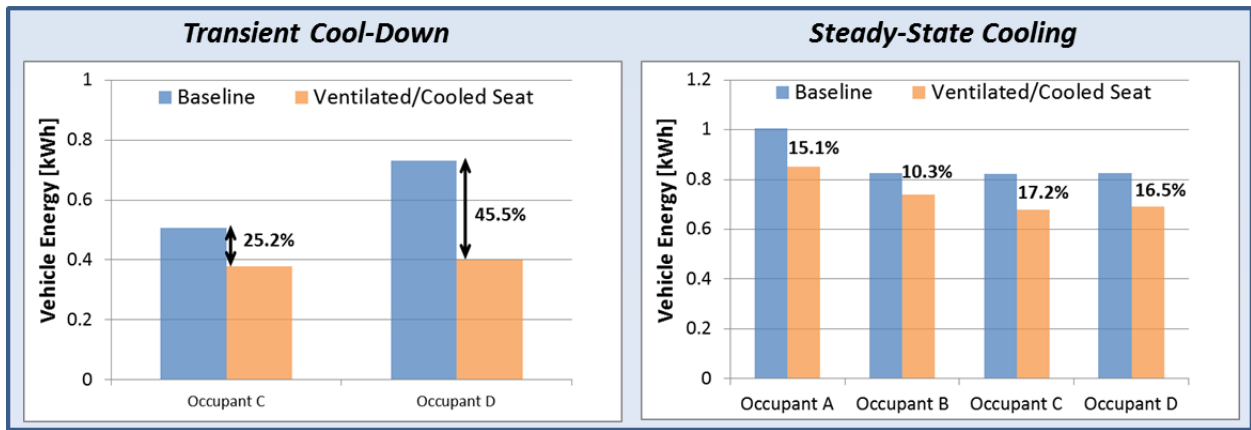


Figure II-67: Transient and steady-state cooling tests using ventilated/cooled seats compared to baseline. Results are specific to each occupant that performed the test.

Phase I Winter Technology Evaluation Results

A summary of the cold weather baseline testing results is provided in Figure II-68. For both transient warm-up and steady-state heating, the combined heater core and PTC electrical heater energy into the cabin between the two vehicles had a strong linear correlation with least-squares coefficients of determination (R^2) of 0.996 and 0.988, respectively. The linear baseline correlation was used for calibrating the vehicles during technology performance evaluations.

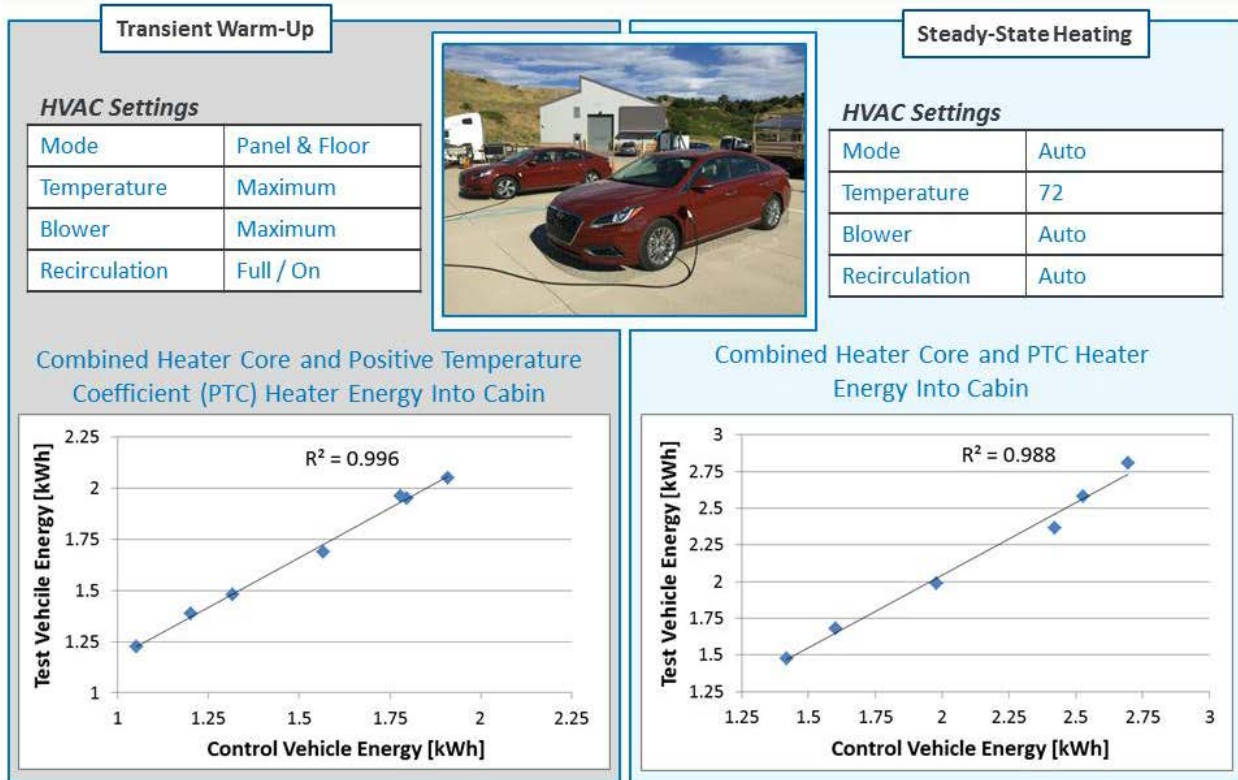


Figure II-68: Summary of Phase I cold weather baseline testing

Next, a combination of contact and non-contact heated surfaces was tested. The results for transient and steady-state heating using heated surfaces are provided in Figure II-69. Testing of the heated surfaces for three different occupants resulted in a 1% to 2% increase in energy use for the transient warm-up period and a 29%–59% decrease in energy use for the steady-state heating period. The variation in energy savings obtained

during the steady-state period is due to the subjective nature of engineering evaluations of thermal sensation. The minor penalty of heated surfaces on transient heating performance can be partially or completely eliminated when used in conjunction with grid-connected thermal preconditioning. Therefore, the benefits of heated surfaces are enabled by preconditioning and allow the vehicle to operate in the steady-state heating condition where large potential benefits are possible. For this reason, heated surfaces will be included in the full system package in Phase II.

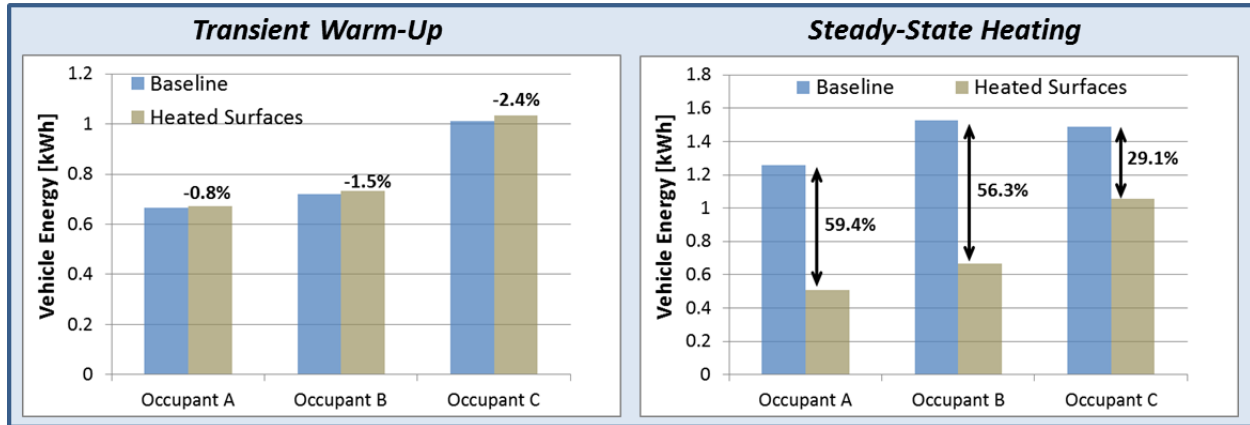


Figure II-69: Transient and steady-state heating tests using heated surfaces compared to baseline. Results are specific to each occupant that performed the test.

The final winter technology evaluation was defogging performance of heated windshield and door demisters compared to the baseline vehicle HVAC system defogging. The results for the time taken to clear the fogged windshield in addition to the average power needed for defogging compared to the baseline is provided in Figure II-70 and represents an average of three tests. The heated windshield and door demister combination was able to clear the windshield in an average of 16.5 minutes compared to an average of 20.5 minutes for the baseline system, providing a 19.5% improvement in time to clear the windshield. During the tests, the heated windshield and door demister system was able to reduce energy consumption by 67.8%. In addition, the combined system maintained a 24.5% reduction in energy consumption while delivering moderate heating to the occupant compared to the baseline. Due to the significant reductions in the time to clear the windshield and energy use, in addition to the ability of the system to decouple occupant heating and defogging tasks, the heated windshield and door demister technology will be included in the Phase II full system package.

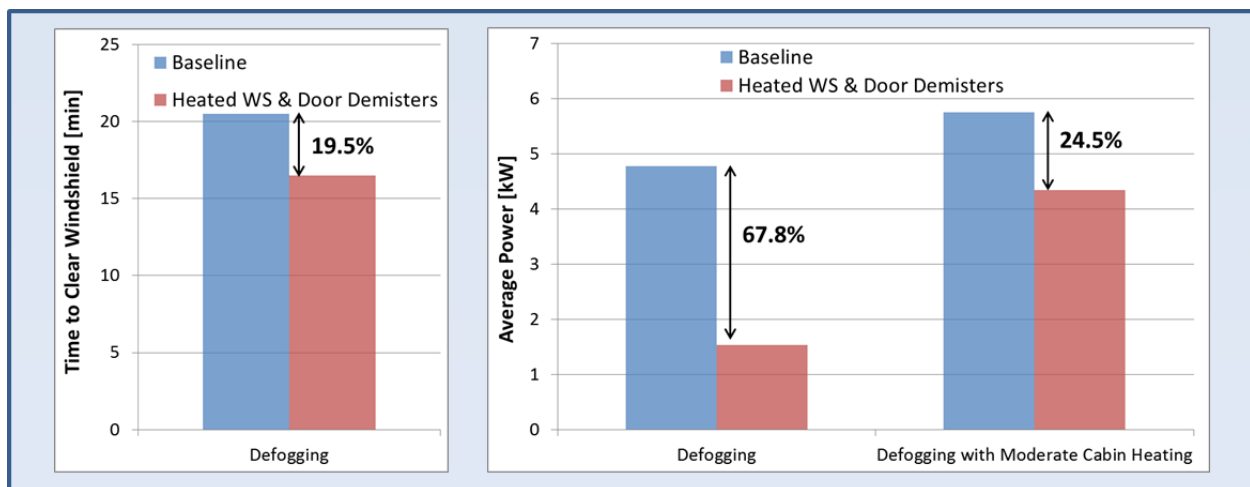


Figure II-70: Cold weather defogging performance of heated windshield and door demisters compared to baseline

Candidate Thermal Load Reduction Technology Go/No-Go Decision Matrix

Data collected during both cold weather and warm weather Phase I testing were used as the primary method for completing the Phase I Go/No-Go decision matrix provided in Figure II-71. Technologies that will be integrated into the Phase II complete thermal load reduction system are highlighted in green.

Candidate Technology	Transient Improvement	Steady-State Improvement	Go/No-Go for Phase II
Glass Package A	24 %	5 %	No-Go
Glass Package B	33 %	9 %	No-Go
Glass Package C	43 %	13 %	Go
Ventilated/Cooled Seats	25 to 46 % (occupant specific)	10 to 17 % (occupant specific)	Go
Solar Reflective Paint	5 %	16 %	Go
Heated Surfaces	-1 to -2% (occupant specific)	29 to 59 % (occupant specific)	Go
Heated Windshield & door demisters	20 % improvement in time-to-clear 25 - 68 % estimated energy savings dependent on cabin heating settings		Go

Figure II-71: Go/No-Go decision matrix for selection of technologies for Phase II thermal load reduction package

Conclusions

Through collaboration between NREL and the project partners, Phase I individual thermal load reduction technologies were designed, manufactured, and evaluated. Two vehicles were instrumented for both cold and warm weather testing at NREL's test facility, and test methods were developed to capture the performance of all technologies. Three solar control glazings, solar reflective paint, and ventilated/cooled seats were evaluated in warm weather conditions. Heated surfaces, and a heated windshield combined with door demisters were evaluated in cold weather conditions. Glass package C, ventilated/cooled seats, solar reflective paint, heated surfaces, and heated windshield and door demisters were selected for Phase II integration. While glass packages A and B showed significant energy savings over the baseline for cooling, glass package C was selected as the top performer.

During FY16, Hanon Systems evaluated the baseline performance of the 2016 Hyundai Sonata PHEV climate control system, providing valuable data necessary for HVAC system model development and validation to experimental data. In addition, NREL completed the development of vehicle and HVAC system models for use in future Phase II national-level analysis tasks.

Finally, NREL and project partners successfully transitioned from *Phase I: Technology Design and Development* to *Phase II: Technology Integration and Validation with the completion of the Phase I candidate technology Go/No-Go decision matrix and initiation of Phase II technology integration*. With continued collaboration between NREL, HATCI, PGW, Hanon Systems, Sekisui, PPG Industries, and Gentherm, the project aims to complete Phase II of the project in FY17. Phase II technology integration and complete system vehicle performance evaluations will be led by HATCI, providing experimental results in hot and cold field conditions, as well as controlled climate chamber testing. In addition, NREL will perform an analysis to estimate the EV range impact of the complete thermal load reduction package at the national level.

II.7.C. Products

Presentations/Publications/Patents

1. Kreutzer, C., Rugh, J. "Design and Implementation of a Thermal Load Reduction System in a Hyundai PHEV." Poster presentation at U.S. Department of Energy Vehicle Systems Simulation, Integration and Testing Annual Merit Review, Arlington, VA, June 8, 2016.

II.7.D. References

1. United States Department of Energy. "EV Everywhere Grand Challenge Blueprint." January 31, 2013.
2. Rask, E. "Argonne National Laboratory Advanced Powertrain Research Facility Data." Presentation at the Vehicle Systems Analysis Technical Team (VSATT) meeting, April 2, 2014.
3. Jeffers, M.; Chaney, L.; Rugh, J. "Climate Control Load Reduction Strategies for Electric Drive Vehicles in Warm Weather." SAE Technical Paper 2015-01-0355, 2015, doi: 10.4271/2015-01-0355.
4. Jeffers, M.; Rugh, J. "Electric Drive Vehicle Climate Control Load Reduction." Presentation at 2015 Department of Energy Vehicle Technologies Office Annual Merit Review, June 9, 2015, Arlington, VA.
5. Rugh, J. "Electric Drive Vehicle Climate Control Load Reduction." Vehicle and Systems Simulation and Testing 2014 Annual Progress Report.
6. Rugh, J.; Chaney, L.; Lustbader, J.; Meyer, J.; Rustagi, M.; Olson, K.; Kogler, R. "Reduction in Vehicle Temperatures and Fuel Use from Cabin Ventilation, Solar-Reflective Paint, and a New Solar-Reflective Glazing." SAE Paper 2007-01-1194. Presentation at the 2007 SAE World Congress, April 16-19, 2007, Detroit, MI.
7. Dieck, R.H., Steele, W.G., Osolsobe, G. Test Uncertainty. ASME PTC 19.1-2005. New York, NY: American Society of Mechanical Engineers. 2005.

II.8. Unitary Thermal Energy Management for Propulsion Range Augmentation [DE-EE0006840]

Sourav Chowdhury, Principal Investigator

MAHLE Behr Troy Inc.
350 Upper Mountain Road
Lockport, NY 14094
Phone: (716) 439-2799; Fax: (716) 439-3168
E-mail: Sourav.Chowdhury@us.mahle.com

John Jason Conley, DOE Program Manager

National Energy Technology Laboratory
3610 Collins Ferry Road
P.O. Box 880
Morgantown, WV 26507-0880
Phone: (304) 285-2023
E-mail: John.Conley@netl.doe.gov

Start Date: November 1, 2015
End Date: September 30, 2016

II.8.A. Abstract

Objectives

- To design a unified, flexible, robust and efficient thermal management system which reduces the load on the vehicle traction battery, and therefore, increases the electric propulsion range of a state-of-the-art EV in heating ambients with a specific goal of 15% range improvement at -10C.
- To positively impact the environment by lowering refrigerant usage by about 50%.
- To design the system comprehending the packaging restrictions, long-term durability and manufacturing requirements already established in the automotive industry.

Accomplishments

- A major accomplishment during this period is installation of the braze furnace and verification of the process parameter capabilities per design.
- A selection of material for flux-free brazing was made from laboratory trial runs.
- Many braze runs were conducted to produce flux-free and fluxed heat exchanger parts. While flux heat exchangers were pressure-tested and ready to use in the system tests, flux-free parts require further development. Several parameters for flux-free brazing were established.
- Proof-of-concept Multi-Mode Flow Controller (MMFC) design was completed and tested. Go-No-go criteria set forth for proof-of-concept version were passed with demonstration of valving in all modes of UTEMPRA.
- Significant improvements were made to eliminate leakages from hot to cold loops during certain modes and pump rates observed with the proof-of-concept MMFC hardware. These changes improve the function as well as commercial cost of the controller.
- UTEMPRA bench system testing plan is completed including plan for hardware upgrade of NREL test loop and test matrix development.
- NREL model of UTEMPRA system has been improved and tested for different system modes. NREL model was also used to understand the effect of possible leakage from high temperature to low temperature loops - the results were used to influence the MMFC design.
- System control work has been initiated by MAHLE with assistance from FCA.

Future Achievements

- MMFC finalized prototype will be made for the vehicle.
- NREL will conduct bench verification tests of UTEMPRA system with assistance of MAHLE. MAHLE will provide all necessary parts (heat exchangers, compressor, pumps and expansion valve) and NREL will provide upgraded system hardware.
- MAHLE will complete development of the control logic and UTEMPRA controller hardware.
- Fiat 500e vehicle will be outfitted with UTEMPRA system hardware and controller.
- Fiat 500e vehicle will be tested in the MAHLE climatic wind tunnels in various simulated weather conditions and control parameters will be adjusted.
- FCA will perform the range verification testing of the UTEMPRA vehicle to confirm if the objective of the project is met.
- MAHLE will continue to develop flux-free brazing process for UTEMPRA heat exchangers.

II.8.B. Technical Discussion

Background

Grid Connected Electrical Drive Vehicles (GCEDEV) are finding their limited and weather-dependent drive range, higher cost and limited battery life as the key hurdles to achieving wide consumer acceptance. There is a strong need to reduce the significant energy drain and resultant drive range loss due to auxiliary electrical loads of which the climate control is the predominant one. Studies show that thermal sub-systems together can reduce the drive range by as much as 40% under cold ambients such as below -10C. Currently, this heat is generated purely using resistive heating. Regaining a part of this range would significantly improve the attractiveness of electric vehicles (EVs) among consumers. This project develops a unifying strategy that satisfies diverse thermal and design needs of the auxiliary loads in EVs. This strategy will address the issues related to long term durability, robustness and mass manufacturing and cost.

Introduction

The UTEMPRA system comprises a semi-hermetic refrigeration loop and a coolant network for thermal energy distribution and waste energy harvesting. The refrigeration loop, shown schematically in Figure II-72 consists of an electric Compressor, a Thermostatic Expansion Valve (TXV), a Liquid-cooled Condenser (LCC) and a Chiller, latter two have the same function as the condenser and the evaporator in a traditional refrigeration loop. Instead of exchanging heat with air, these heat exchangers exchange heat with coolant and, therefore, act as sources of hot and cold coolant streams.

The coolant network utilizes two coolant pumps and valve arrangements that help distribute the energy to the vehicle HVAC system to and other thermal loads (battery and power electronics etc.). In the Cooling Mode, the cold coolant is conveyed from the chiller to the HVAC Cooler for cabin cooling and dehumidification. When needed, after the Cooler, this same coolant stream can be directed to cool the ESS. A Front-end Heat Exchanger (FEX) rejects the heat from the hot coolant coming from LCC to the ambient. In the Heating Mode, the hot coolant from LCC is directed to an HVAC Heater for cabin heating. Downstream of the HVAC Heater, this coolant can be directed to the ESS to maintain its temperature at normal levels.

Further, the since power electronics produce waste heat, the coolant from LCC can pick-up this heat on its way to the HVAC heater thereby re-using the waste energy and improving the EV range. Also, in this mode, the cold coolant stream is directed to the FEX to absorb energy from the ambient. Therefore, the Cooling Mode is akin to the standard A/C operation while the Heating Mode is the Heat Pump (HP) mode. The heat exchangers, pumps and compressor will be sized to meet the full thermal needs of the vehicle.

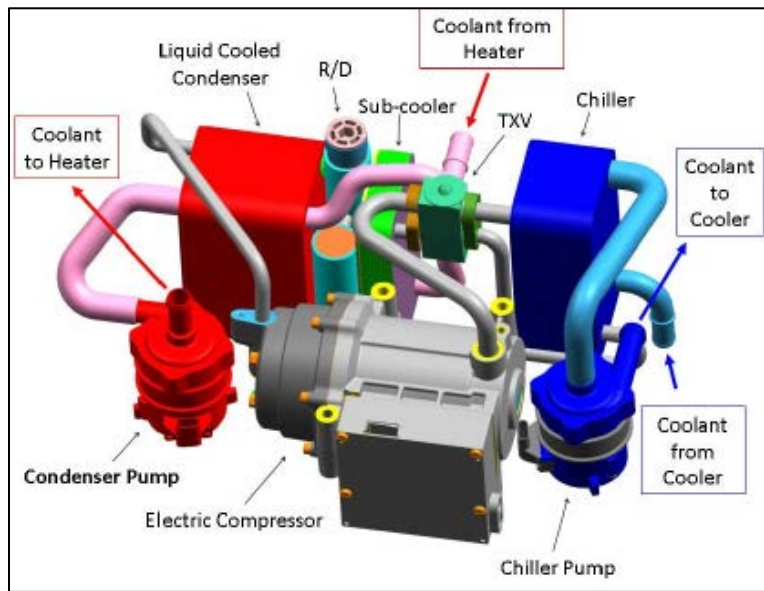


Figure II-72: Schematic of a sample configuration of the UTEMPRA refrigerant loop

With its unique flexibility in design and integration of the coolant architecture, the UTEMPRA system significantly simplifies and unifies the thermal management system in the EVs. It replaces the separate Condenser and a low temperature Radiator in the vehicle front-end with a single heat exchanger, thereby increasing its capacity and effectiveness due to higher available air pressure head. Further, it eliminates the need for separate refrigeration and/or coolant loop for the Energy Storage System (ESS) and power electronics & electric motor (PEEM) cooling and thereby significantly reduces the total refrigerant charge, pumping power, and overall system mass and cost. In summary, the UTEMPRA system serves as a thermal ‘platform’ within the EV architecture as it enables other future thermal & electrical load management strategies such as vehicle idle-stop energy savings, phase-change material (PCM) -based thermal storage, etc.

Approach

The GCEDV identified for this study is Fiat 500e all-electric vehicle. There are three thermal loops present in this vehicle that need to be combined into the UTEMPRA system: (a) Cabin air conditioning loop (b) Battery heating/cooling loop (c) Power electronics and electric motor cooling loop. This vehicle has a dual-purpose refrigerant vapor compression loop for cabin air cooling and providing active cooling to traction battery via a refrigerant-to-coolant heat exchanger (Battery Chiller). The vapor compression loop runs R-134a refrigerant and has an electric compressor, a standard refrigerant-to-air evaporator and standard TXV. Heating of the cabin air is achieved using a 5kW PTC-based electric air heater located in the HVAC module. In addition to being actively cooled by the Battery Chiller, the battery is also actively cooled by coolant circulating in a loop between the battery and a front-end battery radiator receiving forced ambient air flow across it. Figure II-73 below is a schematic of the thermal loops in this vehicle.

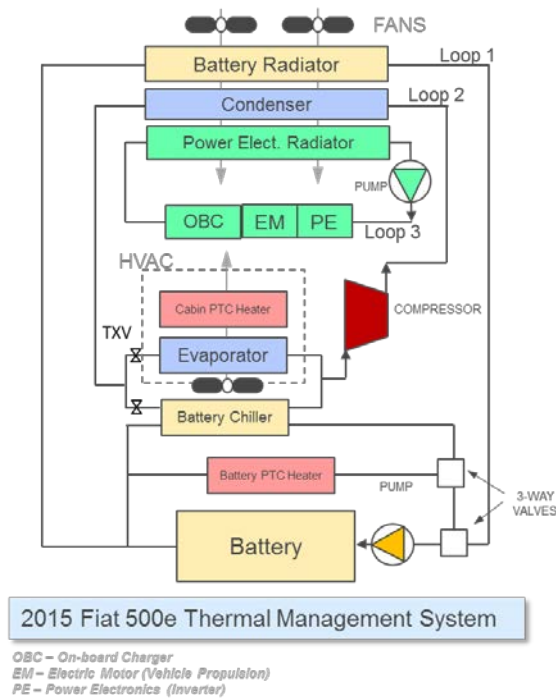


Figure II-73: Thermal management of the Fiat 500e.

Based on prior experience in heat pump loop design, vehicle requirements review and initial component flow versus pressure drop testing, the full coolant and refrigerant flow loop was created (Figure II-74).

One part of the circuit is the refrigeration unit with a liquid-cooled condenser, chiller, Thermostatic expansion valve (TXV), and electric-drive compressor. The coolant flowing through the liquid-cooled condenser is always hot (50 to 65C) while that through the chiller is always cold (5 to -15C). The Multi-Mode Flow Controller (MMFC) which is a fluid manifold with integrated "on-off" valves is located in the coolant network such that the refrigerant-to-coolant heat exchangers reside on its upstream side and the components which will receive the coolant flows from them are on its downstream side.

A positive temperature coefficient (PTC) coolant heater which contains a temperature-controlled resistive heating element is required as, in extreme cold ambients (below -12C), the heat generated from heat pump mode may be insufficient or the heat pump may even be inoperable. In that case the PTC heater will be turned on to provide supplemental heat. This heat combined with the heat absorbed from the ambient by the FEX, if any available, will be ‘pumped’ up using the refrigeration unit to the hot-coolant circuit wherefrom it will be distributed to the destination components.

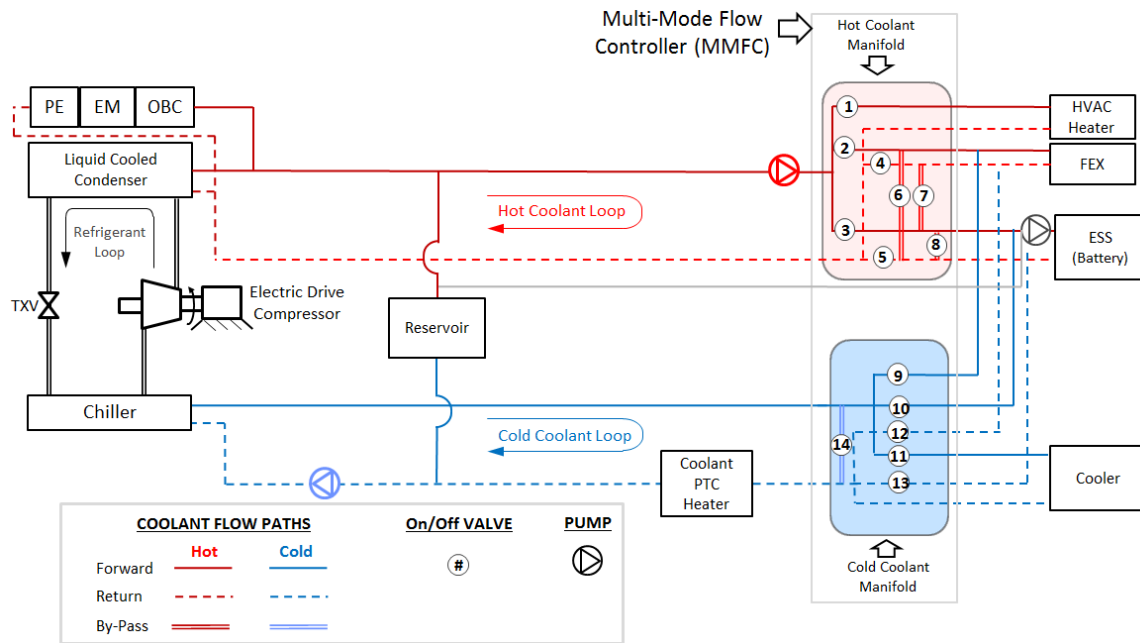


Figure II-74: UTEMPRA Coolant loop architecture

Results

The build of the controlled atmosphere braze (CAB) furnace was completed by end of December, 2015. After the completion of build activities, debug and preliminary verification activities began at the supplier’s location. Through January 2016, temperature profiles, oxygen levels, dew point and conveyor speeds were verified by the supplier culminating in the validation braze run. After successful braze run, the furnace was disassembled, painted, packed and shipped. Following this, the MAHLE Lockport facility received the shipment of furnace parts in March 2016 and installation and verification runs were completed by April 2016. Figure II-75 is a picture of the furnace during installation in Lockport.

MAHLE conducted several trial braze runs in the laboratory with a benchtop glass furnace and "T"-samples of different commercially available braze materials acquired during the period of this report. Figure II-76 indicates the benchtop furnace and the "T" sample outcomes. The benchtop furnace was capable of limiting the free-oxygen in the braze atmosphere to desirable levels. Supplier C flux-free braze material was selected eventually, and MAHLE is conducting full braze trials with heat exchanger components made with this material.



Figure II-75: Controlled atmosphere braze furnace installed in MAHLE Lockport facility

Laboratory Glass Furnace Tube Glass Research Furnace used for fluxfree material development and evaluation	Supplier A	Supplier B	Supplier C
	<p>Notes:</p> <ol style="list-style-type: none"> 1. Fillet size is very small 2. Surface melting is not sufficient 3. Good surface wetting is not noticed 4. Surface discoloration is not noticed 5. Fillet formation between bottom AA3003 and brazing sheet is not noticed 	<p>Notes:</p> <ol style="list-style-type: none"> 1. Fillet size is desired 2. Surface melting is sufficient 3. Good surface wetting is noticed 4. Surface discoloration is noticed 5. Fillet between bottom AA3003 and brazing sheet is not uniform 6. 3 minutes dwell at peak brazing temperature is needed for surface activation 	<p>Notes:</p> <ol style="list-style-type: none"> 1. Fillet size is desired 2. Surface melting is sufficient 3. Good surface wetting is noticed 4. Surface discoloration is noticed 5. Fillet between bottom AA3003 and brazing sheet is uniform 6. Surface activation occurred before peak temperature achieved

Figure II-76: MAHLE Benchtop glass furnace (left) and T-sample braze outcomes.

NREL and MAHLE collaborated to improve the CoolSim simulation model with calibrated heat exchanger models. NREL verified the baseline cabin model by comparing the results of the wind tunnel tests with simulation results (Figure II-77). NREL also verified the mode operations of the UTEMPRA system with CoolSim model. Further work on this will be conducted as we develop the control logic of the system.

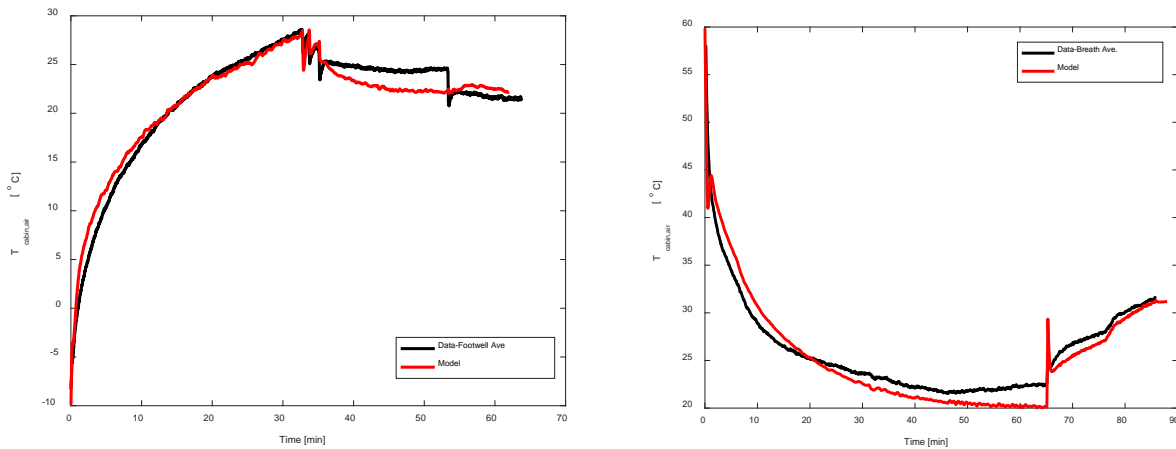


Figure II-77: Comparison of the tunnel test data (Baseline) and CoolSim cabin simulation results: Left - warm-up; Right - cool-down cases

During the trial runs of the MMFC, leakage of coolant via MMFC valves was identified as an issue in the proof-of-concept design. MAHLE worked with NREL to understand the impact of leakage on the performance of the system especially in cooling mode. Based on past experience in testing, MAHLE identified a range of coolant leakage (0.1 to 0.3 LPM) through the common reservoir that may start to affect the performance and system capacity. The UTEMPRA model was used to estimate the effect of coolant leakage in that range between high and low temperature loops on the system performance. The model was updated to include a preset leakage rate. The leakage was modeled through valves in the coolant network. The analysis showed significant performance degradation if leakage is allowed and helped in evaluation and selection of valves and manifold design (Figure II-78).

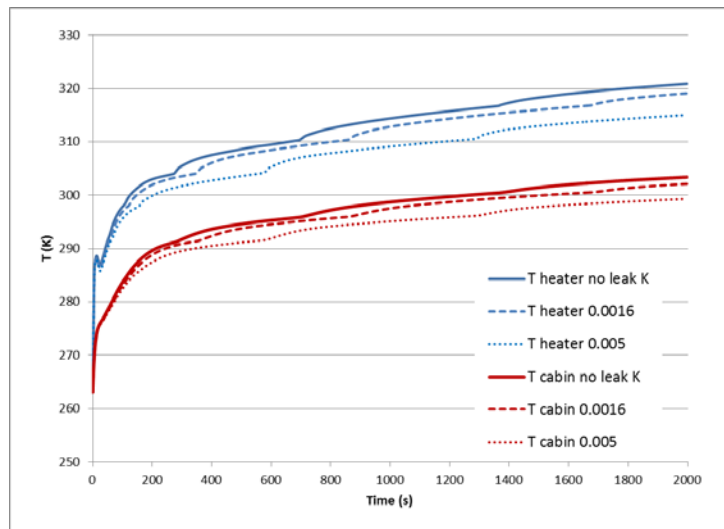


Figure II-78: Effect of leakage (numerical values are coolant leakage mass flow rates – kg/sec) level on heater air discharge temperature

Norgren demonstrated the MMFC proof-of-concept design in a coolant flow bench setup. The MMFC demonstration passed the function and cost criteria for project Year 1 Go-No-go in October 2015. Later, further tests at different mode and pump settings indicated that leakage of coolant was occurring from the high temperature to the low temperature coolant loops in the UTEMPRA system. Norgren investigated the possibility and designs of check valves to mitigate the leakage issue. While check valve solution was functionally effective, the design was not commercially viable and somewhat reduced the system efficiency by adding constant coolant pressure drop to the system. MAHLE and Norgren came up with a different strategy to ensure leakage is prevented without extra pressure drop. During the summer of 2016, the Team worked on a

novel concept of using three-way valves to replace check valves and a number of the two-way valve solenoid operators. The concept is to utilize higher system pressure to help keep the valves shut even during the pressure unbalance situations. This prevents the valves from internally leaking when higher pressures are seen in the outlet side of the valves than on the inlet side and stops fluid from cross flowing between the hot and cold loops.

Conclusions

1. NREL modeling and past testing experience with heat pump systems indicate that the leakage of coolant in certain UTEMPRA modes will have to be eliminated to prevent loss of thermal efficiency of the system.
2. Improvements made during the extended period of braze furnace design were successful in enabling the furnace to meet the crucial parameters of the braze atmosphere.
3. In addition to controlling the furnace atmosphere dew-point and oxygen level, and choosing the correct material system, several techniques such as furnace loading, braze fixturing, etc. are found to contribute to a successful braze run. MAHLE is continuing to understand these different aspects of flux-free brazing.
4. Criteria of commercial viability influenced the improvements in MMFC design. This resulted in a novel approach to use system high pressure drop to open and close the on-off valves.

II.8.C. Products

UTEMPRA System components will be the products that are the outcome at the end of the project:
(a) Heat Exchangers (five types) (b) Compressor (c) Multi-mode Flow Controller (MMFC) (d) Control Algorithm and Software

Presentations/Publications/Patents

1. None

II.8.D. References

1. None.

II.9. Electric Phase Change Material Assisted Thermal Heating System (ePATHS) [DE-EE0006444]

Dr. Mingyu Wang, Principal Investigator

MAHLE Behr Troy Inc.
350 Upper Mountain Road
Lockport, NY 14094
Phone: (716) 439-2493
E-mail: Mingyu.Wang@us.mahle.com

David Anderson, DOE Program Manager

Vehicle Technologies Office
Phone: (202) 287-5688
E-mail: David.Anderson@ee.doe.gov

Start Date: October 1, 2013
End Date: January 1, 2017

II.9.A. Abstract

Objectives

- Thermal Energy Storage (TES) system can store sufficient thermal energy to heat the Electric Vehicle (EV) cabin for an extended period of time. Depending on the sizing of such a system, the TES can provide up to 100% of the thermal energy necessary to heat the cabin during typical commuter driving. For this project, the goal is to design and develop a prototype TES system targeting to improve the electric drive range by 20% in cold ambient conditions. The project scope includes the development of an advanced PCM (Phase Change Material) along with the component and system architecture for integration into a Grid Connected Electric Drive Vehicle (GCEDV) environment to provide cabin thermal comfort. The system performance will be demonstrated at both a bench and vehicle level.
- In operation, the TES system will incorporate a high temperature PCM that will be housed in a standalone container and will seamlessly integrate with the existing charge control architecture. Energy from the electric grid will provide the charging energy to heat the TES system while the EV is being charged at home or at an EV charge station. The TES will be heated via an electrical resistance heater during the plug-in charging cycle. An intelligent TES charge control algorithm will be implemented.
- The basis of the TES is a PCM storage unit. Innovative to this unit is that it incorporates a PCM that has up to 50% more latent heat during phase change than PCMs on the market today. Further, the storage unit will be insulated to minimize parasitic energy loss while the vehicle is parked.

Accomplishments

- System, Components Design and Development:
 - A prototype TES unit, the ePATHS PCM heat exchanger, was built and evaluated on a standalone, custom built test bench. PCM thermal storage capacity met design target. The completed bench with the TES unit was delivered to Oak Ridge National Laboratory (ORNL) for confirmation testing. A test report was issued by ORNL confirming the thermal storage capacity of the unit.
 - Resistive coolant heater was established as the final PCM thermal charging method during bench testing.
 - A major new design of PCM heat exchanger was completed. This second generation design (or GEN-2 design) allows improved outlook toward commercialization and also resolves engineering issues revealed by the initial design.

- Integration of ePATHS into Ford Focus Electric has been completed. On-vehicle software debugging and preliminary testing is ongoing.
- PCM Materials Development
 - Entropy Solutions has completed the development of the second PCM, DPT-83, with a latent heat of 340~350 J/g and a melting temperature of 83°C. Pilot scale production process has been developed and validated. Sufficient DPT-83 has been delivered to MAHLE Lockport Technical Center for thermal storage testing. This is in addition to the previously reported development of DPT-68. As such, the contract deliverable of one PCM material has been met and exceeded.
 - DPT-68 and aluminum material compatibility study has been ongoing for 7 months. Results up to date show no reason for compatibility concerns. However, the test duration is insufficient to make judgment over a 15-year vehicle life, since no accelerated corrosion test protocol is available. DPT-83 has been under test for 2 months. Initial results are good, but similar test limitation applies.
 - Commercialization study for the PCM materials has been completed. DPT-83 can be produced competitively. However, initial capital investment is required to enable its commercialization.
- Program management:
 - Milestones for BP-2 were met. DOE authorized continuation into budget period 3.
 - ePATHS was presented at 2016 Annual Merit Review.
 - DOE site visit to Lockport, NY was completed.
 - The Thermal Division of Delphi has been acquired by MAHLE. Novation for the project is in progress.
 - BP-3 project execution is behind timeline by 4 months due to PCM heat exchanger redesign and delays in DPT-83 synthesis. The project is targeted to be closed in the second quarter of 2017. A request for a no-cost extension for the project will be made to DOE.

Future Achievements

- ePATHS will be tested in climatic tunnel and on the road for range extension evaluations.
- After completion of test, Ford Focus Electric will be delivered to Ford for engineering evaluation.
- The final demonstration vehicle, Ford Fusion Energi, a PHEV, will be rebuilt with the ePATHS system and tested in climatic tunnel and on the road for range extension evaluations.
- Range extension analysis will be completed based on climatic tunnel and road testing by MAHLE, and subsequently confirmed by ORNL.
- Final demonstration to DOE.

II.9.B. Technical Discussion

Background

Climate control poses a severe challenge for battery electric vehicles (BEVs), plug-in hybrid electric vehicles (PHEVs), extended range electric vehicles (EREVs), and even hybrid electric vehicles (HEVs). Cabin heating, depending on the size of the vehicle and the environmental conditions, typically requires 3.2 to 6.5 kW of battery power at the ambient of -10°C to meet transient and steady state comfort requirements. For the larger sized electric vehicles of various genres (xEV), the required battery power may be even greater. The battery power used to generate the heating, either through a heat pump or direct resistive heating, leads to dramatically depressed driving range of xEVs. It is estimated that the range of a BEV can be reduced 50% or more, depending on the drive cycle. It is essential, therefore, to develop a reliable, cost-competitive, and more energy efficient occupant heating system that can help reduce traction battery load and maintain the vehicle electrical driving range without sacrificing occupant comfort.

Introduction

The term “Phase Change Material” (PCM) is used to describe materials that use phase changes (e.g., melting) to absorb or release relatively large amount of latent heat at essentially constant temperature. In general, when the temperature becomes warmer than the freeze point, PCMs liquefy and absorb and store heat. Conversely, when the temperature decreases, the material will solidify and give off heat to warm a medium for productive use.

The MAHLE team has been working with its project partner Entropy Solutions, a leading PCM material supplier in the industry, to custom-develop an advanced PCM material with a latent heat value equal to or greater than 350 J/g and a phase transition temperature near 85 °C (as compared with the latent heat of 334 J/g melting at 100°C for water, and the present commercial PCM latent heat of ~200 J/g), and integrate the PCM material into an innovative, self-contained system to provide charging and discharging of heat to support BEV cabin heating for passenger comfort. The ePATHS project aims to develop a light-weight, compact, and scalable TES system to meet a wide range of grid connected vehicles’ heating needs. MAHLE is working with its OEM partner, Ford Motor Company, to integrate the ePATHS system into a Ford Focus electric vehicle and a Ford Fusion plug-in hybrid vehicle to demonstrate its capability and commercial viability. The development of the ePATHS system is also supported by the analysis and testing capabilities from Oak Ridge National Laboratory (ORNL) to achieve optimization in performance, packaging, weight and other key metrics.

Approach

System Architecture Improvement

The ePATHS system was designed to store heat using power from the electric grid and release heat to warm up vehicle cabin during driving in low temperature ambient conditions. The objective was to facilitate range extension for Battery Electric Vehicles (BEV). The PCM heat exchanger is the core of the ePATHS system. It contains the PCM heat storage medium and internal heat transfer surfaces that allow heat to be added to the PCM material using hot coolant provided by a resistive coolant heater, or removed from the PCM material by circulating a lower temperature coolant stream. A pump is used to provide the pressure head for coolant circulation. Figure II-79 shows a system that also incorporates a configurable CapHX for deep heat recovery from the PCM heat exchanger.

The system of Figure II-79 has been mechanized to achieve three modes of heating: PCM discharging, energy recovery, and PTC heating, along with a fourth mode of PCM charging. An actuated configuration valve was prototyped to allow the CapHX function as a single-parallel heat exchanger attached to either the PCM loop or the PTC loop of the BEV, allowing PCM heating or PTC heating. The valve also allows the CapHX to function as two separate heat exchangers, with the front half attached to the PCM loop to preheat the incoming cold air, and the rear half in the PTC loop to allow final heating of the airstream to fulfill the requirements of cabin heating. This is known as the energy recovery mode of operation.

Improvements to the system design have been made based on the learning from the completed bench testing and vehicle trial runs. Due to the limited capability of heat to penetrate into the interior of the PCM heat exchanger from the exterior surfaces, surface heating was found to be ineffective in sustaining the required charging rate. A high charging rate would result in excessive surface heater temperature exceeding its specification. To operate safely, the heating rate had to diminish gradually to near zero as the PCM temperature rose to the high limit of the charge temperature (120°C). This increased the total charge time beyond the acceptable range. On the other hand, the method of charging by a high temperature coolant steam was found to be effective, as long as heat loss along the way to the PCM heat exchanger is minimized. With the PCM heat exchanger designed to be highly effective in transferring heat between the PCM and the coolant stream, charge rate became a non-issue.

Preliminary test runs of the ePATHS system in the Ford Focus Electric vehicle revealed coolant migration between the vehicle PTC heating system and the ePATHS heating system. The two coolant systems communicated during operating mode transitions. Replacing the PTC side check valve with an actuated isolation valve allowed the system to operate properly.

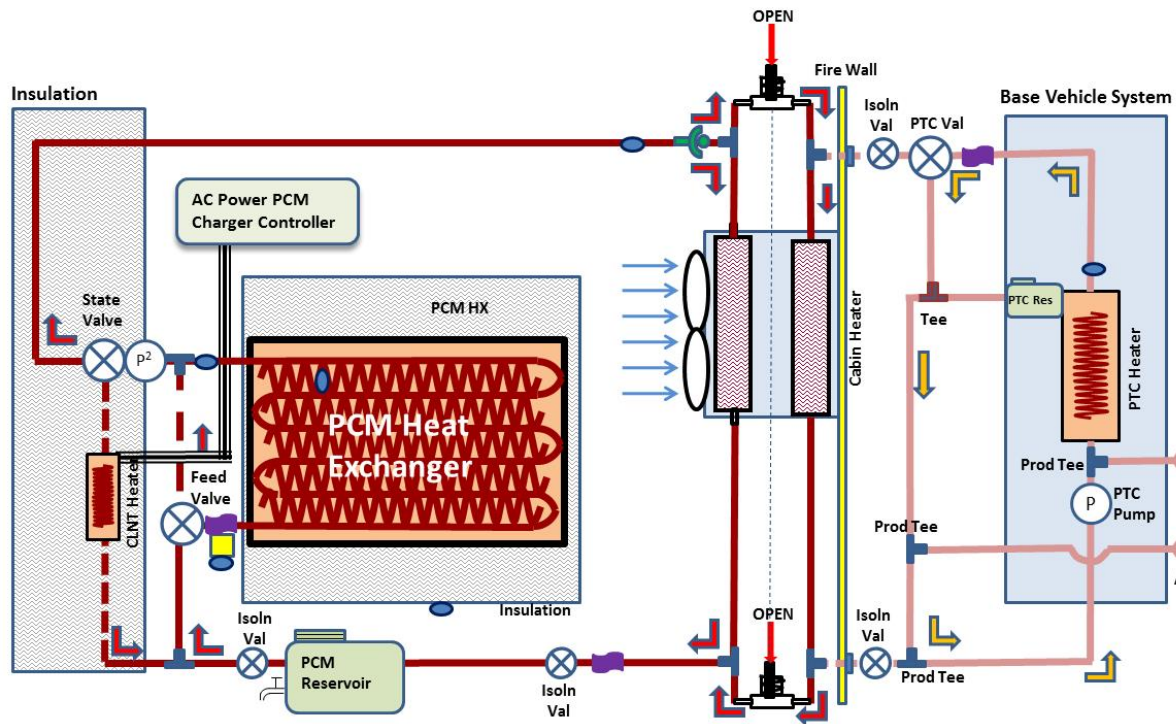


Figure II-79: Improved ePATHS System Design

Phase Change Materials Development

The main progress in PCM materials development is in the synthesis of DPT-83, which has a phase change temperature of 83°C and a latent heat in the range 335~350 J/g, depending on the purity of the product. Compared with DPT-68 synthesized during the prior reporting period, DPT-83 is more difficult to produce in the laboratory. A great deal of effort was invested in streamlining the synthesis pathways and the determination of a proper catalyst. The separation and purification of the desired product was proven to be equally challenging. However, all the challenges were overcome and sufficient amount of product was produced for the final demonstration vehicle.

A commercialization study was carried out for the DPT-83. It was determined that competitive pricing may be achieved to supply to the automotive market. The barrier to commercialization is in the initial capital investment. A dedicated production facility needs to be built to achieve lowered price.

Table II-13: Sample and Exposure Time for DPT-68 Material Compatibility Study

Sample Name	Start Date	Total Exposure Time (Hrs.)	Total Exposure Time (≈Months)
Virgin AA3003_1	02/19/2016	4992	7
Virgin AA3003_2	02/19/2016	4992	7
Dry Flux Sample_1	03/18/2016	4296	6
Dry Flux Sample_2	03/18/2016	4296	6
Wet Flux Sample_1	03/18/2016	4296	6
Wet Flux Sample_2	03/18/2016	4296	6

Preliminary indications show that DPT-83 and DPT-68 are materially compatible with aluminum heat exchangers. For the DPT-68 material, a compatibility study has been maintained uninterrupted with several

prepared aluminum coupons (as shown in Table II-13) soaked in 150°C melted material for the last 7 months. No meaningful material loss or gain was detected in the coupons. While it is optimistic that there should be good material compatibility, it is very difficult at the moment to be conclusive due to the lack of an accelerated test method. Until such a test is identified and carried out, the risk of material loss after an extended period of time cannot be ruled out.

A similar compatibility study for the DPT-83 was also initiated. At the moment, the age of the test is about two months old.

PCM Heat Exchanger Development

The PCM thermal storage heat exchanger is a key component of the ePATHS system. Figure II-80 shows the first generation design of the full sized PCM heat exchanger. The GEN-1 design is based on automotive radiator technology. Multiple brazed radiator units were assembled and encased in an aluminum shell and an insulation jacket. The radiators' finned side forms the PCM containing cavity along with the encasing shell. The coolant tubes and distribution tanks provide the structural support for the extended heat transfer surfaces. Through design optimization, good heat transfer was achieved between the coolant stream in the coolant tubes and the PCM in contact with the fins.



Figure II-80: GEN-1 Radiator-Type PCM Thermal Storage Module

While the heat transfer performance of the GEN-1 design was quite satisfactory, commercialization issues were identified. The design was not amenable to mass production at low cost as several steps of manual assembly were required. Along with some design considerations to improve heat transfer performance and structural integrity, a plate-type heat exchanger was pursued for the GEN-II design.

The plate-type PCM heat exchanger design bears similarity with the automotive chillers and oil coolers. A pair of plates stacked back-to-back forms the PCM containing chamber, and stacking two of the pairs together further forms a coolant flow channel. Necessary heat transfer enhancement on both the coolant side and the PCM side has been designed in.

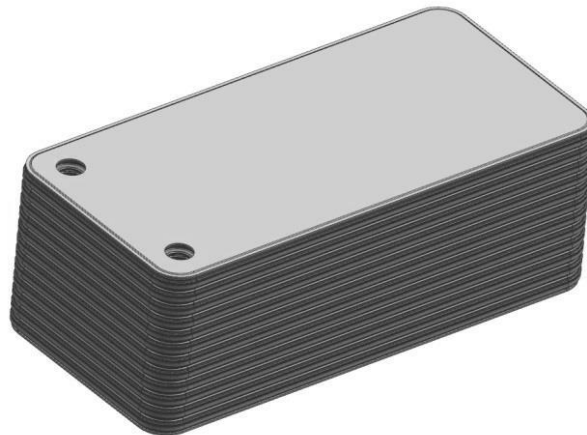


Figure II-81: Plate-Type PCM Thermal Storage Module

The plate-type PCM heat exchanger design is intended to be modular. At the individual module level, dimensional flexibility is achieved by changing the number of plates assembled into the module. The largest number of the plates is only limited by the brazing capability of the production facility and takt time requirement. However, in the other two dimensions, flexibility is limited once the stamping tooling design is frozen.

To obtain a large enough PCM thermal storage system to meet the design objective of 20% range extension of the present project, the so-called modular construction technique was used. Multiple cell-level modules out of the braze oven are plumbed together to form a super storage system capable of storing enough PCM material and heat to meet the project specification. Parallel and serial plumbing of the units are used to optimize coolant flow distribution and pressure drop.

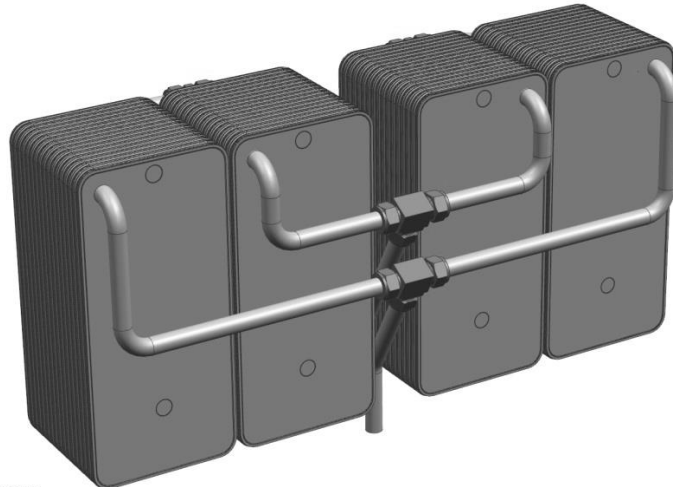


Figure II-82: PCM Thermal Storage with Four GEN-2 Modules with Parallel-Serial Plumbing

Preliminary bench and vehicle testing with the GEN-2 PCM heat exchanger show that all the design criteria have been met. The design demonstrated enough flexibility to allow services on HEVs and PHEVs, which require relatively smaller amount of PCM for thermal storage, and on BEVs, which require larger amount of PCM. The product can also serve other thermal storage needs on conventional vehicles as well as in adjacent markets such as residential and commercial markets.

GEN-1 PCM Heat Exchanger Bench Test

Bench testing of GEN-1 ePATHS thermal storage was completed at MAHLE Lockport Technical Center in October 2015. Subsequently, the test bench was shipped to Building Technologies Research and Integration Center (BTRIC) at the Oak Ridge National Laboratory (ORNL) for confirmation testing. Figure II-83 shows the bench constructed for this project.

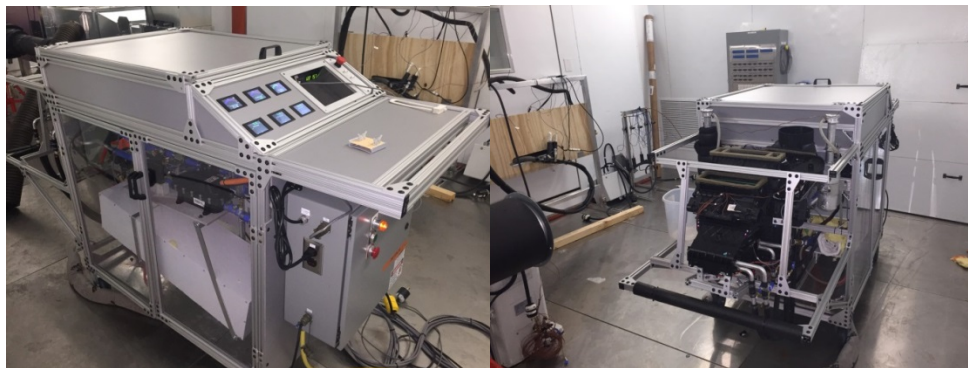


Figure II-83: Photos of the ePATHS Bench Prototype Hardware in ORNL's BTRIC Test Chamber

The ePATHS bench tests assessed three main aspects of operation of the device. (1) The time and energy needed to fully charge the PCM heat exchanger; (2) The energy output by the PCM heat exchanger during Mode 1 (PCM heating only) and Mode 2 (PCM heating with transition to PTC heating) operations; (3) The performance of the insulation system for the PCM thermal storage. The discharge evaluation is the primary means to assess the ePATHS' capability to maintain cabin comfort.

The bench system was equipped with two separate PCM heating systems, as described in the 2015 Annual Progress Report. The surface heating method, while accurate in terms of energy accounting, failed to meet the charging time requirement (< 2 hours). The alternate charging method of hot coolant PCM heating worked very well and was designated the mainstream design for PCM charging. The hot coolant PCM heating method takes advantage of the high exchange effectiveness between the coolant stream and the PCM, which as a basic requirement of the ePATHS specifications.

The total amount of thermal energy storage in the PCM heat exchanger was projected to be 12.7 MJ between the temperatures of 25°C and 120°C based on the latent heat value of 340 J/g. The total energy also includes the sensible energy of the PCM, aluminum, and coolant. The electrical energy input during the charging process was mathematically integrated and found to be 12.2 MJ (as shown in Table II-14). ORNL testing confirmed MAHLE Lockport Technical Center's energy storage evaluation.

Table II-14: PCM Charging Capacity Validation

Cases	Units	Energy_120	Energy_60	Energy_25	Heat_120~60	Heat_25~60	Total
Projection with h-340 j/g	Mj	15.8	6.4	3.2	9.5	3.2	12.7
	kWh	4.40	1.77	0.88	2.64	0.88	3.52
Surface Heater	Mj	15.0	6.9	2.8	8.1	4.1	12.2
	kWh	4.17	1.93	0.78	2.24	1.15	3.39

The thermal loss evaluation was performed by charging the PCM to 100°C and soaking the PCM heat exchanger in a temperature controlled ambient chamber. Both the ambient temperature and the PCM temperature were logged for a period of 15 hours. Since the temperature change is in the sensible range, energy loss was easily calculated. As shown in Table II-15, ORNL's soak test showed a total energy loss of 8% over an eight-hour working day under the ambient condition of -10°C. In the lower PCM temperature range, such as below the phase change temperature, the heat loss was estimated to be around 4% over an eight-hour period. The ePATHS project design target was a 10% loss over an eight-hour period.

Table II-15: Thermal Loss Evaluation during Cold Soak (Cooling from 100°C to 72.6°C)

Temperature Change (°C)	27.4
Time (hr)	14.8
Total Energy Storage, kJ (120-50°C) for 20kg PCM	11418
Energy Loss, kJ (Based on 18.2 kg Actual PCM mass)	1701
Percent Energy Loss/Hour	1 %
Percent Loss Expected During 8 Hour Cold Soak	8 %

Conclusions

The MAHLE project team and its partners have taken the ePATHS project through the bench testing phase to vehicle demonstration phase during the past year. This was enabled by progresses in PCM material synthesis

and PCM heat exchanger engineering development. Major advance was made in the synthesis and pilot production of the DPT-83 PCM material, with sufficient amount delivered to MAHLE Lockport Technical Center for application validation. A fundamental redesign of the PCM heat exchanger was completed and validated that will provide strong support for its commercialization. The GEN-2 PCM heat exchanger is more reliable, less costly to fabricate, and more flexible to configure for both high capacity and low capacity applications. The ePATHS system has been integrated into Ford Focus Electric vehicle. Thermal performance testing and driving range evaluation is ongoing in the climatic tunnels.

II.9.C. Products

Presentations/Publications/Patents

1. LaClair, T., Gao, Z., Abdelaziz, O., Wang, M. et al., "Thermal Storage System for Electric Vehicle Cabin Heating - Component and System Analysis," SAE Technical Paper 2016-01-0244, 2016, doi: 10.4271/2016-01-0244.
2. Wang, M., Wolfe, E., Craig, T., Laclair, T. et al., "Design and Testing of a Thermal Storage System for Electric Vehicle Cabin Heating," SAE Technical Paper 2016-01-0248, 2016, doi:10.4271/2016-01-0248.

II.9.D. References

1. N/A

SUPERTRUCK

II.10. Volvo SuperTruck [DE-EE0004232]

Pascal Amar, Principal Investigator

Volvo Technology of America
7825 National Service Road
Greensboro, NC 27409
Phone: (336) 895-5256
E-mail: pascal.amar@volvo.com

Roland Gravel, DOE Program Manager

Vehicle Technologies Office
Phone: (202) 586-9263
E-mail: Roland.Gravel@ee.doe.gov

Start Date: June 2011
End Date: June 2016

II.10.A. Abstract

Objectives

- Demonstrate 50% increase in freight efficiency [ton-mi/Gal] compared with a ‘best in class’ MY 2009 highway truck.
- Demonstrate 50% brake thermal efficiency on an engine dynamometer.
- Demonstrate pathway towards 55% brake thermal efficiency.

Accomplishments

- Demonstrated 88% increase in freight efficiency [ton-mi/Gal] compared with a ‘best in class’ MY 2009 highway truck, measured on-road over a variety of road profiles, surpassing the 50% goal.
- Demonstrated an advanced powertrain capable of 50% brake thermal efficiency on an engine dynamometer, and tested the same engine on-road in the demonstration vehicle.
- Presented pathway to engine concept exceeding 56% brake thermal efficiency based on simulations and experimental data, exceeding the initial goal.

Future Achievements

This project ended in FY 2016, however Volvo will continue to evaluate potential freight efficiency improvements using the demonstrator vehicle as a research platform.

II.10.B. Technical Discussion

Background

SuperTruck is a 5-year research and demonstration program with the objective to identify technologies that could significantly reduce fuel use by Class 8, long haul trucks. The program focuses equally on diesel engine efficiency and vehicle efficiency.

Introduction

Volvo's SuperTruck project was divided into 2 main phases. The first phase developed a concept evaluation vehicle which was used to demonstrate and validate candidate technologies for improved freight efficiency during 2013. The second phase delivered a final SuperTruck demonstrator comprising the technologies selected to exceed 50% improvements in freight efficiency compared with the 2009 baseline.

Phase I was completed in late 2013, when the technologies deployed on the concept evaluation vehicle were tested on-road and chassis dynamometer and demonstrated 43% freight efficiency improvements and 41% fuel economy improvement. The powertrain installed in the chassis had previously demonstrated 48% Brake Thermal Efficiency in engine test cell.

Phase II was completed during this reporting period, with the final testing of the demonstrator equipped with a 50% BTE capable powertrain. The complete vehicle demonstrated an average freight efficiency of approximately 188ton-mile/gal i.e. an 88% improvement in freight efficiency compared with the MY 2009 baseline, thereby exceeding the program goal of 50% improvement.

Approach

The SuperTruck project developed multiple concepts simultaneously in order to achieve and exceed the aggressive efficiency goals of the program. The engineers faced a significant challenge to define the optimal combination of powertrain, aerodynamics and cooling package in the limited time of the project. In order to facilitate concept selection and design iterations the Volvo team used complete vehicle simulations to gain quantitative insight into trade-offs or synergies between the new technologies. This approach yielded a fully integrated, highly efficient complete vehicle. This simulation platform was also used to size the hotel mode system based on customer trucks usage data, and it helped the software team optimize the predictive energy management controller. The results of this approach are discussed in the following section.

Results

Powertrain Development

The complete powertrain system, including the complex Rankine Waste Heat Recovery (WHR) system, demonstrated 50% BTE on an engine dynamometer before it was installed into the demonstration vehicle. Road testing confirmed stable operation of the WHR system which proved capable of producing power on a flat highway cycle despite the low average road load and exhaust temperatures. The powertrain performed well during the entire SuperTruck road test campaign, delivering the expected fuel economy improvements and driving performance.

Several components included in this powertrain (turbo compound, wave piston, fuel injection) were transferred to an industrialization project and are scheduled to be available in all 11L and 13L engines sold by Volvo in North America starting 2017.

Parasitic Loads

The development of more efficient accessories occurred across multiple work packages in the project. We evaluated many advanced concepts e.g. variable power steering pumps, electronic controls, variable speed engine fan, clutched air compressor, variable oil and water pumps, externally regulated alternators, and electric A/C compressors. Most of these are installed on the SuperTruck demonstrator. Predictive controls are also used to minimize the fuel economy impact of belt-driven auxiliaries.

Lightweight

Some technologies included in this project save fuel but increase weight, thereby reducing payload capacity. A multi-disciplinary approach was used to offset this negative impact and demonstrate further improvement in payload capacity without sacrificing existing attributes such as safety, durability, driver environment, etc. The

team evaluated new materials, designs or manufacturing concepts for use in all parts of the truck, including the potential to use more environmentally friendly materials or to improve material properties. The Net result of all weight additions and reductions on the demonstrator vehicle was 3, 200 lbs. The largest contribution to this weight reduction came from a joint development with Metalsa of a chassis ladder assembly 45% lighter than the baseline with equal or better performance.

Complete Vehicle Aerodynamics

Aerodynamic optimization of the tractor and trailer was a key contributor to overall project freight efficiency improvement, and the team achieved an impressive 40% reduction of the aerodynamic drag for the complete vehicle. The team strived to apply the lessons learned from this project, which resulted in new SmartWay 'elite' trailer aerodynamic packages launched in 2014 and improved roof, bumper and chassis fairings available on Volvo highway tractors starting 2015.

Idle Reduction

This task was divided into four main sub-tasks: 1) Engine-off energy management system, 2) Energy storage system, 3) Climate management system, and 4) Thermally efficient cabin. The resulting concept is a fully integrated hotel load system which provides seamless operation whether the engine is running or off. The energy is stored in energy-dense batteries that are recharged using solar energy produced by photovoltaic panels on the roof of the cab and electricity generated by alternators during deceleration to take advantage of free kinetic energy. The cooling is performed using a dual-zone, 24V air conditioning system to cool the bunk and driving areas selectively when possible. Heating is done with a conventional fuel-fired heater integrated into the cab's climate control system. In order to minimize the energy required to keep the driver cool the cabin insulation was enhanced and windows were removed in the bunk and replaced by lights powered by the roof-mounted solar panel to simulate daylight. The solar panel also powers an exhaust fan which removes hot air from the ceiling of the cab when internal temperature necessitates.

Pathway to 55% Brake Thermal Efficiency

In addition to delivering a successful result for this objective, Volvo and our University partners were able to assist close to two dozen graduate and undergraduate students with funding in support of the work they provided. Cutting edge combustion modeling, fuel mechanism research, and engine simulations were developed in the program and have advanced the industry understanding of these topics.

Conclusions

During this fiscal year the team focused on validation of the technologies integrated into the concept vehicle and demonstration of its performance. A closed track evaluation was performed in Uvalde TX at the Continental proving grounds on the 8.2 mi oval. During four days we compared various configurations of camera/mirrors and accumulated approximately 500 test miles. The fuel economy improvement, averaged over multiple laps, was 69%. Combined with a measured 10% payload increase this yields a freight efficiency of 188 ton-mi/Gal, i.e., an 88% improvement over the MY 2009 baseline. A real world route was also included in the validation tests. The trip consisted of mainly interstate with some secondary roads and city driving. Traffic conditions ranged from highway cruise speeds to traffic jams, and the tests included stops for food and fuel typical of normal truck driving. During the highway tests the SuperTruck showed a fuel economy improvement greater than 70% over baseline. All vehicle systems (HVAC, Electrical, Cooling, etc.) performed flawlessly during verification, despite the vehicle having limited miles of shake-down reliability testing.



Figure II-84: Volvo's SuperTruck concept vehicle
Source: Volvo Technology of America

Overall the truck has accumulated over 5,000 miles of fuel economy testing to date with no hardware failures. It has demonstrated consistent improvements in fuel economy, its drivers are satisfied with the performance, and it generates a lot of questions and excitement at every truck stop during on-road test campaigns.

II.10.C. Products

Presentations/Publications/Patents

1. None

II.10.D. References

1. None

TIRES

II.11. A System for Automatically Maintaining Pressure in a Commercial Truck Tire DE-EE0005447

John Maloney, Principal Investigator

The Goodyear Tire and Rubber Company
200 Innovation Way
Akron, OH 44316-0001
Phone: (330) 796-5146
E-mail: john.maloney@goodyear.com

David Ollett, DOE Program Manager

Office of Energy Project Management
National Energy Technology Laboratory (NETL)
626 Cochrans Mill Road
Pittsburgh, PA 15236-0940
Phone: (412) 386-7339
E-mail: David.Ollett@netl.doe.gov

Start Date: October 1, 2011

End Date: September 30, 2016*

*No-cost extensions have changed the original end-date of this project from September 30, 2014

II.11.A. Abstract

Objectives

- Increase overall commercial fleet fuel efficiency
- Improve tire wear and service life
- Decrease fleet tire maintenance cost and compliance with federal safety regulations.

Accomplishments

Overall

- The AMT manufacturing and testing processes continued to be refined and the team focused on product, process, and people-readiness for the assembly and testing of our Lab, and Customer Focus Tires
- Over road trials were carried out. Various combinations of AMT tires, from as-molded without system components to system pumping tires, were placed on the truck before the full system tires with functioning regulators
- Goodyear stopped the internal regulator iteration of this project in January 2016 and moved forward with a valve stem method/iteration of this project instead
- Goodyear focused on product testing, process, assembling AMT products for customer vehicle testing, and AMT product industrialization
- Goodyear proceeded successfully into on-vehicle testing to date with the following milestones
 - 16 AMT tires are now in operation at Goodyear's testing facility across two trucks, along with 8 control tires.

- Over 3 million miles of AMT tire durability evaluation on Goodyear's test trucks.
- 2 retread tires ready to be applied (114,000, and 135,000 original miles respectively)
- Focus account testing (customer vehicles)
 - 24 AMT tires, w/TPMS Systems for monitoring, installed Feb 11-13 (109,000+ miles)
 - 24 Control tires, w/TPMS Systems, installed March 3, 2016 (120,000+ miles)
- All test facility and customer vehicles have Tire Pressure Monitoring Systems installed allowing engineers to track vehicle location, tire pressure, and temperature
- Goodyear continues to monitor the performance of the AMT tires and contrasts with the performance of the control tires.

Components

- Pump Tube

The team continues to work with our pump tube supplier, to meet pump tube specifications. Current discussion have been on tolerances and pump tube cost. The team is working with the supplier on options to reduce the pump tube component cost.
- Filter
 - Experienced separation of the rubber over-molded filter dock and peristaltic pump tube cover strip, during wheel testing. Goodyear sent the over molder spec to try in place of rubber
 - System tires were assembled and placed in durability testing to test adhesion.
 - Project stopped January 2016.
- Regulator and Dock
 - Significant improvements were made to the docks and regulators. Docks were proven and tested with rubber removable seals, which went on to be used for System Tire Assembly. All components, include tire peristaltic pumping system performed well in static conditions. However, when assembled, and tested in a dynamic condition on a road wheel, the system of components failed to meet expectations.
 - Project stopped January 2016
- Regulator Attachment
 - New iteration docks were delivered by supplier which had curved base to improve high speed attachment and wear issues. New dock clamps were manufactured to support curved docks. Goodyear developed a new passage connector insert process for removable seal docks.
 - Project stopped January 2016
- Control Valve Interconnections

The valve stem product contains (2) interconnect tubes which Goodyear optimized for quality and performance of the tubes, and their fittings
- Process
 - The quick pump system test for QC check of full system tires was proven to perform successfully. Goodyear developed an end of line test on the AMT Assembly cell to check for pump tube flow and for leaks prior to the quick pump QC check
 - Goodyear modified our manufacturing process to convert over to the manufacture of valve-stem AMT Products.
- Goodyear focused on improving the AMT Assembly process in our Proof-of-Concept AMT Cell:
 - Improvements to the dome and pump tube fitting assembly process
 - Improvements made to the dome pre-molding process to eliminate lights in the cured AMT Product
 - Reducing cure time study – curing tires at higher cure temperatures, at a reduced cure time
 - Team is analyzing the dome area for total amount of cure

- Control valve test stand –Goodyear has a quantity of (2) test stands to validate AMT control valves for testing. All control valves are validated over the operating pressure ranges, and efficiencies calculated.
- AMT Product Industrialization
 - The team continues to focus on the industrialization of the AMT product:
 - Establishing product and process specifications
 - Product cost analysis
 - Facility Specifications
 - Process requirements based upon projected demand
 - Operational expense
 - Working with a facilities planning consultant engineer
 - Developing an overall process and product cost model
 - Working with the marketing team for gate process and develop the business case.

Future Achievements

Overall

- Continue on road vehicle tests
- Lab test tires for product release requirements
- Large volume fleet evaluation development tire build
- Continue to optimize AMT generation 2 system installation equipment.

II.11.B. Technical Discussion

Background

Pressurized air in the tire cavity naturally escapes by diffusion through the tire and wheel, leaks in tire seating, and through the filler valve and its seating. As a result, tires require constant maintenance to replenish lost air. Since manual tire inflation maintenance is both labor intensive and time consuming, it is frequently overlooked or ignored. By automating the maintenance of optimal tire pressure, the tire's contribution to the vehicle's overall fuel economy can be maximized.

Introduction

Under-inflated tires significantly reduce a vehicle's fuel efficiency by increasing rolling resistance (drag force). The Air Maintenance Technology system developed through this project replenishes lost air and maintains optimal tire cavity pressure whenever the tire is rolling in service, thus improving overall fuel economy by reducing the tire's rolling resistance. The system consists of an inlet air filter, an air pump driven by tire deformation during rotation, and a pressure regulating device.

Approach

The work is divided into three phases. The objectives of first phase, Planning and Initial Design, resulted in an effective project plan and to create a baseline design. The objectives for the second phase, Design and Process Optimization, are: to identify finalized design for the pump, regulator and filter components; identify a process to build prototype tires; assemble prototype tires; test prototype tires and document results. The objectives of Phase 3, Design Release and Industrialization, are to finalize system tire assembly, perform full release testing and industrialize the assembly process.

Results

Table II-16: Milestones

Phase	Milestone	Iteration	Description	Month	Date Achieved
1. Planning and Initial Design (Concept Scoping)	M01	1	Revised work plan & budget accepted by DOE & Goodyear	01	31-Oct-11
	M02	1	Initial System, component & process specifications complete	06	31-Mar-12
2. Design and Process Optimization (Prototype Development)	M03	1	Initial simulation and modeling complete	09	30-Jun-12
	M04	1	First iteration system assemblies complete	11	31-Aug-12
	M05	1	Evaluation of first design complete	12	30-Sep-12
	M06	2	Second iteration system assemblies complete	17	28-Feb-13
	M07	2	Go/No go decision based on evaluation of refined design	18	31-Mar-13
	M08	3	Third iteration system assemblies complete	23	31-Aug-13
	M09	3	Go/No go decision for on-vehicle trial	24	30-Sep-13
	M10	3	On-vehicle trial initiated-San Angelo (a)	27	31-Dec-13
	M11	4	Fourth iteration system assemblies complete - Eaton 1	31	21-Apr-14
	M12	4	Go/No go decision based on evaluation of refined design	32	19-May-14
	M13	5	Fifth iteration system assemblies complete - Eaton 2	33	16-Jun-14
	M14	5	Go/No go decision based on evaluation of refined design	34	7-Jul-14
	M15	5	Delivery of latest iteration of Eaton regulator/filter components (b)	41	24-Feb-15
3. Design Validation	M16	1	Delivery of control valve components begins for fleet testing assembly (b, c ,d)	49	15-Oct-15
	M17	1	Assembly of fleet evaluation tires commences (e)	52	1-Jan-16
	M18	1	Qualification testing completed prior to fleet (customer) evaluation	52	15-Jan-16
	M19	1	Go/No go decision based on evaluation of refined design	52	18-Jan-16

	M20	1	Fleet evaluation tire shipments begin (f)	53	1-Feb-16
	M21	1	DOE project completed. Approximately 5 months fleet evaluation completed	60	30-Sep-16

Footnotes:

(a) Check valve test - non-functioning regulator. Continuous test. Tires with functioning regulators will be deployed (see M15)

(b) Functioning regulators / control valves

(c) Goodyear Akron / San Angelo qualification testing: ~ 13 weeks, leading to M19 (Go/No go)

(d) Approximately 50/month (delivery to begin prior to M19 to be ready for fleet trial-some risk involved)

(e) Approximately 15/week (assembly to begin prior to M19 to be ready for fleet trial-some risk involved)

(f) First group of tires to be assembled and ready to ship per M19 decision. Deployment to account Feb 2016-May 2016. Expected duration 18 mos.

Note: If M19 decision is a 'No go', additional iterations would be needed. Additional iterations could consume an additional 7-17 weeks.

Conclusions

During FY 2016, the Goodyear AMT team focused on two areas - overcoming AMT component issues so that the project was able to proceed, and on test facility and customer fleet testing of AMT products prior to scale-up.

Critical issues related to the dock and regulator of the AMT design were identified in 2013. These challenges caused several delays to the project, though Goodyear is very pleased that it draws to a satisfactory close on September 30, 2016. Goodyear worked closely with the component vendor in attempting to solve the dock and regulator problems using a wide variety of design adjustments. Ultimately, an alternate design, "valve stem" was used to circumvent the design challenges altogether, allowing Goodyear to proceed to assembly and customer fleet testing. With testing currently underway, the DOE Vehicle Systems project will provide a robust dataset from which to proceed into commercialization.

Goodyear looks forward to bringing this project to market on an industrial scale, currently working on facility specifications, process requirements based upon projected demand, and developing an overall process and product cost model.

II.11.C. Products

Presentations/Publications/Patents

Presentations

1. N/A

Publications

1. N/A

Patents

Goodyear currently has fifty four (54) US Patents involving Air Maintenance Technology (AMT). Sixteen (16) patents were granted during FY16. Goodyear has additional patent applications filed with the US Patent office.

39th Patent issued: US 9,199,518 - Issued 12/1/15

Abstract: A method of assembling an air pump in a tire is provided including: opening an axial air passageway of an elongate flexible air tube at one end; inserting one by one a plurality of one-way check valves into the air passageway from the one end to form an axial array of spaced apart check valves along the air passageway, each check valve having an external nominal width greater than a nominal width of the air tube passageway; establishing a press fit engagement between each check valve and air tube internal sidewalls defining the air passageway to place each check valve at a respective preferred position within the air passageway; retaining the check valves in the respective preferred positions within the air passageway by radial pressure from the air tube internal sidewalls and closing the one end of the flexible air tube.

40th Patent issued: US 9,205,712 - Issued 12/8/15

Abstract: An air maintenance tire includes an air inlet housing affixed to the inner liner of a tire. An elongate sidewall air pumping passageway is incorporated within a first tire sidewall. An intake conduit and an elongate tubular inlet conduit are provided having a quick connect/disconnect latching attachment to sockets formed by the air inlet housing.

41st Patent issued: US 9,205,714 - Issued 12/8/15

Abstract: A self-inflating tire assembly includes an air passageway in the tire that is operable to be sequentially flattened by the tire footprint in a direction opposite to a tire direction of rotation to pump air from an inlet device through the passageway to an outlet device for direction into the tire cavity. A valve device for a tire is also disclosed. The valve device includes an insert mounted in the tire, a valve body mounted within the valve insert; wherein the valve body has a first, second and third chamber, wherein a first and second check valve is positioned in the first and second chamber. A pressure membrane is received within the valve body, and positioned to open and close the third chamber. The pressure membrane is in fluid communication with the tire cavity and the third chamber of the valve body. A spring is received within the third chamber and is positioned to exert force upon the pressure membrane to bias the pressure membrane position relative to the channel in the open position.

42nd Patent issued: US 9,216,619 - Issued 12/22/15

Abstract: An air maintenance tire and pump assembly includes a tire having a tire cavity, first and second sidewalls extending from first and second tire bead regions, respectively, to a tire tread region, an elongate substantially annular air passageway enclosed within a bending region of the sidewalls, the air passageway operatively closing and opening, segment by segment, as the bending region of the sidewalls passes adjacent a rolling tire footprint to pump air along the air passageway, an air inlet port assembly coupled to, and in air flow communication with, the air passageway at an inlet air passageway junction, the air inlet port assembly being operable to channel inlet air from outside of the tire into the air passageway, the air inlet port assembly including an inlet control valve and an outlet tee structure positioned 180° opposite the inlet control valve in the air passageway for moving air into the tire cavity, the inlet control valve including two inlet check valves for ensuring air flow only into, and not out of, the inlet control valve, the air passageway, a corresponding plain tee inlet structure, and the tire cavity.

43rd Patent issued: US 9,216,620 - Issued 12/22/15

Abstract: An air maintenance tire includes an air inlet housing affixed to the inner liner of a tire. An elongate sidewall air pumping passageway is incorporated within a first tire sidewall. An elongate air tube is contained within the first sidewall and has an elongate elliptical internal air passageway. The air tube is configured having a substantially on-side mushroom-shaped sectional shape extending radially into the first tire sidewall formed by a radially inward tube cap and a radially outward tube stem. Inlet and intake conduits connect into sockets of the inlet housing and a pressure regulating valve system within the inlet housing controls pressurized air flow from the tube internal air passageway into the tire cavity.

44th Patent issued: US 9,259,975 - Issued 2/16/16

Abstract: The invention relates generally to a pneumatic rubber tire which contains an outer, annular, circular groove which contains a flexible tube bonded to the walls of the groove.

45th Patent issued: 9,259,981 – Issued 2/16/16

Abstract: An air maintenance tire assembly and method of operation includes a pressurized air supply assembly for supplying pressurized air to a tire cavity through an elongate outward projecting, valve stem passageway. An elongate centrally disposed shaft within the valve stem reciprocally moves axially in the valve stem internal air passageway between a passageway-opening axial position and a passageway-closing axial position. A pressure regulator is provided to move the elongate shaft axially between the passageway-opening and passageway-closing positions responsive to a detected air pressure level within the tire cavity.

46th Patent issued: 9,272,586 – Issued 3/1/16

Abstract: A valve stem-based air maintenance tire assembly and method of operation is provided employing a tire mounted air pumping system. The assembly includes a rim-mounted pressure regulator positioned within a tire cavity opposite an inward end of a tire valve stem to selectively open and close pressurized air flow from a valve stem internal passageway into the tire cavity. An elongate valve stem shaft is mounted within the valve stem air passageway and reciprocally moves axially to close off and open the valve stem air passageway to create or close a pressurized air path into the tire cavity as needed.

47th Patent issued: US 9,302,556 - Issued 4/5/16

Abstract: An air maintenance tire and air pump assembly includes a sidewall and a tire cavity for maintaining pressure; an elongate tubular air passageway enclosed within a flexing region of the sidewall, air passageway, the air passageway operably closing segment by segment in reaction to induced forces from the tire flexing region as the flexing region of the tire wall rotates adjacent a rolling tire footprint, the elongate air passageway having at least one check valve device seated within the axial air passageway; and a relief valve assembly comprising a chamber body, a valve, a piston, and a silicone ring, the valve having a valve body and a valve head, the valve head, deforming to release over-pressurized air from the tire cavity to atmosphere.

48th Patent issued: 9,327,560 – Issued 5/3/16

Abstract: A tire having a tire cavity is disclosed, wherein the tire has a bi-directional pump assembly including a pump passageway having an inlet end and an outlet end, and being operative to allow a portion of the pump passageway near a tire footprint to substantially close and open the pump passageway. The tire includes a valve assembly having a valve housing, wherein a diaphragm is mounted in the valve housing forming an interior chamber, and wherein the diaphragm is responsive to the pressure of the tire cavity. The interior chamber has a first hole in fluid communication with the inlet end of the pump passageway, a second hole in fluid communication with the outlet end of the pump passageway, and a third hole in fluid communication with the outside air. The valve housing has a passageway in fluid communication with the tire cavity and the outlet end of the pump. The valve assembly further includes an inlet control valve having a valve bottom positioned over the third hole and operative to open and close the third hole to allow air to enter the system. The inlet control valve has a first end connected to the diaphragm, and a resilient member biases the inlet control valve into the open position.

49th Patent issued: 9,327,561 – Issued 5/3/16

Abstract: A tire having a tire cavity is disclosed, wherein the tire has a bi-directional pump assembly including a pump passageway having an inlet end and an outlet end, and being operative to allow a portion of the pump passageway near a tire footprint to substantially close and open the pump passageway. The tire includes a valve assembly having a valve housing, wherein a diaphragm is mounted in the valve housing forming an interior chamber, and wherein the diaphragm is responsive to the pressure of the tire cavity. The interior chamber has an inlet in fluid communication with outside air, and an outlet in fluid

communication with inlet and outlet of the pump passageway. The diaphragm is positioned over the outlet and operative to open and close the outlet. A resilient member biases the diaphragm into the open position.

50th Patent issued: 9,327,562 – Issued 5/3/16

Abstract: A pumping mechanism is used with a pneumatic tire mounted on a wheel rim to keep the pneumatic tire from becoming underinflated. The pumping mechanism includes a plurality of pumps forming a linear belt and subsequently being attached circumferentially to the wheel rim, a plurality of pump holders interconnecting the plurality of pumps in a linear configuration, and a control valve for controlling inlet air into a tire cavity of the pneumatic tire.

51st Patent issued: 9,333,817 – Issued 5/10/16

Abstract: A pneumatic tire comprises a sidewall, an annular tire cavity, and a hydraulic actuator connected to the sidewall inside the annular tire cavity, wherein the hydraulic actuator has a flexible reservoir for containing a hydraulic fluid, and an opening allowing hydraulic fluid to enter the reservoir and to exit the reservoir. Further, the hydraulic actuator comprises a lever arm connected to the sidewall and holding the flexible reservoir between the lever arm and the sidewall, wherein the lever arm comprises a fluid channel allowing hydraulic fluid to flow from the reservoir through the opening out of the lever arm.

52nd Patent issued: 9,333,816 – Issued 5/10/16

Abstract: An air maintenance tire assembly includes a tire having an elongate valve stem projecting outward from the tire cavity and a tire sidewall having an elongate sidewall groove formed therein and housing an elongate air tube. A connecting tube extends between the air tube and the valve stem, the connecting tube having an internal connecting air passageway for directing air forced along the air tube air passageway into the internal valve stem passageway as the tire rolls over a ground surface.

53rd Patent issued: 9,340,076 – Issued 5/17/16

Abstract: A tire assembly and method includes one or more elongate air passageway formed within a tire component, such as a tire sidewall. The air passageway is configured as a series or string of elongate cavities, adjacent cavities connected end to end by an elongate connecting channel. The connecting channel is dimensioned having a channel diametric size smaller than a cavity diametric size. Positioned within the tire component, the air passageway sequentially collapses segment by segment as each of the cavities pass sequentially over a rolling tire footprint. Air is pumped by the sequential air passageway collapse with the smaller dimensioned connecting channel(s) acting as valve components to directionally keep the pumped air moving between an air passageway air inlet and an air passageway air outlet and from there into the tire cavity

54th Patent issued: 9,365,084 – Issued 6/14/16

Abstract: A self-inflating tire assembly includes an air tube connected to a tire and defining an air passageway, the air tube being composed of a flexible material operative to allow an air tube segment opposite a tire footprint to flatten, closing the passageway, and resiliently unflatten into an original configuration. The air tube is sequentially flattened by the tire footprint in a direction opposite to a tire direction of rotation to pump air along the passageway to a regulator device. The regulator device regulates the inlet air flow to the air tube and the outlet air flow to the tire cavity.

II.12. Improved Tire Efficiency through Elastomeric Polymers Enhanced with Carbon-Based Nanostructured Materials

Georgios Polyzos, Principal Investigator

Oak Ridge National Laboratory
One Bethel Valley Road
Oak Ridge, TN 37831-6054
Phone: (865) 576-2348; Fax: (865) 574-9407
E-mail: polyzosg@ornl.gov

David L. Anderson, DOE Program Manager

U.S. Department of Energy
Phone: (202) 287-5688
E-mail: David.Anderson@ee.doe.gov

Start Date: January 2016
End Date: December 2017

II.12.A. Abstract

In materials science of elastomers the influence of manufactured nanomaterial filler particles is of utmost significance for the performance of innovative elastomer products, i.e., passenger and commercial tires with ultralow rolling resistance but high traction. Advances in both performance areas are imperative for the development of improved tire efficiency to meet DOE's fuel consumption reduction target of 4%, all while maintaining or improving wear characteristics of the tire. Recent research efforts focus mainly on the development of composite tires based on carbon black and silica. The project goal is to replace existing fillers (such as carbon black and silica) with higher performance materials (viz., graphene and silica nanofibers). The proposed approach capitalizes on the recent advances in nanomaterial and graphene synthesis and functionalization by our group and suggests a promising avenue for the amalgamation of cutting-edge nanotechnologies that can be utilized toward DOE's technical targets. The project will enable the fabrication and testing of scalable structures, which are anticipated to demonstrate unprecedented improvements in the rolling and wear resistance of tires used in the automotive industry. The successful implementation of the project will deliver scalable composite materials and will provide processing conditions that can be utilized in advanced tire manufacturing for breakthrough fuel savings.

Objectives

- To reduce hysteretic losses. Well-defined structures of self-assembled graphene layers will be uniformly dispersed in the elastomer matrix. The unique geometrical configuration of the graphene fillers makes them the most promising carbon-based fillers for breakthrough reduction of the rolling resistance.
 - To reduce the rolling resistance.
 - To replace existing fillers (such as carbon black and silica) with higher performance materials.
 - Tailor the viscoelastic properties.
 - Improve the fuel economy (mpg) of vehicles.
- To sharply enhance the wear resistance of the tire without compromising its viscoelastic properties.
 - Improve the tear resistance.
 - Design of new materials with tailored and complementary properties that will provide parallel improvements.
 - Enable fabrication techniques that can be scaled in manufacturing environment.

Accomplishments

- We have functionalized graphene nanoplatelets (GnPs) in order to impart them with the appropriate surface functionalities that will introduce cross-linkages between the GnPs and the elastomer matrix and therefore, will result in a thermodynamically favorable mixture.
 - Successfully exfoliated graphene nanoplatelets. The exfoliated GnPs are a few atomic layers thick. The GnPs can be exfoliated at large scale quantities.
 - The functionalization of the fillers is uniform.
 - Functionalized GnPs readily available for dispersion in the elastomer matrix.
 - Synthesized silica nanofibers with diameter less than 100nm. We employed nano-indentation techniques to measure the modulus values of the silica nanofibers in order to verify that there are no defects in their structure.

Future Achievements

- Define the processing conditions in order to well-disperse GnPs in the elastomer matrix.
 - Define the GnPs volume fraction in order to achieve 4% fuel saving.
 - Define the silica nanofiber volume fraction in order to achieve increase in the tear resistance.

II.12.B. Technical Discussion

Background

In the United States road vehicles account for more than 80% of motorized transportation and are considered to be the driving force for the steep growth in oil demand [1]. Several studies have indicated the importance of the tire rolling resistance for significant reductions in fuel consumption. The rolling resistance can be responsible for up to 25% of the energy required to drive at highway speeds [2] and a 10% reduction in tire rolling resistance yields fuel savings 1-2% [1,3]. The above-referred results are in excellent agreement with the research conducted for the California Energy Commission, which concluded that approximately 1.5 to 4.5% fuel consumption could be saved by using low resistance tires [4]. In response to Vehicle Technologies funding opportunity announcement we proposed to develop innovative nanocomposite materials that will reduce the fuel consumption by reducing the tire rolling resistance. The targeted fuel consumption reduction will be at least 4% compared to the state-of-the-art, while maintaining traction and wear resistance.

Introduction

The rolling resistance of a tire is the force required to overcome hysteretic losses. The latter, defined as the energy dissipated during the stress-strain cycles of the polymer matrix, are significantly reduced when the polymer chains are adsorbed (and thus being less mobile) on the surface of the filler [5]. Recent studies [6] have shown that graphene oxide (GO) can reduce the rolling resistance when dispersed in elastomer matrix. The rolling resistance of styrene-butadiene rubber (SBR) filled with 0.6vol. % GO was found to be approximately 10% and 40% lower than that of silica-SBR and carbon black-SBR composites at 60°C, respectively. In the proposed work superior to GO filler particles will be utilized. Namely, well-defined structures of atomically thin self-assembled graphene layers (graphene nanoplatelets) will be uniformly dispersed in the elastomer matrix. The unique geometrical configuration of the graphene nano-platelet fillers (~1000 m²/g surface area) makes them the most promising carbon-based fillers for breakthrough reduction of the rolling resistance.

Parallel improvements in material properties, often originating from competing mechanisms, can be achieved when synergistically combining fillers with complementary properties. For instance, the hysteretic losses can be reduced by the incorporation of GnPs at low concentrations (~1vol.%); however, the abrasion and tear resistance (wear resistance) of the tire is optimal when the filler concentration is approximately 20-25vol.% [5]. A significant increase of the GnPs concentration will eventually increase the rigidity (brittleness) of the elastomer matrix and will compromise the elastic properties and traction of the tire. To sharply enhance the wear resistance of the tire without compromising its viscoelastic properties (i.e. traction) we propose to disperse an additional to graphene filler in the elastomer matrix. We have developed a unique approach for

synthesizing high tensile strength flexible silica nanofibers. Silica fibers with nanoscale diameters (~50-100nm) have an intrinsically low incidence of defects. The nanofibers will be cross-linked to the elastomer matrix to form robust flexible interfaces that will provide a reinforcement network with extraordinary mechanical integrity and wear resistance.

Approach

Exfoliated GnPs were obtained from suspensions of graphene oxide (GO), reduced graphene oxide (rGO), and graphite powder using high shear mixing. For comparison, graphene was synthesized using chemical vapor deposition techniques (CVD Gr) according to our previous studies [7, 8]. The thickness of the CVD Gr was calculated based on Raman spectra. Measurements were performed over three different spots. The Raman spectra indicate the growth of defect-free single layer (one atom thick) graphene [9]. High shear mixing and ultrasonic agitation of graphite in an aqueous suspension can yield large quantities of exfoliated GnPs. Graphite flakes are made of multi-layer agglomerated graphene. Using high shear mixing techniques the graphite flakes were successfully exfoliated into a few layer thick GnPs. Exfoliated GO and rGO flakes were also fabricated. These 2D materials have the same crystal structure as the graphene; however, defects in their crystal structure (i.e. C-O-C, OH, COOH) and be utilized to impart them with surface functionalities and therefore to better disperse them in the elastomer matrix. A detailed interpretation of the Raman band peaks and the determination of the layer thickness can be found in reference [9]. According to the shape of the Raman peaks the thickness of the exfoliated platelets is comparable to the thickness of a few single layers (Figure II-85).

Results

Covalently functionalized graphene that can be conjugated to the SBR polymer chains was developed. The GnPs fillers are reduced graphene oxide (rGO) nanoplatelets. We applied a method that can easily be scaled up and reduce the processing steps and cost. Commercially available graphene oxide (GO) was reduced and functionalized with sulfur (S) groups. The functional groups will induce covalent bonds with the elastomer matrix and will promote the dispersion of the fillers. In order to accurately characterize and quantitatively measure the chemical functionalities on the GnPs surface we employed a combination of techniques such as, energy dispersive x-ray spectroscopy (EDX), x-ray photoelectron spectroscopy (XPS), thermogravimetric analysis (TGA), and Fourier transform infrared spectroscopy (FTIR).

EDX element mapping was used to verify the uniform distribution of the chemical functionalities on the GnPs surface. The sulfur atoms that are responsible for the filler-elastomer crosslinking are uniformly distributed on the surface of the GnPs. Quantitative element analysis can be derived from the EDX spectra. However, the element percentages according to the EDX analysis do not accurately correspond to the element percentages on the surface of the sample due to the penetration depth of the electron beam. Therefore, we employed XPS techniques in order to precisely calculate the concentration of the surface chemical functionalities. The samples were mounted onto double-sided tape and introduced into the XPS instrument through a vacuum pumped load-lock. Survey scans were acquired to determine all elements present. In order to access the reproducibility of the functionalization process, two functionalized samples were measured.

TGA with mass spectrometer measurements were performed on the GO, rGO and functionalized rGO. The TGA data indicate the degradation temperature of the organic functionalities and thus allow us to determine the maximum mixing temperature in order to not degrade our filler material. The onset of the degradation process for the functionalized rGO samples indicates that a mixing temperature up to 150°C is safe in order to not degrade the chemical functionalities on the surface of the fillers.

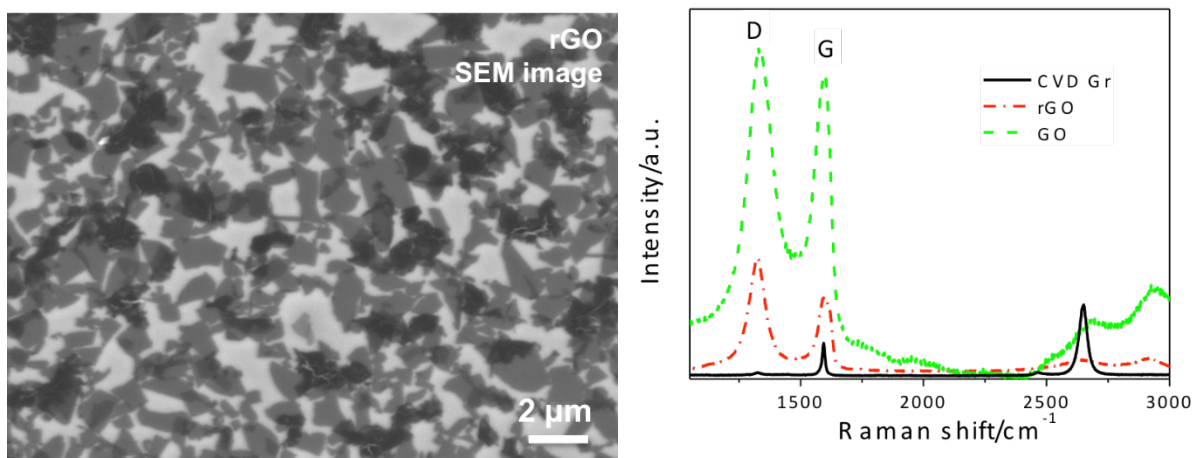


Figure II-85: SEM image of exfoliated rGO. Summarized Raman spectra of the exfoliated platelets. The spectrum of the CVD synthesized graphene is also included.

The silica nanofibers were synthesized using a polyvinylpyrrolidone-pentanol emulsion system. Briefly, polyvinylpyrrolidone (PVP) was dissolved in pentanol by sonicating at 50°C. To this solution, water, sodium citrate, ethanol and a small amount of ammonium hydroxide were added, and the solution was vortex for a few minutes. Then the solution was allowed to react for 16 hours. To separate the silica fibers from the reaction mixture, the mixture was centrifuged at 5000 rpm for a few minutes. The supernatant containing unreacted reagents was discarded, and the residue was washed with ethanol and water 2-3 times, and each washing was followed by centrifugation to remove the washing solvent.

The fibers were deposited on a silicon wafer in order to perform scanning electron microscopy (SEM) measurements. Silicon wafer was used to avoid charging on the silica fiber surface. SEM images revealed the formation of fibers with an average diameter smaller than 100 nm and length of 5-10 μm (Figure II-86). The high modulus values of the silica fibers indicate that there are no defects in their structure. The SiO₂ content on their surface is approximately 90%.

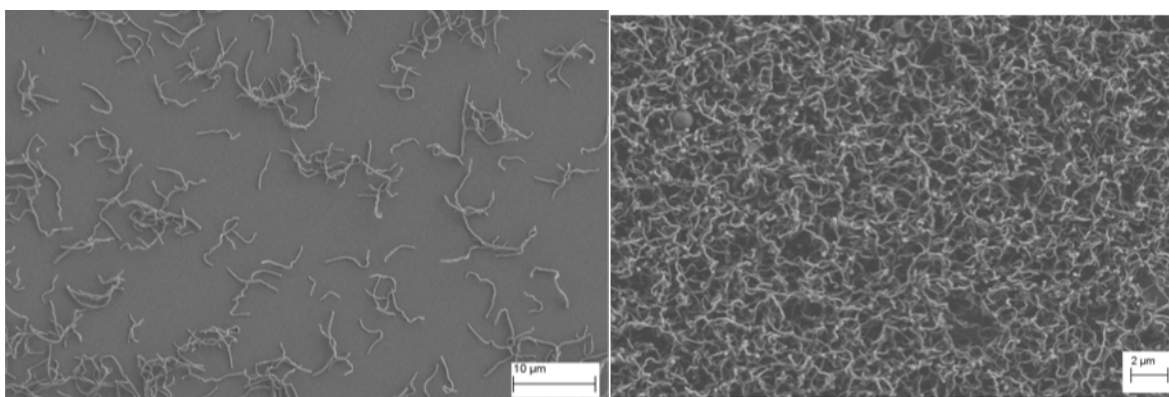


Figure II-86: SEM images at different magnifications of the synthesized silica nanofibers.

The milestones and the status of the milestones are shown in Table II-17.

Table II-17: Deliverables or Milestones

Deliverable or Milestone	Projected Completion Date	Status	Actual/ Expected Date of Completion	TDM Lead
Fabrication of exfoliated GnPs with tailored properties	March, 2016	Completed	March, 2016	David Anderson
Demonstrate silica nanofibers with diameter smaller than 100 nm according to SEM measurements	March, 2016	Completed	March, 2016	David Anderson
Functionalized GnPs readily available for dispersion in the elastomer matrix	June, 2016	Completed	June, 2016	David Anderson
The nanofibers should demonstrate modulus values greater than 50GPa	June, 2016	Completed	June, 2016	David Anderson
Define the processing conditions in order to well-disperse GnPs in the elastomer matrix	September, 2016	Ongoing	September, 2016	David Anderson
Define the silica nanofiber volume fraction in order to increase the tear resistance	December, 2016	Ongoing	December, 2016	David Anderson
Define the GnPs volume fraction in order to achieve 4% fuel saving	December, 2016	Ongoing	December, 2016	David Anderson
Increase in the tear resistance of the elastomer composite	December, 2016	Ongoing	December, 2016	David Anderson
Go/No-Go Gate: Demonstrate the feasibility to fabricate composite elastomer materials that demonstrate reduced hysteretic losses (sufficient to achieve at least 4% fuel savings), and at the same time exhibit improved tear strength.				

Conclusions

Two types of new filler material with complimentary properties were developed in order to reduce the rolling resistance of tires without compromising the wear properties. The filler materials are based on graphene nanoplatelets and silica nanofibers. The silica nanofibers were synthesized using a polyvinylpyrrolidone-pentanol emulsion system. Their average diameter is smaller than 100nm. The graphene nanoplatelets were exfoliated into a few single layers and were functionalized with sulfur based functional groups in order to be crosslinked with the elastomer matrix. The functionalization of the fillers is uniform. The ongoing work is associated with the optimization of the processing conditions in order to well-disperse the filler material in the elastomer matrix and to define the filler volume fractions in order to achieve 4% fuel saving. Tailoring the nanoscale properties associated with the physical characteristics of filler-filler and filler-elastomer interactions is an effective route for the design and fabrication of composite tires with unprecedented performance.

II.12.C. Products

Presentations/Publications/Patents

1. Hydrogen and Fuel Cells Program and Vehicle Technologies Office Annual Merit Review and Peer Evaluation Meeting (AMR), Washington DC, June 6-10, 2016.

II.12.D. References

1. J.A. Carpenter Jr., J. Gibbs, A.A. Pesaran, L.D. Marlina, K. Kelly, "Road transportation vehicles" MRS Bulletin 33, 439-444, 2008.
2. B.E. Lindemuth, "An overview of tire technology", Chapter 1 in "The pneumatic tire", U.S. Department of Transportation, National Highway Traffic Safety Administration, February 2006.
3. T. Markel, A. Brooker, V. Johnson, K. Kelly, M. O'Keefe, S. Sprik, K. Wipke, "ADVISOR: a systems analysis tool for advanced vehicle modeling" J. Power Sources 110, 255-266, 2002.
4. California Energy Commission, Fuel-Efficient Tires and CEC Proceeding Documents Page, www.energy.ca.gov/transportation/tire_efficiency/documents/index.html (accessed January 2008).
5. T.J. LaClair, "Rolling resistance", Chapter 12 in "The pneumatic tire", U.S. Department of Transportation, National Highway Traffic Safety Administration, February 2006.
6. Y. Mao, S. Wen, Y. Chen, F. Zhang, P. Panine, T.W. Chan, L. Zhang, Y. Liang, L. Liu, "High performance graphene oxide based rubber composites" Scientific Reports 3, 2508, 1-7, 2013.
7. I. Vlassiouk, M. Regmi, P. Fulvio, S. Dai, P. Datskos, G. Eres, S. Smirnov, "Role of Hydrogen in Chemical Vapor Deposition Growth of Large Single-Crystal Graphene" ACS Nano 5, 6069-6067, 2011.
8. I. Vlassiouk, P. Fulvio, H. Meyer, N. Lavrik, S. Dai, P. Datskos, Sergei Smirnov, "Large scale atmospheric pressure chemical vapor deposition of graphene" Carbon 54, 58-67, 2013.
9. Thermo Scientific Application Note AN52252 "The Raman Spectroscopy of Graphene and the Determination of Layer Thickness" by Mark Wall, Thermo Fisher Scientific, Madison, WI, USA.

WIRELESS POWER TRANSFER

II.13. High Efficiency, Low EMI and Positioning Tolerant Wireless Charging of EVs [DE EE0005963]

Rakan Chabaan, Principal Investigator

Hyundai America Technical Center, Inc.
6800 Geddes Road
Superior Township, MI 48198
Phone: (734) 337-2305; Fax: (734) 629-0690
E-mail: [rchabaan@hatci.com](mailto:rhabaan@hatci.com)

Lee Slezak, DOE Program Manager

Vehicle Technologies Program
Phone: (202) 586-2335
E-mail: Lee.Slezak@ee.doe.gov

Start Date: October, 2012
End Date: December, 2016

II.13.A. Abstract

Objectives

- The objective of this project is to develop, implement, and demonstrate a wireless power transfer system that is capable of the following metrics.
- Total system efficiencies of more than 85% with minimum 20 cm coil-to-coil gap.
- System output power at least 6.6 kW; but design system capable of 19 kW for future study.
- Maximum lateral positioning tolerance that can be achieved while meeting regulatory emission guidelines.

Accomplishments in Phase III

- Successfully implemented charger-to-vehicle communications with closed loop current control, and charged electric vehicle from 0 to 100% state-of-charge using wireless charging system at ~6.8 kW output.
- Total system (grid to DC output) efficiency: 91% at 6.6kW output.
- Obtained test results in areas of misalignment performance, electromagnetic field emissions, foreign object effect, thermal performance, and AC power quality.
- Started testing of wireless charging system at independent test lab (Idaho National Labs), expect completion by end of 2016.

Future Goals

- Finish testing wireless charging system, at Idaho National Labs and at Hyundai.
- Finish building fleet of five wireless-charge enabled vehicles (Kia Soul EV).
- Run Durability Test on remaining vehicles and demonstrated to DOE management.

II.13.B. Technical Discussion

Background

Wireless charging for electric vehicles is an alternative to plug-in conductive chargers. The main advantage of wireless charging is simplicity and minimum driver intervention and therefore, the user does not have to plug in the charger or even exit the vehicle. This offers increased convenience and safety but also opens the door to wireless chargers integrated into the infrastructure for semi-dynamic and dynamic charging.

Introduction

This project is a joint effort between Hyundai America Technical Center, Mojo Mobility, and Department of Energy. We are currently in the last phase. Since last year, we have worked on finishing the communications and control development, graphical user interface, and finalizing the CHAdeMO charging protocol software so that the system is compatible with the vehicle battery management system. Currently, with a press of a button, the vehicle can be charged automatically.

In recent months we have focused more effort on testing, characterizing system performance, and finding unique issues and observations which will be useful to know in future developments.

Approach

Our system topology, in terms of power flow, is shown below in Figure II-87.

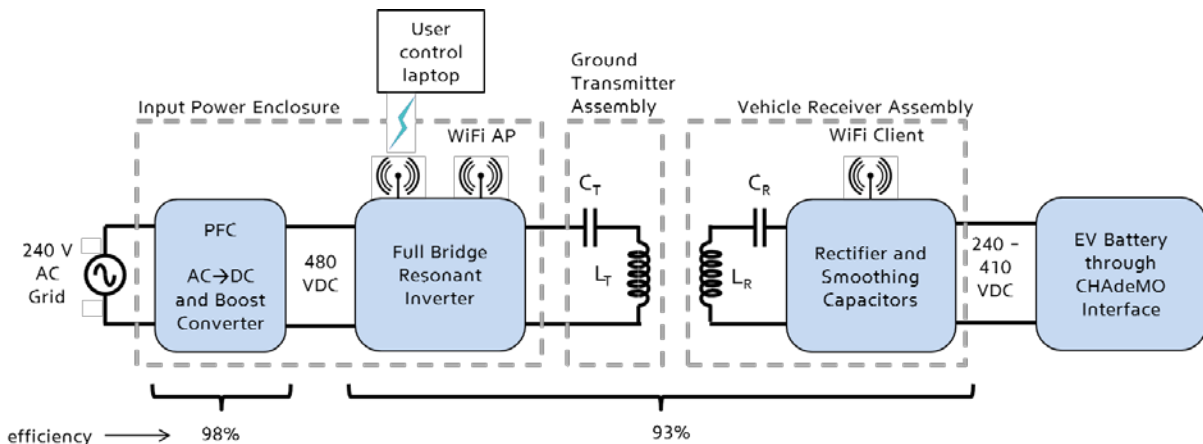


Figure II-87: Wireless Charging System Topology

Input power is 240VAC single phase which is converted and boosted to about 480VDC. This becomes input for Resonant Inverter which feeds 85 kHz current into resonance circuit. After receiver resonant circuit, there is passive rectifier and smoothing capacitors which feed into the DC high voltage bus on the vehicle. The charging circuit accommodates the full range of vehicle battery voltage.

Based on preliminary packaging study, the vehicle receiver coil assembly is designed to be placed just in front of the front axle of the Kia Soul EV, as shown in Figure II-88.

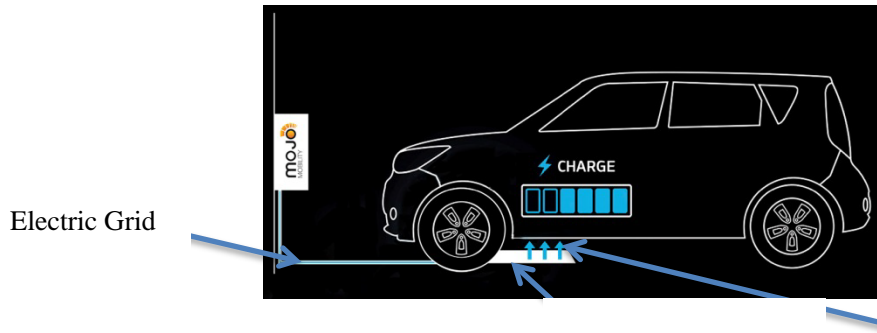


Figure II-88: Coil Placement Under Kia Soul EV
 The location chosen for the vehicle-side coil assembly shown in figure.

The new coil design for the third generation system is described in Figure II-89. In this report, the x-axis is defined to be along the length of the vehicle; and the y-axis is along the width of the vehicle.

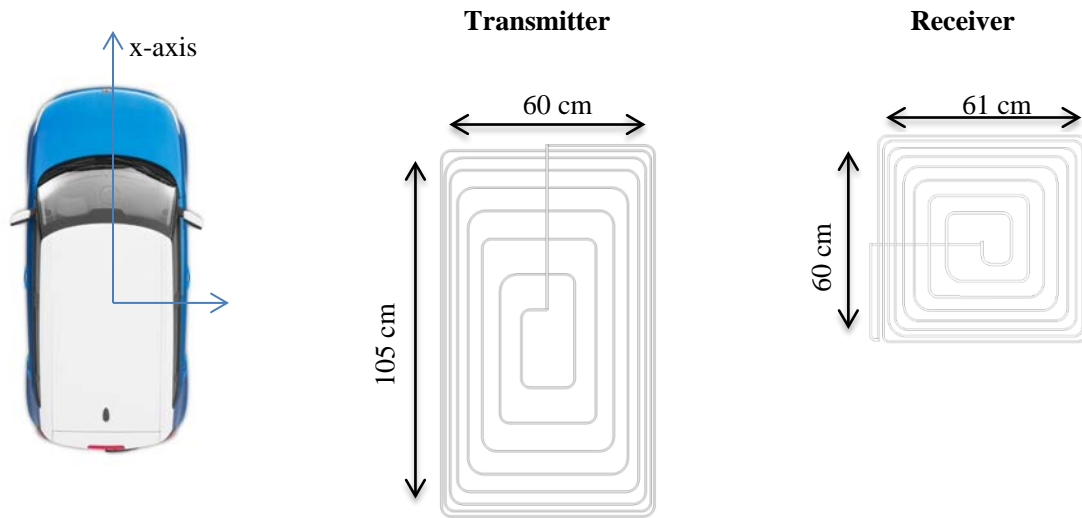


Figure II-89: Coil Design
 The coil design and dimensions. [1]

The coil was laid out using 7 AWG Litz wire in a plastic template. The ferrite tiles completely cover the coil without any empty regions in the middle.

The AC/DC converter and Resonant Inverter boards are actively air-cooled. Besides that, there is no cooling device for the coils or receiver-side electronics. At power levels above 6.6 kW, however, thermal issues will become more important.

The coils are packaged in an ABS plastic enclosure. The receiver-side electronics are enclosed in an aluminum housing which mounts on top of the receiver coil assembly, as shown in Figure II-90.

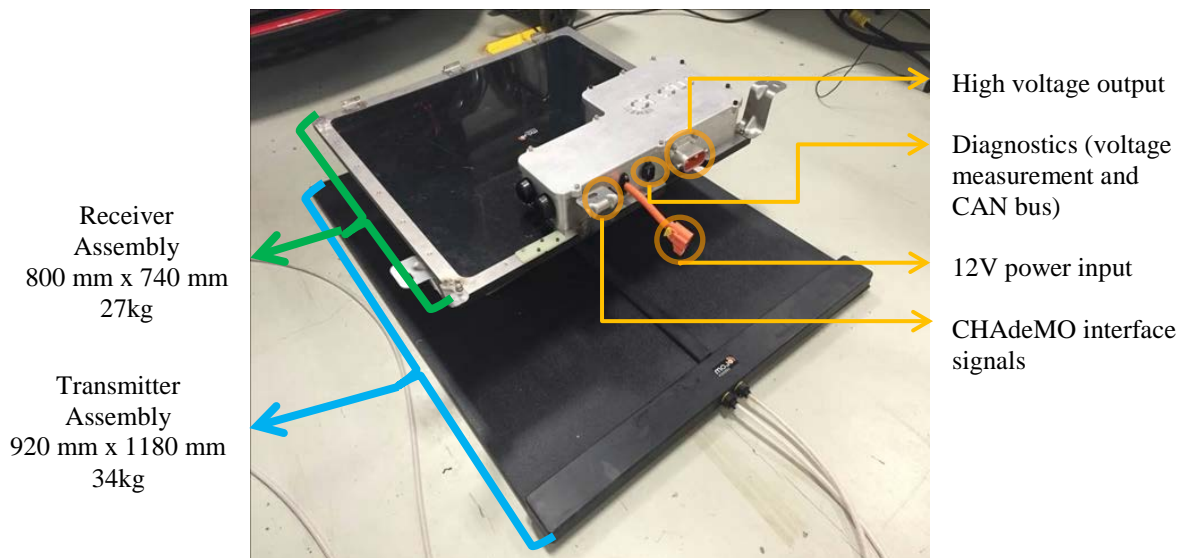


Figure II-90: Transmitter & Receiver Assemblies

The transmitter assembly, which contains a coil and resonant capacitors, sits on the floor. It has 2 wires which connect to the Input Power Box. The receiver assembly mounts to the underside of the vehicle and contains the rectifier and smoothing capacitors before connecting to the vehicle high voltage bus. The receiver assembly additionally has a power input from the 12V lead-acid battery in order to power the digital electronics including Wi-Fi communications.

Results

The system was tested by charging the Kia Soul EV from 0 to 100% state-of-charge. The wireless charging system exhibited stable performance across the range of battery voltages and effectively communicated with the battery management system to output the desired amount of charge current into the high voltage battery.

One of the concerns related to wireless charging is electromagnetic emissions which have an effect on human safety. The International Commission on Non-Ionizing Radiation Protection (ICNIRP) has published guidelines regarding electric and magnetic field limits which are considered safe for humans [2]. Although there are other organizations with guidelines in the same scope, ICNIRP is one of the most commonly referenced organizations regarding electromagnetic limits for human safety.

During wireless charging testing at Hyundai Technical Center, data was collected (using Narda EHP-200A field analyzer) to evaluate magnetic and electric fields levels in and around the vehicle. Measurements were taken inside on the driver seat, outside near the driver and passenger doors, and several locations around the front of the vehicle. Measurements were taken while coils were in aligned configuration as well as a misalignment configuration.

All field levels were below the ICNIRP 2010 limits except for some measurements near the front of the vehicle. Figure II-91 shows measurements locations for which we have reported results and Figure II-92 shows the values at or above limits guidelines. The magnetic field levels were below the limits; however, the electric field levels need further improvement. Additionally, we observe from the data that the misalignment condition generates the worst-case field levels so testing must include misalignment.

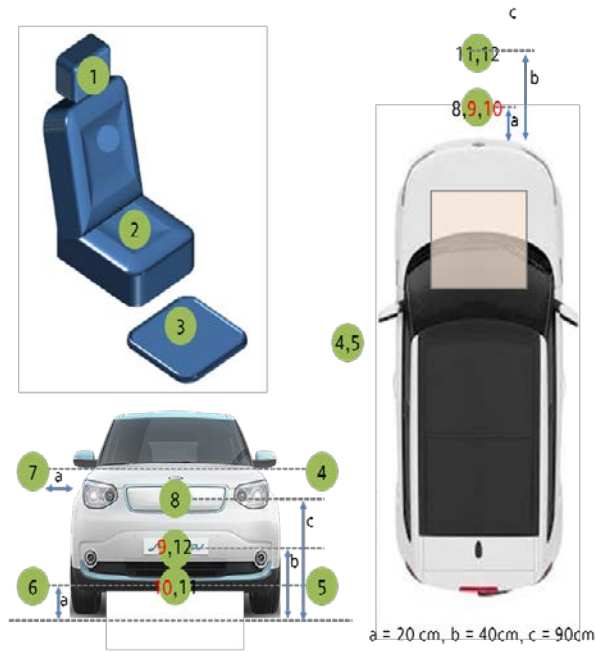


Figure II-91: EMF Measurement Location

The illustration shows the 12 measurement locations which are referenced below in Figure II-92. The numbers highlighted red were locations which exceeded the ICNIRP limit.

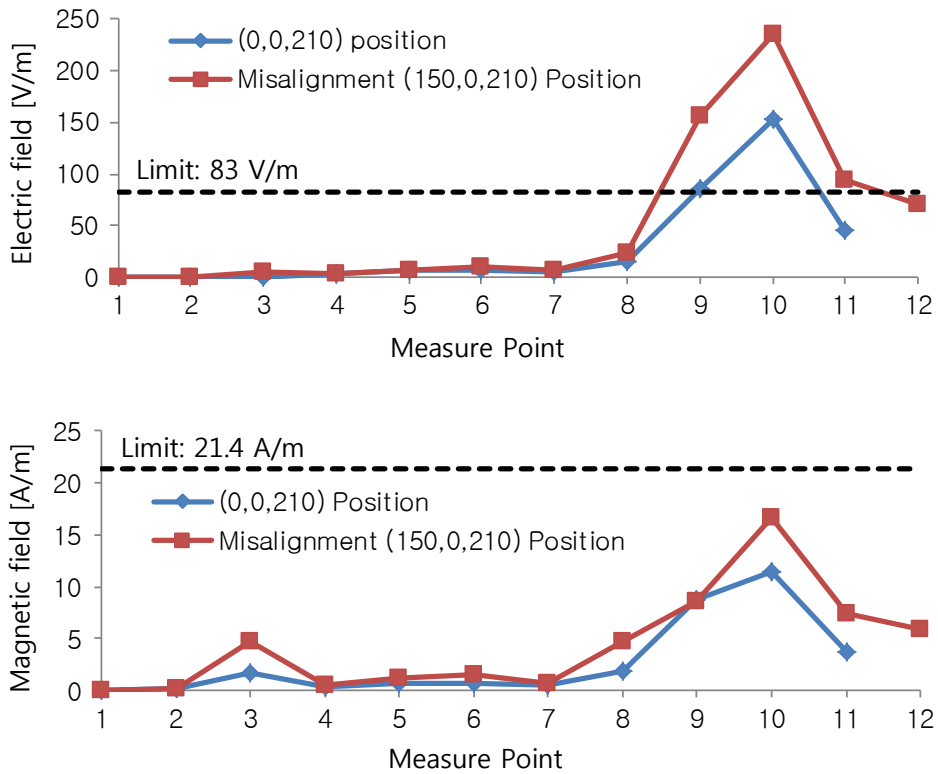


Figure II-92: Electric and Magnetic Field Levels around the Vehicle

The charts above show the electric and magnetic field level measurement along with ICNIRP 2010 limits. The measurement points 1 through 12 are illustrated above in Figure II-91.

Test Condition: 7.0kW output power; 21 cm coil-to-coil gap. Measurements were taken while coils were aligned as well as in misalignment case where transmitter assembly is shifted 150 mm toward driver side.

Another concern regarding wireless charging is overheating. Magnetic fields between the coils are a necessary part of the technology, however, it creates a potential for eddy currents and heating of conductive objects in the vicinity of the power transfer. We recorded temperature of the vehicle receiver assembly using an infrared camera. Over 3.5 hours, the temperature nearly reached steady-state around 50°C, as shown in Figure II-93.

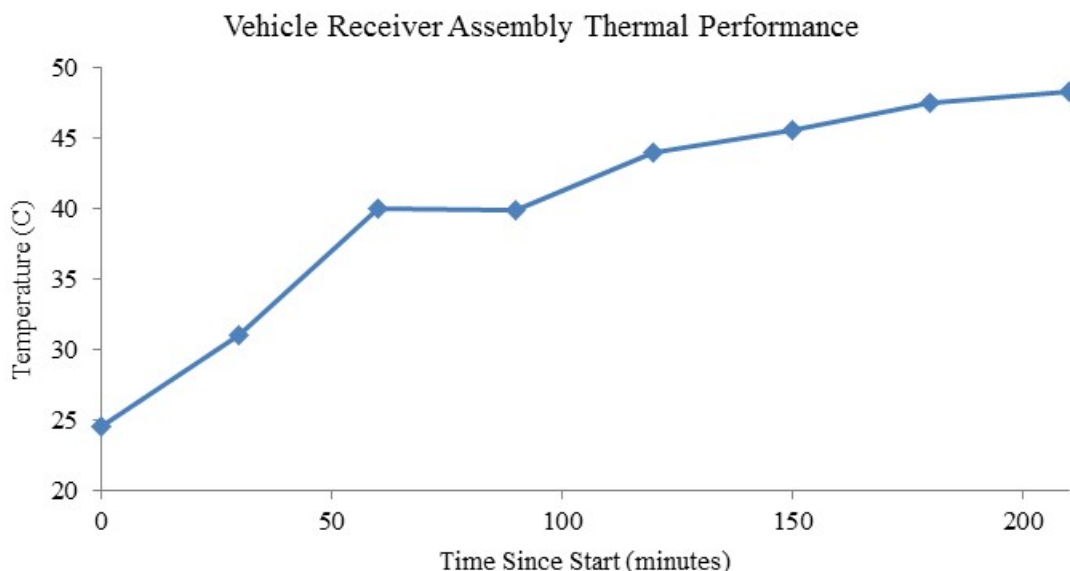


Figure II-93: Temperature Rise of Vehicle Receiver Assembly

Starting from room temperature, the charging system was operating nearly continuously for 3.5 hours. However, there was an 8 minute pause after 1 hour, which explains the brief plateau after 1 hour. An infrared camera was placed on a stand and directed towards the vehicle receiver assembly. Snapshots were taken every 30 minutes. The average output power during this test was 6.8kW.

Conclusions

In previous reports, we have proven the performance of our system’s power electronics, coil, and magnetic designs up to about 10kW with 91% grid-to-battery efficiency. In this report, we demonstrate successful interaction with the battery management system for charging the vehicle at all state-of-charge levels. We also show electromagnetic field levels and temperature rise of the vehicle receiver assembly during charging. The results are very positive, however, in the testing process we have also identified specific technology areas and components that deserve attention in future work. For example, we observed interference with the AM radio quality during wireless power transfer. This and other observations are important notes and learning experience for us which will allow for successful development in the future.

II.13.C. Products

Presentations/Publications/Patents

1. Partovi, Afshin. IDTechEx; November 2015; Santa Clara, CA.
2. Chabaan, Rakan. 2016 DOE Vehicle Technologies Program Annual Merit Review and Peer Evaluation Meeting; April 2016; Washington.
3. Chabaan, Javaid, Partovi, Eliashberg, Ho, and Shams. Hyundai Motor Group Conference; September 2016; Superior Township, MI.

II.13.D. References

1. Kia Soul EV top view. Electric Cars 2016. “2016 Kia Soul EV Review and Price”.
2. International Commission on Non-Ionizing Radiation Protection. “Guidelines for limiting exposure to time-varying electric and magnetic fields (1 Hz to 100 kHz)”. 2010.

II.14. Wireless Charging of Electric Vehicles [FOA #667]

Omer C. Onar, Principal Investigator

Oak Ridge National Laboratory
 Power Electronics and Electric Machinery Group,
 National Transportation Research Center
 2360 Cherahala Boulevard
 Knoxville, TN 37932
 Phone: (865) 946-1351; Fax: (865) 946-1262
 E-mail: onaroc@ornl.gov

Lee Slezak, DOE Program Manager

Vehicle Systems Program
 Vehicle Technologies Office
 Phone: (202) 586-2335
 E-mail: Lee.Slezak@ee.doe.gov

Start Date: October 2015

End Date: October 2016

II.14.A. Abstract

Wireless power transfer (WPT) is a paradigm shift in electric-vehicle (EV) charging that offers the consumer an autonomous, safe, and convenient option to conductive charging and its attendant need for cables. With WPT, charging process can be fully automated due to the vehicle and grid side radio communication systems, and is non-contacting; therefore issues with leakage currents, ground faults, and touch potentials do not exist. It also eliminates the need for touching the heavy, bulky, dirty cables and plugs. It eliminates the fear of forgetting to plug-in and running out of charge the following day and eliminates the tripping hazards in public parking lots and in highly populated areas such as shopping malls, recreational areas, parking buildings, etc. Furthermore, the high-frequency magnetic fields employed in power transfer across a large air gap are focused and shielded, so that fringe fields (i.e., magnetic leakage/stray fields) attenuate rapidly over a transition region to levels well below limits set by international standards for the public zone (which starts at the perimeter of the vehicle and includes the passenger cabin). Oak Ridge National Laboratory's approach to WPT charging places strong emphasis on radio communications in the power regulation feedback channel augmented with software control algorithms. The over-arching goal for WPT is minimization of vehicle on-board complexity by keeping the secondary side content confined to coil tuning, rectification, filtering, and interfacing to the regenerative energy-storage system (RESS). This report summarizes the work performed by the Oak Ridge National Laboratory, Toyota Research Institute of North America, Toyota Motor Engineering and Manufacturing North America (TEMA), Cisco Systems, Clemson University, and Evatran on the wireless charging of electric vehicles which was funded by Department of Energy under DE-FOA-000667. In this project, ORNL is the lead agency. Over the course of the project, ORNL and Toyota TEMA worked closely on the vehicle integration plans, compatibility, and the interoperability of the wireless charging technology developed by ORNL for the vehicles manufactured by Toyota. These vehicles include a Toyota Prius Plug-in Hybrid electric vehicle, a Scion iQ electric vehicle, and two Toyota RAV4 electric vehicles. The research include not only the hardware integration but also the controls and communication systems development to control and automate the charging process for these vehicles by utilizing a feedback channel from vehicle to the stationary unit for power regulation.

Objectives

The main objective of this project is to coordinate multi-party team for the design, development, and fabrication of WPT grid side unit (GSU), coupling coils, and the vehicle side power conditioning units. The GSU includes the active front-end rectifier with power factor correction (PFC), high-frequency power inverter, and the high-frequency isolation transformer whereas vehicle side unit includes a resonant tuning capacitor, a bridge rectifier, a filter circuit, and the additional relays and contactors that are used to timely respond to the charging request or to comply with the charging protocols that a vehicle may have (CHAdeMO, J1772, or direct battery connection). The objective of this work is to demonstrate a fully automated charging process

including the alignment, start charging, stop charging, and the emergency and orderly shutdown procedures while meeting at least 6.6kW power transfer over 160 mm magnetic airgap while exceeding an overall (end-to-end) efficiency of 85%. After integrating ORNL developed WPT technology into demonstration vehicles, an additional objective was to validate the system operation in an independent testing laboratory (Idaho National Laboratory) for field testing of this technology which will assist in system improvements and standards development. In this project, Evatran was the commercialization partner and under ORNL guidance worked on cost and component optimization and fabrication of GSUs and also the primary and secondary coils. Evatran also worked on vehicle integrations in coordination with ORNL and other partners. Clemson University ICAR Center was the demonstration site for phase #2 deliverables of the project. Clemson University, in collaboration with Cisco Systems, also supported the radio communications developments and radio integrations to the vehicles and the WPT equipment on the vehicles. Finally, Toyota Motor Corporation is the vehicle OEM partner provided the vehicles and collaborated with ORNL on the vehicle integrations. One last objective of this project was to demonstrate in-motion wireless charging on Toyota RAV4 vehicles to prove feasibility and collect data.

Accomplishments

- Coordinated hardware and software updates, hardware developments, as well as project strategies with partners.
- ORNL outfitted two Toyota RAV4 EVs with WPT hardware. The first vehicle is tested in the lab and test results collected meeting the efficiency and fringe field targets. The second RAV4 with a GSU were shipped to Idaho National Laboratory for independent testing and evaluation and also characterization of the system with different battery state-of-charge (SOC) levels, misalignment, and power transfer levels.
- The second RAV4 integration is completed. Based on the lessons learned from INL testing and ORNL's re-evaluation of the system power stages, resonant tuning configuration, and the impact of the high-frequency isolation transformer voltage and current ratio, and with the additional testing performed by ORNL, ORNL achieved 20 kW power transfer at 162 mm airgap, with 95% DC-to-DC efficiency (from inverter DC input to vehicle battery). The active front-end rectifier with power factor correction (PFC) stage was excluded from the high power tests since it was initially designed to meet the 6.6 kW of the project goal and it was limited at that power level.
- ORNL also built a dynamic wireless charging track in the lab with two transmit coils and demonstrated in-motion WPT. ORNL also analyzed the impact of resonant tuning configuration on the peak power and energy transfer. The interactions with the steel vehicle body and the steel frame of the traction drive motors were explored.

Future Achievements

Project has been extended till the end of December 2016 without any additional cost. During this time frame, ORNL will explore the opportunities to demonstrate vehicle agnostic operation of the system.

II.14.B. Technical Discussion

Background

Wireless charging of electric vehicles has the potential to eclipse conductive chargers because of its flexibility and convenience to the customer. Use of private and secure radio communications, especially vehicle to infrastructure (V2I), and standardization means that any vehicle would be able to charge at any location. The wireless charging process can be totally transparent to the customer, which would increase the use of opportunity charging with the appropriate infrastructure. The goals and accomplishments of this project during the performance period covered several advancements and integrations in areas including coils, control systems, vehicle integrations, and the site preparations. Through this project, ORNL and partners developed a deep understanding of WPT, real vehicle implementations, control system design and communications for closed loop regulation of power transfer, and the design improvements for higher performance and cost

effectiveness. During the course of this CRADA, hardware and software updates, technology developments, as well as the project strategies are coordinated with the partners.

Introduction

During the FOA #667 project, the team improved the overall operation of the active front-end rectifier with power factor correction, high-frequency power inverter, high-frequency isolation transformer, and the efficiency of the primary and secondary electromagnetic resonance induction coupling coils. Hardware and software developments completed and system is designed to be interoperable with five different vehicles with different charging protocols, target voltage, current, power levels, ramp rates, and response times. A single hardware is built to be interoperable with software changes for each different vehicle. At the end of phase #2, 6.6kW power transfer to Scion iQ EV with >85% end-to-end efficiency while meeting the electric and electromagnetic field limits indicated in International Commission on Non-Ionizing Radiation Protection (ICNIRP); i.e., <6.25 μT and <83 V/m was demonstrated. The team successfully demonstrated the wireless charging operation of both the Toyota Prius Plug-in and Scion iQ EV. The demonstrations featured wireless communications, alignment system, charging initiation and ramping, full charging, and emergency shut down procedures.

Approach

For the Toyota RAV4 EV integration, team had the flexibility of accessing all battery management system (BMS) commands and monitoring functions. The overall integration architecture is similar to that of the Scion iQ EV with the exception of the output contactors to the battery side. For the direct battery connection, a reference current is applied to the battery in current regulation mode while monitoring the battery maximum voltage limit. This mode of operation is illustrated in Figure II-94. For Scion iQ, which required CHAdeMO charging protocol, additional relays and a minimum load resistor was utilized in order to timely respond to a charge request with a reference voltage applied to the CHAdeMO input connectors. WPT system also has to meet the ramp up time and current ripple amplitudes required by the CHAdeMO protocol. These were not needed in Toyota RAV4. However, the charge enable relay has to be enabled within the BMS and the limitations defined in BMS (maximum current, voltage, SOC, temperature) must be monitored. The operational block diagram of the direct battery or CHAdeMO connection of vehicle side WPT equipment is given in Figure II-94.

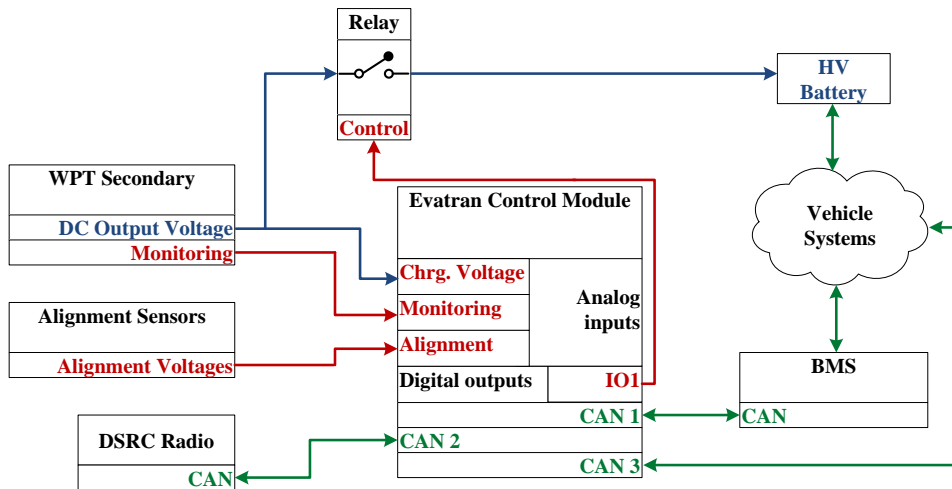


Figure II-94: Operational block diagram of the direct battery or CHAdeMO connection of vehicle side WPT equipment.

Results

As mentioned earlier, one of the Toyota RAV4 vehicles was integrated and tested to collect results and analyze the performance. These initial results were obtained with a smaller (unmatched, but interoperable) coil on the vehicles side. At 162 mm airgap with 220V AC input voltage, the power flow and efficiency across 5 power

conversion stages with 6 input and output voltage and current pairs are presented in Figure II-106. According to these results, active front-end rectifier with power factor correction, high frequency inverter, high frequency isolation transformer, primary and secondary coupling coils, and the vehicle side rectifier and filter efficiency recorded 97.41%, 97.94%, 97.05%, 94.17%, and 97.70%. End-to-end efficiency of the system is recorded 85.18% whereas dc-to-dc efficiency from inverter input to the vehicle battery terminals resulted in 89.51%. In order to deliver 6.6kW power to the vehicle battery, 7.76kW power is drawn from the utility grid. Voltage, current, active power (P), reactive power (Q), apparent power (S), power factor (λ), and the power angle (ϕ) for all power conversions strategies, in addition to the primary coil voltage and the primary side tuning capacitor voltage are presented in Figure II-95. Operational waveforms with expanded views for the high frequency elements (inverter, transformer, and the coils) are presented in Figure II-96 whereas Figure II-97 shows the operational waveforms for low frequency items (grid side AC input, DC link, and vehicle battery voltage and current).

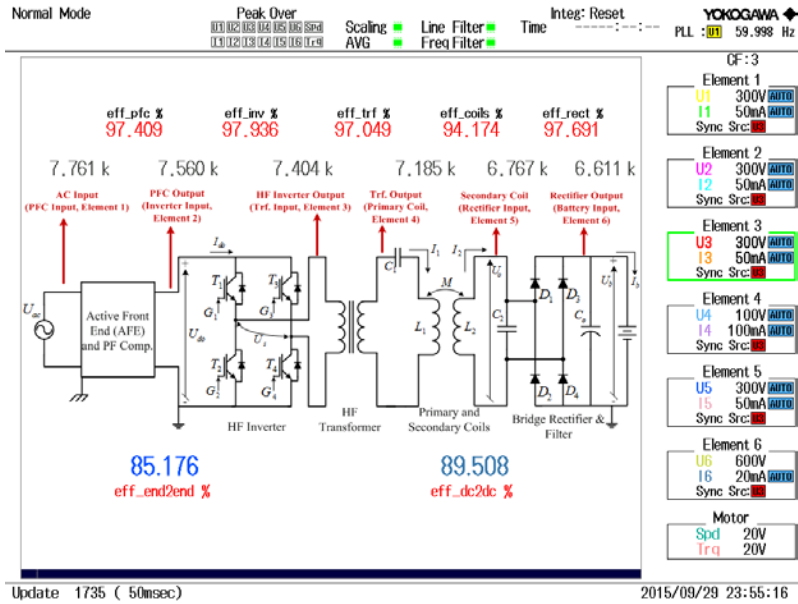


Figure II-95: Toyota RAV4 EV test results: Power flow and efficiency across 5 power conversion stages.

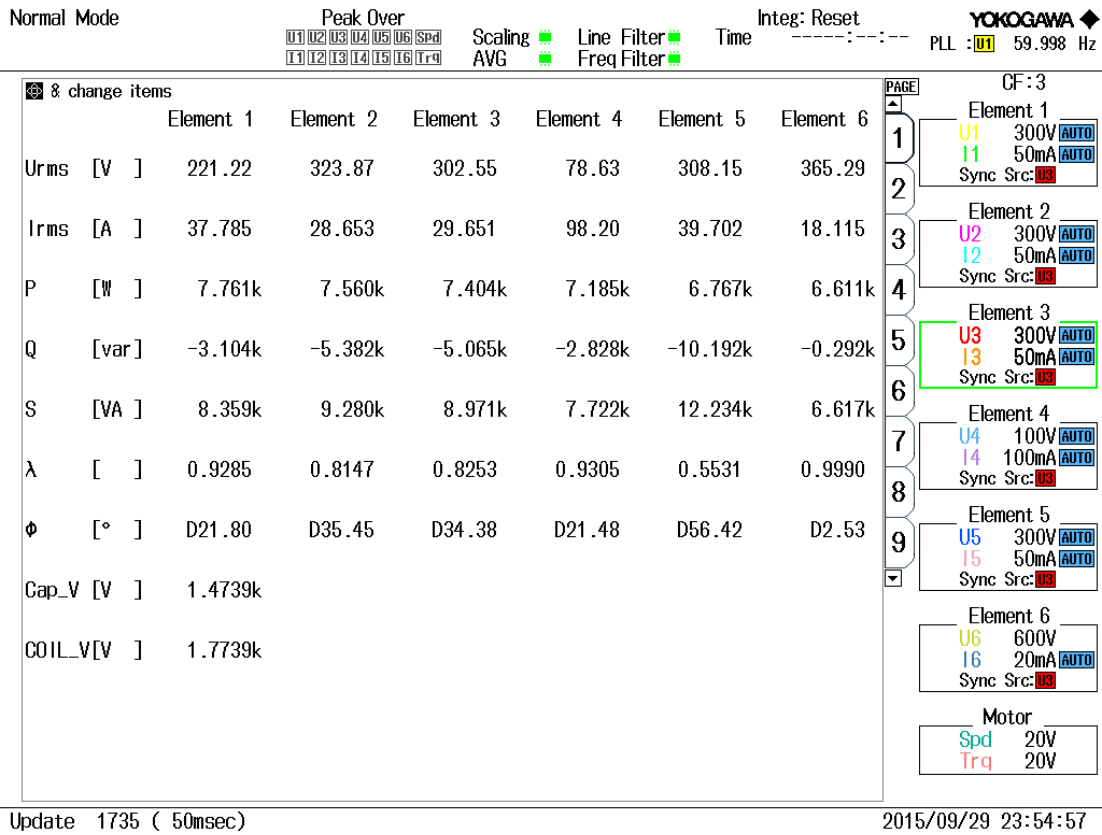


Figure II-96: Test results across all power conversion stages as well as the primary coil and tuning capacitor voltages.

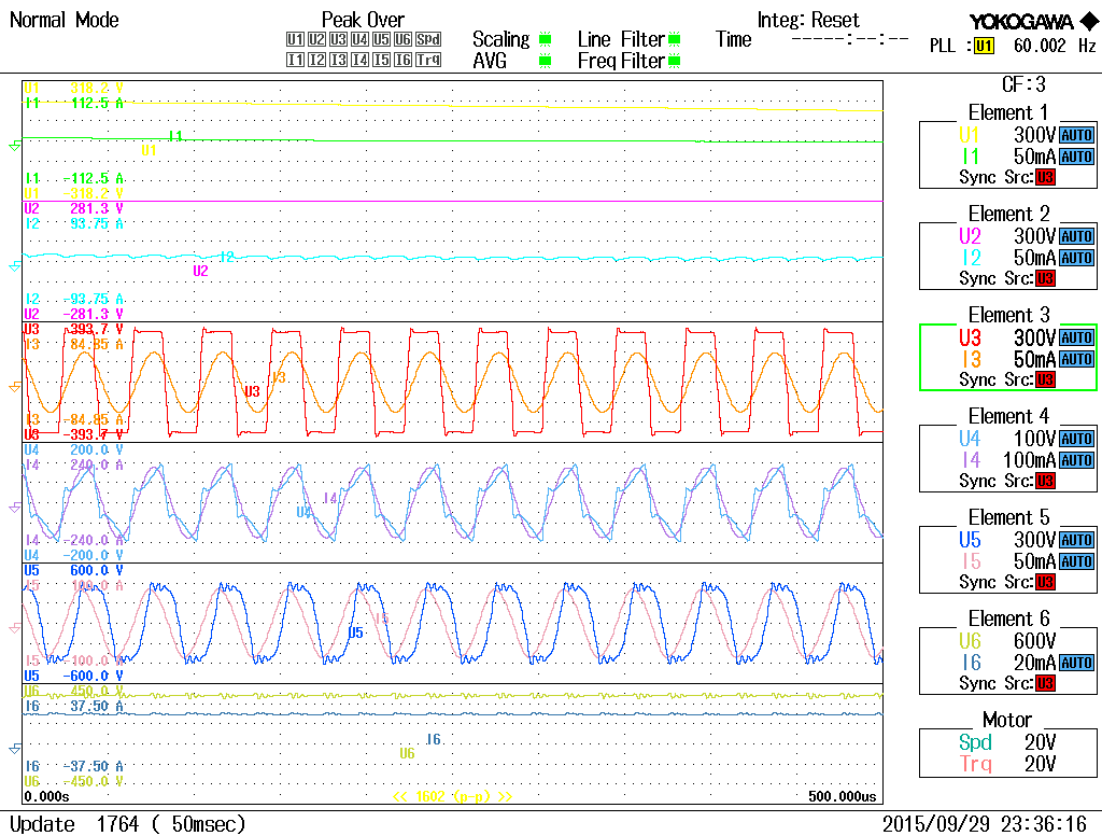


Figure II-97: Operational waveforms for high frequency elements (inverter, transformer, coupling coils).

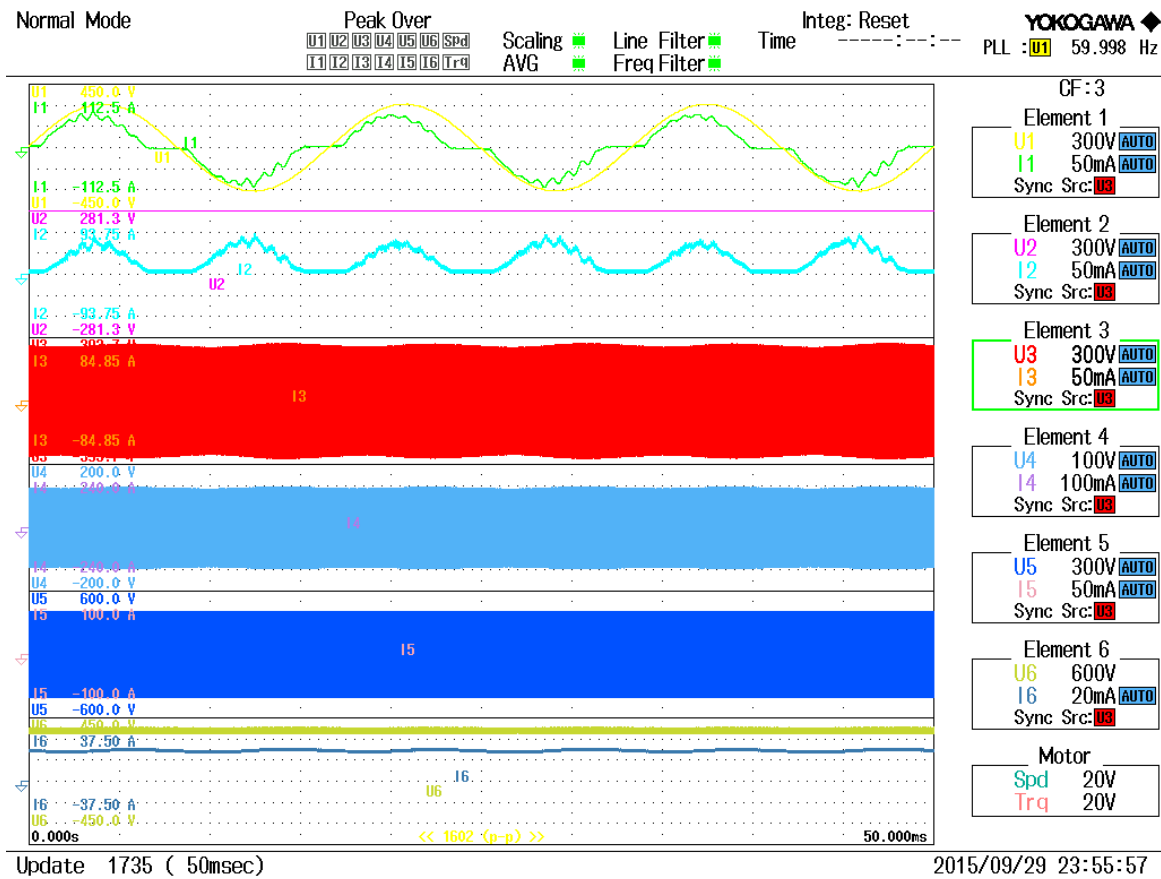


Figure II-98: Operational waveforms for low frequency elements (AC grid input, DC link, vehicle battery).

Based on the test results given in Figure II-95 and Figure II-96, ORNL team identified that all of the power conversion stages are at least 97% or more efficient except the coil-to-coil efficiency. ORNL evaluated that the reduced coil-to-coil efficiency is due to the dimensional difference in primary and secondary coils. On vehicle side, initially, team used a secondary coil that is shorter by 2 inches from each side which reduces the coupling and the efficiency. According to SAE J2954 TIR definition, unmatched coils are interoperable coils and the efficiency expectation of systems with interoperable coils is 80% instead of 85%. Due to the smaller size secondary coil, not all the field generated by primary coil can be captured by secondary. This results in higher fringe field emissions (Magnetic field). The matched and interoperable (unmatched) coils are given in Figure II-99.

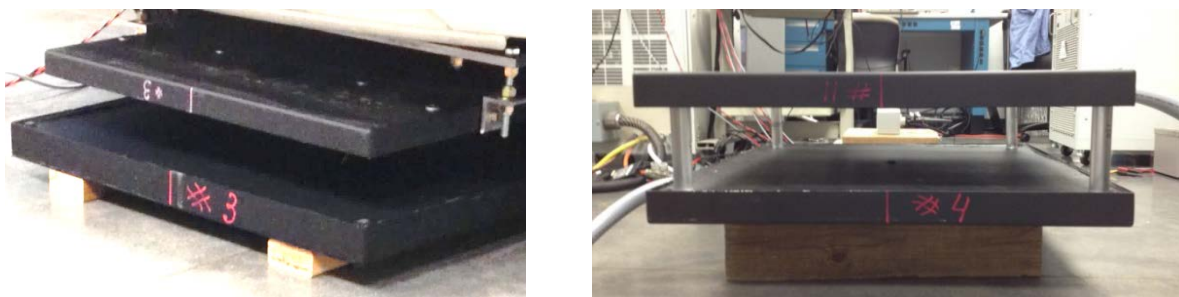


Figure II-99: Unmatched (interoperable) coils on the left and matched coils on the right.

Toyota RAV4 EV laboratory test setup photograph is shown in Figure II-100.

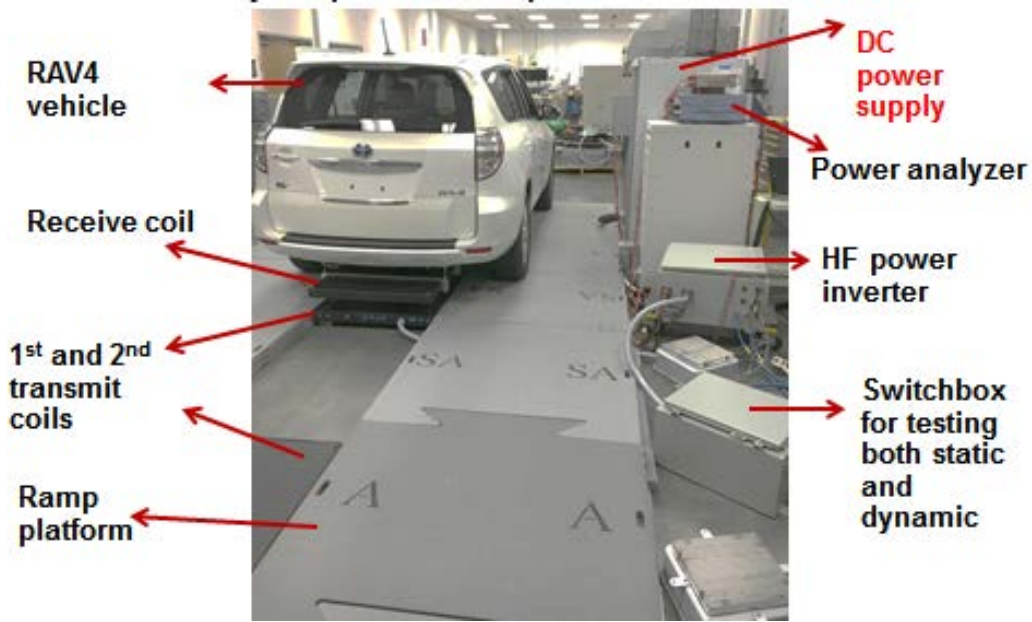


Figure II-100: Laboratory test setup with RAV4 with matched coils.

While taking this step, team also eliminated the PFC stage, which was initially designed at 6.6kW, in order to identify the actual system maximum power, which was designed to be much higher than 6.6kW. When the tests are repeated, it is seen that the coil-to-coil efficiency with the matched coils are improved from 94.17% to 98.1%.

With the SS tuning and matched coils, coil-to-coil efficiency as well as the efficiency of other stages were improved due to the reduced reactive power that the inverter had to handle earlier with poor power factor. For 6.6kW, the tests were repeated and the updated test results are shown in Figure II-101.

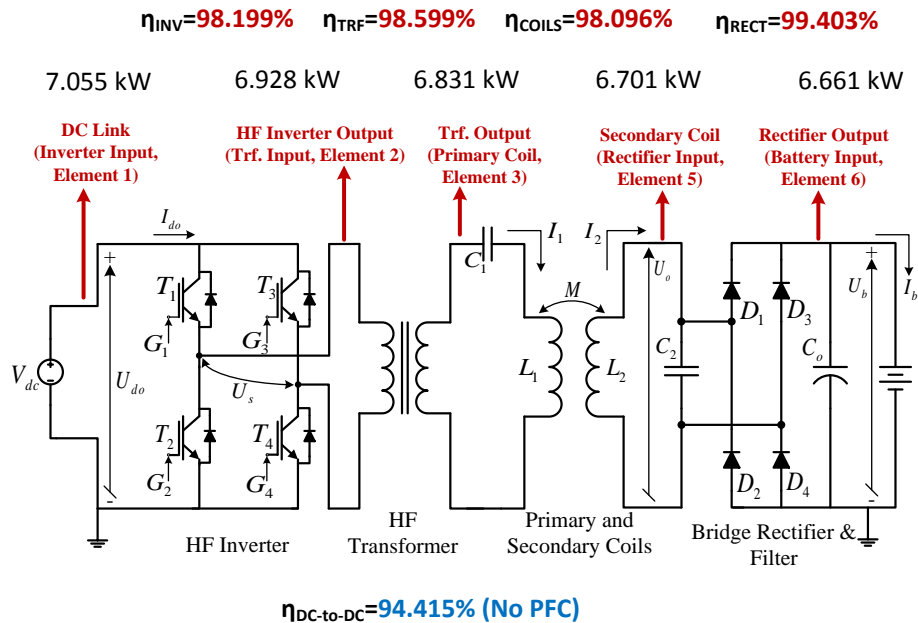


Figure II-101: Updated test results with matched coils and SS tuning with improved efficiencies.

With the findings based on the tuning configuration and coupling coils, the team tested the WPT integrated Toyota RAV4 vehicle up to ~20kW load power transfer after changing the resonant tuning configuration from series-parallel (SP) to series-series (SS). The key to achieve 20kW power transfer was also the high frequency transformer turns ratio adjustment. Other than the physical limitations on the battery maximum power, WPT system maximum power is limited by a factor of parameters including the inverter input voltage (450V maximum), primary coil current on the 2 AWG Litz wire (115A), and the voltage across the tuning capacitors (700V for each capacitor in the series string). With the transformer turns ratio adjustment, the inverter input voltage was reduced for the same amount of power delivery, allowing for higher power transfer without reaching the limit. To represent this relationship, the transformer turns ratio, inverter input voltage, primary coil current, and the load power are illustrated in Table II-18.

Table II-18: Impact of High Frequency Transformer Turns Ratio on System Limits and Maximum Power

Transformer turns ratio [#]	Inverter input voltage [V]	Primary coil current [A]	Voltage across the tuning capacitor [V]	Load power [kW]
10:3	437	62.43	921.69	9.015
8:3	442.56	65.48	966.77	12.034
7:3	438.58	67.43	995.50	14.042
6:3	417.67	69.49	1026	16.053
5:3	424.76	71.18	1050.9	20.122

Test results for 20kW power transfer are provided in Figure II-102.

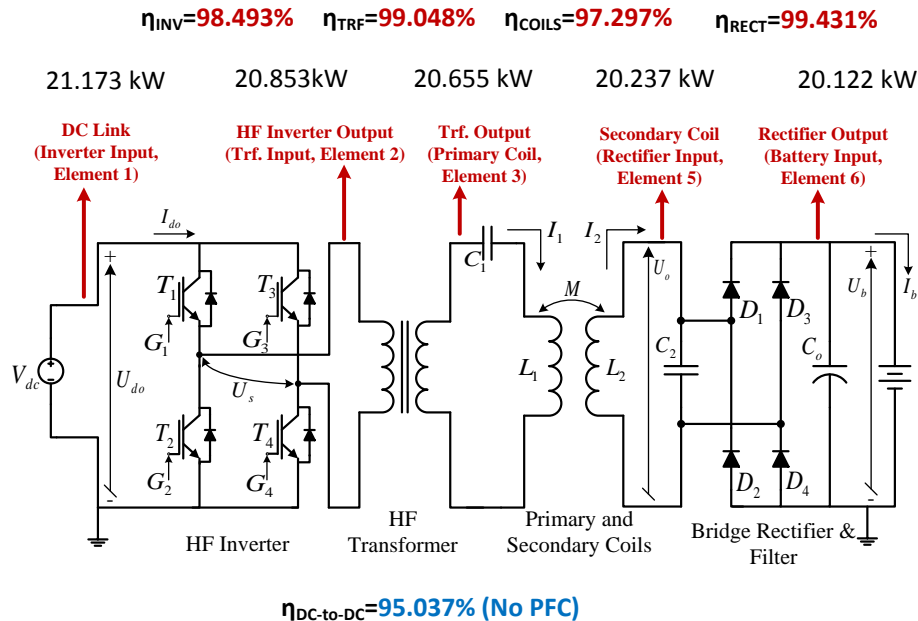


Figure II-102: High power (20kW) transfer efficiency test results by power conversion stage for Toyota RAV4.

This feature of the transformer turns ratio and the maximum power, allows the system designer to optimize the system for a target load power. With this feature, even the light load efficiency can be high if the system is optimized for that target power. Similarly, when the system is set to higher power light-load efficiency drops but efficiency at rated power increases. End-to-end efficiency vs. power for different target power levels are shown in Figure II-103. In Figure II-104, the power vs. efficiency of the system power stages are shown when

the system is optimized for 20kW power transfer. According to this figure, it is observed that the efficiencies of the high frequency transformer and the vehicle side rectifier are independent to the load power; however, the efficiencies of the inverter and the coupling coils increase with the load power and reaches to maximum at the rated power.

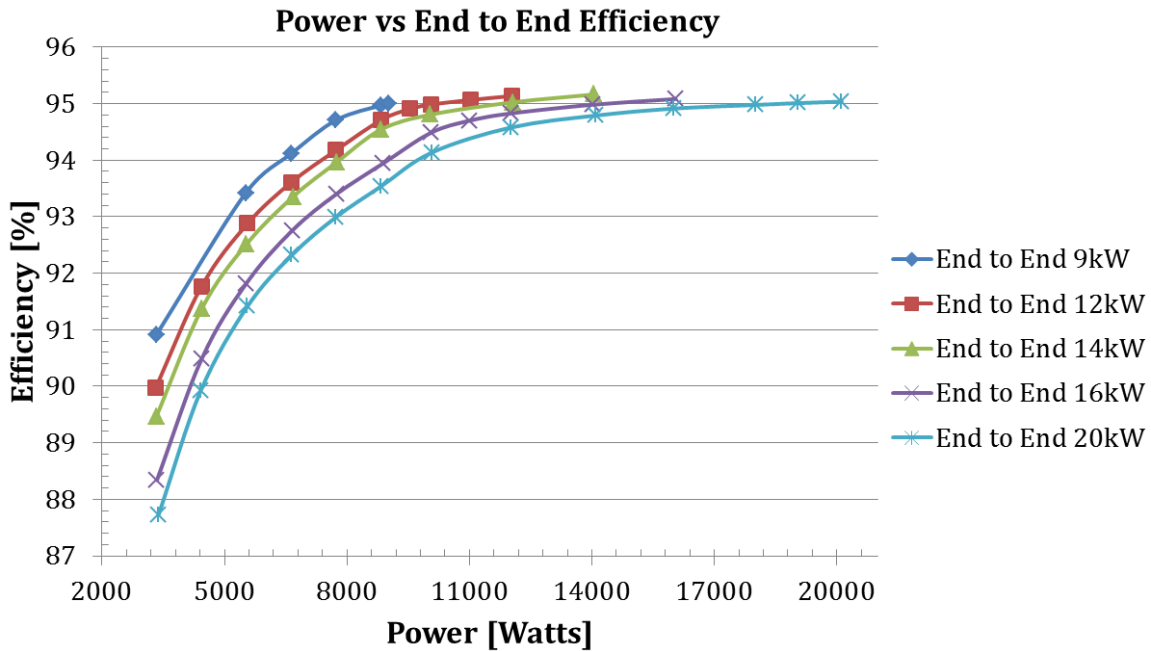


Figure II-103: End to End Efficiency versus Power for Toyota RAV4.

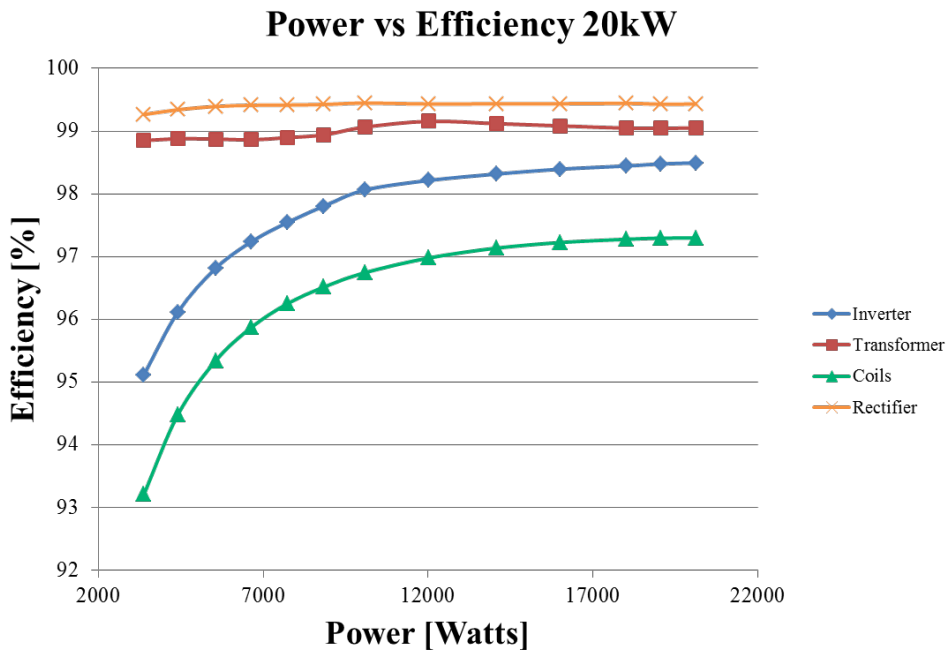


Figure II-104: Efficiency of power stages vs. power when the system is optimized for 20kW power transfer.

It should be noted that all of these tests are performed at 162 mm magnetic airgap (152 mm clearance from the surface of the secondary coil to the ground). In order to test the system performance at higher magnetic airgaps, the airgap was first increased to 184 mm (22 mm increase) to check the system limitations. Since all critical measurements were within the limits, the airgap was then increased to 206 mm (an additional 22 mm increase, 44 mm increase in total). The higher airgap tests were performed at 14kW target power to the vehicle

battery pack. The increase in the airgap, reduction in efficiency, primary power factor, and the primary coil current in these conditions are shown in Table II-19.

Table II-19: Impact of Higher Magnetic Airgap on System Limits

Airgap [mm]	Increase above the nominal [mm]	Primary coil current [A]	Primary coupler power factor [#]	Inverter input voltage [V]	Coil-to-coil efficiency [%]	End-to-end efficiency [%]	Load power [kW]
162	0	68.67	0.9605	371.49	97.083	94.98	14.029
184	22	93.20	0.9484	390.64	96.40	93.83	14.43
206	44	115.68	0.6658	350	94.24	90.79	14.45

Using the same test setup show in Figure II-100, team also demonstrated a dynamic (in-motion) wireless charging system for the Toyota RAV4 EV using the switchbox to energize two transmit coils at the same time. In this setup, two transmit coils are connected series at the output of the system instead of a single coil. One coil length of space is left in between the two transmit coils. The layout of the track is given in Figure II-105.

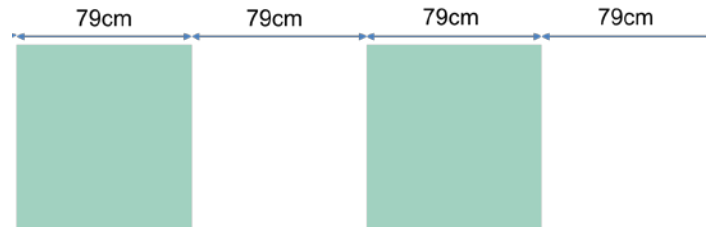


Figure II-105: Track layout for the dynamic wireless charging setup with two coils (green squares).

The energy transfer with both the SS and SP tuned coils are investigated. The power variations with respect to the relative vehicle side coil position are given in Figure II-106 for both the SS and SP tuned configurations. According to this figure, the ramp-up and fall-down skirts are wider in SP tuning configuration. Additionally, the peak power is higher. All these factors contribute to the higher energy transfer to the vehicle battery while the vehicle is in motion. Assuming 50 miles per hour constant travel speed and perfect lateral alignment, for SS tuning, 97.2 Watt-seconds (joules) are transferred to the vehicle battery by taking the time integral of the power vs. time curve. The same time integration for the power vs. time curve of the SP tuning configuration results in 281.08 Watt-seconds (joules). This corresponds to about 3 times higher energy transfer to the vehicle battery.

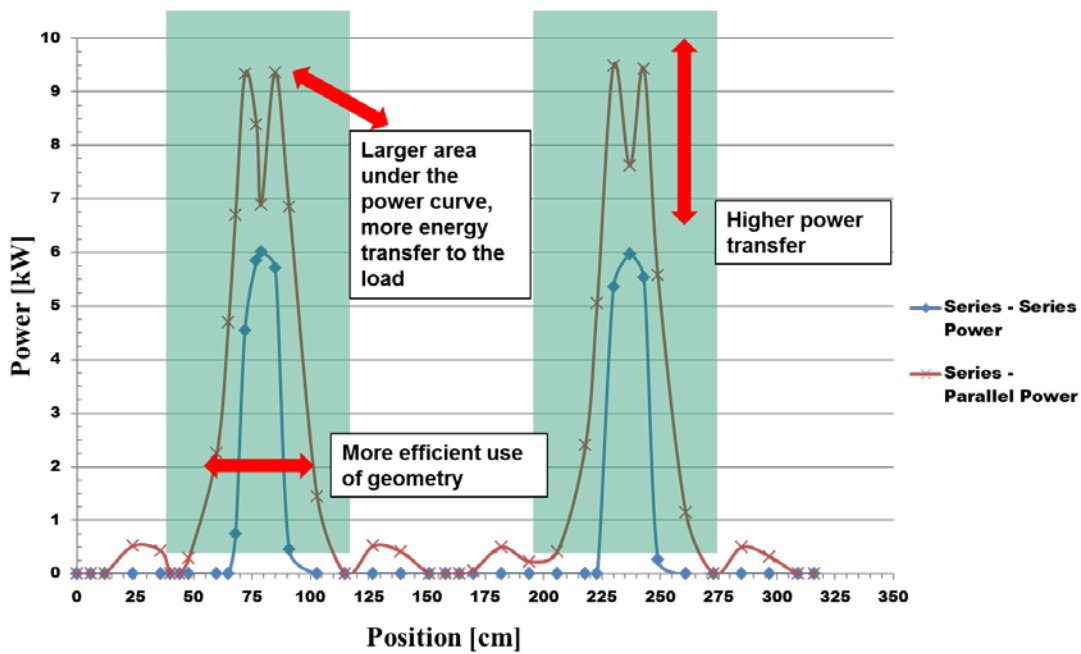


Figure II-106: In-motion wireless charging test results: Power vs. position and comparison of SS and SP tuning configurations.

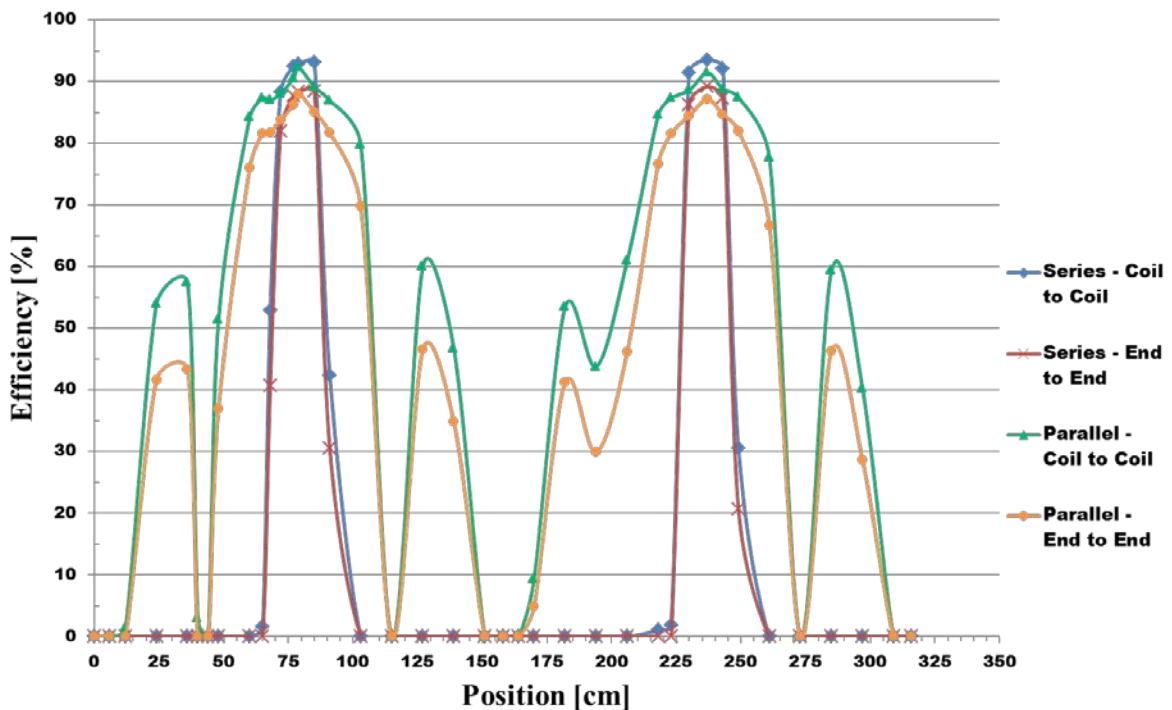


Figure II-107: In-motion wireless charging test results: Efficiency vs. position comparisons for SS and SP tuning configurations.

As observed from Figure II-106, the SS tuning results in very drastic increase and reduction in power transfer with alignment. The efficiency graph on Figure II-107 also confirms this characteristic. This results in limited energy transfer to the vehicle since the power vs. time (or power vs. position) curve has smaller area under the curve. This is due to the fact that SS tuning tunes out the primary and secondary coil self-inductances almost perfectly and this results in small remaining impedance in the system after compensation. However, in SP tuning, the reflected impedance from secondary side is different since parallel secondary tuning cannot perfectly tune the secondary self-inductance since the load is in parallel with the tuning capacitor. Therefore, the impedance vs. frequency characteristics are wider and allow for wide misalignment tolerance. Furthermore, peak power with SS tuning is limited to 6kW when fully aligned with one of the coils because in misaligned

cases worst case peak primary current is 94A. Since maximum current is limited to 120A, it is ideal to leave about 30A margin for possible current increases with lateral misalignments during driving.

Having these characteristics, the SP configuration is used for the dynamic tests. In order to evaluate the energy transfer, the power vs. position characteristics should be converted to power vs. time characteristics so that the time integral of the power curve can be calculated in order to calculate the energy. Assuming 50 MPH constant speed over the track, this speed corresponds to 2235 cm/seconds. Therefore, it takes 141 ms to complete the track of 2 coils (and a space in between) with a total length of 316 cm. Taking the numerical time integral of these curves, such that $E = \int_0^t P(t)dt$, it is found that SS tuning results in 97.2 Watt-seconds (Joules) of energy transfer whereas SP tuning results in 281.08 Watt-seconds (Joules) of energy transfer to the vehicle battery pack.

When the laboratory tests were repeated with the Toyota RAV4 EV, it was seen that the experimental results with the vehicle were slightly different from the experimental results with the manual move of the receive pad over the transmit coils. The difference was not on the power or the energy that the vehicle receives but it was on the inverter output power due to partial cross-coupling with the vehicle body. This is a future work to investigate further and this effect can be minimized or eliminated by fast communications and sequentially energizing the transmit pad while keeping them turned-off while the other vehicle parts are coupling.

Conclusions

In this phase of the project, ORNL team exceeded the original project goal of 6.6kW power transfer with 85% efficiency with >20kW power transfer with 95% dc-to-dc efficiency (92-93% expected with PFC). In addition to the initial project goal of 160 mm magnetic airgap, team also tested the system at 184 mm and 206 mm magnetic airgap levels without exceeding any of the system limitations. The impact of the turns-ratio of the transformer on the system limitations was also analyzed in order to reach 20kW power transfer. In addition, the team demonstrated an in-motion wireless charging system with the Toyota RAV4 EV with tuning configuration comparisons and their impact on energy transfer. Team also achieved an understanding of the potential impact of the vehicle body material.

II.14.C. Products

Publications/Patents

Publications (including conference and journal papers)

1. M. Chinthavali and Z. Wang, "Sensitivity analysis of a wireless power transfer (WPT) system for electric vehicle application," in *Proc., IEEE Energy Conversion Congress and Exposition (ECCE)*, September 2016, Milwaukee, WI.
2. M. Chinthavali, Z. Wang, and S. Campbell, "Analytical modeling of wireless power transfer (WPT) systems for electric vehicle application," in *Proc., IEEE Transportation Electrification Conference and Expo (ITEC)*, June 2016, Dearborn, MI.
3. M. Chinthavali, O. C. Onar, S. L. Campbell, and L. M. Tolbert, "Integrated charger with Wireless Charging and Boost Functions for PHEV and EV applications," *IEEE Transactions on Industry Applications*, submitted for review.
4. K. Colak, E. Asa, M. Bojarski, D. Czarkowski, and O. C. Onar, "A novel phase shift control of semi-bridgeless active rectifier for wireless power transfer," *IEEE Transactions on Power Electronics – Special Issue on Wireless Power Transfer*, vol. 30, no. 11, pp. 6288-6297, May 2015.
5. J. M. Miller, P. T. Jones, J. –M. Li, and Omer C. Onar, "ORNL experience and challenges facing dynamic wireless power charging of EVs," accepted for publication, *IEEE Circuits and Systems Magazine*, March 2015.
6. J. M. Miller, O. C. Onar, and M. Chinthavali, "Primary side power flow control of wireless power transfer for electric vehicle charging," accepted for publication, *IEEE Journal of Emerging and Selected Topics in Power Electronics – Special Issue on Wireless Power Transfer*, March 2014.

7. J. M. Miller, O. C. Onar, C. White, S. Campbell, C. Coomer, L. Seiber, R. Sepe, and A. Steyerl, "Demonstrating dynamic wireless charging of an electric vehicle: The benefit of electrochemical capacitor smoothing," *IEEE Power Electronics Magazine*, vol. 1, no. 1, pp. 12-24, March 2014.
8. O. C. Onar, S. L. Campbell, L. E. Seiber, C. P. White, and M. Chinthavali, "Vehicular integration of wireless power transfer systems and hardware interoperability case studies," *IEEE Energy Conversion Congress and Exposition (ECCE)*, September 2016, Milwaukee, WI.
9. M. Chinthavali, S. L. Campbell, O. C. Onar, Z. Wang, C. P. White, and L. E. Seiber, "Vehicular integration of wireless power transfer systems and hardware interoperability case studies," accepted for presentation, *IEEE Energy Conversion Congress and Exposition (ECCE)*, September 2016, Milwaukee, WI.
10. O. C. Onar, S. L. Campbell, M. Chinthavali, L. E. Seiber, and C. P. White, "A high-power wireless charging system and integration for a Toyota RAV4 electric vehicle," *IEEE Transportation Electrification Conference and Expo (ITEC)*, June 2016, Dearborn, MI.
11. M. Chinthavali, O. C. Onar, S. L. Campbell, and L. M. Tolbert, "All-SiC inductively coupled charger with integrated plug-in and boost functionalities for PEV applications," *IEEE Applied Power Electronics Conference and Exposition (APEC)*, March 2016, Long Beach, CA.
12. O. C. Onar, M. Chinthavali, S. Campbell, L. Seiber, and C. White, "ORNL Research on Wireless Charging of Electric Vehicles," SAE Hybrid Symposium, February 2016, Anaheim, CA.
13. P. T. Jones and O. C. Onar, "Impact of wireless power transfer in transportation: Future transportation enabler, or near term distraction," in *Proc., IEEE International Electric Vehicle Conference (IEVC)*, December 2014, Florence, Italy.
14. J. -M. Li, P. T. Jones, O. Onar, and M. Starke, "Coupling electric vehicles and power grid through charging-in-motion and connected vehicle technology," in *Proc., IEEE International Electric Vehicle Conference (IEVC)*, December 2014, Florence, Italy.
15. L. Tang, M. Chinthavali, O. Onar, S. Campbell, and J. Miller, "SiC MOSFET based single phase active boost rectifier with power factor correction for wireless power transfer applications," in *Proc., IEEE Applied Power Electronics Conference and Exposition (APEC)*, March 2014, Fort Worth, TX.
16. O. Onar, M. Chinthavali, S. Campbell, P. Ning, C. White, and J. Miller, "A SiC MOSFET based inverter for wireless power transfer applications," in *Proc., IEEE Applied Power Electronics Conference and Exposition (APEC)*, March 2014, Fort Worth, TX.
17. O. C. Onar, S. Campbell, P. Ning, J. M. Miller, and Z. Liang, "Fabrication and evaluation of a high performance SiC inverter for wireless power transfer applications," in *Proc., IEEE Workshop on Wide Bandgap Power Devices and Applications (WiPDA)*, pp. 125-130, October 2013, Columbus, OH.
18. P. Ning, J. M. Miller, O. C. Onar, and C. P. White, "A compact charging system for electric vehicles," in *Proc., IEEE Energy Conversion Congress and Exposition (ECCE)*, pp. 3629-3634, September 2013, Denver, CO.
19. M. S. Chinthavali, O. C. Onar, J. M. Miller, and L. Tang, "Single-phase active boost rectifier with power factor correction for wireless power transfer applications," in *Proc., IEEE Energy Conversion Congress and Exposition (ECCE)*, pp. 3258-3265, September 2013, Denver, CO.
20. O. C. Onar, J. M. Miller, S. L. Campbell, C. Coomer, C. P. White, and L. E. Seiber, "Oak Ridge National Laboratory Wireless Power Transfer Development for Sustainable Campus Initiative," in *Proc., IEEE Transportation Electrification Conference and Expo (ITEC)*, pp. 1-5, June 2013, Dearborn, MI.
21. P. Ning, O. Onar, and J. Miller, "Genetic algorithm based coil system optimization for wireless power charging of electric vehicles," in *Proc., IEEE Transportation Electrification Conference and Expo (ITEC)*, pp. 1-8, June 2013, Dearborn, MI.
22. O. C. Onar, J. M. Miller, S. L. Campbell, C. Coomer, C. P. White, and L. E. Seiber, "A novel wireless power transfer for in-motion EV/PHEV charging," in *Proc., IEEE Applied Power Electronics Conference and Exposition (APEC)*, pp. 3073-3080, March 2013, Long Beach, CA.
23. P. Ning, J. M. Miller, O. C. Onar, C. P. White, and L. D. Marilino, "A compact wireless charging system development," in *Proc., IEEE Applied Power Electronics Conference and Exposition (APEC)*, pp. 3045-3050, March 2013, Long Beach, CA.

24. M. Chinthavali, O. C. Onar, and J. M. Miller, "A wireless power transfer system with active rectification on the grid side," in *Proc., Conference on Electric Roads and Vehicles (CERV)*, February 2013, Park City, UT.
25. J. M. Miller, C. P. White, O. C. Onar, and P. M. Ryan, "Grid side regulation of wireless power charging for plug-in electric vehicles," *IEEE Energy Conversion Congress & Exposition (ECCE)*, pp. 261-268, September 2012, Raleigh, NC.
26. J. M. Miller and O. C. Onar, "Oak Ridge National Laboratory In-motion wireless power transfer system," *1st Conference on Electric Roads and Vehicles (CERV2012)*, February 2012, Part City, UT.
27. M. Pickelsimer, L. Tolbert, B. Ozpineci, and J. M. Miller, "Simulation of a Wireless Power Transfer System for Electric Vehicles with Power Factor Correction," in *Proc., IEEE International Electric Vehicle Conference (IEVC)*, pp. 1-6, March 2012, Greenville, SC.
28. O. C. Onar, "Recent Advances in Wireless Power Transfer Systems," IEEE Applied Power Electronics Conference and Exposition, Industry Special Session on Recent Development in Wireless Power Transfer, March 2015, Charlotte, NC.
29. J. M. Miller (Moderator), Ted Bohn, O. C. Onar, J. Taiber, and M. de Rooji, "Wireless Power Transfer: Facts and Fictions," RAP Session at the IEEE Applied Power Electronics Conference and Exposition, March 2015, Charlotte, NC.
30. O. C. Onar, "Electric Vehicles without Plugging-In," Presentation at the University of Tennessee Science Forum, November 2014, Knoxville, TN.
31. O. C. Onar, "Electric Vehicles without Plugging-In," Presentation to the Technical Society of Knoxville, November 2014, Knoxville, TN.
32. O. C. Onar, "Electric Dreams: Sustainable Mobility without Plugging-in," Coil Winding, Insulation, Electrical Manufacturing Conference and Expo, September 2014, Chicago, IL.
33. O. C. Onar, "ORNL Dynamic Wireless Power Transfer Systems," University of Tennessee-Knoxville, ESE599 Seminar, Bredesen Center for Interdisciplinary Research and Graduate Education, invited by Center Director, September 2014.
34. O. C. Onar, "Charge on the go: In-motion Wireless Power Transfer Systems and Its Effect on the EV Market," ORNL Transportation Science Seminar Series, Invited by FEERC Center Director Robert Wagner, July 2014.
35. O. C. Onar (ORNL, panelist and panel organizer), Kevin Bai (Kettering University, panelist), Roger Burns (OLEV Technologies, panelist), and Konrad Woronowicz (Bombardier, panelist), Pavol Bauer (panel session chair), *IEEE Transportation Electrification Conference and Expo (ITEC) Panel Session on Wireless Power Transfer Systems for PEV Charging Applications*, June 2014, Dearborn, MI.
36. O. C. Onar, Madhu Chinthavali, J. M. Miller, and P. T. Jones, "ORNL Developments in Stationary and Dynamic Wireless Charging," IEEE Applied Power Electronics Conference and Exposition, Industry Session on Key Vehicle Power Electronics, March 2014, Fort Worth, TX.
37. O. C. Onar (ORNL, panelist), T. Bohn (ANL, panelist), S. Stanton (ANSYS, panelist), J. Muhs (WiTricity, panelist), J. Curry (Qualcomm Inc., panelist), Matt Roush (WWJ's Tech Report, CBS, moderator), *Wireless Power Transfer Workshop*, organized by IEEE, ANSYS, University of Michigan, and DOE GATE Center for Electric Drive Transportation, March 2014, Dearborn, MI.
38. O. C. Onar, "ORNL WPT Developments," USCAR Electrical and Electronics Technology Team Meeting, March 2014, Southfield, MI.
39. O. C. Onar, "ORNL Wireless Power Transfer Technology," Friends of the ORNL (FORNL) Meeting, February 2014, Oak Ridge, TN.
40. O. C. Onar, "ORNL WPT Developments," International Forum on Eco-Friendly Vehicle and System Forum (IFEV), Distinguished Speaker at the Plenary Session, October 2013, Daejeon, Korea.
41. O. C. Onar, J. M. Miller, and P. T. Jones, "ORNL Developments in Stationary and Dynamic Wireless Charging," *IEEE Energy Conversion Congress & Exposition (ECCE) Special Session on: Advances in Wireless Power for Electric Vehicles*, September 2013, Denver, CO.
42. P.T. Jones and O.C. Onar, "Considerations for Deployment of In-Motion Wireless Power Transfer Technologies in Transportation" SAE 2014 Hybrid and Electrical Vehicle Symposium Feb 2014 La Jolla, CA.

43. J. M. Miller and O. C. Onar, "Short Course on Wireless Power Transfer (WPT) Systems," Educational short course at the *IEEE Transportation Electrification Conference and Expo (ITEC)*, June 2013, Dearborn, MI.
44. J. M. Miller (panel session chair), O. C. Onar (ORNL, panelist and panel organizer), A. Daga (Momentum Dynamics, panelist), David Schaltz (WiTiricity, panelist), and S. M. Lukic (North Carolina State University, panelist), *IEEE Transportation Electrification Conference and Expo (ITEC) Panel Session on Wireless Power Transfer Systems for PEV Charging Applications*, June 2013, Dearborn, MI.

Patents / Pending Patents:

1. ID-2250 – A Loosely Coupled Air Core Transformer with Improved Efficiency Operation, US Patent [8,310,202](#)
2. ID-2637 – Coupling Coil ac Resistance Minimization, US Patent Application [13/526,662](#)
3. ID-2638 – Regulation Control and Energy Management Strategy for Wireless Power Transfer, US Patent Application [13/484,404](#)
4. ID-2639 – WPT EVSE Installation and Validation Tool, US Patent Application [13/526,659](#)
5. ID-2667 – Wireless Power Transfer Electric Vehicle Supply Equipment Installation and Validation Tool, US Patent Application [13/544,058](#)
6. Vehicle to Wireless Power Transfer Coupling Coil Alignment Sensor, [U.S. Patent no: 9,260,026](#)
7. ID-2768 – WPC Using Point of Load Controlled High Frequency Power Converters, US Patent Application [13/739,198](#)
8. ID-2813 – Off-Resonance Frequency Operation of Wireless Power Transfer US Patent Application [13/447,447](#)
9. ID-2956 – Buffering Energy Storage Systems for Reduced Grid and Battery Stress PCT patent application [US13/027578](#)
10. ID-3196 – Overvoltage Protection System for Wireless Power Transfer Systems, US Patent# [14/631,903](#).

II.14.D. References

1. Please refer to the publications listed above.

ZERO EMISSION CARGO TRANSPORT 1

II.15. Zero Emission Drayage Trucks Demonstration [EE-0005961]

Matt Miyasato, Principal Investigator, Deputy Executive Officer

South Coast Air Quality Management District
21865 Copley Drive
Diamond Bar, CA 91765
Phone: (909) 396-3249; Fax: (909) 396-3252
E-mail: mmiyasato@aqmd.gov

Brian Choe, Co-Principal Investigator, Program Supervisor

South Coast Air Quality Management District
Phone: (909) 396-2617; Fax: (909) 396-3252
E-mail: bchoe@aqmd.gov

Lee Slezak, DOE Program Manager, Vehicle Systems Manager

U.S. Department of Energy
Phone: (202) 586-2335
E-mail: Lee.Slezak@ee.doe.gov

Start Date: October 1, 2012
End Date: September 30, 2017

II.15.A. Abstract

Objectives

- The objective of this project is to develop and demonstrate eleven zero emission capable heavy-duty drayage trucks based on four different architectures, consisting of two battery electric drivetrains and two plug-in hybrid electric drives with all-electric range capability, to promote and accelerate deployment of zero emission cargo transport technologies.
- This project will also collect and analyze vehicle performance and O&M data to evaluate technical feasibility and market viability of zero emission truck technologies in drayage operations.

Accomplishments

- Completed five battery electric trucks (BETs) with four currently in demonstration with fleet partners at the Ports of Los Angeles and Long Beach
- First plug-in hybrid electric truck (PHET) is completed and undergoing validation testing
- Two BETs, one each from TransPower and US Hybrid, has been tested on chassis dynamometer at University of California, Riverside (UCR)
- Continue to collect and analyze vehicle performance and operational data.

Future Achievements

- Complete and deploy the remaining five vehicles in revenue drayage service for demonstration
- Complete validation testing including chassis dynamometer testing.

II.15.B. Technical Discussion

Introduction

On-road heavy-duty diesel trucks are one of the largest sources of diesel particulate matter and NOx emissions in the South Coast Air Basin. The impact on air quality and public health is more pronounced in the surrounding communities along the goods movement corridors near the Ports of Los Angeles and Long Beach, and next to major freeways in Southern California. As a measure to reduce the impact and to meet federal ambient air quality standards, South Coast Air Quality Management District (SCAQMD) has been working with regional stakeholders, including the Ports of Los Angeles and Long Beach, to promote and support the development and deployment of advanced zero emission cargo transport technologies. In 2012, SCAQMD received a \$4.17 million grant from the DOE Zero Emission Cargo Transport Demonstration Program to develop and demonstrate zero emission capable drayage trucks based on four different electric drive architectures in real world drayage environment. The main objective is to promote zero emission truck technologies to fleet operators, the end users, by demonstrating that electric drayage trucks are capable of supporting demanding drayage operations reliably. This project is also to collect and analyze vehicle performance and O&M cost data to evaluate the benefits over conventional diesel trucks and assess their market viability in drayage operations.

Approach

This project will develop eleven zero emission and near-zero emission heavy-duty drayage trucks for demonstration based on four different architectures, consisting of two types of battery electric vehicles (BEVs) and two types of plug-in hybrid electric vehicles (PHEVs) with all-electric range capability. Initial project scope had a total of thirteen trucks including Vision Motor’s fuel cell hybrid electric trucks and Balqon’s BETs but these two companies have since dropped out due to financial hardships and limited resources. With the departure of Vision Motors and Balqon, TransPower and US Hybrid, locally based EV system developers and vehicle integrators in Southern California, have been selected to develop plug-in hybrid electric trucks with all-electric range, in addition to the BETs they are already building under this project as summarized in Table I-

Table II-20: 2012 Zero Emission Drayage Truck Demonstration Portfolio

Technology Provider	Architecture	No. of Trucks
TransPower	BEV	4
US Hybrid	BEV	2
TransPower	PHEV	2
US Hybrid	PHEV	3
Total		11

Upon completion, these trucks will be deployed in revenue drayage service for up to two years of demonstration with fleet partners at the Ports of Los Angeles and Long Beach. During the demonstration, vehicle performance and O&M data will be collected and analyzed by National Renewable Energy Laboratory (NREL) to evaluate technical feasibility and market viability of the technologies to support drayage operations. In addition, each technology will be tested on chassis dynamometer at the UCR for performance validation.

Battery Electric Trucks

a) TransPower

TransPower will develop four Class 8 BEV drayage trucks for demonstration. The motive power will be provided by a dual motor system with two 150 kW motors, coupled to an automated manual transmission (AMT) with proprietary software for high vehicle performance and improved efficiency. Also, TransPower will use an innovative Inverter-Charger Unit (ICU) that combines the functions of both vehicle inverter and battery charger to reduce the size and cost of power electronics.

Figure II-108 shows an illustration of the TransPower BEV system, which is comprised of:

- 300 kW dual motor assembly coupled to an AMT
- Two ICUs, each rated at 150 kW for motor control and 70 kW for charging
- 215 kWh lithium iron phosphate battery pack, air cooled
- 70 to 100 miles of range in normal drayage operation
- Recharge time of 3-4 hours with one 70 kW ICU

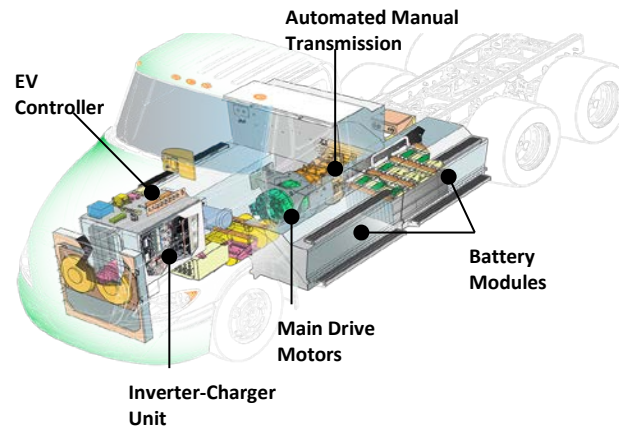


Figure II-108: TransPower BEV System

b) US Hybrid

US Hybrid will develop two Class 8 BEV drayage trucks. Each truck will be powered by a 320kW induction motor with a direct drive control to provide sufficient power and torque to support drayage operations.

Figure II-109 shows an illustration of the US Hybrid BET, which is equipped with:

- Direct drive powertrain with a 320 kW induction motor
- Lithium-ion battery pack with 240 kWh in total capacity, air cooled
- 60 kW on-board charger
- 70 to 100 miles of range in normal drayage operations
- Recharge time of 4-5 hours with 60 kW on-board charger

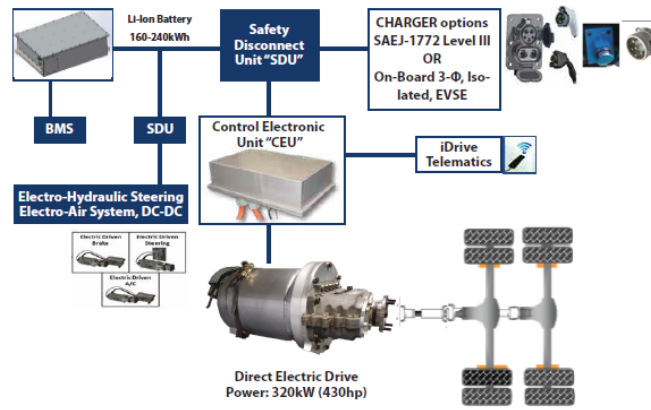


Figure II-109: US Hybrid BEV System

Plug-In Hybrid Electric Trucks

a) TransPower

Two Class 8 plug-in hybrid electric trucks will be developed by TransPower with a targeted operating range of 150-200 miles, including 30-40 all-electric miles. The hybrid technology is based on the ElecTruck™ system TransPower has developed for their BETs with a CNG auxiliary power unit (APU) as a range extender.

Figure II-110 shows an illustration of the TransPower’s PHEV system, which will be comprised of:

- Series hybrid system with a 3.7L CNG engine-generator
- 300 kW dual motor assembly coupled to 10-speed AMT
- Two ICUs, each rated at 150 kW for motor control and 70 kW for charging
- 155 kWh lithium iron phosphate battery pack, air cooled
- 30-40 all-electric miles, and 150-200 miles of total range in normal drayage operations

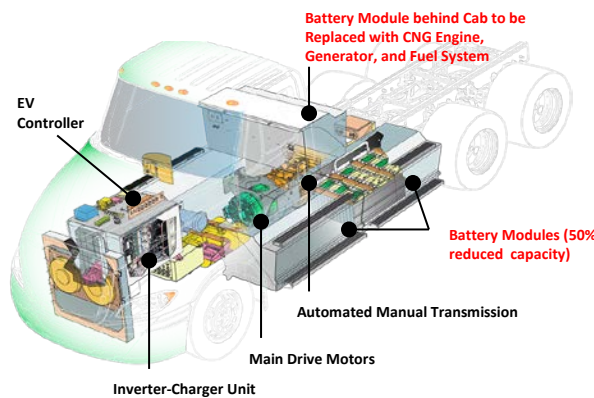


Figure II-110: TransPower PHEV System

b) US Hybrid

US Hybrid will develop three Class 8 plug-in hybrid electric drayage trucks for demonstration. US Hybrid will convert exiting LNG trucks with 8.9L ISLG engine into PHETs with all-electric range capability. The hybrid

system will be designed to provide comparable power and torque to those from larger 12L or 15L engines to support a full range of drayage operations.

Figure II-111 shows the proposed US Hybrid PHEV topology, which will be comprised of:

- Parallel hybrid system with 8.9L LNG engine-generator
- 240 kW powertrain with an automatic transmission
- 240 kW motor control unit and 20 kW on-board charger
- Lithium-ion battery pack with 80 kWh in total capacity, air cooled
- 30-40 all-electric miles, and 150-200 miles of total range in normal drayage operations

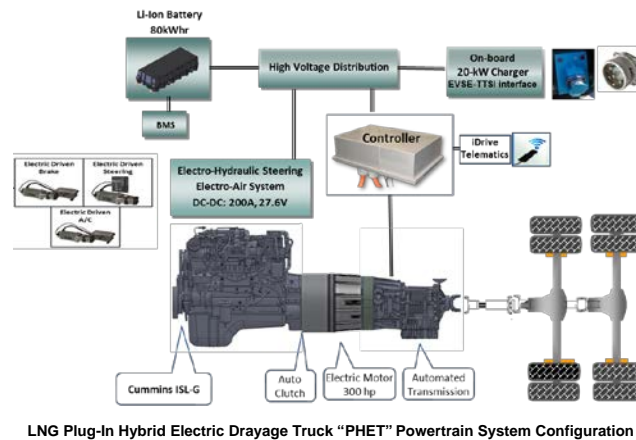


Figure II-111: US Hybrid PHEV System

Results

Battery Electric Trucks

The project has made steady progress in FY 2016. TransPower has maintained three of their four BETs in drayage service with the fourth truck just upgraded with new battery cells and advanced battery management system (BMS). US Hybrid also deployed their first BET in drayage service in July 2016 after extensive testing for validation, including chassis dynamometer testing in October 2015. The achievements in FY 2016 are further discussed below.

a) TransPower

TransPower has successfully maintained three of their four BETs, EDD2 through EDD4, in drayage service without much downtime throughout 2016. Also, TransPower completed an upgrade of EDD1, their first BET which had been sidelined due to unreliable battery cells and BMS, with higher density battery cells and advanced and more reliable BMS in September and is currently undergoing on-road testing for validation. As of September 2016, the four BETs have collectively accumulated over 27,000 miles, including 18,600 miles in drayage service under this project.

EDD trucks continue to generate interest within the local and national trucking industry. After starting out with only two fleets for demonstration, namely TTSI and SA Recycling in January 2015, many more fleet operators have since signed up for demonstration, including Cal Cartage, National Retail Transportation, Knight Transportation, PASHA, and 3 Rivers Trucking. Feedback from fleet operators described the trucks as quiet, clean and easy to drive especially in the stop and go traffic at the ports. The 80-mile range with average

payloads works well for short haul applications, especially with close-to-port operators like Cal Cartage who can complete as many as 4 or 5 container “moves” or “turns” daily from the port terminals to their yard.



Figure II-112: TransPower EDD Trucks

As shown in Table II-21 which summarizes daily average use and performance data reported by NREL, EDD trucks averaged 5 hours per day of operation, covering 40-50 miles of distance with 2-2.5 kWh/mi in fuel efficiency. The EDD trucks spent over 50% of their operating hours idling, mostly while waiting in queues to load and unload cargo containers at the port terminals. This type of operation is typical for short-haul drayage trucks operating at the Ports of Los Angeles and Long Beach, and they are ideal match for electric trucks which, unlike conventional diesel trucks that have to keep their engine running for AC and other amenities during such operations, can use a small amount of battery power for AC and other auxiliary loads with zero tailpipe emissions, thus providing significant fuel savings as well as considerable benefits in air quality and public health.

Table II-21: TransPower EDD Trucks Average Daily Use

Parameter	EDD2	EDD3	EDD4
Time (hr)	4.91	5.02	5.19
Distance (mi)	50.35	40.94	45.74
Energy Efficiency (kWh/mi)	1.96	2.47	2.14
Regeneration Energy (kWh)	17.81	17.60	12.90
Average Speed (mph)	11.64	8.85	10.50
Average Driving Speed (mph)	22.21	18.62	19.51
Idle Time (hr)	2.64	2.82	2.84
Start SOC (%)	97.12	96.44	83.79
End SOC (%)	57.48	52.04	49.38
Air Conditioning Energy (kWh)	2.49	3.70	2.50

TransPower also completed an upgrade of EDD1 with a new battery product and more reliable BMS. The new batteries for EDD1, cylindrical cells of an advanced design with 60% higher energy density, are installed into four battery boxes, two on each side of the truck, providing a total of 311 kWh in capacity with a similar weight and footprint of the existing 215 kWh system used in other EDD trucks. The truck is currently

undergoing on-road testing for validation and is expected to be re-deployed in drayage service with TTSI for longer drayage runs to warehouses and distribution centers in the Inland Empire region, approximately 50-60 miles east of the Ports of Los Angeles and Long Beach.



Figure II-113: TransPower EDD1 with new battery cells and BMS

b) US Hybrid

US Hybrid has also made good progress in FY 2016, having deployed their first BET (Figure II-113) in drayage service with TTSI in July 2016 after extensive evaluation, including chassis dynamometer testing at the University of California, Riverside in October 2015. The testing was conducted over UDDS and Port Truck Drayage Cycles with 72,000 lbs. GCW in test weight. Preliminary test results showed the truck had performed well, demonstrating 3.0 kWh or less per mile in energy efficiency and 72 miles of range with a fully loaded container.

US Hybrid has also conducted extensive on-road testing with the truck, including highway driving for validation and optimization. The testing also included pulling a fully loaded trailer over the Vincent Thomas Bridge, a suspension bridge located in the San Pedro Bay Port complex with a steep 7% grade. US Hybrid BET demonstrated sufficient power to manage the 7% grade bridge with a full load while maintaining observed speed limits. As noted earlier, this truck is now deployed in drayage service with TTSI since late July. Based on initial feedback, TTSI drivers are generally impressed with the smooth ride, low cabin noise, and steady power delivery. The truck had a minor issue with its AC compressor which has since been fixed with an upgrade.



Figure II-114: US Hybrid BET

Plug-In Hybrid Electric Trucks

With both PHEV technologies added in midstream in late 2015, there aren't any demonstration trucks deployed in drayage service for either technology. However, both TransPower and US Hybrid have made good progress, especially with US Hybrid in FY 2016. US Hybrid completed their first PHET in May and has since been testing the vehicle for validation and optimization. TransPower has also completed vehicle and system design, leveraging their experience and knowledge gained from the development of a hybrid catenary truck in a separately-funded project. The achievements in FY 2016 are further discussed below.

a) TransPower

With the contract executed in December 2015, TransPower has since completed vehicle and system design for the PHEV trucks and also continued testing a prototype CNG generator in a separately-funded hybrid catenary truck, to characterize and fine tune engine control for maximum efficiency with minimum impact on emissions. TransPower will utilize the test results to improve and refine the auxiliary power unit for their PHETs to be developed in this project. TransPower is also constructing a dyno test cell using all of the parts and features of the production article generator sets to run calibration testing of custom engine control software. This test cell will be installed into a trailer outside their facility in Poway CA to provide a controlled testing environment with an added level of safety, noise abatement, and security.

TransPower has ordered and received most of the long lead components except for the batteries. Voltronix, their battery supplier, recently notified TransPower that they could not guarantee a continued supply of 300 Ah lithium iron phosphate cells TransPower was planning to use for the trucks. As a result, TransPower has decided to use the new, higher density cells, which are used in the EDD1 truck upgrade, for the PHETs as well. However, this decision to switch battery cells will not cause much delay in the project schedule because TransPower has already procured enough of the new cells for both PHETs. Based on the current projection, TransPower expects to complete the first PHET by December 2016.

b) US Hybrid

US Hybrid completed their first PHET in May 2016 and is currently running validation testing with the truck. The powertrain, which is based on a parallel hybrid architecture with a Cummins 8.9L ISLG engine, has demonstrated sufficient power and torque, even comparable to those of larger Cummins ISX12 and ISX15 engines, to support a full range of demanding drayage duty cycles without penalties in fuel economy and emissions that are typically associated with larger engines. Upon successful demonstration of the system, US Hybrid aims to market the system to drayage fleets as a viable technology to convert LNG trucks with the 8.9L ISLG engine, which is known to be underpowered to support heavy-duty drayage operations. US Hybrid plans to deploy their first PHET in drayage service with TTSI in early 2017 after more testing has been completed, including a chassis dynamometer testing at the UCR.



Figure II-115: US Hybrid PHET

II.15.C. Products

Presentations/Publications/Patents

1. None

II.15.D. References

1. None

II.16. Hydrogen Fuel-Cell Electric Hybrid Truck Demonstration [EE0005978] & Houston Zero Emission Delivery Vehicle Deployment [EE0005979]

Andrew J. DeCandis, Principal Investigator

Houston-Galveston Area Council
3555 Timmons Lane, Suite 120
Houston, TX 77027
Phone: (832) 681-2589; Fax: (713) 993-4508
E-mail: Andrew.DeCandis@h-gac.com

Lee Slezak, DOE Program Manager

Office of Energy Efficiency and Renewable Energy
Phone: (202) 586-2335
E-mail: Lee.Slezak@ee.doe.gov

Start Date: October 1, 2012
End Date: September 30, 2017

II.16.A. Abstract

Objectives

EE0005978

- Accelerate the introduction and penetration of electric transportation technologies (ETT) into the cargo transport sector.
- Demonstration of at least three (3) Class 8 zero-emission port drayage trucks
 - Vehicles will be selected through a Call for Projects process.
 - Vehicles will meet or exceed all applicable federal and state emission requirements and safety standards.
- Operate vehicles under real world conditions at or near the Port of Houston to measure and demonstrate operational cost-effectiveness and commercial viability.

EE0005979

- Accelerate the introduction and penetration of electric transportation technologies (ETT) into the cargo transport sector.
- Deployment of thirty (30) all-electric delivery trucks.
- Project vehicles will be selected through a Call for Projects process. Vehicles will be operated by selected fleet operators including large national fleets and progressive regional fleets with delivery operations.
- Testing and data collection for vehicles in real-world conditions to measure and demonstrate operational cost-effectiveness and commercial viability.

Accomplishments

EE0005978

- Worked with USDOE to finalize a project modification to manufacture and deploy three (3) zero-emission Class 8 zero-emission trucks.

- Worked with Gas Technologies Institute (GTI) to modify contract language to account for issues of timing and budgeting. This is ongoing.
- US Hybrid worked to begin construction on the three (3) zero-emission Class 8 zero-emission trucks. This is ongoing.

EE0005979

- Completed delivery of all eighteen (18) contracted vehicles from OEM Workhorse to United Parcel Service (UPS).
- All of the delivered vehicles for this portion of the project have now been registered by UPS with the State of Texas and have been deployed to routes within the Houston-region.
- Continued to solicit local fleets through a Call for Projects to solicit fleet partners for the remaining twelve (12) all-electric delivery vehicles.
- This solicitation resulted in the submission of twelve (12) additional vehicles to be purchased by UPS and manufactured by BYD. At this time, discussions are being held with USDOE regarding the acceptability of the solicitation.

Future Achievements

EE0005978

- Full deployment and demonstration of at least three Class 8 zero-emission port drayage trucks.
- Release of technical report on cost-effectiveness of Class 8 zero-emission trucks in regional fleet(s).

EE0005979

- Contract with additional fleet(s) to deploy the final twelve (12) all-electric delivery vehicles.
- Reduce emission of 4,180 tons of criteria pollutants over the two-year project deployment phase.
- Reduce emissions of greenhouse gases by 75 MMTCE over the two-year project deployment phase.
- Reduce over 250,000 gallons of diesel fuel over the year project deployment phase.
- Release of technical report on cost-effectiveness and emission reductions related to vehicle deployment.

II.16.B. Technical Discussion

Background

EE0005978

The Houston-Galveston Area Council (H-GAC) is partnering with a project team (including a regional fleet and zero-emission Class 8 truck OEM) for a Zero-Emission Class 8 Drayage Truck Demonstration Project. The primary objective of the project is to accelerate the introduction and penetration of electric transportation technologies into the cargo transportation sector. The project will deploy vehicles, establish required fueling infrastructure, and demonstrate that vehicles will meet or exceed all emissions requirements.

To meet this objective, the grant will support development and demonstration of three Class 8 zero-emission trucks in the Houston-Galveston-Brazoria NAAQS 8-hour ozone nonattainment area. The project will demonstrate vehicle operations, collect data, and report on project results for a period of two years after deployment.

Long-term benefits of the program may include improved air quality in highly traveled areas in the Houston region and particularly near the active port facilities. Additionally, fleets may realize savings on fuel expenditures and can work towards meeting sustainability and corporate social responsibility goals.

EE0005979

The Houston-Galveston Area Council (H-GAC), Center for Transportation & the Environment (CTE), have partnered to establish the Houston Zero Emission Delivery Vehicle Demonstration Project. The primary objective of the project is to demonstrate the effectiveness of all-electric delivery vehicles to perform at the same level of operation as similarly sized diesel delivery vehicles, while reducing vehicle emissions and petroleum consumption.

To meet this objective, this project will support the deployment of 30 all-electric delivery trucks in the Houston-Galveston-Brazoria NAAQS 8-hour ozone nonattainment area.

Vehicles selected through a Call for Projects process will be demonstrated by selected national, regional, and/or local fleets. All vehicle deployment and operation of the vehicles will occur with the Houston-Galveston region. In addition to the deployment of delivery vehicles and charging infrastructure, the project will demonstrate vehicle operations, collect data, and report on project results for a period of two years after deployment.

Introduction

EE0005978

This project supports ongoing efforts to reduce criteria pollutant emissions, greenhouse gas emissions, and fossil fuel use among drayage truck vehicles within the Houston region. As the project team works to create a demonstration of three zero-emission Class 8 drayage trucks, the vehicles will be monitored and fleet operators will be surveyed in order to measure and demonstrate operational cost-effectiveness and commercial viability of the trucks.

EE0005979

The primary objective of this project is to deploy thirty zero-emission all electric trucks and demonstrate the effectiveness of the all-electric delivery vehicles to at the same level of operation as similarly sized diesel delivery vehicles while reducing vehicle emission and petroleum consumption.

The vehicles deployed will be selected through a Call for Projects process and will be deployed on delivery routes in the Houston-Galveston area. Large national fleets and progressive regional fleets that operate diesel and gasoline delivery vehicles in the region have been the initial targets for fleet deployment and testing. Integration of all-electric vehicles into their fleets will result in both emission and noise reductions over diesel and gasoline counterparts. The fleets will also reduce their reliance on petroleum-based fuels and realize significant cost savings.

Approach

EE0005978

Vehicles eligible to respond to the Call for Projects included zero-emission heavy-duty Class 8 drayage trucks. The vehicles were required to be cargo-carrying on-road trucks with an expected gross vehicle weight rating of at least 80,000 lbs. Project vehicles were required to be designed and used for the sole purpose of moving and/or delivering cargo, freight, goods. The vehicles were also required to be on-road legal and used under real-world drayage freight movement activities or through port or intermodal rail yard property for the purpose of loading, unloading or transporting cargo, such as containerized, bulk or break-bulk goods.

Project vehicles were required to be zero emission and use an electric motor for all of the motive power of the vehicles, including battery electric, fuel cell, and hydrogen hybrid electric fuel cell vehicles. The vehicles were also required to meet or exceed all applicable federal or state emission requirements and safety standards.

Testing

Qualitative evaluations and quantitative documentation for the tested parameters will be collected during the program using a combination of an on-board data collection system and input obtained by surveying drivers and maintenance personnel. These findings will be included in the monthly, quarterly and final reports.

Testing Variables

- Vehicle Operations
 - Daily Mileage
 - Operating Time
 - Payloads
 - Speed
 - State of Charge
 - Auxiliary Loading
 - Maintenance Costs
- Charging Operations
 - Daily Charge Times
 - State of Charge
 - Energy Consumption
 - Utility Costs
 - Maintenance Costs

Demonstration Period

The project will include a two-year demonstration of the zero-emission Class 8 vehicles under real world conditions.

Infrastructure Requirements

Recharging/refueling infrastructure needed for this project will be located to allow the proper charging of the trucks utilizing the facility.

Commercialization

The experience and data collected from this project will help validate hydrogen and/or electric as a feasible alternative fuel options. Confirming durability and driver acceptance are also key results expected from this demonstration that would advance commercialization of zero-emission Class 8 vehicles.

EE0005979

CTE has worked with fleets and OEMs selected through the Call for Projects to plan, select, and model routes on which the vehicles have been deployed. CTE will do the same for the fleet selected for the remaining 12 vehicles. The project team installed and tested vehicle charging stations in preparation for vehicle deployment. With the demonstration period in progress, the project is now conducting a series of tests to validate vehicle performance against the model and is currently collecting operational data for these first 18 vehicles.

As a result of the Call for Projects process, UPS and Workhorse were selected as the initial fleet/vehicle team for this project. UPS has accepted and deployed 18 of the project's 30 vehicles. H-GAC has recently evaluated an additional fleet for the final 12 vehicles and hope to move forward with these new vehicles as soon as UPS and USDOE come to an agreement on a mutually agreeable vehicle for this project. The following information pertains to this project.

System Description

Workhorse has developed a new chassis for this project and for the commercial market. The W88 chassis is designed to meet the needs of a wide range of customers. At the same time, it is a universal chassis from an operations perspective.

The vehicle is 100% electric powered by a 120kWh battery pack giving it a useful range of 80 miles in a typical 120-150 stop per 8-hour package delivery shift. The range of the Workhorse truck will be more than adequate to cover the 50 to 65 mile per day routes in Houston. The vehicle has no transmission--it is a direct drive to the differential making it very efficient. The electric motive drive is a 2200NM regenerative drive capable of powering a 23,000-pound vehicle from a dead stop up a 23% incline.

Top speed of the vehicle is limited to 65 mph. Typical differential ratios are 4.78 to 1 and 5.1 to 1 for the direct drive. The vehicle has a supervisory controller that interfaces with the Battery Management System, the Body Control Module, and the Brake Module, and the charging system to control the vehicle. There is an onboard level two J1772 charger, either 7KW or 18Kw depending on the customer preference. The vehicle can also be fitted with inductive charging.

Testing

UPS as well as any additional recipient fleet, in partnership with CTE and Workhorse, will report vehicle and charger specifications and will collect operational and maintenance data for vehicles. Data collected may include powertrain and battery operational data. Additionally, data from non-electric fleet vehicles may be required for comparative analysis. All information collected shall be provided to CTE. CTE will analyze the data and summarize for submittal to DOE.

Testing Variables

- Vehicle Operations
 - Daily Mileage
 - Operating Time
 - Payloads
 - Speed
 - State of Charge
 - Auxiliary Loading
 - Maintenance Logs
- Charging Operations
 - Daily Charge Times
 - State of Charge
 - Energy Consumption
 - Utility Costs
 - Maintenance Logs
- Data Collected will be used to calculate a number of analytical factors, including, but not limited to:
 - Fuel Efficiency (i.e., \$/mile, kWh/mile, etc.)
 - Cargo Ton-Miles/Vehicle
 - Cargo Ton-Miles/Fleet
 - Reduction in Petroleum Consumption
 - Reduction of Green House Gas Emissions (Million Metric Tons of Carbon Equivalent (MMTCE)/year)
 - Reduction of Criteria Pollutant and Toxic Emissions
 - Expected Life Cycle Benefit Analysis

Demonstration Period

The project will include a two-year demonstration of each all-electric truck under real world conditions.

Data Collection Strategy

The 18 Workhorse vehicles were tested for durability and are equipped with data collection and monitoring systems to track variables from the battery management, drive system, cooling systems, etc. Coast-down testing was used to determine projected energy usage per mile; use case testing was accomplished to verify that vehicle energy usage is consistent with projected usage. Limits of charge and discharge were set as to ensure that the main battery will operate to its projected life without overstressing it.

Real time data is sent to a server for storage and analysis and parameters are modified as necessary to insure the vehicle performs to its design parameters.

Vehicles prototypes are tested on steep hills and anticipated normal driving conditions locally to get baseline data before TRC testing. Data is collected to determine energy usage per mile under various driving conditions and compared to predicted models to determine battery life, range, acceleration etc. Major vehicle maintenance for production vehicles can be performed at Workhorse dealers across the country.

Infrastructure Requirements

Each vehicle comes with a water-cooled J1772 level 2 charger on-board. The charger is typically 12kWh, 220 Vac. Vehicles may be optionally equipped with 25KW induction charging.

Commercialization

It is believed that the vehicles used in this project will result in a positive business case on a total cost of ownership basis for UPS and other selected fleets. This is due to the lower cost of electricity and lower maintenance costs as compared to fuel and maintenance of diesel medium- and heavy-duty vehicles.

Results

EE0005978

The new project team has been convened and is working to finalize agreements with GTI and the local fleet. Significant site preparation has been complete. Fueling infrastructure is on-site, however no equipment has yet been installed. US Hybrid has partially managed the project vehicles. To date, no performance data has been collected.

Expected results:

H-GAC anticipates the following actions to occur as a result of this project:

- increased adoption of zero-emission Class 8 technology for drayage fleets
- increased adoption of technology for regional port operators as a result of outreach and exposure to the project
- increased adoption of technology through other outreach and education efforts to ports in other areas, through DOE meetings, participation in DOE Clean Cities/Clean Fleets partnership programs

EE0005979

The project team has contracted with United Parcel Service (UPS) to for the purchase of eighteen (18) all-electric delivery vehicles. These vehicles are fully manufactured and deployed within the Houston region. Performance data for these vehicles is currently being collected however the data has, to date, not been sufficiently analyzed.

Expected results:

H-GAC anticipates the following actions to occur as a result of this project:

- Reduction of petroleum use in the demonstration period during and after the project activities
- Reduction of greenhouse gases, criteria pollutants, and toxic emissions

- Demonstration and evaluation of market viability
- Opportunity to increase adoption of the demonstration technologies
- Expansion of U.S. manufacture and production of electric vehicles and U.S. suppliers of batteries and equipment for electric vehicles

Conclusions

EE0005978

This project will produce on-road experience and gather data which will serve to accelerate the introduction and penetration of electric transportation technologies. Specifically, at least three zero-emission Class 8 trucks will be deployed into the drayage cargo transportation sector. Current delays in project initiation will require an aggressive timeline for manufacture of advanced vehicle technologies and the establishment of adequate fueling and/or charging infrastructure in early 2017.

EE0005979

This project will produce on-road experience and gather data which will serve to accelerate the introduction and penetration of electric transportation technologies. Specifically, 30 zero-emission all-electric trucks will be deployed across the Houston region. The project has experienced delays due to financial challenges faced by the originally intended OEM and in identifying appropriate routes in the Houston area as a result of typically longer travel routes. We will continue to analyze and report the demonstration data for 18 existing all-electric vehicles while continuing to work to finalize the remaining 12 vehicles.

II.16.C. Products

Presentations/Publications/Patents

1. None to Date

II.16.D. References

1. None

ZERO EMISSION CARGO TRANSPORT 2

II.17. San Pedro Bay Ports Hybrid & Fuel Cell Electric Vehicle Project [DE-EE0006874]

Joseph Impullitti, Program Supervisor

South Coast Air Quality Management District
21865 Copley Drive
Diamond Bar CA 91765
Phone: (909) 396-2025; Fax: (909) 396-3252
E-mail: jimpullitti@aqmd.gov

Adrienne Riggi, Program Manager

National Energy Technology Laboratory (NETL)
Phone: (304) 285-5223
E-mail: Adrienne.Riggi@netl.doe.gov

Start Date: October 1, 2014
End Date: September 30, 2019

II.17.A. Abstract

Objectives

- Reduce criteria pollutants in South Coast Air Basin by reducing diesel emissions from transportation and movement of goods
- Accelerate introduction and penetration of zero and near-zero emission fuel cell and hybrid technologies in cargo transport sector
- Execute a joint project with the Port of Los Angeles and Long Beach consisting of demonstration, data collection and analysis of seven fuel cell and hybrid trucks on five different vehicle architectures.

Accomplishments

The San Pedro Bay Ports Fuel Cell and Hybrid Electric Vehicle Project has experienced many delays due to contracting with South Coast Air Quality Management District's (SCAQMD) technology partners and securing funding agreements with SCAQMD's financial partners. In Q4 2015 contracts with U.S. Hybrid (USH) and TransPower (TP) were executed and those projects were kicked off; in Q2 2016 contracts with GTI and CTE were executed and the projects have started. The delay in executing a funding agreement for \$2.4M with the California Energy Commission (CEC) has prevented the CTE project from performing tasks associated with CEC funds. The CEC and the State's Department of General Services have finally come to an agreement on their differences and the funding contract has been fully executed. Now that all of the contracts have been executed and the program is fully funded we expect our progress to improve and SCAQMD's technology partners to pull their schedules ahead where possible.

Future Achievements

- Going forward, in Q4 2016 US Hybrid will be ready to demonstrate its first fuel cell truck and in Q1 of 2017 TransPower will be ready with their first fuel cell truck.
- Hydrogen refueling with a temporary station is being planned and will be ready by January 2017 to begin demonstration of US Hybrid and TransPower trucks.
- The GTI and CTE trucks, CNG Hybrid and Fuel Cell respectively will both be ready for demonstration in Q4 of 2017.

II.17.B. Technical Discussion

Background

The I-710 and CA-60 highways are key transportation corridors in the Southern California region that are heavily used on a daily basis by heavy duty drayage trucks that transport the cargo from the ports to the inland transportation terminals. These terminals, which include store/warehouses, inland-railways, are anywhere from 5 to 50 miles in distance from the ports. The concentrated operation of these drayage vehicles in these corridors has had and will continue to have a significant impact on the air quality in this region whereby significantly impacting the quality of life in the communities surrounding these corridors. To reduce these negative impacts it is critical that zero and near-zero emission technologies be developed and deployed in the region. A potential local market size of up to 46,000 trucks exists in the South Coast Air Basin, based on near-dock drayage trucks and trucks operating on the I-710 freeway. In areas with historically poor air quality like the South Coast Air Basin, zero-emission transportation technologies are being considered and may become standard. The SCAQMD, California Air Resources Board (CARB), and Southern California Association of Governments (SCAG) are the agencies responsible for preparing the State Implementation Plan required under the federal Clean Air Act. These agencies have stated that to attain federal air quality standards the region will need to transition to broad use of zero and near zero emission energy sources in cars, trucks and other equipment (SCAG et al, 2011). The SCAG 2012 Regional Transportation Plan also lays out a long-term vision of a phased adoption of zero and near-zero emission technologies to meet air quality goals. The current near-dock rail yard development project known as the Southern California International Gateway (SCIG) has been the subject of significant public concern regarding air quality impacts from the project and may ultimately result in the use zero emission trucks and other equipment. The planned expansion of the existing near-dock rail yard known as the Intermodal Container Transfer Facility (ICTF) is expected to face pressures similar to the SCIG to employ zero emission technologies.

Introduction

The proposed project area is known as the Los Angeles Goods Movement and Industrial Corridor. This area is adjacent to the Ports of Long Beach and Los Angeles, the busiest port complex in North America. The area is in an industrial setting with diesel truck activity mingled with a variety of uses including residences, schools, daycares and senior centers. The area is also a known Environmental Justice Community made up of predominantly low-income and minority populations.

The proposed technologies, fuel cell range extenders and hybrid electric trucks, face many challenges in the process of commercialization: proper sizing of the fuel cell stack, battery and fueling system; system integration and packaging of power train components and systems for safe, efficient and economical deployment of the technologies are just a few of the challenges. Many options exist in sizing the energy systems for these type of vehicle architectures – making the battery, engine or fuel cell dominate in size; plug in charging versus operation in charge sustaining mode and sizing of the energy storage system. Considerations for the power requirements of vehicle under load and providing enough onboard energy to attain the range requirements for the drayage operation and duty cycles all come into play in the design of the energy storage and power systems. Another challenge is to design the energy and power train systems described above and then integrate them into a vehicle for safe and efficient operation that can be made economical in volume and series production.

Approach

The technical objective of our proposed application is to address some of the challenges of developing the fuel cell range extended and hybrid truck platforms with the cost and time constraints of this FOA. By bringing together small to medium sized vehicle integrator contractors along with global manufactures and developers we offer the best in innovation and experience in this project. Transportation Power, International Rectifier and U.S. Hybrid, who are extremely cost effective in demonstrating proof of concept and exploring design variants in a timely fashion; BAE Systems and Ballard Power Systems a global defense and security company and an international fuel cell manufacturer who both have experience in developing fuel cell transit buses. Together our project contractors offer the opportunity to explore design variations concurrently and address many of the challenges mentioned above in a timely and cost effective manner. Some of the metrics that will be used to

evaluate the design variants of the five fuel cell range extended and hybrid architectures are: Operational capabilities, Energy usage and efficiency, Fueling/charging requirements and Costs compared to diesel powered trucks.

ZECT 2 Projects:

BAE Systems will develop a battery electric truck with a hydrogen fuel cell range extender. The vehicle will operate in electric mode at all times and all speeds until the battery energy system reaches a lower operating state of charge level, at which point the hydrogen range extender would be activated to supplement power.

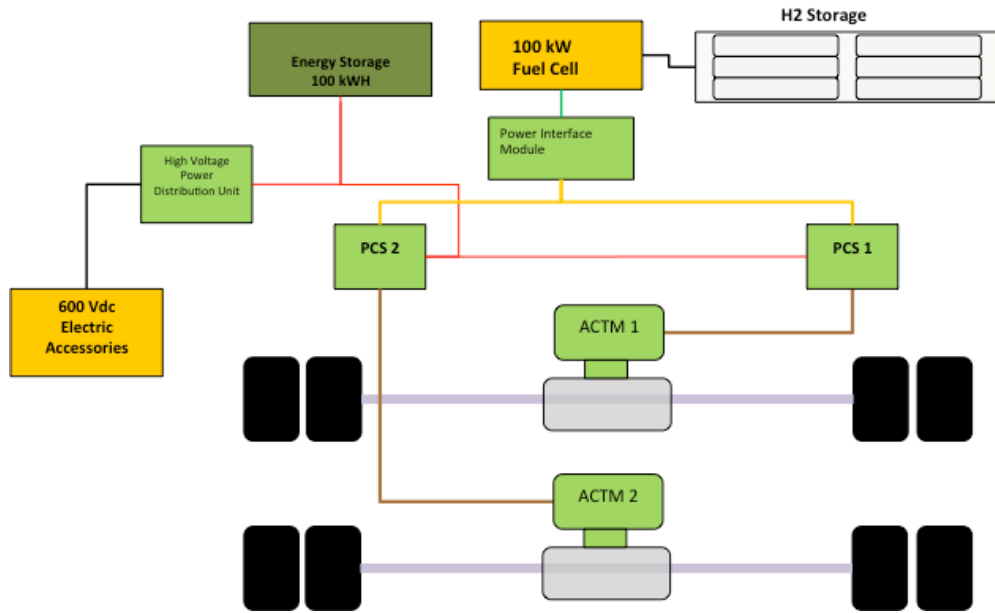


Figure II-116: Block diagram of BAE Systems battery electric truck with hydrogen fuel cell range extender

TransPower will develop two battery electric trucks with hydrogen fuel cell range extenders. These trucks will employ a small fuel cell and stored hydrogen. One truck will be equipped with a 30 kW fuel cell and one with a 60 kW fuel cell, enabling a direct comparison of both variants.

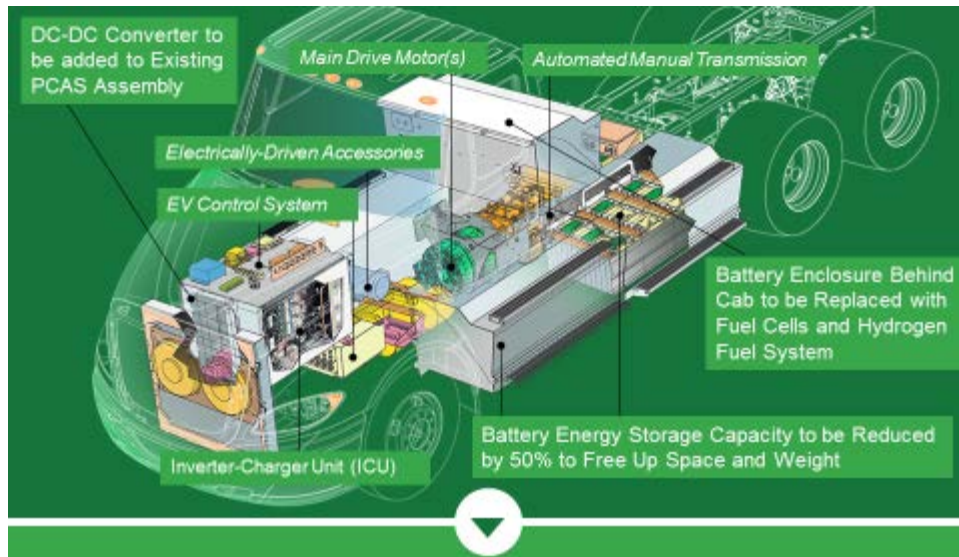


Figure II-117: Changes to baseline TransPower battery electric truck for fuel cell range extender variants

U.S. Hybrid will develop two equivalent battery electric trucks with an on-board hydrogen fuel cell generator. Each truck is estimated to have 20 kg of hydrogen storage at 350 BAR with an estimated fueling time under 10 minutes.

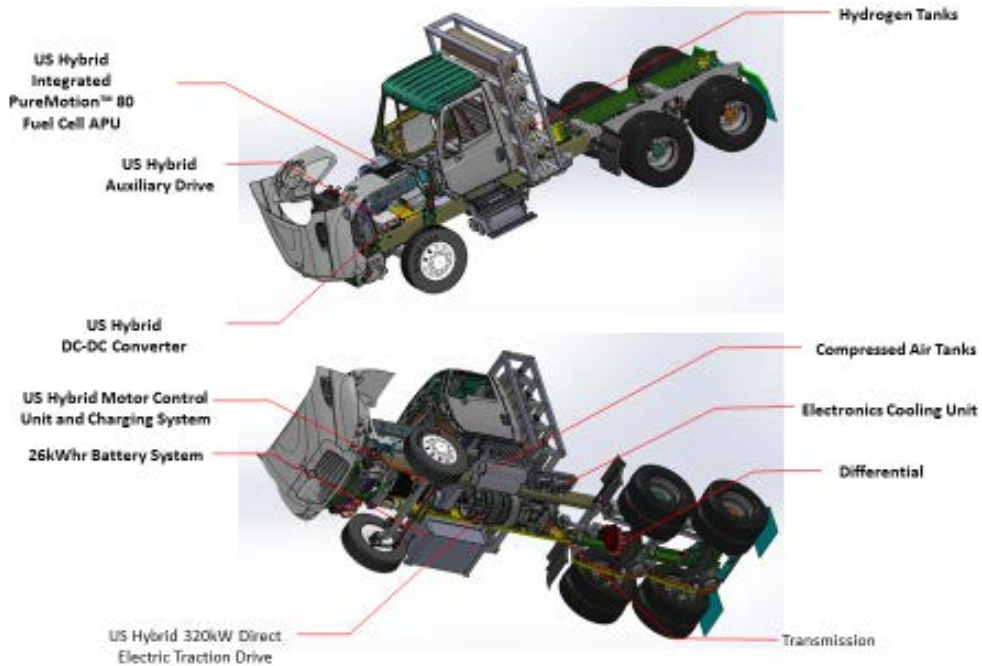


Figure II-118: U.S. Hybrid battery electric truck with on-board fuel cell generator

BAE Systems and Kenworth will develop one hybrid battery electric truck with CNG range extender and catenary capability. The proposed technical concept provides an all-electric mode, a catenary electric mode to operate on a catenary system developed by Siemens and in a conventional hybrid mode using CNG.

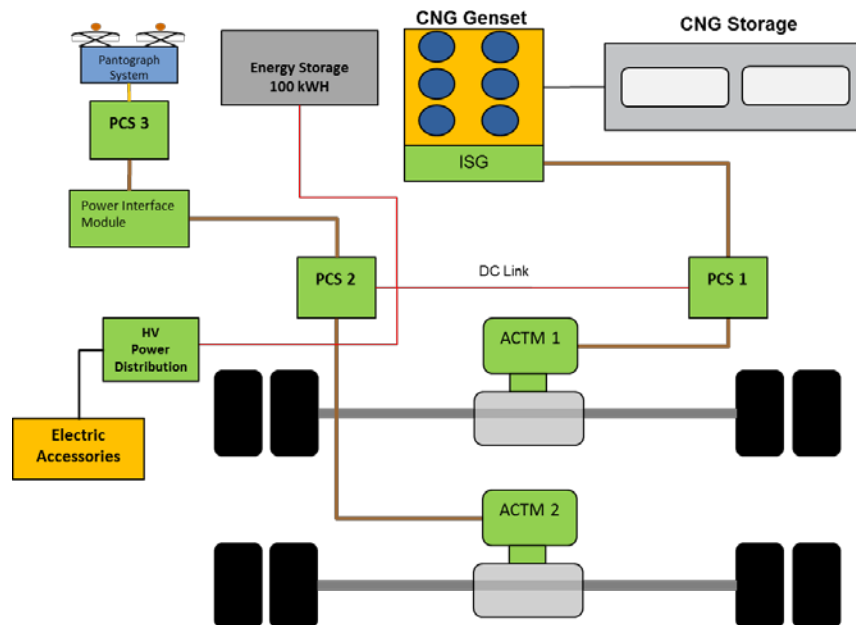


Figure II-119: Block diagram of BAE Systems and Kenworth hybrid electric truck with CNG range extender

International Rectifier (IR) had planned to develop one plug-in hybrid-electric truck and an ultra-fast charger for use in or near the ports as part of the project. In August of 2015 Infineon Technologies AG and International Rectifier Corporation announced that Infineon would acquire International Rectifier. After the acquisition Infineon declined to continue developing the truck as part of the ZECT project. SCAQMD has been working to identify a new technology partner to replace International Rectifier after its departure.

Results

Our technology partners have made some progress with the most coming from USH and TP because of their earlier start in Q4 2015. While CTE and GTI projects were just started in the last two months they plan to pull ahead their schedules in order to be more aligned with the other project partner's budget periods.

TransPower

- Project is on schedule with all major components procured and to be delivered by August 2016.
- Truck chassis are scheduled to be delivered in mid-July
- Both trucks to be completed by the end of 2016.

US Hybrid

- Project is on schedule.
- MATLAB modeling completed in May 2016
- Procurement and fabrication of subsystems completed in June 2016
- Vehicle integration for both trucks already underway with completion schedule by October 2016
- Chassis dyno test scheduled in Oct/Nov 2016

CTE and GTI

Both CTE and GTI projects were kicked off in the June and July of 2016. The Kenworth and BAE Systems team have proactively looked at ways to pull the schedules of both projects ahead and limit risk on each of them. To mitigate risk the team has identified items that are new and critical items that need to be understood and defined to complete the vehicle design as well as the form, fit and function in the truck platform. The items include mechanical and electrical interface verification and validation of components for compatibility within each system. These items include:

- Vehicle accessories (Kenworth)
- Fuel cell engine (Ballard)
- High voltage output for electric accessories (BAE Systems)
- Test of propulsion components to validate the models and simulations and verify all data (BAE Systems)

The components are all known and used by respective team members on their individual projects but have not been integrated together on a common platform. The design of the vehicle and the subsystems are slated to be completed by end of Q2 2017. However, without the availability of the physical components to conduct limited testing and interface verification it will be challenging to complete the design phase. The procurement of key components is currently assigned in BP2. To maximize the team's ability to complete the vehicle design and successfully transition to a build, install and integration phase we need to allow the team to procure some critical system components in advance; this applies to both CTE and GTI projects.

III. Vehicle Technology Evaluations

III.1. Advanced Vehicle Testing Activity

James Francfort, Principal Investigator

Idaho National Laboratory
 P.O. Box 1625
 Idaho Falls, ID 83415
 Phone: (208) 526-6787; Fax: (208) 526-0828
 E-mail: James.Francfort@inl.gov

Lee Slezak, DOE Program Manager

Phone: (208) 586-2335
 E-mail: Lee.Slezak@ee.doe.gov

Start Date: October, 2013
 End Date: Ongoing

III.1.A. Abstract

Objectives

- Provide efficiency, maintenance, and lifecycle cost data for advanced hybrid electric vehicles (HEVs), plug-in hybrid electric vehicles (PHEVs), battery electric vehicles (BEVs), and advanced internal combustion engine vehicles.
- Provide real-world usage data from advanced technology vehicles for use in research, modeling, and planning.
- Benchmark battery performance and life in HEVs, PHEVs, and BEVs to support progress in battery development and aid understanding of vehicle battery degradation.
- Support New York State Energy Research Development Authority's (NYSERDA) electric vehicle charging station deployment project.

Accomplishments

- Advanced Vehicle Testing and Evaluation
 - Three new models deployed in testing program
 - Baseline performance reports
 - On-road operation summary reports
 - Mileage and fuel reports
 - Maintenance and operations costs reports
 - Battery benchmarking reports
 - BEV fast charging capability reports
- NYSERDA Electric Vehicle Supply Equipment (EVSE) Demonstration Project Quarterly reports published.

Future Achievements

- Continue rapid HEV, PHEV, and BEV mileage accumulation and benchmarking activities with a focus on new technologies.
- Correlate battery performance degradation to battery cycling from on-road testing.
- Partner with original equipment manufacturers to collect extensive field data through collaboration.

III.1.B. Technical Discussion

Background

The Advanced Vehicle Testing Activity (AVTA) is the only activity tasked by the U. S. Department of Energy (DOE) to conduct field evaluations of light-duty vehicles that use advanced technology systems and subsystems to reduce petroleum consumption. A secondary benefit of these advanced technology systems is a reduction in exhaust emissions.

Most of the advanced technology vehicles tested by AVTA have some degree of electrified propulsion, including electric motors and advanced energy storage systems. However, other vehicle technologies that employ advanced designs, control systems, or other technologies with production potential and significant petroleum reduction potential are also considered viable candidates for testing by AVTA.

The AVTA light-duty activities are conducted by Idaho National Laboratory (INL) for DOE. INL has responsibility for technical direction and management, along with data collection, analysis, and test reporting, for work performed under the Advanced Vehicle Testing and Evaluation Project performed by Intertek Testing Services North America. INL is supported in this role by various subcontracts for specific tasks when greater value can be achieved for DOE. The AVTA sections of this task jointly cover the testing work performed by INL, in addition to work over which INL maintains technical oversight. When appropriate, AVTA partners with other governmental, public, and private sector organizations to provide maximum testing and economic value to DOE and the United States' taxpayers via various cost-sharing agreements.

Introduction

AVTA is evaluating grid-connected plug-in electric vehicle (PEV) technologies in order to understand their capabilities to significantly reduce petroleum consumption when compared to traditional internal combustion technology. PEVs are becoming more common throughout the United States, including many companies and groups that are proposing, planning, or have already started the introduction of PEVs into their fleets.

It should be noted that grid-connected PEVs include several vehicle/energy storage powertrain types that include BEVs (or simply electric vehicles), such as the Mercedes B-Class Electric and Kia Soul electric vehicle; PHEVs, such as the Ford Fusion Energi; and extended-range electric vehicles (EREVs), such as the Chevrolet Volt and BMW i3 REx. Current PHEV batteries tend to have between 4 and 18 kWh of energy storage and current BEVs tend to have more than 20 kWh.

AVTA also tests HEVs and vehicles with advanced internal combustion engines or other advanced technologies that can displace petroleum consumption through increased efficiency. Low emissions capability is also a consideration for these advanced technologies.

AVTA makes extensive use of data loggers in vehicles and in charging infrastructure to collect a variety of vehicle and infrastructure performance parameters. Experience has shown that automated data collection in fleet environments is the only way to ensure accurate and complete data are collected.

The concept of advanced onboard energy storage and grid-connected charging raises a number of questions, and answering these questions require detailed data sets, such as those collected in the AVTA program. These unknowns include the life and performance of these larger batteries as they are used over the life of a vehicle, the amount and location of charging infrastructure required to sustain PEV penetration, consumer driving and charging behavior patterns, and the actual petroleum displacement achieved.

Approach

Advanced Vehicle Testing Activity Fleet Testing

Under the Advanced Vehicle Testing and Evaluation Project, three basic types of test methods are used to evaluate vehicles and their subsystems, each of which is discussed in detail in the following subsections.

Baseline Performance Testing

To understand the capabilities of a vehicle when it is new and to independently verify performance ratings, vehicles are tested on a closed track and a chassis dynamometer. These tests are completed following published procedures and are highly controlled for comparability across vehicles and powertrain types. Track testing characterizes performance metrics such as acceleration, constant-speed range, braking, and fuel consumption (which can include electricity, gasoline, or any other fuel used) throughout the operating range of the vehicle. The vehicles are also coast-down tested to determine dynamometer coefficients, which are used during the various urban and highway dynamometer test cycles. Note that AVTA dynamometer testing is conducted by Argonne National Laboratory at their Advanced Powertrain Research Facility. AVTA shares vehicles with other testing entities, leveraging capability and testing expertise to reduce costs to DOE. Reports are published to document how the vehicles performed during each test, with a focus on fuel consumption.

Accelerated Testing

For experimental vehicles or cutting edge technologies, dedicated drivers are used to complete a series of drives and charges (for PEVs) on city and highway streets. This testing often is used to ensure PEVs can accomplish several charge and drive cycles during a single day. For some vehicles, this can include more than 5,000 miles of operation per month.

Fleet Testing

For most production advanced vehicles, AVTA partners with various fleets that utilize light-duty vehicles in high-mileage missions (e.g., document couriers or taxis). This allows testing to be performed at the lowest possible cost to DOE and ensures the vehicles will be tested with a wide variation in drive cycles. AVTA partners with government, private, and public fleets for fleet testing because these fleets are often the earliest adopters of advanced technology vehicles. Note that AVTA fleet testing normally does not include operation by the general public due to the level of management and the data collection costs needed to ensure strict reporting for data quality assurance.

PHEVs and EREVs can operate on gasoline, even when the vehicles' battery packs are not charged. Therefore, with some exceptions, fuel use reporting is normally broken down into different operating modes to better understand the petroleum displacement potential under different usage scenarios. The modes by which operation is broken down are as follows:

- **Charge-Depleting Mode:** During a trip, electric energy in the traction battery pack provides either all-electric propulsion or electric-assist propulsion throughout the entire trip.
- **Charge-Sustaining Mode:** During a trip, no electrical energy is available in the PHEV or EREV traction battery pack to provide any electric propulsion support beyond normal HEV types of operations.
- **Combined Charge-Depleting and Charge-Sustaining Mode:** For this mode, electrical energy is available in the traction battery pack at the beginning of a trip. However, during the trip, the PEV battery is fully depleted and the vehicle functions like a hybrid vehicle for the remainder of the trip.

Breaking down operation into these modes and characterizing the usage patterns is useful for understanding a technology's petroleum displacement potential and the results realized under the usage scenario the vehicle was placed in for rapid mileage accumulation.

For all vehicles, data are recorded on a second-by-second basis during driving and charging, such that energy can be precisely tracked. The conditions under which the vehicle was operated are documented and presented

with the fuel and energy consumption data. Throughout the mileage accumulation process for each vehicle, subsystems of interest, particularly traction batteries, are tested for performance. Reports are generated to document battery capability and degradation over the life of the vehicle.

New York State Energy Research Development Authority Electric Vehicle Supply Equipment Demonstration Project

Data were captured from 482 vehicle charging ports throughout the State of New York beginning in October 2013; data collection is presently ongoing. INL processes the charging data that are provided by several models of EVSE into a database that is used to generate reports and help answer questions about charging behavior. This system readily allows the data to be reduced by several different metrics that can be used to describe the charging station.

Results

Advanced Vehicle Testing Activity Fleet Testing

The accelerated testing of HEVs, PHEVs, BEVs, and internal combustion engine vehicles is performed by Intertek Testing Services North America in Phoenix, Arizona. Intertek is working with INL on data collection, analysis, reporting, and procedure development. Ninety-one advanced technology vehicles were operated as part of the AVTA test fleet in 2015. Several models continued testing from previous years, while two new models were introduced. The new models are listed as follows, along with their technology of interest:

- 2016 Chevrolet Impala Bi-Fuel (advanced engine with compressed natural gas/gasoline operation)
- 2016 Chevrolet Volt (battery, electric drive, and gasoline range extender).

All vehicles with high-voltage traction batteries were tested for battery performance when they were new and four times throughout the test duration. Figure III-1 shows the battery capacity for 2013 Ford Focus Electric that continued testing in 2016. The full results of battery testing are compiled into battery testing results reports. Vehicles having other advanced systems undergo similar subsystem testing.

Additionally, the new vehicles were tested on a closed test track for performance following a break-in period. A new test vehicle fitted with measurement instrumentation is shown in Figure III-2.

Dynamometer testing follows track testing to give consistent conditions for performance and energy consumption measurements that can be used too fairly compare models. Data from these tests were compiled into reports that detail the vehicle specifications and performance and energy consumption both from the track and dynamometer testing. Following testing, the vehicles were instrumented with data logging equipment and released to fleets for mileage accumulation. On-road usage reports were compiled for each test vehicle to show how each vehicle was used and the resulting fuel and electrical energy consumption. The distribution of electrical energy consumption is shown for a 2015 Chevrolet Spark Electric Vehicle in Figure III-3.

Electronically logged data are continuously sent from the vehicles to INL servers and are processed daily. These data are used for specific subsystem studies at INL; they also have been provided to other national laboratories to support their modeling and simulation efforts. All reports referenced in the discussion of the project results were posted on the INL AVTA website (<http://avt.inl.gov>).

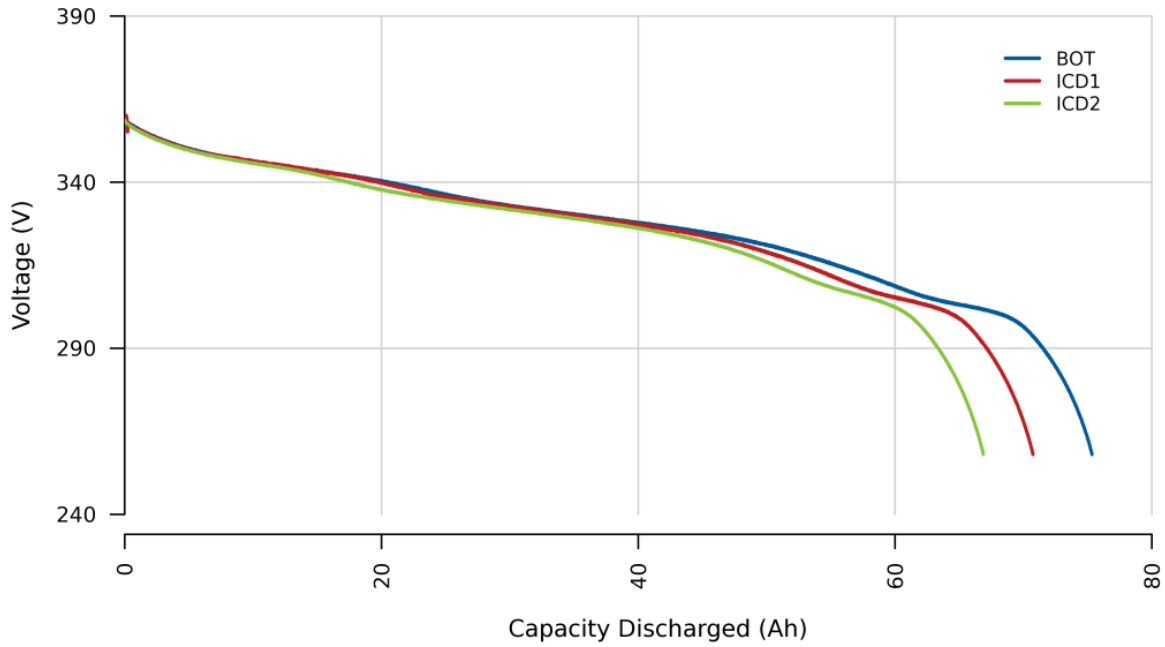


Figure III-1: Battery capacity data shown for a 2013 Ford Focus Electric. The data shown are from tests performed at 4,000; 14,000; and 60,000 miles. Two additional tests will be performed prior to completion of testing to characterize battery performance through the life of the battery.

INL



Figure III-2: A 2014 BMW i3 electric vehicle fitted with testing and measurement equipment for track testing.

Intertek Testing Services North America

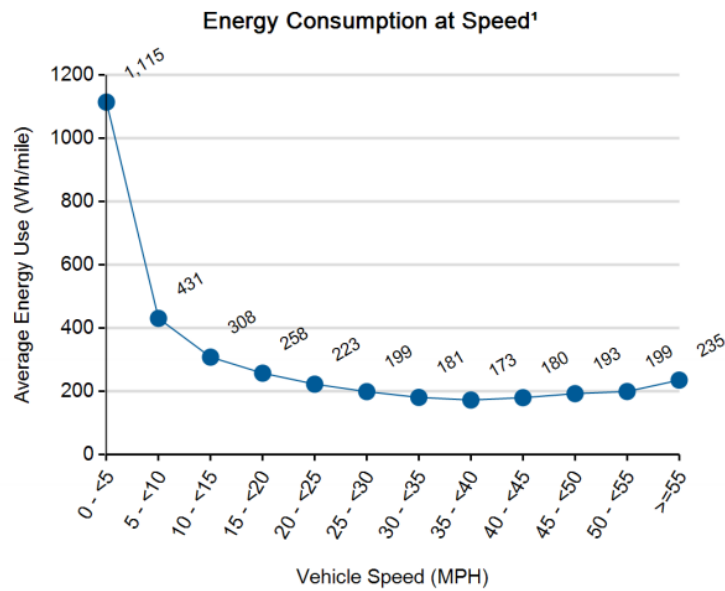


Figure III-3: Electrical energy consumption data are shown for a 2015 Chevrolet Spark electric vehicle. The data shown are from on-road operations logged over several thousand miles.

INL

New York State Energy Research Development Authority Electric Vehicle Supply Equipment Demonstration Reporting

As of March 2016, this project had deployed 482 electric vehicle charging ports in the state of New York. Data were collected from several distinct EVSE networks spread over five geographic districts. Aside from geographic location, the EVSE were also distributed among several fee structures, venues (e.g., retail, workplace, and hotel), access type locations (i.e., public and private), and land-use types (e.g., urban, suburban, and rural). INL’s reporting includes an overview for all EVSE; it also slices the data to examine variation in usage for each of the factors listed above. In Fiscal Year 16, one year of data was received and reports have been produced for three quarters. The final quarter is ongoing at the time of this writing. EVSE in New York City have the highest average energy consumed per event, at almost 13 kWh, and have longer charge times than any other region. This suggests that the vehicles charging in New York City begin charging events with more depleted or larger batteries. The use of EVSE ports, by land use type, is shown in Figure III-4.

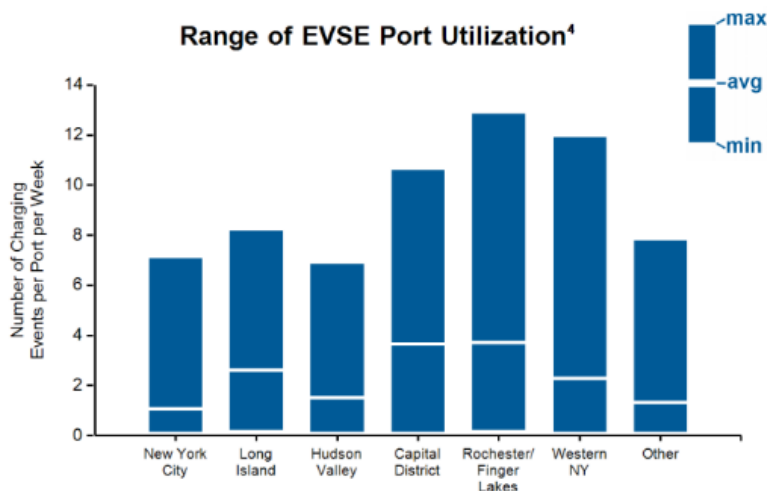


Figure III-4: The range and mean of EVSE port use is shown by region.

INL

Conclusions

AVTA will continue to provide the real-world testing needed to benchmark DOE technology investments, including the critical tasks of determining suitability for deployment, lifetime performance, and lifecycle costs of new technology components and vehicle systems. This testing provided information used to help understand the infrastructure requirements, operating costs, and petroleum displacement of PEVs, other alternative fuels, and HEVs, as well as proper placement of supporting infrastructure. The quality of the vehicles and the batteries (i.e., expected operational life) has improved significantly and fleets have been found that can significantly accumulate high per-vehicle mileage. Hybrid and internal combustion engine vehicle fleet testing mileage targets are set at 195,000 miles per vehicle. The PHEVs entering testing will accumulate 160,000 miles per vehicle and the BEVs will operate for 30,000 miles per vehicle. These targets are a combination of the practical limits of mileage accumulation and the period of interest (i.e., about 3 years) for the new technologies. Though the durability of these vehicles has improved significantly, the need for on-road testing is still very relevant to understand off-cycle performance and how on-road usage compares to standardized test procedures.

III.1.C. Products

Presentations/Publications/Patents

2. "Mileage Accumulation and Fuel Economy, Series of Fact Sheets," INL/MIS-14-32657, Idaho National Laboratory, 2016.
3. "Vehicle Specifications and Testing Results, Series of Reports," Idaho National Laboratory, Intertek Testing Services North America, 2016.
4. "Battery Pack Laboratory Testing Results, Series of Reports," INL/MIS-14-31587, Idaho National Laboratory, 2016.
5. "Maintenance and Repair History, Series of Fact Sheets," Idaho National Laboratory, 2016.
6. "Operating Costs, Series of Fact Sheets," INL/MIS-14-32657, Idaho National Laboratory, 2016.
7. "Plug-In Hybrid Electric Vehicle On-Road Usage and Performance Summary, Series of Fact Sheets," INL/MIS-11-22875, Idaho National Laboratory, 2016.
8. "Electric Vehicle On-Road Usage and Performance Summary, Series of Fact Sheets," INL/MIS-15-36519, Idaho National Laboratory, 2016.
9. "Hybrid Electric Vehicle On-Road Usage and Performance Summary, Series of Fact Sheets," INL/MIS-15-36685, Idaho National Laboratory, 2016.
10. "DC Fast Charging at Different Temperatures, Series of Fact Sheets," INL/MIS-16-38450, Idaho National Laboratory, Intertek Testing Services North America 2016.
11. "Steady State Vehicle Charging Fact Sheet, Series of Fact Sheets," INL/MIS-15-34055, Idaho National Laboratory, 2016.
12. "NYSERDA Electric Vehicle Charging Infrastructure Report, Quarterly Reports," INL/MIS-14-31250, Idaho National Laboratory, 2016.
13. "Cold Weather On-Road Testing of a 2015 Nissan Leaf," INL/EXT-16-39028, Idaho National Laboratory, 2016.
14. "PEV Workplace Charging Costs and Employee Use Fees," INL/MIS-15-37525, Idaho National Laboratory, 2016.
15. "The History of Electric Cars," INL/MIS-16-39608, Idaho National Laboratory, 2016.

III.2. Medium- and Heavy-Duty Field Testing

Kenneth Kelly and Bob Prohaska

National Renewable Energy Laboratory
15013 Denver West Parkway, MS 1633
Golden, CO 80401
Phone: (303) 275-4465
E-mail: Kenneth.Kelly@nrel.gov

David Anderson and Lee Slezak

Phone: (202) 287-5688 (David Anderson)
E-mail: David.Anderson@ee.doe.gov
Phone: (202) 586-2335 (Lee Slezak)
E-mail: Lee.Slezak@ee.doe.gov

Start Date: Ongoing
End Date: Ongoing

III.2.A. Abstract

Objectives

The main goal of this project is to test and/or validate advanced propulsion technologies in medium- and heavy-duty vehicle applications and to provide data and results from independent evaluation to help facilitate transitioning these vehicles from the research and development /prototype stage into the marketplace. This will be accomplished by means of the following:

- Testing and analyzing near-term advanced technologies in vehicles and comparing them to conventional technologies in vehicles in similar service
- Providing data and feedback to the research and development community (including other offices and programs within the U.S. Department of Energy [DOE]) to guide technology development that will lead to fuel-saving commercial products.

Accomplishments

Smith Newton Plug-In Electric Delivery Truck Field Evaluation with Frito-Lay N.A.

- Refined facility power simulation model to evaluate managed charge opportunity at Frito-Lay's Federal Way facility and applied a facility power model to evaluate benefits of onsite integrated solar arrays
- Performed well-to-wheels greenhouse gas (GHG) analysis of electric vehicles (EVs) operating in the Federal Way fleet compared to broad national averages
- Presented research results at the IEEE 2016 Transportation Electrification Conference and Expo in Dearborn, Michigan
- Compiled findings and results into a National Renewable Energy Laboratory (NREL) technical report.
- Completed Parker Hannifin Hydraulic Hybrid Refuse Truck Case Study with Miami-Dade County
- Completed in-field data collection of hydraulic hybrid vehicles (HHVs) and conventional vehicles, including over 34,000 miles of 1-Hz automated side loader refuse truck driving data
- Performed preliminary analysis of vehicle operation and performance of conventional diesels and both first-generation (MY13) and second-generation (MY15) hydraulic hybrids

- Completed chassis dynamometer testing of a conventional diesel refuse truck and a compressed natural gas (CNG) HHV refuse truck at NREL's Renewable Fuels and Lubricants (ReFUEL) laboratory.

Proterra Fast Charge Battery Electric Transit Bus Field Evaluation with Foothill Transit

- Performed preliminary analysis on vehicle operation and performance of battery electric buses (BEBs) as compared to conventional CNG buses operating in Foothill Transit's fleet
- Provided analysis and results in support of California Air Resources Board-funded Foothill Transit Battery Electric Bus Demonstration Results technical report
- Presented preliminary results on BEB performance at the IEEE 2016 Transportation Electrification Conference and Expo in Dearborn, Michigan.

CGI/EV2G Electric School Bus

- Provided baseline school bus data from 40 vehicles operated in two California school districts to the Fleet DNA project
- Developed a representative "school bus" drive cycle using NREL's Drive-Cycle Rapid Investigation, Visualization, and Evaluation (DRIVE) drive cycle evaluation tool
- Coordinated with NREL's Grid Integration team to conduct testing of the EV2G school bus at the Energy Systems and Integration Facility (ESIF) and ReFUEL laboratory
- Completed chassis dynamometer testing of the TransPower EV2G school bus at NREL's ReFUEL laboratory
- Completed IEEE 1547 and SAE J3068 interconnection testing at ESIF
- First EV2G school bus placed into service at Torrance (California) Unified School District.

Odyne Hybrid Systems Plug-in Hybrid Utility Truck Field Evaluation with Duke Energy

- Completed project kick-off meeting in April 2016 with Odyne Hybrid Systems and Duke Energy's Fleet Director
- Identified vehicles and locations for in-field data collection.

BYD Battery Electric Transit Bus with Wireless Charging Field Evaluation with Long Beach Transit

Completed project kick-off meeting in August 2016 with BYD and Long Beach Transit fleet managers.

Future Achievements

Smith Newton Plug-In Electric Delivery Truck Field Evaluation with Frito-Lay N.A.

Project complete.

Parker Hannifin Hydraulic Hybrid Refuse Truck Case Study with Miami-Dade County

- Complete chassis dynamometer testing of diesel HHV at NREL's ReFUEL laboratory
- Analyze emissions and fuel economy results of dynamometer testing
- Collect and analyze maintenance data as provided by Miami-Dade County Public Works and Waste Management Department
- Compile findings and publish final technical report (FY17).

Proterra Fast Charge Battery Electric Transit Bus Field Evaluation with Foothill Transit

- Plan to perform chassis dynamometer testing of a BEB and a conventional CNG bus at the California Air Resources Board's Los Angeles, California, test facility

- Continue analysis and comparison of performance between BEBs and CNGs including investigating the impact of temperature on efficiency
- Develop and validate BEB in the Future Automotive Systems Technology Simulator (FASTSim) vehicle model and investigate energy storage requirements for additional transit routes
- Compile findings and publish final technical report.

EV2G Electric School Bus

- Completion of next five EV2G bus conversions and delivery of the buses to the school districts
- Monitor introduction of buses into service
- Collaborate with TransPower to collect and analyze six EV2G school buses in use with three school districts as they are deployed through November 2016
- Use field and dynamometer test data to create a validated EV2G school bus FASTSim model to evaluate bus design parameters on all school bus data in Fleet DNA
- Compile findings and publish final technical report of project status and outcomes.

Odyne Hybrid Systems Plug-in Hybrid Utility Truck Field Evaluation with Duke Energy

- Collect field data from Odyne hybrid utility bucket trucks and hybrid utility vans with comparable conventional baseline diesel vehicles with similar duty cycles
- Perform laboratory chassis dynamometer testing of a hybrid utility bucket truck and comparable baseline conventional diesel
- Develop and validate plug-in hybrid electric vehicle (PHEV) FASTSim utility vehicle model to investigate energy storage sizing and controls
- Compile findings and publish final technical report in 2017.

BYD Battery Electric Transit Bus with Wireless Charging Field Evaluation with Long Beach Transit

- Collect field data from BEBs and conventional CNG vehicles operating in Long Beach Transit's fleet
- Perform detailed data analysis of in-use data to quantify performance and efficiency of BEB technology
- Develop and validate a BEB FASTSim vehicle model and investigate energy storage requirements and charge management strategies
- Collect and analyze vehicle charging data for conductive and wireless charging (when in service)
- Compile findings and publish final technical report.

III.2.B. Technical Discussion

Background - General

The DOE's Vehicle Technologies Office funds an array of research and development projects to develop technologies and subsystems for advanced vehicles. Testing, validating, and providing data and analysis of real-world service requirements and performance of vehicles and systems can help accelerate the transition of DOE's and other energy-saving technologies into widespread marketplace adoption. To accomplish this, DOE's Vehicle Systems Program provides a process to document testing, validating, and benchmarking the advanced technologies and provide data and technology evaluations from an unbiased source. The information provided by this project is vital to original equipment manufacturers and system integrators to optimize advanced vehicle systems for energy savings, performance, and cost while meeting vocational requirements. The project also provides independent information to fleets to aid them in making purchase decisions that will be appropriate for the unique operational characteristics of a given vocation. Data and results are provided to

other researchers, including DOE-funded programs, to help understand real-world technology requirements and component performance and feed vehicle systems modeling efforts.

Approach

This project will cooperate with fleet and/or original equipment manufacturer partners to select, test, and validate advanced technologies in commercial vehicle applications. Specific technologies will be selected based on (1) their potential for reducing fuel consumption, (2) their potential for widespread commercialization, and (3) interest at DOE (including the 21st Century Truck Partnership and other DOE programs). After a technology area has been identified, NREL will collect vehicle data on system performance, maintenance (if applicable), and/or operational costs relating to the new technology. The data will be analyzed, and the results will be presented to DOE and the project teams. The potential for improvement in real-world service, including operational costs, maintenance, and emissions, will be compared to data collected from conventional technology vehicles.

The approach for the FY16 medium- and heavy-duty field evaluation projects included:

- Working cooperatively with commercial fleets to collect operational, performance, and cost data for advanced technologies
- Characterizing vehicle drive/duty cycles
- Analyzing performance and cost data during a period of 6 months to 1 year or more
- Testing and analyzing in-use performance of advanced technologies in a laboratory setting to duplicate observed real-world conditions
- Developing validated vehicle systems models and investigating power train design parameters for a variety of medium- and heavy-duty vocations
- Producing fact sheets and reports on advanced heavy-duty vehicles in service
- Providing updates on new advanced technologies to DOE and other interested organizations as needed.

Smith Newton Plug-In Electric Delivery Truck Field Evaluation with Frito-Lay N.A.

Background and Introduction

NREL's Fleet Test and Evaluation Team has found medium- and heavy-duty vehicle fleets to be good candidates for deploying low-emitting advanced technologies because of their large numbers, high vehicle miles traveled—and consequently high petroleum fuel consumption and emissions—and frequent operation in large population centers, as well as common return-to-base fueling regimes and consistent driving routes.

Previous testing and analysis conducted by NREL have illustrated the influence of drive cycle and vehicle usage on both energy consumption (from liquid fuels and high-voltage hybrid battery packs) and exhaust (or well-to-wheels) emissions. Drive cycle has also been shown to influence the all-electric range of battery EVs, the charge-depleting range of PHEVs, and the potential fuel economy benefit of hybrid EVs (HEVs). Accordingly, fleet customers can benefit from a further understanding of advanced vehicle technology deployment to minimize fuel consumption and emissions. It has also been shown that large-scale deployments of EVs in a localized area can lead to power quality and power cost issues.

Results

Initial Fleet Identification and Selection

During FY13, NREL engaged with Frito-Lay North America (FLNA) and Smith to establish a program to evaluate the performance of plug-in electric delivery vans in direct comparison to conventional diesel vehicles.

Based on the availability of comparable vehicles, NREL and FLNA decided that the FLNA Federal Way, Washington, fleet depot would be the ideal target site for research. Table III-1 lists the diesel vehicles that were instrumented with data loggers.

Table III-1: Federal Way vehicles monitored

Manufacturer	Model	Isaac ID	Comm. Protocol	FLNA ID	Year
International	4200 SBA 4X2	14	J1708	E06636	2005
International	4200 SBA 4x2	15	J1708	E06644	2003
International	4700 4x2	16	J1708	E04126	2001
International	4200 SBA 4X2	17	J1708	E09471	2005
International	4200 SBA 4x2	25	J1708	E09390	2006
Hino	HINO 238	26	OBD2	E27205	2012
International	4200 SBA 4x2	27	J1708	E09595	2007
International	4200 SBA 4X2	28	J1708	E09392	2005
International	4700 4x2	29	J1708	E04128	2001

Initial Route and In-Vehicle Data Collection

Data collected from the nine diesel vehicles provide the baseline to which Smith EV performance was compared. NREL gathered data from the 10 Smith EVs stationed at Federal Way during the 17 days of logging in 2014 (April 16 to May 1) and found correlations among FLNA diesel and EV operations. The routes for both sets of vehicles span similar ranges across the territory served by the Federal Way depot (Figure III-5) and the average daily driving distance is also very similar with the diesel vehicles averaging 38.2 miles per day and the EVs averaging 32.5 miles per day. Additional daily performance statistics for both the conventional diesels and the EVs are shown in Figure III-7.

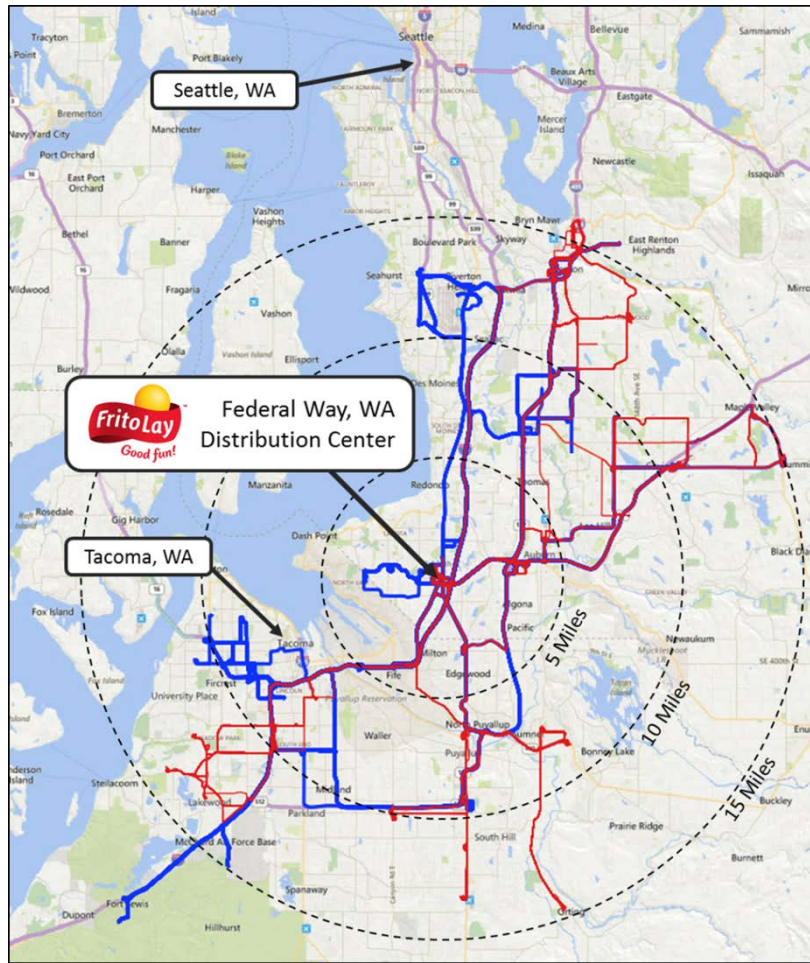


Figure III-5: Comparison of diesel (blue) and EV (red) routes
 Image: Robert Prohaska/NREL

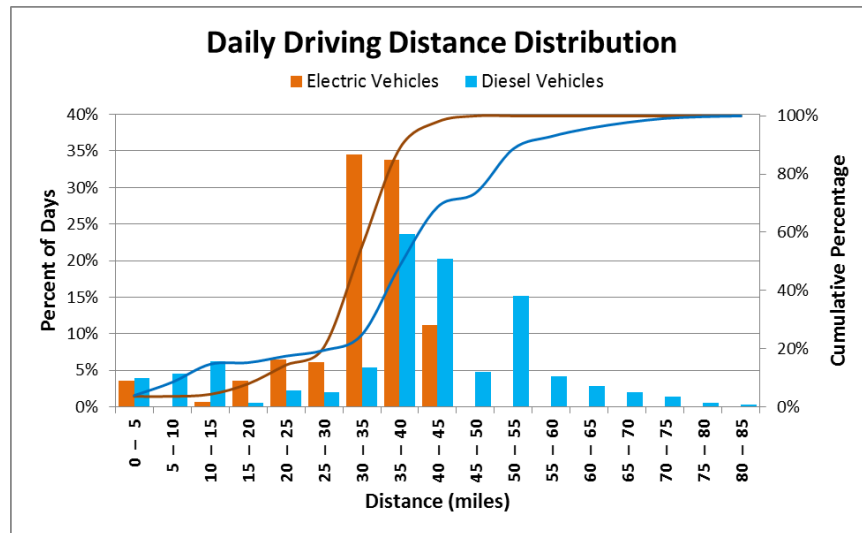


Figure III-6: Federal Way Smith Newton EV and conventional diesel daily driving distance distribution
 Image: Robert Prohaska/NREL

Daily Averages	Diesels	σ	EVs	σ
Average driving time (hours)	1.51	0.31	1.54	0.45
Average total distance (miles)	38.23	12.76	32.50	10.40
Average speed (mph)	25.18	6.84	21.48	4.23
Average fuel consumed (gallons)	4.97	1.58	1.21a	0.35a
Gallons / 100 miles	13.11	1.08	3.81a	0.53a
Average energy consumed (kWh)	187.24a	59.49a	45.66	13.12
kWh / mile	4.99a	0.33a	1.40	0.20
Average fuel economy (mpge)	7.63	0.59	24.09b	2.85b
Average number of stops	44.25	13.74	43.28	14.47
Average number of stops / mile	1.35	0.76	1.38	0.41
Average kinetic intensity (1 / mile)	0.54	0.37	0.70	0.23

a 37.656 kWh per gallon of diesel fuel

b Miles per gallon equivalent (mpge) assumes 90% charger efficiency.

Figure III-7: Federal Way Vehicle Daily Performance Metrics Shown with Standard Deviations (σ)

One way to quantify the energy efficiency of EVs is to look at their daily average DC energy consumption per mile on a kilowatt-hour basis. The distribution of kilowatt-hours per mile shows energy used to drive the vehicle and power any auxiliary loads, such as lights and climate control, but does not necessarily represent the total energy consumed by the system. Losses occur in the EVSE, the onboard AC-DC charger, and the onboard DC-DC converter during charging. In this study, the researchers used a combined 90% efficiency to account for losses between the AC supply and end-use driving, which means that for each 1.11 kWh of energy from the AC charging station that is plugged into the vehicle, only 1.0 kWh of energy is converted into usable DC energy on the vehicle. Figure III-8 shows the distribution over a multi-week period of the daily driving kilowatt-hour per mile energy consumption of the 10 Federal Way EVs. The average DC energy consumption for the Federal Way EV fleet, including the use of accessory loads during operation, was found to be 1.40 kWh/mi, and the average daily energy consumption for this study was found to be 45.7 kWh, with an average daily driving distance of 32.5 miles.

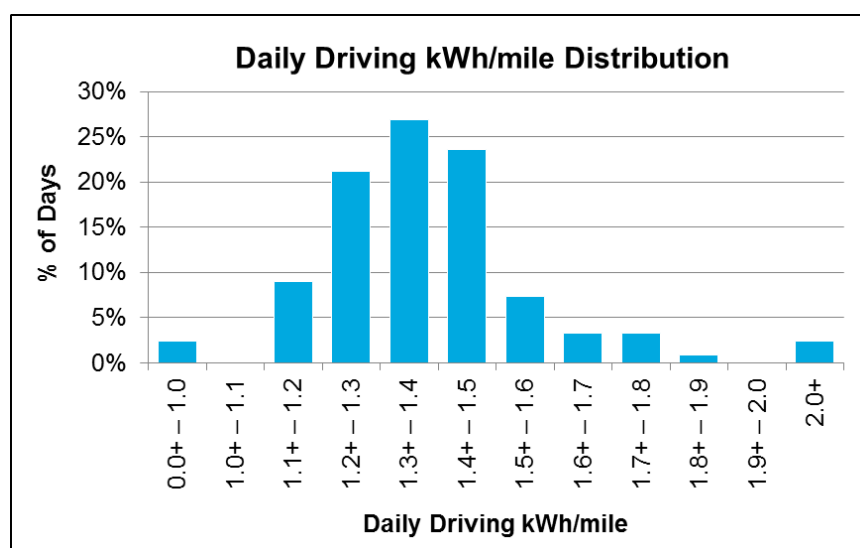


Figure III-8: Federal Way Smith Newton EV DC energy consumption per mile, data collected 4/14--5/14

Image: Robert Prohaska/NREL

Traveling on similar routes as the diesel trucks, FLNA’s Federal Way EVs operated at much higher fuel efficiencies. As shown in Figure III-9, the EVs at times exceed 25 miles per diesel gallon equivalent (mpgde), resulting in nearly three times the distance traveled of the diesels on an energy basis. The diesel equivalence was calculated using the Alternative Fuels Data Center energy density for a gallon of low-sulfur diesel fuel. With the diesel trucks averaging 7.63 mpgde at \$3.85/gal, the average diesel price in Seattle at the time of data collection, and the EVs averaging 23.3 mpgde at \$0.102/kWh, the average delivered price per kilowatt-hour FLNA paid in 2013, the same ratio in fuel economy applies to fuel savings for EVs. FLNA spent \$0.507 for every mile driven with diesel trucks versus \$0.159 for every EV mile. As fuel prices continue to fluctuate, the relative per-mile energy savings of the EVs over the diesels varies. Assuming the same AC energy cost of \$0.102/kWh and the same vehicle and charger efficiencies, the break-even cost per mile fuel price was found to be \$1.212/gallon. At this price per gallon of diesel fuel, the energy cost to operate the diesels and the EVs would be the same. This metric can be useful for fleet managers as they try to optimize their operations with widely varying fuel prices.

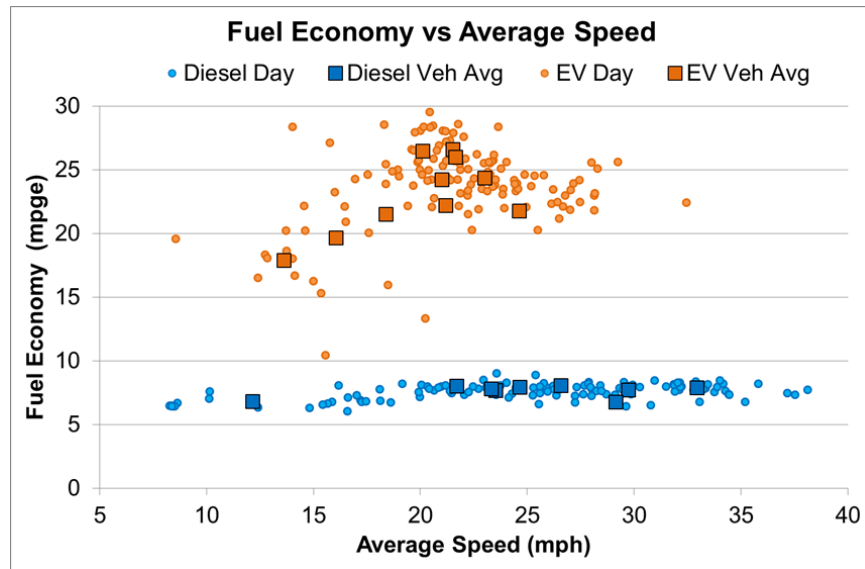


Figure III-9: Fuel economy vs. average speed for Federal Way depot diesels and EVs
 Image: Robert Prohaska/NREL

Further examination of average energy efficiency as a function of kinetic intensity shows that in this application, kinetic intensity is not a strong indicator of fuel economy for either the conventional diesels or the EVs as there is a wide range of kinetic intensity levels for a given level of equivalent fuel economy. The relationship between energy consumption per mile and kinetic intensity is shown in Figure III-10.

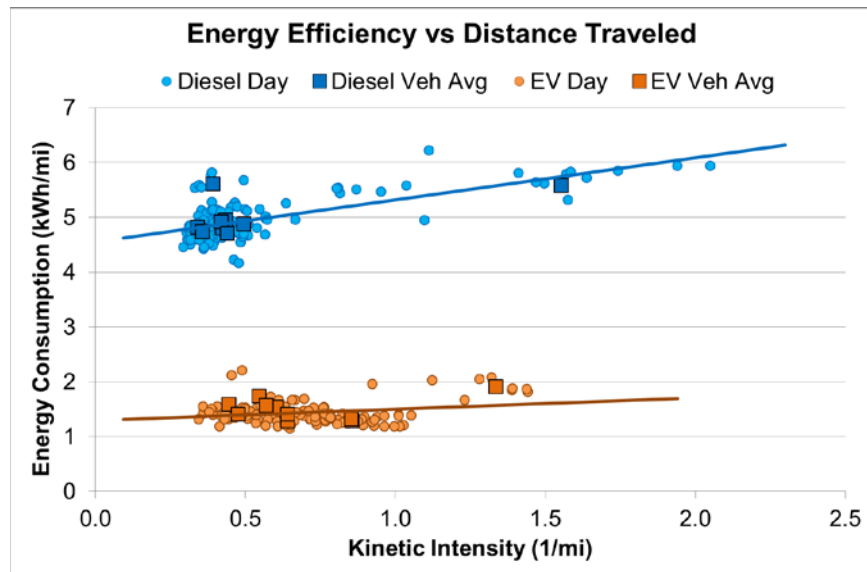


Figure III-10: Energy efficiency vs. kinetic intensity for Federal Way depot diesels and EVs

Image: Robert Prohaska/NREL

While the level of kinetic intensity alone may not be a strong predictor of overall energy consumption for this fleet, daily driving distance is correlated to energy consumption for both the EVs and the diesel vehicles. As seen in Figure III-11, a strong correlation exists between the daily distance traveled and the total amount of energy each vehicle consumed with neither vehicle type varying significantly in efficiency as a function of daily distance. Just as shown in Figure III-9 and Figure III-10, the EVs demonstrate a higher efficiency across the spectrum of operation. With such a strong correlation between energy consumption and distance travelled, fleet managers can use this type of information to forecast energy use over longer periods of time based on projected mileage. This simple relationship is key to understanding the benefits a fleet can recognize through electrification. In this specific operation, the more an EV is driven within the limits of its battery capacity, the more energy saved as compared to the diesel, thereby increasing the cost benefit of electrification.

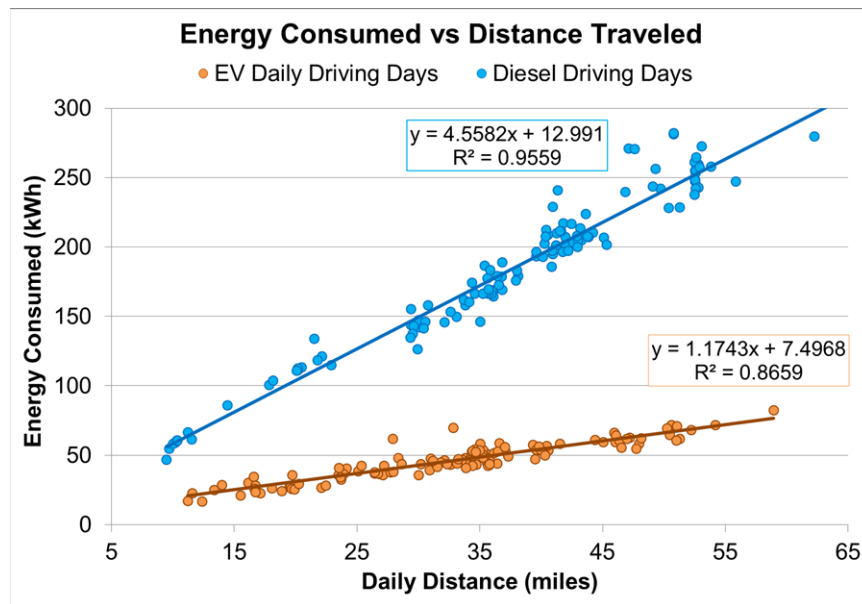


Figure III-11: Energy consumption as a function of daily distance traveled

Image: Robert Prohaska/NREL

FLNA fleet managers could improve their operational efficiency by dispatching the EVs on routes closer to their maximum range to maximize the electrification advantage. As seen in Figure III-12, 79% of EV trips required less than 55 kWh of the available 80 kWh. However, fleet managers are aware that longer routes may increase the driver’s range anxiety and will increase the possibilities for incomplete trips. Figure III-13 shows the average savings per EV based on distance travelled and average diesel fuel price. Using the annual distance traveled of 8,488 miles as a baseline, fleet operators could save on average an additional \$750 per year per vehicle with an average fuel price of \$3.79 per gallon by increasing the annual distance driven of the EVs by just 25%, to 10,610 mi. This increased use would result in an average daily energy consumption of approximately 57 kWh. At a diesel fuel price of just \$2.25 per gallon, this 25% additional mileage would result in an average annual per-vehicle savings of \$322. The average savings per EV assumes a cost of \$0.102/kWh, which was the average electricity charge from FLNA’s utility bill during this evaluation, and the vehicle efficiencies outlined in Figure III-7.

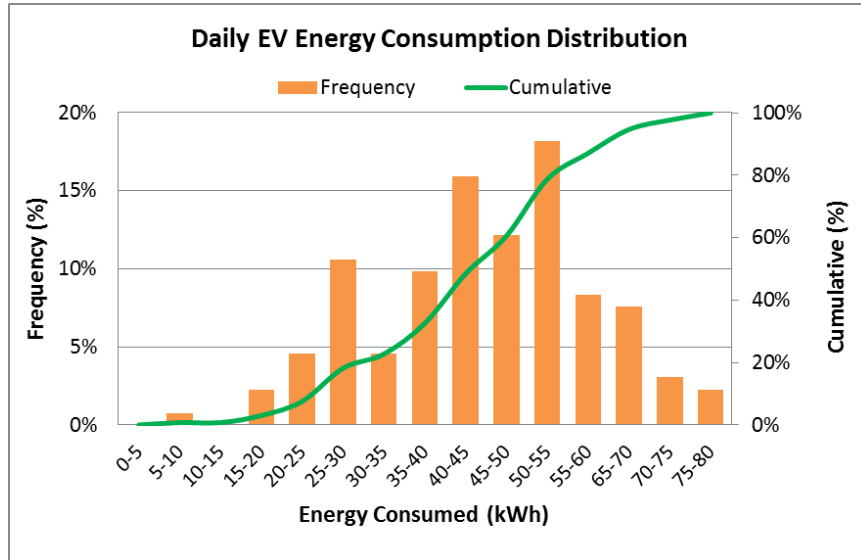


Figure III-12: Distribution of daily EV energy consumption

Image: Robert Prohaska/NREL

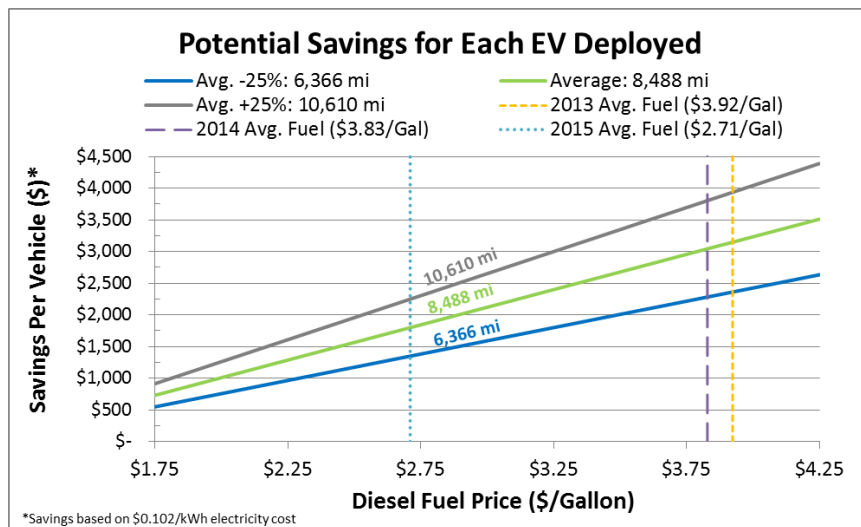


Figure III-13: Cost savings of EVs over conventional diesels based on average annual mileage and fuel price, assuming an electricity cost of \$0.102/kWh

Image: Robert Prohaska/NREL

While EVs show a significant savings on a per-mile basis, their incremental cost over conventional diesels is a significant barrier for most fleets. For example, New York State’s EV voucher incentive program lists the incremental cost of an 80-kWh Smith Newton at \$86,791 over the cost of a comparable conventional vehicle. While they do offer a \$60,000 voucher, there is a significant up-front cost to consider when purchasing an EV.

Vehicle Emissions

One of the potential benefits of EV adoption is a reduction in GHG emissions compared to conventionally powered diesel vehicles, as EVs emit no tailpipe GHG. However, significant emissions can be produced upstream depending on the local energy source distribution; this is sometimes referred to as the “extended tailpipe.” The power is supplied to the Federal Way facility by Puget Sound Energy (PSE), which reported a 2014 carbon dioxide equivalent (CO₂e) emissions intensity of 450.58 g/kWh. This emissions intensity includes all PSE-generated and purchased power measured at the generation source (non-distributed). The 2014 generation source distribution is shown in Figure III-14. Once electric energy is generated, it must be moved to areas where it will be used through transmission and distribution. The National Electrical Manufacturers Association considers normal transmission and distribution losses to be between 6% and 8% from the power generation source to the end user’s site. Using the Energy Information Administration’s 2013 transmission and distribution loss of 7.2%, we arrive at a CO₂e emissions intensity level of 485.54 g/kWh for energy at the FLNA facility from PSE. Factoring in the charging efficiency losses discussed earlier, the Smith EVs average 759.06 grams of CO₂e emissions per mile traveled.

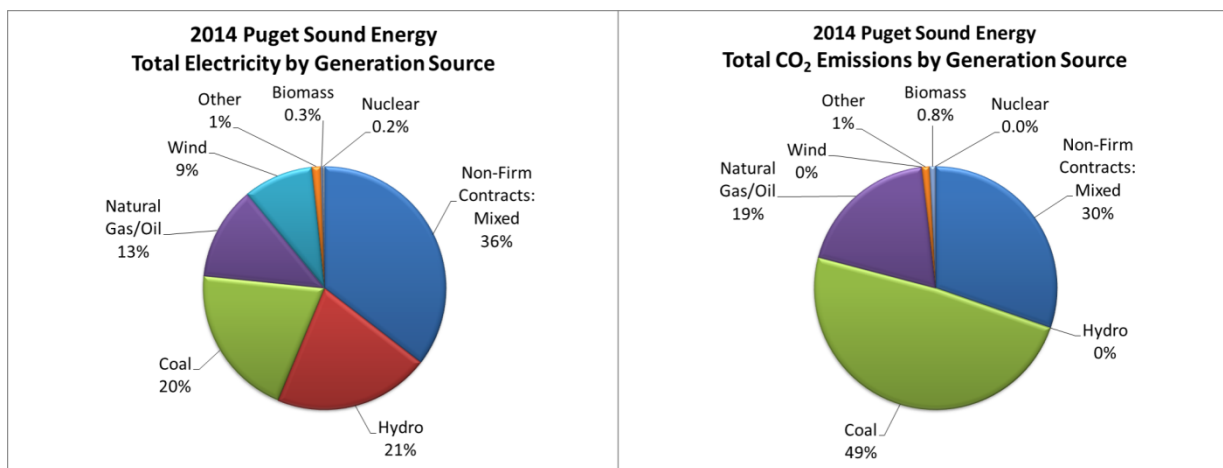


Figure III-14: 2014 PSE total electricity (kWh) by generation source and CO₂ emissions (metric ton)

Image: Robert Prohaska/NREL

Using Argonne National Laboratory’s Greenhouse Gases, Regulated Emissions, and Energy Use in Transportation (GREET) Model’s CO₂e emissions for the delivered, national energy generation source distribution, we find the CO₂e emissions are 613.12 g/kWh, which equates to 958.51 g CO₂e/mi using the Smith EV average energy efficiency including the charger and inverter efficiency losses. The average CO₂e emissions from the EVs can then be compared to the conventional diesels operating in Federal Way using the using GREET’s well-to-wheels analysis tool. Using the national low-sulfur diesel values and the diesel vehicle energy efficiency from GREET, the emissions are 1,414.93 g CO₂e/mi. The EVs, using PSE’s source distribution, emit 46.4% less CO₂e emissions per mile travelled than the diesel vehicles, and using the national energy source distribution, the EVs emit 32.3% less CO₂e per mile. With an average annual distance travelled of approximately 8,488 miles, each EV deployed at the Federal Way site saves approximately 6.136 tons per year of CO₂e emissions compared to a conventional diesel vehicle (see Figure III-15).

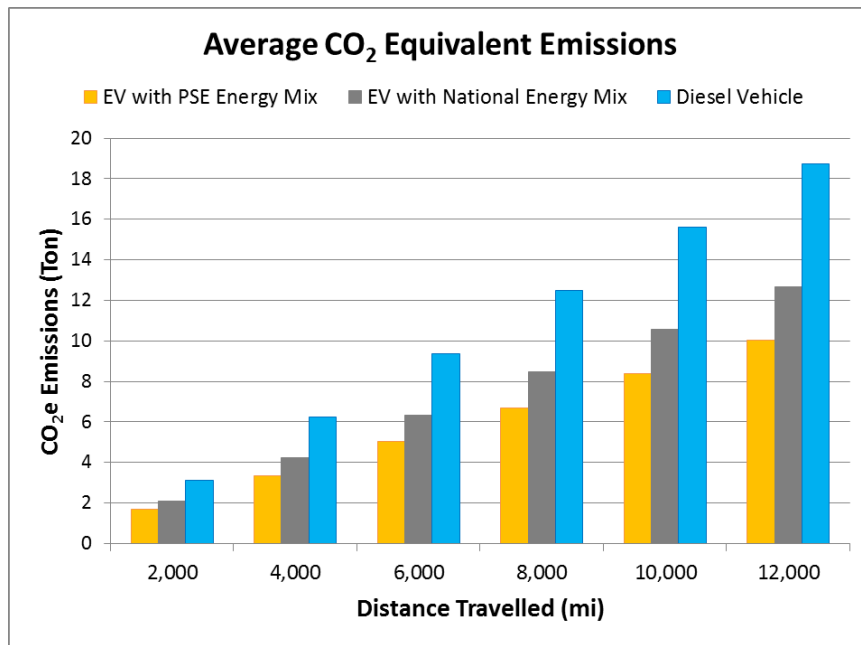


Figure III-15: Average CO₂e emissions by energy source and distance travelled based on Federal Way delivery vehicle operation

Image: Robert Prohaska/NREL

Facility Power Model

Continuing the work performed in FY15, researchers continued to develop and refine a representative facility power model to evaluate the opportunities inherent in managed charging and integration of onsite renewable energy generation sources. The differences between opportunity charging, delayed charging, and managed charging are graphically shown in Figure III-16.

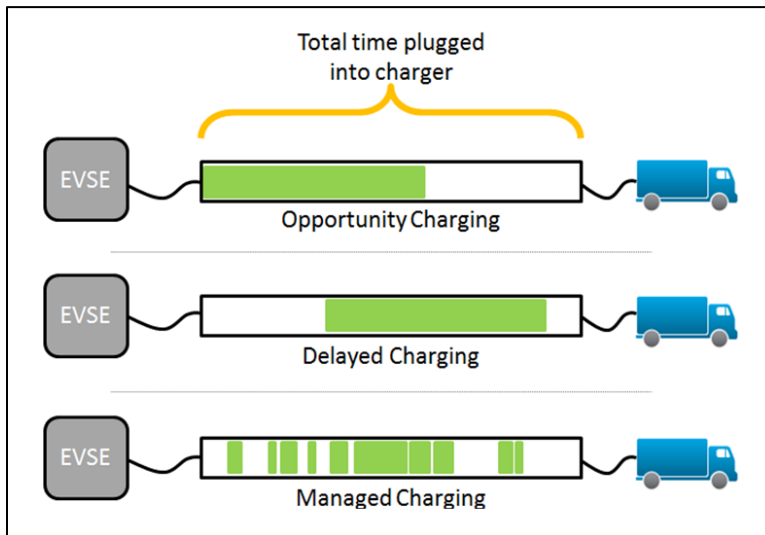


Figure III-16: Opportunity charging, delayed charging, and managed charging.

Image: Robert Prohaska/NREL

When considering managed EV charging at a facility, it is important to understand the timing of different loads. For example, at the Federal Way facility there is a significant overlap in peak facility loads and peak charging loads, which combine to increase the peak demand charge. This overlap allows for the reduction of peak demand charges by shifting the vehicle charging to later in the day with an active charge management system. The amount of time the vehicle is charging can be shifted depending on the current state of charge

(SOC) and the amount of time before the vehicle is dispatched again. While the model shows what is theoretically possible, there are currently limitations in terms of real-world implementation as the managed charging model relies on an up-to-date dispatch schedule and, more importantly, communication of the vehicle’s SOC when it returns to the depot. This feature is not currently available on the Smith Newton vehicles.

FY15 analysis included the use of NREL’s PVWatts® Calculator to characterize the energy available at the Federal Way facility with a 100-kW solar array based on its orientation relative to the sun (Figure III-17).

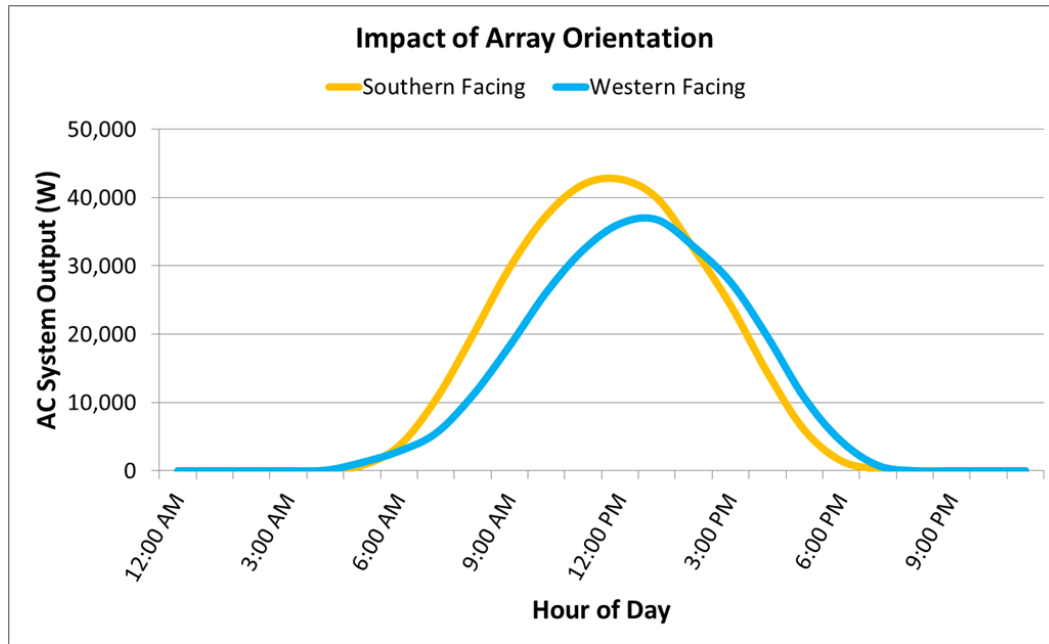


Figure III-17: Average hourly output of 100-kW AC system based on array orientation at Federal Way facility
 Image: Robert Prohaska/NREL

Integrating this PVWatts solar profile into the facility power model, the offset between daily peak solar and daily peak demand loads can be seen in Figure III-18. In this three-day period, the difference between the dashed blue line and the solid green line shows the benefit of integrating a 100-kW solar array into the Federal Way facility with a managed charging routine. The black line indicates the power load requirements of the facility only, not including the electric vehicle supply equipment (EVSE). Even when the western-facing array is modeled, it is evident from Figure III-18 that the facility peak demand loads are offset by several hours from the solar peak loads, thereby minimizing the benefit in reducing peak loads as seen in the direct overlap of the blue and green lines for the majority of the day.

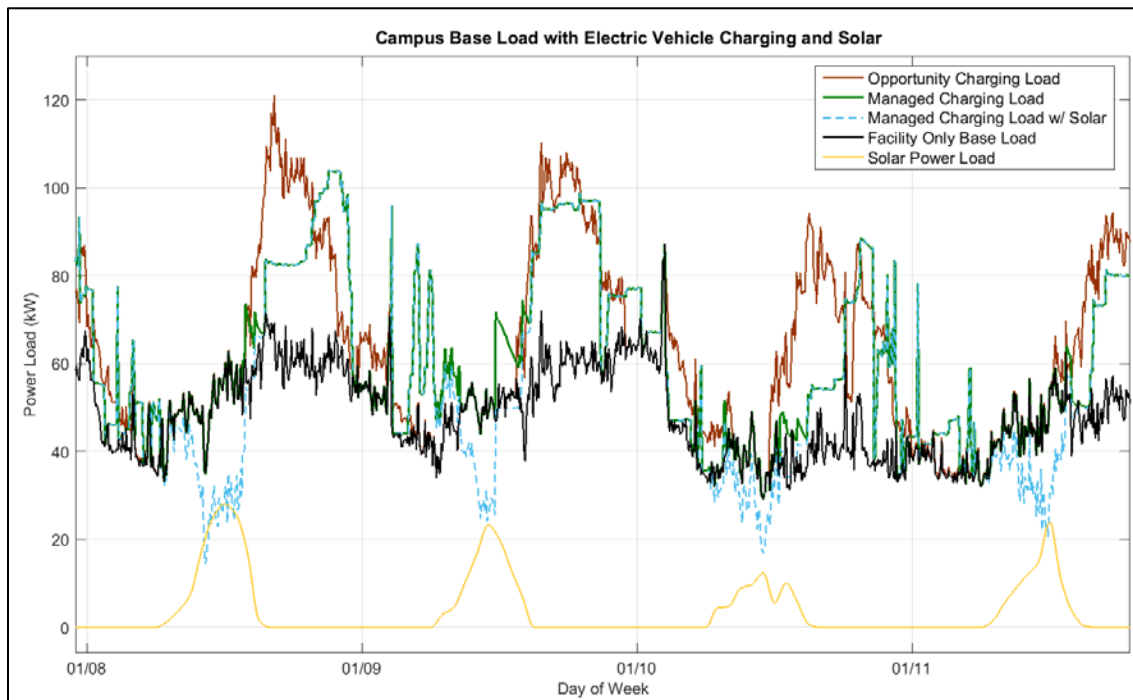


Figure III-18: Campus net load with simulated 100-kW PV array and managed EV charging

Image: Robert Prohaska/NREL

Considering the operational characteristics of the EV fleet at Federal Way, the relatively low peak demand charges in the Seattle area, and the low average solar potential in the Pacific Northwest as shown in Figure III-19, our analysis showed that from a financial perspective, the Federal Way facility is not a strong candidate for integration of onsite solar. For locations with greater solar resource potential and a different EV dispatch schedule, there could be better opportunities to offset vehicle charging loads through the use of onsite solar. To demonstrate the impact of greater solar resources, a western-facing 100-kW solar array was modeled using the solar resource profile of a FLNA location in Casa Grande, Arizona, in conjunction with the same Federal Way facility model. The results are shown in Figure III-20. This simulated solar profile for Casa Grande equates to 149,246 kWh of annual output. As before, the difference between the solid green line and the dashed blue line indicates the added benefit of the solar array. Values less than zero, as seen on day 1/10, indicate opportunities to sell back power to the grid. While the solar resource potential is much greater in Arizona, without large-scale onsite energy storage capacity, there is very little impact on the overall peak power loads due to the offset between EV charging times and peak solar loads.

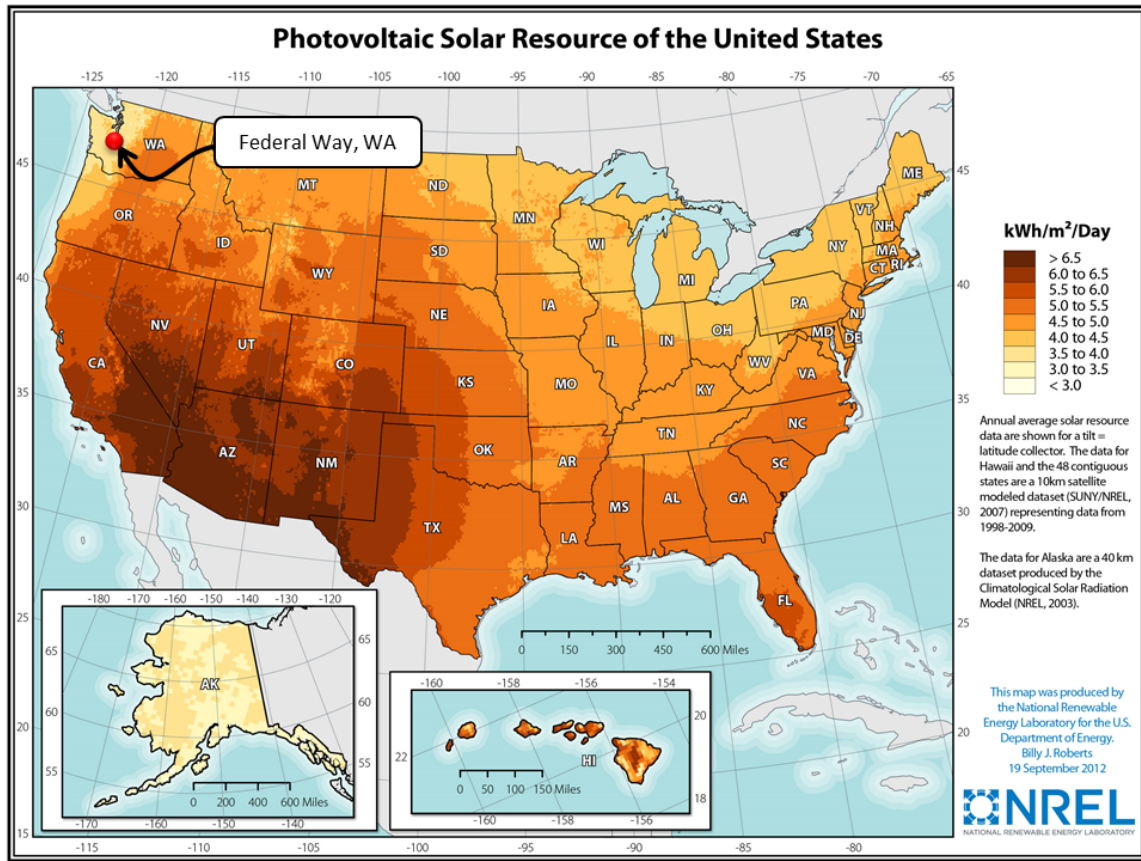


Figure III-19: Solar energy potential. National map shows low solar resource potential near Federal Way

Image: http://www.nrel.gov/gis/images/eere_pv/national_photovoltaic_2012-01.jpg

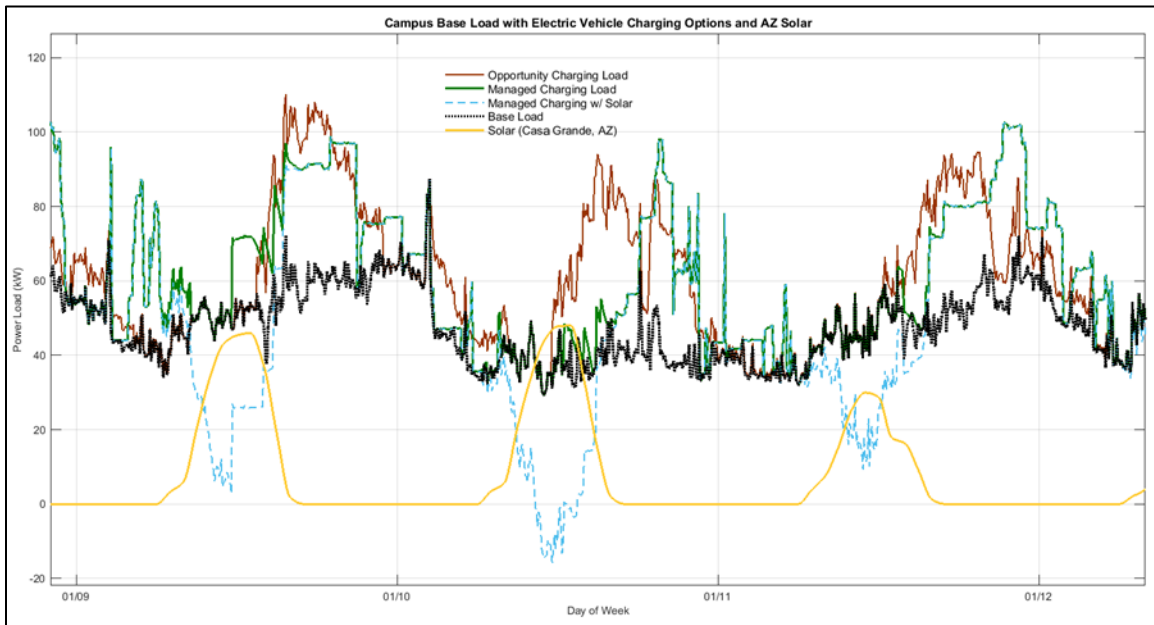


Figure III-20: Campus net load with simulated 100-kW PV array using Casa Grande solar resource profile and managed EV charging

Image: Robert Prohaska/NREL

Therefore, to truly maximize the benefit of onsite solar to reduce peak power loads, the solar peaks must align with the demand peaks. To demonstrate the benefit of aligning peak solar times with peak power demand times, the western-facing Casa Grande solar profile used in Figure III-20 was shifted 6 hours ahead. This simulated 6-hour time shift puts the facility peak loads and the solar output in better alignment. As seen in Figure III-21, the “Managed Charging w/ Solar” power load line (shown in red) has much lower values when compared to the “Managed Charging Load” line (without solar) (shown in green).

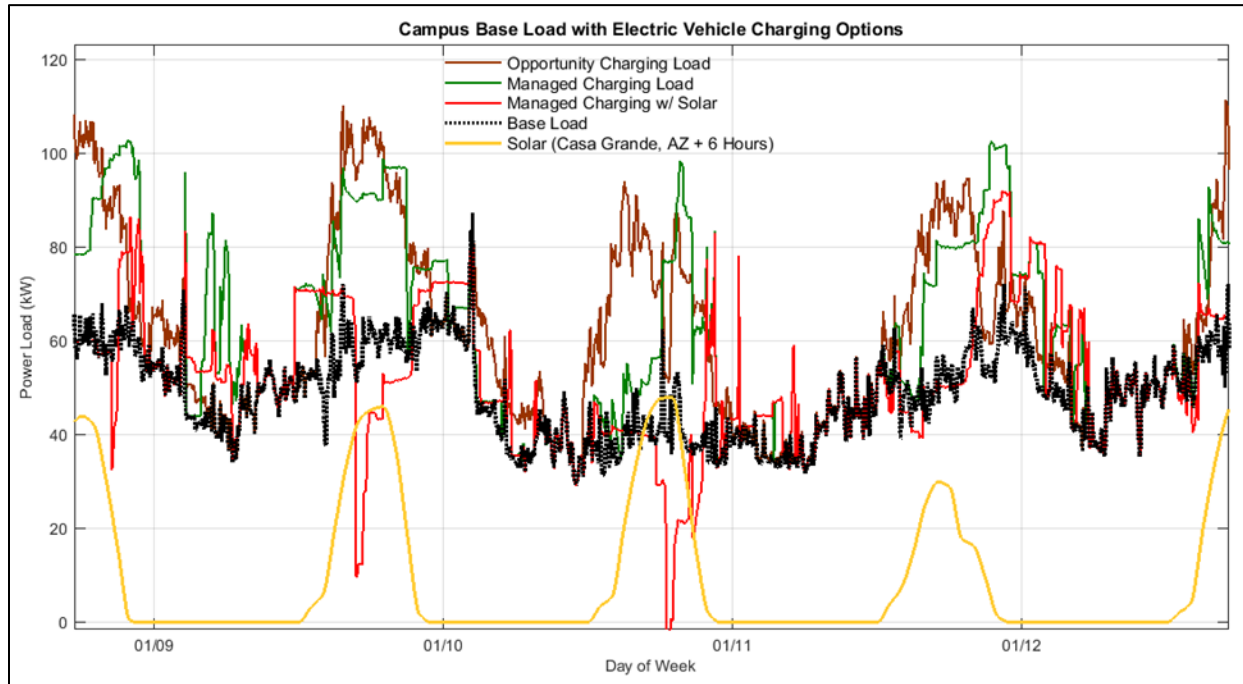


Figure III-21: Campus net load with managed EV charging and simulated 100-kW PV array using a 6-hour time shifted Casa Grande solar resource profile

Image: Robert Prohaska/NREL

This modeling exercise, while not representative of the Federal Way FLNA operation, demonstrates the potential benefits of integrating onsite renewables in the right application. With flexible vehicle dispatching, managed charging, and high solar resources, it is possible to offset a substantial amount of the demand charges that would otherwise be incurred with the integration of EVs into a facility.

Conclusions

This fleet evaluation of FLNA’s Federal Way Smith electric delivery vehicles shows that the success of advanced vehicle technologies for medium- and heavy-duty vehicles is highly dependent on the drive cycle characteristics as well as the general operation of the vehicles. The way in which vehicles are dispatched and operated on the road will dictate how well a specific technology, such as electrification or hybridization, can perform in a fleet setting. As discussed, the route characteristics and requirements of the observed fleet made electrification a viable choice to reduce fleet energy consumption and emissions. Just as energy efficiency is highly dependent on a vehicle’s duty cycle, emissions savings with electrification is highly dependent on the power generation source.

Specific to plug-in EVs, considerations for peak demand charges and charging infrastructure requirements as well as the time required for charging between shifts must be taken into account for successful deployment of electric delivery vehicles. It is imperative for fleet managers to collect and analyze real-world data describing how their vehicles are operated before attempting to adopt a new technology into their fleet.

Traveling on similar routes as the diesel trucks, FLNA’s Federal Way EVs operated at much higher fuel economies. The EVs drove nearly three times as far on the same energy as the diesels, at times exceeding 25 mpg. The diesel trucks averaged 7.7 mpg at \$3.85/gal—roughly the average in Seattle at the time of this

report—and the EVs averaged 23.3 mpge at \$0.102/kWh; thus, the same ratio in fuel economy applies to fuel savings for EVs. FLNA spent \$0.50 for every mile driven with diesel trucks compared to \$0.15 for every mile driven by an EV.

Electricity costs roughly \$2,470 per EV each year on average, whereas FLNA spent nearly \$6,000 per diesel truck in fuel costs (assuming an average of slightly more than 4 gal/day/truck at \$3.85/gal).

Due to the significant overlap in facility and charger peak demand times and relatively lower peak demand charges in the area, managed charging would save FLNA on average only \$270–\$370 per month across Federal Way’s 10 vehicles based on current power prices, thereby reducing the overall utility bill 6%–12%.

Presentations/Publications/Outreach

1. Project Startup: Evaluating the Performance of Frito Lay’s Electric Delivery Trucks. April 2014 (<http://www.nrel.gov/docs/fy14osti/61455.pdf>)
2. R. Prohaska, A. Ragatz, M. Simpson, and K. Kelly. 2015. “Medium-Duty Plug-In Electric Delivery Truck Fleet Evaluation.” IEEE Transportation Electrification Conference and Expo (ITEC 2016). NREL/CP-5400-66055 (<http://www.nrel.gov/docs/fy16osti/66055.pdf>)
3. R. Prohaska, A. Ragatz, M. Simpson, and K. Kelly. 2016. “Medium-Duty Plug-in Electric Delivery Truck Fleet Evaluation.” Presented at IEEE Transportation Electrification Conference and Expo (ITEC 2016). NREL/PR-5400-66755 (<http://www.nrel.gov/docs/fy16osti/66755.pdf>)

Parker Hannifin Hydraulic Hybrid Refuse Truck Case Study with Miami-Dade County

Background

Working with the Southeast Florida Clean Cities Coalition, NREL has partnered with Miami-Dade County’s Public Works and Waste Management Department (PWWMD) to evaluate the on road-performance of Parker Hannifin’s RunWise hydraulic hybrid system on refuse trucks.

With a fleet of 190 refuse vehicles, Miami-Dade County’s PWWMD provides waste collection and recycling services to more than 320,000 households in unincorporated Miami-Dade County and eight municipalities in southern Florida—Aventura, Cutler Bay, Doral, Miami Gardens, Miami Lakes, Palmetto Bay, Pinecrest, and Sunny Isles Beach. It processes more than 1.2 million tons of waste a year, with 240,000 tons of material being processed into a biomass fuel. The county owns an advanced waste-to-energy facility operated by Covanta. The 77-megawatt facility produces enough energy to run the plant and meet the electrical needs of approximately 45,000 homes.

Miami-Dade County is a long-recognized leader in its commitment to reducing GHG emissions. It has an impressive track record of implementing numerous programs and policies that contribute to the regional GHG reduction target of 80 percent below 2008 levels by 2050.

Miami-Dade County operates the largest municipal hybrid fleet in the State of Florida and has the third largest municipal hybrid fleet in the United States. In April 2010, the County’s PWWMD began testing a prototype hydraulic hybrid diesel refuse truck and in December 2010 placed an order for five more vehicles as a “seed fleet” to replace conventional diesel trucks. In 2012 Miami-Dade purchased 29 MY13 HHVs with federal funding from the U.S. Environmental Protection Agency’s “National Clean Diesel Campaign” helping pay for 15 of the 29 trucks (Figure III-22). In 2015, the county ordered an additional 29 MY15 HHVs for a total of 64 hydraulic hybrid refuse trucks.



Figure III-22: Miami-Dade County’s first generation (MY13) hydraulic hybrid refuse trucks at the 58th St. PWWMD facility
 Robert Prohaska / NREL 32729

The Parker RunWise hydraulic hybrid system is not strictly parallel or series in architecture, but a combination of both styles. System specifications are shown in Table III-2. It is a dual path system capable of transmitting power hydraulically or mechanically or a combination of both. The systems’ Power Drive Unit (PDU), as seen in Figure III-23, which replaces the conventional transmission, offers two lower speed hydrostatic modes: hydrostatic low (0–25 mph) and hydrostatics high (25–40 mph), as well as mechanical drive for higher speeds (40 mph and above). The PDU is able to mix power input from both the diesel engine and the hydraulic motor to the wheels, to the hydraulic motor from the wheels for regeneration, or from the hydraulic motor to the engine flywheel to restart the engine as the system shuts off the diesel engine when it is not needed (Figure III-24).

Table III-2: Hybrid Propulsion-Related System Specifications

Category	Hybrid System Description
Manufacturer	Parker Hannifin Corporation
Transmission	Parker Power Drive Unit (3-Mode)
Drive mode max power	335-hp C24 Variable Displacement Bent-Axis Hydraulic Pump/Motor
Regen mode max power	335-hp C24 Variable Displacement Bent-Axis Hydraulic Pump/Motor
Energy storage	Composite Bladder Accumulator (MY13) Steel Vessel Accumulator (MY15) 3,500–4,000 psi nominal pressure range 5,400 psi max pressure

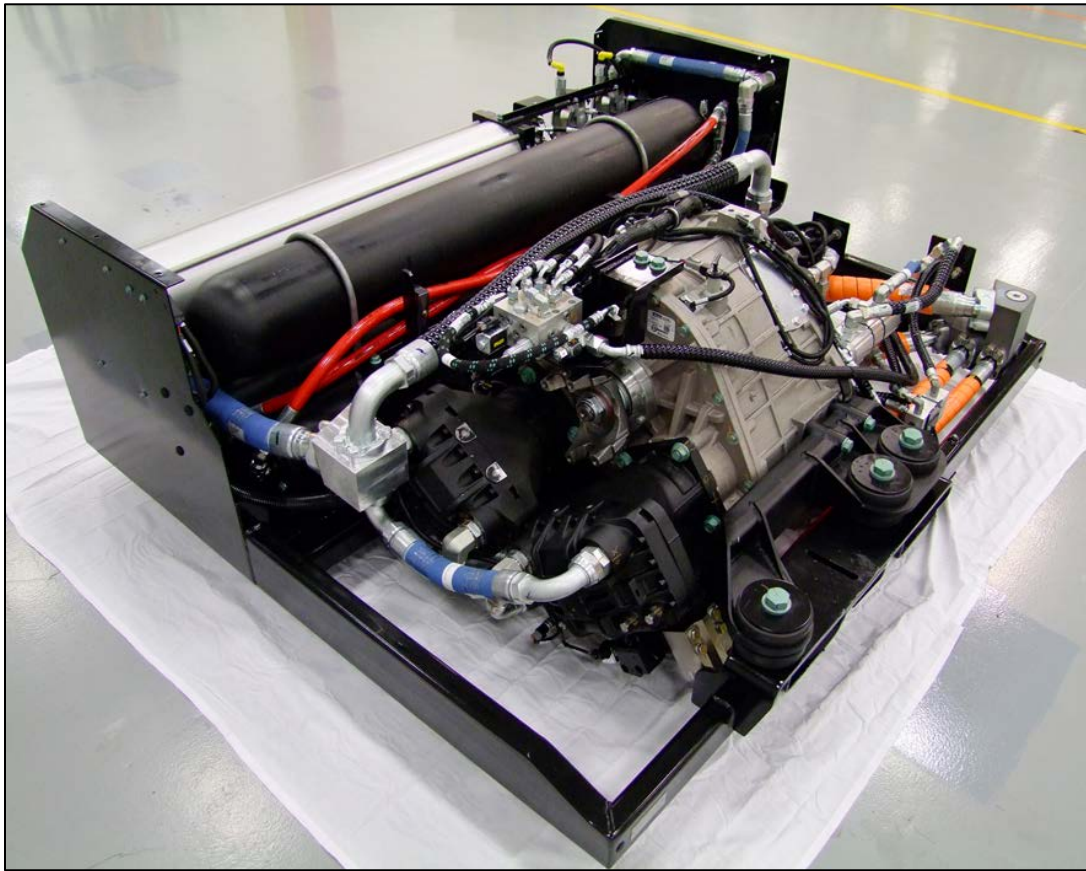


Figure III-23: MY15 Parker Hannifin RunWise hybrid system shown out of vehicle chassis
 (Image Courtesy: Parker Hannifin 39154)

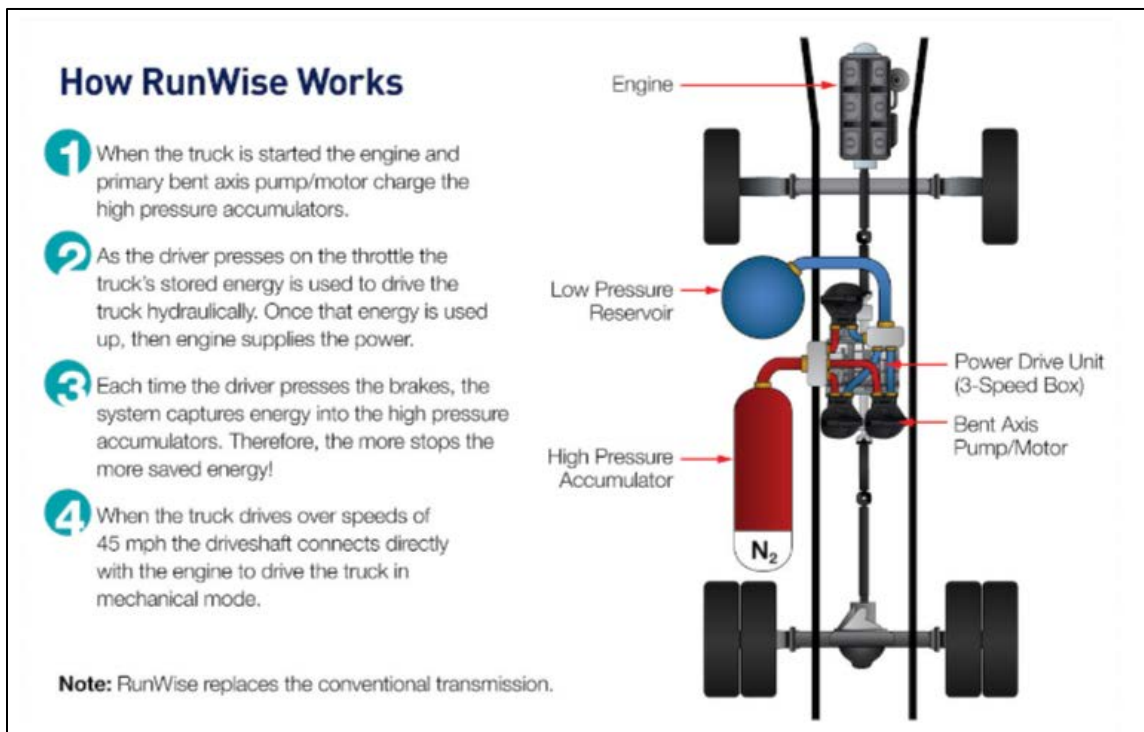


Figure III-24: Parker Hannifin RunWise hybrid system schematic
 (Image: NREL 34464)

Introduction

This field evaluation project discusses an in-use evaluation of first generation MY13 and second generation MY15 HHV refuse vehicles in service in Miami-Dade County. Continued laboratory chassis dynamometer testing is planned for FY17 to validate the in-field findings and quantify both fuel and emissions savings over standard chassis dynamometer cycles.

Host Site Profile—Miami-Dade County PWWMD

The host site in Doral, Florida, is a large service facility serving all Miami-Dade county PWWMD vehicles as seen in Figure III-21. This home terminal offers not only service and repair facilities but also onsite refueling of both diesel fuel and diesel exhaust fluid. The residential waste collection schedule in Miami-Dade County is based on two pick-ups per week, either Monday and Thursday or Tuesday and Friday depending on location. All collected waste is taken to either a transfer station or directly to the local Covanta waste-to-energy plant.



Figure III-25: Overview of the Miami-Dade PWWMD 58th St location

Image source: Google Earth

Approach

The technical approach for this project follows the general approach for conducting fleet evaluations described above. The specific technical approach for the Miami-Dade County Hydraulic Hybrid Refuse Truck Case Study includes the following:

- Initial fleet identification and selection
- Technology partnership
- Initial route and in-vehicle data collection
- Follow-up route and in-vehicle data collection
- Twelve-month fleet data (maintenance/operations) collection.

Detailed results from discussion and results from each of these steps are covered in the following section; a high level project timeline is shown in Figure III-26.

		2014				2015				2016				2017			
Task		Q1	Q2	Q3	Q4	Q1	Q2	Q3	Q4	Q1	Q2	Q3	Q4	Q1	Q2	Q3	Q4
Initiate Project	Submit Project Proposal to Miami-Dade	█															
	Project Kick-off Meeting					█	█										
	Execute Technology NDA							█									
Data Collection	Initial Field Data Collection						█										
	Secondary Data Collection								█								
	Initial Maintenance Data Collection										█						
	Final Maintenance Data Collection														█		
Test & Analysis	Data Analysis							█	█	█	█						
	Dynamometer Testing										█						
	Modeling & Simulation															█	
Results	Finalize Analysis																█
	Generate Final Technical Report																█

Figure III-26: High level project timeline

Image: Robert Prohaska/NREL

Results



Figure III-27: Three configurations of refuse trucks from which data were collected

Photo by Robert Prohaska/NREL

Starting in March 2015, NREL researchers deployed nine data logging devices, Isaac Instruments DRU900/908, (Figure III-28) with global positioning system antennas and J1939 controller area network (CAN) bus connections to the Miami-Dade fleet. For data collection on the MY15 HHVs, Parker provided NREL with a custom database configuration file to decode proprietary messages, such as accumulator SOC, pressures, and temperatures from the hydraulic hybrid system.



Figure III-28: Installation location of on-board Isaac data logger
 Photo by Robert Prohaska/NREL

Initial drive cycle analysis of the in-use data was performed to gain a better sense of how the vehicles are driven on a daily basis. The first component of this evaluation was to confirm that the hybrid vehicles and the conventional vehicles from which data were collected were being operated similarly and on comparable routes (Figure III-29).



Figure III-29: Neighborhood detail showing global positioning system vehicle routes
 Image: Robert Prohaska/NREL

Two strong indicators for the kinematic comparison are daily average kinetic intensity and daily average driving speed. As seen in Figure III-30, there is substantial overlap between the three data sets (MY13 HHV, MY15 HHV, and conventional diesels). The plots shown in Figure III-31 further reinforce the consistency in

overall operation between vehicle platforms. It was determined that the MY13 data would not be included in the broader analysis as that platform represents older technology no longer available from the manufacturer.

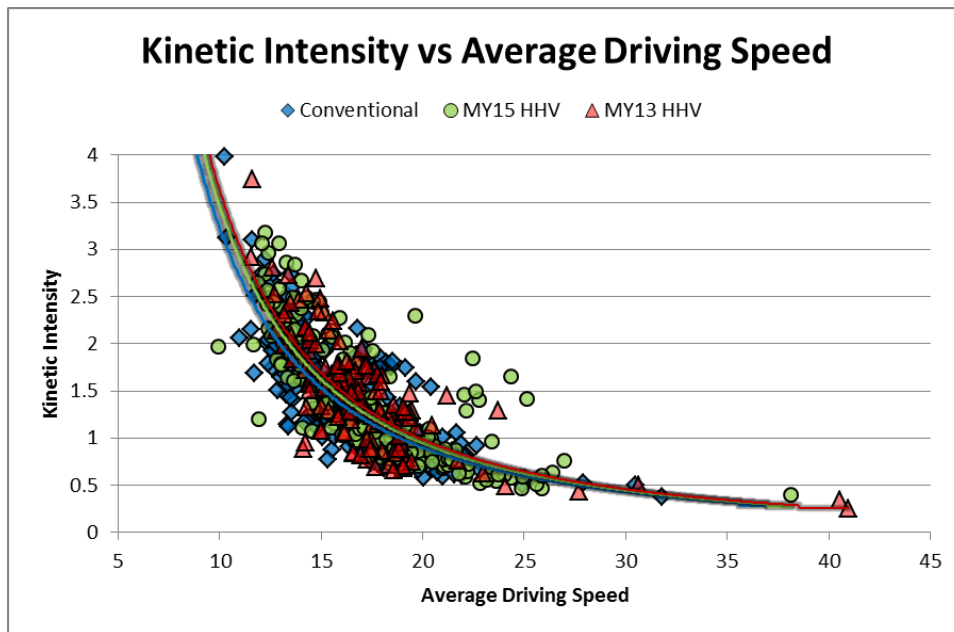


Figure III-30: Kinetic intensity vs. average driving speed
Image: Robert Prohaska/NREL

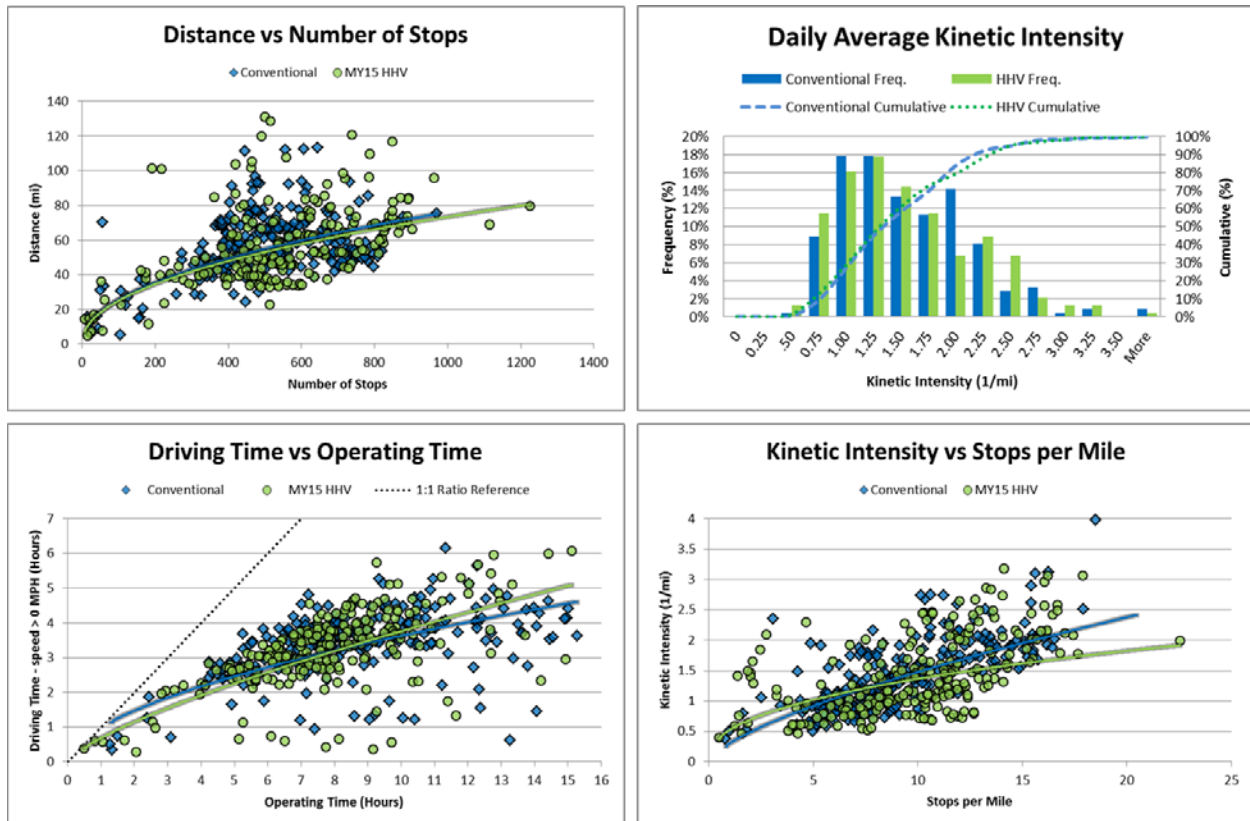


Figure III-31: Multiple scatter plots and a histogram demonstrating the similarities between the operation of the HHVs and the conventional diesel automated side loader refuse trucks
Image: Robert Prohaska/NREL

The average fuel economy of both the MY15 hybrid vehicles and the conventional diesels, in general, decreases as kinetic intensity increases. Figure III-32 shows the average fuel economy for different levels of kinetic intensity. The shaded regions indicate the standard deviation of each data set.

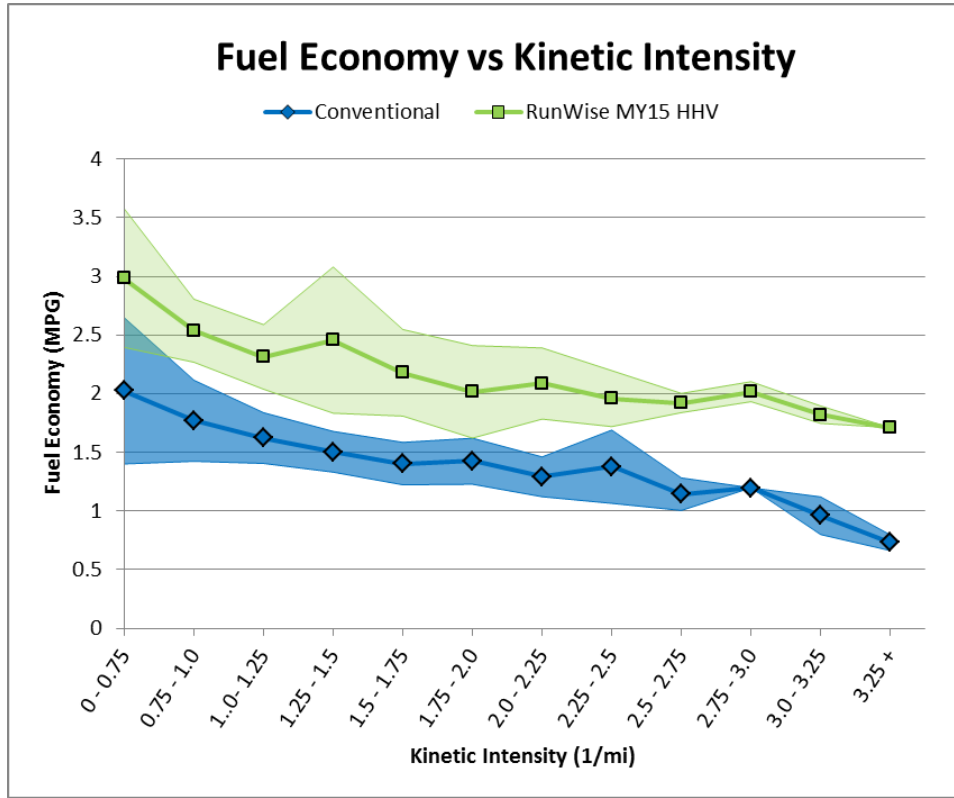


Figure III-32: Fuel economy vs. kinetic intensity shown with standard deviation ranges
 Image: Robert Prohaska/NREL

An initial comparison of the in-use torque vs. speed engine map of the MY15 HHVs to that of the conventional diesels shows that the usage profile for the engine in the HHV is different from that of the conventional vehicle. The MY15 HHVs (Figure III-33) show two primary concentrated areas, one at low speed and torque, near idle and another between 1,500 and 2,000 rpm at a torque level just about 1,200 Nm. The conventional diesel engines (Figure III-34) have a much broader average operating region and do not exhibit the same concentrated operating zones as the MY15 HHVs. Future analysis will compare the fuel consumption rates in these engine operating areas in conjunction with operational duty cycle information.

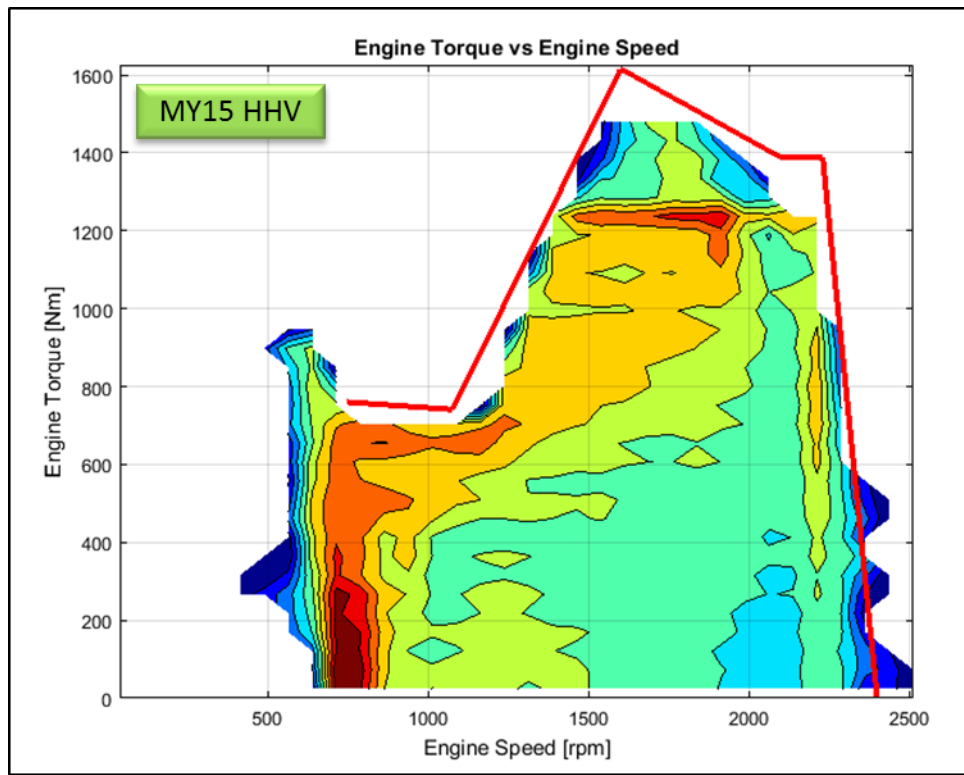


Figure III-33: MY15 HHV Cummins ISL 9, 380-hp, 8.9-L diesel engine operating heat map. Color indicates frequency of data points.

Image: Robert Prohaska/NREL

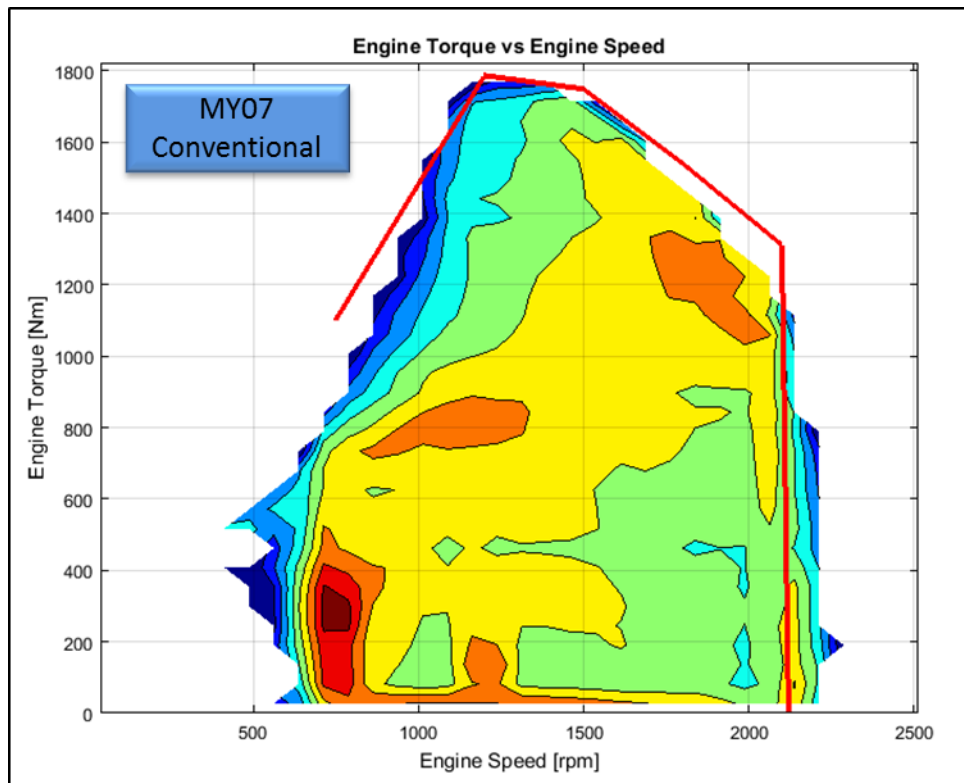


Figure III-34: MY07 Caterpillar C11 ACERT, 335-hp 11.1-L conventional diesel engine operating heat map. Color indicates frequency of data points.

Image: Robert Prohaska/NREL

Initial analysis of the 1-Hz in-use MY15 HHV data shows an interesting dynamic between engine speed and wheel-based vehicle speed (Figure III-35). Due the system architecture of the hydraulic hybrid system, the two hydrostatic gears operate across the range of engine speeds and vehicle speeds up until about 40 mph (64 kph) when the direct drive mechanical gear is engaged. This shows up on the heat plot as a concentrated linear line.

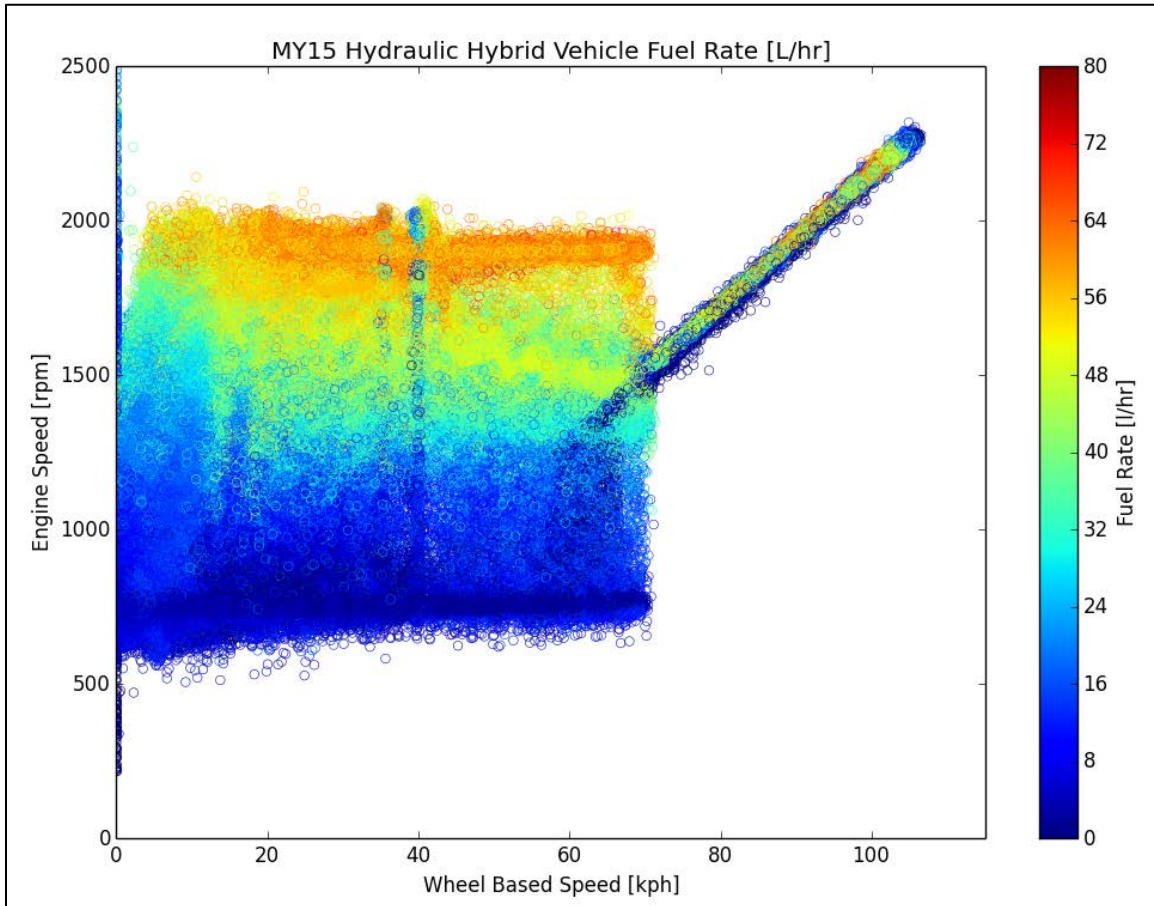


Figure III-35: MY15 HHV engine fuel rate as a function of engine speed and wheel-based vehicle speed
 Image: Robert Prohaska/NREL

Figure III-36 shows the same fuel rate parameter as a function of engine speed and wheel-based vehicle speed for the conventional vehicles. In this plot the six forward gears of the automatic transmission are clearly shown as distinct bands. Both Figure III-35 and Figure III-36 are shown on the same color scale. The conventional vehicle consistently shows a higher fuel rate (darker red) at engine speeds over 1,500 rpm across the spectrum of vehicle speeds, potentially indicating opportunities to reduce the engine size on the HHVs.

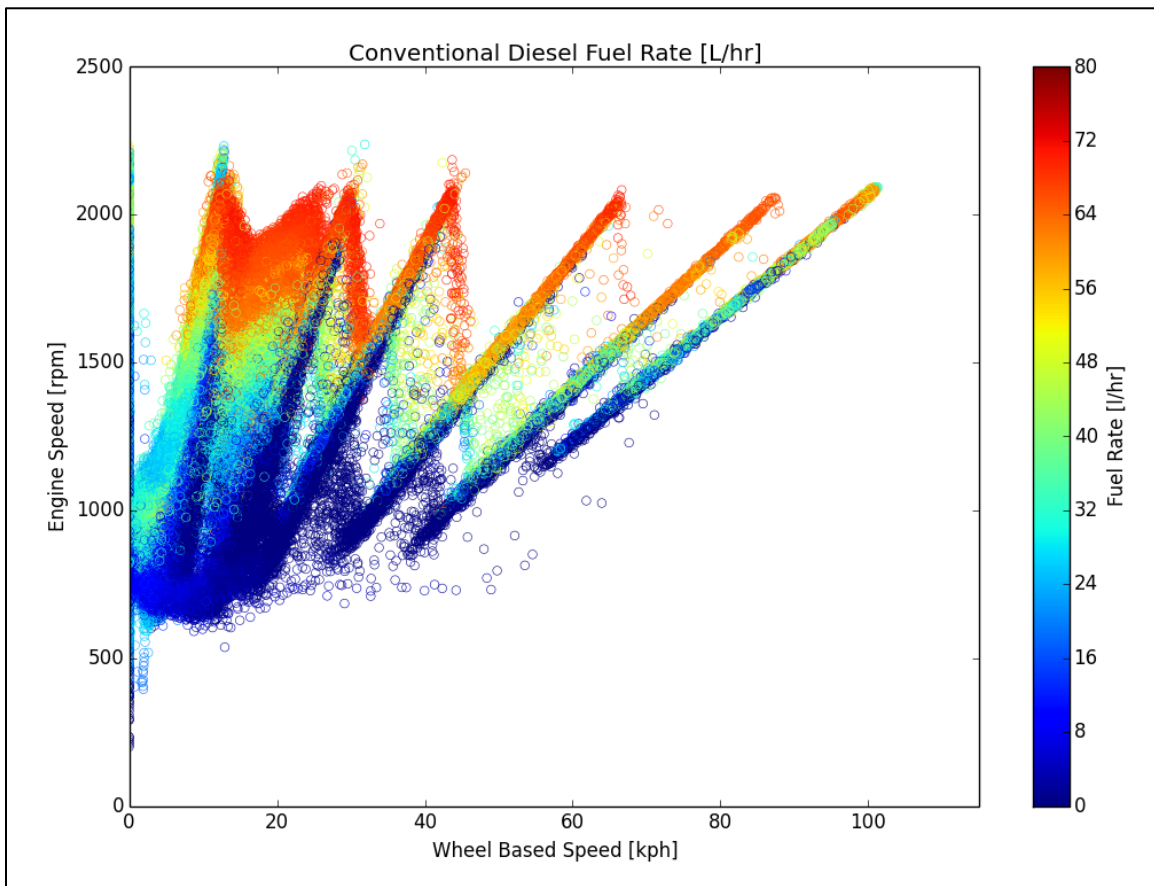


Figure III-36: Conventional vehicle diesel engine fuel rate as a function of engine speed and wheel-based vehicle speed
 (Image: Robert Prohaska/NREL)

Dynamometer Testing

NREL is in the process of conducting chassis dynamometer tests of a conventional diesel refuse hauler, an MY15 diesel HHV and an MY15 CNG HHV to provide a comparison of fuel use and emissions under controlled conditions. Vehicle details and specifications are shown in Table III-3.

Table III-3: Vehicle specifications for chassis dynamometer testing

	Conventional Diesel	Hydraulic Hybrid Diesel	Hydraulic Hybrid CNG
Vehicle Source	City of Denver, Parks & Recreation	Parker Hannifin Engineering Development Vehicle	Parker Hannifin Demonstration Vehicle
Fuel Type	Diesel	Diesel	CNG
Engine	MY15 Cummins ISX12, 12L	MY12 Cummins ISL, 8.9L	MY12 Cummins ISL-G, 8.9L
Aftertreatment	DOC, DPF, SCR	DOC, DPF, SCR	Three-Way Catalyst
Horsepower Rating	350 hp	380 hp	320 hp
Transmission	Allison 4500 RDS	Parker RunWise	Parker RunWise
Transmission Fwd. Gears	6 with 2 Overdrive	2 Hydrostic, 1 Mechanical	2 Hydrostic, 1 Mechanical
Rear Axle Rating	4.56:1	4.33:1	4.33:1

Based on the in-field data collected from the Miami-Dade fleet, the following test cycles were selected for the chassis dynamometer testing:

- Neighborhood Refuse Truck
- Urban Dynamometer Driving Schedule – Heavy Duty (UDDS-HD)
- Heavy Heavy-Duty Diesel Truck (HHDDT) Composite
- NREL Miami-Dade Refuse Custom

Figure III-37 shows how these test cycles compare to the collected field data and one another in terms of average driving speed and kinetic intensity. Each gray circle represents one day of driving. The three trend lines represent the three configurations from which field data were collected: MY13 HHVs, MY15 HHVs, and MY07 conventional diesels.

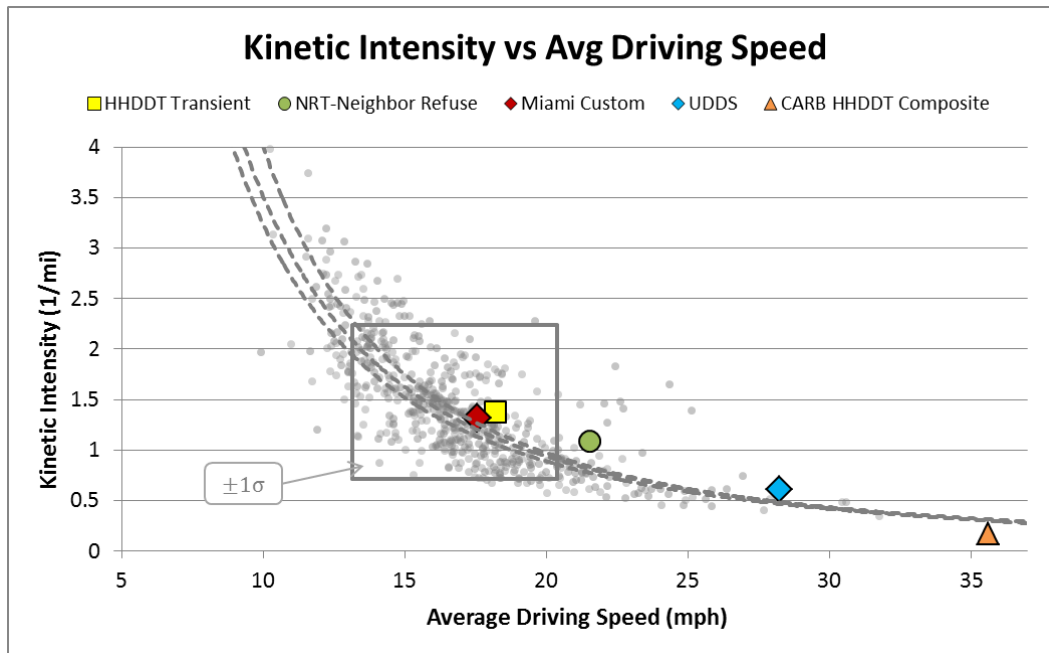


Figure III-37: Field data from MY13 HHVs, MY15 HHVs, and Conventional diesels shown with select chassis

Image: Robert Prohaska/NREL

Working with local fleet representatives from the City of Denver Parks and Recreation department, a 2015 Peterbilt refuse truck was tested at NREL’s ReFUEL laboratory. The vehicle, equipped with a 350-hp Cummins ISX12 12-L diesel engine (Figure III-38) was tested on a variety of drive cycles while researchers measured fuel consumption with gravimetric weigh tanks, criteria exhaust emissions using a Fourier transform infrared spectroscopy (FTIR) gas analyzer and high-speed J1939 CAN data.



Figure III-38: City of Denver 2015 Peterbilt with ISX 12
 Photo by Robert Prohaska/NREL

In conjunction with work being performed for the California Air Resource Board, Parker Hannifin loaned NREL its 2013 CNG HHV demonstration vehicle for benchmark testing, which is configured with the same MY15 RunWise HHV system (Figure III-39). While the CNG hybrid configuration is the same as the diesels where the RunWise system replaces the conventional transmission, there are currently no CNG HHVs fielded. Researchers tested this CNG HHV vehicle on the four test cycles listed above while monitoring fuel consumption with a Coriolis fuel flow meter, exhaust emissions with an FTIR gas analyzer, and high-speed CAN data.



Figure III-39: 2013 AutoCar E3 MY15 HHV refuse truck with Cummins ISL-G engine at NREL's ReFUEL laboratory
 Photo by Dennis Schroeder / NREL 38576

Conclusions

Preliminary analysis of the in-field data indicates an average fuel economy improvement of 52% with the second-generation HHVs over the 2007 conventional diesels when operated on similar routes. The analysis also shows evidence of Parker Hannifin's stated improved efficiency due to quicker acceleration rates for a given level of fuel consumption.

Analysis of the dynamometer fuel consumption and emissions out from the conventional diesel, CNG HHV, and the MY15 HHV diesel will be completed in FY17.

More data will need to be collected and analyzed to draw a full conclusion on the maintenance implications of this technology.

Presentations/Publications/Outreach

1. Local and Federal Government Partnership Progresses, Southeast Florida Clean Cities Coalition, November 2015 (<http://sfregionalcouncil.org/wp-content/uploads/2015/11/CCFall2015Newsletter.pdf?fbisphpreq=1>)
2. Project Startup: Evaluating the Performance of Hydraulic Hybrid Refuse Vehicles (<http://www.nrel.gov/docs/fy15osti/65013.pdf>)
3. NREL Evaluates Performance of Hydraulic Hybrid Refuse Vehicles. NREL Highlights in Research & Development. September 2015. (<http://www.nrel.gov/docs/fy15osti/64825.pdf>)

Proterra Fast Charge Battery Electric Transit Bus Field Evaluation with Foothill Transit

Background and Introduction

In March 2014, Foothill Transit began operating a fleet of battery electric buses (BEBs) in its service area in the San Gabriel and Pomona Valley region of Los Angeles County, California. The BEBs were purchased through a \$10.2-million grant under the Federal Transit Administration’s Transit Investments for Greenhouse Gas and Energy Reduction (TIGGER) program. These electric buses, produced by Proterra, Inc., as the BE35 model, are 35-foot-long composite body buses that are capable of being charged on-route via Eaton 500-kW fast chargers. NREL’s Fleet Test and Evaluation Team is evaluating the in-service performance of 12 fast-charge BEBs compared to conventional CNG buses operated on similar routes by Foothill Transit. Launched in 2015 in conjunction with a previously funded California Air Resources Board research project, this study aims to improve understanding of the overall usage and effectiveness of fast-charge electric buses and associated charging infrastructure in transit operation.

Results

In early 2015, Proterra provided researchers at NREL with over 92,000 miles of 2-Hz in-use raw operation data from 12 electric transit buses operating in Foothill Transit’s fleet. These data were from four separate time periods to balance out potential effects of seasonality and changes in ridership (Figure III-40).

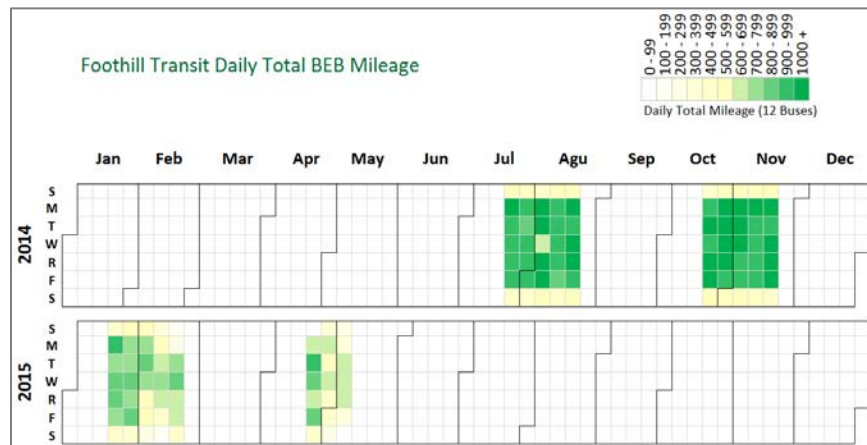


Figure III-40: Data collection periods shaded according to daily mileage accumulation for all 12 BEBs

(Image: Robert Prohaska/NREL)

Successful deployment of advanced vehicle technologies is highly dependent on correctly matching the technology with an appropriate duty cycle. There are many ways to characterize a vehicle’s duty cycle, but by focusing first on the kinematics of daily operation, one can better understand how vehicles are operating and begin to understand the drive cycle requirements of the duty cycle. The term duty cycle refers to the operational cycle of the vehicle, which includes how, when, and where the vehicle is dispatched; how many riders are picked up; how often the vehicle is recharged, etc. The term drive cycle describes the kinematics, or motion, of the vehicle. Each drive cycle will include a number of metrics characterizing the vehicle’s behavior, such as maximum speed, average speed, distance traveled, frequency of stops, acceleration rates, idle time, etc.

Figure III-41: shows a typical drive cycle speed trace for a BEB in operation on Line 291, which Foothill dedicated to BEB-only operation. Three separate charge events with an average duration of 5 to 6 minutes are included in this figure and are marked accordingly, along with the relative location (North or South Loop). The North and South Loops make up the full route for Line 291. The purple line shows the vehicle speed trace of the bus while the blue line shows the battery pack SOC; both of these metrics use the left vertical axis. The red line, with the vertical axis on the right, shows cumulative distance. When examining the change in slope of the battery SOC curve on the portion of the figure labeled “North Loop,” we can see varying degrees of discharge rates. These variations are attributed to the slight amount of road grade on Line 291—the north end of the loop is approximately 300 feet (92 m) above the Pomona Transit Center. The outbound portion of the North Loop,

starting at approximately 4:18 p.m. with a battery pack SOC of 80% shows a faster discharge rate (steeper slope of the blue line) than the return trip on the same loop due to the bus gaining elevation. The second half of the North Loop has a slower discharge rate (shallower slope of blue line) as the bus returns to the Pomona Transit Center with a battery pack SOC of approximately 32%. While 300 feet is not a significant amount of elevation change over 4.7 miles (approximately half of the North Loop), there is a noticeable effect on the power required for operating the BEB, which demonstrates the importance of road grade when considering energy storage requirements.

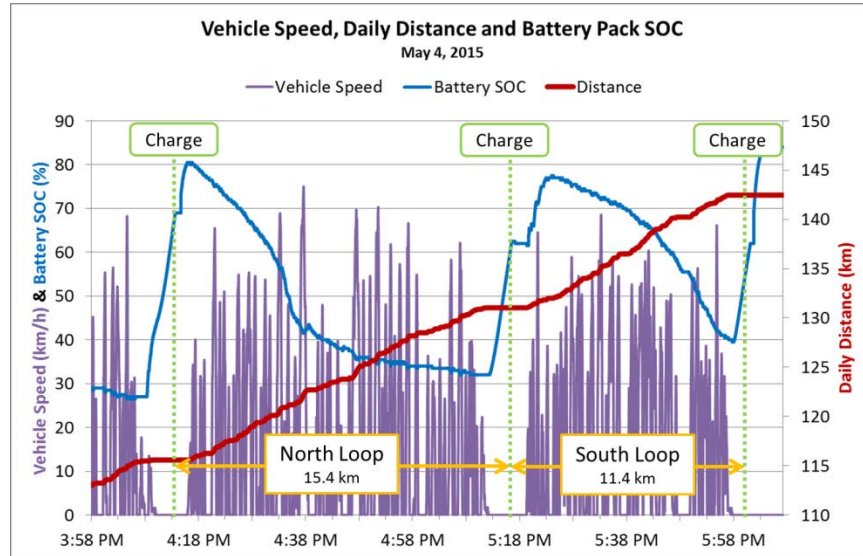
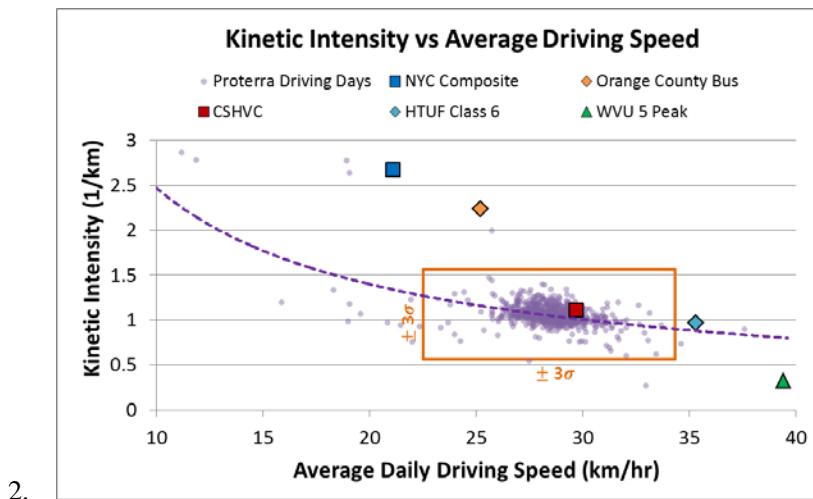


Figure III-41: Vehicle speed, battery pack SOC, and distance for one typical “loop” on Line 291 with three charge events shown

Image: Robert Prohaska/NREL

One metric often used to describe the drive cycle of a particular vehicle is kinetic intensity. Kinetic intensity is a relative measure of driving aggressiveness and is based on the relationship between the energy used for accelerating a vehicle versus the amount of energy used to overcome aerodynamic drag. Comparing daily average kinetic intensity to average driving speed (Figure III-42), we can see that since the BEBs operate on a dedicated route, there is very little variation in the data set as 99.7% of all the values fall within the orange rectangle representing values within ± 3 standard deviations from the mean.



2.

Figure III-42: Kinetic intensity vs. average driving speed for all Protterra BEBs with $\pm 3\sigma$ reference box. Standard test cycles are also shown.

(Image: Robert Prohaska/NREL)

Looking at the frequency of stops on a distance basis as a function of acceleration, one can see in Figure III-43 that the BEBs average 3.7 stops per mile (2.31 stops per kilometer) and have a slightly higher average rate of deceleration than acceleration.

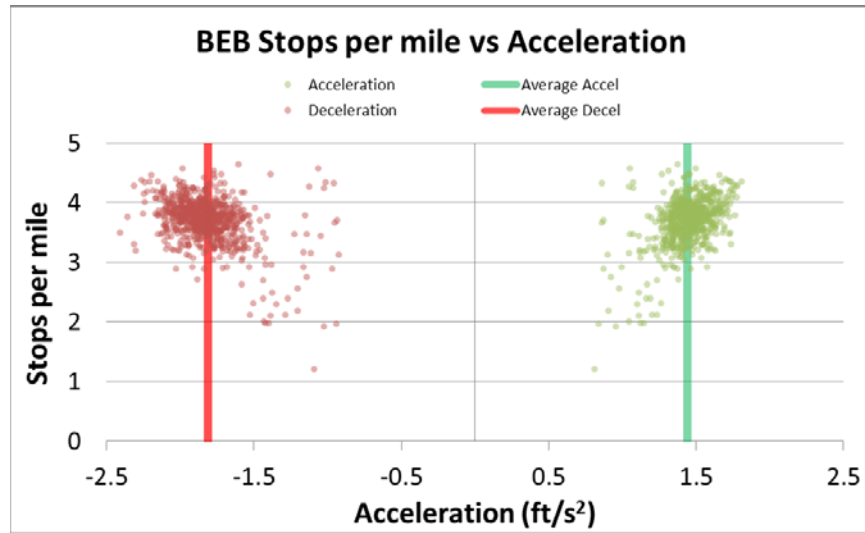


Figure III-43: Average daily acceleration rates vs. stops per mile

Image: Robert Prohaska/NREL

Figure III-45 shows a typical day of operation for a single BEB on Line 291. The bus operates continuously from 5 a.m. through 11 p.m. for a total of 250 km and is charged a total of 18 times with the battery SOC never dropping below 45%. Figure III-45 shows that this charging behavior is consistent with the larger fleet operation where the average battery pack SOC is equal to 75.4% and the battery pack rarely drops below 50% SOC.

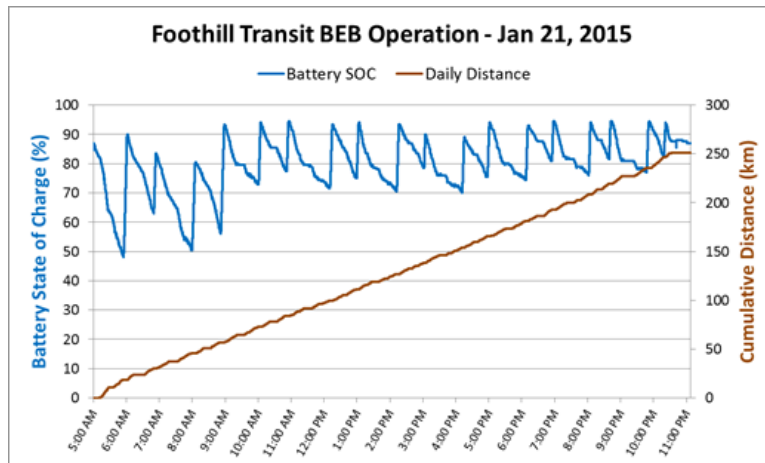


Figure III-44: Typical day of operation showing average battery pack SOC and cumulative distance travelled

Image: Robert Prohaska/NREL

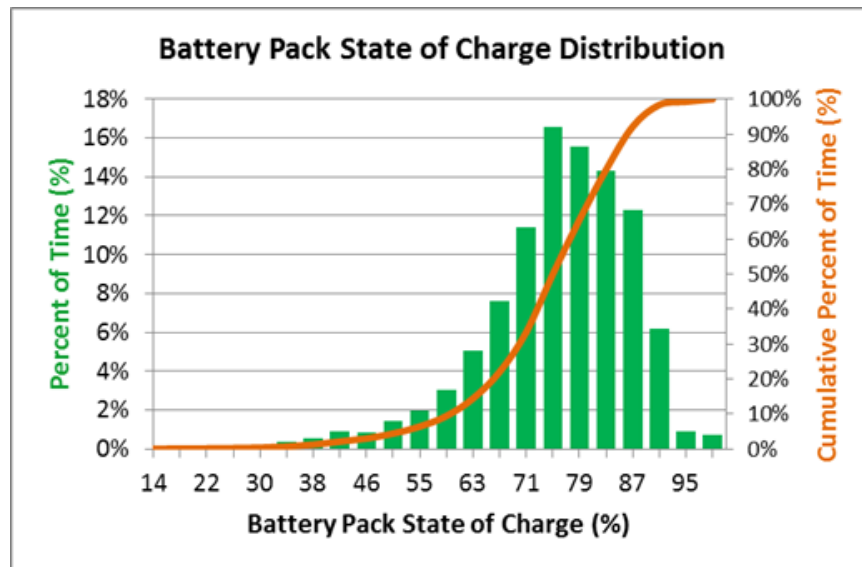


Figure III-45: Vehicle-reported SOC for all BEBs over the entire data reporting period

Image: Robert Prohaska/NREL

This battery pack SOC distribution curve also indicates the potential opportunities to optimize deployment of the BEBs on Line 291 as the buses spend less than 6% of their time at an SOC less than 55%. Operationally, the buses could be charged less frequently on route, which would allow drivers to get back on schedule if they are delayed. Systematically, there is a potential opportunity to reduce the size of the energy storage system on the vehicles running this particular route to reduce weight and purchase price.

The BEBs deployed on this electrified route demonstrated an overall average efficiency of 1.34 kWh/km. On an equivalent energy basis, this equates to 7.43 kilometers per diesel liter equivalent. This average efficiency was calculated using data provided by Proterra from July 2014 through June 2015 using the charging energy delivered to the battery packs of the BEBs and the total distance travelled. The overall fleet average efficiency includes the energy required to operate all accessory loads such as the heating, ventilating, and air conditioning (HVAC) system and fluctuates in response to average temperature, as seen in Figure III-46.

The average monthly temperatures are from National Oceanic and Atmospheric Administration measurements taken at the Ontario, California, airport, which is approximately 15 km from the Pomona Transit Center, where the BEBs are charged. The monthly BEB fleet efficiency fluctuates relative to average temperature with efficiency dropping when temperatures are higher and the buses require use of air conditioning as well as when temperatures drop, requiring the use of the electric heater. The months of highest efficiency have average high temperatures less than 25°C and average low temperatures greater than 11°C, requiring the least amount of energy for passenger comfort.

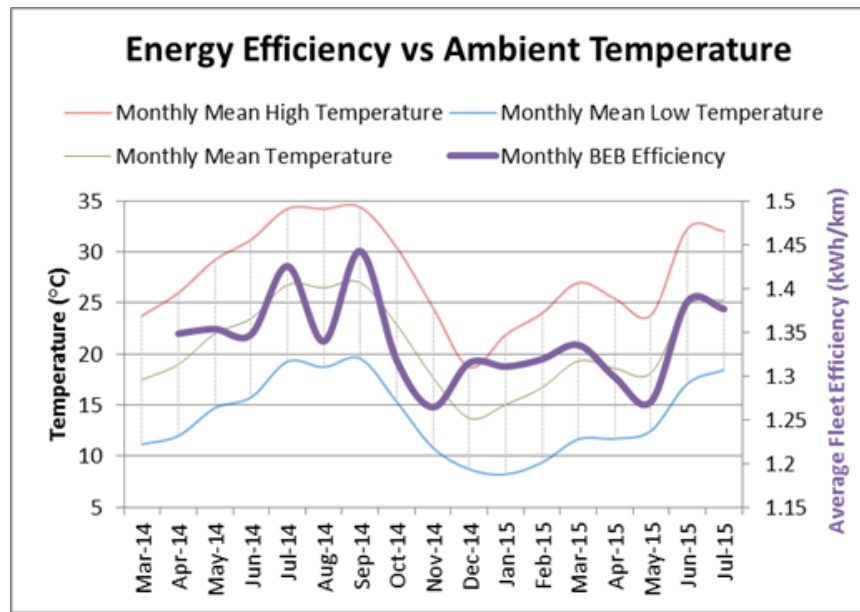


Figure III-46: BEB energy efficiency vs. mean, mean maximum, and mean minimum temperatures
 Image: Robert Prohaska/NREL

Vehicle Comparison – CNG & BEB

Figure III-47 shows the strong relationship between daily operating time and daily driving time of the BEBs in purple and the CNG vehicles in red. The BEBs on their dedicated route demonstrated an R2 value of 0.9655 for the linear fit trend line, which shows that on average the vehicles are only in motion about 48% of the time they are in operation while the CNG vehicles are much more scattered and in general are moving proportionally more when they are in operation.

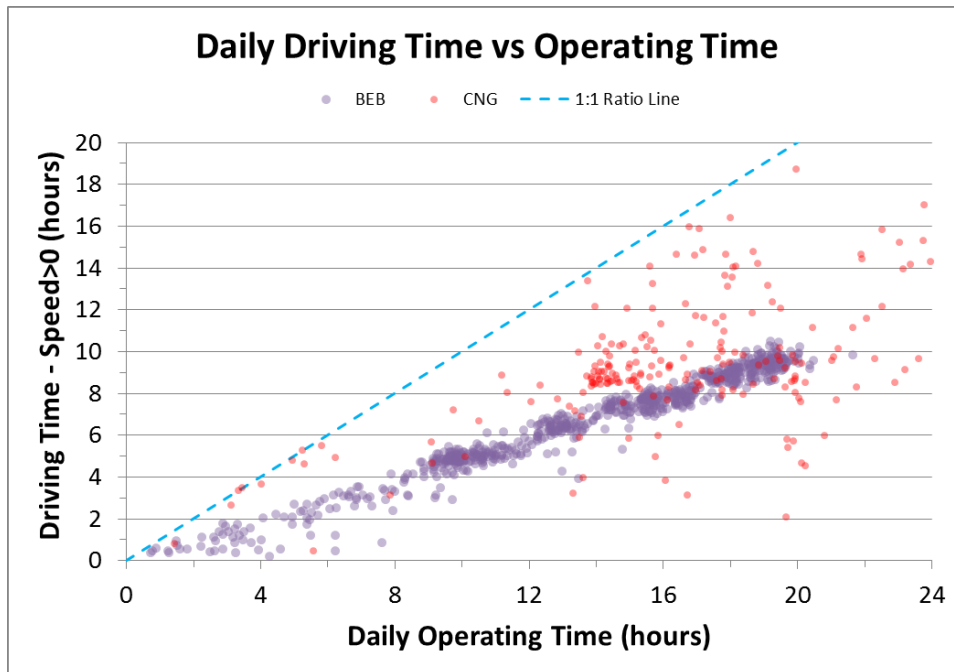


Figure III-47: Distribution of driving time where speed is greater than zero vs. amount of time when system is “ON” for BEBs and CNG vehicles
 Image: Robert Prohaska/NREL

Figure III-48 shows the number of stops per day as a function of daily distance travelled for both the BEBs and CNGs. In general the routes that the CNGs are deployed on are longer and require fewer stops than the electrified BEB line 291.

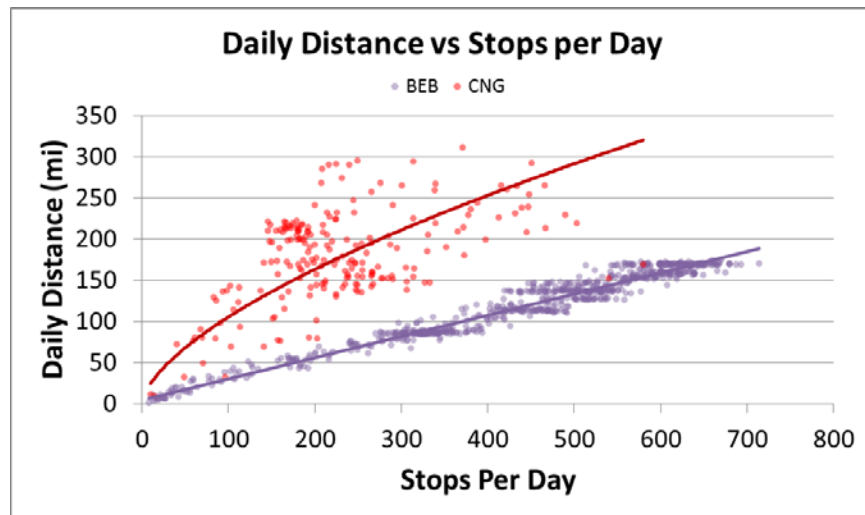


Figure III-48: BEB and CNG daily distance vs. stops per day

Image: Robert Prohaska/NREL

Conclusions

Only initial data analysis has been completed to date and, while the BEBs have demonstrated an energy efficiency of 1.34 kWh/km, road grade and non-tractive energy demands such as HVAC can have a significant effect on overall energy efficiency and must be taken into account when determining the feasibility of deploying advanced technologies. Researchers will continue to analyze the in-field data of the CNG vehicles for a more robust comparison.

While the data showed seasonal variation in energy efficiency, additional analysis is required to accurately define the thermal load characteristics of these BEBs to isolate the HVAC system power requirements specific to this operational duty cycle.

Future Research

Future research will be done to compare the dedicated BEB Line 291 in detail to a broader set of Foothill Transit routes using in-use data collected from conventional compressed natural gas buses randomly dispatched throughout the Foothill Transit service area. Through modeling and simulation, researchers will be able to identify other routes that would be well suited for electrification. In addition to further benchmarking the operational efficiency of BEBs against compressed natural gas buses using in-field data, researchers plan to perform controlled chassis dynamometer testing in partnership with California Air Resources Board to characterize efficiency over a range of drive cycles. Researchers also plan to investigate the impacts of HVAC requirements on energy efficiency and identify areas for potential improvement.

Presentations/Publications/Outreach

1. Project Startup: Evaluating the Performance of Electric Buses. April 2016. NREL/FS-5400-66142 (<http://www.nrel.gov/docs/fy16osti/66142.pdf>)
2. R. Prohaska, L. Eudy, and K. Kelly. "Fast Charge Battery Electric Transit Bus In-Use Fleet Evaluation." ITEC 2016: IEEE Transportation Electrification Conference and Expo. Dearborn, Michigan. NREL/CP-5400-66098. May 2016 (<http://www.nrel.gov/docs/fy16osti/66098.pdf>)

3. R. Prohaska, L. Eudy, and K. Kelly. “Fast Charge Battery Electric Transit Bus In-Use Fleet Evaluation.” ITEC 2016: IEEE Transportation Electrification Conference and Expo. Dearborn, Michigan.
4. L. Eudy, R. Prohaska, K. Kelly, and M. Post. Foothill Transit Battery Electric Bus Demonstration Results. NREL/TP-5400-65274. January 2016 (<http://www.nrel.gov/docs/fy16osti/65274.pdf>)
5. NREL Evaluates Performance of Fast-Charge Electric Buses. NREL Highlights in Research & Development. September 2016. (<http://www.nrel.gov/docs/fy16osti/67057.pdf>)
6. K. Kelly. “Medium- and Heavy-Duty Vehicle Duty Cycles for Electric Powertrains.” Applied Power Electronics Conference. Long Beach, CA NREL/PR-5400-66228. March 2016. (<http://www.nrel.gov/docs/fy16osti/66228.pdf>)
7. C. Morris. NREL Report: Battery-Electric Buses are Four Times More Fuel-Efficient than CNG. Charged Electric Vehicles Magazine. February 23, 2016 (<https://chargedevs.com/newswire/nrel-report-battery-electric-buses-are-four-times-more-fuel-efficient-than-cng/>)

CGI / EV2G School Bus Case Study

Background

NREL’s Fleet Test and Evaluation Team is leveraging investment of the Clinton Global Initiative (CGI) technical and project team with funding from the California Energy Commission (CEC) and the South Coast Air Quality Management District (SCAQMD). The CGI project will upfit and deploy six EV school buses and place them into service at three separate California school districts by the 2016/17 school year. NREL’s Fleet Evaluations Team and Vehicle Grid Integration Team will collaborate on field data and testing and analysis that support DO’s grid integration efforts and vehicle technology evaluations. The project will provide data to the Fleet DNA database and contribute to the knowledge base on school bus duty cycles and their electrification potential.

Introduction

NREL is currently funded by DOE to collect operational data on conventional school buses in the districts receiving electric vehicle-to-grid (EV2G) buses and on the EV2G buses once they are all deployed beginning in the end of the fourth quarter of 2016 and continuing into the 2016/17 school year. The project will document vehicle performance and cost of operation of all six CGI electric school buses with vehicle-to-grid (V2G) capability and contribute to TransPower's bus conversion efforts through the duty cycle characterization and vehicle systems analysis of current conventional and hybrid vehicles in service. Table III-4 gives the TransPower EV2G bus specs.

Table III-4: EV2G School Bus Specifications

Chassis/Body	1996 medium-duty DT466 chassis conversions International/Bluebird buses
Motor	Permanent magnet 3-phase electric 150-kW peak, 110-kW continuous
Transmission	6-Speed autoshift manual (5 speeds used)
Battery	115.2 kWh total (92.1 usable)
Curb/Gross Vehicle Weight	17,000/25,500 lbs.

Approach

The technical approach for this project follows the general approach for conducting fleet evaluations described above. The specific technical approach for the EV2G school bus project includes the following:

- Initial route and in-vehicle data collection
- One school year of EV2G fleet data collection
- Energy Systems Integration Facility (ESIF) V2G evaluation, including IEEE 1547 and J3068 testing
- Dynamometer testing representative of school bus in-use service conducted at NREL’s ReFUEL test facility
- Develop validated FASTSim EV school bus model and conduct design parameter investigation.

Results

Progress to Date

Initial Fleet Identification and Selection

During FY15, NREL engaged with CGI to conduct an analysis of real-world school bus duty cycles. NREL coordinated with Napa Valley Unified School District (NVUSD) and Torrance Unified School District (TUSD) to gather needed baseline data for the planned EV2G retrofit demonstration project in those districts. Zonar, the telematics provider for TUSD, agreed to provide in-kind 1-Hz data for 2 weeks on the TUSD 32-bus fleet to NREL for the purpose of this evaluation. NREL worked with NVUSD to identify eight buses as targets for data logger installation based on TransPower EV bus potential route operation and completed the instrumentation plan in April 2016. NREL reported on the NVUSD and TUSD baseline bus utilization data gathering to the Statistics Working Group on June 24, 2015.

Initial Route and In-Vehicle Data Collection

Data collected from the school districts were used to produce data products to help TransPower understand the usage environment its product will be placed into. Figure III-49 shows a histogram of daily distances traveled by buses in NVUSD and TUSD fleets. Note that 80% of observed days had fewer than 50 miles driven, and less than 10% of days had greater than 70 miles driven. The TransPower EV2G bus is designed to have a 70-mile range. Previous EV evaluations have shown a significant impact of road grade on EV energy consumption. Future analysis will be conducted to evaluate driving range constraints subject to actual route road grades.

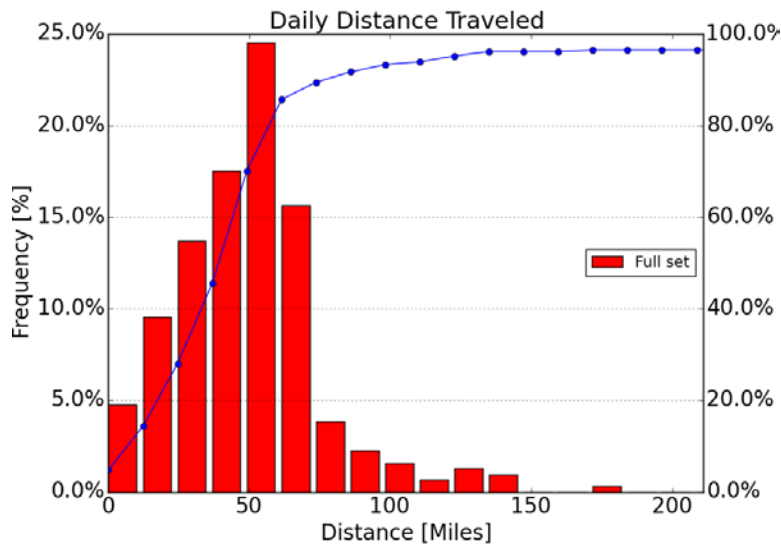


Figure III-49: School bus distance driven daily

Figure III-50 shows a histogram of the average speed driven by buses in the NVUSD and TUSD fleets. NVUSD had lower average trip speeds than TUSD, but also had more trips at higher average speeds, likely due to longer distance drives in rural areas of the district.

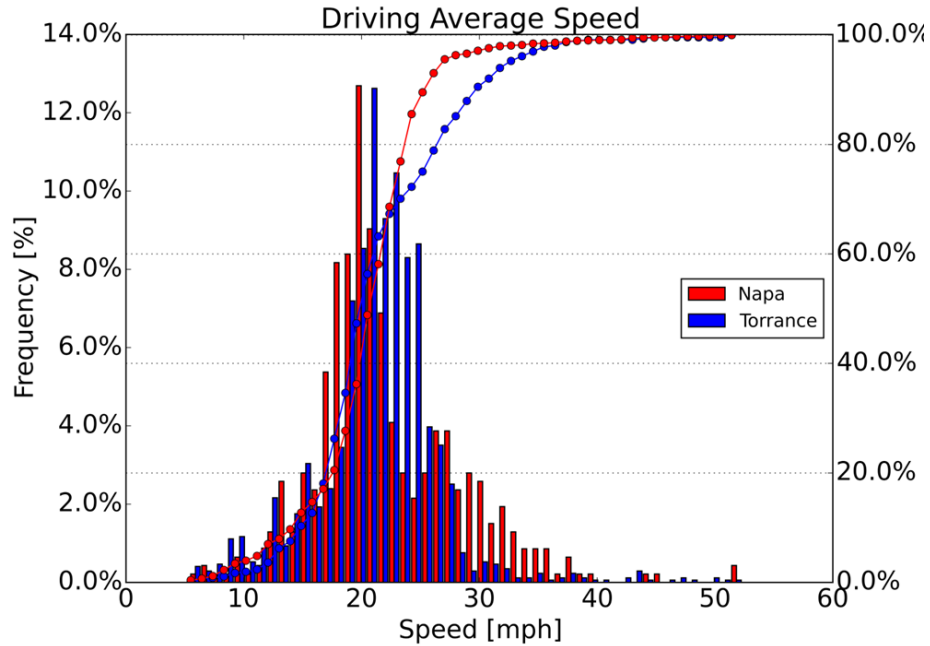


Figure III-50: School bus average speed driven

NREL evaluated the in-use drive cycle data to select three representative dynamometer test cycles that bracket the observed bus drive cycles and developed a custom NREL School Bus Cycle using the Drive-Cycle Rapid Investigation, Visualization, and Evaluation (DRIVE) tool. The chosen cycles included Orange County Transit Authority bus cycle (OCTA), Rowan University Composite School Bus Cycle (RUCSBC) and California Air Resources Board Heavy Heavy-Duty Truck (HHDDT). Figure III-51-Figure III-54 shows the speed traces of each test cycle and the NREL custom School Bus Cycle. Table III-5 lists the cycle statistics of the test cycles.

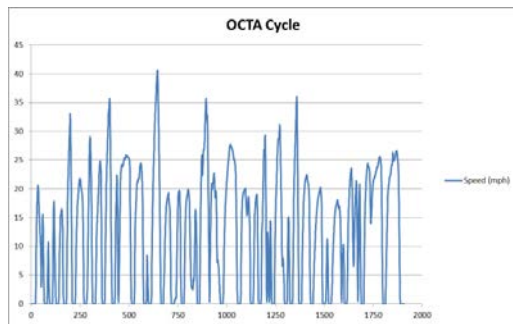


Figure III-51: OCTA Dynamometer Test Cycle

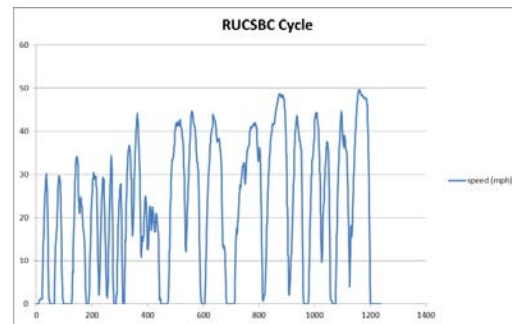


Figure III-52: RUCSBC Dynamometer Test Cycle

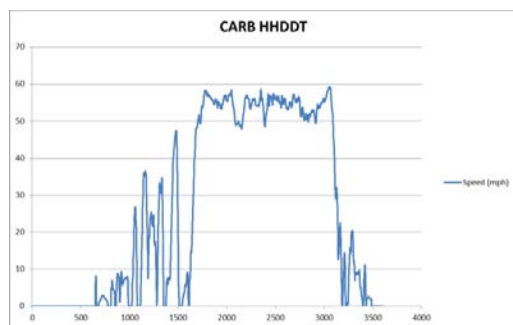


Figure III-53: CARB HHDDT Dynamometer Test Cycle

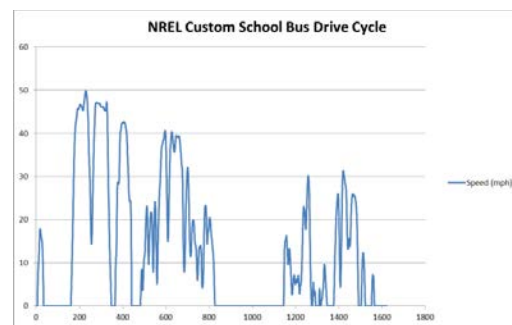


Figure III-54: NREL Custom School Bus Dynamometer Test Cycle

Table III-5: EVG2 Dynamometer Results

Test Cycle	OCTA	RUCSBC	HHDDT	NREL Custom School Bus
Max Speed (mph)	40.6	49.7	59.3	49.9
Average Speed (mph)	15.7	26.6	35.6	22.6
Stops per Mile	4.7	1.4	0.5	1.9
Kinetic Intensity (1/mile)	3.6	1.7	0.2	1.3

A TransPower school bus was delivered to NREL for planned grid integration testing at the Energy Systems Integration Facility and power train efficiency testing on the heavy-duty chassis dynamometer at the ReFUEL lab from May through August 2016. The ReFUEL testing included four warm repetitions of each of the previously discussed test cycles.

Table III-6 gives the KWH/mile energy consumption results from the dynamometer testing. Figure III-55 shows the chosen test cycles compared to NREL’s library of school bus data in Fleet DNA. Figure III-56a and Figure III-56b show the EV2G school bus on the dynamometer at the ReFUEL laboratory.

Table III-6: EV2G School Bus DC KWH/mile

Test Cycle	OCTA	RUCSBC	HHDDT	NREL Custom School Bus
Average	1.28	1.56	1.33	1.34
Standard Deviation	0.03	0.02	0.06	0.03

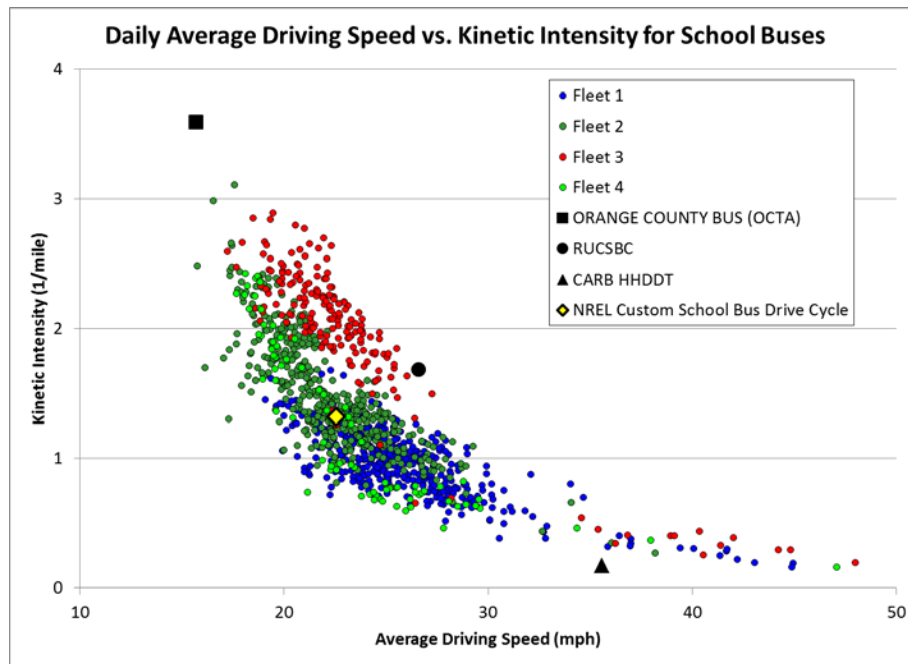


Figure III-55: Daily average driving speed vs. kinetic intensity for school buses field data and dynamometer cycles



(a)



(b)

Figure III-56: (a and b) EV2G bus at the ReFUEL laboratory

While the ESIF testing was focused on testing relative to grid integration standards (IEEE 1547) funded under a separate task, AC charge to DC discharge efficiency was tested and is of interest to this discussion. AC to DC charging efficiency was determined to be 95.6% while AC charge to DC discharge efficiency was determined to be 87.8%. This round-trip efficiency from the grid must be taken into account when calculating the energy the school district must pay for to operate the buses. Table III-7 gives the kWh/mile energy consumption results from the dynamometer testing with the 87.8% efficiency taken into account.

Table III-7: EV2G Dynamometer Results with Charging Efficiency Considered

Test Cycle	OCTA	RUCSBC	HHDDT	NREL Custom School Bus
Average	1.45	1.78	1.52	1.53



Figure III-57: EV2G bus at ESIF

Conclusions

This project is an ongoing study. The first of six EV2G school buses has only been deployed for 1 week. Field data collection of conventional school buses added to the library of data in Fleet DNA and confirmed that the design of the bus was for an adequate range to accomplish 80%–90% of observed bus days. Laboratory testing at ESIF and the ReFUEL dynamometer confirmed that the bus energy consumption and efficiency are in the design intent region to attain the expected range. Monitoring of the buses for the school year will enable those initial conclusions to be tested with more in field data.

Publications

Only initial field data have been collected to date in addition to the laboratory test results just completed; therefore, no technical publications have been produced at this time. However, the following working group meeting presentation was reported.

EV V2G School Bus Demonstration Project Baseline Vehicle Duty Cycle Data Collection; Quarterly Stakeholder Meeting, TransPower – Poway, CA Wednesday, June 24, 2015.

Odyne Hybrid Systems Plug-in Hybrid Utility Truck Field Evaluation with Duke Energy

Background and Introduction

Odyne Systems of Waukesha, Wisconsin, produces a power take-off (PTO)-based plug-in hybrid vehicle system for medium- and heavy duty vocational vehicles in the utility and maintenance sectors. The Odyne system, which interfaces with Allison 2000, 3000, and 4000 series transmissions provides both tractive power for driving as well as power for auxiliary loads such work tools and HVAC. The system interfaces through the stock transmission's PTO port, which feeds power to a double-ended electric motor shaft attached to the PTO clutch on one side and the hydraulic pump on the other. The Remy HVH250 electric motor is rated at 56 horsepower for continuous use and 95 horsepower for peak power and is also used to capture up to 40 kW of energy during regenerative braking that is transferred back into the system for improved fuel economy when traveling to a jobsite. The vehicles are configured with 28.4-kWh battery packs from Johnson Controls. Once onsite, the PTO clutch can be disengaged and the electric motor can drive the hydraulic work equipment, HVAC, and electric accessories without the need to idle the engine (Figure III-58).

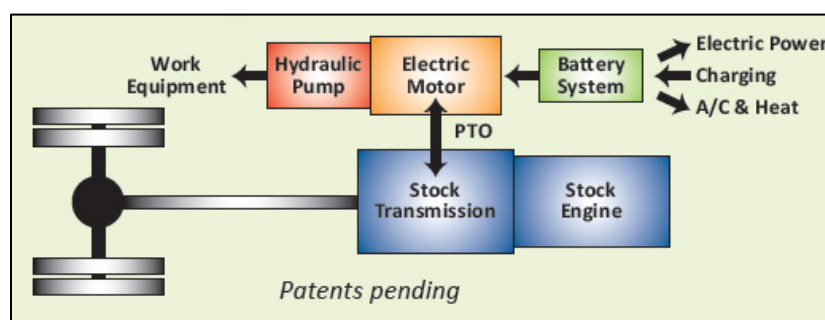


Figure III-58: Odyne parallel hybrid architecture schematic

Image: Courtesy Odyne Systems (NREL 34049)

Duke Energy, based in Charlotte, North Carolina, is the third largest electric power holding company in the United States based on kilowatt-hour sales. Its regulated utility operations serve approximately 4 million customers located in five states—North Carolina, South Carolina, Indiana, Ohio, and Kentucky—representing a population of approximately 11 million people. Duke Energy is striving to make PHEVs and EVs its only new vehicle purchases by 2020. In support of this initiative Duke Energy has partnered with Odyne Systems for its new utility truck purchases. Duke Energy currently operates PHEV fuel tanker vehicles, aerial bucket trucks, and underground utility vans in their fleet.

This project will focus on characterizing the duty cycle and operating characteristics of both conventional diesel and PHEV aerial bucket trucks and utility vans in Duke Energy's fleet. NREL researchers will evaluate on-road and off-road energy efficiency and performance of these vehicles. NREL will also perform chassis dynamometer testing of a hybrid PHEV aerial bucket truck to characterize and compare the energy efficiency over a variety of drive cycles as compared to a conventional diesel vehicle. Additionally, researchers hope to evaluate the off-cycle/stationary energy and emissions savings associated with electrification of auxiliary loads.

Approach

The technical approach for this project follows the general approach for conducting fleet evaluations described above. The specific technical approach for the Odyne Hybrid Systems–Duke Energy Case Study includes the following:

- Initial fleet identification and selection
- Technology partnership
- Initial route and in-vehicle data collection

- Follow-up route and in-vehicle data collection
- Chassis dynamometer testing
- Modeling and simulation with field validated models.

Results

Progress to Date

Technology Partnership

Odyne Hybrid Systems has agreed to support this research project by providing technical information into the operation of its hybrid system as well as access to test vehicles for chassis dynamometer testing.

Initial Fleet Identification and Selection

With the support of representatives from Odyne Hybrid Systems, NREL met with Duke Energy's director of fleet operations and was able to establish the project framework for this research project. Duke Energy is interested in this research to better quantify the fuel savings it has seen with the Odyne Hybrid System, to more objectively evaluate the performance of its newest vehicles, and to promote fuel savings technology in the utility vehicle vocation.

Duke Energy, a member of the Edison Electric Institute Utility Fleet Working Group, is headquartered in Charlotte, North Carolina and distributes power to over 7 million customers with a service territory of over 100,000 miles (Figure III-59). As of October 2015, Duke Energy was operating 57 plug-in electric vehicles including 13 Odyne Hybrid utility trucks.

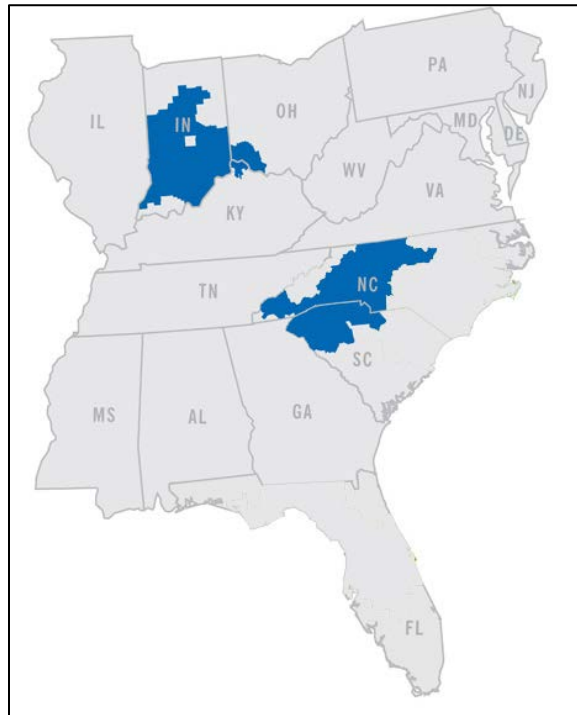


Figure III-59: Duke Energy service territory

(Image: <https://www.duke-energy.com/rates/DE-service-territory.asp>)

NREL researchers plan to instrument aerial utility vehicles similar to the vehicle in Figure III-60, at multiple locations in North Carolina and South Carolina in the first and second quarters of FY17. These will be a combination of Odyne hybrid vehicles and conventional diesels. Unlike other fleet evaluations with a central terminal, these vehicles are spread out across the Duke Energy service area so they can quickly respond to reported outages or repairs. Following the data collection and preliminary analysis of the aerial utility vehicles,

NREL researchers will collect in-use data on underground utility vehicles operating in Duke Energy's fleet. These underground utility vehicles will be a combination of Odyne hybrid vehicles and conventional diesels. The latest order of Odyne underground utility vehicles is expected to be put into service by Duke Energy starting in the first quarter of FY17.



Figure III-60: Odyne Hybrid Systems aerial bucket truck

Image: Courtesy Odyne Systems (NREL 34043)



Figure III-61: Odyne Hybrid Systems underground utility vehicle

Image: Courtesy Odyne Systems (NREL 34042)

Conclusions

This project is just beginning in FY 2016.

Presentations/Publications/Outreach

None produced to date.

BYD Battery Electric Transit Bus with WAVE Wireless Charging Field Evaluation with Long Beach Transit

Background and Introduction

In the third quarter of 2016, Long Beach Transit placed an order for ten 40-ft BEBs from BYD Motors (Figure III-62), the U.S. subsidiary of BYD Auto Co., a Chinese automobile manufacturer. These 10 fully electric buses are expected to be in full revenue service by the end of the first quarter of 2017. This project will focus on comparing the in-use performance and efficiency of the 40-ft BEBs to conventional CNG vehicles currently operating in Long Beach Transit's fleet, in partnership with work being funded by the Federal Transit Agency, reliability, maintenance, and operating costs will be evaluated and compared to the conventional CNG vehicles. This project will also focus on characterizing the in-use performance and efficiency of the WAVE wireless charging system, which is expected to be installed at the Long Beach Convention Center in FY17.

Results

A project kick-off meeting was held in Long Beach, California, in late August 2016, with representatives from NREL, BYD, Federal Transit Agency, and Long Beach Transit. Representative from Long Beach Transit provided updates on the procurement of the 10 BEBs and the associated charging infrastructure required at its facilities to support the buses. During this kick-off meeting, conventional CNG vehicles were identified and a preliminary timing plan for FY17 data collection was proposed. It was determined that data from the 10 BEBs will be collected using BYD's onboard instrumentation and telematics, and data will be collected from the conventional CNGs by NREL.



Figure III-62: BYD 40-ft BEB at Long Beach Transit

Image: Robert Prohaska/NREL

Conclusions

A project kick-off meeting was held in August 2016; therefore, no significant technical results or conclusions are available for FY 2016.

Clean Cities Partnership Zion National Park Shuttle Bus Electrification

Background and Introduction

With support from Clean Cities, NRELs Field Test and Evaluation Team evaluated the drive-cycle characteristics of a fleet of propane-powered shuttle buses operating at Zion National Park. The National Park Service (NPS) originally deployed the propane buses (see Figure III-63) in 2000 to reduce congestion along the park's main traffic corridor. As the propane-powered fleet ages and associated maintenance costs rise, NPS is working with NREL to use this drive-cycle information to optimize the conversion of 14 of its propane buses to run on electricity. Leveraging existing tools and capabilities, NREL supplied the NPS with data and information to be used in their upcoming request for proposal solicitation.



Figure III-63: Zion NPS propane-powered bus connected to a non-powered passenger trailer

Photo by Robert Prohaska/NREL

Results

Researchers collected data from nine buses operating in the park over a multi-month period that spanned the spring and summer seasons. CAN bus operational data from the propane buses were collected via onboard data loggers to understand dispatching patterns, evaluate the effect of road grade on system requirements, and determine optimal power and energy storage requirements based on the fleet's unique operation. Using Global Navigation Satellite System (GLONASS)-enabled global positioning system units, researchers were able to characterize the route's road grade despite the tall and narrow canyon walls that typically interfere with global positioning system signals as seen in Figure III-64.

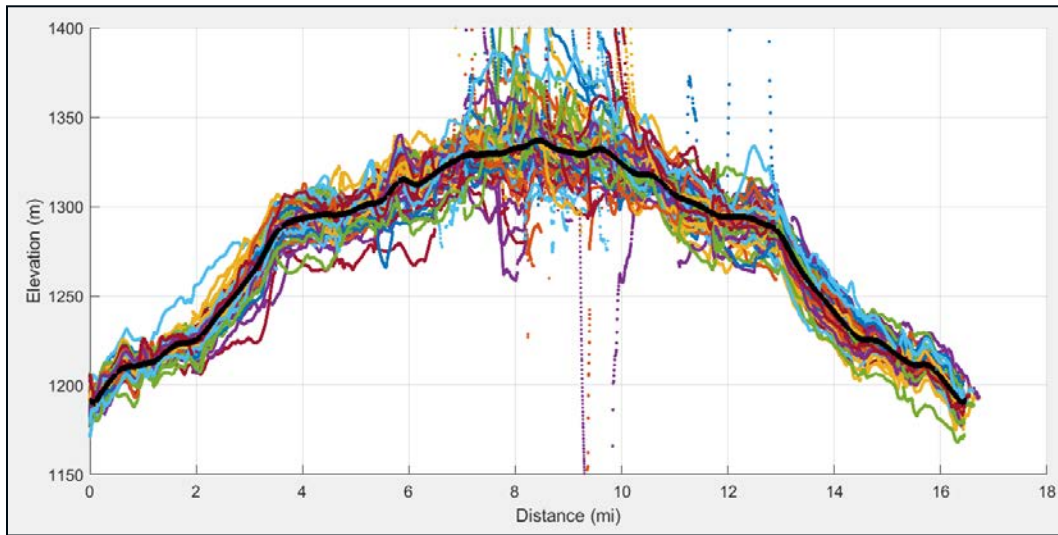


Figure III-64: Median fit road grade profile from GLONASS-enabled global positioning system over 63 trips.

Image: Adam Ragatz/NREL

Table III-8: Spring schedule high-level summary statistics from propane powered buses.

Metric	Average Daily Value	Standard Deviation
Distance (miles)	124.82	42.73
Work (kWh)	276.12	92.68
Average Speed (mph)	10.25	1.74
Average Driving Speed (mph)	16.80	0.62
Maximum Speed (mph)	31.15	1.96
Kinetic Intensity (1/mi)	1.31	0.08
Average Bulk Fueling MPG*	3.019	0.184

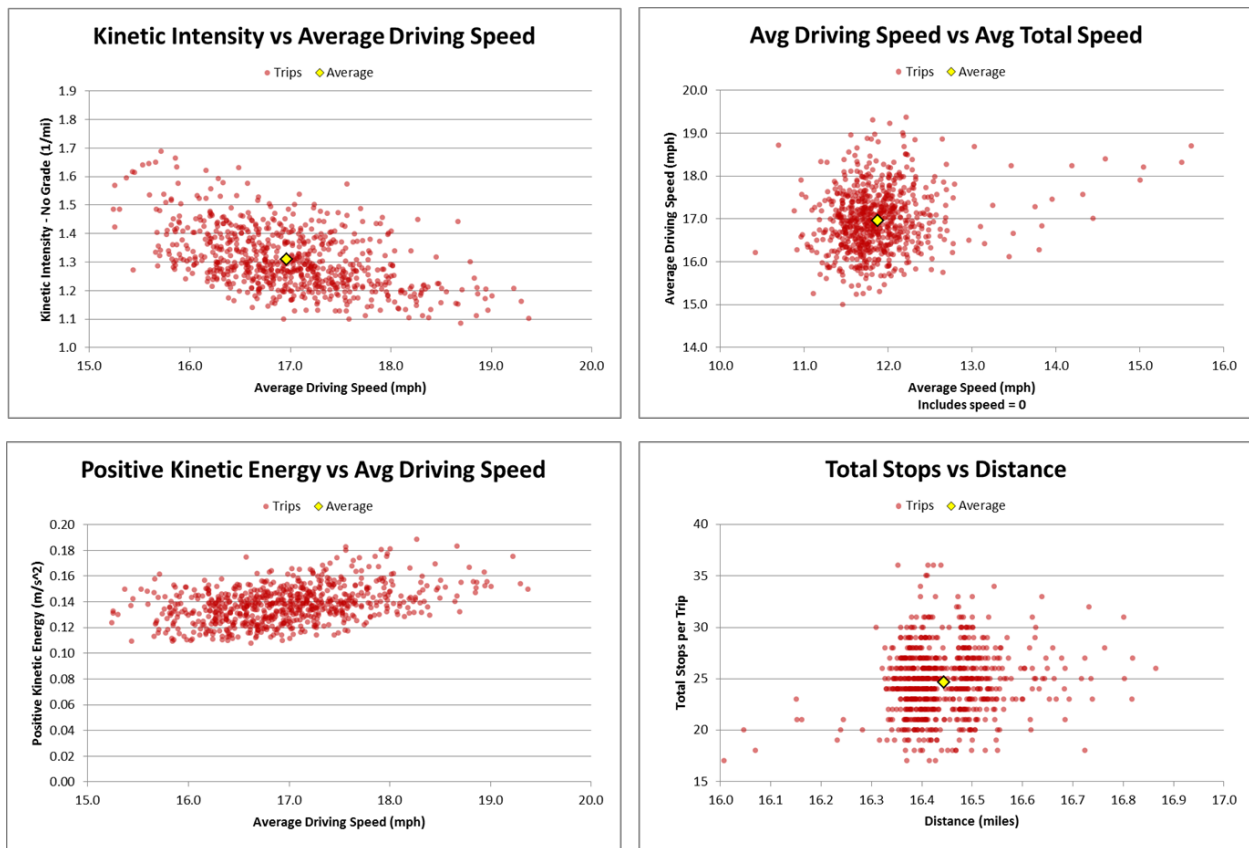


Figure III-65: Multiple scatter plots demonstrating the highly repetitive driving behavior of the propane-powered buses
 (Image: Robert Prohaska/NREL)

Conclusions

As this was primarily a data gathering and sharing activity, there are no formal conclusions to present at this time. The NPS has included in its request for proposal NREL's raw and processed data as well as recommendations from lessons learned on prior fleet deployments.

Presentations/Publications/Outreach

1. NREL Evaluates Propane-to-Electricity Shuttle Bus Conversion at Zion National Park. (<http://www.nrel.gov/transportation/news/2016/33707.html>)
2. NREL Evaluates Replacing Propane Shuttle Buses at Zion National Park with EVs. Charged Electric Vehicles Magazine. July 29, 2016. (<https://chargedevs.com/newswire/nrel-evaluates-replacing-propane-shuttle-buses-at-zion-national-park-with-evs/>)
3. NREL Evaluates Propane-to-Electricity Shuttle Conversion at Zion Park. July 19, 2016 (<http://ngtnews.com/nrel-evaluates-propane-to-electricity-shuttle-conversion-at-zion-national-park/>)
4. NREL Supports Propane-to-Electricity Shuttle Bus Conversion at Zion National Park. July 18, 2016 (<http://www.greencarcongress.com/2016/07/20160718-nrel.html>)

Battery Ownership Model Medium-Duty HEV Battery Leasing & Standardization

Background and Introduction

In the summer of 2014, principals at Eaton discussed with DOE’s Vehicle Technologies Office that standardization and leasing batteries could make the medium-duty HEVs more cost attractive and perhaps revive the U.S. market. The Vehicle Technologies Office provided guidance to NREL to focus its Battery Ownership subtask to investigate the economics of leasing standardized battery packs for medium-duty HEVs. Preliminary analysis was performed, and researchers consulted with industry representatives to collect necessary information for assessing the merit of leasing standardized batteries for medium-duty HEVs.

Results

Researchers found that the economics of leasing may be better than owning batteries but would depend on how much standardization could reduce the incremental cost of HEVs compared to conventional diesel vehicles. Battery standardization strategies were then investigated to identify how they could impact the total cost of ownership based on a representative drive cycle and assumed usage criteria. Figure III-66 shows an example of the system architecture modeling that became the foundation for sizing components for all total cost of ownership calculations.

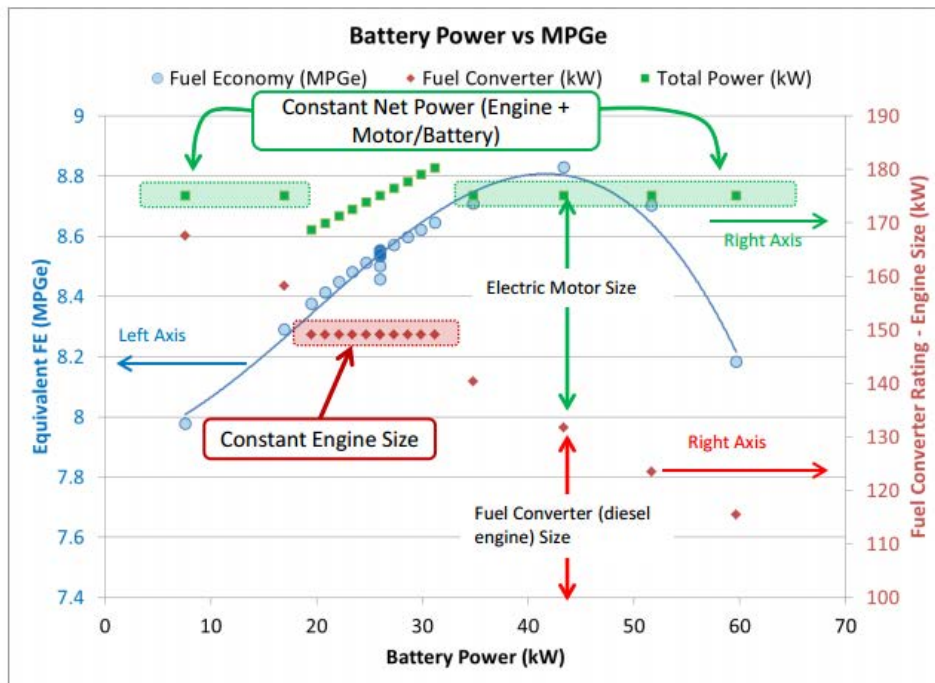


Figure III-66: FASTSim vehicle simulator results showing impact of different component sizes.

Image: Robert Prohaska/NREL

The primary focus of the work in this report was to further quantify cost benefits of standardized batteries for medium-duty HEVs.

Key Findings:

- Incremental costs of hybrid electric drive systems vary by manufacturer and vehicle type and range from \$12,000 to \$35,000 for Class 5 delivery vehicles relative to a conventional medium-duty vehicle.
- U.S. new vehicle registrations of Class 4-6 HEV step vans are projected to be less than half of all U.S. step van new vehicle registrations through 2020 and are expected to range from 1,000 – 4,000 per year.

- At 1,000 batteries/year, there is no value to standardization.
- At 5,000 batteries/year, there is only a 2% value to standardization (communications interface).
- At 10,000 batteries/year, there is a 7% cost benefit with standardization. Standardizing module housing and bus bars are most beneficial.
- At 50,000 and 100,000 batteries/year, there is a 13% to 16% cost benefit to standardization.
- Leasing looks better than direct ownership over a short (3-year) time horizon.
 - Leasing shifts expenses from capital to operating expenses, which is favorable in the short term, but always increases the total cost of ownership over the long term.
 - Leasing may be attractive to some fleet operators with constraints on capital expenses for purchasing new vehicles.
- The strongest factors affecting the total cost of ownership and payback period are:
 - Fuel prices
 - Annual mileage driven
 - Incremental cost of HEV
 - Incremental fuel savings benefit of HEV.
- There is a steep decrease in per-battery price for volumes between 1,000 and 10,000 per year (50% reduction).
- The potential Class 5 medium-duty HEV market is not large enough to reach the benefit of 10,000 batteries/year.
- Greater value may be obtained by applying strategies across a wider range of products such as other medium-duty vehicle platforms, full electric vehicles, and light-duty HEVs.

Drawing on the experience of Ricardo experts that have done a battery standardization study for the California Energy Commission, interim results of the joint effort by Ricardo and NREL were shared with DOE and Eaton via a web meeting on December 23, 2015. Subsequent to the web meeting, the additional total cost of ownership analysis was added for this final milestone report.

This work was performed by the members of Energy Storage and the Vehicle Simulation Teams in the Transportation and Hydrogen Systems Center and members of Vehicles Analysis Team in Ricardo Inc.

Presentations/Publications/Outreach

1. K. Kelly, K. Smith, Jon Cosgrove, R. Prohaska, A. Pesaran, J. Paul and M. Wiseman. Battery Ownership Model Medium Duty HEV Battery Leasing & Standardization. NREL/MP-5400-66140. (<http://www.nrel.gov/docs/fy16osti/66140.pdf>)

Medium- and Heavy-Duty Vehicle Duty Cycles for Electric Powertrains

Background and Introduction

NREL's Fleet Test and Evaluation Team has extensive in-use vehicle data demonstrating the importance of understanding the vocational duty cycle for appropriate sizing of EV and power electronics components for medium- and heavy-duty EV applications. This presentation at the 2016 Applied Power Electronics Conference in Long Beach, California, included an overview of recent EV fleet evaluation projects that have valuable in-use data that can be leveraged for sub-system research, analysis, and validation. Peak power and power distribution data from in-field EVs were presented for four different vocations, including Class 3 delivery vans, Class 6 delivery trucks, Class 8 transit buses and Class 8 port drayage trucks, demonstrating the impacts of duty cycle on performance requirements.

Results

Understanding the vocational duty cycle is critical for appropriate sizing of EV components for medium-duty and heavy-duty plug-in EV applications. NREL has extensive in-use data for these types of vehicles.

NREL field data show the ratio between peak power and continuous power requirements varies by vocation (motor specs). Battery electric transit bus data results are shown in Figure III-67 and Figure III-68 for reference.

- Transit Bus ~ 160 kW / 60 kW (2.7) | 220 kW / 120 kW (1.8)
- Delivery Van ~ 70 kW / 55 kW (4.0) | 70 kW / 55 kW (1.3)
- Delivery Truck ~ 90 kW / 40 kW (2.3) | 150 kW / 80 kW (1.9)
- Class 8 Drayage Tractor ~ 300 kW / 90 kW (3.3) | 300 kW / 240 kW (1.25)

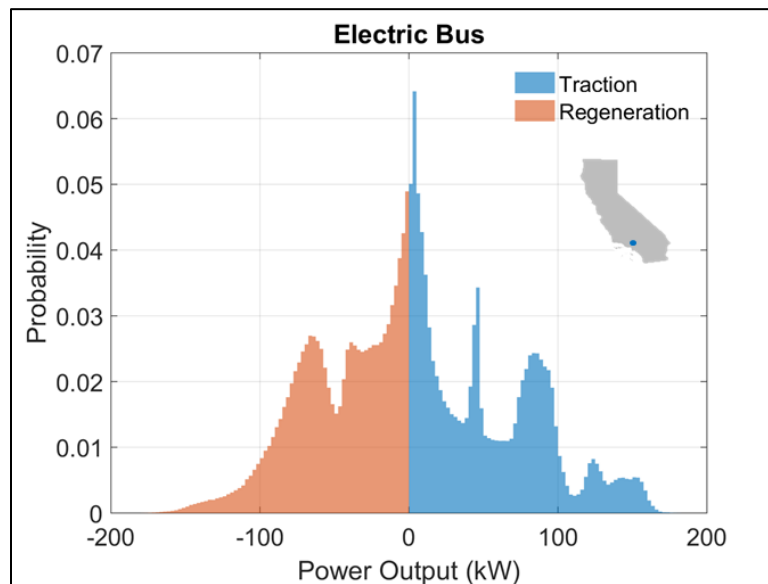


Figure III-67: Probability distribution of traction and regeneration power output from electric transit buses

Image: Eric Miller/NREL

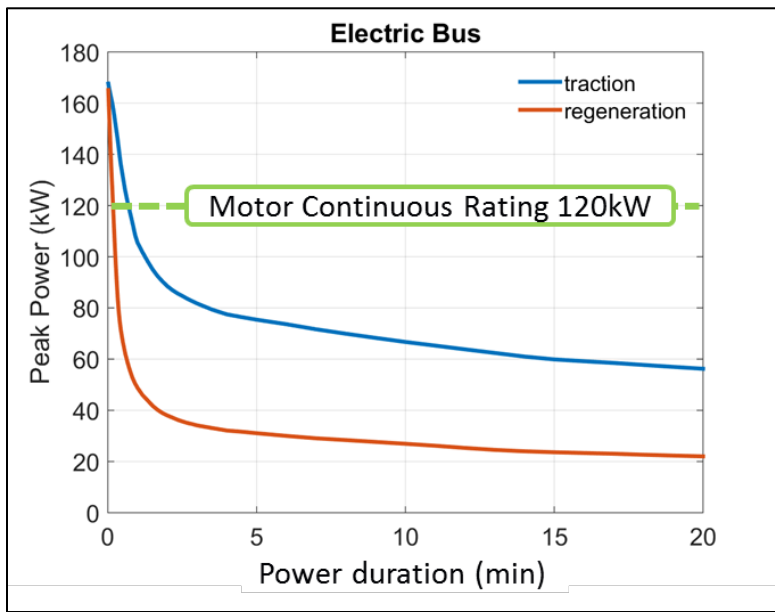


Figure III-68: Peak power duration for traction and regeneration power from electric transit buses
 (Image: Eric Miller/NREL)

Power electronics must be designed to handle power and heat requirements for both traction and regenerative power.

Presentations/Publications/Outreach

1. K. Kelly, K. Bennion, E. Miller, and R. Prohaska. "Medium- and Heavy-Duty Vehicle Duty Cycles for Electric Powertrains." Applied Power Electronics Conference. Long Beach, CA. March 2016. NREL/PR-5400-66228. (<http://www.nrel.gov/docs/fy16osti/66228.pdf>)

NREL's Drive Cycle Analysis Tool (DriveCAT) Web Application

Background and Introduction

NREL's Fleet Test and Evaluation Team has extensive in-use vehicle data demonstrating the importance of understanding the vocational duty cycle when selecting advanced mobility technologies. As part of the research and development process of refining advanced technology system architecture, researchers and developers are often looking for statistically representative drive cycles for modeling, simulation, and dynamometer validation. NREL has years of experience distilling large amounts of in-use duty cycle data into representative drive cycles using the Drive-Cycle Rapid Investigation, Visualization, and Evaluation (DRIVE) tool. Until the creation of NREL's Drive Cycle Analysis Tool (DriveCAT), there has not been easy open source access to both NREL's custom-generated drive cycles and the standard test cycles. Having a consolidated common access website hosting NREL's representative cycles in addition to regulation-focused cycles from agencies such as the California Air Resources Board and EPA give researchers the ability to compare and contrast drive cycles while being able to quickly and easily select the most appropriate drive cycle for their application.

Results

An initial DriveCAT mock-up was created and approved by NREL communications staff for full development. The first version of the website features 19 drive cycles available for download as well as a select number of drive cycle statistics that will help researchers in selecting the appropriate drive cycle for their research. The 19 cycles are a mixture of NREL custom generated cycles as well as more commonly used drive cycles from California Air Resources Board and EPA. A screen shot from the initial website is shown in Figure III-69. Initial feedback from industry partners has been very positive as no single, open source easy-to-use site like this previously existed.

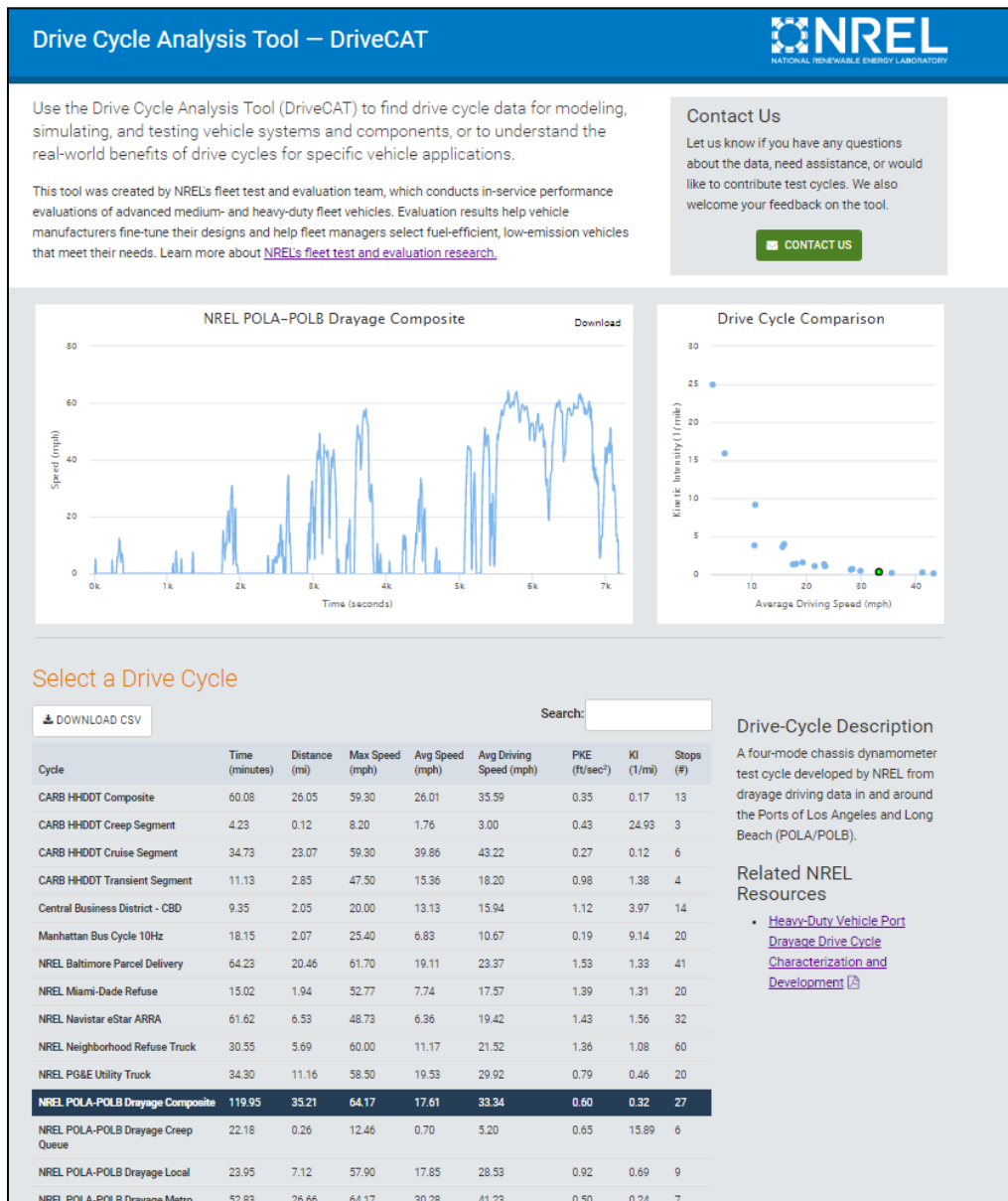


Figure III-69: Screen shot from NREL's DriveCAT website
Image: Robert Prohaska/NREL

Presentations/Publications/Outreach

1. K. Kelly, R. Prohaska, A. Ragatz, and A. Konan. (2016). NREL DriveCAT - Chassis Dynamometer Test Cycles. National Renewable Energy Laboratory. www.nrel.gov/transportation/drive-cycle-tool

III.3. Zero Emissions Cargo Transport Data Collection and Analysis

Kenneth Kelly and Bob Prohaska

National Renewable Energy Laboratory
15013 Denver West Parkway, MS 1633
Golden, CO 80401
Phone: (303) 275-4465
E-mail: Kenneth.Kelly@nrel.gov

David Anderson and Lee Slezak

Phone: (202) 287-5688 (David Anderson)
E-mail: David.Anderson@ee.doe.gov
Phone: (202) 586-2335 (Lee Slezak)
E-mail: Lee.Slezak@ee.doe.gov

Start Date: Ongoing

End Date: Ongoing

III.3.A. Abstract

Objectives

The primary objective for this project is to reduce criteria pollutants in the South Coast Air Basin by reducing diesel emissions from the transportation and movement of goods from the ports to intermodal and warehousing facilities throughout Southern California. The project is being led by the South Coast Air Quality Management District (SCAQMD) in conjunction with several fuel cell and hybrid electric vehicle powertrain providers, and the National Renewable Energy Laboratory (NREL). The overall technical objective is to accelerate the introduction and penetration of heavy-duty fuel cell and hybrid electric vehicles into the cargo transport sector which will help us achieve the primary objective to substantially reduce criteria pollutants and as a side benefit reduce petroleum consumption and greenhouse gases. NREL's role in the project is to collect in-use data, serve as the central data repository, and perform analysis of the vehicle performance and cost of operation over the vehicle demonstration phase. The majority of this effort will take place during the last year of the 3-year effort in the demonstration phase. In this first year, however, NREL coordinated with SCAQMD and several fleet operators at the Port of Long Beach collect a substantial set of baseline in-use vehicle data and developed representative duty cycles that will be provided to the technology developers.

Accomplishments

- Provided detailed data collection protocols for baseline, hybrid electric, and fuel cell vehicles.
- Collected baseline data from 30 heavy-duty drayage diesel tractors from over 550 days and 36-thousand miles of operation.
- Developed a re-usable methodology for statistically determining duty cycle driving modes based on k-medoid clustering analysis.
- Completed analysis of baseline duty cycles and developed several drive cycles representing various modes of operation including: creep, port/near-dock, local driving, highway driving.
- Published SAE technical paper: "Heavy Duty Vehicle Port Drayage Drive Cycle Characterization and Development" to be presented at the SAE Commercial Vehicles Engineering Congress – Oct 2016.

Future Achievements

- Coordinate with each of the technology providers to established data collection processes
- Capture sample data from each provider as the vehicles are initially deployed
- Conduct analysis of vehicle performance and cost of operation
- Provide interim results to SCAQMD and each technology provider
- Publish final report on performance and cost of operation of each technology upon the completion of the demonstration



III.3.B. Technical Discussion

Heavy-Duty Vehicle Port Drayage Drive Cycle Characterization and Development

Background and Introduction

In an effort to better understand the operational requirements of port drayage vehicles and their potential for adoption of advanced technologies, National Renewable Energy Laboratory (NREL) researchers collected over 36,000 miles of in-use duty cycle data from 30 Class 8 drayage trucks operating at the Port of Long Beach and Port of Los Angeles in Southern California. These data include 1-Hz global positioning system location and SAE J1939 high-speed controller area network information.

Results

Initial analysis was focused on characterizing the different operating modes of drayage operation based on the geography of where trips originated and ended. Researchers hypothesized that the vehicle trip kinematics were highly correlated to the geographic attributes of trip. Four distinct regions and an “other region” (Figure III-70) were created to represent the primary locations of drayage trips. All of the trips were then categorized based on the geographic location of their start and stop location into one of the 25 possible groups and a geospatial analysis was run on all of the trip data.

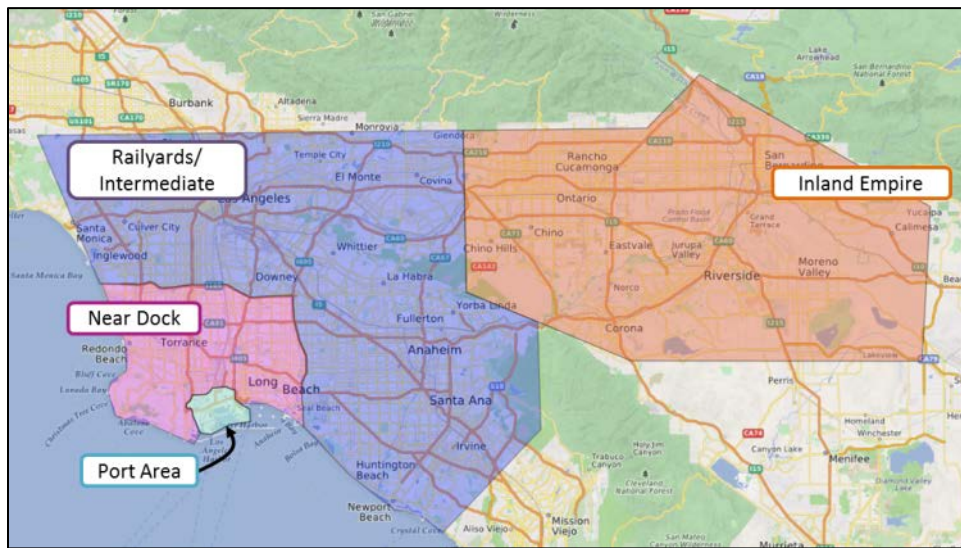


Figure III-70: Geographic regions for trip-level origin and destination analysis.

(Image: Robert Prohaska/NREL)

This trip-level geospatial origin and destination analysis indicated that of the possible 25 combinations of start and end locations, 74% of the mileage, 75% of the fuel and 83% of operating time could be accounted for in just six of the combinations as follows:

- From: Port Area | To: Port Area
- From: Near Dock | To: Near Dock
- From: Port Area | To: Near Dock
- From: Near Dock | To: Port Area
- From: Near Dock | To: Inland Empire
- From: Inland Empire | To: Near Dock

However, further trip-level drive cycle analysis of the origin and destination method indicated that while the vehicles may start and stop their trips in the same region, the trip activity could vary widely with trip maximum speed and average driving speed as shown in Figure III-71.

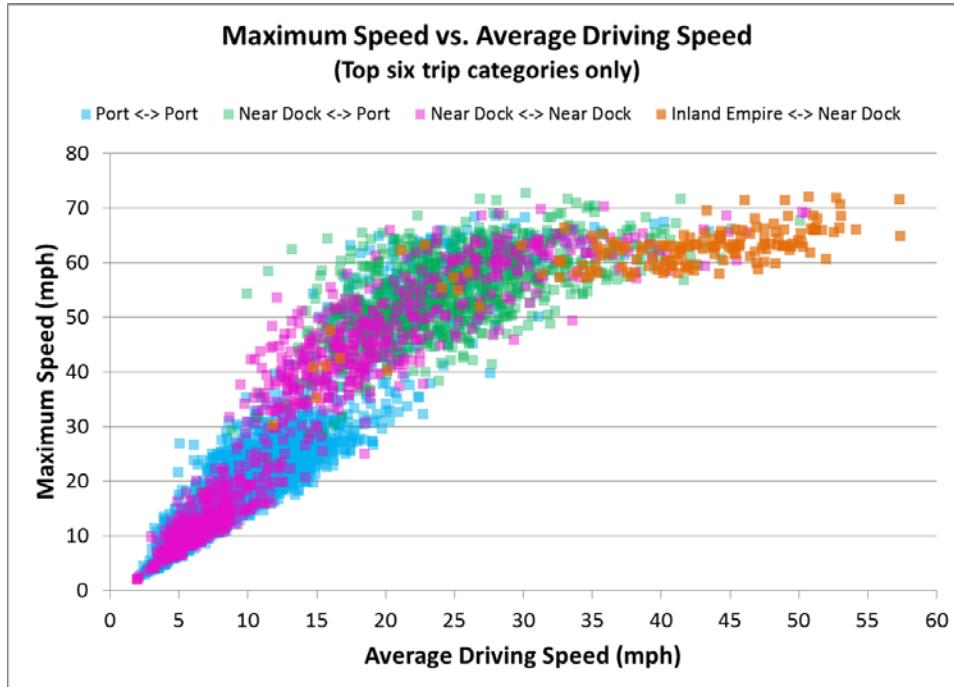


Figure III-71: Trip results from the top categories identified in the origin and destination analysis

(Image: Robert Prohaska/NREL)

Using the same trip-level data, a clustering analysis was performed to organize the data into functional groupings that would better describe the different drive cycle components. Clustering is the process of placing statistically similar data in the same cluster and dissimilar data in different clusters. The first step in the clustering analysis was to identify the optimal number of clusters in the data set to describe the data, using the mean shift method of cluster selection. It was determined that there are four clusters in the data set. The mean shift method uses a non-parametric iterative algorithm to identify the optimal number of clusters by creating a temporary window around data points, calculating the mean value of those surrounded data points, and then shifting the window location to the new mean and iterating until it converges on the mean of the cluster. A k-medoids clustering analysis was then performed using the partitioning-around-medoids method. The k-medoids algorithm is a non-hierarchical clustering algorithm related to the k-means algorithm. Both the k-means and k-medoids algorithms are partitional and attempt to minimize the distance between points in a cluster and a point designated as the center of that cluster. K-medoids was selected over the more commonly used k-means, as it is based on the most centrally located data point in each cluster, the medoid, rather than the most centrally located average value of all the points in the cluster; because of this, k-medoids is also less sensitive to outliers

Using the k-medoid clustering results one can see that each of the four clusters have minimal overlap with neighboring clusters and all data within a cluster are similar. When compared to the region and destination method shown in Figure III-71, the k-medoid clustering approach offers a much better method for partitioning the kinematic data for drive cycle analysis, as shown in Figure III-72.

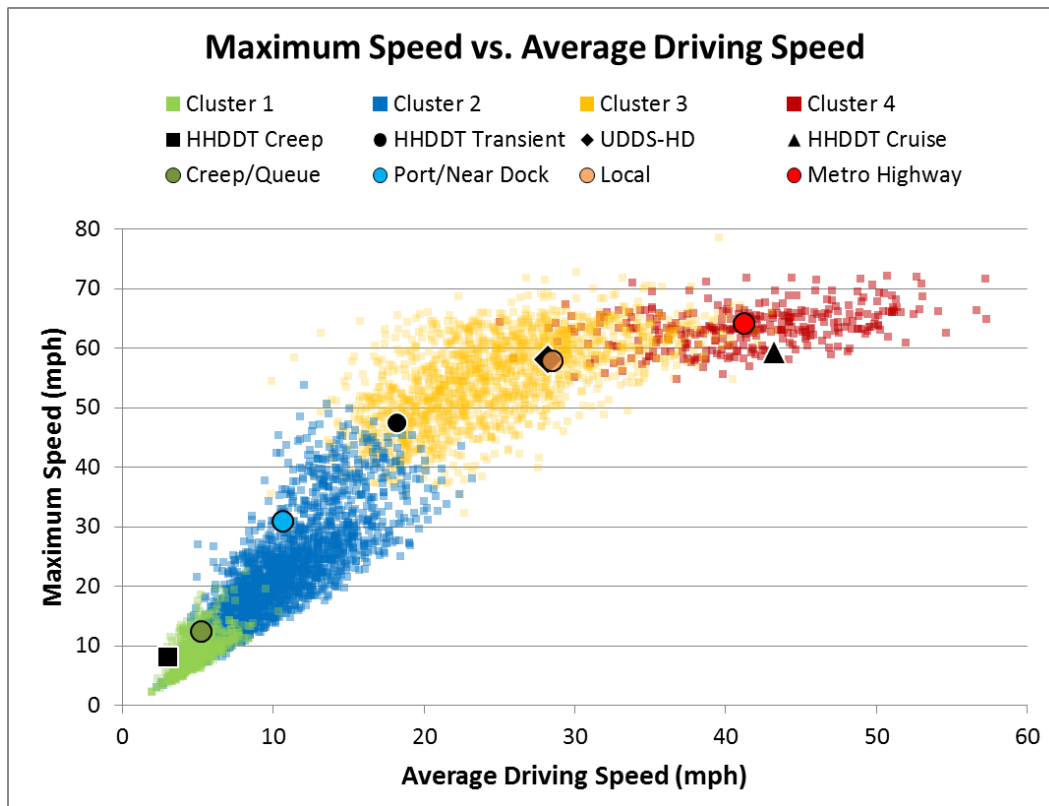


Figure III-72: Trip level maximum speed vs. average driving speed

(Image: Robert Prohaska/NREL)

Looking at the distribution of the clustered data as a function of characteristic acceleration and aerodynamic speed (Figure III-73), the principal components of kinetic intensity, one can see that the clusters still exhibit distinct separation from one another and that Cluster 1 has on average the highest level of kinetic intensity and Cluster 4 has the lowest. A high kinetic intensity ratio represents driving with more energy used for accelerations (higher characteristic acceleration) while a low kinetic intensity value is indicative of driving at more constant speeds (higher aerodynamic speeds).

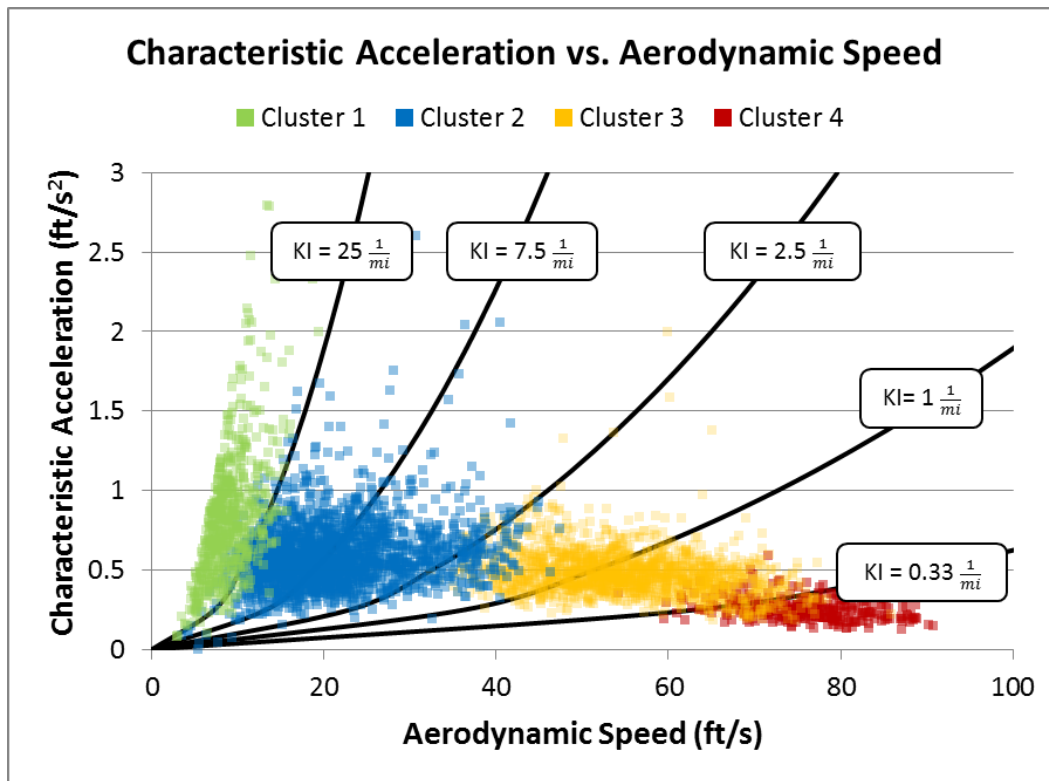


Figure III-73: Constant kinetic intensity curves shown with characteristic acceleration and aerodynamic speed
(Image: Robert Prohaska/NREL)

Having partitioned the data into four distinct clusters based on a multivariate drive cycle clustering analysis, NREL researchers used the drive cycle generation portion of DRIVE to generate representative drive cycles. DRIVE uses a deterministic multivariate hierarchical clustering method to generate representative drive cycles from the source data of each cluster. The custom cycle developed for Cluster 1 is the shortest, lowest speed cycle and has the highest kinetic intensity. This cycle is most similar to the Heavy-Heavy Duty Diesel Truck (HHDDT) Creep standard cycle and represents trips where vehicles would be waiting in line with short durations of driving followed by extended stationary idle time. Cluster 2's representative drive cycle includes segments of extended idle as well as medium speed driving components. This cycle is representative of trips that primarily start and end either in the Port Area or in the Near Dock area. The custom cycle for Cluster 3 is representative of local higher speed, shorter trips that start and/or end in the Port area and the Near Dock area. The representative drive cycle for Cluster 4 is the longest cycle of the four and has the highest average speed and lowest average kinetic intensity. This cycle is representative of vehicles making longer, higher speed trips on the metropolitan area highways, originating near the Ports and ending in the Inland Empire.

When considering how the four individual drive cycles together represent the real-world data collected at the POLA and POLB, all four of the cycles can be run in a sequence as shown in Figure III-74 as the NREL LA/LB Drayage Composite drive cycle. The results can then be analyzed directly or synthesized using a similar method to that in the U.S. Environmental Protection Agency's Title 40 Code of Federal Regulations §1037.510, where the results of each emissions test are weighted by the distance travelled over that specific cycle.

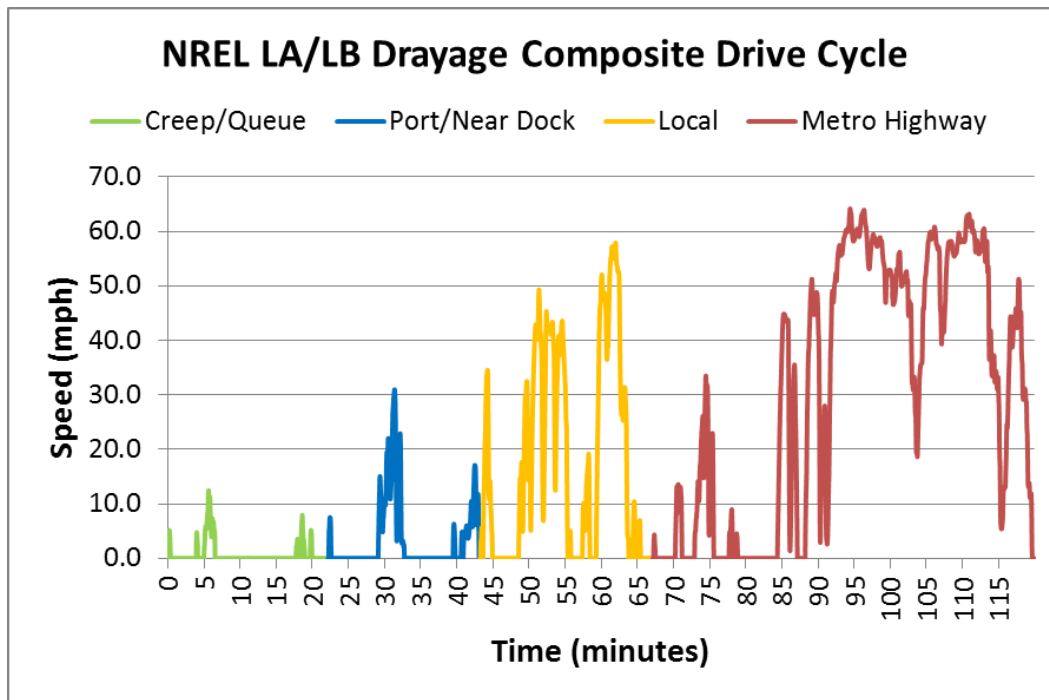


Figure III-74: Four component LA/LB drayage composite drive cycle
 (Image: Robert Prohaska/NREL)

Conclusions

NREL’s role in the project is to collect in-use data, serve as the central data repository, and perform analysis of the vehicle performance and cost of operation over the vehicle demonstration phase. The majority of this effort will take place during the last year of the 3-year effort in the demonstration phase. During this first year of the project NREL focused on gathering baseline vehicle data and developing representative drive cycles. NREL researchers collected over 36,000 miles of in-use duty cycle data from 30 Class 8 drayage trucks operating at the Port of Long Beach and Port of Los Angeles in Southern California. These data include 1-Hz global positioning system location and SAE J1939 high-speed controller area network information. NREL applied a statistical data clustering technique known as k-medoids clustering to segment the in-use baseline vehicle data into 4 operational modes including creep, port/near-dock, local driving, highway driving. An individual drive cycle was developed for each of the 4 modes along with a single composite cycle. The drive cycle analysis will be provided to the project participants for use in powertrain optimization and will be presented at SAE 2016 Commercial Vehicle Engineering Congress in October 2016.

III.3.C. Products

Presentations/Publications/Outreach

1. R. Prohaska, A. Konan, K. Kelly and M. Lammert. Heavy-Duty Vehicle Port Drayage Drive Cycle Characterization and Development. SAE 2016 Commercial Vehicle Engineering Congress NREL/CP-5400-66649 August 2016. (<http://www.nrel.gov/docx/proofs/66649.pdf>)

III.4. Analysis Process for Thermal Load Reduction Off-Cycle Credit Technologies

Cory Kreutzer, Principal Investigator

John P. Rugh, Task Leader

National Renewable Energy Laboratory (NREL)

15013 Denver West Parkway, MS 1633

Golden, CO 80401

Phone: (303) 275-4413; Fax: (303) 275-4415

E-mail: John.Rugh@nrel.gov

David Anderson, Lee Slezak, DOE Technology Managers

Vehicle Technologies Office (VTO)

Phone: (202) 287-5688, (202) 586-2335

E-mail: David.Anderson@ee.doe.gov, Lee.Slezak@ee.doe.gov

Start Date: 2016

End Date: 2016

III.4.A. Abstract

Objectives

- Develop an analysis process to determine fuel use and CO₂ emissions in the United States from the operation of vehicle air conditioning systems
- Calculate the potential reduction in fuel use and CO₂ emissions for four of the solar/thermal technologies in the 2017–2025 light-duty vehicle greenhouse gas (GHG) regulation

Accomplishments

- Developed thermal models for three light-duty vehicle types: compact, mid-size sedan, and sport utility vehicle (SUV)
- Used U.S. Department of Transportation (U.S. DOT) National Household Travel Survey (NHTS) data to characterize time-of-day and duration-of-trips for vehicles in the United States
- Used an NREL-developed methodology to assign national vehicle registration weighting to typical meteorological year (TMY) weather locations, followed by down-selection to 206 U.S. locations

Future Achievements

- Simulate vehicle air conditioning (A/C) operation in three U.S. weather locations: hot – Phoenix, Arizona, moderate – Golden, Colorado, and cold – Minneapolis, Minnesota
- Calculate evaporator thermal loads and use an air conditioning (A/C) model to determine the accessory load on the engine
- Use vehicle simulations and real-world drive cycles to calculate the annual fuel use and CO₂ emissions due to A/C operation for the baseline vehicles in three cities
- Complete the national-level analysis using all 206 locations and apply weighting factors to calculate aggregate national estimations for solar/thermal A/C fuel use and CO₂ emissions



III.4.B. Technical Discussion

Background

In the 2017–2025 Light-Duty Vehicle Greenhouse Gas Emission Standards and Corporate Average Fuel Economy Standards (CAFE), menu-based off-cycle credits are available for solar/thermal control technologies because their impacts are not measured on the standard fuel economy drive cycles. The credits provide incentive for automobile manufacturers to incorporate technologies that reduce real-world fuel use and emissions. The magnitudes of the credits are defined in Table III-9.

Table III-9: Solar/Thermal Control Technology Off-Cycle Credits

Thermal Control Technology	Car (g CO ₂ /mi)	Truck (g CO ₂ /mi)
Glass or Glazing	Up to 2.9	Up to 3.9
Active Seat Ventilation	1.0	1.3
Solar Reflective Paint	0.4	0.5
Passive Cabin Ventilation	1.7	2.3
Active Cabin Ventilation	2.1	2.8

Introduction

The goal of the project is to develop a process to calculate national-level fuel use from A/C operation and determine the national-level grams of CO₂ emissions per mile reduction for four of the solar/thermal control technologies identified in the off-cycle credit menu. The four solar/thermal control technologies evaluated are solar control glazing, solar reflective paint, and both passive and active ventilation. Active seat ventilation, the fifth solar/thermal technology, is known to enable a reduction in A/C loads; however, including this technology was beyond the resources of this project.

The development of the off-cycle credit technology analysis process leverages previous work from NREL's light-duty vehicle A/C fuel use methodology (1) and heavy-duty vehicle thermal load and idle reduction analysis process (2). NREL also leverages thermal and vehicle simulation analysis tools that have been developed under recent DOE VTO Vehicle Systems' projects. These tools include: CoolCalc, a rapid heating, ventilation, and cooling (HVAC) load estimation software (3); CoolSim, a MATLAB/Simulink thermal modeling framework (4); and FASTSim, a high-level advanced vehicle powertrain systems analysis tool (5).

Approach

The analysis process used for the solar/thermal off-cycle credit calculations is provided in Figure III-75. Three main components were used in the analysis modeling process, starting with a vehicle thermal model used to calculate the evaporator thermal load. Next, an A/C system model was used to convert evaporator thermal load into an engine accessory load. Finally, a vehicle performance model was used to convert the accessory load to associated fuel use and GHG emissions.

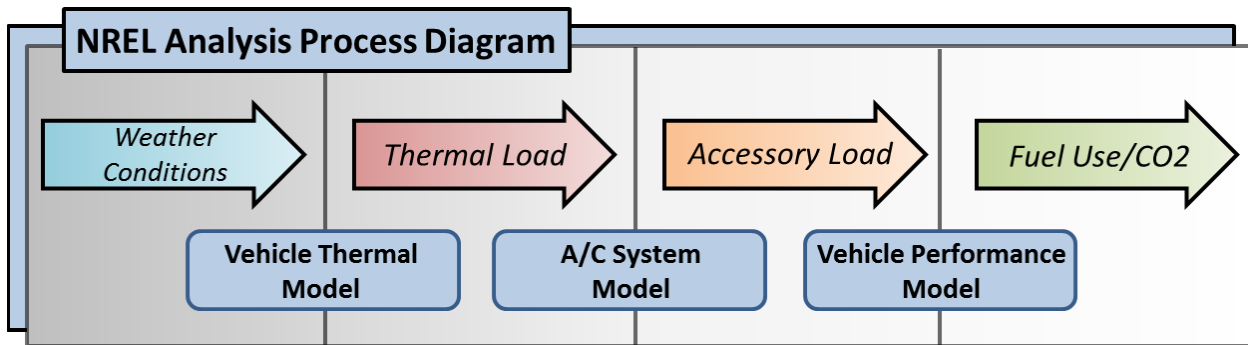


Figure III-75: Analysis process used for solar/thermal off-cycle credit calculations

Vehicle Thermal Model

Thermal models were built using CoolCalc software (3). CoolCalc is a simplified, physics-based HVAC load estimation tool that requires no meshing, has flexible geometry, and excludes unnecessary detail. The model simulates heat transfer between the vehicle and an environment defined by TMY weather data for select locations in the United States. The model calculates the cabin interior heat transfer and the evaporator capacity required to maintain the interior cabin air temperature at a user-defined set point. Prior to implementing the vehicle thermal models for the analysis, the U.S light-duty vehicle fleet was simplified into three vehicle types: compact, mid-size sedan, and SUV. Using Polk automotive registration data (6), detailed vehicle body type classifications were collapsed into three bins resulting in a compact, mid-size sedan, and SUV, with registration numbers based weightings of 18%, 30%, and 52%, respectively.

The development of the three thermal models started with geometric construction of the vehicle of interest in CoolCalc. The CoolCalc geometric rendering of the mid-size sedan is shown in Figure III-76. Next, material properties and wall constructions were defined for the solid and glazing vehicle surfaces and an HVAC system object was implemented. The three models were then validated against previous experimental thermal soak and cooldown data collected at NREL.

CoolCalc defaults to a fixed vehicle orientation relative to solar coordinates. Defining the vehicle orientation with respect to the sun presented a challenge because the orientation of a parked or moving vehicle has a significant impact on the resulting thermal load. To determine the impact of orientation on thermal loads, three cities (Golden, Phoenix, and Minneapolis) were evaluated for annual A/C thermal load with the vehicle facing the north, south, east, and west orientations. The A/C thermal loads in the east direction deviated by only -0.5% from the four-direction average (the least deviation compared to other directions) and was therefore determined to be the most representative and selected for the analysis.

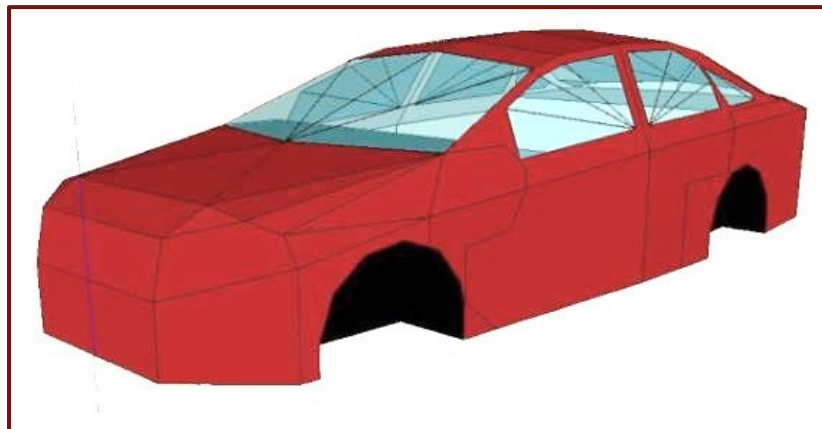


Figure III-76: CoolCalc geometric rendering of a mid-size sedan

The CoolCalc thermal models were used to calculate vehicle interior temperatures during a thermal soak and evaporator thermal load during A/C operation. The A/C control strategy was defined to maintain an equivalent interior air temperature of 72°F (22.2°C). To approximate a single, national-level recirculation strategy, a 95% vehicle cabin air recirculation percentage was used when the ambient temperature was greater than 35°C and 0% recirculation when the ambient temperature was less than 35°C. Five vehicle configurations were evaluated: the baseline configuration and the four solar/thermal control technology configurations.

Table III-10 defines the baseline and thermal control glazing properties used in the analysis.

Table III-10: Baseline and Solar Control Glazing Direct Solar Transmittance (Tds, %)

Configuration	Windshield	Tempered glazings: sedan – all and SUV in front of B Pillar	Tempered glazings: SUV behind B Pillar
Baseline (Tds, %)	41.9	45.1	16.6
Thermal Control (Tds, %)	33	33	16.6

The radiative properties of the baseline vehicle paint were calculated using PPG Industries color trend market analysis data (7) and the Lawrence Berkeley National Laboratory Pigment Database (8). The baseline average paint color had a solar-weighted absorptance of 64.1%, which included 60.9% absorptance in the near infrared spectrum (NIR). In the 2017–2025 GHG emissions regulation, the U.S. Environmental Protection Agency (EPA) defined a solar reflective paint as having less than a 35% absorptance (greater than 65% reflectance) in the NIR. To calculate the solar-weighted absorptance of the solar reflective paint configuration, the baseline ultraviolet and visible absorptances were retained and the NIR absorptance was changed to match the EPA's 35%. The resulting solar-weighted solar reflective paint absorptance was calculated to be 48.3%.

To determine the representative air infiltration rate of a vehicle in a passive ventilation configuration, the parameter was swept in a CoolCalc thermal model of a mid-size sedan. In a previously conducted passive ventilation test program conducted at NREL, an air temperature reduction of 3.5°C was measured due to lowering the door windows two centimeters during a thermal soak experiment (9). Similar temperature reductions were measured due to a passive ventilation configuration implemented in a Chevy Cobalt test program. Evaluation of the CoolCalc thermal model identified an infiltration rate of 4.8 air change per hour (ACH) during a thermal soak that resulted in a 3.5°C temperature reduction. Therefore, in the off-cycle credit technology analysis, an infiltration rate of 4.8 ACH represented passive ventilation.

Similarly, in a recent thermal load test program conducted at NREL, a just-in-time ventilation strategy was found to be effective at reducing the soak temperature in an electric vehicle (10). Using the HVAC blower to ventilate the cabin 15 minutes prior to vehicle operation, the average cabin air temperature was reduced by 7°C. Using a CoolCalc thermal model of the mid-size sedan, a 65 cfm flowrate for 15 minutes resulted in a temperature reduction similar to the experimental data. Therefore, a 65 cfm infiltration rate 15 minutes prior to the drive was used in the off-cycle credit technology analysis to represent active ventilation in the mid-size sedan. Ventilation flow rates for the compact and SUV models were subsequently scaled based on their cabin volumes in relation to the mid-size sedan.

Locations

To create a vehicle population weighting factor for weather data throughout the U.S., county vehicle registrations were assigned to the closest TMY3 weather station dataset. Due to the large number of TMY3 locations (more than 900), it was required to reduce the number of representative locations. The representative TMY3 locations were reduced by sequentially removing the location with the smallest registrations and reassigning them to the nearest remaining location. In addition, a criterion was established to retain at least one location per state. Figure III-77 shows the initial, 900+, and final 206 TMY3 locations (Alaska and Hawaii not shown).

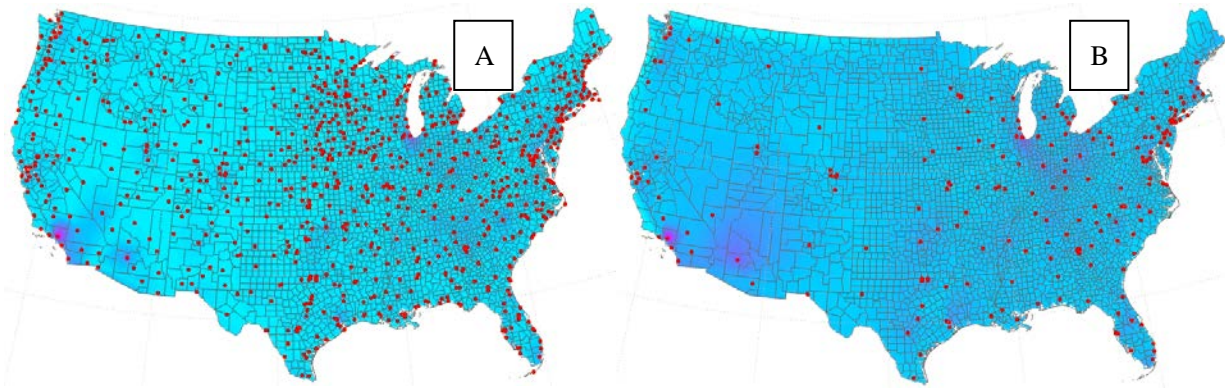


Figure III-77: Initial (A) and final (B) TMY3 locations used in the thermal model

Vehicle Usage

Time of Day

Information from the 2009 NHTS (11) was used to determine how U.S. drivers use their vehicles. The vehicle types that represent the majority of light-duty vehicles were selected: automobile/car, van, SUV, and pickup truck. Due to diurnal fluctuations in the environment, the time of day a vehicle is used strongly influences the interior temperatures at the start of the drive and also the thermal loads necessary to cool the vehicle. NHTS frequency-of-trips data were sorted into 60-minute intervals for the entire day, and time-based groupings were determined by trip start time. The distribution was represented by three groups and the average time within the group was calculated, roughly representing morning, mid-day, and evening drive events. The resulting start time and corresponding weighting factors to be applied to the results are shown in Table III-11.

Table III-11: Time of Day of Travel

Time Range	0:00–9:00	9:00–16:00	16:00–24:00
Average Time	7:06	12:35	18:26
Weighting Factor	0.183	0.476	0.341

Thermal Soak Duration

The length of time a vehicle soaks in the sun prior to a drive also influences the interior temperatures at the start of the drive and the thermal loads necessary to cool the vehicle. Using the NHTS survey time between trips data, all trips were divided evenly into two groups to represent the following vehicle thermal conditions: partially soaked and fully soaked. For the partially soaked vehicle trips, the time between trips ranged from 0 to 50 minutes with an average of 17 minutes. Table III-12 shows the soak time and weighting for the two groups.

Table III-12: Time Spent Between Trips

Time Range (min)	0–50	50–full day
Average Time (min)	17	232 (~ 4 hr)
Weighting Factor	0.50	0.50

In CoolCalc, the partial soak case was represented by a predrive that ended 17 minutes before the drive of interest. Therefore, the vehicle cabin experienced a 17-minute solar soak after the interior was cooled by the vehicle A/C prior to the target drive event. Data were unavailable for the frequency in which vehicles are parked in the shade or in buildings compared to outside, and therefore these use cases are assumed to be represented by the partially soaked case.

Trip Duration

The length of a drive is important because it partially determines how much of the drive time is in a transient cool-down mode where A/C loads are higher than for steady-state operation. For the trip duration analysis, the NHTS trip duration data were sorted into 15-minute intervals and trips greater than 30 minutes were grouped into a single bin. The average trip duration within each group was calculated along with the group weighting factor. The three resultant trip durations represent a high-frequency short drive, a medium duration drive typical of a commute, and finally a long-duration drive. Table III-13 shows the trip duration bins and weighting factors.

Table III-13: Trip Duration

Time Range (min)	0–15	15–30	30+
Average Time (min)	7.2	18.4	49.4
Weighting Factor	0.508	0.31	0.182

A/C System Model

An A/C system model of a representative MY2007 vehicle was developed using CoolSim software (4). The model converts the evaporator thermal load determined in the CoolCalc thermal model to an accessory load on the vehicle engine.

The A/C system selected for the analysis used R134a refrigerant with a belt-driven (mechanical) fixed displacement compressor with a pulley ratio of 1.37. The superheat was controlled by a thermal expansion valve. The compressor displacement was 200 cm³. The model control strategy ensured the evaporator air discharge temperature was maintained at 3°C by clutch cycling the compressor. When a low or high system pressure limit was exceeded, a clutch disengaged the compressor for duration of at least five seconds. The authors acknowledge that some vehicles employ an automatic temperature control strategy that overcools the supply air and subsequently reheats it to attain a target vent air temperature. This reheat strategy results in significant A/C operation and the implication of not considering it will underpredict A/C fuel use. Simulating reheat was beyond the scope of this analysis but could be included in future work.

A CoolSim model typically executes at real-time, which is prohibitively slow for a fully coupled annual analysis with CoolCalc. To facilitate the GHG analysis, a decoupled approach was chosen where CoolCalc independently calculated the effect of the energy-saving solar/thermal technologies on the A/C evaporator load and CoolSim computed the A/C system coefficient of performance (COP) for each of the evaporator capacity demands. Such a decoupled approach was complicated by the fact that the required evaporator capacity was dynamically affected by the drive-cycle conditions. The solution was to create a 7-dimensional (7D) A/C system COP map to post-process CoolCalc results at each timestep for each of the drive cycles. It should be noted that such an approach is based on the assumption that instantaneous A/C system COP is equivalent to those obtained from an A/C system map. To check this assumption, a separate study was done comparing dynamically obtained values of energy removed from the cabin with those computed using the mapped approach. The difference for the 18.4-minute drive cycle was found to be within 10%, which was considered an acceptable accuracy due to the prohibitive computational times for a coupled analysis. The parameters and values used for the CoolSim performance mapping process are provided below:

- Engine speed: 800, 1,400, 2,000, 2,500, 3,000 [rpm]
- Evaporator inlet temperature: 15, 32.5, 50 [°C]

- Evaporator inlet relative humidity: 20, 50, 80 [%]
- Condenser inlet temperature: 15, 30, 45 [°C]
- Condenser inlet relative humidity: 20, 50, 80 [%]
- Vehicle velocity: 0, 12, 26 [m/s]
- Evaporator capacity: 1,000; 3,000; 5,000; 8,000 [W]
- Output – compressor power, system COP.

To illustrate the premapped CoolSim results, Figure III-78a shows evaporator capacities computed by CoolSim in comparison with those requested from CoolCalc over a range of engine speeds. The remaining parameters were as follows: vehicle velocity 12 [m/s], ambient temperature 30°C, evaporator inlet air temperature 32.5°C, ambient relative humidity 50%, and evaporator air inlet humidity 50%. As can be seen in Figure III-78a, the system is not always capable of producing the requested capacity because fixed displacement compressor capacity is a function of engine speed. For example in an extreme case of low engine speed of 800 rpm, the system delivered 5kW of evaporator capacity where a potential request up to 8kW is possible. To resolve the conflict, CoolCalc’s maximum thermal load capacity was limited to 6kW, which avoids unachievable capacity demands in most cases.

Figure III-78b shows a subsurface of the 7D COP map as a function of the requested capacity and engine speed for the same set of conditions used for capacity evaluation. The results of the CoolSim simulations were also compared to the SAE Improved Mobile Air Conditioning Cooperative Research Program Life Cycle Climate Performance results (12) and were found to be in agreement. The system COP computed by CoolSim is based on compressor power. After the compressor power was calculated, an average condenser fan power of 75W was added to the vehicle model when the A/C system was in operation. Since the HVAC blower was assumed to be operating at all times when the vehicle was operated regardless of A/C operation, a 150-W load was incorporated into the base accessory load.

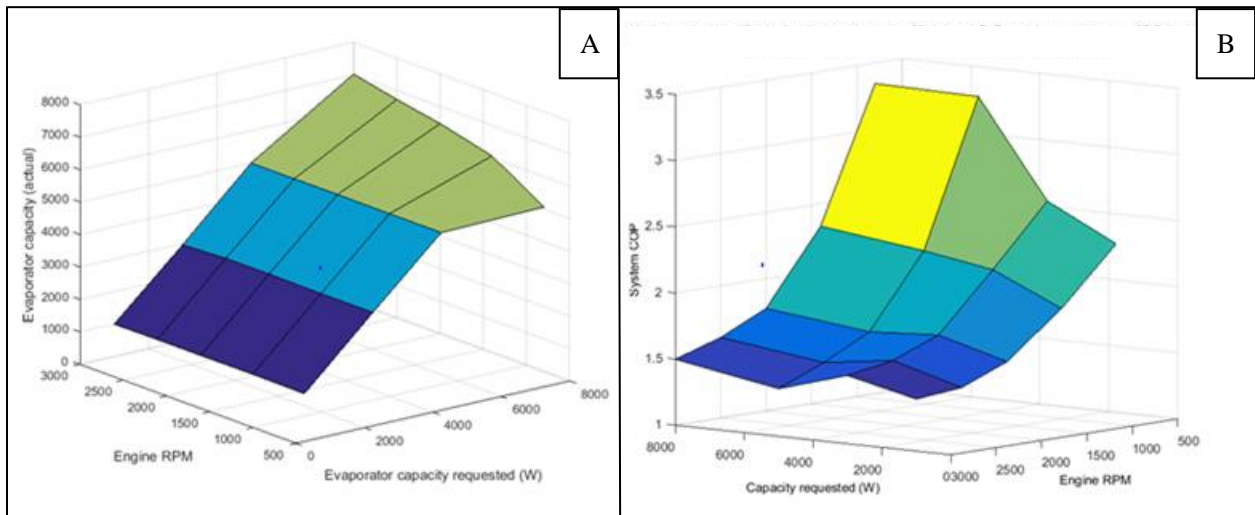


Figure III-78: Actual versus requested evaporator capacity (A), and COP versus capacity and engine rpm (B)

Vehicle Fuel Use Model

Vehicle models were developed in FASTSim (5) for each of the three representative vehicle platforms in order to calculate the impact of the A/C compressor mechanical load on vehicle fuel use and GHG emissions. FASTSim is a simplified vehicle simulation tool that enables the user to define powertrain components including engine and electric motor as well as battery and auxiliary loads. FASTSim is validated for hundreds of vehicles and vehicle performance can be calculated over standard and real-world drive cycles.

NREL's Transportation Secure Data Center (TSDC) was used to evaluate and identify a representative drive cycle for each of the three drive lengths (13). For each of the three representative drive durations, all drive

events from the TSDC with drive times similar to the target drive time were selected and aggregate statistics computed. Thereafter, the cycle that best represented the group was selected. The selected representative drive cycle for the 18-minute drive is shown in Figure III-79a. Vehicle speed was used to determine engine speed in FASTSim for use in the A/C model and was also used for calculating external velocity in the CoolCalc thermal model.

Once representative drive cycles were selected, the FASTSim models of the three vehicles were used to evaluate vehicle performance over a range of accessory loads for each of the cycles. A vehicle performance map was created with fuel use as a function of drive cycle, vehicle type, and accessory load. The impact of the A/C load on fuel economy for the three vehicles on the 18.4-minute drive cycle is shown in Figure III-79b.

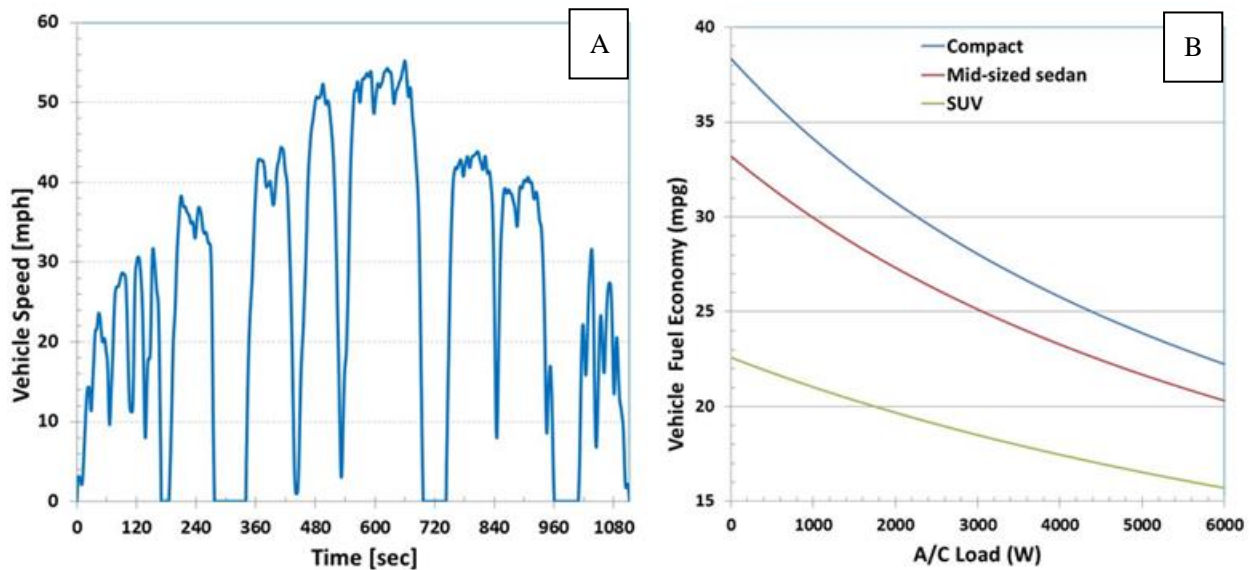


Figure III-79: Real-world vehicle speed profile for the 18.4-minute drive (A), and vehicle fuel economy as a function of A/C load for three vehicles over the 18.4-minute drive (B)

National A/C Fuel Use Analysis Process

The thermal model will be used to calculate the evaporator thermal load for a vehicle with and without the solar/thermal control technologies, representing a total of five configurations. In order to incorporate representative national vehicle use cases, multiple CoolCalc simulations will be performed that varied the location, dwell time, drive duration, time of day, and vehicle type. A full factorial analysis of the vehicle use cases results in 18,540 simulations. For each simulation, the HVAC map defined in the A/C System Model section will be used to calculate an accessory load and the vehicle map described in the previous section will be used to calculate vehicle fuel use.

Due to the large number of simulations necessary, NREL's Windows-based, high-performance computing system will be used for parallel simulation (14). The CoolCalc simulation results will be aggregated using post-processing and appropriate weighting factors will be applied to incorporate the relevancy of each use case simulated. To account for different locations and weather environments, the results will be weighted by the registered vehicles assigned to each location as previously described. With this process, the national-weighted fuel use and CO₂ emissions will be calculated for baseline vehicles and vehicles incorporating each of the four solar/thermal technologies. The impact of the solar/thermal technologies will then be computed by taking the difference between the solar/thermal vehicle and the baseline vehicle performance.

Results

The analysis is on-going. As an initial check, the fuel use and GHG emission results for the baseline vehicle in three cities will be calculated and compared to literature.

Conclusions

NREL researchers developed an analysis process to calculate the impact of the solar/thermal off-cycle credit technologies available in the EPA's 2017–2025 Light-Duty Vehicle Greenhouse Gas Emissions and CAFE standards. Such credits include glazing, solar reflective paint, and both passive and active cabin ventilation. NREL leveraged thermal and vehicle simulation analysis tools, including CoolCalc, CoolSim, and FASTSim. Using the U.S. DOT NHTS data, U.S. light-duty vehicle driving behaviors and weighting factors were characterized and integrated into the analysis. These factors included time-of-day of travel, trip duration, and time between trips. In addition, U.S. locations were selected and weighting factors were generated based on light-duty vehicle registrations. Researchers plan to calculate the grams of CO₂ per mile reduction for each solar or thermal control technology in the United States.

Acknowledgements

Co-authors: Bidzina Kekelia, Gene Titov: NREL

III.4.C. Products

Presentations/Publications/Patents

1. DOE Fuel Economy Working Group status presentation, July 29, 2016
2. 2016 SAE Thermal Management Systems Symposium presentation, October 20, 2016
3. 2017 SAE World Congress technical paper (planned)

III.4.D. References

1. Rugh, J.; Hovland, V.; Andersen, S. "Significant Fuel Savings and Emission Reductions by Improving Vehicle Air Conditioning," Mobile Air Conditioning Summit, Washington, D.C., April 14-15, 2004.
2. Lustbader, J.; Kreutzer, C.; Kekelia, B.; Jeffers, M.; Schilling, S. "VTCab, Rapid Vehicle HVAC Load Estimation Tool." DOE Annual Report, 2015.
3. Lustbader, J.; Kreutzer, C.; Jeffers, M.; Adelman, S., et al. "Impact of Paint Color on Rest Period Climate Control Loads in Long-Haul Trucks." SAE Technical Paper 2014-01-0680, 2014, doi:10.4271/2014-01-0680.
4. Kiss, T.; Lustbader, J. "Comparison of the Accuracy and Speed of Transient Mobile A/C System Simulation Models." SAE International Journal of Passenger Cars—Mechanical Systems (7), August 2014; pp. 739–754; doi:10.4271/2014-01-0669.
5. Brooker, A.; Gonder, J.; Wang, L.; Wood, E. et al. "FASTSim: A Model to Estimate Vehicle Efficiency, Cost and Performance." SAE Technical Paper 2015-01-0973, 2015, doi:10.4271/2015-01-0973.
6. "2014 Polk Vehicle Registration Database." IHS Automotive, driven by Polk. <https://www.ihs.com/btp/polok.html>.
7. "Automotive Color Trends." PPG Industries. <http://corporate.ppg.com/Color/Color-Trends/Automotive-Color-Trends.aspx>, accessed 7/2016.
8. "Lawrence Berkeley National Laboratory Pigment Database." Lawrence Berkeley National Laboratory. <http://coolcolors.lbl.gov/LBNL-Pigment-Database/database.html>, accessed 7/2016.
9. Rugh, J.; Farrington, R. "Vehicle Ancillary Load Reduction Project Close-Out Report: An Overview of the Task and a Compilation of the Research Results." NREL/TP-540-42454, 2008.
10. Jeffers, M.; Chaney, L.; Rugh, J. "Climate Control Load Reduction Strategies for Electric Drive Vehicles in Warm Weather." Proceedings of 2015 World Congress and Exhibition, Paper #2015-01-0355, Society of Automotive Engineers, Detroit, MI, April 21-23, 2015.
11. "National Household Travel Survey, 2009." Oak Ridge National Laboratory, <http://nhts.ornl.gov>, accessed 5/2016.

12. Papasavva, S.; Hill, R.W.; Brown, O.R. "GREEN-MAC-LCCP: A Tool for Assessing Life Cycle Greenhouse Emissions of Alternative Refrigerants." SAE Technical Series Paper 2008-01-0829, 2008.
13. "Transportation Secure Data Center." National Renewable Energy Laboratory, http://www.nrel.gov/transportation/secure_transportation_data.html, accessed 7/2016.
14. "Information for Users of the WINHPC system," National Renewable Energy Laboratory, <https://hpc.nrel.gov/users/systems/winhpc>, accessed 5/2016.

III.5. Advanced Technology Vehicle Lab Benchmarking (Level 1 & Level 2)

Kevin Stutenberg, Principal Investigator

Argonne National Laboratory
9700 South Cass Avenue
Lemont, IL 60439
Phone: (630) 252-6788; Fax: (630) 252-3443
E-mail: kstutenberg@anl.gov

Lee Slezak, DOE Program Manager

U.S. Department of Energy
Phone: (202) 586-2335
E-mail: Lee.Slezak@ee.doe.gov

Start Date: October 1, 2015
End Date: September 30, 2016

III.5.A. Abstract

Objectives

- Provide independent evaluation of advanced automotive technology via benchmarking of advanced technology conventional vehicles (CVs), hybrid electric vehicles (HEVs), plug-in hybrid electric vehicles (PHEVs), battery electric vehicles (BEVs), and alternative fuel vehicles (AFVs) for the Vehicle Technologies Office of the U.S. Department of Energy (DOE).
- Establish the baseline for state-of-the-art automotive technology in powertrain systems and components through acquisition of independent and publicly available test data and analysis.
- Disseminate vehicle and component testing data to partners of the DOE, such as other national laboratories, the U.S. Council for Automotive Research (USCAR), OEMs, suppliers and universities.
- Provide data to support both codes and standards development and powertrain simulation model development and validation.

Accomplishments

- Level 1: Noninvasive technology assessments accomplishments
Completed technology assessment of advanced technology vehicles of multiple classes and fuel types. These included:
 - 2015 VW E-Golf (BEV)
 - 2015 Mercedes Benz B-Class Electric (BEV)
 - 2015 Chevrolet Impala Bi-Fuel (Alternative Fuel)
 - 2016 Chevrolet Volt (PHEV)
- Level 2: Invasive technology assessments
Completed technology evaluation of the 2014 BMW i3 with range extending engine
- Evaluation of Impacts of Active Transmission Warm-up technologies
- Analysis and Reporting: Development of advanced data management and reporting methods

Future Achievements

- Continued evaluation of advanced technology powertrain systems and components in order to provide independent and public data and analysis to the DOE's Vehicle Technologies Office and its partners. .

III.5.B. Technical Discussion

Background

Since its inception, the Advanced Powertrain Research Facility (APRF) has been testing advanced-technology vehicles to benchmark the latest automotive technologies and components for the U.S. Department of Energy (DOE). The staff has tested a large number of vehicles of different types, such as advanced technology conventional vehicles (CVs), hybrid electric vehicles (HEVs), plug-in hybrid electric vehicles (PHEVs), battery electric vehicles (BEVs), and alternative fuel vehicles (AFVs).

Introduction

Since the late nineties, the researchers at the APRF have developed a broad and fundamental expertise in the testing of the next generation of energy-efficient vehicles. Over this period of time, many methods of vehicle instrumentation and evaluation have continuously been refined. Two levels of instrumentation and testing exist today. The first level (Level-1) involves comprehensive, but non-invasive, instrumentation of a vehicle, leaving the vehicle unmarked after the testing. Typically, these L1 vehicles enter Idaho National Laboratory's (INL) fleet testing as part of the DOE's Advanced Vehicle Testing Activity (AVTA). The second level (Level-2) involves comprehensive invasive instrumentation of a vehicle and its powertrain components, which leaves the vehicle with irreversible alterations, but provides an in-depth assessment of the technology.

This report summarizes the Level-1 and Level-2 benchmark activities of FY 2015. The first section describes the test approach for the benchmark work followed by a second section which highlights some select test results and analysis.

Approach

Vehicle Acquisition

The Level 1 benchmark program leverages the DOE's AVTA activities. Through this program, INL in collaboration with Intertek Testing Services, procures new advanced-technology vehicles to evaluate through accelerated fleet testing. As part of the evaluation, these vehicles are benchmarked at Argonne National Laboratory's APRF. Figure III-80 illustrates the AVTA process.

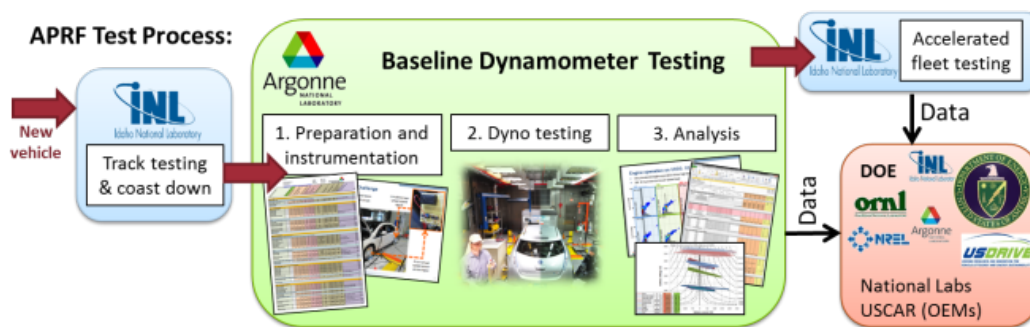


Figure III-80: Advanced Vehicle Testing Activity process.

Further information on the AVTA is available at <http://avt.inel.gov/>.

Additional test vehicles to those supplied within the AVTA program can be acquired for Level 1 evaluation in addition.

Level 2 vehicles are acquired by Argonne directly from dealerships. The typical Level 1 instrumentation is so invasive and complete that the vehicles are typically not road worthy at the completion of the program. The Level-2 test vehicles are maintained by Argonne to be used in future studies to support DOE investigations.

General Test Instrumentation and Approach

Typically, Argonne receives Level 1 test vehicles on loan; therefore, the vehicles need to leave the test facility in the “as-received” and road worthy condition. This requirement limits instrumentation to sensors that can be easily installed and removed without leaving any damage.

Despite this limitation, Argonne strives to achieve the maximum level of instrumentation to facilitate relevant data collection. If the vehicle has an internal combustion engine, instrumentation is applied to measure the engine speed, fuel flow and engine oil temperature (achieved through dipstick instrumentation). For electrified vehicles, a power analyzer is used to record the voltage and current from the high voltage energy storage system. If the vehicle requires charging, the electric power from the grid to the charger is measured. Furthermore, any sensors that can be fitted without permanent damage to the vehicle, such as temperature sensors, are typically included in locations of interest (a battery pack vent, for example). Additional APRF instrumentation focuses on the particular or unique technology, or technologies that enable the increased energy efficiency of the powertrain. A final aspect of Level 1 instrumentation is the recording of messages from the vehicle’s information buses, the content of which varies widely from vehicle to vehicle. This is completed by determining and recording both transmitted diagnostic and broadcast network messages.

The Level 2 benchmark, which included in-depth, testing, and analysis of new and emerging vehicle technologies, is specific to each vehicle. The particular Level 2 instrumentation is therefore described in the results and analysis section of the Level 2 vehicles of this report.

Advanced Powertrain Research Facility

In order to evaluate a vehicle in a variety of real-world conditions, the 4WD chassis dynamometer of the APRF is EPA 5-cycle capable. The test cell includes a thermal chamber and an air-handling unit with a large refrigeration system that enables vehicle testing at the EPA “Cold CO Test” ambient temperature of 20°F (-7°C), the standard test temperatures of 72°F (25°C), and the “SC03” test temperature of 95°F (35°C). Additionally, ambient test temperatures of 0°F (-17°C), and 40°F (4.5°C) may be used. All temperatures can be evaluated with or without solar emulation lamps providing up to 850 W/m² of radiant sun energy. The test cell is shown in Figure III-81.

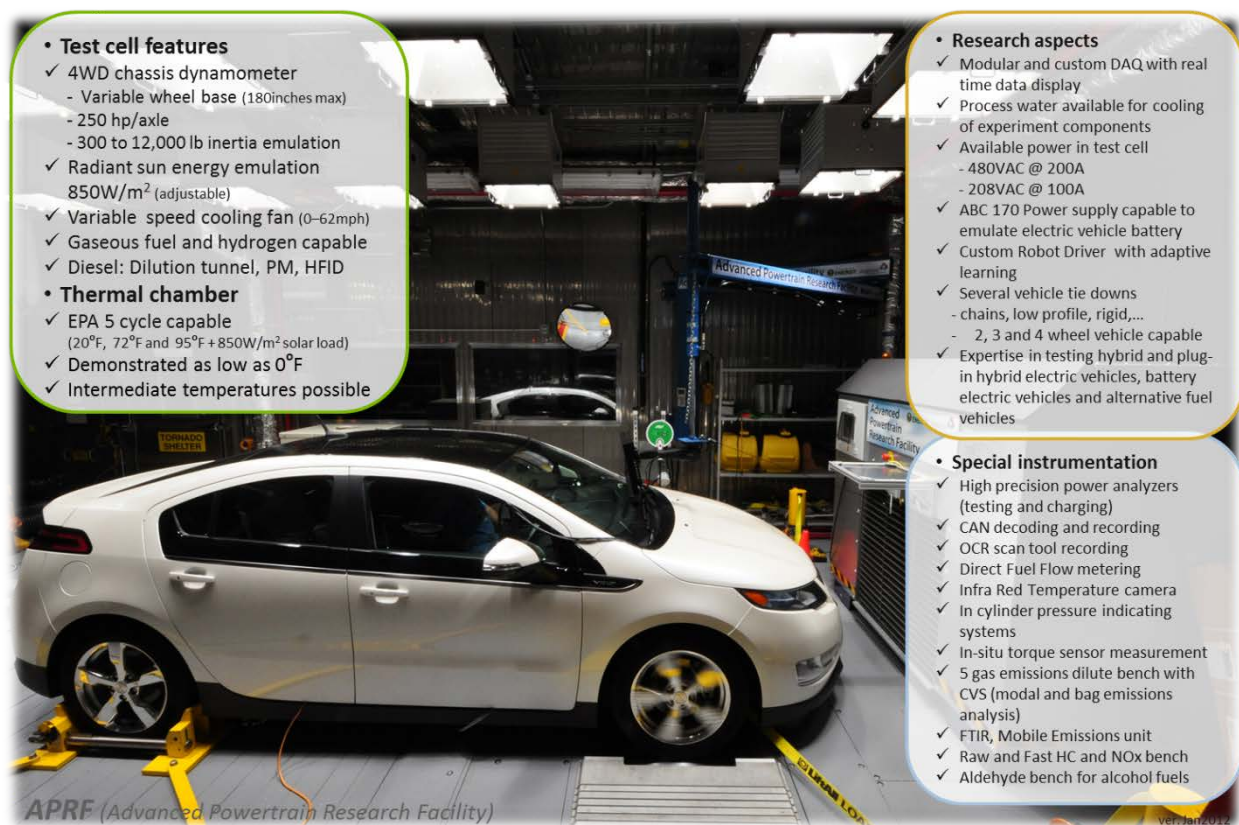


Figure III-81: Illustration of the chassis dynamometer in thermal chamber long with facility capabilities

The APRF benchmark program goes well beyond the standard tests performed for EPA certification of fuel economy and emissions. To fully characterize the powertrain and the individual components the instrumented powertrains are tested on a wide range of ambient temperatures, drive cycles, performance tests and vehicle/component mapping tests.

Purpose of Benchmarking

A major goal of the benchmarking activity is to enable petroleum displacement through data dissemination and technology assessment. The data generated from the vehicle testing as well as the analyses are shared through several mechanisms, such as raw data, processed data, presentations and reports.

The independent and public data is a foundation enabling the development of rigorous and technology neutral codes and standards. The data also serves to develop and validate several modeling and simulation tools within the DOE system (i.e., Autonomie ...) as well as outside (i.e., EPA Alpha model, University modeling, and economic models). These activities in turn impact the modification of test plans and instrumentation for current and future test vehicles. Partners in the testing include U.S. manufacturers and suppliers, through the U.S. Council for Automotive Research. Many of the research activities of the DOE rely on the benchmark laboratory and fleet testing results to make progress towards their own goals. Figure III-82 details some of these DOE research activities and partners.

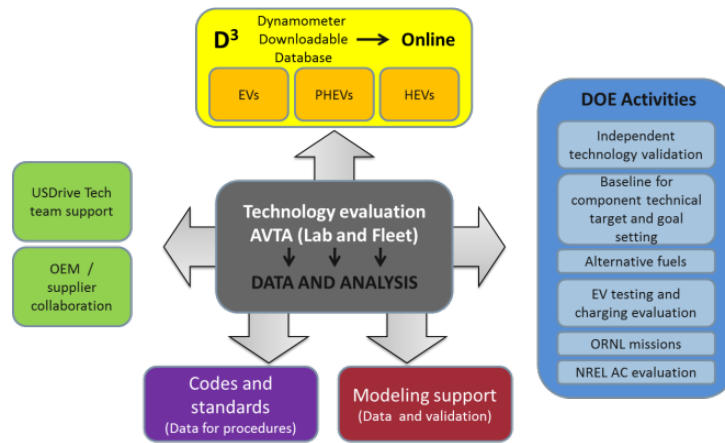


Figure III-82: Data dissemination and project partners

Downloadable Dynamometer Database (D3)

D3 is a public web portal of highly detailed accurate public and independent vehicle test data, of critical utility in the research community. This web-based portal to Argonne vehicle test data is designed to provide access to dynamometer data that are typically too expensive for most research institutions to generate. Shared data is intended to enhance the understanding of system-level interactions of advanced vehicle technologies for researchers, students, and professionals engaged in energy-efficient vehicle research, development, or education. Figure III-83 shows the structure and content of the database.

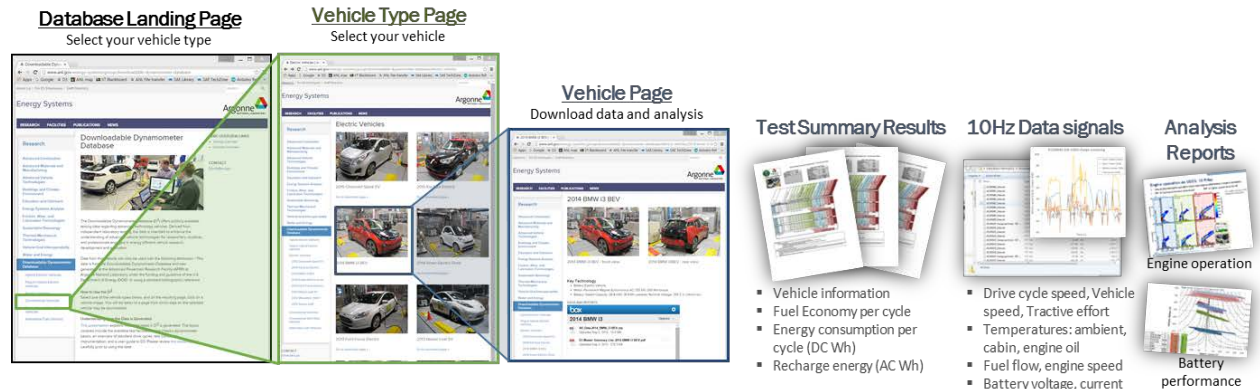


Figure III-83: Map of Downloadable Dynamometer Database content

Vehicle Technology Evaluations in Review

2015 VW E-Golf (AVTA)

Vehicle Description

The eGolf is Volkswagen entry in the 100+ mile (20~25kWh) battery electric vehicle category. The electric powertrain with the battery pack adds about 400 lbs. compared to the base conventional vehicle model. The battery system is air cooled. The specifications of the vehicle are listed in Table III-14

Table III-14: 2015 VW E-Golf specifications

Architecture	Battery Electric Vehicle
Motor*	Synchronous AC Permanent Magnet Electric Motor 85kW (115hp) / 270Nm (199 lb-ft) torque
Battery*	Li-ion, 24.2 kWh stated capacity, 323V Nominal
EPA Label Fuel Economy (mpg)+	126 City, 105 Highway, 116 Combined

* manufacturer's data
 ^ www.fueleconomy.gov

Points of Interest

Impact of ambient temperature on energy consumption

Figure III-84 shows the energy consumption of the eGolf for different drive cycles and ambient temperature conditions. The vehicle was conditioned for over 12 hours at the target ambient temperature and the four tests (UDDS cold start, UDDS hot start, Highway, and US06) are run consecutively. The climate control system was set to maintain a temperature of 72F in the cabin. The ambient temperature of 72F is the reference test as the car spend no energy on heating or cold the cabin. The largest increase in energy consumption occurs at the coldest temperature right after the start of the test. The electric heater has to warm up the cold cabin during this first test. During the second test, the heater only has to maintain the cabin temperature which requires less energy. The energy consumption penalty is reduced on more energy intense drive cycles, such as the highway and the US06, as proportionally more power is required to move the vehicle compared to the city drive cycle. The air conditioning compressor power needed to cool the car during hot testing is significantly lower compared to the electric heater power usage.

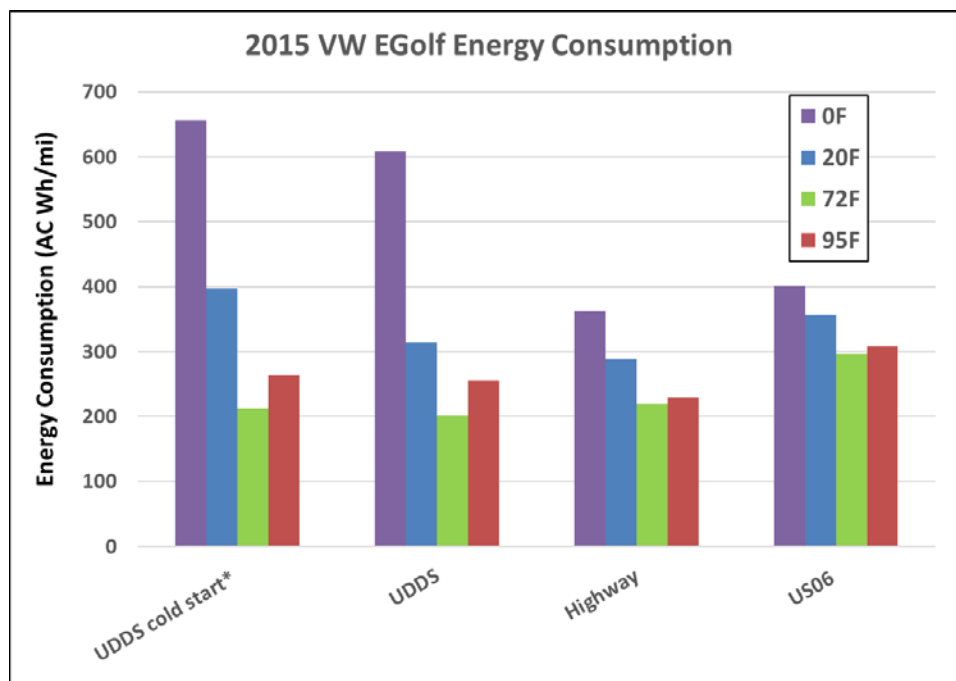


Figure III-84: eGolf electric energy consumption for different drive cycles across different temperatures

Impact of ambient temperature on the battery system

Ambient temperature has a significant impact on the high voltage battery system. The polarization curves for the four different target temperature tests are shown in Figure III-85. The battery system resistance, which is represented by the slope of the polarization curve, increases which colder temperatures. At 0F the system resistance is twice as high at 0.10 ohm as compared to the resistance at 72F temperatures. The higher resistance along with the higher average power draw, which is caused by electric heater usage and higher powertrain losses at 0F, can be observed in the polarization curves. Less regenerative braking power is stored in the battery as the heater uses some of the power immediately. The mean current level at 0F is around 10A compared to a mean current level closer to 0A at 72F as illustrated in the histograms of Figure III-85.

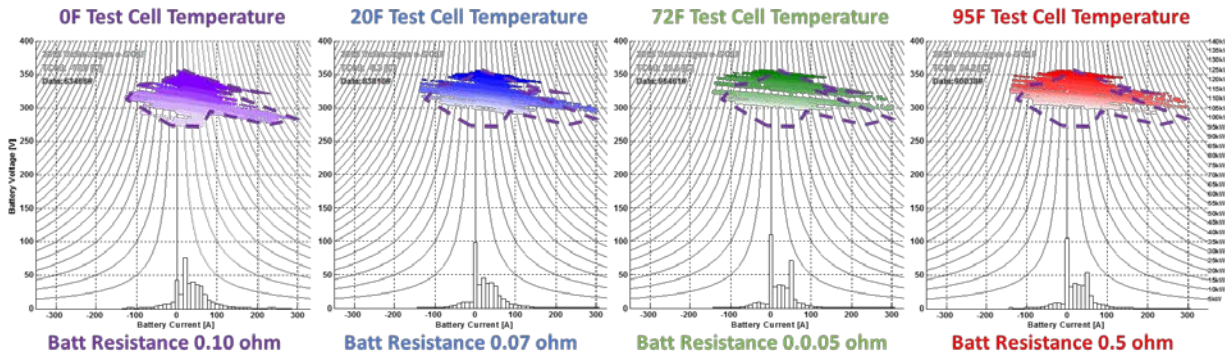


Figure III-85: eGolf battery polarization curves across different temperatures

2015 Mercedes Benz B-Class Electric (AVTA)

Vehicle Description

The battery electric B-class from Mercedes Benz is another modern battery electric vehicle evaluated this year. The motor power is higher than most other battery electric vehicles. The technical specifications are listed in Table III-15.

Table III-15: 2015 Mercedes Benz B-Class Electric specifications

Architecture	Battery Electric Vehicle
Motor*	AC Induction Motor 177 HP (131 kW); 251 lb-ft (340Nm)
Battery*	Li-ion 28 kWh capacity, "Range Extending" Option - 32kWh
EPA Label Fuel Economy (mpg)+	85 City/ 82 Highway/ 84 Combined

* manufacturer's data
 ^ www.fueleconomy.gov

Points of Interest

Range extending option investigation

The B-class has a range extender option which enables 32kWh of battery energy compared to the standard 28 kWh. Figure III-86 shows the data from the SAE J1634 multi-cycle shortcut test which is used to determine the energy consumption and range of battery electric vehicles. The test is started with a fully charged battery pack. The extended range test starts the battery system at a voltage of 343V which is 6 volts higher compared to the standard charge which starts the battery at 337V. The test is ended when the vehicle cannot maintain the 60 mph speed when the battery pack is depleted. The extra range from the extended range charge option is clearly visible in Figure III-86. This higher voltage results in a usable battery energy of 34.8 kWh compared to 31.1 kWh in the standard operation.

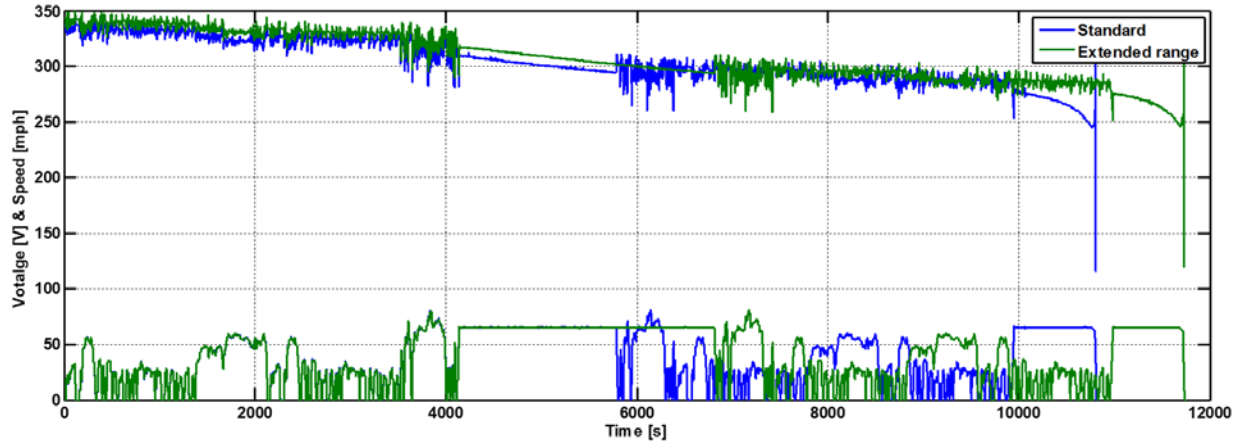


Figure III-86: B-class electric energy consumption for different drive cycles across different temperatures

Battery system resistance as a function of battery temperature

The B-class was tested at ambient temperatures of 72F, 95F with 850 W/m² of solar load emulation, 20F and 0F on the SAE J1624 multi cycle shortcut test sequence shown Figure III-86. The average battery system resistance and battery pack temperature was calculated for each test. The results are shown in Figure III-87. At the battery resistance is triple for the first 0F test and double for the first 20F test as compared to the 0.1 ohm at 72F.

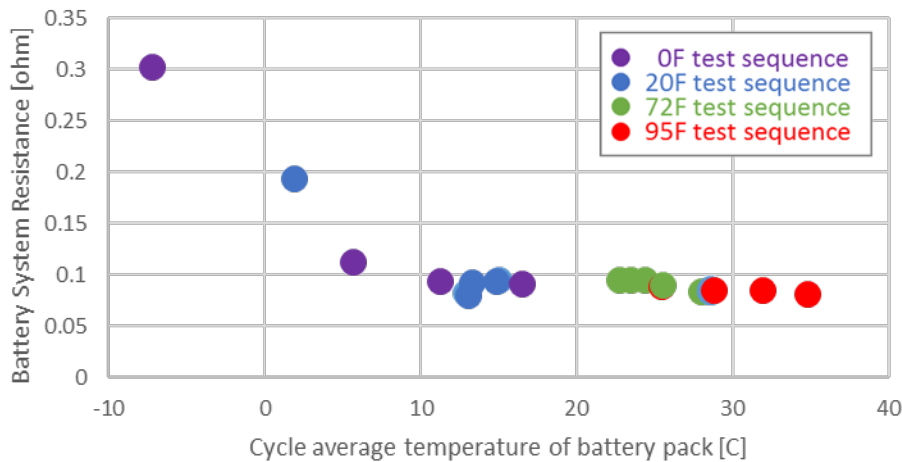


Figure III-87: B-class battery system resistance as a function of battery temperature

2015 Chevrolet Impala Bi-Fuel (AVTA)

Vehicle Description

With the 2015 Chevrolet Impala Bi-Fuel, General Motors offered a model of Impala with a factory option for a compressed natural gas bi fuel variant equipped by Quantum Motors. The vehicle was offered as a bi-fuel vehicle, with operation occurring on CNG or gasoline based on the drivers selected state. The conversion included installation of required CNG components, including a 3600psi CNG tank, fueling lines, modified intake manifold for port CNG injection, along with updates to the 3.6L V6 to ensure durability such as hardened valves and valve seats. The vehicles default mode is CNG, with transfer to gasoline operation occurring following depletion of the CNG reserve, or driver demand.

Table III-16: 2015 Chevrolet Impala Bi-Fuel Specifications

Architecture	Midsized Conventional, FWD
Engine*	3.6-Liter V6, Bi-Fuel Gasoline/ CNG DOHC 232 hp / 218 lb.-ft. (CNG) 258 hp / 244 lb.-ft. (Gasoline)
Transmission*	6 Speed Automatic
EPA Label Fuel Economy (mpg)^	16 city / 24 hwy / 19 combined (CNG) 17 city / 25 hwy / 20 combined (Gasoline)

* manufacturer's data

^ www.fueleconomy.gov

Vehicle Instrumentation

Test vehicle instrumentation focused on a comparison of vehicle operation, energy use, and emissions while in CNG and gasoline operation. Instrumentation captured major systems operation, and the impacts of these systems operation on the vehicle system as a whole.

Liquid fuel flow measurements were made with a positive displacement fuel scale, while gaseous fuel flow measurement was completed with a Coriolis mass flow meter. Diagnostic (OBD and manufacturer specific) and broadcast CAN messages were captured during testing, with parameters such as: engine and transmission component speeds, engine torque, pedal position, engaged transmission gear, pedal positions, gaseous fuel system operation states and pressure. The low voltage electrical system was instrumented to capture accessory energy use. Additionally, measurements were captured from the APRF facilities, including dynamometer parameters, and emissions measurements of CO, CO₂, NO_x, THC, and CH₄.

Test cycles completed include UDDS, Highway, and US06 cycles at the test temperatures of 20F, 72F, and 95F with 850 W/m² of solar emulation. Additional maximum performance and mapping testing was completed at 72F to determine vehicle capabilities.

Points of Interest

Vehicle operation- CNG vs Gasoline highlights

An overview of the effects on vehicle fuel economy, in miles per gallon energy equivalent to certification fuel, and emissions derived from testing can be found in Table III-17 and Figure III-88 below.

Table III-17: Fuel Economy and Emissions of 2015 Chevrolet Impala Bi-Fuel at 72F ambient

	Fuel Consumption (MPGe)		Emissions (g/mile)									
	Gasoline	CNG	CO2		CO		Nox		THC		CH4	
			Gasoline	CNG	Gasoline	CNG	Gasoline	CNG	Gasoline	CNG	Gasoline	CNG
UDDS cold start	19.2	18.3	465.6	365.5	1.407	1.492	0.007	0.004	0.013	0.025	0.007	0.068
UDDS	21.5	20.9	423.1	328.0	0.603	0.275	0.016	0.004	0.003	0.005	0.002	0.017
Highway	37.4	36.3	241.6	188.2	0.127	0.118	0.004	0.001	0.000	0.001	0.000	0.003
US06	21.5	21.6	398.3	310.9	9.878	1.190	0.010	0.012	0.007	0.021	0.008	0.064
US06 City	12.4	12.7	666.5	533.4	31.278	3.158	0.029	0.032	0.023	0.071	0.030	0.211
US06 Highway	27.1	27.0	321.5	247.3	3.757	0.628	0.004	0.007	0.003	0.007	0.002	0.022

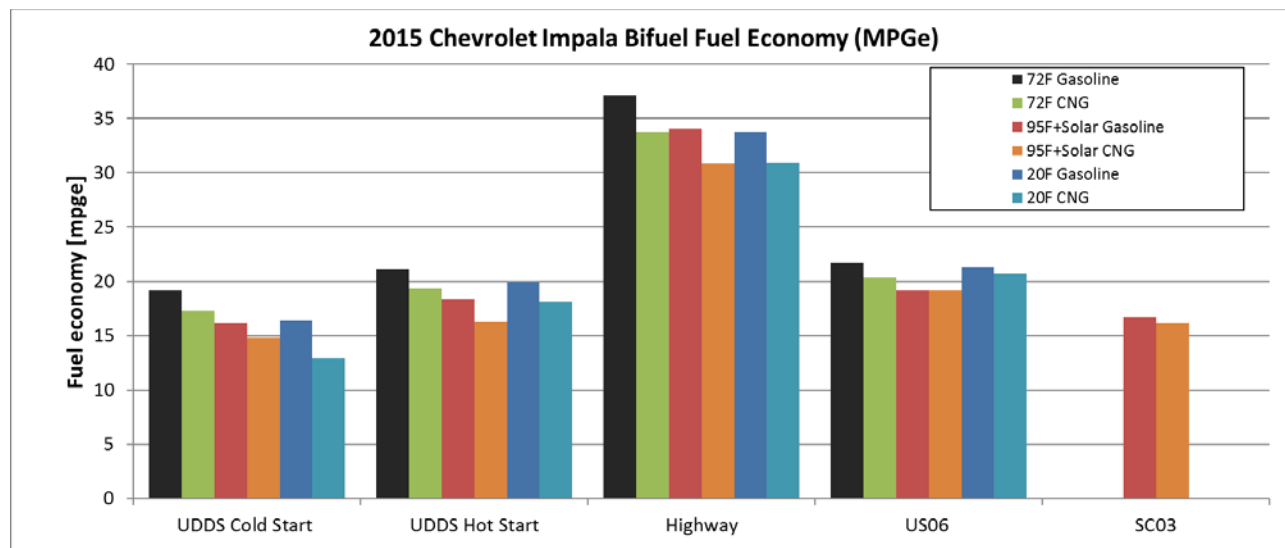


Figure III-88: Fuel Economy of the 2015 Impala Bi-fuel at varying ambient temperatures

A consistent reduction in CO2 tailpipe emissions, ranging from 30-35% dependent on drive cycle and test cell temperature was found. As can be seen the reduction in emissions for CO, NOx, THC, and CH4 was quite variable, as at the low level of emissions found small peaks in vehicle emissions created a large impact on overall cycle.

2016 Chevrolet Volt (AVTA)

Vehicle Description

The 2016 Chevrolet Volt offers a second generation of the extended range electric vehicle first released by General Motors in 2011. The vehicle powertrain was thoroughly redesigned, including the HV battery, electric drive system, and IC engine.

Table III-18: 2016 Chevrolet Volt specifications

Architecture	EREV: Extended Range Electric Vehicle
Engine*	0.65L In-line 2, PFI, DOHC 28kW (37.5 hp) Generator Output- 26.6 kW at 5000rpm
Transmission*	1 Speed
Motor*	Synchronous PM Electric Motor 125 kW [170 hp] / 250Nm [184 lb-ft]
Battery*	Lithium Ion 18.8 kWh Net Capacity
EPA Label Fuel Economy (mpg)^	117 combined 72 miles EPA estimated EV Range

*Manufacturer's data

^ www.fueleconomy.com

Vehicle Instrumentation

As vehicle energy use was of key interest on this vehicle, high voltage instrumentation was an area of particular focus. Instrumentation included a high voltage tap and current measurements at multiple locations. These current measurement locations included: at high voltage battery pack, A/C compressor, the PTC heater, the range extending generator, and the low voltage supply from the vehicles DCDC converter.

Points of Interest

Energy source for cabin heat at 20F ambient temperatures

Figure III-89 shows a comparison of a full depletion on city certification cycle at 72F and 20F ambient conditions. The Volt operates in electric mode for the full depletion duration at the 72F test conditions. The climate control system was set at 72F for the 20F test and as a results the internal combustion engine is operating on every UDDS test. Note that 8 consecutive UDDS cycles were run continuously and a key start occurred on the 9th test which could explain the higher electric usage for the 20F test sequence.

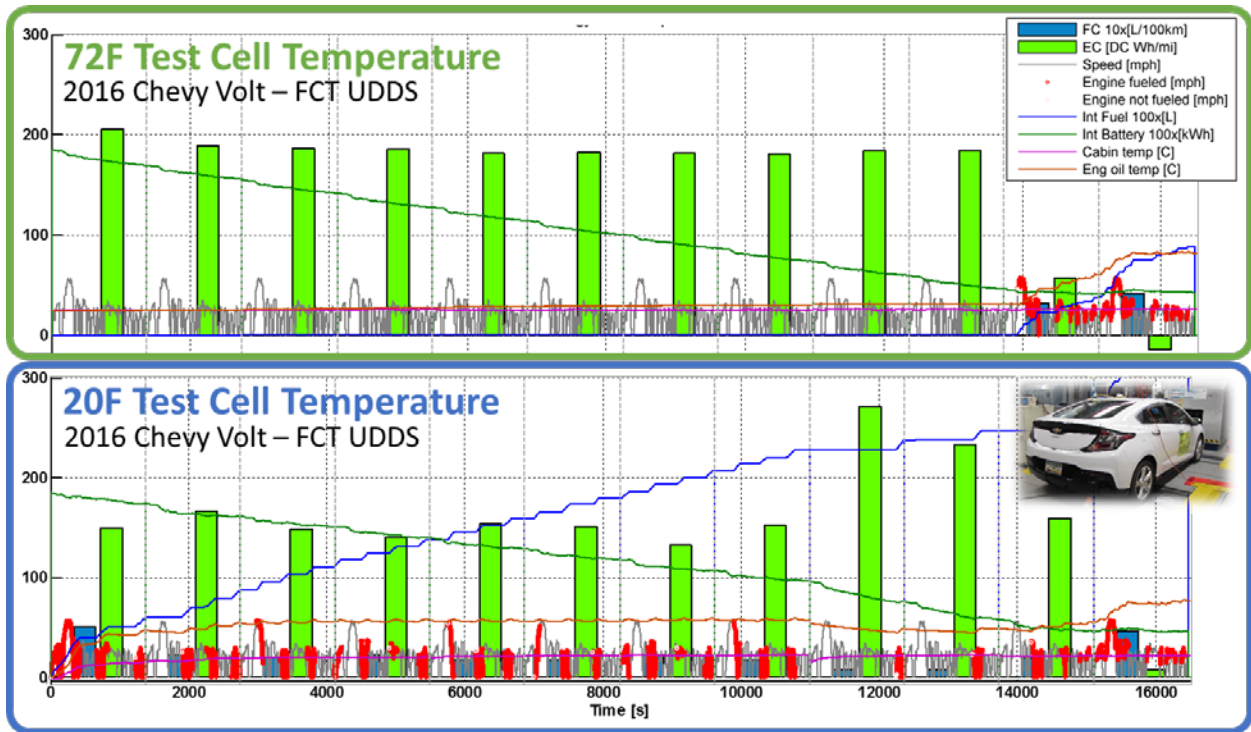


Figure III-89: Full charge test on the UDDS cycle at 72F and 20F for the 2016 Volt

The engine operation for the 72F and 20F test sequence is shown in Figure III-90. It is evident that the engine operates at lower power level around 5kW in the 20F test condition compared to 15kW at 72F. This engineering trade-off was made to provide heat from the powertrain to the cabin.

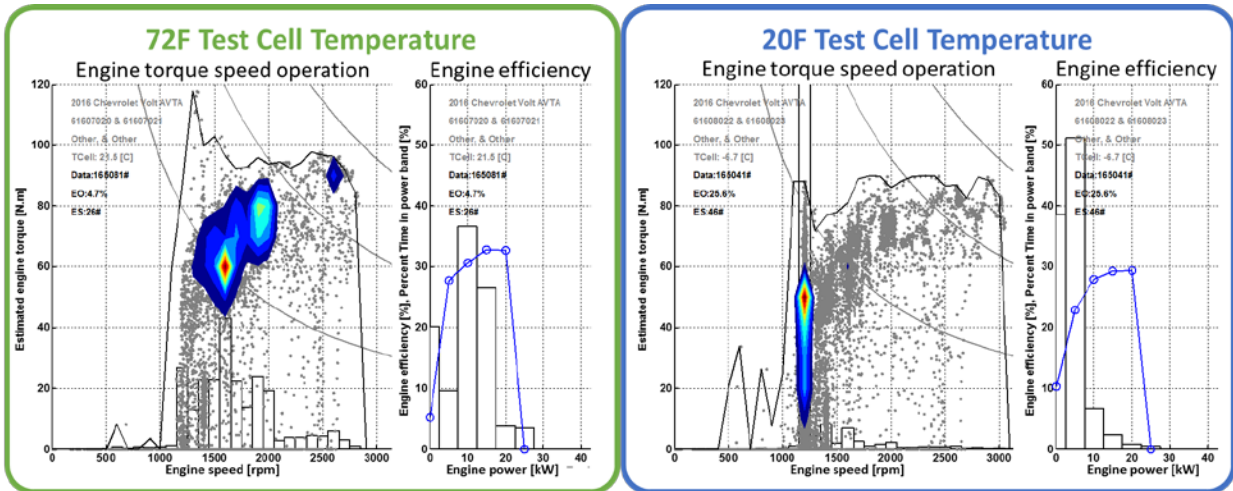


Figure III-90: Engine operation of the international combustion engine from the testing shown in Figure III-89

Level 2- Invasive testing: 2014 BMW i3 with Range Extending Engine

Vehicle Description

The BMW i3 is available both an electric vehicle (referred to later as BEV) and a plug-in hybrid vehicle that to an optional range extender (referred to as REx). During the FY 2015, both versions of this model have been tested at the APRF through vehicles supplied by the AVTA program. Additionally, the level 2 test vehicle was a 2014 BMW i3 REx, allowing for leveraging of components and testing knowledge between the two testing regimes. Table III-19 gives the specifications of the BMW i3 with optional range extending engine (REx).

Table III-19: 2014 BMW i3 Rex Specifications

Architecture	BEV-X: Battery electric vehicle with range extending engine
Engine*	0.65L In-line 2, PFI, DOHC 28kW (37.5 hp) Generator Output- 26.6 kW at 5000rpm
Transmission*	1 Speed
Motor*	Synchronous PM Electric Motor 125 kW [170 hp] / 250Nm [184 lb-ft]
Battery*	Lithium Ion 18.8 kWh Net Capacity
EPA Label Fuel Economy (mpg)^	117 combined 72 miles EPA estimated EV Range

*Manufacturer’s data

^ www.fueleconomy.com

This vehicle represents one of many battery electric vehicles to recently reach the market, though equipped with several unique features leading to a desire for in depth evaluation. Of key interest was a low power, 28kW range extending generator option for the standard BEV. This generator, directly mounted to the engine, provides electric power as a series hybrid only upon depletion of the high voltage battery. Figure III-91 shows the vehicle mounted on the 4WD chassis dynamometer at the Advanced Powertrain Research Facility undergoing testing.



Figure III-91: 2014 BMW i3 REx mounted in APRF for evaluation.

Vehicle Instrumentation

In contrast to the instrumentation implemented on vehicles through the AVTA program, invasive instrumentation provided an in-depth signal list which allows the measure the full energy flow across different components within the powertrain. The fitment of additional sensors, capture of additional vehicle parameters, and an extensive barrage of testing reveals the powertrain operation and component maps. The full instrumentation is detailed in last year's report which includes specific sections on the high voltage and low voltage instrumentation, the cooling system instrumentation, the exhaust system instrumentation, the cabin climate control instrumentation, the power electronics instrumentation and the engine instrumentation.

Overall Powertrain Operation

The i3 operates like a standard battery electric vehicle in charge depletion mode. Once the battery is depleted the range extending engine generator provides electric power to achieve charge sustaining operation. The test results at 72F are presented in Figure III-92.

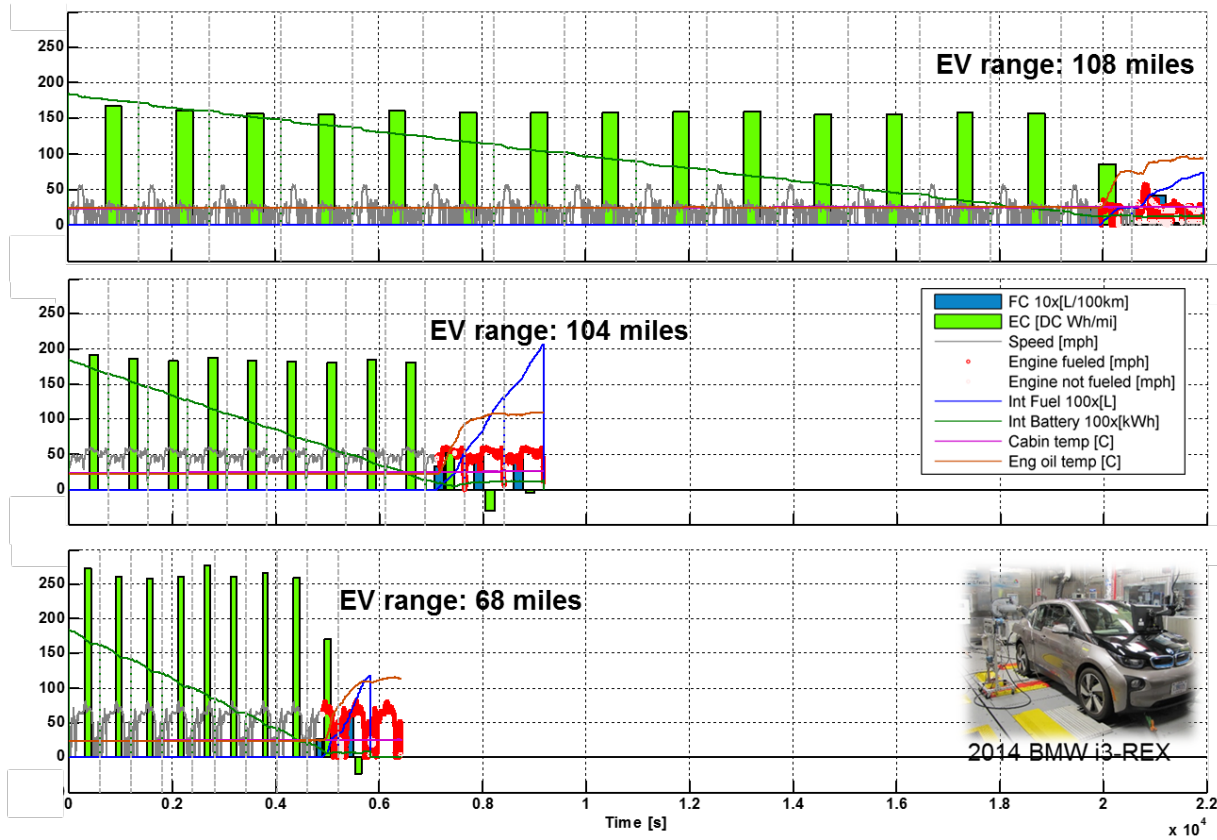


Figure III-92: Full charge test at 72F on the UDDS, the highway and the US06 cycles

The BMW i3 operates as a series hybrid electric vehicle in charge sustaining mode Figure III-93 and Figure III-94 provide some insight into this series hybrid operation. Compared to plug-in hybrid like a Volt, the maximum engine power of 28kW is very low. As a result the engine operates more frequently in charge sustaining mode to provide the average electric power needed for propulsion. A Prius operates its engine a quarter of the time on a UDDS cycle at 72F while the BMW i3 uses its engine about half the time in charge sustaining mode in the same conditions. Figure III-93 shows that the engine often operates at a constant speed while adjusting the load to achieve a power level. At lower vehicle speeds the engine appears to follow the vehicle speed which could improve the acoustics of the engine to driver.

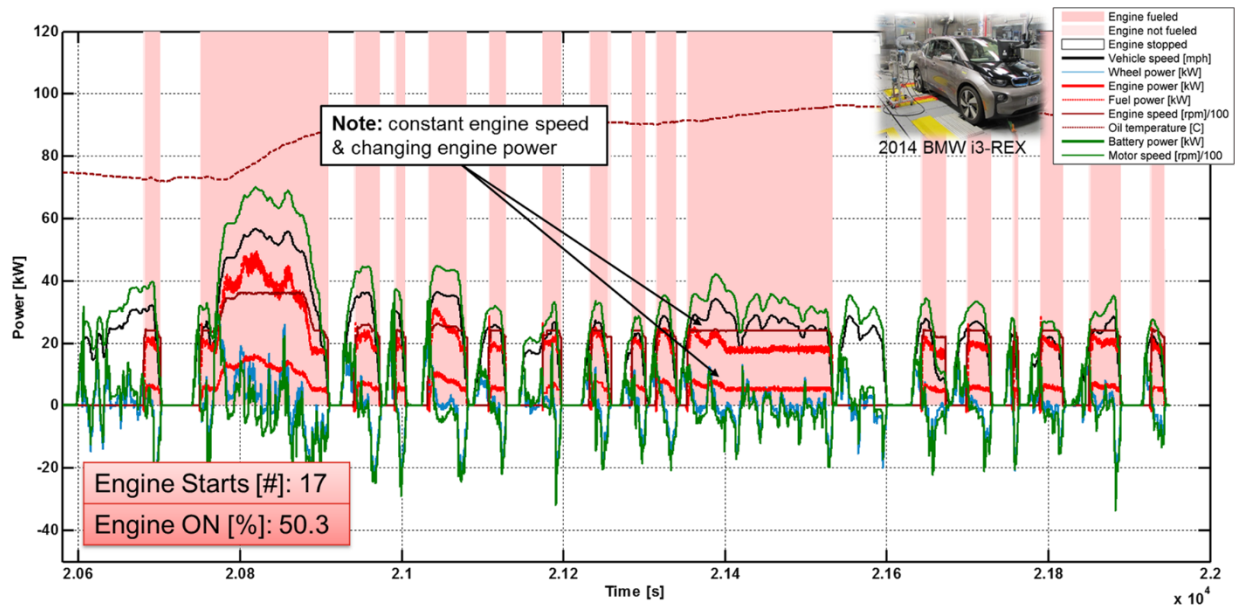


Figure III-93: Overview of charge sustaining operation

The range extending engine appears to have three preferred operating speeds while driving on the US certification drive cycles as illustrated in Figure III-94. That data is derived from a charge sustaining test sequence using the UDDS, highway and US06 drive cycles. The two major engine operating areas are 2400 rpm for 5 to 8 kW of electric power and 2550 rpm for 10 to 20 kW of electric power. A third operating point at 4500 rpm is used to generate 20 to 25kW electric power. This third operating speed is used in aggressive and high speed driving like the US05 drive cycle. The engine to electric power path is around or slight over 30% efficient.

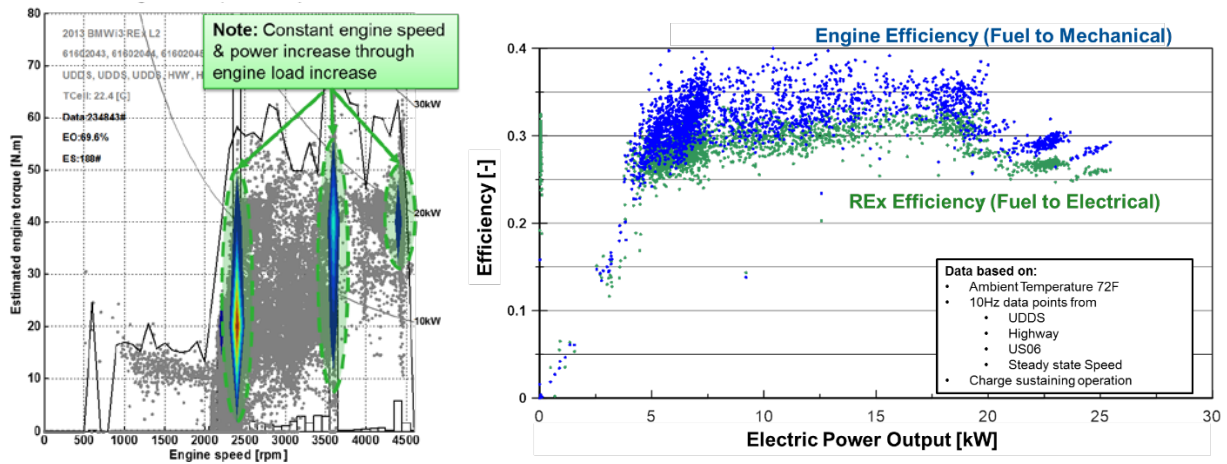


Figure III-94: Range extended engine operation and efficiency

Technology Assessments and Analysis

Battery Electric Vehicle Energy Consumption Comparison

The Advanced Powertrain Research Facility benchmarked 9 different models of battery electric vehicles and 3 plug-in hybrid electric vehicles in the last two years. Figure III-95 illustrates an example of the findings of this activity. It quantifies the variation in electric range depending on driving cycle, ambient temperature and accessory use. On average, compared to 72F, the range penalty in city driving is 51% at 20F and 18% at 95F, due mainly to the power consumption of cabin heating or cooling. Cabin and powertrain thermal preconditioning during vehicle charging can increase the city range at 20F by 5%. Heat pump systems are most active at off-cycle test conditions, such as 40F test temperature, providing real-world range benefits.

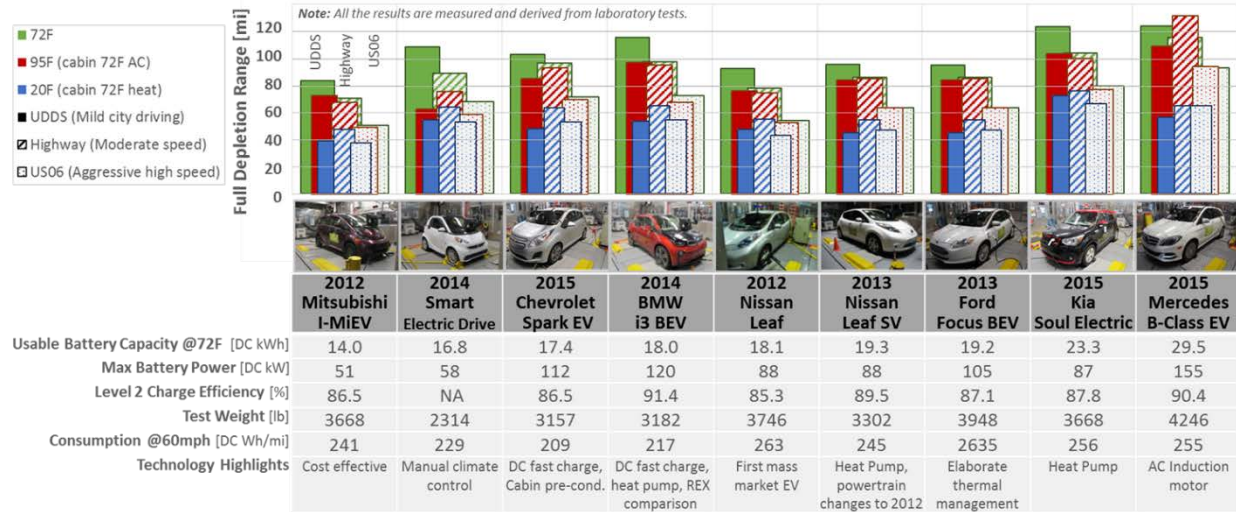


Figure III-95: Overview of Battery Electric Vehicles Range

Advances in Data Management and Reporting Methods

Data Management Methods

Prior to the start of this century, when the first mass production hybrid vehicle was released, the APRF has been performing technology evaluations on advanced vehicle technologies. As vehicle technologies have advanced, methods of capturing and processing data have advanced as well, most recently with the capture of data from vehicle diagnostics and broadcast CAN. Data sets have grown considerably in size, a breadth of information available, and the possibility of cross comparison of a high number of vehicle technologies has been found to produce insightful results.

Over the last fiscal year, the APRF has refined the methods to mine and develop reports from the data sets. Software has been tailored to produce consistent data formats, and allow for a quick search and comparison of the effects of varying measurement data on vehicle energy use. In the short term, these efforts have focused on producing a consistent reporting methods for the test results, as can be seen in the reports posted on the APRF website, found on the downloadable dynamometer database at www.anl.gov/d3. Additionally, a laboratory supported structure allowing for quick data distribution has been established with D3, with integration of cloud based file storage allowing for simple uploading of data sets and reports.

The APRF plans to continue with development of this searchable database in upcoming fiscal years, producing research results based on the findings, all the while adding to the available data for mining with testing completed within this project. A summary of reports systems developed in FY16 can be found below

Standardized APRF Single Test Summaries

In the past, APRF testing summaries structured as a table of information displaying relevant test information for the round of tests completed on that single vehicle. This test summary was useful in that it allowed for a quick summary of information, and a reference for the specific test numbers that could be referenced for further analysis. Unfortunately, this display method does not allow to quickly visualize the test data.

To support this need, a reporting template was developed to summarize specific vehicle tests. These summaries provide a test overview and test cell setup, with all relevant vehicle, fuel, and dynamometer information. The summary also provides a display of the vehicle energy use over the driven cycle, split into major components impacting energy consumption. An additional page provides tabulated data for the cycle of key metrics related to energy consumption, once again focusing on major components impacting energy use. An example of the report can be seen in Figure III-96. These test reports are available for tests cycles posted to APRF's D3 website, and extended versions are available to DOE's collaborative partners.

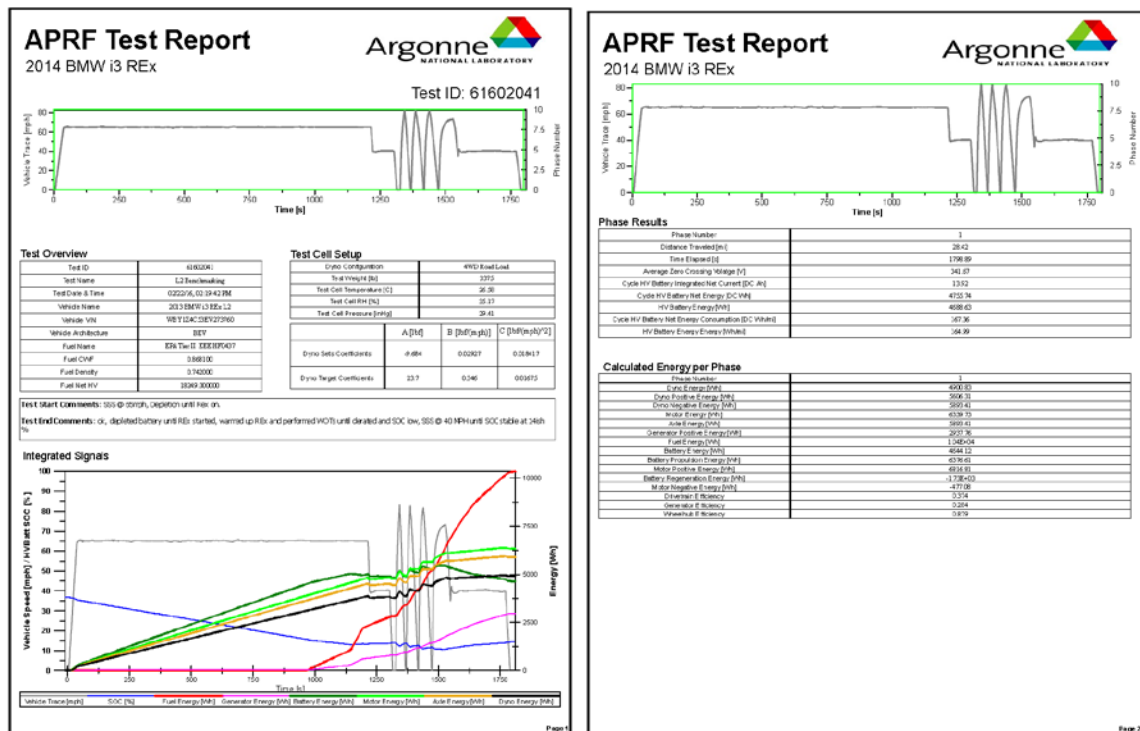


Figure III-96: Example of the APRF single cycle report

PHEV Full Charge Test Reporting

Full charge tests are often performed on plug in hybrid vehicles to provide an understanding of how the vehicles powertrain blends electric and hybrid operation. This operation dictates the energy savings potential of the specific plug in hybrid, dependent on the vehicle demands for that specific driving cycle.

A summary report has been developed to display this operation of plug in hybrid vehicles, and calculate specific quantities from the SAE J1711 standard, such as the charge depleting range, distance to a transition cycle, and distance at the first engine start. The report also provides vehicle energy consumption, from both fuel and electricity on a per cycle and per mile basis, in a tabulated form. As this report will be generated for most plug in hybrid vehicles currently on the market from the independent test data from the APRF, it will act as a useful reference for plug in hybrid operation at a range of temperatures and energy demands. An example of this report is displayed in Figure III-97.

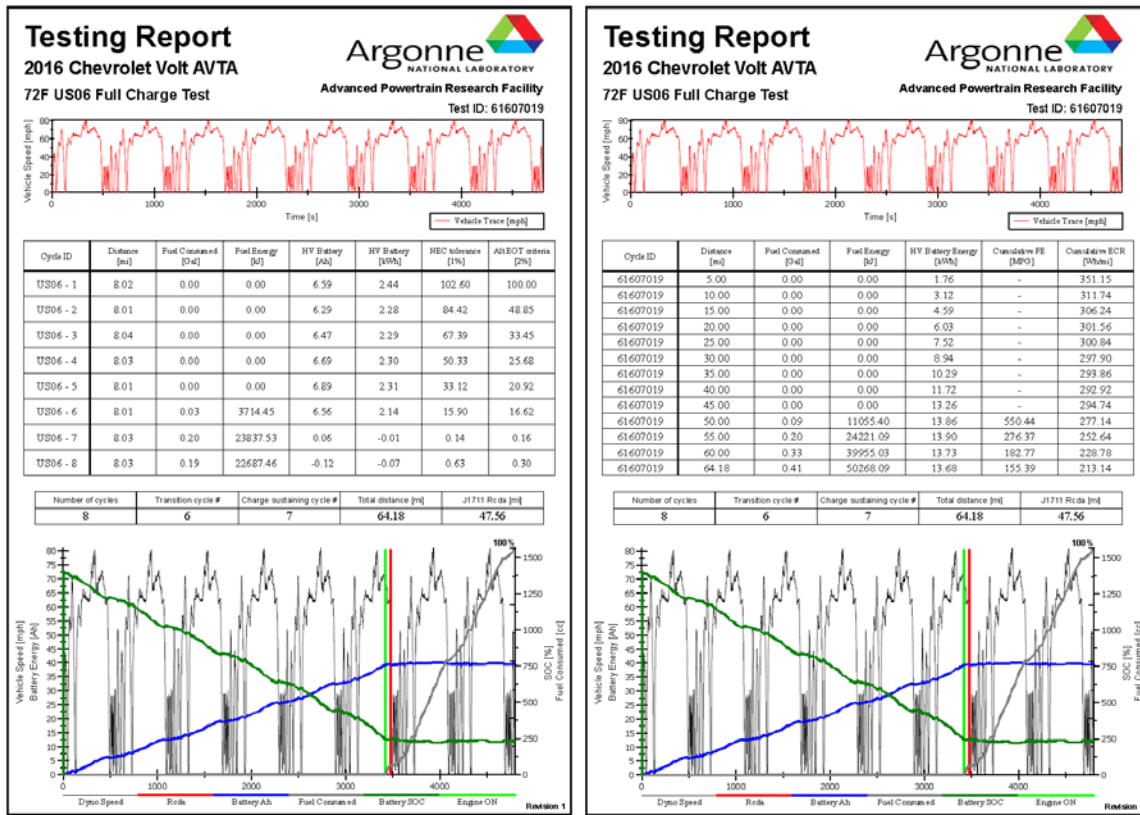


Figure III-97: Example of a Full Charge Test (FCT) summaries for PHEV's

Electric Vehicle Charge Reporting

The APRF testing provides data on charging. In order to properly quantify the energy use impacts of electric vehicles on domestic energy use in the future, energy use should be considered from its development to end use. In addition to measuring a vehicles energy use while driving, the APRF has been capturing data during charging. Instrumentation used during drive cycle operation has been utilized during these tests, providing the ability to determine energy consumption from the supply point to the vehicles energy storage system.

A summary report was developed to provide a condensed analysis of energy use during a vehicles charge. These "Charge Reports" summarize the test cell conditions seen by the vehicle during the charge event, give an overview of the vehicle on tests, and provide insight into vehicle energy use and efficiency, by component. Additionally, they bring in key parameters from the prior days driving, such as prior testing consumption in Wh, and Ah. A summary a recharge report is shown in Figure III-98.

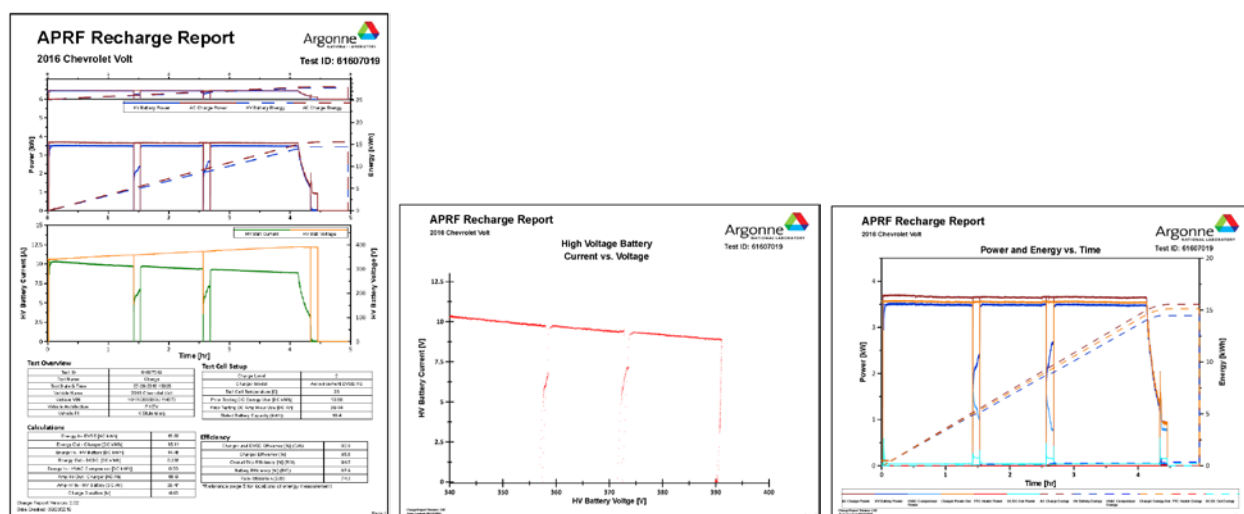


Figure III-98: Example sheets from an APRF Recharge Report

Conclusions

The APRF benchmarked a range of advanced technology vehicles. The 2016 Chevrolet Volt and the 2015 BMW i3 REx provide two different approaches to battery range extender vehicles. The Mercedes Benz B-class electric vehicle integrated range extending charging mode. The added energy consumption in cold temperatures is still a challenge for electric vehicles. The Chevrolet Impala bi-fuel demonstrates the tailpipe CO₂ reduction potential of natural gas. The test results and analyses were distributed through several mechanisms such as reports, presentations, and sharing of raw data. Several new analysis routines accelerate analysis tasks and improved the quality of data shared with DOE partners and the public. Finally, the laboratory benchmark data and the test vehicles enabled the development of several automotive testing standards, an active transmission warm up project, research in the connected and automated vehicle world, and a study focusing on a comparison of real world vs certification performance of blended PHEVs. For more in-depth work regarding this and many additional advanced vehicles, the reader is pointed toward the Argonne Downloadable Dynamometer Database at www.anl.gov/D3.

III.5.C. Products

Presentations/Publications/Patents

1. Henning Lohse-Busch, "Off-Cycle Factors for Advanced Vehicle (xEV) Range and Energy Consumption", SAE 2015 Government/Industry Meeting, Washington DC, January 21-23, 2015
2. Henning Lohse-Busch, "Vehicle Electrification Increases Efficiency and Consumption Sensitivity", SAE ICE2015 12th International Conference on Engine and Vehicles, Keynote speech, Capri, Italy September 13-17, 2015
3. Namwook Kim, Jongryeol Jeong, Aymeric Rousseau, Henning Lohse-Busch, "Control Analysis and Thermal Model Development for Plug-In Hybrid Electric Vehicles", SAE Journal Article, 2015-01-1157
4. Jay Anderson, Scott Miers, Thomas Wallner, Kevin Stutenberg, Henning Lohse-Busch, Michael Duoba, "Performance and Efficiency Assessment of a Production CNG Vehicle Compared to Its Gasoline Counterpart", SAE Technical Paper 2014-01-2694
5. Namwook Kim, Aymeric Rousseau, Daeheung Lee, Henning Lohse-Busch, "Thermal Model Development and Validation for 2010 Toyota Prius", SAE Technical Paper 2014-01-1784
6. Namdoo Kim, Aymeric Rousseau, Henning Lohse-Busch, "Advanced Automatic Transmission Model Validation Using Dynamometer Test Data", SAE Technical Paper 2014-01-1778
7. Jake Bucher, Thomas Bradley, Henning Lohse-Busch, Eric Rask, "Analyzing the Energy Consumption Variation during Chassis Dynamometer Testing of Conventional, Hybrid Electric, and Battery Electric Vehicles", SAE Journal Article 2014-01-1805

III.6. Road and Lab Coordinated Assessment of Active Transmission Warm-up

Shawn Salisbury, Principal Investigator

Idaho National Laboratory
 P.O. Box 1625
 Idaho Falls, ID 83415
 Phone: (208) 526-3430; Fax: (208) 526-0828
 E-mail: Shawn.Salisbury@inl.gov

Eric Wood

National Renewable Energy Laboratory

Forrest Jehlik, Simeon Iliev

Argonne National Laboratory

Start Date: October 1, 2015
 End Date: September 30, 2016

III.6.A. Abstract

Objectives

Active transmission warm-up systems are recognized by the EPA to have fuel saving benefits that are not captured by standard fuel economy test methods. Vehicles with these systems receive a credit to reflect these fuel savings benefits. The credit is based upon several assumptions. This project uses dynamometer and on-road testing of several vehicles, coupled with modeling and simulation, to determine the real-world benefit of active transmission warm-up.

Accomplishments

- Dynamometer testing of a 2011 Ford Fusion was performed at ANL's APRF. A custom test plan was developed, including standardized drive cycles to understand vehicle-level fuel economy, as well as steady state speed tests used to provide data for a thermally sensitive transmission efficiency map. Testing was also performed with the transmission pre-heated to have an initial understanding of the effects of active transmission warm-up systems.
- From the 2011 Ford Fusion testing, a thermally sensitive vehicle model was created, and an initial active transmission warm-up model was developed. The vehicle model was simulated over standardized fuel economy testing and real-world drive cycles from the NREL Transportation Secure Data Center to understand the real-world fuel economy benefit that would be seen by the 2011 Ford Fusion with a hypothetical transmission warm-up system.
- On-road and dynamometer testing was completed on production Ram 1500 pickup trucks equipped with the active transmission warm-up system. This testing provided data that will be used to calibrate the active transmission warm-up model to provide simulation results that are more representative of production vehicles. This testing also highlighted that system implementation is highly important, as the active warm-up systems had differences between the truck on which dynamometer testing was conducted and the truck on which on-road testing was conducted.

Future Achievements

- A production 2015 Ford Taurus equipped with an active transmission warm-up system will undergo dynamometer and on-road testing to provide further information on system operation and benefit. The results of this testing will provide a more complete picture of active warm-up systems in current production vehicles. This will be used to refine the active warm-up operation in the vehicle model for more accurate simulation results.
- Present project findings to the DOE Fuel Economy Working Group.

III.6.B. Technical Discussion

Background

The Environmental Protection Agency (EPA) and National Highway Traffic Safety Administration (NHTSA) Corporate Average Fuel Economy (CAFE) program for 2012-2025 fuel economy and greenhouse gas standards calls for 4-5% annual improvement. By 2025, these improvements equate to 54.5 MPG on the unadjusted 2-cycle test method. In the final standard, the EPA recognize that certain technologies yield fuel economy improvements in the real world that would not be captured during standard EPA fuel economy test procedures. Vehicles using these "off-cycle" technologies are granted emissions and fuel economy credits. Vehicle manufacturers have directed significant funding and effort toward developing and deploying these technologies in the US in order to increase their fleet fuel economy.

There is strong interest in both government and industry to understand the fuel-saving potential of technologies that are difficult to assess with standard laboratory certification cycles. More specifically, the Department of Energy (DOE) and regulatory bodies, like the EPA, want to maximize real-world fuel savings, and manufacturers want to get credit for actual fuel savings achieved.

Introduction

A technology for which off-cycle credits are currently granted is active transmission warm-up. The active transmission warm-up systems in currently available production vehicles use a heat exchanger to transfer heat from the engine coolant to the transmission oil. The technology reduces the amount of time spent driving with the transmission oil below normal operating temperature, a condition known to decrease transmission efficiency. The major benefit of this technology would be realized at temperatures below the temperature of EPA testing, so an efficiency credit is granted for vehicles utilizing the technology.

The derivation of the credit for active transmission warm-up is documented by the "Joint Technical Support Document: Final Rulemaking for 2017-2025 Light-Duty Vehicle Greenhouse Gas Emission Standards and Corporate Average Fuel Economy Standards". Using a simulation study performed by Ricardo, as well as a number of assumptions, the efficiency gains are estimated at 0.58%. This translates into absolute benefits of 1.5 gCO₂/mile for cars and 3.2 gCO₂/mile for light-duty trucks.

Existing DOE laboratories have the capability to perform rigorous engineering evaluation of off-cycle fuel savings potential using laboratory testing, on-road testing, real-world drive cycle analysis, and simulation. This project is performed in collaboration between Idaho National Laboratory (INL), Argonne National Laboratory (ANL), and the National Renewable Energy Laboratory (NREL), to assess the real-world fuel saving benefit of active transmission warm-up systems at a national level.

Approach

The Road and Lab Coordinated Assessment of Active Transmission Warm-up project includes experimental vehicle chassis dynamometer and on-road tests conducted over a wide range of temperatures and loads. These tests are used to develop simplified models from the experimental data, which are then used to demonstrate real-world economy over a broad range of drive cycles and ambient temperatures.

Vehicle Dynamometer Testing

All dynamometer testing for this project is performed at ANL in the Advanced Powertrain Research Facility (APRF). The first portion of this project involved testing of a 2011 Ford Fusion that had been fully instrumented for previous projects at ANL. The instrumentation can be seen in Figure III-99. A test plan was developed with standardized drive cycles to capture vehicle fuel efficiency as well as steady state speed tests to determine transmission efficiency across varying operating speeds, torques, gears, and torque converter states as the operating temperature increases. This vehicle does not have a transmission warm-up system, but a portion of the testing was performed with the transmission pre-warmed prior to the testing to provide an initial understanding of active transmission warm-up benefit. The pre-warming was achieved with electric transmission heating pads used to raise the transmission temperature prior to the start of the test.

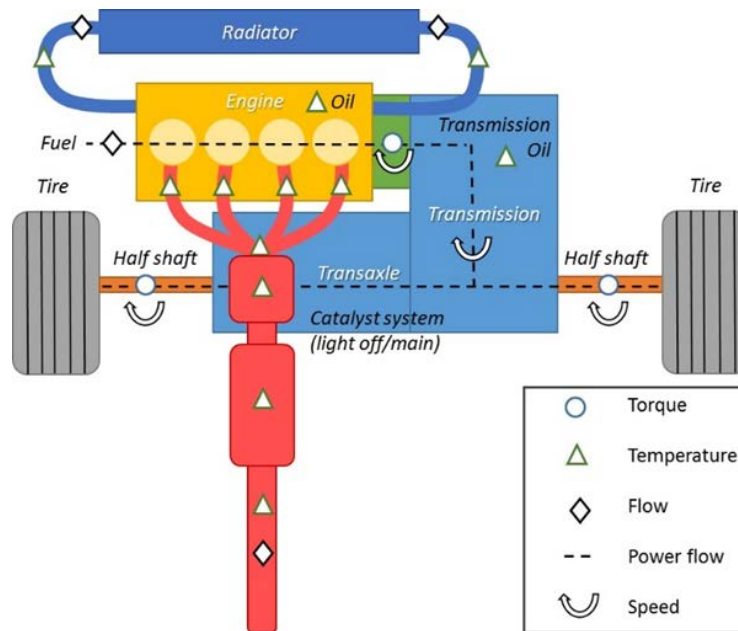


Figure III-99: Diagram of 2011 Ford Fusion drivetrain and sensors installed on the vehicle.

ANL

The project also includes dynamometer testing of two production vehicles equipped with active transmission warm-up systems. Each vehicle is tested on a series of standardized drive cycles. Approximately half of the tests have the transmission warm-up system active, and the remaining tests are performed with the system manually disabled. Testing occurs in a temperature-controlled test cell at 72°F and 20°F so off-cycle fuel economy benefits of active transmission warm-up can be determined directly. In addition, the transmission temperature profiles with active warm-up can be used to calibrate the thermally sensitive vehicle model. This testing has been completed for a 2015 Ram 1500 pickup and is currently underway for a 2015 Ford Taurus.

On-Road Vehicle Testing

The same production vehicle models tested on the dyno undergo on-road testing at INL on the roads in and around Idaho Falls, Idaho. The vehicles drive a prescribed route a number of times over the course of several weeks to capture operation in a wide range of operating temperatures. Half of the test drives are performed with the active transmission warm-up system enabled, and the rest with the system manually disabled. CAN data is collected and analyzed for each test drive to determine fuel economy and transmission oil temperature profiles for each test. As of this writing, the 2015 Ram 1500 pickup truck has been tested, and the 2015 Ford Taurus is to be tested after dynamometer testing is complete. Figure III-100 shows the method used to disable the active transmission warm-up system on the 2015 Ram 1500, which involves clamping off the line that sends hot engine coolant to the transmission oil heat exchanger.

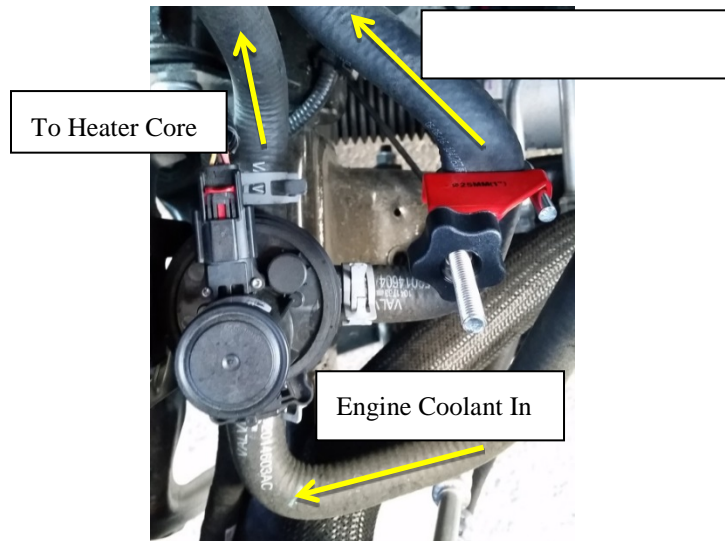


Figure III-100: Engine coolant routing from the engine block to the transmission heater. The red fluid line clamp in the photo is used to stop coolant flow and disable the active transmission warm-up operation.

INL

Modeling and Simulation

Using the results of dynamometer testing, a vehicle model was created to capture the effect of transmission warming of the 2011 Ford Fusion. The results of the testing were used to calibrate a simplified response surface and build a lumped parameter thermal model to describe the transmission efficiency and thermal response relative to any given speed, load, and ambient temperature input. This model, especially the operation of the transmission warm-up system, is then calibrated and refined using the data collected during the production vehicle testing.

The thermally sensitive vehicle model is simulated over millions of miles of real-world driving in various environmental conditions. The results of the simulations are aggregated by road type and ambient temperature to generate average fuel consumption rates for the full range of road type and ambient temperature combinations, a sample of which is shown in Figure III-101. These average fuel consumption values are weighted using vehicle miles traveled data from the Federal Highway Administration’s Highway Performance Monitoring System to calculate a national average fuel economy. This process is conducted twice using the vehicle model with and without active transmission warm-up in order to understand its impacts on a national level.

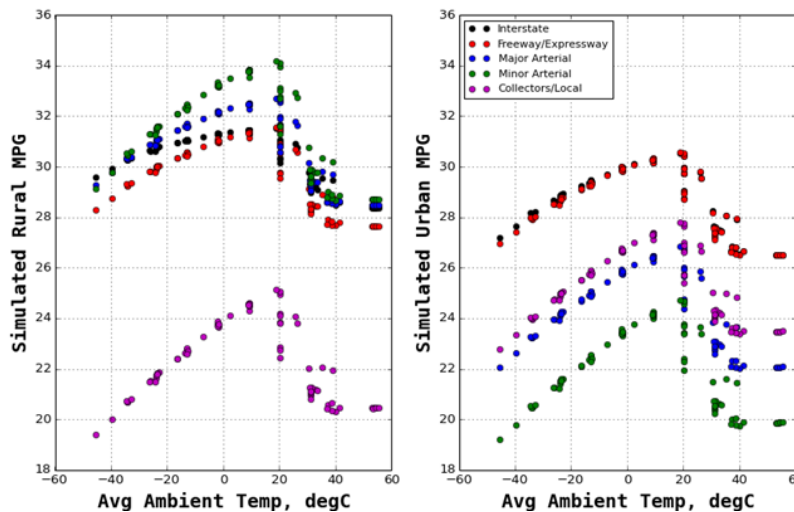


Figure III-101: Sample fuel economy variation by road type and ambient temperature.

NREL

Results

From the initial testing of the 2011 Fusion, a vehicle model was developed that included a transmission model with thermally sensitive mechanical efficiency, shift schedule, and torque converter control. A hypothetical active transmission warm-up model was also added to the model based upon testing with the transmission pre-warmed. Figure III-102 shows a simulation of back-to-back UDDS cycles and the resulting temperature profiles of different vehicle components, including transmission oil temperature with and without active warm-up.

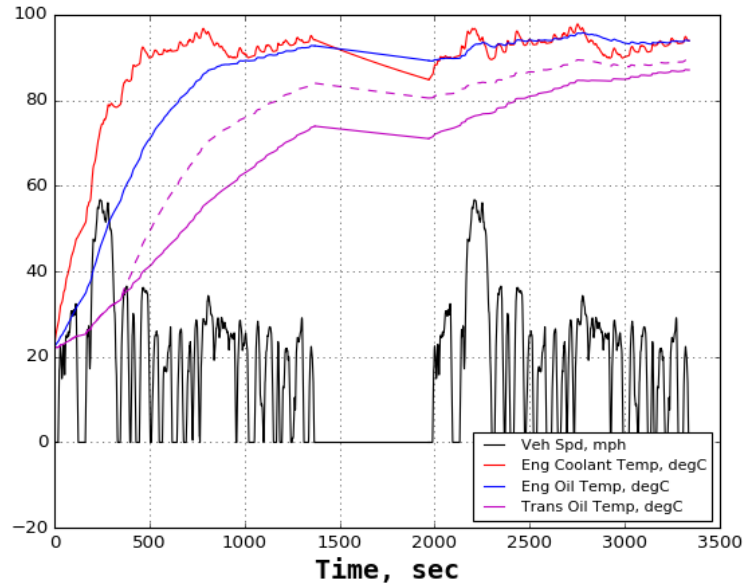


Figure III-102: The simulated operation of the thermally sensitive vehicle model over two consecutive UDDS cycles. The magenta lines show the difference between no transmission warming, solid line, and active warming, dashed line.

NREL

These models of the Fusion with and without active warm-up were then simulated on the EPA certification drive cycles as well as real world cycles from NREL’s Transportation Secure Data Center. The results of these simulations, as well as the results from the dynamometer testing of the actual vehicle are shown in Table III-20.

Table III-20: Results of dynamometer testing and model simulation of 2011 Ford Fusion with pre-warmed transmission and hypothetical active warm-up system, respectively. A positive fuel economy benefit corresponds to a decrease in fuel use.

Vehicle	Test	Ambient Temp, °C	Start Condition	Fuel Economy Benefit
2011 Ford Fusion (w/ APRF transmission preheating)	UDDSx1	+22°C	Cold Start	+0.96%
	US06x1	+22°C	Cold Start	+0.32%
	UDDSx1	-7°C	Cold Start	+2.46%
	US06x1	-7°C	Cold Start	+6.53%
2011 Ford Fusion (w/ modeled active transmission heating)	EPA 2-cycle	+22°C	Mixed	+0.37%
	EPA 5-cycle	Mixed	Mixed	+0.36%
	Real world sims	Mixed	Mixed	+0.50%

During dynamometer testing at colder temperatures, there was a larger benefit of the active transmission warm-up system. On the US06 cycle at 7°C, the Fusion’s fuel economy increased 6.5% due to pre-heating the transmission. In all dynamometer test cases, including at warm ambient temperature, active transmission warm-up provided a fuel economy benefit. Due to this, it is necessary to compare the real world benefit to that of the on-cycle certification testing to understand the true “off-cycle” benefit—the real-world “off cycle” credit will be the difference between the two. In the case of the Fusion with a hypothetical transmission warm-up, the off-cycle benefit would be estimated at 0.14% (0.5% real world benefit minus 0.36% on-cycle benefit).

After testing of both production vehicles is complete, the model will be adjusted and calibrated based upon the testing results, especially the modeled operation of the active warm-up system. The on-road and dynamometer testing of the Ram 1500 pickup truck yielded interesting results due to different implementations of the active warm-up system. The truck tested on the dynamometer at the APRF was a 2016 Ram 1500 with a 5.7L V8, and the active warm-up system was thermostatically controlled. When the engine coolant reaches operating temperature, the thermostat opens so coolant can flow to the transmission oil heat exchanger. The transmission oil temperature profiles of this vehicle with and without active transmission warm-up at an ambient temperature of 22°C can be seen in Figure III-103.

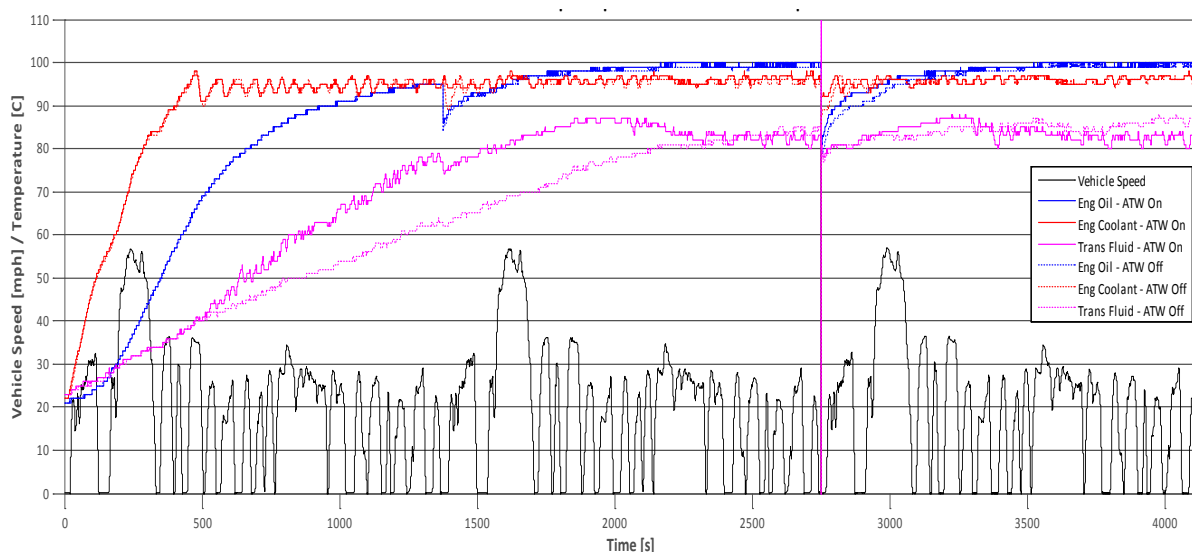


Figure III-103: 2016 Ram 1500 component temperatures during dynamometer testing over three consecutive UDDS cycles with active transmission warm-up on and disabled. Transmission temperature is shown in magenta, with the solid line representing active warm-up on, and the dotted line representing warm-up disabled.
ANL

The difference in transmission oil temperature between tests with the active warm-up system on and off for the 2016 Ram is fairly small. In the specific tests from the above figure, the maximum difference between the transmission temperatures is 20°C. The fuel economy benefits from the 2016 Ram tests, summarized in were variable and sometimes negative, meaning the fuel use was higher when the warm-up system was active. This could be due to variability in testing, active warm-up system implementation, or a number of other factors.

Table III-21: Results of 2016 Ram 1500 dynamometer testing at various temperatures to determine the fuel economy benefit of active transmission warm-up. A positive fuel economy benefit corresponds to a decrease in fuel use due to active transmission warm-up.

Vehicle	Test	Ambient Temp, °C	Start Condition	Fuel Economy Benefit
2015 Dodge Ram (w/ active transmission heating)	UDDSx1	+22°C	Cold Start	+0.75%
	UDDSx1	-7°C	Cold Start	-0.70%
	US06x1	-7°C	Cold Start	-3.25%

ANL

The on-road Ram testing used a 2015 Ram 1500 that had the same drivetrain as the vehicle tested on the dynamometer, but had a different implementation of active transmission warm-up. The road tested truck had a 3-way valve that could modulate the flow of engine coolant between the heater core and transmission heater at any point. This implementation allowed the transmission oil to be heated much quicker. The two tests shown in Figure III-104 were conducted at similar ambient temperatures, and the transmission was significantly colder during tests when the active warm-up system was disabled.

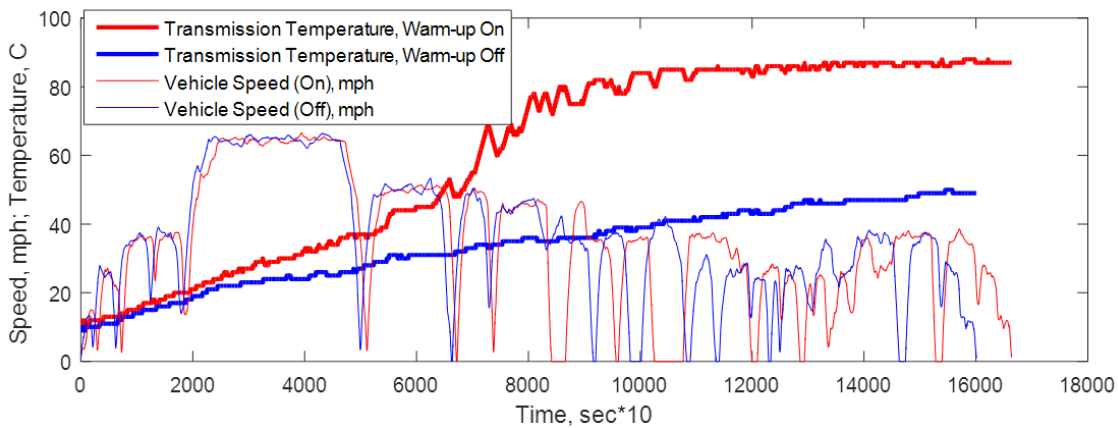


Figure III-104: Results of on-road testing from two tests at approximately the same ambient temperature. The thick red and blue lines show transmission oil temperature with active warm-up on and disabled, respectively.

INL

Fuel economy was calculated for each test run with the truck, but a difference between active and disabled transmission warm-up could not be determined. The variability of on-road testing can be large, and differences of a few percent can easily become lost in that variability.

The differences between the active warm-up system implementation from the two trucks led to very different transmission temperature profiles, and these two systems could have very different fuel economy benefits. Testing of the 2015 Ford Taurus will provide a more complete understanding of the implementations and operations of active warming systems available in today’s production vehicles. This understanding will be used to calibrate the vehicle model and its transmission warm-up profiles to better understand the fuel saving capability of active warm-up systems.

Conclusions

Researchers from three national labs, INL, ANL, and NREL, have collaborated to perform on-road and dynamometer testing of several vehicles to develop thermally sensitive models capable of simulating the real-world fuel economy benefit of active transmission warm-up systems. The results of testing and simulation

performed so far have suggested that active transmission warm-up does have a fuel economy benefit, but current results represent a single implementation of the system in a single vehicle. Testing of production vehicles with active transmission warm-up systems is currently underway to understand the implementation and operation of those systems. This testing will be used to build a more representative active warm-up model and provide more accurate results. Results of the final simulations will be presented to the DOE Fuel Economy Working Group.

III.6.C. Products

Presentations/Publications/Patents

1. “Road and Lab Coordinated Assessment of Active Transmission Warm-up.” Idaho National Laboratory, Argonne National Laboratory, National Renewable Energy Laboratory, INL/MIS-16-39824.

IV. Modeling and Simulation

IV.1. Evaluation of Dynamic Wireless Charging Demand

Jan-Mou Li, Principal Investigator

Oak Ridge National Laboratory
2360 Cherahala Boulevard
Knoxville, TN 37932
Phone: (865) 946-1461
E-mail: lij3@ornl.gov

David Anderson, DOE Program Manager

Vehicle Systems
Phone: (202) 287-5688
E-mail: David.Anderson@ee.doe.gov

Start Date: October 1, 2015
End Date: September 30, 2016

IV.1.A. Abstract

Objectives

This project aims to accelerate future deployment of EV and needed infrastructure through a better understanding of dynamic wireless charging demand. Results generated from this project should be able to facilitate:

- An optimal investment of dynamic wireless charging (DWC) infrastructure for charging-in-motion services,
- Extension of battery lifespan and reduction of battery size while increasing driving range simultaneously, and
- Demand response of smart grid application

Accomplishments

A novel traffic-based power demand (TBPD) framework to identify where the DWC infrastructure has better to be deployed is established. Advantages of this framework include

- Not only numbers and types of vehicle but also their spatial distribution of power demands are taken into consideration for the optimization;
- Both travel (from point to point) and parking (in between travels) can be simulated for the charging demand estimation;
- Directional power demand can be estimated.

Future Achievements

This project has been concluded at the end of FY16.

IV.1.B. Technical Discussion

Background

The services of charging-in-motion (CIM) require DWC infrastructure deployed on public roads to extend battery lifespan and reduce battery sizes while increasing driving range simultaneously. Since it would be financially infeasible to have such investments serving only few vehicles, estimation of power demand in real world applications will be valuable to the deployment. We develop a novel traffic-based power demand (TBPD) framework to estimate the demand since not only number and type of vehicles but also their spatial distribution of power demands have to be considered for the optimization. Monte Carlo simulations are incorporated into the proposed framework to estimate both number and type of vehicles as well as their speed profiles in a road network. Spatial distribution of power demands is derived with the simulated speed profiles and lays a foundation for the optimization. An example of applying the proposed framework in a corridor in Chattanooga, TN is demonstrated for further discussion. Based on the power demand estimation, it is found that road segments between slightly upstream to and farther downstream from a stop line are ideal candidates to server the purpose.

Introduction

Electric vehicle (EV) is a promising option for emission reduction from the transportation sector while growing the economic. However, price and limited driving range are still well-accepted factors preventing EV from mass adoption. Dynamic wireless charging (DWC) technology [1-8] enables EVs to be charging-in-motion (CIM). Even though the concept remains almost the same as discussed in [1], contemporary developments in DWC technology (e.g. [2] and [3]) have been evolved significantly. DWC technology aims to charge EV simultaneously while the battery pack is discharging for driving. Such a capability enables smaller operating voltage window that can increase life span of battery, and allows us to use a smaller battery (energy) for a same service level or, at least theoretically, to reach unlimited driving range as suggested in [4] and [5]. These features address the two barriers of EV adoption, i.e. cost of EV and range anxiety, that are essential to growth of EV penetration.

To protect battery and to extend its life span, modern EVs have some state of charge (SoC) management logic [9-12] to control charging and discharging within a designated voltage range, similar to the area between dashed lines shown in Figure IV-1 [9]. It shows a voltage profile of a half cell consisting of LiFePO₄ and lithium metal as the electrodes. The region between dashed lines is the designated operational range of a battery. The range could be varied depending on the application and battery materials. It is preferred to charge and discharge batteries within this region for two reasons: 1) majority of the battery energy is inside this region and 2) structure of electrode materials is less stable outside this region. That is, the cut-off voltage has better to be controlled between the upper bound (3.6V in Figure IV-1) and lower bound (3.3V in Figure IV-1) by a battery management system which benefits the battery calendar life albeit battery underutilization. As an example, Xie et al. [10] proposed a charging algorithm that reduces SoC swing and average SoC level of the battery array, which has been proven helpful in extending battery bank cycle life. Both Kaneko et al. [11] and Lacey et al. [12] reinforced that the lower the average SOC, the lower the degradation of lithium ion cells.

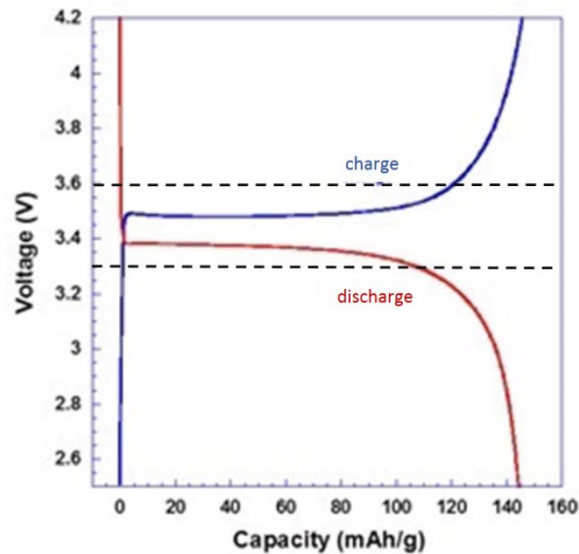


Figure IV-1: Voltage curve versus battery capacity [9]

Estimation of driving range extension with different designs of DWC for an individual EV can be found in literature. According to their analysis on three inductive power transfer (IPT) configurations in consideration of traffic intensity (in terms of speed), power demand and vehicle speed, Yilmaz et al. [6] suggested that a spaced loop configuration can drastically increase coupling between roadbed and pickup coils. Smaller loop sizes were preferred because that can reduce the supply voltage requirements and the magnetization reactive power.

Standard speed profiles (e.g. UDDS in [4] and [8], HWFET and VAIL2NREL in [4], JC08, HWFET2, and MEEDC in [8]) or those from test tracks (e.g. CU-ICAR in [7]) were commonly used for evaluation of driving range extension. With optimization for three vehicles running under a same driving cycle, Lukic et al. [4] suggested that if there is sufficient IPT track coverage the consumer could be travelling unlimited distances without the need to stop for charge. They suggested which portion of the selected driving schedules should be served with IPT tracks. To map the temporary-based suggestion onto actual road network can be challenging. It is also unclear about how their optimization algorithm can work with vehicles driving individually, especially not following a same driving cycle.

Assuming the maximum energy transfer can be achieved at the location with lowest average vehicle speed, Lorico et al. [7] proposed an optimization algorithm to determine the location of lowest average vehicle speed for three driving cycles with a 500-meter IPT track. They reported increases in driving range of up to 31.6% and 85.7% with 20kW and 40kW IPT ratings respectively. That suggestion is somehow spatial-related but is still unclear about how the selected location can be aligned with lowest average speed segments of the three different driving cycles.

Chopra and Bauer [8] analyzed the effect with cases of idling and in-motion. It was found that up to 194% of range extensions could be achieved (with JC08) when 100% of idle time was spent to charge with a 10 kW contactless power transfer (CPT) system (in 80% efficiency). With a 40kW CPT system, 20% road coverage, and in 80% efficiency, 163% of range extensions could be achieved (with HWFET2). While these results were encouraging, its implement can be challenging because having 20% road covered with DWC systems will be expensive and it is not easy allocating the systems to where vehicles will stop for charging en route.

These studies all showed that the locations of DWC system need to be carefully considered to optimize the efficiency of energy transfer from road to vehicle. However, the approaches based on individual driving cycles may be insufficient to guide a real world deployment because such a system can't be optimized only for few, if any, vehicles that drive with designated driving cycles, not to mention that real world traffic is much more complicated than selected driving cycles.

To facilitate future deployment of DWC systems, a traffic-based power demand (TBPD) simulation framework is proposed in this paper for the demand analysis. Methods included in the framework are briefed in the next section. For a comparison, power demand and energy consumption of a standard driving cycle, i.e. LA92, and a selected speed profile from a traffic simulation are investigated. Potential allocation of DWC systems for a corridor in Chattanooga, TN is discussed based on power demand results from traffic simulations.

Approach

While DWC infrastructure can charge vehicles regardless their moving status, it has better to be allocated in the most demanded road segments. As reviewed previously, approaches with selected driving schedules were common found in literature but may be insufficient for the optimization of DWC investment because they can barely represent the demand in a road segment where DWC infrastructure would be built

Taking best SoC managing practices (as discussed in the introduction section) into consideration, we argue that the most demanded road segments can be located at where accelerations, instead of idling, occurred most frequently. Once DWC infrastructure is available at the location, energy spent on accelerating can be compensated from the infrastructure and then swing of SoC can further be controlled within an even smaller range. The candidate location should be considered with traffic instead of individual vehicles. That is, factors including how many and what types of vehicle travelling from origins to destinations as well as their interactions with the others and traffic controls in a road network have to be involved in the optimization because they all have influence on the acceleration behaviors.

A. Traffic Simulation

The newly proposed traffic-based power demand (TBPD) framework (as illustrated in Figure IV-2) derives the power demand based on driving schedules of every vehicle in traffic at a road segment/network considering travel demand, traffic composition, and traffic control. A basic idea behind the proposed framework is to mimic real world traffic and then to estimate power demand from vehicles in traffic at a study area. Several software packages are available for simulating traffic.

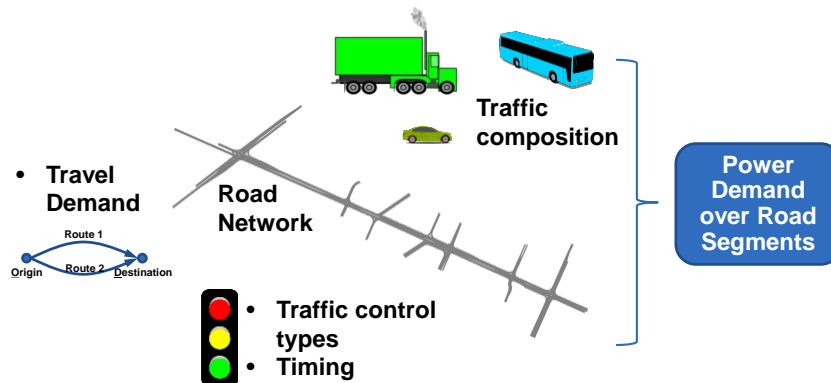


Figure IV-2: The traffic-based power demand (TBPD) framework

More technical details regarding traffic modeling can be found in [13]. Although it might be beyond scope of this paper, the traffic simulations have better been validated in order to have reliable results for a real world application. In addition to validation, Monte Carlo simulation technique [14] can also be required for a more general power demand distribution in the area.

B. Tractive Power

Among many factors having impacts on the power demand, traction should be the primary one. That is, traction to drive a vehicle is a key to determine quantity and rate of energy required under driving conditions. Tractive power can be estimated by a linear relation of base load (P_{base}), rolling resistance (P_{roll}), aerodynamic drag (P_{aero}), gravitational load (P_g), and inertial load (P_{inert}). Such a relation has been well

documented, for example in [15]. Assuming no regenerative brake and auxiliary load are involved, the power required to drive a vehicle can be simplified as,

$$\bar{P} = \frac{\int (P)^{P>0} dt}{\int t^{P>0} dt} \tag{1}$$

where

\bar{P} is the mean of tractive power when tractive power P is positive, and

$$P = P_{base} + P_{roll} + P_{aero} + P_g + P_{init}$$

C. Configurations of Demonstration

The demonstration of analysis with the TBPD framework reported here has been simplified to make validation by the other interested parties possible. Figure IV-3 shows geometry of the selected surface street segment in Chattanooga, Tennessee area. The road segment covers part of Shallowford Rd corridor across Interstate 75. Even though length of the Shallowford Rd segment is only about 1.3 km, it comprises seven signalized intersections.

VISSIM [16], a commercial software package, was used to conduct traffic simulation tasks for the demonstration. The package has capability to model a wide range of vehicle types but only a type of passenger car was modeled based on characteristics of an Accord described in [15] for the demonstration. The vehicle curb weight and coefficients for road load power estimation are listed in Table IV-1.



Figure IV-3: Geometry of the simulated corridor

Table IV-1: Parameters of vehicle for road load power estimation

Vehicle	Accord
Curb Weight (kg)	1,557
A Coefficient (N)	121.9
B Coefficient (N·s/m)	1.83
C Coefficient (N·s ² /m ²)	0.42

Since the road network consists of urban streets, Wiedemann 74 model [17] was applied to control car following behavior during the simulations. Vehicle movements at each intersection were calibrated with actual traffic counts collected on December 20, 2014. A coordinated ring barrier controller was modeled to regulate vehicle movements at those signalized intersections.

By varying random seeds that dominate randomness of stochastic processes in the simulation model, forty-two one-hour samples were drawn for the power estimation. For example, distributions of vehicle arrival and its interval will be different and then the associated traffic flow changes accordingly, when different random seeds are applied. Table IV-2 shows some statistics from results of the 42 Monte Carlo simulations. A total of 213,173 vehicles were simulated. Speed profiles for every vehicles simulated at the system within the hour were captured for estimation of power demand and energy consumption. Judging by the average energy efficiency, i.e. 0.3 kWh per km, the simulation results should be acceptable.

Table IV-2: Statistics from the Monte Carlo Simulations

	Average	Standard Error
Number of cars	5076	67.43
Distance travelled (meters)	740.86	5.72
Ave. Speed (km/hr)	31.07	0.37
Top speed (km/hr)	54.14	0.06
Energy efficiency (kWh/ km)	0.30	0.0068

Results

A. Potential Benefit of DWC Systems

For a comparison with potential benefits reported in literature, we investigated two driving schedules along with hypothetical DWC deployments. Similar to the idling case discussed in [8], a standard driving schedule, i.e. LA92 [18], was selected for demonstrating energy consumption and possible benefit DWC systems may offer. Compared to the FTP driving schedule, the LA92 has a higher top speed, a higher average speed, less idle time, fewer stops per mile, and a higher maximum rate of acceleration. Assuming DWC is available at every location where the test vehicle idled at least one second and the other conditions are all perfect, about 1 kWh (or 6 kWh) can be received from 20kW (or 100kWh) DWC systems along the 9.82 miles/1435 seconds journey.

Different types of dash types in Figure IV-4 represent associated energy profiles with or without charging from hypothetical DWC systems. Without charging en route, 2.66 kWh was consumed to drive an “Accord” car through the driving schedule and is represented by the red dash line in Figure IV-4. Only 1.85 kWh was needed if the car was charged with 20kW DWC systems while idling at least one second. The energy profile is represented by the green dash dot line in Figure IV-4. The purple square dot line in Figure IV-4 represents the energy profile in which it got charged with 100 kW DWC systems while idling at least one second. In that case, the EV’s energy storage system may have a 3 kWh gained from the DWC systems. That can be interpreted as a 100% increase in driving range.

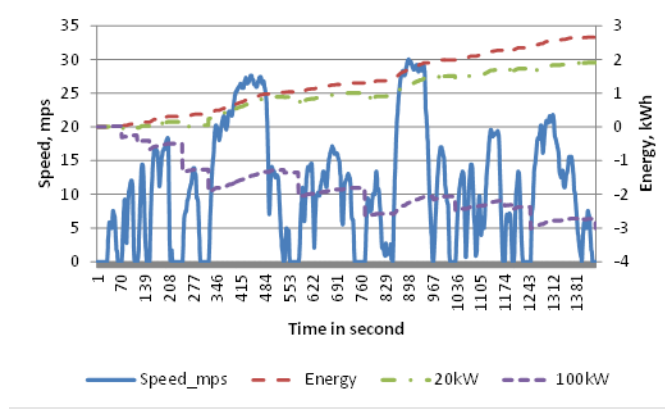


Figure IV-4: LA92 speed and energy profiles

With the same approach, Figure IV-5 show speed and energy profiles for a simulated car driving through the demonstration network. Duration for the car in the network was 142 seconds and it only idled once for three seconds. It drove 1.69 km with a top speed at 55.97 km/hr. 0.22 kWh was consumed to drive the car with the speed profile. The energy profile without CIM is represented by the red dash line in Figure IV-5. Slightly over 0.2 kWh was needed if the car was charged with a 20kW DWC system during the 3-second idling. The associated energy profile is represented by the green dash dot line in Figure IV-5. The purple square dot line in Figure IV-5 represents the energy profile in which the car got charged with a 100 kW DWC system during the 3-second idling. About 0.14 kWh was needed for that case.

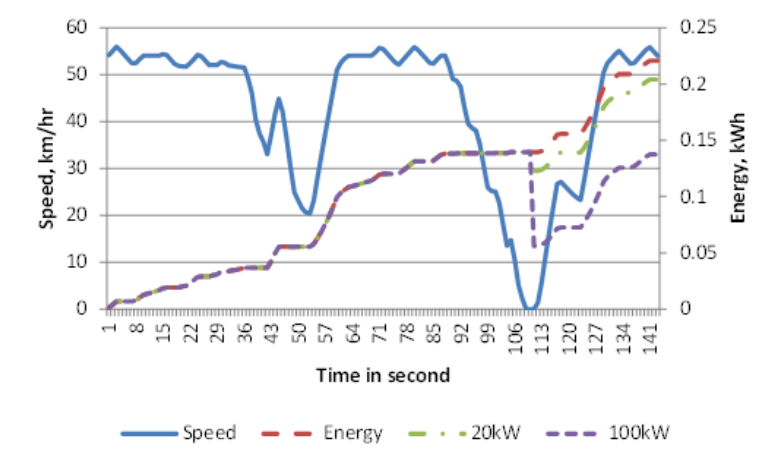


Figure IV-5: Speed and energy profiles of a simulated car charged at idling

B. Spatial Distribution of Simulated Power Demand and Discussion

A major advantage of the proposed TBPD framework is showing where the highest demands can be located in an area. As the example shown in Figure IV-5, DWC systems can help in restoring energy level to a certain degree while travelling through the driving schedule. The challenge is where DWC systems should be deployed in order to charge vehicles during the 3-second idling. Apparently, it would be very difficult to trace back where vehicles idled because that will change from time to time.

To address the challenge, the TBPD framework applies a weighted density approach to aggregate all estimated power demands across locations. Figure IV-6Figure 6 shows a vehicle density map weighted by tractive power of each vehicle based on results from the aforementioned 42 Monte Carlo simulations. The color map in Figure IV-6 represents the demand-weighted density from light yellow (low) to dark red (high).

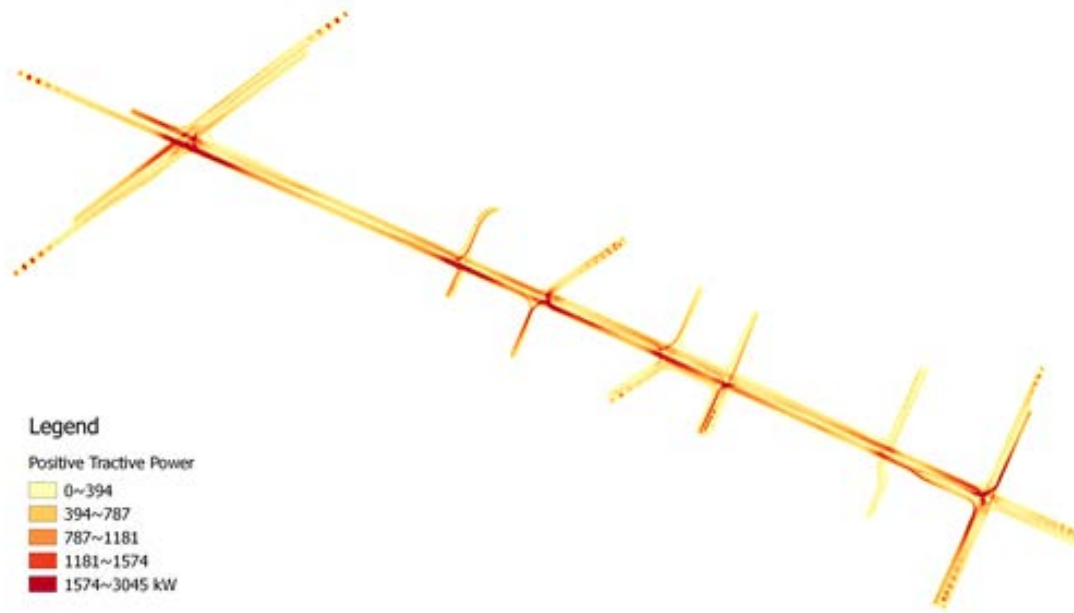


Figure IV-6: Spatial distribution of power demand

Numbers of high power demand location can first be observed from the map. They are of course directional. Those locations may be the best candidates for deployment of DWC systems because they are representing where vehicles applied most tractive power to drive through the network. Assuming DWC is available at five high power demand locations, i.e. eastbound of the left-most four intersections (92, 104, 75 and 56) and southbound of the very right intersection (51), energy profiles with the selected driving schedule can be shown in Figure IV-7. Numbers in the parenthesis represent lengths in meters of the DWC systems at the locations respectively.

Figure IV-7 indicates the simulated car, driving the same speed profile as shown in Figure IV-5, can almost keep a same level of SoC or even can gain about 0.56 kWh with DWC systems in 20kW or 100kW rates at the suggested locations. That is, a car can almost travel effortlessly through the driving schedule with the proposed 20kW DWC systems. With this driving schedule, a 250% increase in driving range may be interpreted if the 100kW DWC systems were in service.

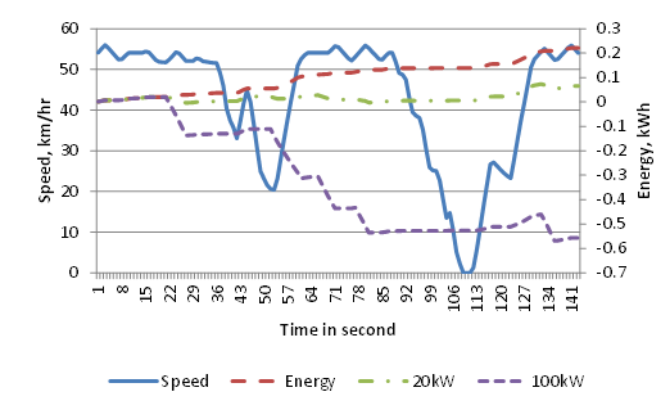


Figure IV-7: Speed and energy profiles of a simulated car charged along its route

It is worthwhile to notice that a major portion in each of those high power demand segments (shown in Figure IV-6) is downstream from a stop line. Those locations are where vehicles were accelerating (to their

desired speeds). It suggests that we may just use energy provided by DWC systems at those locations to accelerate the cars. Such a design may be able to further improve life span of EVs' battery pack.

Conclusions

A new framework to identify where the DWC infrastructure has better to be deployed is proposed. Considerations for the deployment are focused on number of vehicles and their power demands to drive through a study area. We demonstrate advantages of applying the proposed traffic-based power demand (TBPD) framework. It is clearly suggested that DWC systems should cover a certain distance downstream from the stop line. Not only driving range but also life span of battery pack can be increased while realizing this suggestion.

While the spatial distribution of power demand may help in designing DWC infrastructure, to integrate different DWC configurations for the optimization would provide more reliable insight to the deployment. To take the configuration into consideration can provide required information for a thorough cost analysis. On EV side, specification (especially capacity) of EVs' battery pack and their managing strategies should also be part of the optimization. Then an optimal size of battery pack with DWC deployment can be derived.

IV.1.C. Products

Presentations/Publications/Patents

1. Li, J.-M., List, G., and Mashayekhi, M., "Balancing Fuel Economy and Performance of Signalized Intersection - Assessment of Vehicle-Infrastructure Coordination," SAE 2016 World Congress and Exhibition, Detroit, Michigan, April 12-14, 2016.
2. Li, J.-M., J. Li, "Exploratory Spatial Distribution of Dynamic Wireless Charging Demand for EVs", IEEE PELS Workshop on Emerging Technologies: Wireless Power (2016 WoW), Knoxville, Tennessee, October 4-6, 2016.
3. Li, J.-M., "Improvement of Truck Performance with V2I connectivity at Signalized Intersections," SAE 2017 World Congress and Exhibition, Detroit, Michigan, April 4-6, 2017.

IV.1.D. References

1. J. G. Bolger, L. S. Ng, D. B. Turner and R. I. Wallace, "Testing a prototype inductive power coupling for an electric highway system," Vehicular Technology Conference, 1979. 29th IEEE, 1979, pp. 48-56.
2. J. Huh, and C.-T. Rim. "KAIST wireless electric vehicles-OLEV." SAE Technical Paper, No. 2011-39-7263. 2011.
3. O. C. Onar, J. M. Miller, S. L. Campbell, C. Coomer, C. P. White and L. E. Seiber, "A novel wireless power transfer for in-motion EV/PHEV charging," Applied Power Electronics Conference and Exposition (APEC), 2013 Twenty-Eighth Annual IEEE, Long Beach, CA, USA, 2013, pp. 3073-3080.
4. S.M. Lukic, M. Saunders, Z. Pantic, S. Hung, and J. Taiber, "Use of inductive power transfer for electric vehicles," 2010 IEEE Power and Energy Society General Meeting, 2010, pp.1-6.
5. H. H. Wu, A. Gilchrist, K. Sealy, P. Israelsen and J. Muhs, "A review on inductive charging for electric vehicles," 2011 IEEE International Electric Machines & Drives Conference (IEMDC), Niagara Falls, ON, 2011, pp. 143-147.
6. M. Yilmaz, V.T. Buyukdegirmenci, and P.T. Krein, "General design requirements and analysis of roadbed inductive power transfer system for dynamic electric vehicle charging," IEEE Transportation Electrification Conference and Expo (ITEC), 2012, pp.1-6.
7. A. Lorico, J. Taiber, and T. Yanni, "Effect of Inductive Power Technology Systems on Battery-Electric Vehicle Design," IECON 2011 - 37th Annual Conference on IEEE Industrial Electronics Society, 2011, pp.4563-4569.
8. S. Chopra, and P. Bauer. "Driving range extension of EV with on-road contactless power transfer—A case study," IEEE transactions on industrial electronics, vol. 60, no. 1, pp. 329-338, 2013.

9. J. Li, C. Rulison, J. Kiggans, C. Daniel, and D. L. Wood III, "Superior performance of LiFePO₄ aqueous dispersions via corona treatment and surface energy optimization," *J. Electrochem. Soc.* 159 (8), A1152-A1157, 2012.
10. Q. Xie, X. Lin, Y. Wang, M. Pedram, D. Shin and N. Chang, "State of health aware charge management in hybrid electrical energy storage systems," 2012 Design, Automation & Test in Europe Conference & Exhibition (DATE), Dresden, 2012, pp. 1060-1065.
11. G. Kaneko et al., "Analysis of degradation mechanism of lithium iron phosphate battery," *Electric Vehicle Symposium and Exhibition (EVS27)*, 2013 World, Barcelona, 2013, pp. 1-7.
12. G. Lacey and G. Putrus, "Controlling EV Charging Schedules: Supporting the Grid and Protecting Battery Life," *IEEE Vehicle Power and Propulsion Conference (VPPC)*, 2015, pp. 1-5.
13. E. Lieberman, and A. K. Rathi, "Traffic simulation," *Traffic flow theory*, 1997.
14. C. Z. Mooney, *Monte Carlo simulation*. Vol. 116. Sage Publications, 1997.
15. I. M. Berry, *The Effects of Driving Style and Vehicle Performance on the Real-World Fuel Consumption of U.S. Light-Duty Vehicles*, Master's thesis, Massachusetts Institute of Technology, Cambridge, Massachusetts, 2010.
16. PTV Group, *PTV VISSIM*, Version 8, 2016.
17. Wiedemann, R., *Simulation des Strassenverkehrsflusses*. Schriftenreihe des Instituts für Verkehrswesen der Universität Karlsruhe, Band 8, Karlsruhe, Germany. 1974.
18. U.S. Environmental Protection Agency, LA92 "Unified" Dynamometer Driving Schedule, <https://www.epa.gov/emission-standards-reference-guide/la92-unified-dynamometer-driving-schedule>. Accessed: April 15, 2016.

IV.2. Autonomie for Model Based System Engineering

Phillip Sharer, Principal Investigator

Argonne National Laboratory
9700 S Cass Avenue, Bldg. 362
Argonne, IL 60439
Phone: (630) 252-9739

David Anderson, DOE Program Manager

Office of Vehicle Technologies, U.S. Department of Energy
Phone: (202) 287-5688
E-mail: David.Anderson@ee.doe.gov

Start Date: October 1, 2016
End Date: September 30, 2016

IV.2.A. Abstract

Due to even stringent regulations, car manufacturer have to introduce new technologies in the market at an ever increasing rate. In addition, government agencies have had to assess the energy impact of a much large number of technologies and scenarios as part of their R&D portfolio. To do so, researchers and engineers have been increasingly relying on system simulation. The objective of the project is to continue to enhance and maintain Autonomie as needed to support the U.S. Department of Energy (DOE) and the user community as well as expand its ecosystem to assess new technologies (i.e., Connected and Automated Vehicles).

Objectives

- Enhance and maintain Autonomie as needed to support the U.S. Department of Energy (DOE) and the user community
- Expand Autonomie ecosystem

Accomplishments

- Released new versions of Autonomie (R15 and R15SP1) with large number of new features
- Model Based System Engineering (MBSE) Enhancements
Invented a way to select different workflows in Autonomie

Future Achievements

- Continue to enhance Autonomie to support DOE and technology transfer

IV.2.B. Technical Discussion

Background

Autonomie is a plug-and-play powertrain and vehicle model architecture and development environment that supports the rapid evaluation of new vehicle technologies to improve energy consumption through virtual design and analysis in a math-based simulation environment. Autonomie has an open architecture to support the rapid integration and analysis of powertrain/propulsion systems and technologies. This architecture allows rapid technology sorting and evaluation of energy consumption and performance under dynamic/transient testing conditions.

Introduction

To better support the U.S. Department of Energy (DOE) and its user community, several new features have been implemented in Autonomie. Some of the most significant accomplishments are described in this report.

Approach

There are always more ideas for new Autonomie features and enhancements than time to actually implement them. Feedback on which items to prioritize and include is collected in several ways.

First, Autonomie users register suggestions for improving the software or models by email, in person, or through our online issue-tracking system at www.Autonomie.net. Second, direct interaction with partners and sponsors while working on shared projects contributes to collecting new requirements. Finally, DOE studies often drive the improvement of existing capabilities and/or the development of new ones.

Model Based System Engineering (MBSE) enhancements focused on longer-term strategies for the future of vehicle modeling and simulation, such as an emphasis on parallelization for running larger number of simulations. Another emphasis was the integration of tools that, themselves, integrate tools, thereby increasing the breadth of the Autonomie ecosystem.

Results

New Releases

This new releases include multiple patches and usability enhancements that were selected based on user feedback, including:

- Large number of pre-defined vehicles (>150) across multiple vehicle classes, technologies...
- Modified licensing:
 - All licensing and support now done by Argonne, not Siemens
 - Added floating licenses installation (i.e., server based)
- Enhanced packaging:
 - New “light” version for students with limited features and vehicles
- Incorporated software links to third party tools:
 - Updated to run with Matlab R2016b
- Added import features:
 - Users no longer have to retype all of their signal information by hand again and again. They only have to select the signal from a dictionary, and all of the information is populated for them in the signal table.
 - This is also true for parameters.
- Migrated model improvements and new data from studies:
 - Micro hybrids and Integrated Starter Generator Hybrids Vehicle Propulsion Architecture braking strategies now command negative torque to the engine during braking
 - Added new pollutants post-processing to the GREET summary outputs: VOC, CO, PM10, PM2.5, NOx, Sox, BC, POC, CH4, and N2O
 - Added post processing to compute Net Present Value (NPV) and Real Cost of Ownership (RCO)
- Improved speed of performance
- Implemented over 20 other improvements and enhancements

Model Based System Engineering (MBSE) Enhancements

Expanding the Autonomie Workflow Framework and Adding New Workflows

The concept of workflows is part of the design philosophy of Autonomie. While Autonomie has had great success in supporting user-defined workflows for a single vehicle, many additional workflows exist, such as model verification and validation, Design of Failure Modes Analysis (DFMEA) analysis, vehicle validation and correlation, test data quality assurance, system-based hardware-in-the-loop, system-based software-in-the-loop, system-based model-in-the-loop, large-scale study, and large-scale data analysis. Numerous OEMs and even other government entities have used these workflows and would benefit if they were available in Autonomie. This project addresses these additional workflows by creating a new framework to support customized workflows that do not directly involve loading a single vehicle and running a simulation. Before these other workflows are addressed, compatibility with the current workflow must be maintained and demonstrated.

The user begins by choosing the MBSE workflow that matches their requirements (Figure IV-8). Workflows are divided into different categories. The main two are Developer and User.

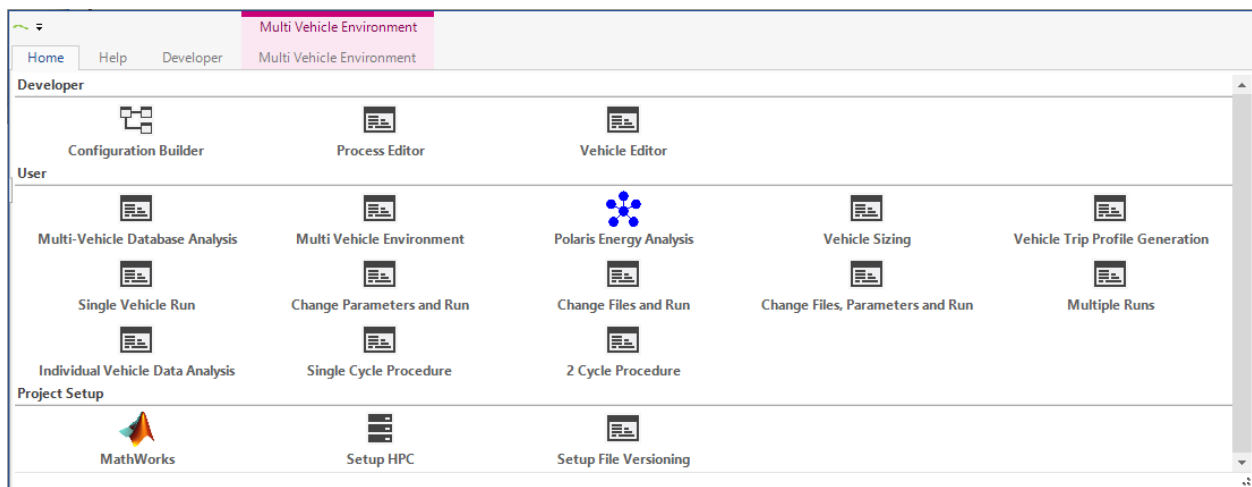


Figure IV-8: Autonomie Available and Future Workflows

For this example, a vehicle simulation on a cycle may be chosen. The workflow is loaded and Autonomie presents to the user a tiled view showing the steps in the current workflow. The workflow starts with Setup Matlab and then progresses to Select a Vehicle, then Initialize the Cycle, Run the Simulation, and finally Data Analysis. The workflow is clear and easy to grasp and informs the user on what steps are involved to accomplish the work. Much of the visual noise has been removed while the core functionality of the tool has been retained. The tiled view is shown in Figure IV-9. This single vehicle workflow was introduced before, but it was refactored this year to work with the new business logic developed for the multiple vehicle run workflow, which is the next workflow to be described. Also, different views were introduced for this workflow, along with a way to easily toggle between them.

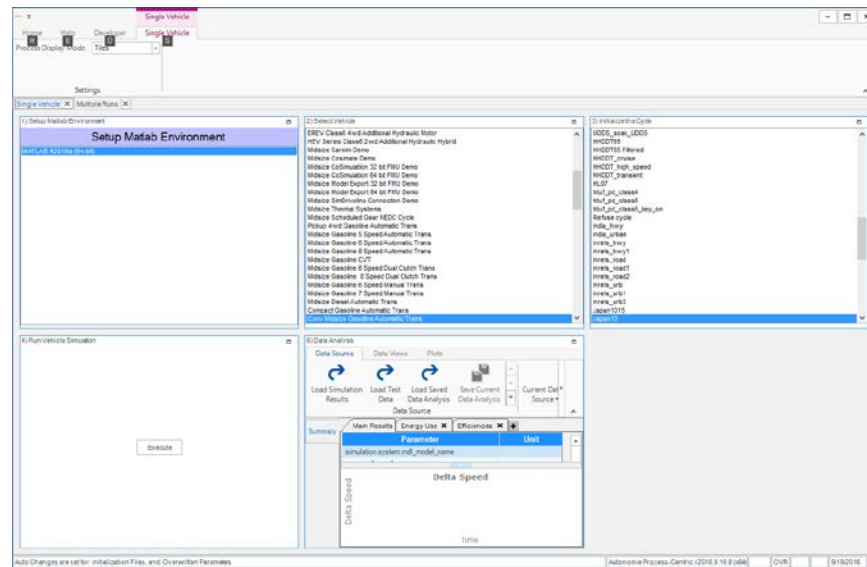


Figure IV-9: Autonomie Single Vehicle Run Titled View

As described previously, because of the way Autonomie is now architected, it is very easy to change from a tiled view to a tabbed view, which is helpful when the number of steps in a workflow is large (Figure IV-10).

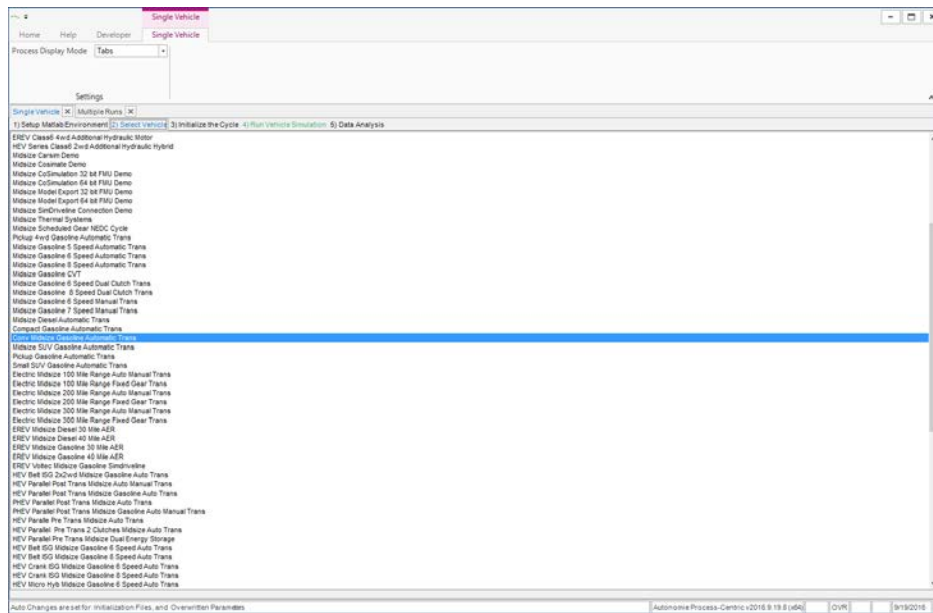


Figure IV-10: Autonomie Single Vehicle Run Tabbed View

This workflow can be extended to include modifying parameters, calibration files, models, and configurations with gradually increasing levels of complexity. The goal is to allow users to have a quick path to completing their work without having to deal with unnecessary complexity. To achieve that goal, we have essentially tailored the user interface to make it simpler and more accessible for users. Basic users have basic views of the vehicle, which expose only those options that they need and hide those they do not need, while developers have advanced views, which expose all the details of the vehicle. We made this modification in response to feedback from the user community and OEMs.

The next workflow is the Multivehicle Run. This workflow could not be implemented in legacy Autonomie because it always forced a user to choose a single vehicle and then deal with the minutia of setting up a single vehicle, even when the user wanted to run a large-scale study with many hundreds of vehicles. Legacy

Autonomie did not scale. The new user interface makes no such requirements on the user. From the start, this user interface was designed to run multiple vehicles. The user interface is shown in Figure IV-11.

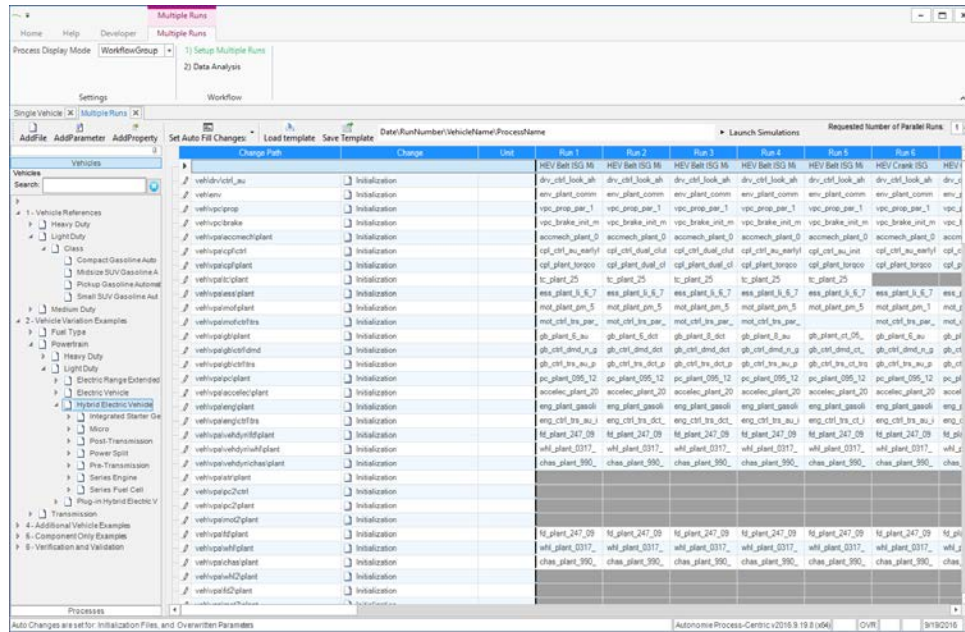


Figure IV-11: Autonomie Multi-Vehicle Run

This user interface and back-end business logic easily scale to hundreds of vehicles. A user can quickly set up a table of vehicles, change parameters and calibration files, and then run each vehicle on many different cycles and procedures. This user interface is ideal for setting up and running medium-scale studies. The methodology and lessons learned here will later be applied to the next level of user interface, which will design studies not at the vehicle level but at the assumption level. This will allow Autonomie to scale from running hundreds of vehicles to running hundreds of thousands of vehicles.

The last view is the Data Analysis workflow (Figure IV-12). This workflow has been redesigned from the ground up to work with the new version of Autonomie. The plotting has been rewritten and streamlined, and new types of plots have been added. These new plots include signal plots, for time-based values; parameter charts, such as bar charts, pie charts, and others for such parameters as energy; efficiency mass and cost; and new scientific plots, such as contour plots, which help users analyze the behavior of components during a simulation run.

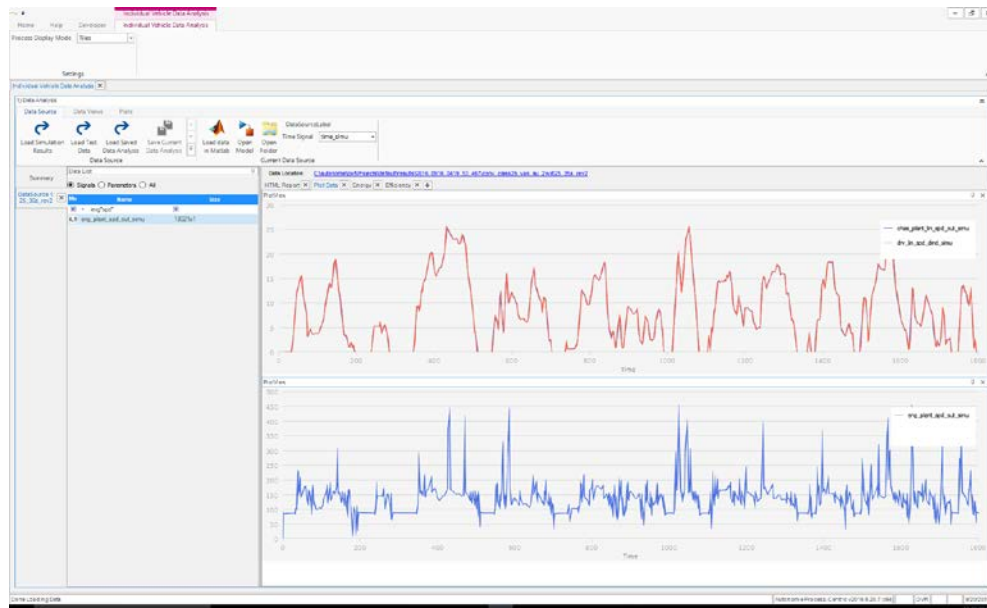


Figure IV-12: Autonomie Data Analysis Workflow

Conclusions

Several versions of Autonomie were released this year; these include numerous new features developed on the basis of the feedback from DOE and the user community. Autonomie for MBSE Workflows is a new future-looking Autonomie, which will let Autonomie scale and adapt to the changes in the industry as new technologies are investigated and added to the DOE research portfolio. For instance, more research is necessary to understand the effect Connected and Automated Vehicle (CAV) technologies will have on either increasing or reducing CO₂. The number of advanced vehicle technologies having a CO₂ impact is only increasing, and Autonomie needs to be capable of handling these new and emerging technologies to assist DOE in evaluating its own potential to improve these technologies and bring them to market.

IV.2.C. Products

- Autonomie REV 15 and REV15 Service Pack 1
- Autonomie for MBSE Workflows

Presentations/Publications/Patents

1. Moawad, A. Rousseau, P. Balaprakash, S. Wild, “**Novel Large Scale Simulation Process to Support DOT’s CAFÉ Modeling System,**” International Journal of Automotive Technology (IJAT), Paper No. 220150349, Nov. 2015
2. Rousseau, “**Plug & Play Architecture for System Simulation,**” SIA System Modeling Conference, Paris, May 2015.
3. Rousseau, S. Halbach, L. Michaels, N. Shidore, Na. Kim, N. Kim, D. Karbowski, M. Kropinski, “**Electric Drive Vehicle Development and Evaluation using System Simulation,**” Journal of the Society of Instrument and Control Engineers, Vol. 53, 2014 (www.sice.jp).
4. S. Pagerit, P. Sharer, A. Rousseau, “**Complex System Engineering Simulation through Co-Simulation,**” SAE 2014-01-1106, SAE World Congress, Detroit, April 2014.
5. N., Kim, A. Rousseau, “**Thermal Model Developments for Electrified Vehicles,**” EVS28, May 2015, Korea.
6. R. Vijayagopal, R. Chen, P. Sharer, S. Wild, A. Rousseau, “**Using Multi-Objective Optimization for Automotive Component Sizing,**” EVS28, May 2015, Korea.

7. R. Vijayagopal, A. Rousseau, **“System Analysis of Multiple Expert Tools,”** [SAE 2011-01-0754](#), SAE World Congress, Detroit, April 2011.
8. S. Halbach, P. Sharer, S. Pagerit, C. Folkerts, A. Rousseau, A., **“Model Architecture, Methods, and Interfaces for Efficient Math-Based Design and Simulation of Automotive Control Systems,”** [SAE 2010-01-0241](#), SAE World Congress, Detroit, April 2010.
9. A. Rousseau, P. Sharer, F. Besnier, **“Feasibility of Reusable Vehicle Modeling: Application to Hybrid Vehicles,”** [SAE 2004-01-1618](#), SAE World Congress, Detroit, March 2004.

IV.3. Connected and Automated Vehicle

Aymeric Rousseau, Project Coordinator
Josh Auld (ANL), Jeffrey Gonder (NREL), Dominik Karbowski (ANL),
Andreas Malikopoulos (ORNL), John Smart (INL), Investigators

Argonne National Laboratory
9700 South Cass Avenue, Building 362
Argonne, Illinois 60439
Phone: (630) 252-7261; Fax: (630) 252-3443
E-mail: arousseau@anl.gov

David Anderson, Jacob Ward, DOE Program Managers
Office of Vehicle Technologies, U.S. Department of Energy
Phone: (202) 287-5688, (202) 586-7606
E-mail: David.Anderson@ee.doe.gov, Jacob.Ward@ee.doe.gov

Start Date: October 1, 2015
End Date: September 30, 2016

IV.3.A. Abstract

Objectives

- Evaluate the potential impact of Connected and Automated Vehicles (CAVs) on transportation energy use under a wide range of scenarios and vehicle technologies
- Assess how CAVs can impact VTO technology R&D and how VTO can help mitigate the potential energy multiplier or maximize its energy reduction depending on the cases

Accomplishments

- Connected with potential providers of light- and medium-/heavy-duty CAVs data from non-DOE-funded real-world demonstration and deployment projects.
- Quantified the energy saving potential of vehicle trip profiles resulting from CAV technologies on multiple powertrain technologies
- Developed a framework with integrated driver, V2X and powertrain models, to complement larger traffic flow models, to allow the co-optimization of powertrain control and vehicle dynamics. Applied the framework to quantify the energy saving potential of platooning and eco-signals.
- Quantified CACC impact on traffic flow and energy using POLARIS
- Assessed the potential for "green routing" (drivers' following the most fuel efficient route) in comparison to actual routes taken for thousands of real-world trips. Initial analysis for conventional powertrain vehicles indicated that 35% of trips (representing 45% of fuel consumption) showed potential for green routing benefit--specifically 13% fuel savings potential within this trip subset.
- Implemented value of travel time in POLARIS behavioral models and quantified the impact on VMT
- Assessed the upper bound opportunity for heavy-duty truck platooning based on consecutive time spent above specific speeds for a large real-world truck operation dataset.
- Quantified the energy and cost saving potential of purpose built CAVs

Future Achievements

All the tasks in this project will continue in FY17 under the new DOE Smart Mobility project within the Connected and Automated Vehicle pillar. The focus will continue to be on assessing the energy impact of new mobility technologies.

IV.3.B. Technical Discussion

Background

CAVs will impact transportation at many levels, including energy, mobility and safety. From an energy point of view, CAVs represent both an opportunity and a challenge. On the one hand, many connected & automated technologies can lead to energy reduction at the individual level (e.g., platooning) or at the system level (e.g., reduced congestion). On the other hand, increased mobility often leads to higher vehicle miles traveled (VMT) and increased energy use. Analysis also becomes more complex as the powertrain become more advanced (e.g., electrification, etc.). In the USA, DOT's AERIS program has been the most ambitious so far at studying CAVs energy implications. A number of programs in the EU, such as EcoMove, Amitran and Cosmo have also tried to address the issues. While these programs made great contributions, they were limited in scope, and models used to assess energy impacts were often inaccurate. For example, MOVES, one of the models used by AERIS, cannot properly model vehicles with advanced controls such as HEVs, as was demonstrated by Kwon et al (2007). Inaccurate energy models pose the risk that savings observed in simulation will not be matched in the real-world implementation. The other common limitation is the small scale of the environment modeled (short section highway sections or a few intersections) and the lack of strategic traveler behaviors (e.g. increased travel due to easier travel). As a result, existing studies have provided qualitative rather than quantitative results.

This proposal leverages high fidelity vehicle energy consumption models along with high fidelity traffic flow simulation tools specifically developed for ITS. Vehicle test data was leveraged to quantify benefits at individual vehicles. Advanced vehicle models developed under the BaSce VTO project will be leveraged to represent current and future technologies including uncertainties (i.e. with and without VTO benefits). Last but not least, the scenarios, including fleet distribution, market penetration will also leverage and expand on the BaSce process to provide energy impact at the national level (AOI 2C).

Introduction

One of the main DOE goals is to develop energy efficient and environmentally friendly transportation technologies to lower petroleum use. While most of the research so far has been performed at the vehicle level, CAVs have the impact to radically change the transportation system. It is critical for VTO to understand the potential energy multiplier from CAVs and how one could mitigate it. In addition to assessing the impact of the large number of technologies under a wide range of scenarios/uncertainties, specific attention will be paid to addressing the impact on VTO R&D activities, including how vehicle design/requirements are impacted.

Approach

The following section describes the tasks that will help us achieve our objectives, leveraging the Road-to-Lab-to-Math (RLM) approach along with high-fidelity simulation:

- How will CAVs technologies impact vehicle design, operation and energy consumption?
- How can Connectivity and Automation be leveraged to reduce total energy use?
- What will be the impact at a regional system level, including potential rebound effects?
- Will future transportation systems affect the benefits of vehicle technologies (I.e. different benefits from vehicle electrification) and should VTO change its targets?

The proposal seeks to improve the accuracy, fidelity and consistent input assumptions for analyzing primary and secondary impacts from various CAVs technologies. The team will build upon and leverage (where appropriate) past and on-going analysis work at external institutions as well as activities at each partnering lab that fall outside of this funding proposal. To address this challenge, this task leveraged numerous VTO's core capabilities and expertise from multiple national laboratories:

- Argonne National Laboratory (ANL):
 - Vehicle energy modeling and control
 - Travel demand, flow and traveler behavior modeling
 - Dynamometer data collection and analysis at APRF
- Idaho National Laboratory (INL): On-road and on-track data collection and analysis for light-duty vehicles
- National Renewable Energy Laboratory (NREL): On-road and on-track data collection and analysis for medium and heavy-duty vehicles as well as green routing
- Oak Ridge National Laboratory (ORNL): Decentralized control for optimizing traffic flow, as well as impact on VMT using geo-demographics

Each project task is described in the following section.

Results

Task 1.1: Light Duty Vehicle On-Road Vehicle Evaluation

The objectives for this task were two-fold: 1) Define data requirements to validate and improve individual vehicle and traffic flow models and assumptions used in aggregate models and 2) identify existing and future non-DOE funded testing/demonstration projects and determine the potential for collaboration.

To accomplish the first objective, INL has conducted interviews with principal investigators over tasks 1.4 through 3 of this project and begun a database to document data needs. Additional interviews will take place in FY17 to produce a more robust compendium of data requirements. This database will be shared with all project participants.

INL's efforts toward the second objectives focused on building a relationship with researchers at the University of Michigan's Mobility Transformation Center (MTC). MTC plans to collect energy-related data from 500 conventional and plug-in electric connected vehicles in the Ann Arbor, MI area. INL provided technical support for this project in FY16 under another VTO-funded project. MTC agreed to share energy-related data with national labs at the completion of the project. MTC has also expressed willingness to share data from its Safety Pilot Model Deployment project, conducted between 2009 and 2012 in Ann Arbor, MI for USDOT. Additionally, INL established contact with TriHydro Consulting, a contractor participating in the USDOT Connected Vehicle Pilot demonstration in Wyoming. Because that project is focused on heavy-duty commercial trucking, further discussions about data sharing were left to NREL. In FY17, INL will build on NREL's relationship with Florida DOT to determine the availability and quality of data collected by FDOT as part of the USCOT Connected Vehicle Pilot demonstration in Tampa, FL.

Task 1.2: Medium and Heavy Duty Vehicle On-Road Vehicle Evaluation

Efforts for this task have focused on identifying and connecting with existing and future non-DOE funded testing and demonstration projects with which to determine the potential for collaboration on CAVs-relevant on-road data. The most promising discussions have been with the Florida DOT and the US DOT Connected Vehicle (CV) pilot demos, most specifically the Wyoming CV demo which targets efficient freight movement across Wyoming on I-80.

In Florida, the state DOT (FDOT) continues to sponsor automated/connected vehicle demonstrations and is the recipient of one of the three CV pilot projects (in Tampa). FDOT provided NREL top level results from a previous Advanced Driver Assistance Systems (ADAS) demonstration that occurred in Tampa, Florida, but granular data (spatial coordinates of vehicle trajectories) were not available. The USDOT CV demo (also in Tampa) is progressing, but similar to the ADAS deployment it concentrates on light-duty vehicles. A second FDOT-sponsored demonstration in the Miami-Dade region assessed the effectiveness of fully connected freight vehicles. The fleet involved the movement of high-value perishables to and from the airport to warehousing facilities. The demonstration was designed as a before-after study with the before data collected in early 2016. The after study, with CV features integrated, was scheduled for later this year but funding to complete the demo is in jeopardy. Even so NREL is investigating the use of the before data as part of its Fleet

DNA analysis. Highly granular spatial data was part of the data collection, but access to the data is still being coordinated. The state of Florida has also legislated a demonstration of fleet platooning, being conducted by the FDOT. NREL is collaborating with FDOT to influence the design of the demonstration and data collection. The demo should occur later in 2016 or early 2017.

NREL also established a dialogue with the USDOT CV Pilot demonstration project in Wyoming which emphasizes commercial freight movement across the state’s primary east-west corridor, Interstate I-80. Having completed the concept definition, Phase I, Wyoming is moving into phase II, project design. Dialogue with the state’s technical integrator, TriHydro Consulting, indicated that the data items will include highly granular spatial information, and some information from the vehicle. However, CAN data such as fuel usage, and engine and transmission control (items that could be valuable to energy analysis) are currently not within scope. TriHydro seemed to think that these could be added with minor technical impact, however any change in scope would need to be coordinated with WYDOT and the USDOT. Access to the CV data for research purposes is planned by USDOT, though no specifics have been provided as to how and when these would be made available. Future efforts in FY17 under the larger DOE SMART Mobility umbrella will include continued interactions with FDOT on their state-sponsored demonstrations, dialogue with USDOT with respect to the CV demos (particularly in Wyoming), and seeking to formalize data sharing agreements in writing.

Task 1.3: Light Duty Chassis Dynamometer Evaluation

This task seeks to investigate and execute methodologies toward testing CAV functionality and behavior in a controlled laboratory setting. The preliminary topic of investigation for this work is adaptive cruise control (ACC), which is a basic, yet relatively widespread form of vehicle automation in terms of controlling acceleration to follow a leading vehicle

A Honda Accord PHEV with a RADAR-based ACC system was chosen as the assessment vehicle for this project. Messages related to the distance between lead and following vehicles, relative speeds, and angular location of the lead vehicle were overridden and passed onto the CAN bus using a man-in-the-middle (MITM) approach. Figure IV-13 shows the vehicle on-dyno, the MITM connections and computer, and a snapshot of the messages related to the ACC system.

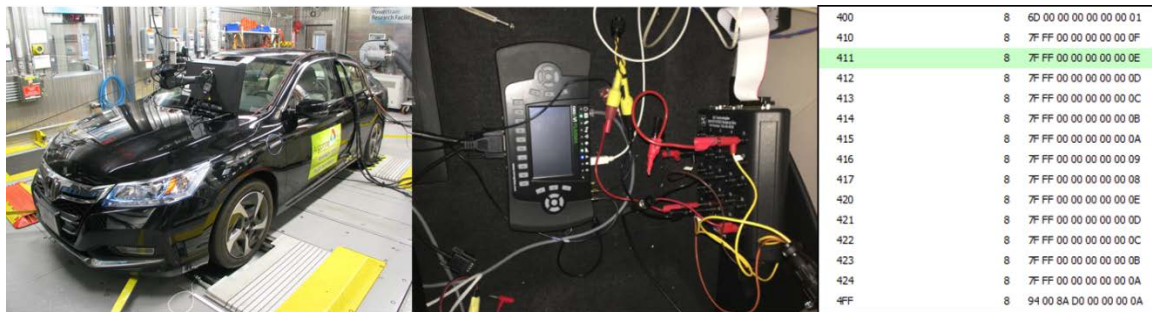


Figure IV-13: Highlighted ACC Project System Components (vehicle on-dyno, MITM computer and connections, data)

Over the course of preparing and decoding the vehicle messages, significant amount of data regarding the Accord ACC system's behavior was collected, example results are shown in Figure IV-14, highlighting the vehicle following using the ACC system.

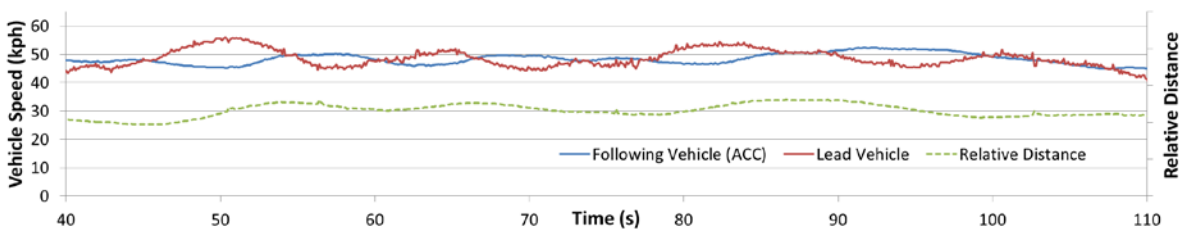


Figure IV-14: On-road ACC data collection of lead/following vehicle speeds and relative distance

Due to difficulties with the final on-dyno translation of CAN messaging and redundancy checking, the ACC Accord is now currently on the dyno for testing and assessment. Results are expected early in FY17 due to the delay. Going forward, this work will be expanded in some form towards other on-going CAVs related projects and will likely incorporate V2X messaging as the next step in the emulation environment development.

Task 1.4: Individual Vehicle Simulations

Connectivity and automation will have an impact on the energy consumption of vehicles: CAVs will probably drive more smoothly, stop less often, and move at faster speeds, thanks to overall improvements to traffic flows. These potential impacts are not well studied, and existing studies tend to focus solely on conventional engine-powered cars. This task intends to address this issue by analyzing the energy impact of various CAV scenarios on different types of electrified vehicles using high-fidelity models. The vehicles—all midsize, one HEV, one BEV, and a conventional—are modeled in Autonomie, a high-fidelity, forward-looking vehicle simulation tool. They are simulated on various CAVs scenarios and modeled by modifications of selected real-world drive cycles (RWDC).

Real-World Driving Cycles were selected from a database of recorded speed traces in the Chicago area. An energetic criteria was used to select RWDCs representing the average driving style. Different changes to the original speed profiles are then applied to represent the connectivity impact: some stops are removed, speed is smoothed, and strong accelerations are saturated. An overall increase in speed is also investigated to represent improved traffic flow. In each case, the distance remains the same as in the original case, representing the same origin and destination.

As shown in Figure IV-15, connectivity and automation reduce energy consumption for all vehicles and the higher the degree of connectivity/automation, the higher the energy consumption reduction. Reductions from 10% to 30% are expected at low speed depending on the degree of connectivity, but much less at higher speeds, where driving is approaching steady-state operations. At lower speeds the conventional vehicle is likely to benefit slightly more from connectivity and automation, as it removes particularly inefficient operations (stops, braking) that are less inefficient for electrified vehicles

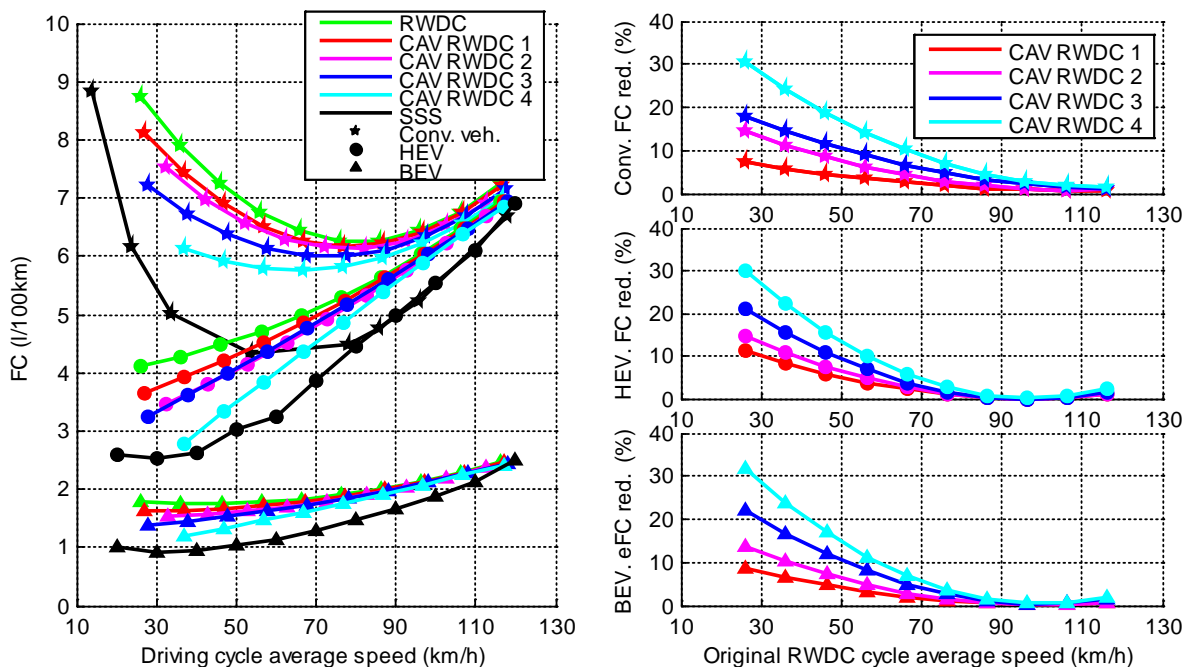


Figure IV-15: Fuel consumption (or equivalent for BEV) for various CAV scenarios: absolute values (left), relative savings to reference case (right)

Task 1.5: Connected Vehicle Simulations

Numerous concepts relying on connectivity and automation have been developed and/or demonstrated, some (s.a. AERIS) with energy efficiency as one of the objectives. As their testing is inherently difficult, modeling is critical for the further development of these technologies their energy impact assessment, in particular in the context of advanced powertrain technologies, some of which rely on advanced control. Traffic flow simulators (e.g. PTV Vissim, Paramics, etc.) are the natural choice to evaluate traffic flow impacts of particular CAV controls, but do not integrate vehicle energy model. This task aims at developing a framework with integrated driver, V2X and powertrain models, to complement larger traffic flow models, thus allowing the co-optimization of powertrain control and vehicle dynamics. The framework will be in Simulink, and an extension to Autonomie, a reference vehicle simulation tool. As a new task in FY16, we focused on modeling two fundamental aspects of driving, with and without connectivity: vehicle following and intersection approach, and establishing some of the foundations of the framework.

In the proposed framework, we will model vehicle travel as longitudinal – turns will be indirectly modeled as a speed reduction. The road will include grade, controlled (traffic light) and uncontrolled (stop sign) intersections, and speed limits. A cohort of several vehicles will be simulated, where vehicle follow each other, with or without connectivity, with or without automation. The lead vehicle will either operate in free flow conditions, following intersection controls and speed limits, or will follow a speed profile, or a hybrid version combining both. It will be possible to generate a scenario directly from a real-world route defined in a digital map. Part or all the vehicles may form a platoon. Each vehicle has its own control logic, using inputs/outputs akin to the ones in a real-world scenario, thus making the framework ideal for development purposes.

The first prototype application is vehicle following as shown in Figure IV-16. We considered a string of trucks, wherein the first vehicle follows a pre-defined highway drive cycle. The following vehicles follow each other either through modelled human interactions (“intelligent driver model”) or through automated driving: adaptive cruise control (ACC) or cooperative ACC (CACC). Both ACC and CACC control strategy aim at keeping a constant time gap with the preceding vehicle. In addition to information about the preceding vehicle, CACC also uses the gap with the vehicle leading the string. The vehicle plant models are modified so that the aerodynamic drag is dependent on the configuration of the platoon. The model can therefore evaluate the benefits of platooning/CACC in a broad range of situations, using wind-tunnel testing data (LLNL) and track testing (NREL).

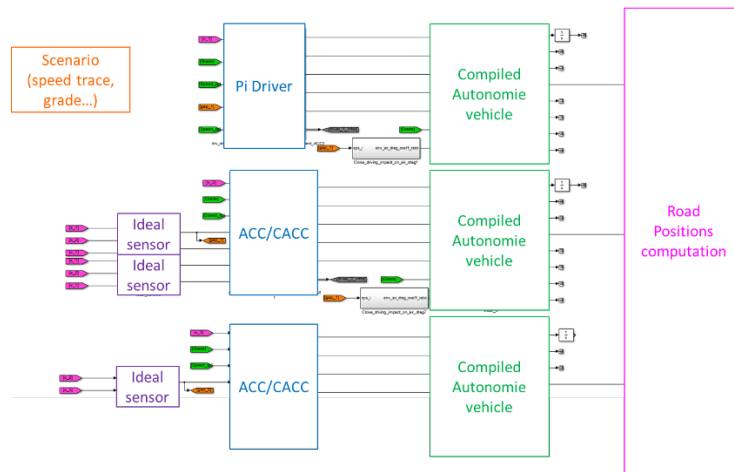


Figure IV-16: Multi-vehicle simulation framework in Simulink

The second application is focused on intersection approach. We implemented a process that generates a model in Simulink of a road with intersections, with an independent model instance for each of them. As the vehicle progresses along the road, a module routes the appropriate signals to the vehicle. The baseline control follows the speed limit, and brakes to a stop at uncontrolled intersections and at controlled ones when the light is red when the vehicle is close. With connectivity and automation, the vehicle also knows the cycle time and phase of the approaching controlled intersection, so it can adjust its approach speed with minimization in mind. We are implementing control algorithms from literature to do just that; the first results will be available in FY17 Q1, before researching additional advanced optimization techniques.

Task 2.1: Large Scale Traffic Flow Impact

The objective of this task over the past year was to update the existing POLARIS traffic flow model to account for macro- and meso-scale impacts of Cooperative adaptive cruise control (CACC) on regional traffic. CACC combines the adaptive cruise control with the vehicle to vehicle communication that allows improved speed control strategies. Forward vehicles communicate information about downstream traffic and provide speed recommendations. The goal of CACC is to improve three metrics associated with a transportation system, namely mobility (reduce congestion), sustainability (reduction in energy used) and safety. These improvements come from reduced headways between vehicles while maintaining traffic flow speed, and thus improving road throughput and avoiding traffic flow breakdowns at high density traffic flows. CACC improves on autonomous adaptive cruise control by allowing vehicle to receive information about lead vehicle earlier that allows to develop better control algorithms (Lu 2011) and keep the following distance close. Additional energy reduction benefits come from reduced drag forces experienced by following vehicles due to reduced air resistance. Updating the POLARIS traffic flow model will allow us to perform energy use analysis on the impacts of CACC at the regional level.

There are several studies that show energy benefits of truck and vehicle platoon in isolated test environments that utilize tightly-coupled platooning. Alam (2010) tested speed control algorithms for follow vehicle that uses information about the road ahead sensed by the lead vehicle. They showed 5-8% fuel efficiency improvement. Computational fluid dynamics simulation performed by Davila (2013) confirm the field studies and show that optimal headway distance to reduce the drag forces is 6-8 meters and potentially lead to 7-15% fuel savings. Similar studies were performed for light duty vehicles (Shida 2009, 2010, Eben 2013, Shladover 2013). Fuel efficiency improvements with CACC using constant-time-gap-following criteria in normal traffic conditions have not yet been demonstrated. Several simulation studies showed that CACC that enables shorter following gaps increases capacity from the typical 2200 vehicles per hour to almost 4000 vehicles per hour at 100 percent market penetration. We studied the impact of CACC vehicles at different market penetration rates on a regional scale by adjusting the capacities of road links according to the values reported in Vander Werf (2002) and Shladover (2012). In their study Vander Werf et al (2002) estimated the effects of CACC using Monte Carlo simulation based approach that utilizes detailed models of vehicle control.

Figure IV-17 shows the relationship between CACC vehicle penetration level (percent of equipped vehicle presented in the traffic flow) and improvement in the road capacity. The capacity of each link is updated at 5-minute intervals according to the average percentage of equipped vehicles traversing the link over the previous interval. While this does not account for the timing of individual vehicles entering/exiting the link and communicating, it does allow for an initial region-level analysis which accounts for distributions of vehicle technology and regional trip patterns. It is important that the traffic flow improvements are implemented in an integrated travel demand model system, as it is possible that improvement in mobility metrics might lead to secondary impacts, such as increase in travel demand. Therefore flow and demand impacts need to be studied simultaneously, as documented in the Task 3.1 update.

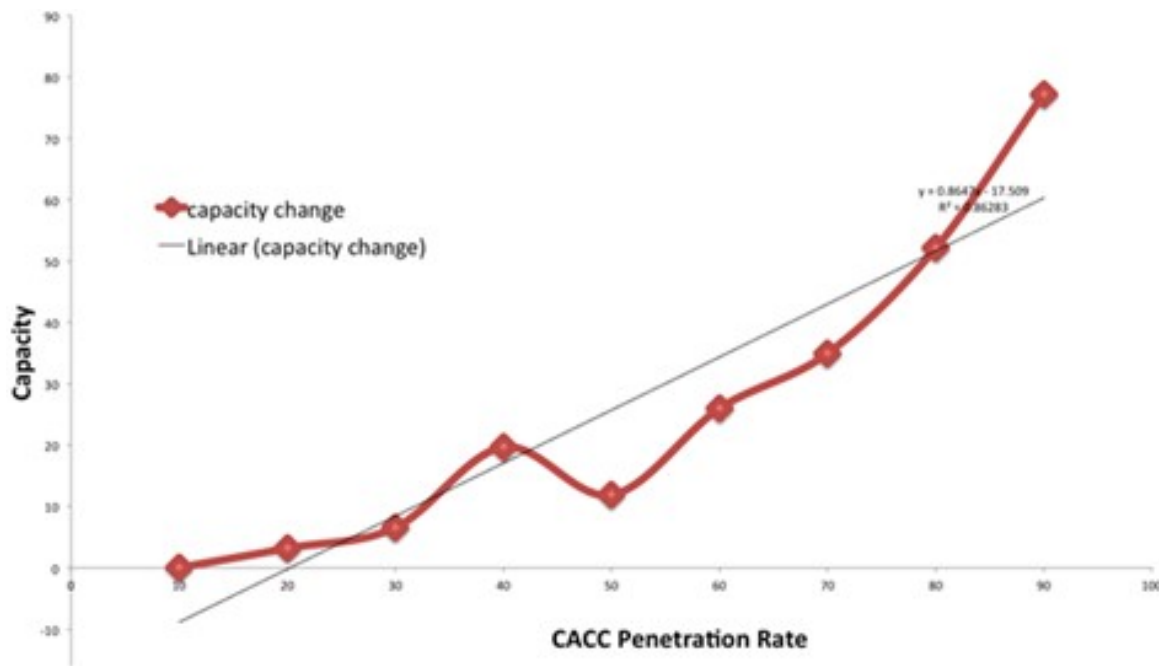


Figure IV-17: Capacity change vs. market penetration of CACC

Task 2.2: Green Routing

The green routing task activities built off of NREL's previous collaboration with General Motors to evaluate green routing and adaptive control fuel saving opportunities for the Chevy Volt (Gonder et al, 2016). The present green routing task focused on application to a high sales volume conventional powertrain vehicle, and applied a fuel consumption estimation model to predict how much fuel the vehicle would consume on any road segment given information about the road segment's functional class category, and the average traffic speed on the road segment at the time of travel (to account for traffic congestion). The analysis then compared the fuel consumption estimate for the identified "greenest" route with that for each actual route taken over a set of real-world travel data for roughly four thousand trips within the state of California. To perform this assessment NREL extracted the origin and destination locations corresponding to each trip, determined possible routes between the origin and destination by querying Google's routing application programming interface (API), and compared these options to the actual route driven.

The analysis revealed that for 78% of the trips the actual route matched one of the API options, but that in the other 22% the driver took a route that deviated from the options given by the API. After applying the fuel consumption estimation model to all of the route possibilities (those suggested by the API and the actual route if different), NREL found that 35% of the trips showed potential for fuel savings (in the others the route taken already aligned with the lowest fuel-consuming route prediction). Interestingly, these 35% of trips accounted for 45% of the estimated fuel consumption from the full set. Among the trips showing potential benefit from alternate routing, the model estimated up to 13% fuel savings from switching to the green route. Compared with the actual route taken, a number of these fuel saving routes would incur some level of travel time increase. However, 60% of the fuel savings comes from route alternatives that are estimated to save both time and fuel. Further efforts on this topic will continue under the larger DOE Smart Mobility Consortium projects, which will include a collaborative INL and NREL task to validate green routing fuel saving predictions with on-road testing.

Task 2.3: Control for Improving Traffic Flow with CAVs

We address the problem of coordinating connected and automated vehicles (CAVs) in merging roadways (Figure IV-18). The region of potential lateral collision of the vehicles is called merging zone and has a length S . There is also a control zone and a centralized controller that can control the vehicles traveling inside the control zone. The distance from the entry of the control zone until the entry of the merging zone is L .

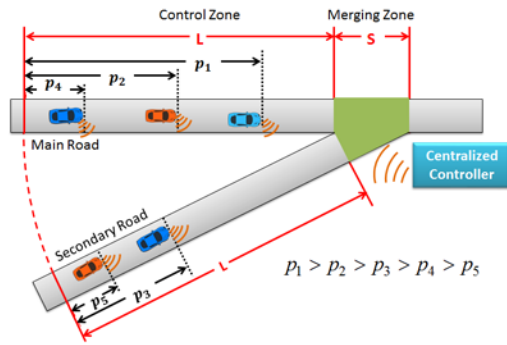


Figure IV-18: Merging Roads with connected and automated vehicles coordinated by a centralized controller

We considered a scenario with 4 CAVs first, in which the vehicles depart from the same position on each road (Figure IV-19a) to validate the approach. Even though the vehicles started from the same initial positions on each road, they were able to derive online their optimal acceleration/deceleration by allowing only one vehicle at a time in the merging zone (Figure IV-19b). Then, we considered the coordination of 30 CAVs moving on two merging roads (15 vehicles on each road) with random initial positions and no limitations on the minimum or maximum speed. The vehicles were able to derive online their optimal control input under the hard safety constraint of avoiding lateral collision in the merging zone (Figure IV-20). The acceleration/deceleration and speed profiles of the vehicles are shown in Figure IV-21a and Figure IV-21b respectively.

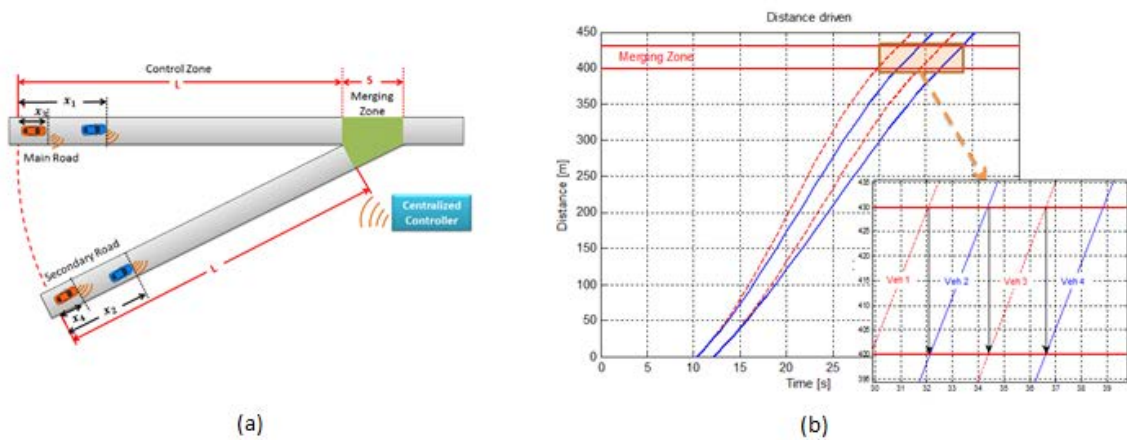


Figure IV-19: (a) Initial vehicle positions on each road for the scenario 1 and (b) position trajectories of the four vehicles for the scenario 1.

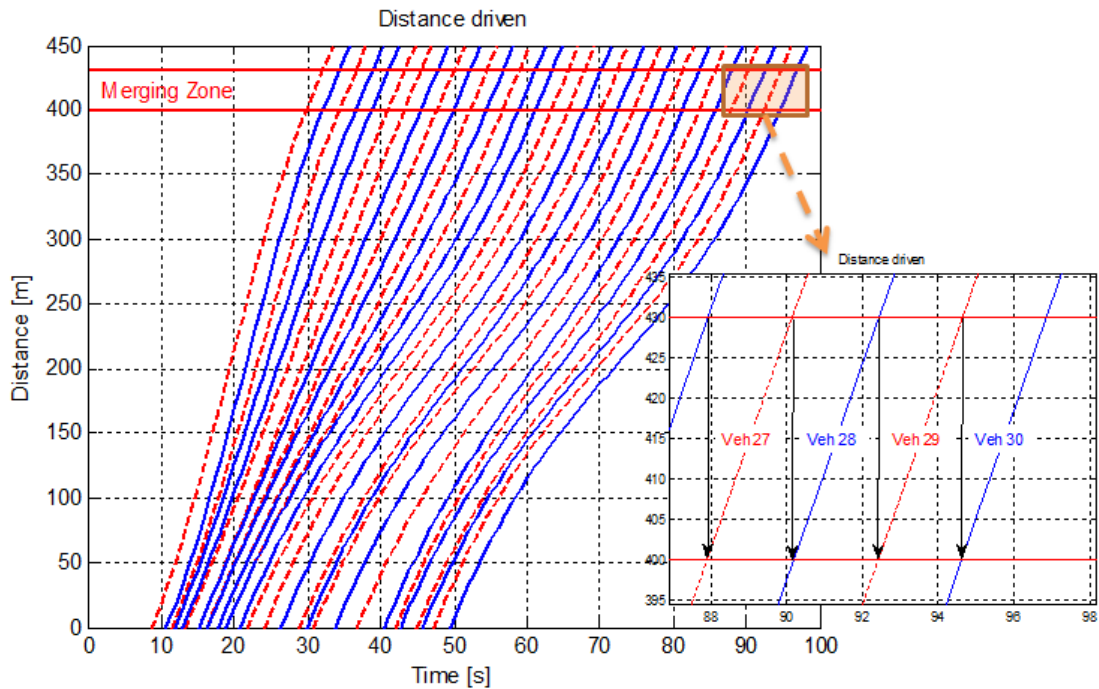


Figure IV-20: Position trajectories of the four vehicles for the scenario 2

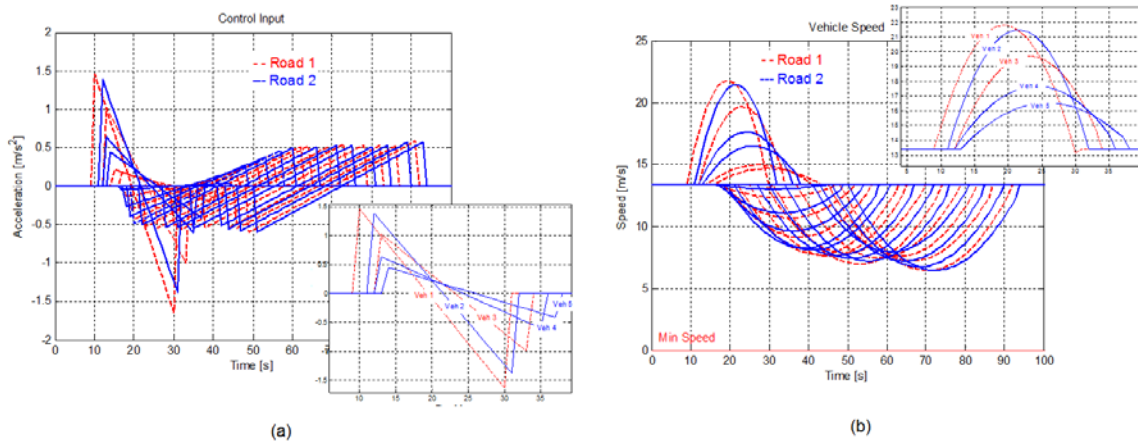


Figure IV-21: (a) Control input and (b) speed profile of the vehicles for the scenario 2

To compare fuel consumption and travel time benefits of vehicle coordination we considered a baseline scenario, in which the vehicles on the secondary road have to stop before the intersection to allow the vehicles in the main road to cross the merging zone. The cumulative fuel consumption is higher in the baseline case compared to the scenario 2 where the vehicles are coordinated (Figure IV-22a). In particular, optimal vehicle coordination improves overall fuel consumption by 52.7% for the scenario 2 compared to the baseline scenario. The total travel time is improved by 7.1% (Figure IV-22b).

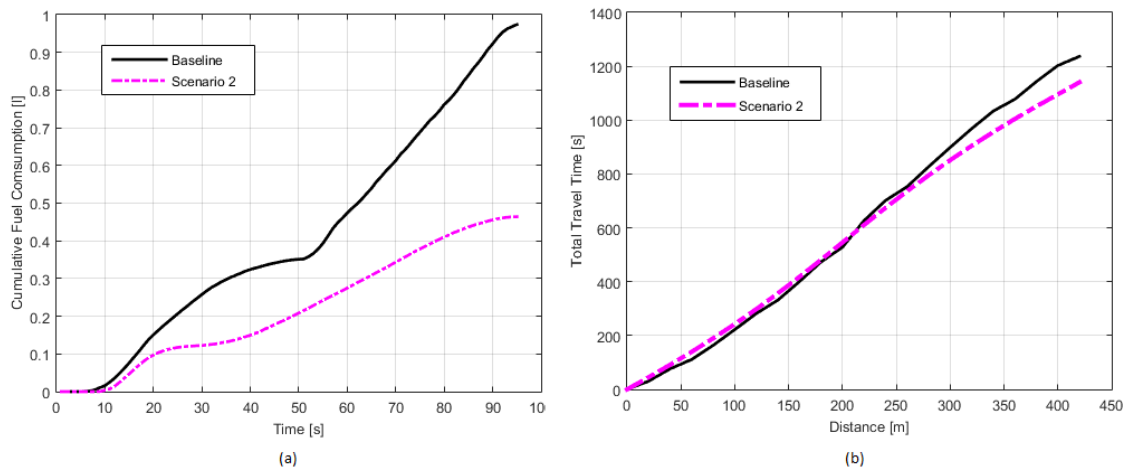


Figure IV-22: (a) Cumulative fuel consumption and (b) travel time.

Task 3.1: Travel Behavior Evolution at the Regional Level and its Energy Impact

In this task we use POLARIS, which includes co-simulation of travel behavior and traffic flow, to study potential impacts of cooperative adaptive cruise control at the regional-level. The preliminary analysis was focused on studying potential impacts, in terms of changes in VMT, over various market penetration levels for a feasible range of changes in travel time sensitivity to determine a potential range of VMT impacts from CACC. In order to demonstrate regional energy use impacts we use the POLARIS model for Ann Arbor, Michigan. The model was connected to the Autonomie vehicle simulation model assess energy impacts of various connected vehicle technologies. Several notable studies on potential CAV travel demand impacts have been conducted recently, including:

- MacKenzie et al (2014): VMT increase of 4-13% with partial vehicle automation and 30-160% for full automation. Assumed value of time at 20% to 50% of the value of time in a conventional vehicle.
- Childress et al (2015): Puget sound ABM. Scenarios included 1) a 30% capacity increase - 3.6% increase in VMT, 2) a 35% decrease in VOTT for the high-income- VMT increase of 5.0%. 3) 100% private AV and 50% reduction in parking cost along with 2 - VMT increased 19.6%.
- Gucwa (2014): San Francisco Bay ABM with capacity increase of 0, 10% and 100% - 4 to 8% increase in VMT (up to 14.5% increase if a zero VOTT for traveling in AV).

This study builds on past work by analyzing potential changes in travel demand due to various CAV deployment scenarios and potential behavior impacts. In this case we utilize a transportation systems simulation model where travel demand and traffic flow are directly and continuously integrated, to model the scenarios. The research incorporates the analysis of demand under a feasible range of travel time valuations identified in the literature, and incorporates research on link capacity changes under various market penetration levels of CACC to formulate the scenarios. The value of travel time change was represented by reducing the travel time parameters in the mode choice and destination choice models inside POLARIS, for travelers assigned to a CACC-enabled vehicle. The scenario setup and results are shown in Table IV-3. Energy results shown in Figure IV-23.

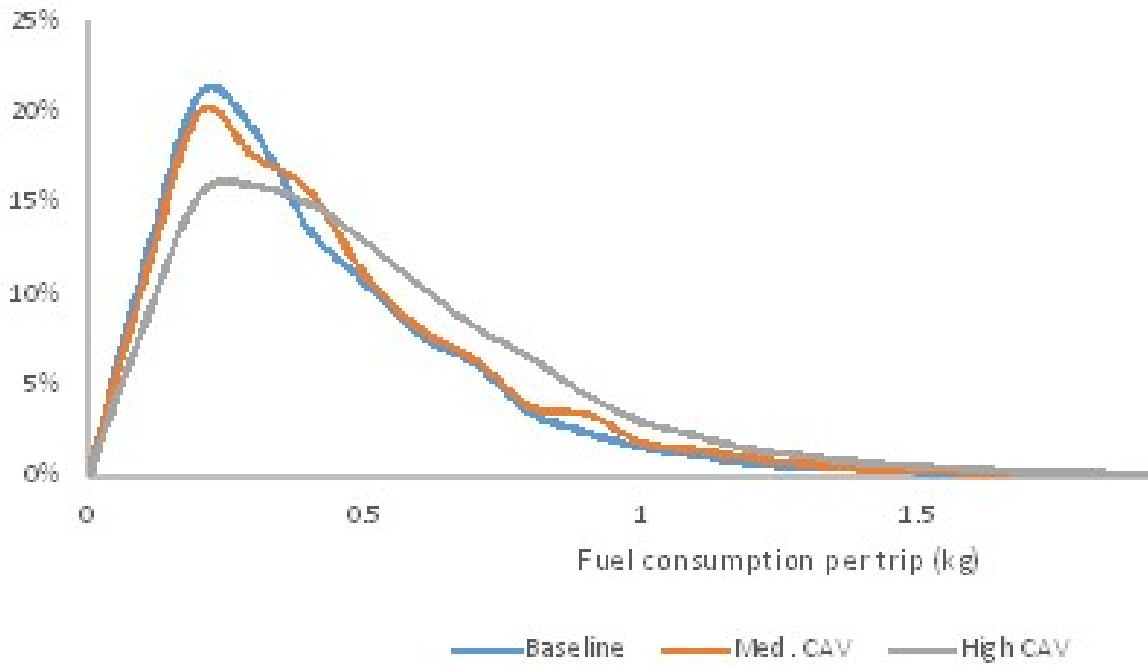


Figure IV-23: Fuel Consumption Impact.

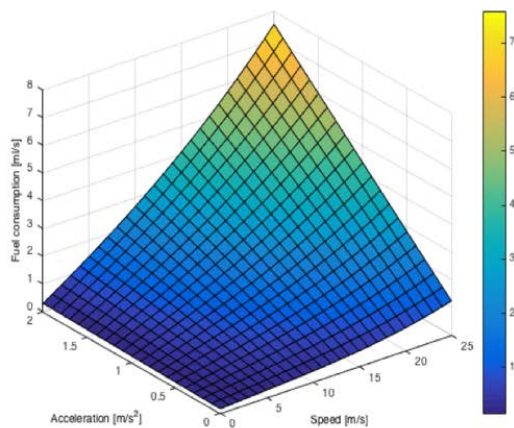
Table IV-3: Scenario Setup and Analysis Results

Scenario Type	Market penetration (%)	Value of Travel Time change (%)	Capacity increase (%)	Auton. Inter. (yes/no)	Vehicle Miles Traveled (million miles), Percent change (%)	Vehicle Hours Traveled (thousand hours), Percent change (%)	Avg. travel time (min), Percent change (%)
1. Baseline	0	0	0	no	5.35, (0.00)	154.7, (0.0)	12.2, (0.0)
2. Capacity increase only	0	0	12	no	5.35, (0.36)	152.2, (-1.6)	12.0, (-1.8)
4. Capacity increase only	0	0	77	no	5.44, (2.04)	147.7, (-4.5)	11.6, (-4.5)
5. VOTT only-low pen.	20	-25	0	no	5.41, (1.34)	157.4, (1.8)	12.4, (1.8)
7. VOTT only-low pen.	20	-75	0	no	5.60, (4.98)	166.3, (7.5)	13.0, (7.1)
8. VOTT only-high pen.	75	-25	0	no	5.64, (5.77)	167.6, (8.4)	13.2, (8.0)
10. VOTT only-high pen.	75	-75	0	no	6.33, (18.59)	202.4, (30.9)	15.8, (29.9)

11. All effects-low pen.	20	-25	3	no	5.42, (1.61)	157.5, (1.8)	12.4, (1.6)
13. All effects-low pen.	20	-75	3	no	5.62, (5.32)	166.3, (7.5)	13.0, (7.1)
14. All effects-med pen.	50	-25	12	no	5.56, (4.32)	160.2, (3.5)	12.6, (3.2)
16. All effects-med pen.	50	-75	12	no	6.01, (12.73)	180.2, (16.5)	14.1, (15.9)
17. All effects-high pen.	100	-25	77	yes	5.87, (10.000)	162.6, (5.1)	12.7, (4.5)
19. All effects-high pen.	100	-75	77	yes	6.84, (28.19)	203.9, (31.8)	15.8, (30.1)

Task 3.2: Evolution of Vehicle Miles Travelled at the National Level

We considered a baseline scenario that we allow us to study the implications of having a mixture of non-CAVs and CAVs on the roads. In this scenario, the non-CAVs on the secondary road will attempt to merge if there is a safe gap between the vehicles on the main road. To evaluate the impact of different penetrations of CAVs on fuel consumption, a polynomial metamodel was implemented (Figure IV-24) that can yield fuel consumption for any type of vehicle with respect to the speed and acceleration. The model will be used to quantify the benefits of coordinating different penetrations of CAVs in specific traffic scenarios, e.g., intersections, merging roadways, speed reduction zones, roundabouts.



$$f_v = f_{cruise} + f_{accel}$$

$$f_{cruise} = w_0 + w_1 \cdot v + w_2 \cdot v^2 + w_3 \cdot v^3$$

$$f_{accel} = u \cdot (r_0 + r_1 \cdot v + r_2 \cdot v^2)$$

v is vehicle speed

u is vehicle acceleration, and

w_i and r_i parameters of the metamodel

Figure IV-24: Polynomial MetaModel

Task 3.3: Impact of Heavy Duty Freight Demand

NREL's efforts under this task have included exploring approaches and identifying potential tools/data sources for investigating possible CAVs' impacts on heavy-duty freight service demand and energy consumption, specifically for Class 8 trucks. In particular, impact of CAV technologies is assessed for (1) low-level CAV technologies (short-term, mainly platooning), and (2) high-level CAV technologies (long-term, including logistics improvement and mode-shifting from other freight transport modes). The main outcomes are identified at the single vehicle and fleet level to properly inform different stakeholders.

The focus in FY16 was on overall methodology and low-level automation, namely platooning. In particular, analysis on real world data (roughly three million miles of driving) assessed the fraction of total heavy duty

VMT available for platooning. This quantification provides an upper bound for the fleet efficiency that can be realized through adoption of low-level automation, with true real-world potential also dependent on truck operators' willingness to platoon. Figure IV-25 illustrates the amount of driving at different speed and time thresholds for a targeted (nightshift trucking) application that could be particularly well suited for platooning opportunity.

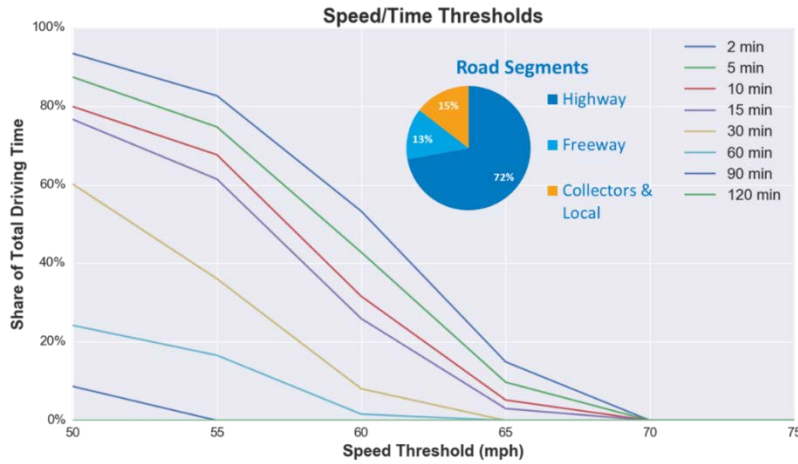


Figure IV-25: Analysis of Platoonable Miles for a Targeted Truck Application

Task 3.4: Impact on Vehicle Design with Autonomie

Connected, and especially automated vehicles have the potential to change the way vehicles are used. In particular, the design of the vehicles in the future may be quite different than they are today. For example, acceleration performance will not be as critical. Safety features may be removed, but comfort items may be added. Vehicles may be designed for particular purposes (right-sizing). In this task, we evaluate the effects on energy consumption of these new design requirements. Several sets of assumptions were defined, based on literature review and existing sizing algorithms used for VTO benefit analysis:

- Reduction of weight related safety features: MR0 - 0kg (no change), MR1 - 60kg (corresponds to removing half of the safety features, going back to 1975), MR2 - 120kg (involve unspecified structural changes)
- Reduction of the demand for acceleration capabilities (0-60mph): AC0 - 8.5 sec (no change), AC1 - 11.2 sec, AC2 - 14.0 sec (If acceleration capabilities reverted to 1982 level)
- Modifications of cycle speed for sizing algorithm: CAV0 - no change, CAV1 - 10% PKE (Positive Kinetic Energy) decrease, same averaged speed, CAV2 - 12% PKE decrease, average speed increased at low speed, stops removed.

Conventional, HEV, PHEV and PHEVs are then sized using modified requirements, and the resulting energy consumption computed in using Autonomie as shown in Figure IV-26. The simulations show that:

- Connectivity and automation reduce vehicle cost to 8-17% and PHEVs have biggest potential due to having more components.
- Design changes for connectivity doesn't impact much on energy consumptions saving. Lab year 2025 high tech assumptions are used for this study, i.e. there is small impact on downsizing owing to the relatively high engine/electric efficiency in the baseline case.

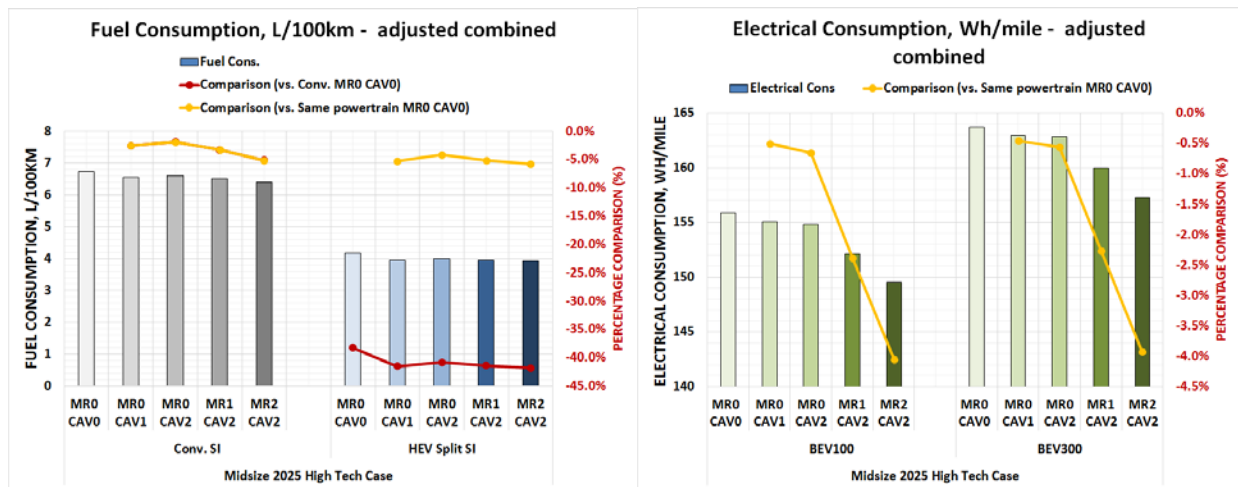


Figure IV-26: Impact on fuel/electricity consumption of alternative CAV designs

Task 3.5: Impact on Vehicle Design with FASTSim

NREL’s efforts under this task have included (1) organizing 1-Hz vehicle travel trajectories captured during household travel surveys conducted in various parts of the country (focusing on datasets that can be linked to known driving conditions at the time of travel), (2) running FASTSim models to estimate fuel consumption of vehicles with particular vehicle designs, and (3) exploring influences of average travel speed and the free flow speed (FFS) of each traversed road segment on the vehicle’s estimated fuel consumption rate.

Figure IV-27 shows the fuel consumption estimates for an example conventional vehicle design over road conditions with different combinations of FFS and average driving speed. The patterns show that for road segments with FFS < 55 mph, the vehicle’s fuel consumption rate decreases with increases in vehicle speed, reaching the minimum rate when the average speed is close to the FFS. For situations with a FFS greater than 55 mph, the average fuel consumption rate initially decreases as the average speed increases, reaches the minimum when average speed is between 50 and 55 mph and then starts gradual increasing with further increases in average speed. This analysis construct makes it possible to compare the relative fuel consumption impact of various vehicle designs under different driving conditions.

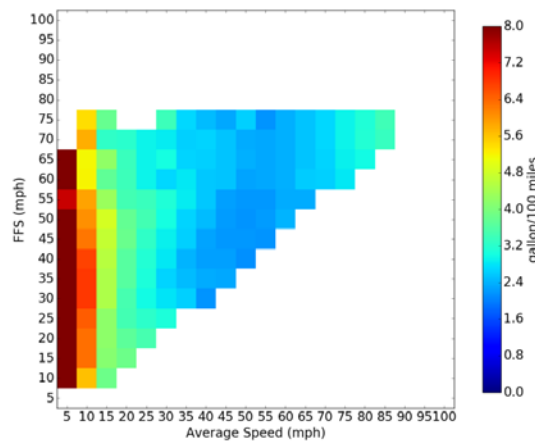


Figure IV-27: Influence of Road Segment Free Flow Speed (FFS) and Average Speed at Time of Travel for an Example Conventional Vehicle Design

Conclusions

Connectivity and Automation have the ability to change current transportation system as we know it. During the first year of the multi-year project, the different National Laboratories involved in the project have started to develop new capabilities to quantify the energy impact of advanced technologies, including emulating virtual environment on vehicle dynamometers, new multi-vehicle framework. In addition, existing capabilities were expanded and adapted to the specific requirements of CAVs, including green routing and merging roadways. The tools were leveraged to provide energy impact of CAVs for multiple powertrain technologies under different scenarios, including smoothed vehicle trip profiles, platooning, eco-signals and value of time. The new capabilities developed in this project and new data sources that are being pursued will be critical to the success of the new DOE SMART Mobility project.

IV.3.C. Products

Presentations/Publications/Patents

1. Karbowski, D., Sokolov, V., Rousseau, A., "Vehicle Energy Management Optimization through Digital Maps and Connectivity", ITS World Congress, October 2015
2. Rousseau, A. "Impact of Connection and Automation on Electrified Vehicle Energy Consumption", SAE Hybrid and Electric Vehicle Technologies Symposium, February 2016
3. Michel, P., Karbowski, D. "Impact of Connectivity and Automation on Vehicle Energy Use", SAE World Congress, SAE 2016-01-0152, April 2016
4. Karbowski, D. "Impact of Connectivity and Automation on the Energy Use of Advanced Vehicles", Automated Vehicle Symposium, July 2016
5. Rios-Torres, J., and Malikopoulos, A.A., "Automated and Cooperative Vehicle Merging at Highway On-Ramps," IEEE Trans. Intell. Transp. Syst., 2016. (forthcoming) (DOI: 10.1109/TITS.2016.2587582)
6. Malikopoulos, A.A., "Online Coordination of Connected and Automated Vehicles," Urban Autonomous Vehicles Roundtable at FedEx Institute of Technology, April, 2016.
7. Rios-Torres, J., and Malikopoulos, A.A., "Energy Impact of Different Penetrations of Connected and Automated Vehicles: A Preliminary Assessment," Proceedings of ACM SIGSPATIAL International Workshop on Computational Transportation Science (IWCTS), 2016. (to appear)
8. Zhang, Y.Z, Malikopoulos, A.A., and Cassandras, C.G., "Optimal Control and Coordination of Connected and Automated Vehicles at Urban Traffic Intersections," Proceedings of the 2016 American Control Conference, pp. 6227-6232, 2016.

IV.4. Vehicle Technologies Benefits on Real-World Drive Cycles Using POLARIS Regional Transportation System Model

R. Vijayagopal, D. Karbowski, Principal Investigators

Argonne National Laboratory
9700 S Cass Avenue, Bldg. 362
Argonne, IL 60439
Phone: (630) 252-6960
E-mail: rvijayagopal@anl.gov

David Anderson, DOE Program Manager

Office of Vehicle Technologies, U.S. Department of Energy
Phone: (202) 287-5688
E-mail: David.Anderson@ee.doe.gov

Start Date: October 1, 2015
End Date: September 30, 2015

IV.4.A. Abstract

Objectives

- Quantify the impact of new technologies on Real-World Driving Cycles (RWDC) and compare the impact to the benefits observed in regulatory cycles.
- Use transportation system models and synthetic drive cycle generation algorithms to generate drive cycles specific for a region.
- Estimate a region-wide transportation energy impact of new technologies by combining the vehicle sales predictions and fuel or energy consumption.

Accomplishments

- This study utilized three different tools developed under multiple projects funded by various agencies:
 - Autonomie
 - POLARIS
 - MA3T
- Vehicle trip profiles generated from the Chicago metropolitan area POLARIS model were used for this study.

Future Achievements

- The generic process developed in the study can be reuse to assess the impact of specific technologies or for different regions.
- In future, a nationwide impact analysis could be conducted if we record or synthesize sample drive cycles for more locations.

IV.4.B. Technical Discussion

Background

The VTO benefit analysis (BaSce) [1] evaluates the impact of various vehicle technologies on regulatory drive cycles on vehicle energy consumption and cost. Since the energy benefits of advanced technologies on standard drive cycle differ from the actual ones on real world driving cycle, it is necessary to quantify their

impact under different driving conditions. To do so, researchers have historically used a set of measured real world driving cycles and vehicle models to assess technologies impact. While that process is very useful, it is difficult to justify the selection of the real world driving cycles. In addition, such a process only allows researchers to consider current driving cycles (I.e., assessing connection and automation (CAVs) impact is not possible). As a result, the objective of the project is to leverage output from a transportation system simulation model (POLARIS) to estimate the impact on a large metropolitan area. While the process currently does not consider the impact of Smart mobility technologies on the vehicle trip profile, it will be leverage in the future to do so.

Introduction

For this study, the real-world vehicle trip profiles are synthesized from Argonne’s transportation system modeling tool, POLARIS. The energy requirement of various types of vehicles, ranging from conventional gasoline vehicles to battery electric vehicles, including various hybrids and alternate fuel vehicles, are considered. There are several challenges in accomplishing this study; however, the primary issue is feasibility of evaluating hundreds of vehicle combinations on thousands of real-world speed traces.

Approach

This study brings together the results of several other DOE-funded projects (Figure IV-28). Autonomie models for this study were developed earlier for the BaSce analysis. They were sized according to all of the technology assumptions for lab years 2010 and 2020. These vehicles are expected to be similar to those of MYs 2015 and 2025, respectively.

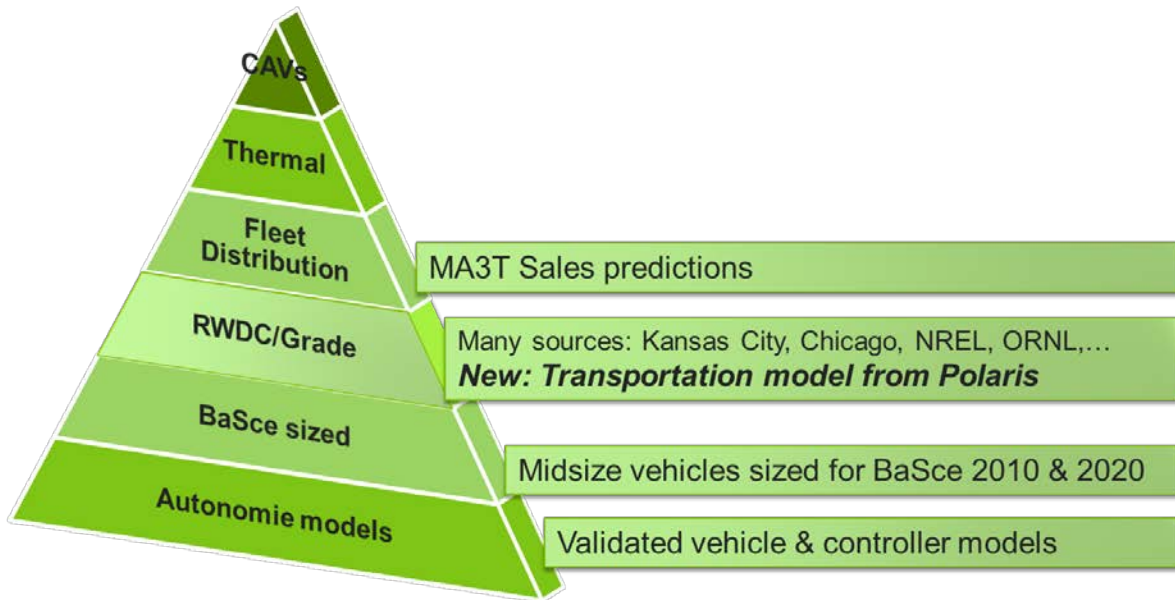


Figure IV-28: Utilization of multiple efforts funded by DOE is necessary for this study.

A vehicle in 2020 could get much better fuel economy than its counterpart in 2010, because of improvements in engine efficiency, light weighting. The new tools introduced in this study are the transportation system simulation tool, POLARIS along with the Vehicle Trip Profile generation tool. The fuel consumption or energy consumption over these drive cycles can be combined with the fleet composition predicted by market penetration tools (i.e., MA3T) to estimate fleet-wide fuel/energy consumption (Figure IV-29). At present, this exercise considers the Chicago Metropolitan area.

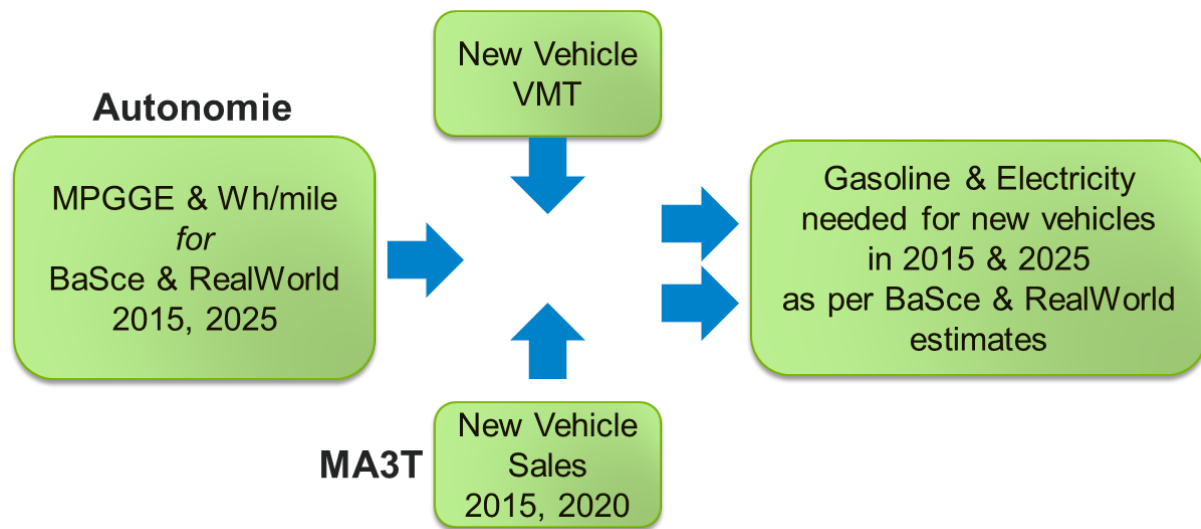


Figure IV-29: Overview of the process to estimate gasoline and electricity demand for vehicles by combining energy consumption, driving behavior, and market share predictions.

Generating Vehicle Trip Profiles from POLARIS

Figure IV-30 shows how the vehicle trip profiles are generated from POLARIS. The input to POLARIS is the transportation surveys that quantifies the number of people and their daily travel routines. POLARIS is able to model the traffic arising from such movement of people. It also gives the average speed for every road segment in the region being modelled. From this information, the Vehicle Trip Profile tool is used to generate a representative drive cycle based on general light duty driving behavior data using techniques that are already available [2].

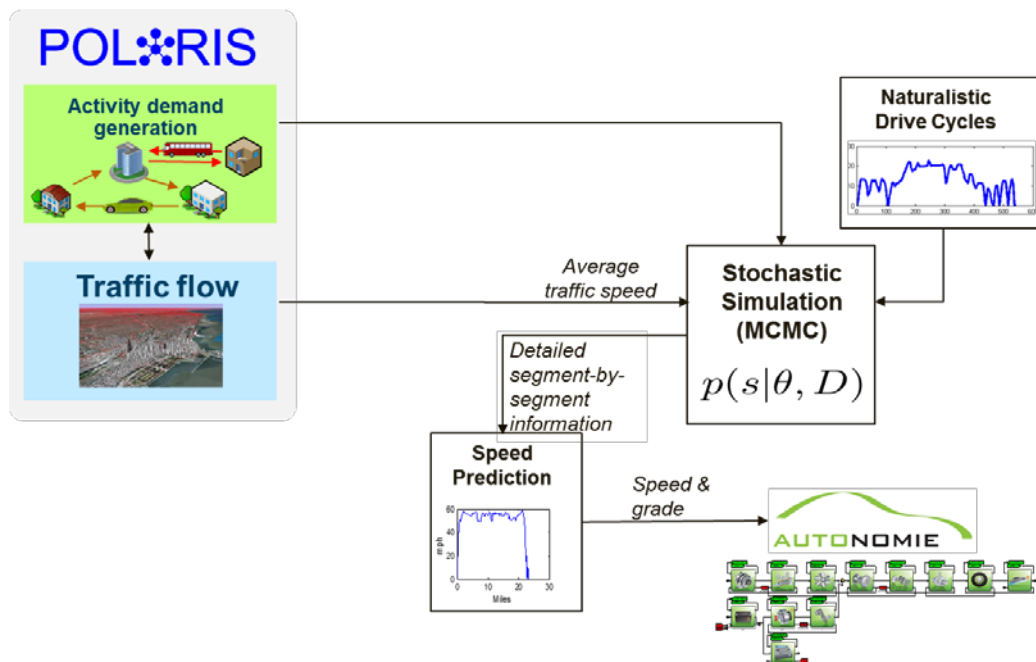


Figure IV-30: Overview of the process to generate real-world cycles from POLARIS.

Simulation Process

This study considers 175 vehicles, involving several powertrains, fuels, vehicle types, and technology choices. POLARIS generated 20,000 drive cycles to represent the driving pattern for the region in and around Chicago. All the vehicle models were developed to represent 2010 and 2020 Lab Year technologies. When these vehicles are evaluated over a drive cycle using Autonomie, we are able to determine the energy impact of every technology over the next 10 years.

Evaluating all of these cycles on all the vehicles will require a total of 7 million simulation runs. A few years ago, this task would have been deemed very difficult because of the simulation time necessary. Even if each simulation ran in a minute, a sequential run of so many simulations would extend over a few years. Parallelization could reduce the time to a few months. With the ability to compile the model and then parallelize the runs, this study can be completed in a few days by using distributed computing capabilities, supported by Matlab and Autonomie.

The accelerated evaluation capabilities come at the expense of some upfront tasks. For speeding up the simulation and reducing the memory requirement, not all available signals are recorded. The signals that are absolutely necessary for analyzing the simulation needs to be determined prior to compilation. Similarly, a few test cases should be devised to verify that the variables that are considered as tunable for the model are, indeed, tunable in the compiled version of the model. In lieu of these efforts needed in compiling the model, we can expect the simulations to get approximately 100 times faster.

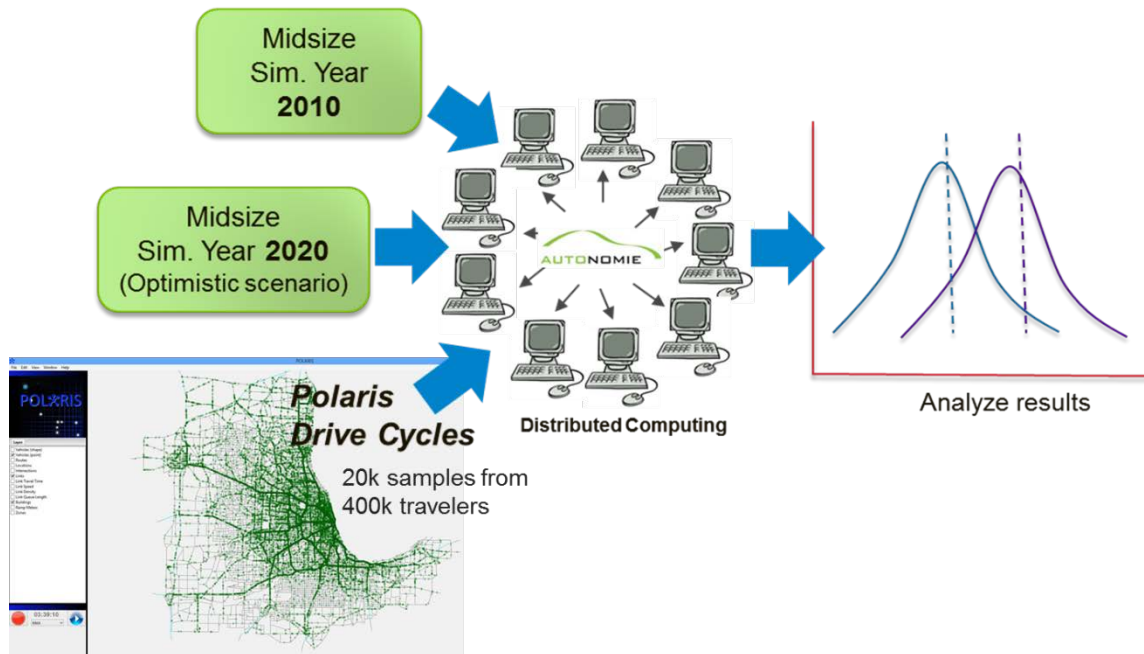


Figure IV-31: Overview of the simulation process involving vehicles from multiple time frames and synthetic drive cycles.

Results

Although the simulations considered cars and trucks with various types of powertrains and fuels, in this report, we will focus on a gasoline-powered conventional vehicle, a split hybrid electric vehicle (HEV), and a plug in hybrid with a 40-mile electric range, equipped with a range extender (EREV-40). For all vehicles, we look at fuel and electrical consumption changes observed on standard US cycles and on cycles generated from POLARIS. The comparisons of these two factors are shown as bar graphs on the top half of the analysis plots of Figure IV-32–Figure IV-34. The blue bar denotes the values observed for technologies available in lab year 2010 (MY 15), and the red bar represents the improved values estimated with technologies that are expected to be available in lab year 2020 (MY 25). A two-dimensional distribution plot is in the lower half of those plots to show how fuel economy or electrical consumption varies when the technology improves over the decade.

The real-world cycles are known to have higher acceleration rates, higher speeds, and higher energy consumption than the regulatory cycles. This is one of the reason behind the lower fuel economy on the real-world cycles. We use the unadjusted regulatory values, and we expect all vehicles to be operating under warmed-up conditions to ensure that the results reflect the sole impact of the drive cycles.

Note that, for this study, the components for vehicles that use electric powertrains are sized to maximize their benefits (regenerative braking for HEVs and electric drive for EREVs) in the UDDS cycle. These vehicles may exhibit better performance on real-world cycles, if they were sized and controlled differently.

In the case of conventional vehicles, the BaSce analysis predicts an improvement of 43% in fuel economy on regulatory cycles. Figure IV-32 shows the mpg variation from about 25 mpg to 36 mpg. On real-world cycles, while the fuel economy average is lower, the percentage improvement observed between the 2010 and 2020 vehicles in real-world cycles is 40%.

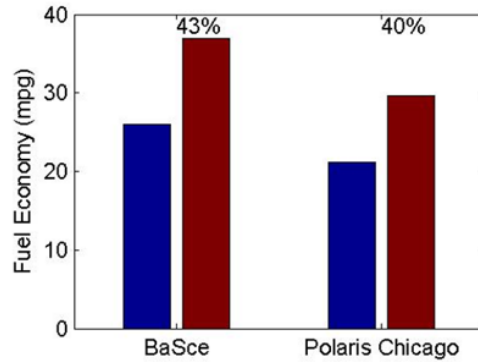


Figure IV-32: Fuel economy improvement on standard and POLARIS Chicago cycles for a conventional vehicle in lab years 2010 and 2020.

In the case of hybrid vehicles, the fuel economy improvements are lower under real world driving conditions than on the standard cycles (respectively 58% vs 68%). In addition, one notes that the fuel economy difference between both set of cycles is smaller than for the conventional vehicles.

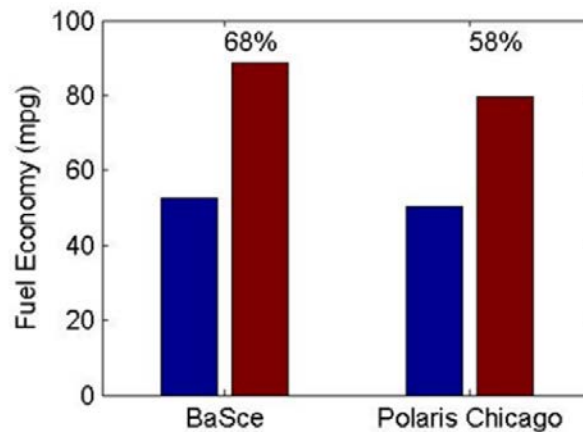


Figure IV-33: Fuel economy improvement on standard and POLARIS Chicago cycles for a HEV in lab years 2010 and 2020.

For EREV-40, most of the POLARIS Chicago cycles can be driven with the stored electrical energy (Figure IV-34). An occasional engine start results in the very high mpg values. The electrical consumption from these vehicles is the more relevant factor to be considered. While regulatory cycles show a 33% reduction in electrical consumption, the POLARIS cycles predict an improvement of 21%. Similar to the other two vehicle categories, EREVs also consume more energy on real-world cycles because of the more aggressive drive cycle characteristics.

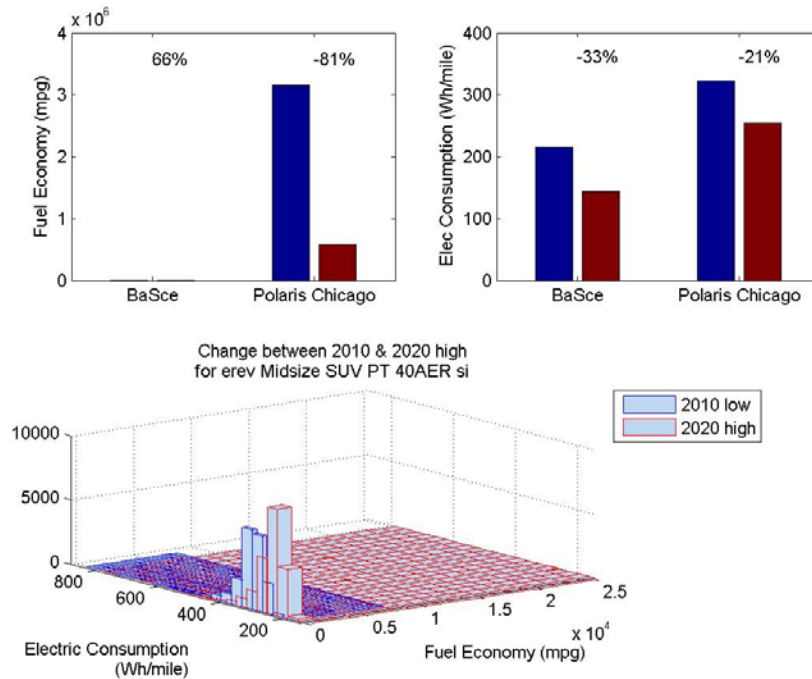


Figure IV-34: Fuel economy improvement on standard and POLARIS Chicago cycles for EREV-40 vehicle in lab years 2010 and 2020.

Extending the results to a nationwide energy consumption

MA3T is a tool developed by Oak Ridge National Laboratory (ORNL) to predict the market penetration of vehicles, based on their fuel economy, cost, and other characteristics (Figure IV-35). In this case, the market penetration predictions are made with regulatory fuel consumption values, as that is likely to be the factor known to consumers. We expect all vehicles to be driven in the same way, as understood from the NHTS data.

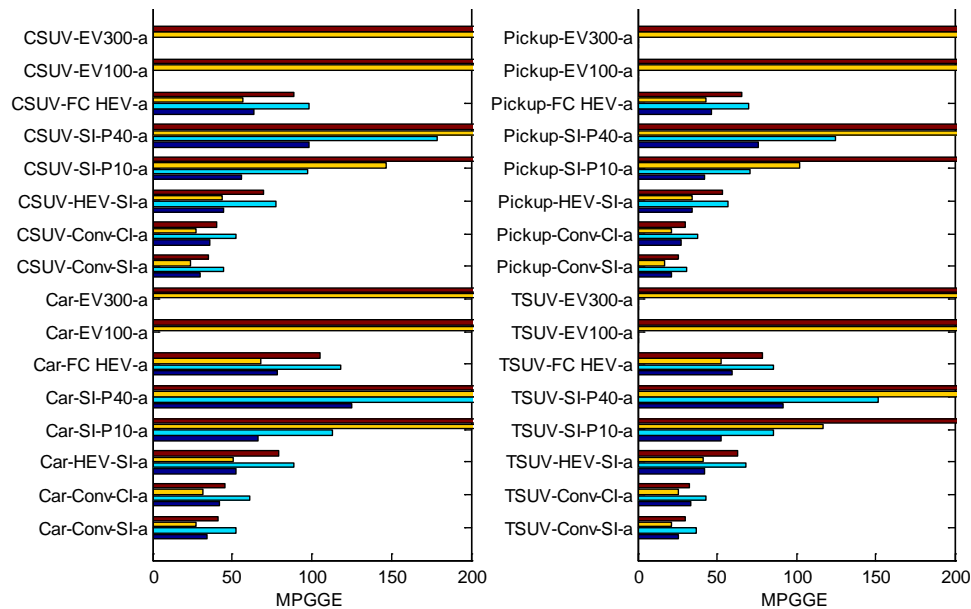


Figure IV-35: Fuel economy estimates for all vehicle types considered in MA3T. Values are truncated at 200 mpgge.

The market share of new vehicles sold in 2015 as well as in 2025 are shown in Figure IV-36. Instead of considering the energy consumed by the entire fleet of vehicles, we will focus on the energy consumed by the new vehicles sold in these particular years. A fleet-level analysis will also be possible, but this requires the simulation of every model year vehicle within the fleet. As a result, the number of simulations needed for this study could be increased by roughly 15 times.

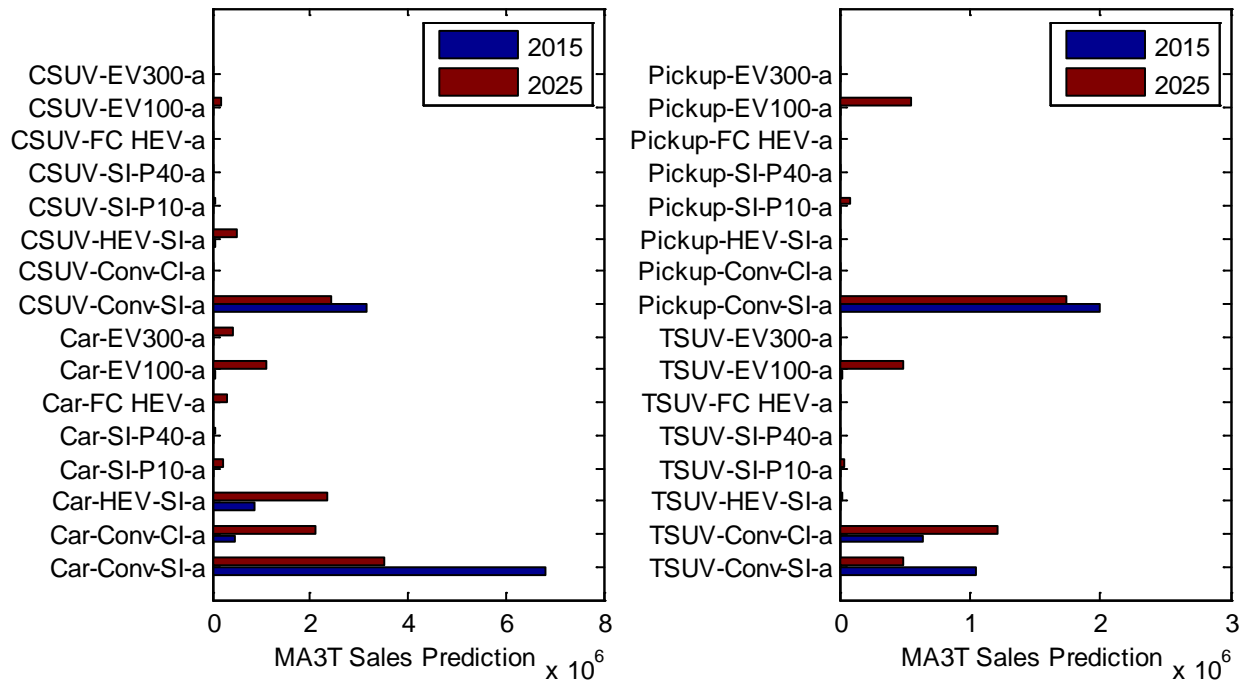


Figure IV-36: The market share predicted for every vehicle class in MA3T.

VMT is computed by combining the market share with driving behavior. In a year, an average car and light truck are expected to be driven 13,852 miles and 15,300 miles, respectively. When we multiply these mileage values with the market share of each type of car and truck, we get the total distance covered by each type of vehicle. The fuel consumed or electrical energy consumed for driving those distances is also estimated by using the known fuel/energy consumption values for each vehicle type. This estimate is as shown in Figure IV-37.

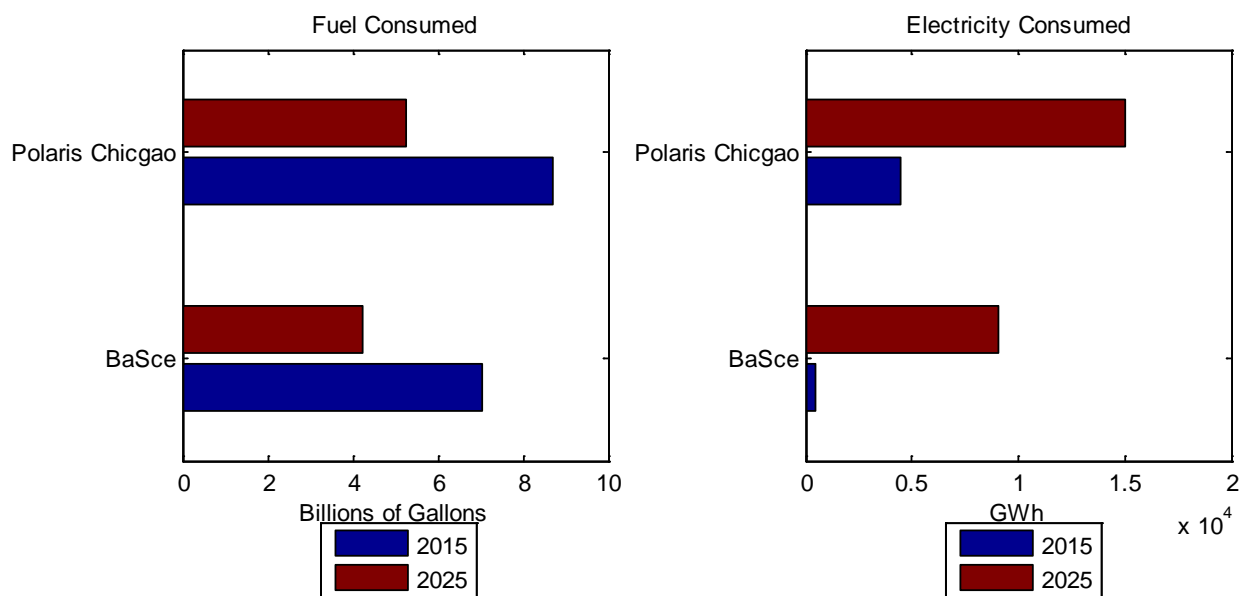


Figure IV-37: Gasoline and electricity needed for automotive applications in years 2015 and 2025.

Conclusions

A new process has been developed to quantify the energy impact of advanced vehicle technologies for real world driving conditions by leveraging multiple tools for transportation system model (POLARIS), vehicle trip profile generation, vehicle energy consumption (Autonomie) and market penetration (MA3T).

Vehicle previously developed to assess the benefits of VTO developed technologies on standard driving cycles were simulated under the set of real world driving conditions and their respective energy consumption benefits compared at the fleet level. The study demonstrated that while the energy consumption under real conditions was expected to increase, the benefits of the different technologies considered between 2010 and 2020 were similar between the standard and the real world cycles. As shown in Figure IV-38, analyses using both regulatory cycles and POLARIS Chicago cycles estimate a 36% reduction in the overall energy consumption

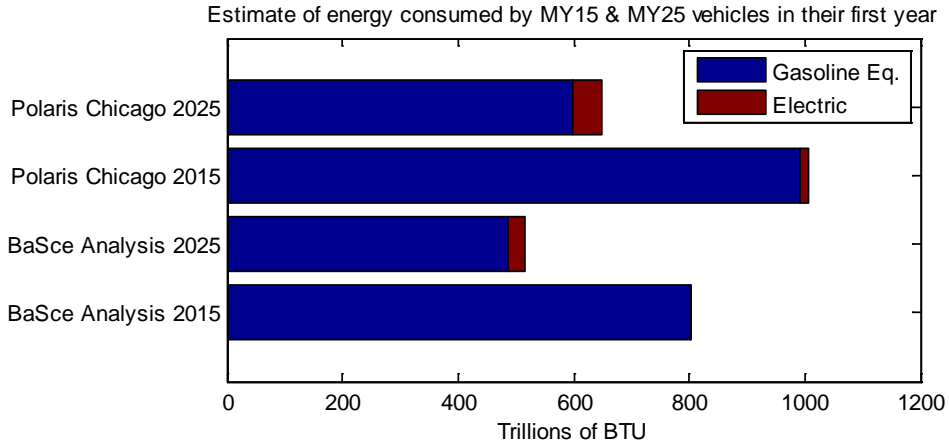


Figure IV-38: Reduction in transportation energy consumption in the next 10 years as vehicles become more efficient.

IV.4.C. References

1. BaSce Analysis, 2015, Report: Assessment of Vehicle Sizing, Energy Consumption and Cost through Large Scale Simulation of Advanced Vehicle Technologies. Available at http://www.autonomie.net/publications/fuel_economy_report.html. Accessed May 4, 2016.
2. Lee. Filipi, "Synthesis and validation of representative real-world driving cycles for Plug-In Hybrid vehicles" Vehicle Power and Propulsion Conference (VPPC), 2010 IEEE, DOI: 10.1109/VPPC.2010.5729040

IV.5. Long-Haul Truck Idle Climate Control Load Reduction & VTCab, Rapid Vehicle HVAC Load Estimation Tool

Jason Lustbader, Principal Investigator

Bidzina Kekelia, Cory Kreutzer, Matt Jeffers, and Sam Schilling, Co-Authors

National Renewable Energy Laboratory

15013 Denver West Parkway

Golden, CO 80401

Phone: (303) 275-4443

E-mail: Jason.Lustbader@nrel.gov

David Anderson, DOE Program Manager:

U.S. Department of Energy

Phone: (202) 287-5688

E-mail: David.Anderson@ee.doe.gov

Lee Slezak, DOE Program Manager:

U.S. Department of Energy

Phone: (202) 586-2335

E-mail: Lee.Slezak@ee.doe.gov

Start Date: October 1, 2015

End Date: September 30, 2017

IV.5.A. Abstract

Objectives

- Develop modeling tools to help quantify the impact of advanced load-reduction technologies and show progress toward at least a 30% reduction in long-haul truck idle climate control loads with a 3-year or better payback period.
- Reduce the risk of advanced technology adoption by improving the quantification of thermal load reduction technology impacts for both design points and national-level estimation.
- Investigate opportunities to reduce truck cab thermal loads through modeling and simulation to decrease the estimated 667 million gallons of fuel used for truck rest period idling.

Accomplishments

- Improved Vehicle Thermal Cab Simulator (VTCab), a standalone version of CoolCalc, by adding a convection model graphic user interface (GUI), a zone and construction painter, an improved COLLABorative Design Activity (COLLADA) file importer that maintains sub-surfaces, and high-performance computer (HPC) parallel simulations (National Renewable Energy Laboratory [NREL] internal only). Eliminated bugs while increasing robustness.
- Completed initial national heating fuel use analysis simulations, which showed that a fuel fired heater with thermal load reduction package (TLRP) could save 973 gallons of fuel per truck annually. While the TLRP provided some fuel savings, its primary benefit was to reduce peak thermal load by 30%, which would improve performance and provide an opportunity for downsizing the heater. These results complement the previous electric air conditioning (A/C) battery idle-off savings of 774 gallons per truck per year. For the A/C system, the TLRP reduced the required batteries by half.
- Cost estimates (based on aftermarket quotes) for the installed combined battery-electric A/C idle-off system, fuel-fired heater, and TLRP were estimated at \$9,000. Simulations show that the payback period of this system is 2 years at \$2.50/gallon and 1.7 years at \$3.00/gallon.

Future Achievements

- Update VTCab so that it provides the full set of features so that the old CoolCalc SketchUp version can be phased out.
- Make further improvements to the national-level fuel use analysis process and add greenhouse gas emissions estimation. Partner with industry to simulate the payback period of various technology configurations, enabling fuel use and payback period-driven design.
- Apply tools to the broader commercial vehicle industry and identify opportunities for climate control and idle load reduction.

IV.5.B. Technical Discussion

Background

A/C and heating are two of the primary reasons for long-haul truck main engine operation when a vehicle is parked. In the United States, trucks that travel more than 500 miles per day use 667 million gallons of fuel annually for rest period idling [1]. This rest period idling is approximately 6.8% of the total long-haul truck fuel use and represents a zero freight efficiency operating condition for the truck. Including workday idling, more than 2 billion gallons of fuel are used annually for truck idling [1]. Even with lower diesel prices, fuel remains one of the largest operating costs for long-haul trucks, and increased volatility of fuel prices provides a significant financial incentive to reduce fuel use. Recent federal, state, and city anti-idling regulations [2] are providing further incentives to reduce truck idling. One example is the idle reduction technology credit in the Heavy-Duty Greenhouse Gas Emissions Standards [3] and the Phase 2 Greenhouse Gas Emissions Standards [4].

By reducing thermal loads and improving efficiency, there is an opportunity to reduce the fuel used and emissions created by idling. Enhancing the thermal performance of cabs/sleepers will enable cost-effective idle-reduction solutions. If the fuel savings from new technologies can provide a 1- to 3-year payback period [2], fleet owners will be economically motivated to incorporate them. This provides a pathway to the rapid adoption of effective thermal and idle load-reduction solutions. Therefore, financial incentive and a need to meet regulations in a cost effective manner provide a pathway to rapid adoption of effective thermal load and idle reduction solutions.

Introduction

NREL's CoolCab project is researching efficient thermal management strategies that keep the vehicle occupants comfortable without the need for engine idling. To achieve this goal, NREL is developing tools and test methods to assess idle-reduction technologies. The heavy-duty truck industry needs a fast, high-level analysis tool to predict thermal loads, evaluate load reduction technologies, and calculate their impact on climate control fuel use over a wide range of temperatures and use conditions.

To achieve an effective solution, NREL first conducted baseline testing of vehicles to quantify their thermal behavior. This information was then used to build and validate a CoolCalc model. CoolCalc is NREL's rapid heating, ventilating, and air conditioning (HVAC) load estimation tool [5]. In FY14, CoolCalc thermal models were then used in conjunction with experimental screening tests to identify promising thermal load reduction technologies. The most promising technologies were combined into a Complete-Cab TLRP. Previous tests showed that this reduced A/C electrical loads by more than 35.7%, exceeding the 30% goal [5]. In FY15, NREL tested the impact of this Complete-Cab TLRP on heat loads using an overall heat transfer coefficient, UA, test procedure. This showed a 43% reduction in heating loads. The Complete-Cab TLRP was then updated with improved insulation (an additional thin layer of advanced insulation with reflective barrier was added to the previously tested thermal insulation package), resulting in a UA heating load reduction of 53.3% [6].

To evaluate the impact of these technologies on fuel use and payback period, NREL has developed a national thermal, climate control load, and fuel use simulation process. This process leverages NREL's VTCab vehicle thermal system modeling tool CoolSim, and vehicle models Future Automotive Systems Technology Simulator (FASTSim) or Autonomie. VTCab is a simplified HVAC load estimation tool that enables rapid exploration of idle reduction and climate control design options for a range of climates. CoolSim is a Simulink-based air conditioning and thermal system modeling tool allowing for detailed system models. Both FASTSim and Autonomie are vehicle simulation tools that allow for impact estimation of parasitic loads on vehicle performance and energy use.

Using this process, a model of the base Complete-Cab TLRP was used to understand the national impact of the climate control load reduction technologies on thermal performance, climate control loads, and fuel consumption, spanning the wide range of use and environmental conditions that occur in the United States. In FY16, the impact on heating fuel use reduction was addressed and the payback period of these systems was evaluated. VTCab was also improved further.

Approach

Overview

The goals of the CoolCab research project are to reduce thermal loads, improve occupant thermal comfort, and maximize equipment efficiency to eliminate the need for rest period engine idling. To accomplish these goals, NREL is closely collaborating with original equipment manufacturers and suppliers to develop and implement commercially viable thermal management solutions. To understand the potential impact of thermal load reduction solutions and to inform their design, NREL's national thermal analysis process is used to simulate thermal loads, electrical loads, fuel use, and emissions.

Rest-Period Climate Control Fuel Use Estimation

To estimate the fuel use of thermal load reduction technologies during rest-period climate control operation, a fuel use estimation process was developed leveraging VTCab, CoolSim, and vehicle models.

VTCab is an easy-to-use, simplified, physics-based HVAC load estimation tool that requires no meshing, has flexible geometry, excludes unnecessary detail, and is less time intensive than more detailed computer-aided engineering modeling approaches. For these reasons, it is ideally suited for performing rapid tradeoff studies, estimating technology impacts, and sizing preliminary HVAC designs. These attributes make VTCab a critical tool for achieving the project goals. It enables rapid evaluation of thermal load reduction technologies, not only at extreme design points, but also over the wide range of weather and use conditions that the vehicles will experience. Each phase of the CoolCab project approach leverages VTCab.

CoolSim is a MATLAB/Simulink-based air conditioning and thermal system modeling tool. It is an integrated single- and two-phase thermal system modeling framework. This integrated approach allows for rapid system analysis and design in a flexible and open modeling environment. This tool provides the performance model for the A/C system, linking thermal loads to electrical or mechanical loads.

NREL uses both FASTSim and Autonomie for vehicle modeling. FASTSim is NREL's rapid vehicle modeling tool and Autonomie is a Simulink-based vehicle model developed at Argonne National Laboratory. The vehicle models provide a link from electrical or mechanical load to fuel use.

A high-level overview of the process is shown in Figure IV-39 and includes the relationship between each step in the process and the associated type of energy evaluated or converted in the step. For national-level analysis, additional components are added to this fuel use estimation process and include national weather station selections, vehicle-miles-traveled (VMT) weighting, as well as high-performance computing and result post-processing steps. Each subtask is described in the following sections.

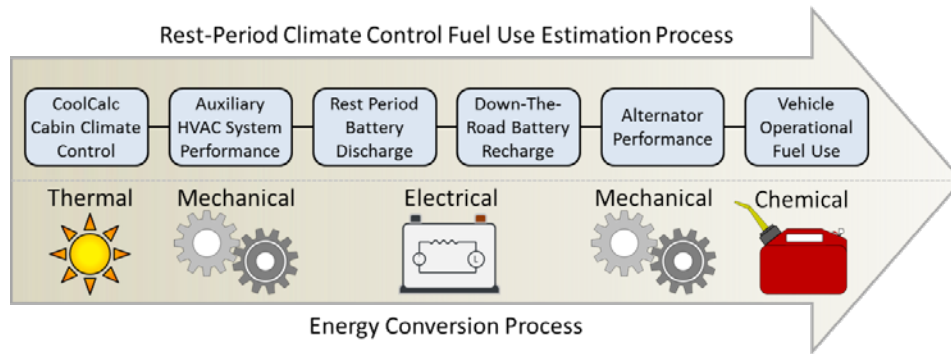


Figure IV-39: Relationship between the rest-period climate control fuel use estimation process and energy conversion

Weather Station Weighting by Truck VMT

The impact of thermal load-reduction technologies on long-haul trucks is dependent on weather conditions. The location and time of year, therefore, are important inputs for a VTCab thermal analysis. VTCab simulations use Typical Meteorological Year weather data to simulate vehicle thermal behavior at many different locations throughout the United States. The distribution of weather stations, however, is not correlated with the distribution of long-haul truck traffic throughout the United States. Thus, the simulation results from each weather station cannot be weighted equally when distilling results into a single, representative national-average value for a technology's impact on rest-period idling. For a national-level VTCab analysis, the results of simulations in different cities are weighted by the fraction of long-haul trucks operating in and around each of those cities. It is assumed that the geographic distribution of trucks during rest periods is proportional to the distribution of on-road truck traffic. Therefore, an analysis was performed to determine the relative importance of each weather station in the contiguous United States in terms of its proximity to long-haul truck traffic.

Truck traffic density data for long-haul trucks were available from the Freight Analysis Framework dataset [5]. The traffic data were uploaded into geographic information system software [5], which divided truck routes into small traffic segments with average number of trucks traveling the segment per day. The truck traffic data were imported into MATLAB for analysis. First, the data were filtered to remove unwanted segments: those pertaining to truck routes outside the contiguous United States and those containing zero truck traffic. The daily average VMT for each segment were calculated from the segment length and the average number of trucks traveling on that route per day. For each route segment, the distance to every weather station was calculated, the closest weather station was identified, and the VMT for the segment were allocated to the closest weather station. The total VMT for each weather station were calculated, and a VMT-weighting was determined for each weather station.

Weather Station Down-Selection

Not every weather station contributes significantly to the results of a national-level analysis because many of the stations represent a very small percentage of the national total VMT. To reduce the time required to run the national-level simulations and to process and analyze the results, an iterative process was used to down-select the list of weather stations. Beginning with the full set of approximately 900 stations (Figure IV-40A), the closest weather station was identified for every route segment. The VMT for each route segment were allocated to the closest weather station, the total VMT per weather station was calculated, and the stations were sorted by total VMT per station. The weather station that represented the fewest VMT was eliminated from the list. For the next iteration, the closest weather station for every segment was again identified, now with one fewer station from which to choose. The segment VMT were applied to the closest weather station and the total VMT per station was recalculated. In this way, the VMT that were originally applied to the eliminated station were reallocated to the next nearest weather station(s), conserving the number of total truck VMT across the United States. The iterative process was continued until only the desired number of weather stations remained. The 200 weather stations remaining in the list are shown in Figure IV-40B. VTCab simulations were performed using weather conditions for each of these stations, and the results were weighted by the final VMT weightings for each station.

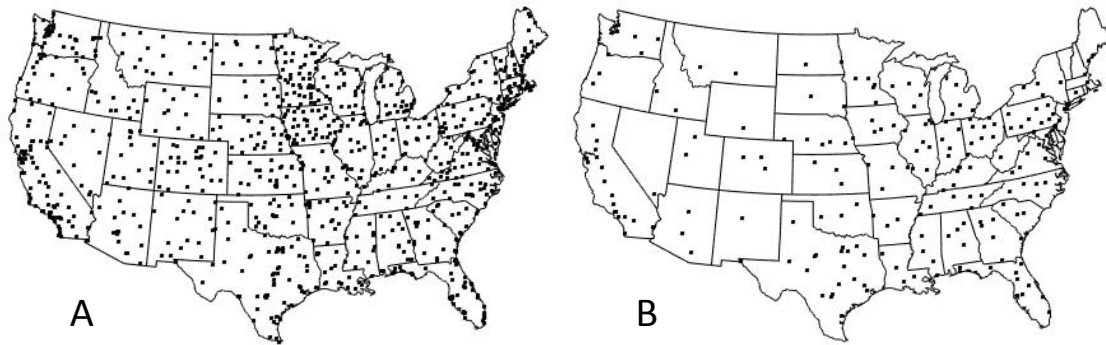


Figure IV-40: Map of weather station locations for A, all stations and B, remaining top 200 stations

VTCab: Cabin Climate Control

After the weather station weighting by VMT, a VTCab model of the vehicle cabin was created and validated with local experimental data. VTCab is a new standalone version of CoolCalc, described in more detail in [5]. The vehicle cabin model contained the thermal load reduction package and the baseline package. An HVAC system was created for the sleeper compartment with heating and cooling target temperatures at 72°F and 65°F, respectively. A high-performance computer was used to perform an annual simulation at each of the 200 down-selected weather locations for both the baseline and TLRP model configurations. The primary outputs of the VTCab analysis were the time-dependent cooling and heating thermal power required to maintain the sleeper compartment target temperature throughout the entire year for each location. These thermal load results were then converted into A/C system electric loads or fuel-fired heater fuel use as described in the subsequent steps.

CoolSim: Auxiliary Electric HVAC System Performance

To convert time-dependent thermal load results for both the complete-cab package and the baseline configuration, a model of a generic example auxiliary electric A/C system was created using the CoolSim modeling tool previously developed [6]. Due to the large quantity of results obtained and the difference in run-time between VTCab and the A/C system model, the A/C system simulations were used to build a detailed performance look-up table. The A/C system was operated at each combination of ambient temperature and flow rate until steady-state operation was achieved. Then the corresponding thermal power demand of the evaporator and the system electrical power consumption were calculated. These were used to generate look-up tables of thermal load and system electrical power consumption as functions of ambient temperature and blower flow rate. The look-up tables were then used to convert VTCab cabin thermal results into A/C system electrical energy consumption at each time step.

Battery Electrical (MATLAB): Rest-Period Battery Discharge

Once the auxiliary A/C system electrical energy consumption was calculated for each time interval, an internal resistance-based battery model was used in conjunction with a battery discharge algorithm to quantify the impact of the A/C system electrical energy consumption on the on-board battery. For the analysis, eight 104-Ah, 12-V group 31 absorbed-glass-mat deep-cycle batteries were modeled based on capacity recommendations from the A/C system manufacturer. The MATLAB/Simulink-based internal resistance battery model was adapted from ADVISOR [7] and selected for its ability to accurately and simply model lead-acid type batteries. For the battery discharge process, data over a 24-hour period for each configuration and location was selected. At the beginning of the 24-hour period, the battery pack was initialized to be fully charged. As the A/C system electrical energy was discharged over the 24-hour period, losses in the HVAC system inverter were included. The battery discharge process then proceeded by calculating the battery state of charge (SOC) throughout the day based on the A/C system energy consumption at each time interval. At the end of the 24-hour period, the final SOC of the batteries was saved for subsequent evaluation. If the loads for the 24-hour period fully depleted the batteries, a full depletion event was saved and the battery pack reinitialized to a full SOC for subsequent depletion. In this case, both a fully depleted and a partially depleted SOC for the 24-hour period were collected.

Battery Electrical (MATLAB): Down-the-Road Battery Recharge

After the discharge process was completed, each discharge event was then cycled through a recharge event. The battery recharge process utilized the same internal resistance battery model described for the discharge process. In addition to the battery model, a battery-charging algorithm was needed to accurately model the battery management system function for the battery pack. A three-phase charging algorithm was selected and included a bulk phase, absorb phase, and float phase. However, because the float phase maintains an existing charged battery, it was omitted in the analysis. Assuming adequate supply from the alternator, the bulk phase of the charging algorithm supplied 0.2 times the C-rate for the battery until the actual current consumption by the battery was reduced to below 90% of the supply current. Thereafter, for the absorb phase, the battery management system held the supply voltage at 14.9 V for 1.5 times the duration of the bulk phase. The charging algorithm was subjected to reduced supply capacity at any time interval if the alternator was unable to provide the necessary power. Due to the coupling of the battery recharge event to alternator and vehicle performance, recharging, vehicle accessory load calculation, and down-the-road fuel use estimations were performed simultaneously and are described in subsequent sections.

Battery Electrical (MATLAB): Alternator Performance

To supply the auxiliary A/C system battery pack with adequate power for recharging during down-the-road operation, a high-capacity engine alternator was modeled. For the model, the performance of a claw-pole brushed alternator was used, and the maximum current output of the alternator as a function of alternator speed in addition to the alternator efficiency as a function of current and speed were used for the analysis. The alternator was sized to have a 275-A rating to adequately charge the batteries over a typical long-haul driving period. To determine the alternator speed at a given engine speed, a pulley ratio of 2.5:1 was used. In addition to the energy needed for recharging the battery pack, additional electrical accessory loads of 0.35 kW on the alternator were included to represent operation of additional vehicle components such as headlights and radio. The 0.35 kW was selected based on the U.S. Environmental Protection Agency (EPA) Greenhouse Gas Emissions Model (GEM) Model Class 8 combination tractor modeling parameters used for heavy-duty greenhouse gas emissions credits [11].

Fuel-Fired Heater

Fuel-fired heaters can be used on long-haul trucks to provide thermal heating loads directly from fuel. The fuel use rate for these systems was calculated by determining the fuel energy density from the lower heating value of diesel and its density. This was then used with an average fuel fired heater efficiency, which was determined based on heater specification sheets. This efficiency was found to be 83.8%, which results in a fuel use rate of 0.03177 gal/kWh. Thermal load requirements from the VTCab model could then be used with this value to determine the heating fuel requirements.

Vehicle Operational Fuel Use Estimation

In order to calculate the vehicle fuel use during the down-the-road auxiliary A/C system battery recharge process, a vehicle model was needed. The vehicle model provided the link between mechanical accessory power demand of the alternator to the fuel used by the engine. For the fuel use estimation process, Autonomie was used with a non-proprietary open-use Class 8 long-haul truck vehicle model developed by Oak Ridge National Laboratory. The vehicle model was modified to match the EPA GEM Model Class 8 combination tractor modeling parameters [11], and electrical accessory loads were disabled for the model. In addition, three Heavy Heavy-Duty Diesel Truck (HHDDT) schedule components were used: HHDDT 65 Cruise cycle, HHDDT Cruise cycle, and the HHDDT Transient cycle. The vehicle model was operated over a range of mechanical accessory loads, vehicle weights, and the three drive cycles. The average fuel consumption at each combination was quantified and was used to generate a fuel performance curve as a function of the input variables. It was determined that the impact of vehicle weight variation due to thermal load reduction technologies on cycle average fuel consumption was insignificant and therefore gross vehicle weight was held constant at 29,000 kg for the analysis.

A visual description of the beginning and end of a single recharge event is provided in Figure IV-41. The recharge process began by selecting a drive cycle and ending SOC from the rest-period discharge sequence. For each time interval in the recharge event, the charge current from the battery-charging algorithm was

determined and added to the additional accessory electrical loads (i_{other}). The combined current demand was then used in conjunction with the cycle averaged engine speed to calculate the alternator efficiency. If the current demand exceeded the maximum current at the specified speed, only the maximum alternator current would be supplied. Next, the vehicle mechanical accessory power was calculated based on the current and bus voltage, in addition to the power regulator efficiency, alternator efficiency, and alternator-to-engine belt efficiency. The accessory power and drive cycle were then used as inputs to the vehicle performance map to determine the fuel use rate. In parallel, the process was repeated at each step without the battery charging electrical load and only accessory electrical loads. The difference between the fuel use with and without the battery charging at each time interval was calculated. The process was repeated for each time interval throughout the recharge process, and the cumulative fuel use difference with and without battery charging was calculated. The entire recharge process was then repeated for each of the three drive cycles. Every ending SOC was saved from the rest-period discharge process. Once the drive cycle specific fuel use for each recharge event was calculated, cycle weighting fractions from the EPA GEM analysis transient cycles of 86% for the HHDDT 65 Cruise, 9% for the HHDDT Cruise, and 5% for the HHDDT [11] were applied to the result to determine a composite fuel use for each recharge event. Finally, the daily electrical HVAC load profile obtained early in the analysis was integrated, and the corresponding fuel use was used to generate a fuel use rate per electrical HVAC energy. This fuel use rate per electrical energy was then applied to the HVAC load profile for the day to generate an approximate fuel use at each time interval for use with additional post-processing tools.

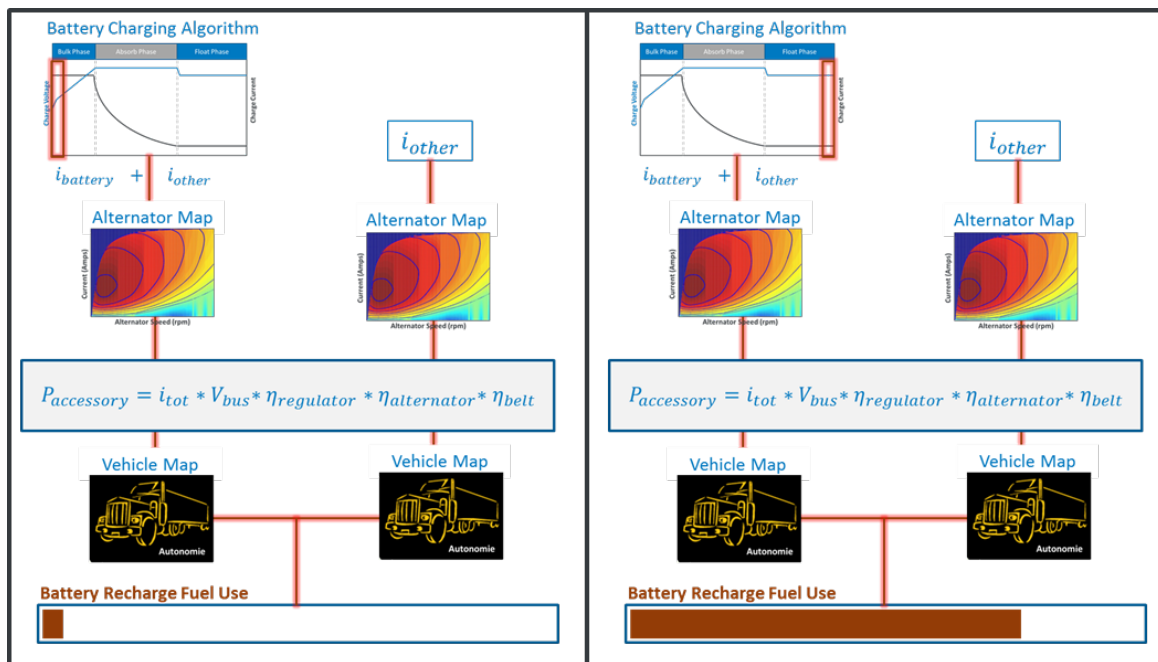


Figure IV-41: Auxiliary A/C system battery pack recharge process sequence for fuel use estimation. A (left), beginning of a recharge event; B (right), end of a recharge event.

Results

VTCab Improvements and New Features

An updated version of VTCab, a SketchUp-independent version of CoolCalc, was completed and released for feedback from industry partners. For rapid preliminary tool development and the demonstration of CoolCalc, use of the SketchUp environment was very beneficial; however, this dependency is also a disadvantage because of updates that are required for CoolCalc to remain compatible with SketchUp as the SketchUp product changes over time. For this reason, development of VTCab was initiated.

The primary purpose of VTCab is to retain and improve upon existing CoolCalc functionality with standalone execution of the software. VTCab is currently being developed to use EnergyPlus as the thermal solver; however, future development could include the addition of a thermal solver developed in the MATLAB/Simulink environment. VTCab provides additional programming flexibility and control while eliminating unnecessary SketchUp tools and features that were not used in CoolCalc projects. VTCab also simplifies the installation process with a single installer, providing a faster and simpler procedure for new users. A picture of the VTCab interface is shown in Figure IV-42A.

The VTCab beta version has all the basic tools needed to build a model from imported geometry, set up parametric variables, and run the model using the GUI.

Various enhancements have been made to VTCab. These include the following:

1. The COLLADA file importer was improved further to maintain all subsurfaces from the original geometry during import.
2. A convection model GUI, Figure IV-42A, was added to VTCab, which easily allows for application of custom convection models to the various interior surface groups: floor, walls, windows, and roof. Example models are provided.
3. Zone and construction painters were added (Figure IV-42B and Figure IV-42C), allowing easy application of construction properties and zone assignment to surfaces. The constructions are built from material objects. The stack of materials determines the construction properties. The construction name, resistance, R-value, thickness, and conductivity are provided for easy selection. Once the desired construction is selected in the list box, it can be applied to surfaces using the paint can icon. Similarly, the zone painter tab allows the user to easily select and assign zones to the surfaces. From this interface, zones can also be added, renamed, assigned colors for rendering, or removed. This is particularly important after importing geometry. After geometry import from a COLLADA file, each surface needs to be assigned to a zone. Rendering the surfaces by construction or zone was added to help the user quickly see the surface properties. In this view, each surface is colored by either its construction or zone assignment.
4. The parametric simulation capability was improved in VTCab. The parametric variables allow the user to define multiple values for a model input parameter (e.g., insulation thickness or conductivity) and evaluate the impact parametrically. Interdependent variables can be grouped together to ensure associated values are simulated together in the desired sequence. Weather files can also be set up as parametric variables (and grouped by state, geographic region, population density, etc.). This feature provides full control over the parameter combinations in the run simulation GUI, up to full factorial parametric simulations. The ability to run these simulations in parallel on an HPC was added. While the parallel HPC simulations are currently an NREL internal-only tool, it is a critical addition to support large national-level simulations.
5. Multiple bugs were identified and resolved and the program robustness was further improved.

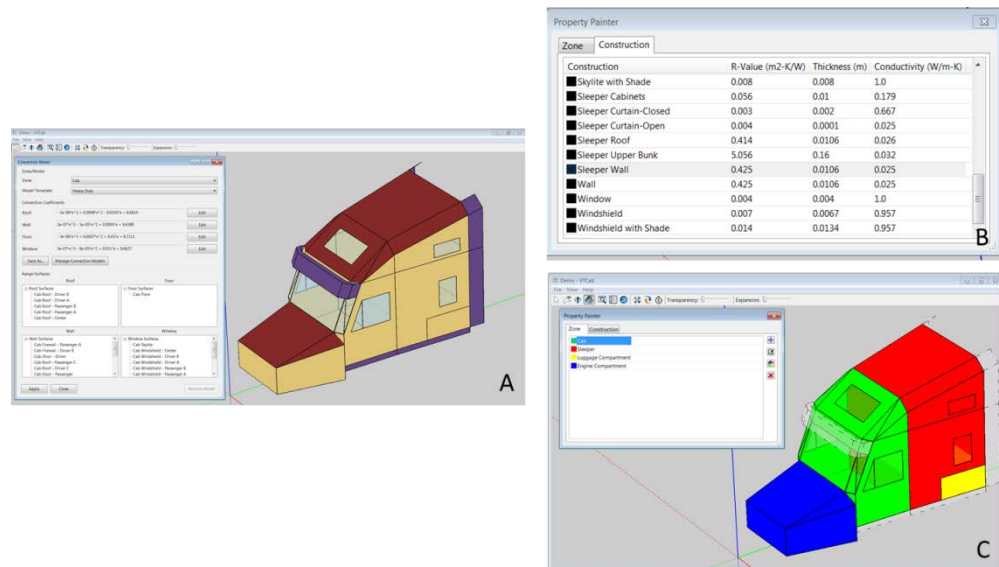


Figure IV-42: VTCab interface: A, convection GUI, B, construction pallet, and C, zone assignment painter

Results—Comparison of Cases

Annual simulations were carried out for the 200 selected locations for unmodified (standard) sleeper cab and a sleeper cab modified with a Complete-Cab TLRP with a "no-idle" electric A/C unit and a fuel fired heater.

For comparison to a baseline system, a number of idling assumptions were made. The number of operational days for a long-haul truck with a rest period was assumed to be 260 annually. This assumption is on the conservative side of prior estimations of 250–300 days [11]. To be consistent with current rest period regulations, a 10-hour rest period within each 24 hours of operation was assumed. These 10 hours were assumed to be equally probable throughout each 24-hour period. This assumption could be replaced with a time-of-day probability when this information is available. Idling fuel consumption of a truck engine was assumed to be 0.8 gal/h [12]. It should be noted that this analysis assumes trucks idle only when there is an HVAC load.

Air conditioning results: VTCab thermal reduction results for the A/C system are shown in Figure IV-43A. The TLRP reduced cooling thermal loads by up to 57%. This reduction in thermal power requirements would result in the same A/C system providing much better cooling performance. This also allows the possibility of reducing the A/C system power capability and thus reducing cost and weight. Using the thermal load requirement and environmental conditions at each one-minute time step, the required A/C power was calculated from the detailed performance map created in CoolSim. This resulted in an average annual coefficient of performance of approximately 1.83. Corresponding daily maximum 10-hour electrical load requirements, shown in Figure IV-43B, were reduced by 46%. This exceeds the initial goal of a 30% reduction in cooling loads.

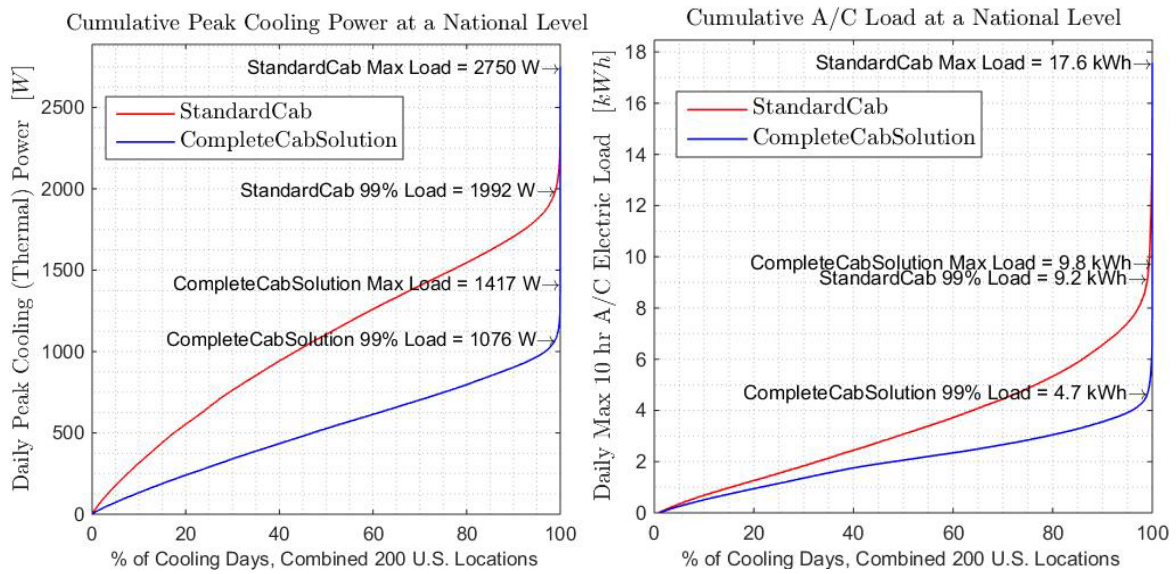


Figure IV-43: A (left), daily peak cooling power for combined cooling loads of 200 US locations and B (right), daily maximum 10-hour window A/C electric loads

Lowering the A/C energy requirement reduces the battery size requirement, which provides significant additional cost savings and incentive for the auxiliary A/C system installation. Assuming an inverter efficiency of 90%, a 9.2-kWh A/C electrical load for a standard cab would need at least eight 104-Ah (≈ 1.25 kWh) batteries. A cab with TLRP would require approximately four batteries to meet 4.7 kWh of A/C electrical load. Assuming that during a 3-year period of use, the pack of batteries has to be replaced once, the cost savings could add up to \$1,400 (see Table IV-4).

Table IV-4: Battery sizing impacts of TLRP

"No-idle" Electric A/C System Configuration	Number of 104 Ah (1248 Whr @ 12V) Batteries	Cost per Battery	Initial Cost Reduction of Electric A/C System	Number of Replacements During 3-year Period	Battery Replacement Cost During 3-year Period	Savings During 3-year Period
Standard electric A/C system	8	\$ 175	\$ -	1	\$ 1,400	\$ -
Electric A/C system with reduced battery pack	4		\$ 700	1	\$ 700	\$ 1,400

Once the electrical discharge demands were known, the battery model was recharged for each day over three drive cycles and the loads were applied to a vehicle model. The drive cycle weighted fuel cost per battery energy used was calculated. This was then used to account for fuel used to recharge the battery as described in detail in the Approach section. The benefits from reducing idle time and cooling loads due to application of these technologies are summarized in Table IV-5.

Table IV-5: A/C national-level fuel use simulation result summary

Truck Configuration	During Rest Periods [hour]	During Rest Periods [gal/yr]	Fuel Price [\$/Gal]	During Rest Periods [\$/year]	Annual Savings in Fuel Costs	3 Year Savings in Fuel Costs
Standard Cab - idling*	989.6	791.7	\$ 2.50	\$ 1,979	\$ -	\$ -
Complete-Cab TLRP-idling	806.9	645.6		\$ 1,614	\$ 365	\$ 1,096
Standard Cab with electric A/C system		34.8		\$ 87	\$ 1,892	\$ 5,677
Complete-Cab TLRP with electric A/C system		17.4		\$ 44	\$ 1,936	\$ 5,807
*Rest period idling hours assume that idling only occurs when an HVAC load is present. If trucks are idled the full duration of rest periods (even after HVAC load goes to zero), then an additional 164 hours per year should be added to the "Annual A/C On Time". This would increase standard cab annual fuel use for cooling by 131.2 gal/year. At nominal diesel fuel price of \$3/gal this would provide an additional savings of \$393.60/year or \$1180.80 in 3 years.			\$ 3.00	\$ 2,375	\$ -	\$ -
				\$ 1,937	\$ 438	\$ 1,315
				\$ 104	\$ 2,271	\$ 6,812
				\$ 52	\$ 2,323	\$ 6,968
			\$ 4.00	\$ 3,167	\$ -	\$ -
				\$ 2,582	\$ 584	\$ 1,753
				\$ 139	\$ 3,028	\$ 9,083
				\$ 70	\$ 3,097	\$ 9,291

Heating results: Figure IV-44A shows the daily peak heating thermal load for the baseline and TLRP simulations. The TLRP provides approximately a 30% reduction in peak heating load. This will improve the heater performance at attaining and maintaining the set point temperature, improving comfort. This load reduction could also be used to downsize the required heater size. From prior testing [6], a 40% reduction in peak power requirement from the TLRP was expected. It appears that the model is underestimating the TLRP benefit. The curtain properties used in the model are a possible cause of less peak load reduction in simulation, but this discrepancy needs to be investigated further. For the purposes of this study, the model is providing a conservative estimate of the heating requirement reduction and thus can be used for further analysis.

Due to the selection of thermal reduction technologies that favor reducing cooling loads over heating loads, the TLRP picks up less solar heat during the day as can be seen in Figure IV-44B. At night, the 30% peak load reduction is achieved. When the sun rises, the solar radiation increases and the baseline cab load drops to zero. The TLRP vehicle's heating load decreases slower due to lower solar gain, and in this case, does not reach zero load. This results in an increased heating time for the TLRP, but still significantly reduces the total heating energy requirement. The reduced solar heat gain is likely due to both the lighter color and the very reflective shades. The goal of this TLRP package was to reduce the battery requirements and thus trade-off some heating load reduction for additional cooling benefit. This is a good illustration of how these tools can be used to make cab thermal design decisions.

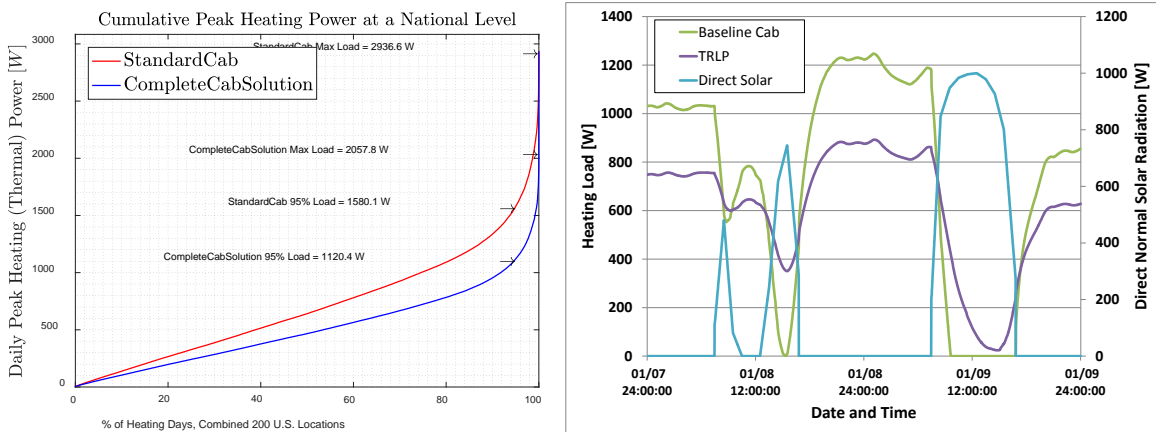


Figure IV-44: A (left), daily peak cooling power for combined cooling loads of 200 U.S. locations and B (right), daily maximum 10-hour window A/C electric loads

Using the heater fuel use as described in the approach section, the fuel savings using the thermal load reduction technologies and the fuel fired heater were calculated. The benefits from reducing idle time and heating loads due to the application of these technologies are summarized in Table IV-6.

Table IV-6: Heating national-level fuel use simulation results summary

Truck Configuration	Annual Heat On Time During Rest Periods [hour]	Fuel Use During Rest Periods [gal/yr]	Diesel Fuel Price [\$/Gal]	Fuel Cost for Heating During Rest Periods [\$/year]	Annual Savings in Fuel Costs	3 Year Savings in Fuel Costs
Standard Cab - idling*	1240.7	992.6	\$ 2.50	\$ 2,481	\$ -	\$ -
Complete-Cab TLRP-idling	1401.5	1121.2		\$ 2,803	\$ (322)	\$ (965)
Standard Cab with electric A/C system		24.3		\$ 61	\$ 2,421	\$ 7,262
Complete-Cab TLRP with electric A/C system		19.7		\$ 49	\$ 2,432	\$ 7,297
			\$ 3.00	\$ 2,978	\$ -	\$ -
				\$ 3,364	\$ (386)	\$ (1,157)
				\$ 73	\$ 2,905	\$ 8,715
				\$ 59	\$ 2,919	\$ 8,756
			\$ 4.00	\$ 3,970	\$ -	\$ -
				\$ 4,485	\$ (514)	\$ (1,543)
				\$ 97	\$ 3,873	\$ 11,619
				\$ 79	\$ 3,891	\$ 11,674

Adding the fuel fired heater quickly saves significant money over idling for heating. Adding the thermal load reduction package saves thermal energy and thus additional fuel over the baseline fuel fired heater. Simulations showed that the fuel fired heater with TLRP saved 973 gallons per truck each year. It should be noted, however, that this TLRP does increase heater on-time. With the assumption of a fixed fuel use rate per time for idling (rather than load dependent), this results in additional idling fuel use for a configuration without a fuel fired heater. The system achieves its design target, but caution should be used with this TLRP design if a fuel fired heater is not part of the idle reduction solution.

Payback period: In order to estimate the payback period of this system, several quotes were obtained for an aftermarket battery electric air conditioning unit. Based on three quotes, an installed cost of \$7,000 for a battery electric air conditioning unit with eight group 31 absorbed-glass-mat deep-cycle batteries was used. The cost of each battery was estimated at \$175, so the TLRP with only four batteries saved \$700 and the system cost was estimated at \$6,300. For the TLRP a cost estimate of \$800 was used. Therefore, the total installed cost for the battery electric A/C system with the TLRP was \$7,100. Based on these same quotes, an estimate of \$1,900 for the total installed cost of a fuel fired heater system was used. Figure IV-45A shows savings of the battery electric A/C system with TLRP over time. A payback occurs in approximately 3 years at a fuel cost of \$3.00/gal. In year 4, the batteries are replaced, which costs half as much as a system without the TLRP. Figure IV-45B shows the savings of the battery fuel fired heater with TLRP. The cost of the TLRP is only included in the A/C system and not in the fuel fired heater plot.

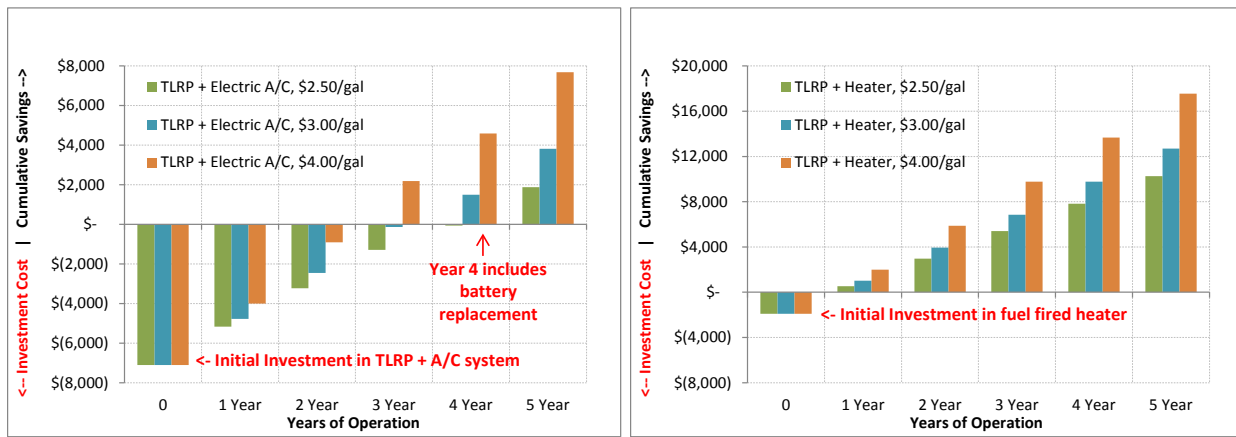


Figure IV-45: A (left), savings for the battery-electric A/C with TLRP and B (right), savings for the fuel fired heater with TLRP

For the combined battery electric air conditioning system, fuel fired heater, and TLRP, the payback period was approximately 1.7 years at \$3.00 per gallon and 2 years at \$2.50 per gallon.

Conclusions

NREL's national HVAC load and fuel use estimation process was used to evaluate a long-haul truck rest-period TLRP coupled with a battery electric HVAC system and fuel fired heater. This process combines VTCab thermal load estimation, CoolSim A/C simulation, and a vehicle performance model (Autonomie or FASTSim). Preliminary analysis performed using these tools showed that adding a thermal load reduction technology package and auxiliary electric A/C system to a standard cab could save up to 774 gallons of fuel annually per truck. At a diesel fuel price of \$3.00/gal, this fuel savings translates into \$6,968 over the first 3 years of operation. In addition to fuel savings, the thermal load reduction package reduces HVAC battery energy requirements by half, thus requiring fewer batteries and lowering the cost. The reduction in peak cooling demand could also allow for reducing the size and/or improving performance of a "no-idle" A/C system. This analysis also showed that a thermal load reduction technology package with fuel fired heater could save up to 973 gallons of fuel annually per truck. While most of the fuel savings is from the low fuel use rate of the fuel fired heater, the TLRP reduced the peak power requirements by approximately 30%. This will improve performance and/or reduce heater capacity. This peak power prediction from the model is lower than expected from test data. While this needs to be investigated further, the prediction is conservative and thus was used for the analysis. It is also important to note that while the thermal load reduction package did significantly reduce total heating energy required, it also reduced heat gain from the sun during cold days, and as expected, increased idle time. This trade-off is consistent with the design priority of the system to reduce cooling loads and overall fuel use for a battery electric, fuel fired heater system. It is a good illustration of the opportunity to use these tools for design of cab load reduction solutions for specific constraints.

Based on quotes, the estimated cost of the combined TLRP with battery electric A/C and fuel fired heater was \$9,000. Based on this initial fuel use analysis, the payback of this system was 2 years at \$2.50/gallon and about 1.7 years at \$3.00/gallon. This achieves the project goal of a 30% long-haul truck rest period climate control load reduction with a 3-year or better payback period. The next steps are to make further improvements to the national fuel use analysis process, address greenhouse gas emissions, and apply the process working closely with industry partners for fuel use driven design of idle off systems. The process can then be adapted to investigate the other commercial vehicle applications.

IV.5.C. Products

Presentations/Publications/Patents

1. Lustbader, J., Kekelia, B., Tomerlin, J., Kreutzer, C., et al. "Long-Haul Truck Sleeper Heating Load Reduction Package for Rest Period Idling." SAE Int. J. Passeng. Cars - Mech. Syst. 9(2):2016, doi:10.4271/2016-01-0258.

2. Lustbader, J., Bidzina K., Tomerlin, J., Jeffers, M., Schilling, S., Titov, G., Kreutzer, C. "Commercial Vehicle Thermal Load Reduction and VTCab – Rapid HVAC Load Estimation Tool." DOE Annual Merit Review, June 8, 2016; VSS075.
3. Lustbader, J., Kreutzer, C. "Systems and Methods for Conditioning an Environment." Alliance for Sustainable Energy, Golden, CO (US), assignee, Patent application US 14/682,874, Oct. 15, 2015.
4. Lustbader, J., Kreutzer, C. "Shield Devices, System, and Methods for Improved Measurement and Detection." Alliance for Sustainable Energy, Golden, CO (US), assignee, Provisional Patent application PROV/15-98, Feb. 2016.
5. VTCab rapid HVAC load estimation tool beta version. Only available to industry and laboratory partners at this time.

IV.5.D. References

1. Gaines, L., Vyas, A., Anderson, J. "Estimation of Fuel Use by Idling Commercial Trucks." 85th Annual Meeting of the Transportation Research Board, Washington, D.C., Jan. 22–26, 2006; Paper No. 06-2567.
2. Roeth, M., Kircher, D., Smith, J., Swim, R. "Barriers to the Increased Adoption of Fuel Efficiency Technologies in the North American On-Road Freight Sector." Report for the International Council for Clean Transportation. NACFE. July 2013.
3. "Greenhouse Gas Emissions Standards and Fuel Efficiency Standards for Medium- and Heavy-Duty Engines and Vehicles, Final Rule." Federal Register 76 (September, 15, 2011): 57106-57513. <https://www3.epa.gov/otaq/climate/regs-heavy-duty.htm>. Accessed 10/2/2016.
4. Lustbader, J., Kreutzer, C., Adelman, S., Yeakel, S., Brontz, P., Olson, K., Ohlinger, J. "Impact of Paint Color on Rest Period Climate Control Loads in Long-Haul Trucks." SAE World Congress, April 8, 2014.
5. Lustbader, J., Kekelia, B., Tomerlin, J., Kreutzer, C., et al. "Long-Haul Truck Sleeper Heating Load Reduction Package for Rest Period Idling." SAE Int. J. Passeng. Cars - Mech. Syst. 9(2):2016, doi:10.4271/2016-01-0258. http://ops.fhwa.dot.gov/freight/freight_analysis/faf/index.htm. Accessed 9/15/2015. <http://grass.osgeo.org/> or QGIS Brighton 2.6.
6. Kiss, T., Lustbader, J. "Comparison of the Accuracy and Speed of Transient Mobile A/C System Simulation Models." SAE International Journal of Passenger Cars—Mechanical Systems (7): August 2014; pp. 739–754, doi:10.4271/2014-01-0669.
7. Johnson, V. "Battery Performance Models in ADVISOR." Journal of Power Sources, (110):2002; pp. 321–329.
8. U.S. Environmental Protection Agency. "Greenhouse Gas Emissions Model (GEM) User Guide." EPA-420-B-11-019. August 2011. <http://www3.epa.gov/otaq/climate/documents/420b11019.pdf>.
9. Lim, H. "Study of Exhaust Emissions from Idling Heavy-Duty Diesel Trucks and Commercially Available Idle-Reducing Devices." U.S. Environmental Protection Agency. EPA420-R-02-025, October 2002.

IV.6. Vehicle Thermal System Model Development in Simulink

Jason A. Lustbader, Principal Investigator

Gene Titov, Co-Author

National Renewable Energy Laboratory

15013 Denver West Parkway

Golden, CO 80401

Phone: (303) 275-4443

E-mail: Jason.Lustbader@nrel.gov, Gene.Titov@nrel.gov

David Anderson and Lee Slezak, DOE Program Managers

Vehicle Technologies Office

Phone: (202) 287-5688, (202) 586-2335

E-mail: David.Anderson@ee.doe.gov, Lee.Slezak@ee.doe.gov

Start Date: October 1, 2014

End Date: September 30, 2017

IV.6.A. Abstract

Objectives

- Develop a flexible, publicly available framework for analysis of electric, hybrid, and conventional vehicle advanced thermal management systems.
 - Use the popular MATLAB/Simulink environment as an implementation platform.
 - Model the vapor compression cycle, coolant, and oil distribution networks in a general manner applicable to variety of loop architectures including: traditional air conditioning (A/C) systems, combined loop systems, heat pumps, organic Rankine cycles, and oil-based cooling loops.
 - Develop a component library that can be used for modeling a full range of modern vehicle thermal management systems and includes compressors, heat exchangers, expansion valves, pumps, valves, heaters, etc.
 - Develop a capability for introducing new refrigerants and make several common ones readily available, including R-134a and HFO-123yf.
 - Collaborate with industry to model and develop energy-saving advanced thermal management systems and their required control strategies.
 - Co-simulate with Simulink compatible vehicle models such as Autonomie.
- Develop tools aimed at analysis and design of advanced thermal management system architectures. Rapidly assess the impact of emerging concepts and technologies with industry partners.
- Apply the analysis tools with industry partners to assess the impact of technologies that reduce thermal load, improve climate control efficiency, reduce vehicle fuel consumption, recover waste heat, and extend range.

Accomplishments

- The National Renewable Energy Laboratory's (NREL's) CoolSim MATLAB/Simulink modeling framework was extended by adding alternative refrigerant modeling capabilities. As an application of this capability, the HFO-1234yf refrigerant was added to the framework and used in simulations of NREL's advanced combined loop system, as well as on a project with an industry partner.
- An internal heat exchanger (IHX) model was added to the CoolSim framework to simulate advanced refrigeration cycle systems. An IHX transfers heat from the condenser outlet to the compressor inlet, increasing the subcooling and making it possible to control the compressor inlet superheat level with less degradation of the evaporator capacity. The IHX model showed up to a 6.5% improvement in coefficient of performance (COP). It was also used on two projects with industry partners.

- The cabin model was improved by accounting for heat transfer in the ducts. Using datasets provided by MAHLE, it was found that significant heat exchange may occur between the flow inside the ducts and either cabin or outside air. The updated cabin model accounts for this type of heat exchange and makes cabin model validation more accurate.
- Using a CoolSim model of NREL's combined coolant loop system, a study of efficient control strategies was performed. The control approach included a mode selection algorithm and controllers for the compressor speed, cabin blower flow rate, and the front-end heat-exchanger coolant bypass. The power electronics and electric machine were pre-conditioned to 55°C for additional energy benefits. A range extension study of an electric vehicle was performed for the Urban Dynamometer Driving Schedule (UDDS) and HWFET2X drive cycles covering the range of ambient temperatures from -20°C to +20°C. Using the Future Automotive Systems Technology Simulator (FASTSim) modeling tool, up to a 16% improvement in range was found for the weighted 45%/55% UDDS and Highway Fuel Economy Test 2X (HWFET2X) drive cycle.
- CoolSim was used on a number of Funding Opportunity Announcement projects with industry partners, including MAHLE, Hanon Systems, Hyundai, and Daimler. It is also being used for U.S. Department of Energy (DOE)-requested analysis of the greenhouse gas reduction credits.

Future Achievements

- Integrate CoolSim and CoolCalc to enable performance simulation of a fully coupled thermal management system, accounting for all the environmental loads.
- Develop an oil loop modeling capability to support projects that include such loops.
- Use CoolSim to identify design improvement opportunities and estimate the impact of advanced thermal management systems on light- and heavy-duty vehicle performance, fuel use, and range extension projects.
- Develop a generic component library including compressors, heat exchangers (refrigerant-to-air, refrigerant-to-coolant, and refrigerant-to-refrigerant), expansion valves, etc. Make the components modifiable and provide calibration harnesses for the users to specialize the components for their needs.

IV.6.B. Technical Discussion

Background

Thermal management systems are increasingly important for effective and efficient advanced heavy- and light-duty vehicle design. Developing flexible and cost-effective tools to understand vehicle thermal trade-offs at the system level is critical to designing advanced electrified traction drive systems and their associated thermal controls. When operating, the A/C system is the largest auxiliary energy consumer in a conventional vehicle. A/C loads account for more than 5% of the fuel used annually by light-duty vehicles in the United States [1]. Climate control loads can have an even larger impact on hybrid electric vehicle (EV), plug-in hybrid EV, and all-electric vehicle performance. Hybrid EVs show a 22% lower fuel economy with the A/C on [2]. For all-electric vehicles, the effect of the climate control system usage is even more severe. Due to a shortage of waste heat, heating of the passenger cabin in EVs has to rely on battery energy. Cooling the cabin can also take a high portion of the energy available in the battery, significantly reducing vehicle efficiency and range. Mitsubishi reports that the range of the i-MiEV can be reduced by as much as 68% when heating and 46% when cooling the cabin over Japan's 10–15 cycle [3]. The Advanced Powertrain Research Facility at Argonne National Laboratory has reported 59.3% and 53.7% reductions in range due to maximum heating and maximum cooling, respectively, for the Ford Focus EV operating on the UDDS cycle [4]. In addition to these climate control impacts, electric-drive vehicles may have additional cooling requirements for the electric traction drive system components including batteries, power electronics, and electric machines.

To address these challenges, more efficient heating and cooling methods and systems are needed for EVs. These methods and systems often involve running the vapor compression system in heat pump mode to reduce the electrical heating power requirements of the cabin. In some advanced concepts, the traditional liquid-

coolant-based thermal management is supplemented with refrigerant-based cooling systems, which can make the thermal management significantly more complex. When developing a thermal management system for an internal combustion engine vehicle, it has traditionally been sufficient to simulate the A/C systems and the liquid-coolant-based cooling systems separately. For advanced vehicles, especially for hybrid and all-electric vehicles, the benefits of interconnectedness of the thermal management and A/C systems outweigh the associated complexity. This requirement motivates the development of a more integrated simulation approach.

More complex advanced thermal management systems allow for various alternative modes of operation that can be selected based on driving and ambient conditions. Investigating a number of system alternatives and determining the best ranges for various operating modes with experimental methods can be very time consuming. A good system simulation tool can greatly reduce the time and expense of developing these complex systems. Thermal system modeling tools should also be able to efficiently co-simulate with vehicle simulation programs and should be applicable for evaluating various control algorithms. The MATLAB/Simulink simulation environment is popular in the automotive industry and is well suited for developing such models while meeting the requirements of dynamic modeling of complex systems.

Introduction

To meet the needs of advanced vehicle thermal system simulations, NREL is building an integrated single- and two-phase thermal system modeling framework in MATLAB/Simulink called CoolSim. This integrated approach allows for rapid system analysis and design in a flexible and open modeling environment. Simulink is a common engineering platform that allows for co-simulation with vehicle models such as Autonomie [5] or in conjunction with FASTSim [6]. NREL previously developed an A/C system simulation modeling framework in MATLAB/Simulink and validated its results against test bench data. To match the wide range of A/C modeling needs, NREL developed models with three different levels of detail: Fully Detailed, Quasi-Transient, and Mapped-Component.

The three models involve different levels of trade-offs between speed and accuracy to meet a wide range of modeling needs. The Fully Detailed model captures the system transient behavior accurately, but it runs at 1/10 of real-time speed [7]. The Quasi-Transient and Mapped-Component models are progressively more simplified while trying to maintain accuracy. These models run at real time and 10 times real-time speed, respectively [8]. The goal of these model versions is to provide faster simulation tools for less detailed, vehicle-focused, drive-cycle-based evaluations of A/C systems. For steady-state conditions, the Quasi-Transient model provides essentially the same accuracy as the Fully Detailed model. The Mapped-Component model does lose some accuracy in steady-state conditions. For the SC03 drive cycle, the averaged results of power and heat exchange rates obtained with the Quasi-Transient model are within 3% of the Fully Detailed model results. The Mapped-Component model results are within 15% of the Fully Detailed model results. For both simplified models, short transients, such as those occurring during compressor cycling, produce the most deviation from the Fully Detailed model. Conversion from the Quasi-Transient A/C system model approach to the other two models is relatively simple within the CoolSim framework. This allows for a new system model to be developed with the Quasi-Transient version before the results are refined using the slower Fully Detailed version or accelerated using the faster Mapped-Component model version.

A CoolSim model of NREL's combined fluid loop (CFL) thermal management system was previously developed, which included both active cooling and heating modes. Comparisons of simulated results with measured data validated the solution approach [9].

This report focuses on the development of a control strategy concept for a HFO-1234yf CFL system using CoolSim. This control approach includes a mode selection algorithm and associated controllers for the compressor speed, cabin blower flow rate, and front-end heat-exchanger coolant bypass. This controlled CFL system model enabled a simulation comparison of the system's efficiency over different drive cycles. The drive-cycle-based thermal-system performance was then used to simulate the impacts on vehicle efficiency and range using NREL's FASTSim vehicle model.

To reduce electric machine warm-up losses and provide additional energy benefit, the PEEM was preheated in this study to 55°C, the temperature set point for the heater air discharge temperature.

Approach

Model description

CoolSim's "Quasi-Transient" modeling method was employed for both refrigerant and coolant circuits in this study. The details of the solution method are discussed in [8]. Both refrigerant and coolant circuits are represented by 0-D volumes connected with 1-D pipes, valves, or orifices. In general, any system component that can provide a flow rate due to a pressure differential can be attached to these 0-D volume blocks. For example, for the coolant loop network topology, these 0-D volume blocks are used as junctions to connect lines for the purpose of the numerical solution. 0-D volume blocks can also be used to model physical components such as expansion tanks and headers in both coolant and refrigerant circuits.

The 1-D pipe block assumes a constant coolant mass flow rate along its length. The flow rate then becomes a simulation state variable. At each time step, the coolant pressure differential across each line is compared to pressure difference between the 0-D junctions that they connect. A numerical method is applied to continuously adjust the coolant mass flow rate in each of the lines. The goal of this method is to match the pressure drop in the line to the pressure difference between the junctions that the line connects. Ideally, sub-iterations would be continued until convergence is reached at each time step of the solution to ensure a diminishing difference between the pressure drop in the line and the pressure difference between the connected junctions. This would result in a steady state solution corresponding to the instantaneous values of boundary conditions at each simulation time step (hence the name, "Quasi-Transient"). To speed up the solution, however, only a single iteration is done in each time step. This was found to be an acceptably accurate approach when the computational time-step is relatively small compared to the system-level thermal response characteristic time. In this case, the solution converges fast enough to account for transients.

To further speed up simulations by increasing the solution time step, the notion of artificial bulk modulus was introduced. This allows for changing the relationship between pressure and density and thus the system "stiffness." By setting the artificial bulk modulus larger than the true bulk modulus of liquids, the numerical stiffness in coolant and liquid portions of refrigerant networks can be reduced. This quasi-transient solution method results in lost accuracy for fast transients (on the order of seconds) such as pump cycling. For steady-state conditions, however, the conservation of mass and energy for each junction and each of the 1-D pipes in the model is ensured. A typical thermal management network is a slowly drifting "quasi-steady" system, especially in cases with constant rpm electric pumps. In such cases, a true conservation of mass and energy will be closely approximated by this method. Details of the coolant loop modeling approach can be found in [9].

In FY 2016 the CoolSim framework was expanded by adding a new HFO-1234yf refrigerant modeling capability, and an internal heat exchanger module. The cabin model was also updated by taking into account heat exchange in ducts.

The HFO-1234yf refrigerant modeling capability required a new set of MATLAB S-functions written in the C-language for the 1-D lines and 0-D volumes, the fundamental blocks of CoolSim models. These functions were, however, developed in a way that allows for easier implementation of new refrigerant capabilities in the future. A system that is schematically identical to NREL's CFL test bench but uses HFO-1234yf refrigerant instead of R134a was modeled. As expected, the HFO-1234yf refrigerant exhibited some performance disadvantages compared to R134a. The loss of system capacity was within 10%, which was consistent with expectations, and helps to qualitatively verify the implementation.

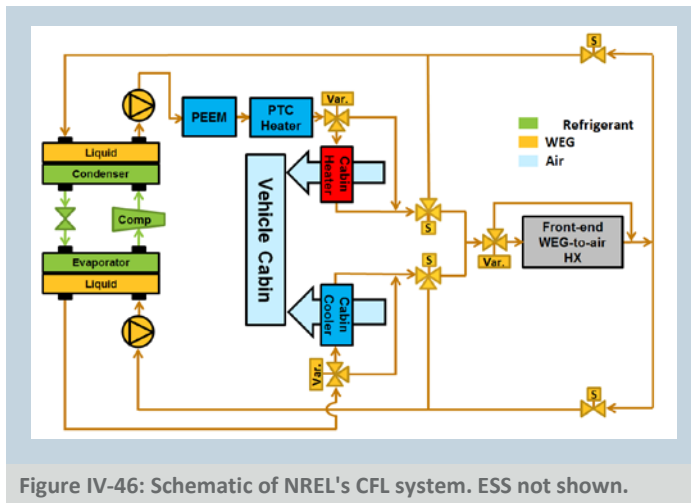
The IHX model allows for analysis of advanced A/C systems that use an IHX. The IHX allows energy to be exchanged between the hot refrigerant liquid at the outlet of the condenser and relatively cold refrigerant vapor at the exit of the evaporator. An exchanger effectiveness approach was used to model the IHX allowing for studies of system performance without detailed information regarding the heat exchanger design. Once the desired effectiveness is determined through CoolSim modeling, a specific IHX design can be chosen that has the desired effectiveness. In the future, a more detailed IHX model will be developed for projects that require such capabilities. In the simulations performed, the IHX predicted up to a 6.5% COP improvement under ideal conditions. The IHX model was also used on two projects with industry partners.

The cabin model was also updated to account for heat exchange in cabin ducts. Three ducted air passes were considered: from cowl to the blower, from the heater outlet to the cabin vents, and from the cabin outlet to the blower (recirculated portion). The heat exchange between the duct air and the duct wall was accounted for using an effectiveness-NTU (Number of Transfer Units) method whereas resistances restricted energy exchange between the duct wall and either the cabin or ambient air. This approach improved verification of the model without needing to consider details such as heat paths inside the instrument panel or engine/motor compartment that would be prohibitively complicated within the scope of CoolSim. By adjusting the values of resistances and parameters of the NTU method, the updated cabin model was successfully validated using data from a partner. In this study, a generic version of the model is used.

Combined fluid loop system

To study control strategies and efficiency gains for warm-up conditions of a CFL system, the updated CoolSim tool was used to build three model versions of NREL's CFL electric-drive vehicle thermal management system and test bench prototype [10] illustrated in Figure IV-46 and Figure IV-47.

- **The Full-CFL:** Shown in Figure IV-46, the Full-CFL system engages a vapor compression cycle based heat pump (HP) to pick up heat from a colder ambient air and deliver this heat to the cabin. It also includes a positive temperature coefficient (PTC) electrical resistance heater and a waste heat recovery sub-loop that recovers heat from the power electronics and electric machine (PEEM).
- **PTC + PEEM:** This system concept maintains heat recovery from the PEEM but excludes the heat pump capability.
- **PTC-only:** This model used a coolant PTC heater that provided cabin heating via a coolant network and a coolant-to-air cabin heater. Losses on the lines were not included, so the system has only small efficiency disadvantages as compared to an air-PTC system.



PEEM preheating to 55°C was assumed for each of the models. This could be achieved using the PTC heating in the high-side coolant loop. Pre-conditioning the PEEM was selected because it is expected to have lower losses than the cabin during pre-conditioning. A separate study is planned to consider benefits of cabin preheating in more detail.

The System Control Strategy

Similar control algorithms were developed for each variant of the system. Two control goals were pursued: a cabin air temperature set point of 22°C and heater air-discharge temperature of 55°C. The cabin air temperature was controlled by cabin blower mass flow rate, and the heater discharge temperature was controlled by compressor revolutions per minute (rpm), PTC power, and front-end heat-exchanger bypass on the coolant-side depending on the mode and the model variant.

The Full-CFL system has multiple modes of operation. For the purposes of this study, the following three heating modes were considered:

- **Mode 1: PEEM heat recovery only**—In this mode, there is sufficient waste heat from the PEEM to heat the cabin and no additional power is needed. If at some point the PEEM approaches its maximum inlet coolant temperature, then some coolant is routed through the front-end heat exchanger to reject heat to the environment and keep the PEEM sufficiently cool.
- **Mode 2: Heat pump with PEEM heat recovery**—In this mode, the coolant accepts heat from the condenser (a coolant-to-refrigerant heat exchanger). The condenser heat is delivered by a vapor compression heat pump that pulls heat from the ambient using the front-end heat exchanger. The coolant then goes through the PEEM, accepting available waste heat. The compressor speed is controlled to regulate the cabin heater exit temperature to 55°C. It is also ensured that the PEEM inlet temperature is below its design limit.
- **Mode 3: Heat pump complemented by PTC heating and PEEM waste heat recovery**—In this mode, the heat pump is operated at its full capacity as long as the COP remains above 1. Coolant exits the condenser and then picks up waste heat from PEEM. The PTC heater is then used to provide additional power to meet the cabin heater exit temperature set point. As long as the heat pump COP is above 1, this provides efficiency benefits over PTC heating.

The control algorithm consisted of two layers. The first layer is a mode selection layer that chooses one of these three modes based on the system and environmental conditions. The second layer control then provides component control, within the mode constraints, to maintain cabin and vent exit temperature set points. Initially, the first-layer control selects either Mode 3 or Mode 2 for a fast cabin warmup. Mode 3 provides the maximum heating power capability; but at warmer temperatures, it can cause large overcapacity and thus overshoot the set point. To determine the initial warm-up mode, an independent study was performed that compared available PEEM waste heat to cabin thermal load for several drive cycles. At below 5°C, Mode 3 was initially engaged, whereas at higher temperatures, Mode 2 was initially used.

The second-layer controls consisted of several PID controllers that maintained a preset cabin air temperature of 22°C, the cabin heater air discharge temperature at 55°C, and the PEEM coolant inlet temperature below 60°C. These controllers included:

- A blower flow rate controller that adjusts the blower mass flow rate to attain and maintain the cabin air temperature set point of 22°C.
- Compressor rpm controller that adjusts compressor rpm in Mode 2 to maintain the preset heater air discharge temperature (this controller is overridden in Mode 3 and the compressor is set at maximum as long as the COP is greater than 1).
- PTC power controller that adjusted complementary PTC power in Mode 3 when the compressor rpm was at its maximum.
- Front-end heat exchanger (FEHX) bypass controller that ensured that the PEEM inlet coolant temperature was below a preset limit in Mode 1 in cases when PEEM waste heat was excessive for cabin heating.
- Coolant pump pulse width modulated controller that maintained the coolant flow rate.

At temperatures below and equal to 5°C, Mode 3 is initially selected for maximum warm-up performance. The system relies on the PTC power controller to maintain the heater air discharge temperature at 55°C while keeping the compressor at maximum rpm if the COP remains above 1. Once the needed PTC power decreases to below 10 watts, the first-layer controls switch to Mode 2, disengaging the PTC and switching to compressor rpm control. When the compressor rpm decreases to below the lower limit (500 rpm), the first-layer controller switches to Mode 1, turning off the vapor compression system and PTC heater relying only on the PEEM waste heat. In Mode 1, the FEHX coolant bypass controller is engaged to prevent the PEEM from overheating by directing a part of the hot coolant to the FEHX so that excess heat can be dissipated to ambient. At ambient temperatures above 5°C, Mode 2 is initially selected to prevent overcapacity and overshoot but otherwise the process is the similar.

The first-layer controls also handle the reverse mode switches going from Mode 1 to Mode 2 and from Mode 2 to Mode 3. If the system is in Mode 1 and the heater air discharge temperature falls below 53°C, the system

switches to Mode 2 (heat pump with PEEM heat recovery); if the system is in Mode 2 and heater air discharge temperature falls below 50°C, the system switches to Mode 3 (heat pump power supplemented by PTC heating and waste heat recovery). The control algorithm also includes time delays and signal treatment to make sure instabilities and overshoots do not cause chaotic system behavior. For example, temperature measurements are taken over a duration of time to make sure a control decision is not made based on a temperature spike. Controller resets were implemented on mode switch events so that the compressor, PTC, and FEHX bypass were engaged at reasonable initial conditions in accordance with the new mode of operation.

An attempt was made to make sure that the control algorithm relies only on measurable variables such as temperatures. However, the blower mass flow rate was adjusted directly to maintain the cabin air temperature (as opposed to controlling blower rpm) due to a lack of reliable blower performance curves. Still, all the control inputs used by the algorithms are either directly measurable on a vehicle or closely related to measurable parameters.

The systems were evaluated over a range of ambient temperatures between -20°C and +20°C. The constraints imposed on the system included:

- Maximum compressor rpm: 8,000 / Minimum compressor rpm: 500
- Maximum blower mass flow rate: 0.14 kilograms per second (kg/s) (~250 CFM)
- Maximum PTC power: 7kW
- Coolant flow rate in both condenser and chiller coolant loops: 0.23 kg/s (~10 liters per minute)
- Cabin air temperature set point: 22°C
- Heater air discharge temperature set point: 55°C
- Initial PEEM temperature: 55°C

The heating load of the cabin was dynamically computed based on the vehicle velocity and ambient temperature. Radiative heat load on the cabin was assumed to be zero (nighttime driving) and the ambient air humidity was 50%. Air recirculation fraction was 85% in all cases.

To test the control algorithm and to accurately estimate the CFL energy savings and range benefits, the three thermal management systems were evaluated over two transient drive cycles. Transient drive cycles are important for capturing the effects on the available PEEM waste heat and the cabin loads. The average commute travel time in the United States is 22.85 minutes [11]. This is a relatively short time period for vehicle warmup and will heavily weight the transient effects over steady state. Consistent with NREL's test CFL bench testing paper [10], drive cycles were selected to match this time period and approximate a realistic mix of urban and highway driving. The UDDS is a city cycle and is 22.9 minutes long. The HWFET cycle represents highway driving, and by running two back-to-back cycles (HWFET2X), a total duration of 25.5 minutes is achieved. For final combined impact estimation, these cycles will be weighted 45%/55% UDDS and HWFET2X.

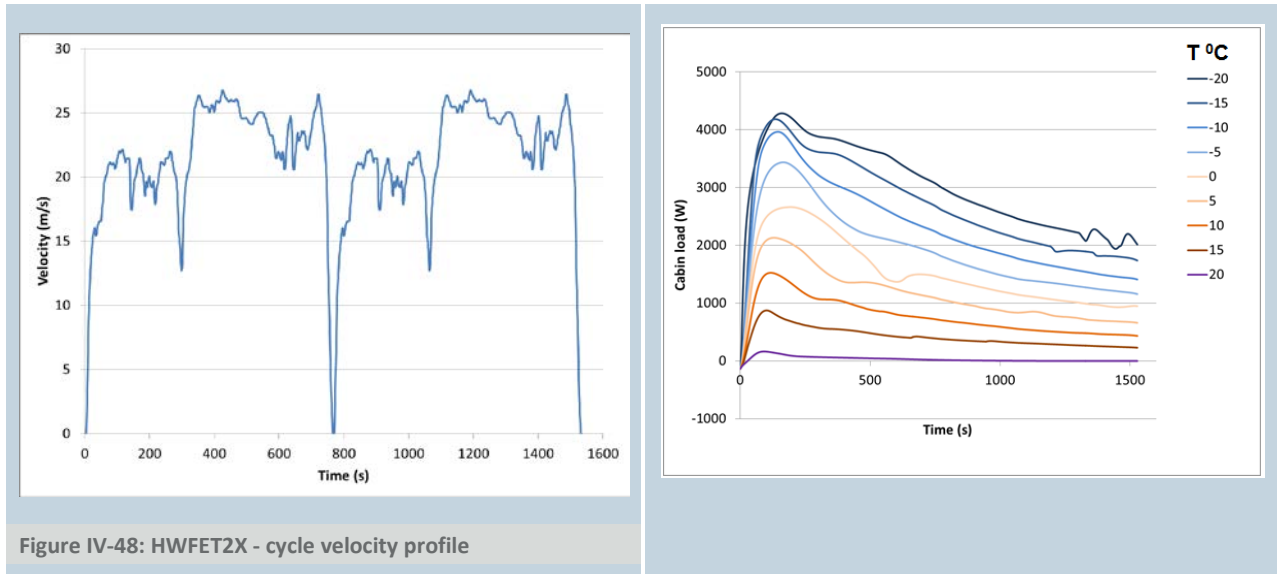
In FASTSim, an example electric sedan model was used to predict PEEM waste heat available over the drive cycles. The heat generation profile and vehicle velocity were then used in CoolSim during the warm-up simulation. This impacted both the waste heat available and cabin load. The total system power required from CoolSim was then imposed as an auxiliary load in FASTSim and the impact on vehicle energy use and range was simulated.

Results and Discussion

HWFET2X Drive Cycle

The HWFET2X drive cycle velocity profile is shown in Figure IV-48. These velocities affect the external cabin heat transfer, and thus, they impact the cabin heat demand. The heat generated from the PEEM operating over the drive cycles was first simulated by FASTSim and is then provided as an input for the simulation.

Figure IV-49 shows the heat delivered to the cabin by the heating system. As shown in the figure, the power initially spikes as the vehicle starts from a cold soak and the controller tries to quickly warm up the cabin and then gradually decreases over the duration of the drive cycle as the vehicle warms. The heating system needs to match the demand, and its control algorithm has to deliver the needed heating capacity in the most efficient manner using various modes of operation.



An example of how the CFL system manages the cabin heating at an ambient temperature of +5°C is shown in Figure IV-50. Mode number is shown in red (left vertical axis) and difference between the cabin heating power need and available PEEM waste heat is shown in blue (right axis). When the blue curve representing this difference reaches zero, PEEM waste heat is sufficient to heat the cabin. The system starts in Mode 3 and quickly warms the cabin by engaging all of the available heating resources (HP, PTC, and PEEM). When the PTC power is no longer needed, the system switches to Mode 2 (heat pump and PEEM heat recovery). At around 850 seconds into the drive cycle, the difference between the needed heat and available PTC power falls below zero. This causes the compressor rpm to fall below 500 and switches the system into Mode 1 (PEEM energy recovery only). The controller then senses a falling vent exit temperature due to increased cabin heating demand and briefly switches to Mode 2, turning the heat pump back on. When the demand decreases again, the compressor rpm once again falls below 500 and the controller switches to Mode 1. From there, it keeps the system in Mode 1 for the rest of the drive cycle due to sufficient waste heat. Figure IV-51 shows the energy difference between the cabin heating power need and heat exchange rate from PEEM to coolant for all of the cases considered. At temperatures below -5°C, the difference is always greater than zero, which indicates that the available PEEM energy is not sufficient for cabin heating at any point during the drive cycle. Starting at 0°C, there is sufficient waste heat were the graph falls below 0. At higher temperatures, this occurs closer to the beginning of drive cycle. At +15°C, PEEM energy is sufficient for cabin heating shortly after the beginning of the drive cycle. At +20°C, PEEM energy is sufficient from the beginning of the drive cycle.

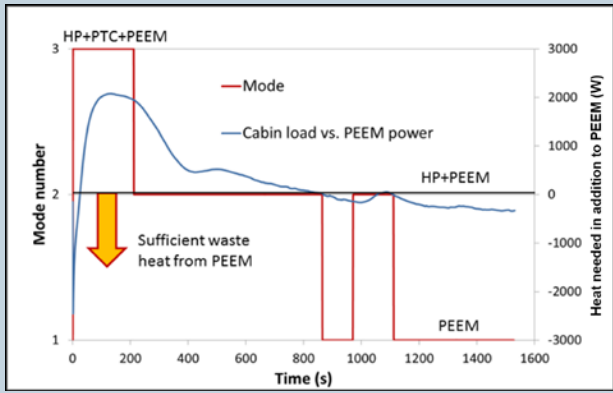


Figure IV-50: HWFET2X – Energy balance and mode selection at +5°C

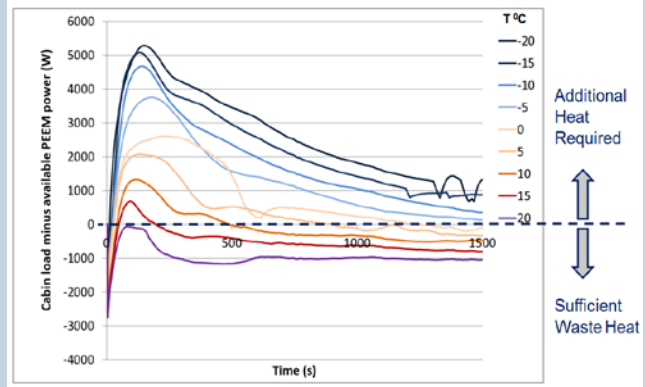


Figure IV-52 and Figure IV-53 show the PTC power and the cabin blower flow rate. The PTC power complements other power sources when there is insufficient heating capacity to maintain the heater air discharge temperature at 55°C. In cases of ambient temperature below -15°C, the PTC power initially stays at a maximum of 7 kW and then gradually decreases to zero. In cases of ambient temperature above 5°C, PTC power is only engaged briefly to speed up the cabin warm-up. The blower flow rate, shown in Figure IV-53, is also initially engaged at full speed at low ambient temperatures to provide maximum heating to the cabin. Its flow rate is then controlled to maintain the cabin temperature at the set point of 22°C.

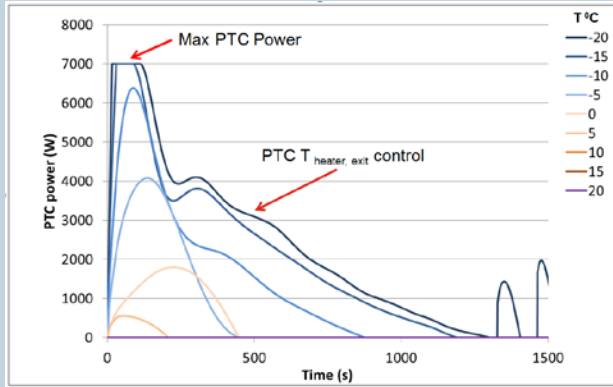
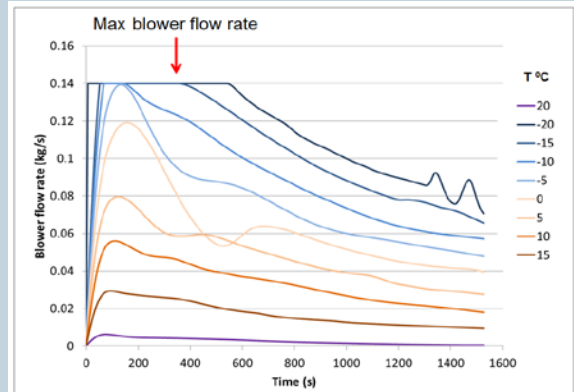


Figure IV-52: HWFET2X – PTC power



Similarly to PTC power, the compressor rpm is controlled to maintain the heater air discharge temperature at 55°C, as illustrated in Figure IV-54 for selected cases. The corresponding compressor power is shown in Figure IV-55. It should be noted that the vapor compression cycle COP behavior was also monitored—and except for the initial 200 seconds, the COP never fell below 1, illustrating that the vapor compression system was used efficiently.

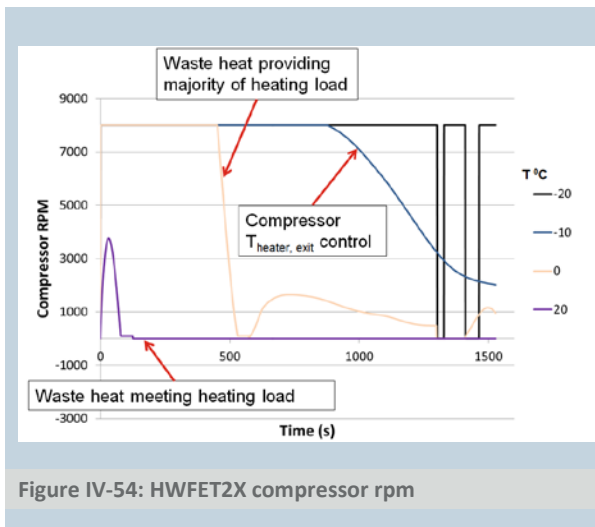


Figure IV-54: HWFET2X compressor rpm

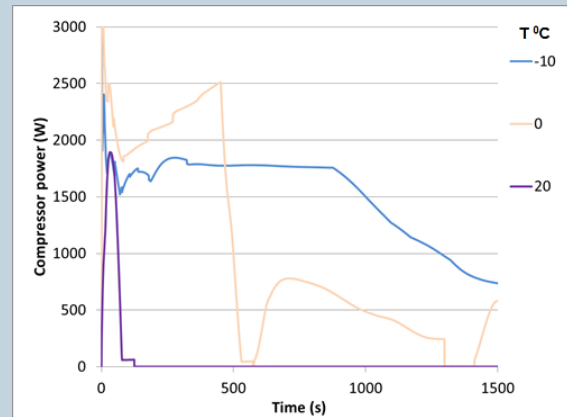


Figure IV-56 and Figure IV-57 show the response of cabin air temperature and heater air discharge temperature to control inputs for a range of ambient temperatures from -20°C to $+20^{\circ}\text{C}$. As can be seen in Figure IV-56, the system attains and maintains a desired cabin air temperature of $+22^{\circ}\text{C}$ at all ambient conditions; however, the time to set point decreases with increasing ambient temperature.

The heater air discharge temperature overshoots the set point initially and then settles at the 55°C set point. The initial overshoot is on the order of 5°C and is a trade-off between a fast controller response causing the overshoot and longer times to set point.

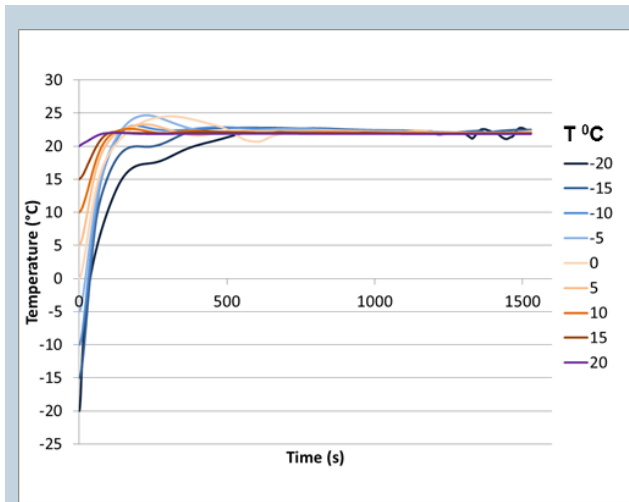
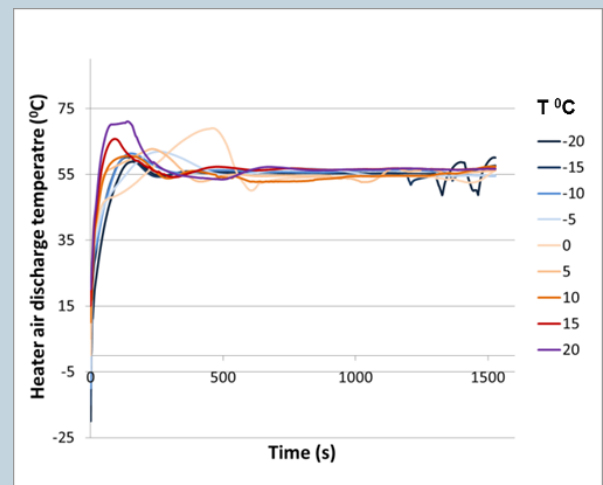


Figure IV-56: HWFET2X – Cabin air temperature



In addition to the Full-CFL simulations, the PTC+PEEM cases were also modeled. Figure IV-58 and Figure IV-59 illustrate the level of energy savings achieved by the Full-CFL and PTC+PEEM system as compared to a PTC-only system.

The Full-CFL and PTC+PEEM systems show considerable energy savings. The Full-CFL system has a maximum savings over the PTC system of more than 80% at an ambient temperature of 10°C . Savings of the PTC+PEEM system continue to increase throughout the range of ambient temperatures, but are up to 20% lower than that of the full system.

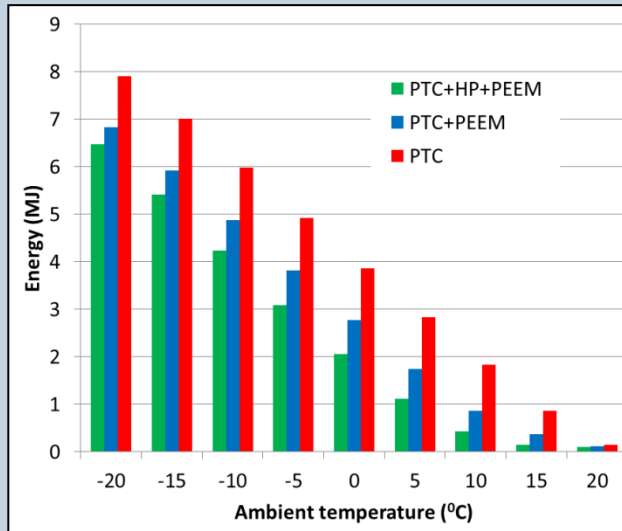
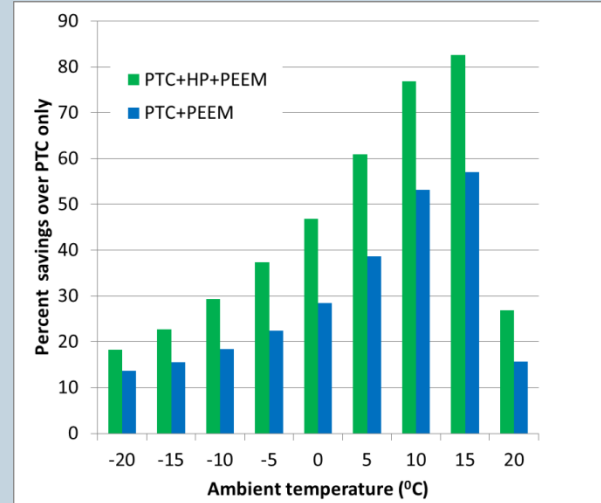


Figure IV-58: HWFET2X – Energy consumed by different system variants



UDDS Drive Cycle

The UDDS drive-cycle vehicle speed is shown in Figure IV-60. A similar study was performed for this drive cycle. Figure IV-61 shows the energy used for cabin heating for each of the system configurations. Similar to the HWFET2X cases, the Full-CFL system shows the maximum benefit and the PTC+PEEM system is about 15% less efficient than the full system.

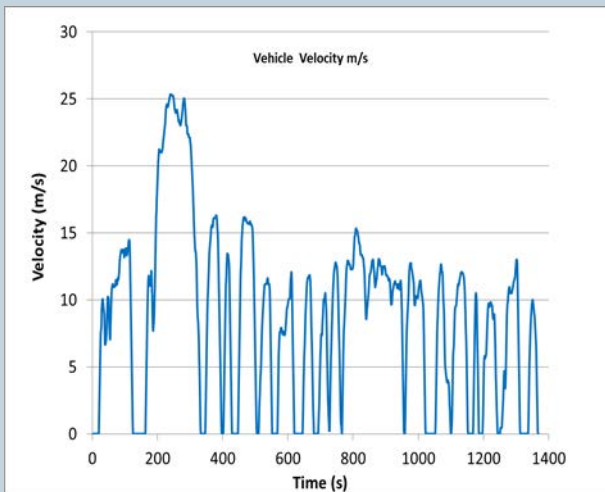
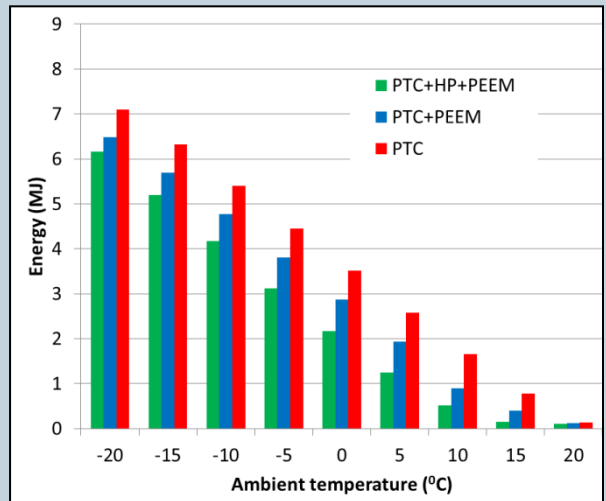


Figure IV-60: UDDS drive-cycle vehicle velocity

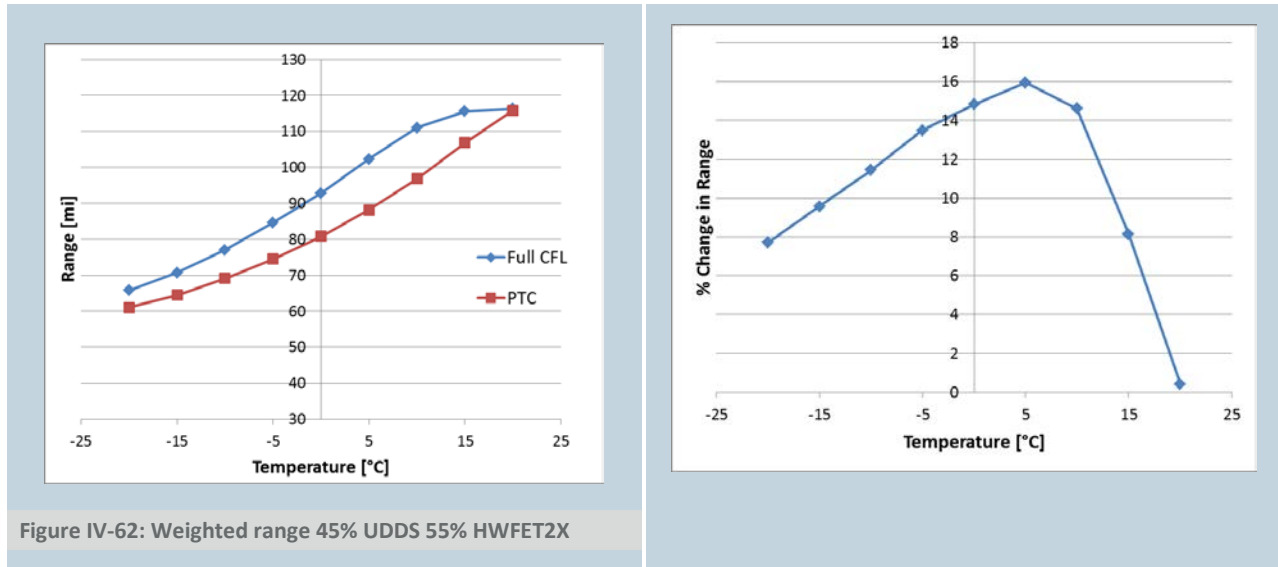


The results for the UDDS cycle are qualitatively similar to that of HWFET2X, but savings are somewhat less due to less PEEM waste heat in the less aggressive cycle.

Range Impact

The thermal system electrical power demand for each drive cycle was calculated in CoolSim. This electrical demand was imposed on the vehicle model in FASTSim as a variable auxiliary load. Due to the lower vehicle speed on the UDDS cycle, the cabin loads were lower. This more than offset the lower PEEM waste heat

availability, resulting in smaller energy requirements. Due to the lower speed, however, the vehicle traveled less distance on the UDSS than the HWFET2X cycle—7.52 miles and 20.52 miles, respectively. Because the thermal loads are based on time and not on distance, this results in a larger thermal load per mile on the UDSS cycle, and thus, a larger impact on vehicle range. To illustrate a combined effect on the vehicle range, Figure IV-62 and Figure IV-63 show weighted averages (45% UDSS and 55% HWFET2X) of the range and percent of range change. Figure IV-62 shows range variation with ambient temperature for the Full-CFL and the PTC-only system. Figure IV-63 shows the range improvements provided by the Full-CFL over the PTC-only system. As can be seen in the in Figure IV-62, a significant benefit is provided by the full system, with a maximum range improvement of 16% at +5°C.



Conclusions

NREL's MATLAB/Simulink thermal modeling framework CoolSim was improved and used to develop a control strategy for an advanced combined coolant loop system concept. Improvements included a new HFO-1234yf refrigerant capability, IHX model, and an updated cabin model that accounts for heat exchange in ducts. The CFL system controls use a two-layer system, with the first layer determining mode and the second layer controlling components within the mode constraints. To determine the impact of the design on the vehicle loads and performance, simulations were done for two drive cycles. The HWFET2X and UDSS drive cycles were selected to represent a mix of typical highway and urban driving, and their duration was similar to the typical commute time in the United States. The controls successfully selected modes of operation and maintained the vent discharge and cabin air temperatures close to set points in a stable manner over the drive cycles. The CFL system showed significant energy savings in both drive cycles. The energy benefit changed with temperature and drive cycle, resulting in reductions from 12% to 80%. PEEM preheating enabled faster cabin warm up and contributed to battery energy savings. Over the drive cycles, the weighted (45% UDSS and 55% HWFET2X) range improvement over the PTC-only system peaked at 16% with an ambient temperature of +5°C and had notable benefits throughout the entire range.

Next steps will include adding traction battery thermal management to the simulations. The A/C control modes will also be added. The heating and cooling loads will then be weighted by national temperature distributions to determine the national-level impact of the CFL system. Other planned improvements to CoolSim include oil loop modeling, more detailed power electronics and energy storage components, a component library, and improved usability. Improvements will allow CoolSim software to be used for a wide range of advanced thermal management systems for electric and traditional vehicles, as well as for advanced subsystems such as organic Rankine cycles.

CoolSim's improved capabilities and NREL's expertise in thermal system modeling are currently used by the following projects:

- MAHLE's UTEMPRA system, which will use CoolSim to assist with control-algorithm development of a combined coolant-loops architecture with 22 modes of operation
- Hannon EV thermal management system, which includes options for thermal energy storage
- Daimler Truck HVAC system modeling
- Hyundai hybrid vehicle energy-efficiency improvement by application of advanced technologies
- ORNL-Cummins Accessory Electrification cooperative research and development agreement
- DOE greenhouse-gas credit development analysis project.

IV.6.C. Products

Presentations/Publications/Patents

1. J. Lustbader; E. Titov; E. Miller. 2016. "Vehicle Thermal System Modeling Framework in Simulink." Presentation. DOE Annual Merit Review, June 8, 2016; VSS134.
2. G. Titov; J. Lustbader; D. Leighton; T. Kiss. 2016. "MATLAB/Simulink Framework for Modeling Complex Coolant Flow Configurations of Advanced Automotive Thermal Management Systems," SAE \ Technical Paper 2016-01-0230, 2016, doi:10.4271/2016- 01-0230.

IV.6.D. References

1. J. Rugh et al. 2004. Earth Technologies Forum and Mobile Air Conditioning Summit.
2. J. Francfort; T. Murphy. 2007. "Operational and Fleet Testing, A. Hybrid Electric Vehicle Testing." Chapter V. Advanced Vehicle Technology Analysis and Evaluation Activities: FY 2007 Annual Report. Washington, D.C.: Vehicle Technologies Program, U.S. Department of Energy, 2007; p. 145.
3. K. Umezu et al. 2010. "Air-Conditioning System for Electric Vehicles (i-MiEV)." 2010. SAE Automotive Refrigerant and System Efficiency Symposium.
4. E. Rask et al. 2014. "Ford Focus BEV In-depth (Level 2) Testing and Analysis." Presentation. DOE Annual Merit Review.
5. "Autonomie." www.autonomie.org.
6. A. Brooker; J. Gonder; L. Wang; E. Wood; et al. 2015. "FASTSim: A Model to Estimate Vehicle Efficiency, Cost and Performance." SAE Technical Paper 2015-01-0973, 2015, doi:10.4271/2015-01-0973.
7. T. Kiss; L. Chaney; J. Meyer. 2013. "A New Automotive Air Conditioning System Simulation Tool Developed in MATLAB/Simulink." SAE International Journal of Passenger Cars—Mechanical Systems 6(2); doi:10.4271/2013-01-0850.
8. T. Kiss; J. Lustbader. 2014. "Comparison of the Accuracy and Speed of Transient Mobile A/C System Simulation Models." SAE International Journal of Passenger Cars—Mechanical Systems (7), August; pp. 739–754; doi:10.4271/2014-01-0669.
9. G. Titov; J. Lustbader; D Leighton; T. Kiss. 2016. "MATLAB/Simulink Framework for Modeling of Complex Coolant Flow Configurations of Advanced Automotive Thermal Management Systems." SAE International World Congress. Paper #2016-01-0230.
10. D. Leighton; J. Rugh. 2014. "Electric Drive Vehicle Range Improvement Using a Combined Fluid Loop Thermal Management Strategy." Presentation at the SAE Thermal Management Systems Symposium, Sept. 22–24, 2014, Denver, CO.
11. A.T. Santos; N. McGuckin; H.Y. Nakamoto; D. Gray; S. Liss. 2011. "Summary of Travel Trends: 2009 National Household Travel Survey." Report # FHWA-PL-11-022, U.S. Department of Transportation, June 2011.

Acknowledgements

Special thanks to industry partner MAHLE and to John Rugh and Lisa Fedorka of NREL.

IV.7. Real World Effectiveness of Engine Start-Stop Systems

R. Vijayagopal, A. Rousseau

Argonne National Laboratory
9700 S Cass Avenue, Bldg 362
Argonne, IL 60439
Phone: (630) 252-6960
E-mail: rvijayagopal@anl.gov

David Anderson, DOE Program Manager

Office of Vehicle Technologies, U.S. Department of Energy
Phone: (202) 287-5688
E-mail: David.Anderson@ee.doe.gov

Start Date: October 1, 2015
End Date: September 30, 2016

IV.7.A. Abstract

Objectives

- The objective of this study is to
- Quantify the effectiveness of technologies that enable idle reduction, using Real World Driving Cycles (RWDC) and compare it to the benefits observed in regulatory cycles.

Accomplishments

- This study developed a modelling and simulation approach to quantify benefits of technologies on real world drive cycles.
- Assuming the impact of technology can be accurately modelled, this approach is faster and cheaper than actual on road testing.
- This study compares the simulation approach and verifies the results using test data from dynamometer testing as well as fleet testing from other independent sources.

Future Achievements

The scope of this project was limited to assessing the effectiveness of start-stop systems, but this process could be extended to measure the impact of other technologies too.

IV.7.B. Technical Discussion

Background

Regulatory testing activities evaluate the impact of various technologies on standard drive cycles (UDDS & HWFET). Since the energy impact of technologies might differ between standard and real world driving cycles, EPA offers additional credits to certain technologies in the current regulatory framework [1]. This is based on the belief that many technologies could offer additional benefits under real world operating conditions. Idle reduction techniques like 'engine start-stop' is one such technology. The objective of this study is to quantify the impact of engine start-stop technologies on Real World Driving Cycles (RWDC).

Introduction

In the US, start-stop systems are made available in some variants of an existing vehicle model. In nearly all cases, the variant uses multiple fuel saving strategies like downsizing or turbo charging the engine, aerodynamic improvements, different transmission etc., so as to minimize the fuel consumption. Argonne has tested multiple vehicles on a dynamometer to measure the start-stop specific fuel consumption benefits (Figure IV-64). Those test results can be downloaded from the D3 database [2]. Because of the multitude of technologies involved, it is not possible to identify the energy impact of start-stop systems.

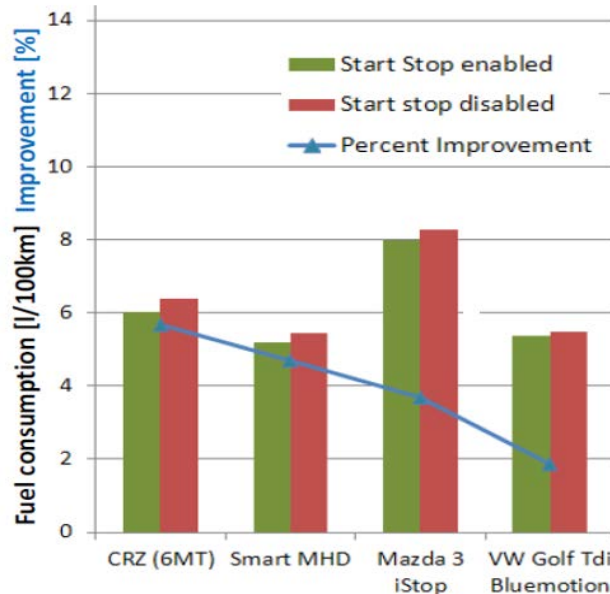


Figure IV-64: Fuel consumption reduction attributable to start-stop systems in four different vehicles

Approach

Vehicle system simulation will be used to quantify the impact of start-stop system across multiple technology implementations and driving cycles. Three midsize vehicle models were built in Autonomie [3] using the same component models to compare their relative fuel saving potential. Each of the vehicles are identical except for the battery and electric machine sizes.

- The conventional vehicle has an alternator to keep the 12V battery charged and the engine idles when the vehicle is not moving. This vehicle is considered as the baseline.
- The micro-hybrid uses the same engine and other components as the conventional vehicle, but it turns the engine off when vehicle comes to a stop, and restarts the engine when the driver releases the brake pedal. This vehicle uses the regular starter to restart the engine. There is no regenerative braking in this vehicle.
- The third vehicle is a Belted Integrator Starter Generator (BISG) with a 7kW motor and li-ion battery pack. This vehicle can do regenerative braking and assist, but the smaller motor limits the hybrid operation.
- The fourth vehicle is Crank Integrator Starter Generator (CISG) with a 15kW motor and li-ion battery pack.
- These vehicles will help quantify the improvements due to idle reduction, regenerative braking and launch assist for engine.

- The real world cycles for this study were obtained from the Transportation Secure Data Center (TSDC) [4] in NREL. Over 8000 daily cycles were recorded from 6 different locations. Since this data is from various transportation studies in cities and suburbs, it may not reflect the driving behavior across United States. The National Household Transportation Survey (NHTS) provides an insight on the driving behavior of people in this country. By sampling down the TSDC data, we can get a fair representation of the national driving behavior [5]. Simulating the four different vehicles on thousands of real world driving cycles yield the real world fuel consumption estimates for these vehicles. The benefits attributable to start-stop technology can then be derived by analyzing the results.

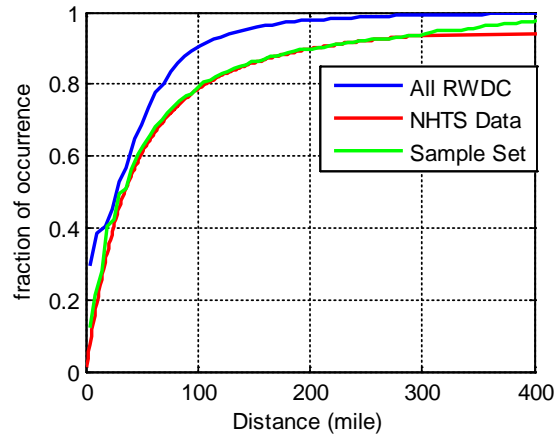


Figure IV-65: Sample sets that conform to the NHTS drive pattern are taken from the pool of real world driving cycles (RWDC)

Simulation Process

All vehicles were simulated in all cycles as the first step. This is a time consuming step, but once this large database is built, it enables the result analysis with respect to various drive characteristics. The parameters that are most interesting for this study are driving distance and idle time in the real world cycles.

Each sample taken from the pool of real world cycle results represent 1000 cycles with driving distances following the same distribution as the NHTS driving distance profile, as shown in figure 2. For each of these samples the fuel consumption obtained for the four vehicles can be computed. To minimize sampling errors, 100 such samples were taken and for each sample the weighted fuel consumption is computed as shown in Figure IV-66.

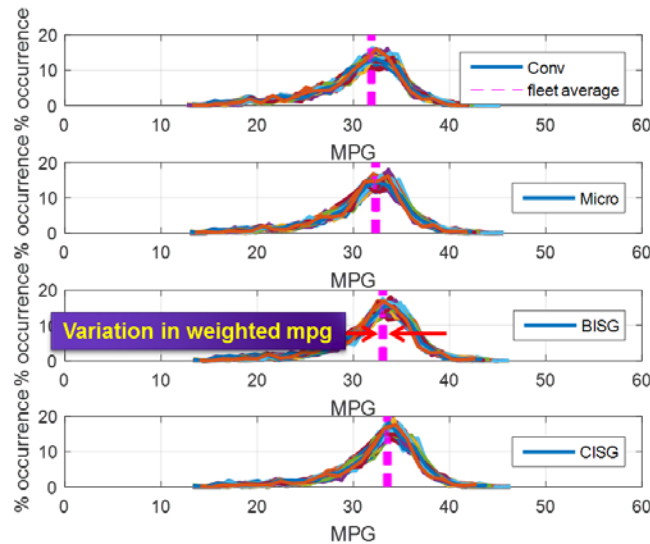


Figure IV-66: Distribution of fuel economy values for four vehicles over 100 sample sets

Results

For every vehicle, the average fuel consumption value from all these samples is taken as the representative fuel consumption. When we compare the fuel consumption reduction, it can be seen that the increase in the degree of hybridization leads to greater reductions in real world fuel consumption. This is shown in Figure IV-67.

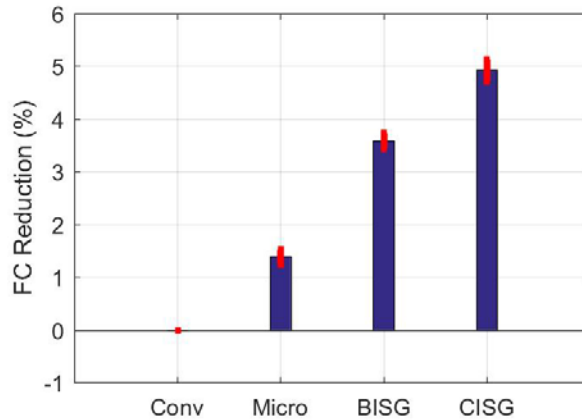


Figure IV-67: FC reductions observed in real world cycles due to various micro/mild hybrid technologies on a generic midsize passenger car

When these benefits are compared against the fuel consumption reduction observed in regulatory cycles, we see that the real world benefits are not as high as that observed in the combined 2 cycle estimates. This comparison is shown in Figure IV-68.

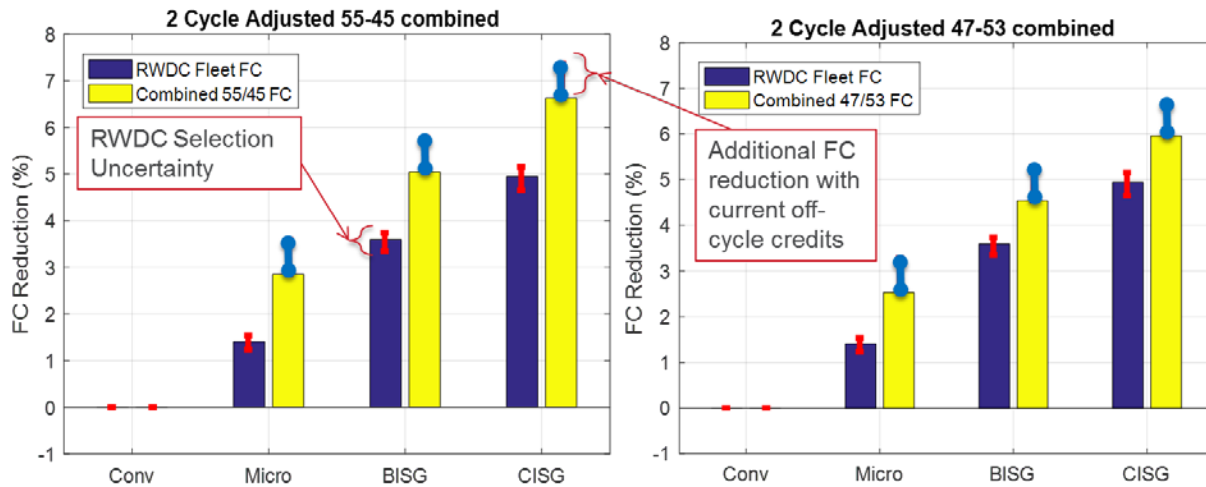


Figure IV-68: Real world benefits compared against the improvements observed in regulatory cycles.

The combined adjusted values are calculated by simulating the fuel consumption observed in UDDS and HWFET cycle and then weighing those values based on the EPA's 2 cycle procedure. Both 55-45 weighting and the 47-53 weighting are considered in this case. Unadjusted improvement values are even higher than these estimates. The red error bars on the real world fuel consumption reduction estimate show the variation that is observed between multiple samples. The blue bar on top of the improvement observed on combined 2 cycle estimates are the additional off-cycle credits offered for the start-stop systems. Based on this sample of real world cycles and for this particular type of vehicle, it is observed that the real world benefits are lower than the ones for the standard driving cycle.

Since idling time has a significant impact on the technology benefits, further analysis was performed for different trip characteristics. The real world fuel savings on shorter drive cycles (<10 miles) was analyzed for this purpose. Shorter cycles tend to be more from city driving based on the stops per mile, idling time, average speed, and other characteristics. This is seen from the cycle characteristics shown in Figure IV-69.

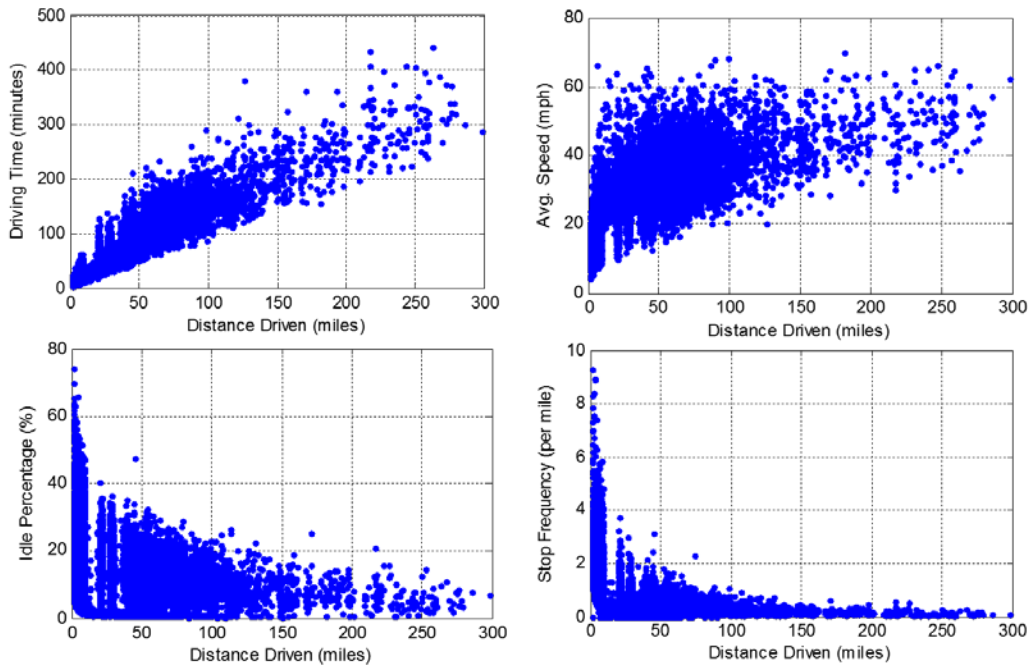


Figure IV-69: Driving distance has a good correlation to many other drive cycle properties.

UDDS cycles is expected to be a good indicator of the city driving conditions. When cycles under 10 miles are considered, we see that the real world benefits match closely with the improvements observed in UDDS cycle. During short trips, the combined 2 cycle procedure under predicts the benefits of the start-stop systems.

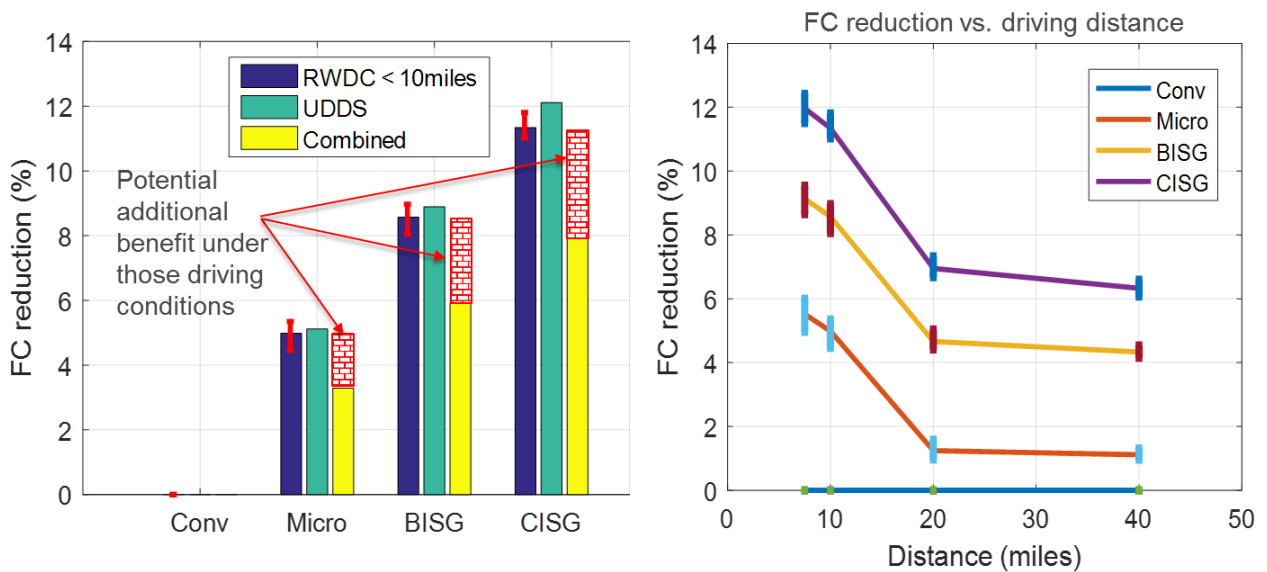


Figure IV-70: Driving distance has a good correlation to many other drive cycle properties.

The red textured region shown in Figure IV-70 shows the potential additional benefits of start-stop vehicles when driven short trips.

Conclusions

In this study, we have developed a process to quantify the impact of individual technologies for multiple real world driving cycles. The analysis for start-stop vehicles demonstrated the critical influence of idling time and driving distance on the benefits. Depending on the type of trip, it was found that start-stop can have smaller or larger fuel displacement compared to the standard test procedure.

IV.7.C. References

1. <https://www.federalregister.gov/documents/2016/09/02/2016-21217/alternative-method-for-calculating-off-cycle-credits-under-the-light-duty-vehicle-greenhouse-gas> accessed on Nov 2016
2. D3 Database, <https://www.anl.gov/energy-systems/group/downloadable-dynamometer-database> accessed on Jan 2016
3. Autonomie, www.autonomie.net accessed on Jan 2016
4. TSDC, www.nrel.gov/transportation/secure_transportation_data.html accessed on Sep 2016
5. N.Shidore,E.Islam, et.al.,"A Large Scale Simulation Process to evaluate Powertrain Technology Targets with Real World Driving", EVS29, June 2016

V. Codes and Standards

V.1. Codes and Standards and Technical Team Activities

James Francfort, Principal Investigator

Idaho National Laboratory
P.O. Box 1625
Idaho Falls, ID 83415-2209
Phone: (208) 526-6787
E-mail: James.Francfort@inl.gov

Lee Slezak, DOE Program Manager

Phone: (202) 586-2335
E-mail: Lee.Slezak@ee.doe.gov

Start Date: October 2013
End Date: Ongoing

V.1.A. Abstract

Objectives

To contribute vehicle, component, fueling, and charging infrastructure testing knowledge gained by Idaho National Laboratory (INL) staff from on-road and laboratory evaluations to industry and government groups developing and modifying standards, codes, best practices, and regulations.

Accomplishments

- Recognition as an industry expert and a voting member of these industry and government committees is a major accomplishment in itself.
- The current committees/organizations that INL staff contribute to include the following:
 - Society of Automotive Engineers (SAE) J2954 Wireless Charging Task Force
 - SAE J2894 Power Quality Requirements for Plug-in Electric Vehicle Chargers
 - National Institute of Standards and Technology's U.S. National Work Group on Measuring Systems for Electric Vehicle Fueling and Sub-Metering
 - U.S. Drive: Vehicle Systems Analysis Tech Team
 - U.S. Drive: Grid Integration Tech Team
 - Electric Power Research Institute – National Electric Transportation Infrastructure Working Council.

Future Achievements

- Continue future participation on various committees and panels, representing U.S. Department of Energy (DOE) interests and providing expertise and testing results from testing of cutting-edge advanced vehicle technologies.
- Continue providing high-fidelity performance testing, analyses, procedure development, methodology validation, reporting, and other support related to the various codes and standards committees INL is part of, as well as the DOE U.S. Drive Grid Interaction Technical Team, the Electric Power Research Institute-sponsored Infrastructure Working Group, and other Codes and Standards (C&S) committees, as directed by DOE.

V.1.B. Technical Discussion

Background

DOE's Advanced Vehicle Testing Activity (AVTA) is part of DOE's Vehicle Technologies Office, which is within DOE's Office of Energy Efficiency and Renewable Energy. AVTA is the only DOE activity tasked by DOE to conduct field evaluations of fueling infrastructure and light-duty vehicle technologies that use advanced technology systems and subsystems in light-duty vehicles to reduce petroleum consumption. A secondary benefit is reduction of exhaust emissions.

Most of the advanced technology vehicles, subsystems, and fueling infrastructure that AVTA tests include the use of electric drive propulsion systems and advanced energy storage systems. However, other vehicle technologies that employ advanced designs, control systems, or other technologies with production potential and significant petroleum reduction potential are also considered viable candidates for testing by AVTA. AVTA and INL's first priority is providing DOE feedback on the performance of advanced technologies that DOE has made funding investments in.

AVTA's light-duty activities are conducted by INL for DOE. INL has responsibility for AVTA's execution, direction, management, and reporting. INL is supported in this role by various subcontracts for specific tasks when greater value can be achieved for DOE if INL conducts research in partnerships with other organizations.

Introduction

DOE's AVTA evaluates grid-connected plug-in electric vehicle (PEV) technology in order to understand the capability of electric grid-recharged electric propulsion technology to significantly reduce petroleum consumption when vehicles are used for transportation. In addition, many companies and groups are proposing, planning, and starting to introduce PEVs into their fleets.

Knowledge gained from 20 years of testing electric drive vehicles, other vehicle technologies, and fueling infrastructure for more than 232 million miles is used by INL staff to contribute to various industry and government groups that are primarily interested in developing policies, standards, codes, and regulations that ensure safety and interoperability within the technology sectors.

Approach

As a member of a technical committee or industry group, participation is intended to contribute to the common body of knowledge being applied to develop standards and other industry practices. Participation is also intended to represent DOE interests.

Results

SAE International

SAE J2954 Wireless Charging Task Force:

INL supports the SAE J2954 committee as a full voting member by providing detailed test results from wireless charging systems and providing detailed test setup information and text that are incorporated into the standard document.

INL is supporting the SAE J2954 codes and standards committee by conducting a two-phase testing program to support knowledge and understanding of wireless charging interoperability requirements. Interoperability is when the ground side and vehicle side of wireless charging are not produced by the same company or are not of the same design. When the two halves of the wireless charging system (i.e., ground side and vehicle side) are of the same design and from the same manufacturer, it is referred to as a matched set.

In Fiscal Year 2016, INL prepared the test plan, measurement equipment, and logistics for testing eight wireless charging systems that were designed and built by three teams comprised of eight manufacturers. The six manufacturers participating and providing wireless charging systems are as follows: Qualcomm, Daimler, Jaguar Land Rover, WiTricity, Nissan, and Toyota. INL's wireless charging test fixture uses fiberglass channel strut structure and non-metallic fasteners to support the vehicle side coil assembly and power electronics (Figure V-1). Fiberglass was specifically chosen because it has no interaction with the magnetic fields of the wireless charging systems, yet it is strong enough to support the components. In contrast, an aluminum or steel structure would have a significant impact on wireless charger performance results due to interaction with the magnetic field. The test fixture also uses a servo-motor driven coil positioning system that accurately positions the ground side coil assembly under the vehicle side coil assembly. This is vital to testing because the coil-to-coil misalignment has a primary impact on system performance.



Figure V-1: Bench testing conducted on eight wireless charging systems to support SAE J2954 codes and standards development.

INL

INL has developed a test host control and data acquisition system (HC/DAS) based in National Instruments LabVIEW. The HC/DAS controls the coil positioning system, the electromagnetic field meter positioning system, the direct current load bank, and all measurement devices, including the multi-channel power meter, the electromagnetic field meter, and the non-contact temperature measurement system. The HC/DAS is designed to conduct testing in a semi-automated fashion to follow the predefined test plan with little intervention from the test operator, yet enable the required flexibility for collaborative evaluation, development, and optimization for advanced prototype wireless charging systems. Additionally the HC/DAS displays real-time data and results to enable real-time development, tuning, and operation of the prototype wireless charging systems. For each test condition (e.g., coil position, power, and voltage) data are recorded from all measurement devices both at a rate of 10 Hz and at an average value over the predetermined sampling time when the wireless charger is operating at steady state. Figure V-2 shows the user interface of the HC/DAS, which displays the real-time and results.

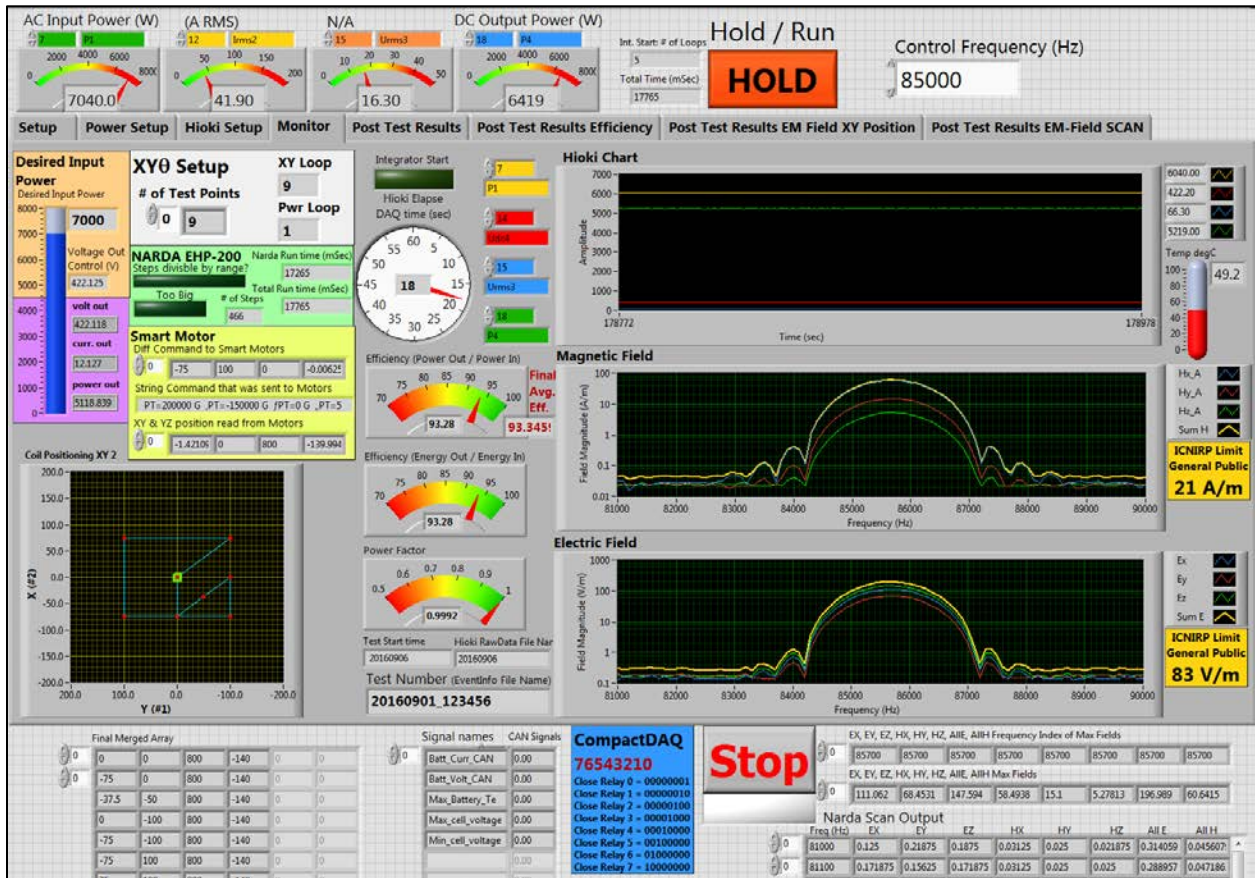


Figure V-2: User interface of the INL developed test HC/DAS that is based in LabVIEW.

INL

During the two phases of testing, multiple performance and safety metrics are measured for comparison between matched and interoperable operation of the same components of the wireless charging systems. These metrics include the following:

- System efficiency
- Power transfer capability
- Power quality
 - Power factor
 - Input current total harmonic distortion
- Magnetic field strength at 800 mm from the center of the wireless charger
- Electric field strength at 800 mm from the center of the wireless charger.

Testing and evaluation investigated the impact of several test conditions on wireless charger performance. These test conditions are aligned with the draft J2954 standard document requirements and classifications for a wireless charging system:

- Coil-to-coil misalignment
 - X: ±75 mm (front to back of the vehicle)
 - Y: ±100 mm (side to side of the vehicle)
- Ground clearance (Z)
 - Z1: 100 mm, 125 mm, 150 mm
 - Z2: 140 mm, 175 mm, 210 mm
 - Z3: 170 mm, 210 mm, 250 mm

- Charge power
 - WPT1: 1.75 kW and 3.5 kW
 - WPT2: 3.5 kW and 7.0 kW
- Output Voltage: 280 V, 350 V, and 420 V.

INL completed bench testing (i.e., off the vehicle) of eight wireless charging systems as matched systems and provided detailed results and findings to the committee to be used for further development and refinement of the draft standard SAE J2954. System efficiency was measured as high as 93% at full power operation. Additionally, all eight wireless charging systems provided the requested power at all operating test conditions across the wide range of misalignment, coil gap, charge power, and output voltage. These results provide an excellent baseline for comparison to interoperable performance and safety.

In Fiscal Year 2017, INL will continue the testing effort by conducting testing on the same eight wireless charging systems; however, it will be done as interoperable pairs instead to determine the performance and safety of the systems.

SAE J2894 Power Quality Requirements for Plug-In Electric Vehicle Chargers:

The SAE J2894 committee is developing requirements and test procedures to ensure PEV chargers do not cause power quality issues on the electric grid and that PEVs can continue to function properly in the presence of power quality issues caused by adjacent loads. The three main purposes of the committee are as follows:

- Identify those parameters of the PEV battery charger that must be controlled in order to preserve the quality of the alternating current service.
- Identify those characteristics of the alternating current service that may significantly impact the performance of the charger.
- Identify values for power quality, susceptibility, and power control parameters that are based on current U.S. and international standards.

INL has supported the J2894 committee through participation in monthly calls and laboratory testing. INL's laboratory testing consists of both steady-state testing and dynamic testing. The purpose of steady-state testing is to determine the overall steady-state behavior of a vehicle as a load on the electric grid. A couple of important test metrics that are acquired during steady-state testing are efficiency, power factor, and the total harmonic distortion in the current. The purpose of dynamic testing is to measure a vehicles dynamic response to grid events and then determine if that dynamic response might be detrimental to the electric power quality or grid stability when a large number of vehicles are charging. Requirements are then added to the J2894 recommended practice to ensure compliant vehicles do not have an undesirable response.

In Fiscal Year 2016, INL has tested four production electric vehicles: 2015 Mercedes B-Class, 2016 Chevrolet Volt, 2015 Ford Fusion, and 2015 Kia Soul. Testing consisted of steady-state tests at many different voltage levels and charge rates and dynamic testing that measured each vehicles response to voltage magnitude deviations, voltage frequency deviations, and voltage distortion among other things (Figure V-3). One area where INL's testing has made a significant impact in Fiscal Year 2016 is in identifying the undesirable response of many PEV chargers to voltage sags. Ideally, during a voltage sag, the amount of current that a vehicle charger is drawing from the grid would decrease during the sag (or at least remain constant) and then return to normal after the voltage sag. The actual response of many production PEVs during a voltage sag is to substantially increase the amount of current the vehicle charger is drawing during the voltage sag (Figure V-3). This response is highly undesirable and the SAE J2894 committee is discussing how this issue should be addressed in the J2894 document.

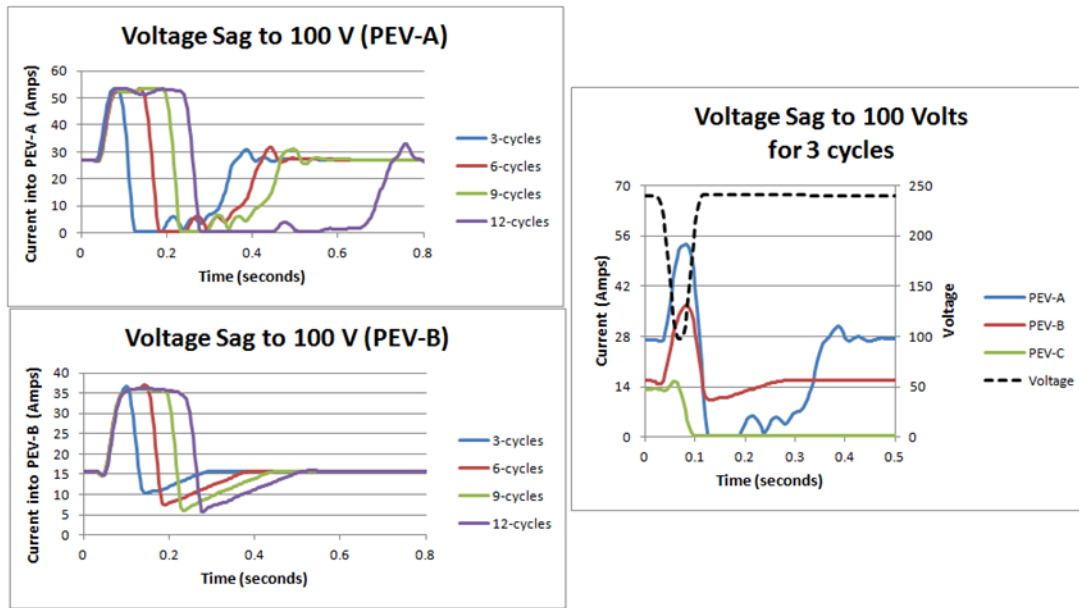


Figure V-3: Steady-state tests at different voltage levels and charge rates.

U.S. Environmental Protection Agency Energy Star

Electric Vehicle Supply Equipment Test Method Development in Collaboration with Energy Star

The U.S. Environmental Protection Agency will be introducing Energy Star ratings for Level 1 and Level 2 electric vehicle supply equipment (EVSE) standby power consumption and power loss during charging. INL is collaborating with the U.S. Environmental Protection Agency and other national laboratories (i.e., Argonne National Laboratory and Lawrence Berkeley National Laboratory) to develop a test method document that details the requirements of the test method, including measurement equipment and detailed test procedures.

INL drafted the measurement equipment requirements, including input and output measurement connection modules that are necessary to safely and effectively measure the input and output current and voltage and the control pilot signal. The specified connection modules alleviate the need to modify EVSE input and output cord sets. Additionally, a controllable load bank is required to draw power through the EVSE at specified current rates. INL also developed and drafted test procedures for evaluation of EVSE for standby power consumption and power loss during charging. Standby power consumption is consumption by the EVSE while not providing current to the vehicle. Standby power consumption is often a result of various EVSE functions (such as status lights, touch screen display, a control module, or a smart grid communication module) drawing power. The measurement of power loss during charging is also detailed in the document. Current is drawn through the EVSE in the same manner as a vehicle charging and at prescribed current levels that are representative of the typical charge levels of production PEVs (i.e., 1.1 kW, 3.3 kW, 6.6 kW, and 10 kW). Input and output power are accurately measured during the steady-state current draw; differences between the two measurements are EVSE power losses during charging. These losses are often due to resistive losses of wire, contacts, and other connections, as well as standby loads that are still present during charging.

In support of developing the test method draft document, INL tested numerous EVSE to validate the test procedures and evaluate alternative measurement methods. Numerous production EVSE were tested using the draft test procedure and the required equipment. The results were analyzed to identify any outlying results or anomalies due to test procedure inconsistencies. No issues were found. Additionally, INL presented at three separate Energy Star webinars to discuss and receive public comments on the draft test method document. The webinars included a proposed alternative method for measuring EVSE loss by a differential measurement technique. After the webinars, INL conducted testing on the same EVSE, but used the proposed differential measurement technique. The results were analyzed and compared with the Energy Star test procedure results. A comparison of the two techniques was conducted and the differential current measurement method was integrated into the draft test method.

National Institute of Standards and Technology

U.S. National Work Group on Measuring Systems for Electric Vehicle Fueling and Sub-Metering:

INL is an original voting member of the U.S. National Work Group on Measuring Systems for Electric Vehicle Fueling and Sub-Metering. This National Institute of Standards and Technology committee developed the design standard, technical specification, metrology, and testing and certification that individual EVSE in the public domain must adhere to if the EVSE meters electricity and is the point of sale. By participating in this standard development, INL staff engineers are helping direct future EVSE testing needs, methods, and procedures.

U.S. Drive (United States Driving Research and Innovation for Vehicle Efficiency and Energy Sustainability)

Vehicle Systems Analysis Tech Team:

INL is a long-time member of the Vehicle Systems Analysis Tech Team due to INL's history of testing that has been performed for DOE. INL staff contributes, via presentations and papers, the results of benchmarking the advanced automotive powertrain components and subsystems from INL's whole vehicle system and component testing. This testing includes fuel use, efficiencies, auxiliary loads, and energy storage results that are subsequently used by other team members as modeling inputs.

Grid Integration Tech Team:

Because of the nature of the infrastructure testing INL performs for DOE, INL is a founding member of the Grid Integration Tech Team. This includes wireless power transfer and conductive charging, direct current fast charging, and INL's data collection, analysis, and reporting on how 8,000 PEV drivers utilize 17,000 Level 2 EVSE and direct current fast chargers.

Electric Power Research Institute – National Electric Transportation Infrastructure Working Council

Infrastructure Working Council:

INL is a 20-year member of the Infrastructure Working Council, which is sponsored by the Electric Power Research Institute and is a group of individuals whose organizations have a vested interest in the emergence and growth of the electric vehicle, plug-in, and hybrid electric vehicle industries, as well as electrification of truck stops, ports, and other transportation and logistics systems. Infrastructure Working Council members include representatives from electric utilities, vehicle manufacturing industries, component manufacturers, government agencies, related industry associations, and standards organizations. The various committees meet several times a year to address electric vehicles, plug-in hybrid electric vehicles, truck stop and port electrification, and infrastructure research and development. INL supports the Plug-in Hybrid and Electric Vehicle Working Group, the Transportation Electrification Committee, and serves on the Infrastructure Steering Committee. Results from INL's testing of vehicles and infrastructure and from data collection with data loggers from 24,000 vehicles and charging infrastructure units is of great interest and support to the Infrastructure Working Council's decision processes.

Conclusions

The intent of this work was to leverage benchmark testing results and staff knowledge gained as a resource for various industry groups that are putting into place industry-lead or government-lead codes, standards, requirements, or best practices.

V.1.C. Products

Presentations/Publications/Patents

The intent of this work was not to publish results as products of INL, because the outcomes are usually the sole intellectual rights of other organizations (e.g., SAE).

The work described in this section will not result in INL patents. The intent of this work is to provide technical support to DOE and industry in development of standards.

V.2. SAE J2907 Performance Characterization of Electrified Powertrain Motor-drive Subsystem

John M. Miller, Principal Investigator and Chair, SAE J2907

JNJ Miller Design Services PLLC
 1100 Mockingbird Lane
 Longview, TX 75601
 Phone: (865) 296-1496
 E-mail: jmmiller35@aol.com

Lee Slezak, DOE Program Manager

Vehicle Systems Program, Vehicle Technologies Office
 Phone: (202) 586-2335;
 E-mail: Lee.Slezak@ee.doe.gov

Start Date: 1 October 2015
 End Date: 30 November 2016

V.2.A. Abstract

Currently, there is no widely accepted standard for specifying the performance of a traction motor designed for use in electrified vehicles whether hybrid, battery electric, fuel cell, or range extended. J2907 is introduced as a TIR - technical information report that establishes a uniform set of test procedures for users and independent testing facilities to validate manufacturer claims in an out-of-vehicle, laboratory environment. This work supports ongoing efforts with J2908 to define and establish unified requirements for measuring hybrid and plug in hybrid electric power levels in-vehicle. Current electric powertrain configurations are widely varied with insufficient criteria to make adequate vehicle to vehicle comparisons. A standard for testing and specifying electric motor ratings is needed to establish a unified consensus for evaluation purposes and validation of manufacturer declared net and maximum 30 minute power. The commonality of J2907 with UN/ECE R85 is considered a benefit to the user community as an updated standard that minimizing confusion, and has global scope.

Objectives

- Define procedures for tests to be done in a laboratory setting to establish a consistent and repeatable mechanism for the assessment of motor net power and maximum 30 minute power.
- Refine existing pre-conditioning procedures for the electric traction drive system (ETDS) that are broadly applicable in the global community as the pre-test warm-up procedure.
 - Revise the pre-test warm-up power level to 20% versus 80%
 - Clarify automotive maximum 30 minute power versus industrial continuous power
 - What is thermal stabilization and does it apply [1]?
- Revised section 1.1 to say that testing is to be performed with manufacturer prescribed operator interface software, including manufacturer supplied production algorithms that are not to be modified.
- Clarify the test durations and filtering requirements of data acquisition needed for accurate and repeatable results.
 - Revise the maximum net power data point duration to be 10s
 - Define data smoothing to be the 10s average vs. 2s moving average
- Deliver J2907 TIR draft by end of October 2016 in preparation for 1st ballot at SAE

Accomplishments

- Obtained industry consensus on ETDS pre-conditioning procedure including:
 - Consensus on laboratory power supply voltage regulation criteria

- ETDS thermal controls criteria and cooling medium
- Laboratory instrumentation accuracy and tolerance requirements harmonized with J2908
- Completed development of out-of-vehicle maximum power procedure and laboratory requirements
 - Specification of dynamometer speed setting, and
 - Speed range and number of testing points, plus
 - Revised UN/ECE R85 setting to full rating of the power converter to 20% of full setting of the power controller until motor temperature stabilizes
 - Reached consensus that torque and speed are to be recorded simultaneously and averaged over a test time of 10s per documented point
 - Revised the maximum net power error band to 5% for the validation criteria
 - Updated net power in the speed range -0.98np to $+1.02\text{np}$ must not deviate more than 4% from the maximum net power in the range
 - Reached consensus on criteria for validation of manufacturer declared maximum net power
- Completed development of laboratory validation of maximum 30 minute power procedure
 - Set the pre-conditioning criteria of a fully equipped ETDS, including all of its assemblies, to an ambient temperature of $25^{\circ}\text{C} \pm 5^{\circ}\text{C}$ for 4 hours
 - Defined the maximum 30 minute power error band to 5%
 - Defined the acceptance criteria that output power after 30 minutes of test time must be within 5% of the initial power.
- Revised definition of repeatability and retests for harmonization with J2908
- Purged all reference to industrial electric motors, specifically the definition of continuous power rating and replaced with a more relevant automotive definition
- Completed conversion of working draft to TIR template in preparation for first ballot by SAE
- Publish document as TIR (pending ballot results) before end of CY2016

Future Achievements

- Work with J2907 Task Force members to identify field trial test sites for evaluation of the TIR
 - Require at least three sites to beta test J2907 TIR using a production ETDS
 - Determine who will pay for the testing and data collection and processing
 - Institute plans for an SAE internet portal that users may archive ETDS test results
 - Advance the J2907 TIR to recommended practice RP provided sufficient number of user sites are identified and completed
- Continue coordination with J2908, especially in areas data collection, filtering, and validation of manufacturer declared power values that meet J2908 requirements
- Publish J2907 as an RP during FY17
 - Revise appendix A1 as mandatory communications sheet to document self-certification
 - Revise appendix A2 as needed during beta testing to document how data acquisition is performed, post processed, and prepared for archiving

V.2.B. Technical Discussion

Background

Electrified vehicles are increasing in market share, and are expected to continue to do so. These advanced vehicles are currently found on dealer lots and in marketing material. They are being compared to conventional vehicles powered by internal combustion engines; whether in light-duty, heavy-duty, or off-road applications. Additionally, these vehicles are being compared with other electrified vehicles which may operate with different voltage levels or powertrain configurations.

Currently there is no widely accepted standard for specifying the performance of a traction motor. It is our intention to be as similar in approach as possible to the existing worldwide standard UN ECE R85 (Uniform provisions concerning the approval of internal combustion engines or electric drive trains intended for the propulsion of motor vehicles of categories M and N with regard to the measurement of net power and the maximum 30 minute power of electric drive trains). In addition, a wide variety of powertrain configurations, as well as limitations arising due to the traction battery, cooling system, or vehicle controls, makes it difficult to predict the net and continuous power of the electric motor, the major component in an electric traction drive subsystem (ETDS), once installed in its application vehicle. The J2907 test procedure provides an accurate assessment of the ETDS performance, under controlled laboratory conditions, using manufacturer supplied equipment settings, as the basis for in-vehicle performance as outlined in SAE J2908.

Due to the inclusion of the inverter and associated production software, the majority of the testing results will reflect the characteristics of the motor in a specific application. The implementation of one motor design in multiple applications or with different inverters or with different algorithms and/or parameterization would require retesting to obtain the motor characteristics that represent the different motor drive systems. The procedures stated in the J2907 document apply whether the ETDS provides direct access to its motor shaft, or access via an integrated gearbox, so that test fixture requirements are minimized.

At this point SAE J2907 should be viewed as a starting point for the standardization of electric traction motor testing. This technology will be evolving as newer and more integrated drive systems become commercially available. It is likely, therefore, that these test protocols will need to be periodically revisited and revised, as the industry matures.

Accordingly, SAE has set a document review cycle of five years to update standards.

Introduction

Ratings of motors intended for electric vehicle traction often do not come with sufficient information to extract meaningful technical data to enable valid performance comparisons. Test procedures are varied among manufacturers and frequently are not explicitly defined when motor characteristics are quoted, resulting in ambiguous and vague specifications that can confuse both consumers and developers.

J2907 was developed to establish a foundation for the standardization of motor tests for electric machines used in electric traction drive systems. Its intent is to specify procedures for tests to be done in a laboratory setting to foster a consistent and repeatable mechanism for the assessment of motor net power and maximum 30 minute power. This facilitates a solid basis for comparisons of different motors as well as a mechanism to establish reliable, repeatable, sanctioned specifications.

The specified tests apply to electric traction drive subsystems as a generic component of vehicle propulsion for light duty passenger cars, motor cycles, and low speed electrified vehicles for which power can be quantified in a laboratory setting and validated by independent testing laboratories.

Approach

The electric drive system under test includes the ETDS comprised of:

- Drive motor with access to its output shaft, either directly or via a gearbox
- Power inverter plus control electronics having MFG supplied production software
- Cables and sensors as needed for operation, data acquisition, and operator interface software
- Any enclosures required to support the operating system
- Entire cooling system that mocks up vehicle usage

Test procedures developed in J2907 are meant to cover an electrified powertrain motor-drive subsystem regardless of end use. Typical applications include fuel cell EV (FCEV), battery electric vehicle (BEV), hybrid EV (HEV), plug-in EV (PHEV), or range extended EV (EREV), regardless of architecture.

Also included within this field of application are ETDS units as may be found in electric motorcycles, scooters, and low speed electric vehicles such as Neighborhood EV's.

Motor only characterization tests are not covered by this document. Instead, appropriate motor test procedures for the characterization of particular electric machine types, such as those illustrated in Figure V-4 below can be found in the IEEE Standards listed below. As such, the field of application is restricted to automotive ETDS units intended for transportation - all reference to industrial motors are removed.

Std. 11 for rail and road vehicles

Draft Std. P1812 for permanent magnet machines

Std. 112 for polyphase induction motors and generators

Std. 115 for synchronous machines

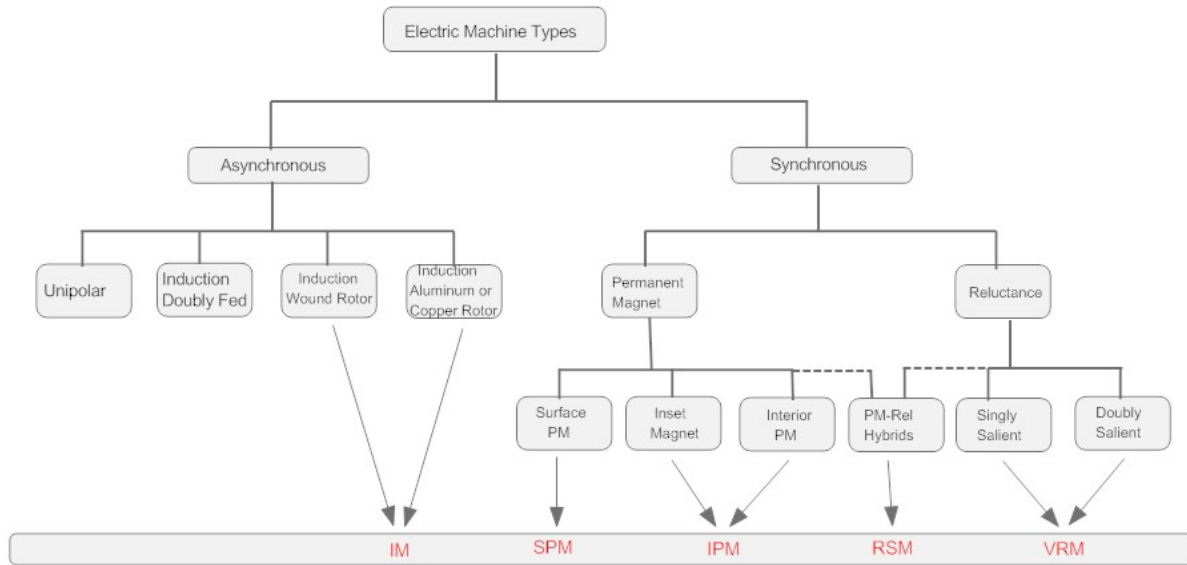


Figure V-4: Types of Electric Traction Motors

The main types of traction motors to be characterized under J2907 are the induction (asynchronous) motor (IM), the interior permanent magnet (IPM), and various types of surface permanent magnet (SPM) machines. Independent testing of manufacturer declared maximum net power and maximum 30 minute power requires the manufacturer to specify the shaft speed, n_p , that peak power was found. Figure V-5 illustrates this speed and corresponding maximum net power (shown as peak power) for the major automotive traction motor types.

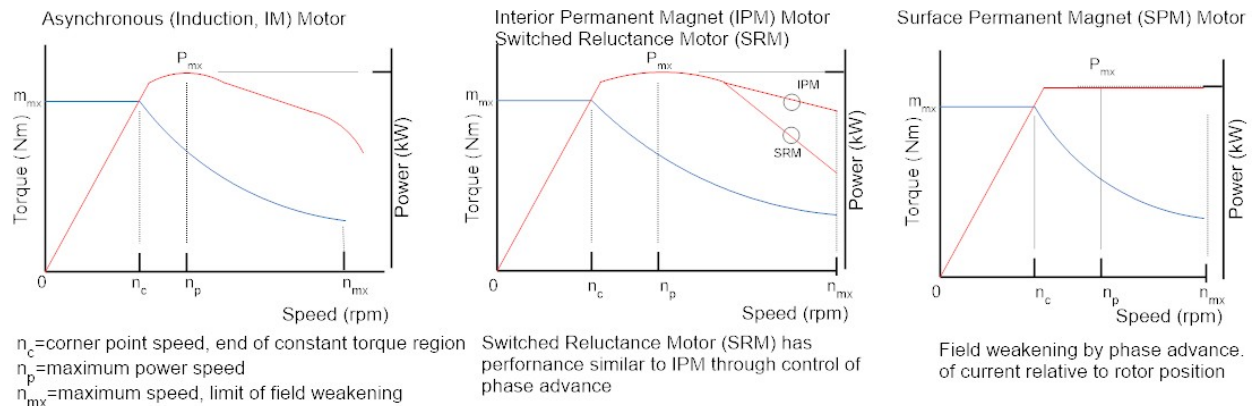


Figure V-5: Torque-speed and power characteristics of selected traction motor types

The sole purpose of the J2907 TIR is the definition of globally accepted test procedures that a user, such as a nationally recognized testing facility (NRTF), would follow to validate manufacturer claims.

Recent experience in the marketplace highlights the importance of internationally accepted procedures to characterize maximum net power and maximum 30 minute power as evidenced by the court claim "Tesla loses ruling over power output disclosure from Norway's Consumer Disputes Commission over how it lists its electric vehicles' power output and may have to pay vehicle owners about \$6,000 per vehicle," over issues stemming from calculation of the Model 2 (P85D) front and rear electric traction motor claimed output power.

"The Norway regulator says that the method in which Tesla disclosed the horsepower output of the two electric motors on its Model S P85D amounted to deceptive advertising." The article is dated 1 July 2016.

Another example is the Motor Trend article describing the launch of the 2016 Toyota PRIUS which states that, "Automakers haven't collectively agreed on a single harmonized procedure to rate their hybrid powertrains. They aim to make it as similar to current engine-only ratings as possible, but hybrid configurations are highly diverse. Toyota's change in rating technique influenced the 2016 Prius' lower system horsepower." An even earlier news alert from M. Hoyer in Machine Design magazine, November 18, 2013 titled "The Misconceptions of EV Motor Testing," noted that: It's time to rethink performance tests on electric motors destined for use in electric vehicles.

Indeed, the automotive industry concurs which supports DOE's commitment to address this need with a pair of standards, J2908 for in-vehicle and J2907 for out-of-vehicle test standards. Progress on development of the initial stages of a standard were published at the DOE AMR 7 June 2016 and also summarized in a short briefing to attendees of a University of Wisconsin-Madison 3 day EV Bootcamp. Figure V-6 highlights architecture, introduction date, torque production mechanism, and excitation source.

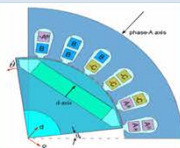
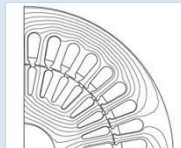
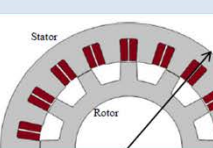
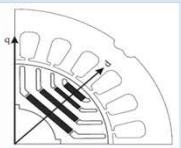
Attribute	Interior PM Motor (IPM)	Induction Motor/Asynchronous (IM)	Switched or Variable Reluctance Motor (SRM, VRM)	Synch-Rel or PM Reluctance (Synch-Rel)
Representative design				
Date of 1 st concept	~1986	1889	1900	1923
Electromagnetic torque, $m_{em} =$	$\frac{3P}{2} \{ \lambda_{pm} I_{qs} - (L_{ds} - L_{qs}) I_{ds} I_{qs} \}$	$\frac{3P}{2} \frac{L_m^2}{L_r} I_{ds} I_{qs}$	$\frac{1}{2} I_s^2 \frac{dL(\theta)}{d\theta}$	$\frac{3P}{2} (L_{ds} - L_{qs}) I_{ds} I_{qs}$
Excitation source	Internal permanent magnets Field weaken via Inverter	All magnetization supplied by power inverter	All magnetization provided by power inverter	Partial magnetization by PM's and field weaken by power inverter

Figure V-6: Basic architectures of electric traction motors

Results

The ETDS must be initialized and preconditioned in accordance with the manufacturer specifications. The ETDS is mounted to a laboratory dynamometer using appropriate fixture such that the motor output shaft, or its extension, is accessible for connection to torque and speed transducers. The ETDS coolant ports, dc power terminals, and controller input connection must also be easily accessible.

The laboratory power supply may be a single bidirectional regulated supply, or unidirectional power supply in combination with energy storage for energy recuperation. ETDS system voltage shall be measured at its dc power connection. For ETDS units operating below 250V the power supply stability tolerance shall not exceed +/-2.5V, and for units operating above 250V the regulation stability tolerance shall not exceed +/-1.25% of the manufacturer specified voltage over a 10s test interval, excluding any short term transients (<100ms).

Figure V-7 illustrates a typical laboratory test configuration for full ETDS evaluation that includes a laboratory power supply, coolant system such as a chiller or representative vehicle coolant system, and related ancillary loads such as dc-dc converter, battery management system BMS if required, controller area network CAN, and any related functions required by the ETDS to function as designed for in-vehicle use.

J2907 Engineering Test Out of Vehicle

Power Supply voltage setpoint per Manufacturer Specification

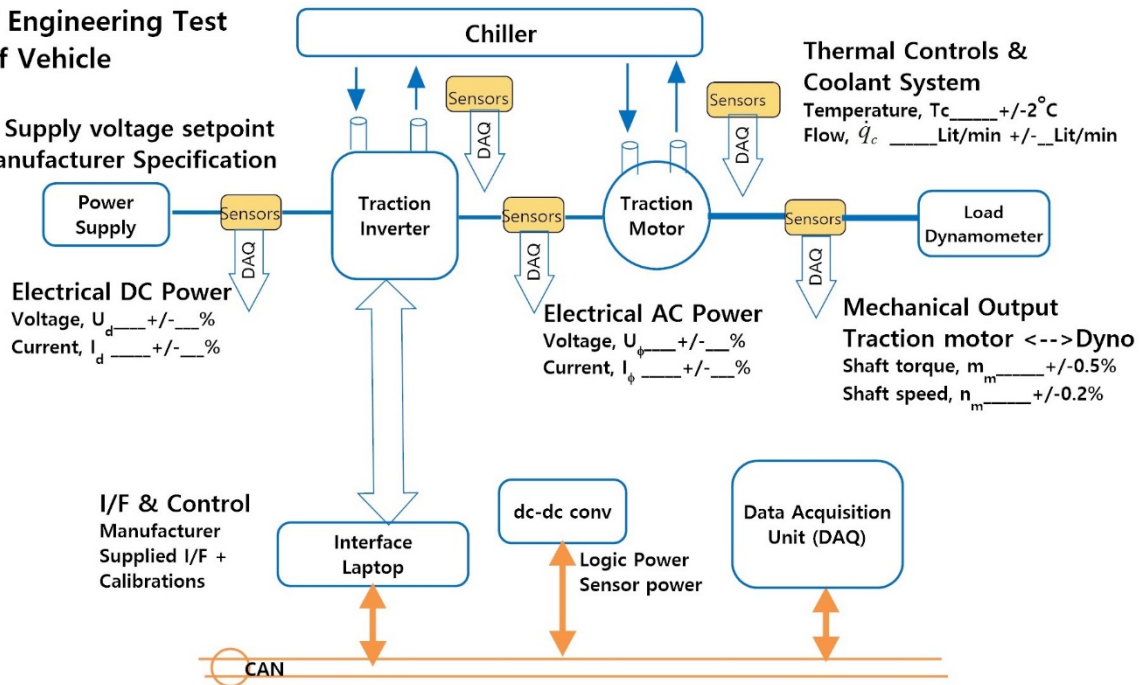


Figure V-7: Functional diagram for bench dynamometer test

Power levels encountered in electrified powertrain testing of passenger vehicle ETDS units will nominally be in the range of 50 kW to 120 kW, but in higher performance vehicles may exceed 250 kW. Recommended instrumentation accuracy is listed in Table V-1.

All measurement equipment, sensors, and power flow analyzers must be traceable and have a calibration record. During the initialization step verify that all equipment (i.e., power analyzers, torque transducer, dynamometer data acquisition system, etc.) have up to date calibrations. Laboratory personnel should review safety documentation and applicable procedures for working in specific dynamometer test cells, and test cell control rooms.

The J2907 Task Force members have agreed, after considerable deliberation and harmonization with J2908 to the instrumentation accuracy and tolerance levels documented in Table V-1.

Table V-1: Instrumentation Tolerance

Sensor/Transducer	Tolerance
VOLTAGE	
Direct, Vdc	+/-0.5%
Alternating, Vrms	+/-0.5%
CURRENT	
Direct, Adc	+/-0.5%
Alternating, Arms	+/-0.5%
TORQUE & SPEED	
Torque, Nm	+/-0.5%
Speed, rpm	+/-0.2%
TEMPERATURE	
Component Temperature, °C	+/-0.5°C
Coolant Temperature, °C	+/-0.5°C

Maximum Net Power Test and Computations

This test is intended to measure the maximum (net) power capability of the ETDS under dynamic power conditions similar to those which are imposed on electrified vehicles in urban driving conditions. The ETDS is operated in the vicinity of its specified corner speed, n_c (rpm) at the manufacturer specified input voltage, coolant conditions, and for appropriate torque and flux commands to its power controller. The ETDS shall operate within its rated capability for all tests.

Operate the ETDS at the maximum torque specified by the manufacturer at a sufficient number of speed points between zero and maximum speed of the ETDS to determine the torque-speed curve. Torque and speed are recorded simultaneously and averaged over a test time of 10s per point. Determine the maximum torque and corresponding speed during the 10s test. The peak power available from the laboratory instrumentation will be at the speed for which power is greater than the previous and subsequent points. The test shall be completed in 5 minutes.

Validation of the maximum net power shall be determined according to (1) where P_{max} occurs at speed n_p .

$$\left| \left(\frac{P_{max}}{P_{declared}} \right) - 1 \right| \times 100 < 5\% \quad (1)$$

Approval requires that net power in the speed range $-0.98n_p$ to $+1.02n_p$ must not deviate more than 4% from the measured P_{max} at speed n_p according to (2). Testing requires a minimum of two measurement points in this range plus the point indicating maximum power.

$$\max_{-0.98n_p < n < 1.02n_p} \left\{ \left| \left(\frac{P_{meas}(n)}{P_{declared}} \right) - 1 \right| \times 100 \right\} < 4\% \quad (2)$$

Maximum 30 Minute Power Test and Computations

The intent of this test is to measure the maximum power capability of the ETDS as validation of its capability to deliver manufacturer stated performance in real world driving conditions.

Operate the ETDS at the manufacturer specified production intent speed for maximum 30 minute power. The ETDS shall operate within its rated continuous capability for the entire test. Monitor and record the motor coolant outlet temperature to insure it remains at the speed used for the measurement. Acceptance criteria requires that output power after 30 minutes of test time must be within 5% of the initial power.

Motor power after 30 minutes of continuous operation shall be calculated according to (3) and (4). The maximum 30 minute power is the average of the initial and final values of power. Test data for maximum 30 minute power shall be logged on a template (paper or electronic) and the average value, $\langle P_{30max} \rangle$, as the average over the 30 minute test run.

$$\langle P_{30max} \rangle = \frac{1}{N} \sum_{k=1}^{N=30} P_{30}(k) \quad (3)$$

Validation of the maximum 30 minute power is determined according to (4).

$$\left| \left(\frac{\langle P_{30max} \rangle}{P_{30declared}} \right) - 1 \right| \times 100 < 5\% \quad (4)$$

For a TIR level standard the data record developed at a testing facility such as supplier or NRTF may also be stored at SAE. Data archive by SAE for TIR results is optional, but mandatory when elevated to RP - recommended practice. No retests are required if the ETDS under test meets the criteria of (1), (2), and (4).

Conclusions

Development of the J2907 standard was necessary because the closest internationally accepted standard is the UN/ECE R85 - Uniform provisions concerning the approval of internal combustion engines or electric drive trains intended for the propulsion of motor vehicles of categories M and N with regard to the measurement of

net power and the maximum 30 minute power of electric drive trains. This existing worldwide standard is becoming outdated and in need of updating for several years now. Moreover, the U.S. has not signed the UN/ECE treaty but manufacturers and suppliers use the R85 procedure which requires the presence of a UN representative to witness testing and to insure instrumentation is certified and calibrated. Consequently, other countries have begun developing their own traction motor rating standards such as China - GB/T 18488.1-2015, Korea, and others to satisfy their need for self-certification.

Publication of the J2907 procedure as a TIR moves this activity into a period of field trials so that users may test and document ETDS performance results according to the criteria established by the task force and listed in (1) through (4). Kicking J2907 off as a TIR also minimizes incurring a false start as may happen if issued as an RP without beta testing. Field trials also validate the need for manufacturer supplied interface software, verification that power controller algorithms are production level and unmodified, that data acquisition accuracy and tolerance are consistent with the stated acceptance criteria for maximum net and 30 minute power, and that test times and limits are appropriate. The result is an ETDS that can be stated as being "tested per SAE" and therefore that motor power rating is self-certified. In addition, the user community as exemplified by task force members, is satisfied that J2907 updates and replaces the R85 procedure and will be less expensive to implement. Feedback from the user community is that J2907 be "a standard that provides an independently verifiable level playing field for all."

Recommendation

The need for field experience was brought up to the J2907 Task Force members with a stated objective of elevating this to an RP level of standard. The immediate feedback was "who pays for the testing?" This question must be addressed in the next two months during which time the J2907 draft is going into first ballot and when it passes SAE will publish as a TIR. The recommendation is that J2907 will not move to RP and Standard until at least three users validate the procedure.

V.2.C. Products

Presentations/Publications/Patents

1. John M. Miller, "SAE J2907 Motor Power Ratings Standards Support," presentation at 2016 DOE Hydrogen and Fuel Cells Program and Vehicle Technologies Office Annual Merit Review and Peer Evaluation, Project ID# VS144, 7 June 2016
2. John M. Miller, "Traction Motor Testing Standard," Electric and Hybrid Vehicle Bootcamp on Electric Machines, Power Electronics, and Energy Storage Systems, a 3-day short course, University of Wisconsin-Madison, Madison, WI, 21-23 June 2016

V.2.D. References

1. Steven L. Rickman, Eugene K. Ungar, "A Physics-based Temperature Stabilization Criterion for Thermal Testing," 25th Aerospace Testing Conference, Oct. 2009
2. Regulation No 85 of the Economic Commission for Europe of the United Nations (UN/ECE), Official Journal of the European Union, 24.11.2006
3. SAE J1349 "Engine Power Test Code - Spark Ignition and Compression Ignition - as Installed Net Power Rating, September 2011

V.3. PEV-Grid Connectivity

Keith Hardy, Director, EV-Smart Grid Interoperability Center, Principal Investigator

Argonne National Laboratory

6900 S. Cass Avenue

Argonne, IL 60439

Phone: (630) 816-7383 (mobile); (630) 252-3088 (ANL); (202) 488-2431 (DC); Fax: (202) 488-2413

E-mail: khardy@anl.gov

Lee Slezak, DOE Program Manager

DOE Vehicle Technologies Program

Phone: (202) 586-2335

E-mail: Lee.Slezak@ee.doe.gov

V.3.A. Abstract

Objectives

Argonne's EV-Smart Grid Interoperability Center in remained focused on technology and standards for vehicle-grid connectivity, communication and interoperability as well as facilitating global harmonization of interoperability requirements/standards. The scope has expanded to include integration with other grid-connected devices because 1) the potential for plug-in vehicles to contribute to and benefit from integration with distributed energy resources and building systems and 2) the potential applicability of Argonne's technology and integration methods to other grid-connected devices and local grids.

This technical direction directly supports the DOE Grid Modernization initiative. Argonne participated in several multi-lab proposals in FY 2015 in response to the lab call issued by the Grid Modernization Laboratory Consortium (GMLC). This resulted in six awards that expanded the center's scope to include cross-cutting (grid-level) and program-specific tasks (for the Vehicle Technologies Program, VT).

Efforts to support standards-related activities have expanded as well due to the GMLC tasks, requiring additional attention to grid-related interface/communication committees of IEEE and developments within associations such as the Smart Grid Interoperability Panel (SGIP) and the GridWise Architecture Council (GWAC). The center's FY 2016 objectives are summarized below and described later in this report.

- Grid Integration
 - Enabling Technologies
 - Demonstrate Common Integration Platform with PEVs and grid-connected devices
 - Demonstrate proof-of-concept and develop prototype Smart Charge Adaptor (SCA)
 - Refine submeters/EUMDs for commercial applications
 - Develop electric fuel metering system for DC charging (i.e., NIST HB 44 compliance)
 - Testbeds
 - Complete Smart Energy Plaza Ø1 to support enabling technology development; sensing, communication and control of networked EVSE, solar and building systems
 - Initiate plans to support grid integration studies; enhance Ø1 capabilities with high power charging and battery storage in a microgrid configuration

- Develop and verify enabling technologies and standards for grid connectivity and communication
- Develop open source solutions for grid integration
- Test communication and control systems in a network of grid-connected devices
- Support harmonization of interoperability standards
- Support interoperability/grid integration activities of the DOE Grid Modernization Initiative

Figure V-8 Objectives

- Grid Modernization
 - Support GMLC foundational tasks
 - 1.2.2 - Interoperability (strategic vision and maturity models)
 - 1.2.3 - Testing Network (intra-lab coordination and external access to data/models)
 - 1.4.1 - Standards and Test Procedures for Interconnection and Interoperability
 - 1.4.2 - Definitions, Standards and Test Procedures for Grid Services from Devices
 - Support VT program-specific tasks
 - GM0062 - Vehicle-to-Building Integration Pathway
 - GM0085 - Systems Research Supporting Standards and Interoperability
- Codes and Standards
 - Continue leadership of SAE J2953 committee (interoperability) and NIST HB44 sub-committee (methodology to measure electric fuel delivery)
 - Participate in SAE committees related to charging/communication
 - Liaise with related IEC/ISO, DIN, IEEE, ANSI committees
- International Cooperation/Harmonization
 - Europe
 - Interoperability; participate in Global InterOP meetings to insure applicability of AC/DC interoperability uses cases, test procedures and test equipment
 - PEV testing; Complete instrumentation and testing of a plug-in hybrid reference vehicle at Argonne, ship to JRC for testing to compare test procedures, analysis and results
 - Continue support of USG initiatives efforts and develop a joint work plan with JRC-E.C.
 - Asia
 - Continue efforts to establish cooperative activities with China that could facilitate harmonization of PEV interoperability standards
 - Facilitate technical discussions with APEC Automotive Dialogue following adoption of the APEC Roadmap for Electric Vehicles in early 2016, which included the establishment of a cooperative EV Interoperability and Research Center

Accomplishments

- Grid Integration
 - Enabling Technologies
 - Demonstrated the Common Integration Platform (CIP.io) and ‘Internet of Things’ (IoT) approach in Smart Energy Plaza Ø1; integrated monitoring, communication, control and visualization of EVSE, building systems and solar array with use cases such as load shedding; authored and published open source interface code for components in the plaza
 - Developed CIP.io interface for and demonstrated proof-of-concept SCA with EVs in Smart Energy Plaza Ø1; refined design and fabricated the alpha prototype SCA
 - Demonstrated 4th generation and developed 5th generation submeters in commercial formats; awarded commercialization contract for FY 2017-18 by DOE Building Technologies Office
 - Completed a proof-of-concept device and design study for a low cost graphic display-user interface for EUMD Rev 5 submeter connected via MODBUS. Potential uses include low cost weatherproof solution to meet NIST Handbook44-3.41 display requirements for commercial dispensing of electricity as a fuel.
 - Refined NIST HB44 electric fuel metering system for AC EVSE
 - In response to the recommendation of the multi-lab grid integration study regarding hardware-in-the-loop, hardware was specified and acquired; modeling is in process
 - Testbeds
 - Completed Smart Energy Plaza Ø1; EVSE, solar and building systems are networked and the common integration platform (CIP.io) has been demonstrated. This capability will be used in FY 2017 for acceptance testing of submeters/EUMDs and alpha prototype SCAs prior to industry/field testing

- Design and construction of Smart Energy Plaza Ø2 was initiated and is expected to be completed in Q1 FY 2017. The additional capabilities will support grid integration studies for VT and GMLC.
- Grid Modernization
 - Foundational Tasks
 - GMLC 1.2.2 - Interoperability; contributed to the strategic vision activity and hosted the first industry/stakeholder meeting in Chicago
 - GMLC 1.2.3 - Testing Network; contributed specifics of grid-related testing capabilities
 - GMLC 1.4.1 - Standards and Test Procedures for Interconnection and Interoperability; contributed the gap analysis for standards related to EV connectivity and communication with the grid
 - GMLC 1.4.2 - Definitions, Standards and Test Procedures for Grid Services from Devices; contributed the EV device template (characterization parameters for grid applications)
 - Program-Specific Tasks
 - GM0062 - Vehicle-to-Building Integration Pathway; contributed to the use case requirements document. Led the development of the "Monitoring, Communication and Control Requirements/Platform & Communication Architecture" document.
 - GM0085 - Research Supporting Standards and Interoperability; same deliverable as GM0062 (initial use cases are common in this phase of the project)
- Codes and Standards
 - Continued as committee chair of SAE J2953 (interoperability) and sub-committee chair of NIST/NCWM Handbook 44-3.41 (commercial dispensing of electricity as a fuel)
 - Contributed test data and feedback to ANSI C63.30 (wireless charging safety; EMC field decay measurement procedure development and validation data from ANL wireless charging tests)
- International Cooperation/Harmonization
 - Europe
 - Interoperability; participated in Global InterOP meetings, awaiting completion of US/EU interoperability test device; programmatic focus on cooperative activities in FY 2017-18 in support of high power DC and wireless charging.
 - PEV testing; completed baseline testing of BMW i3 REx; shipped vehicle to Italy and participated in setup and initial testing
 - The joint ANL-JRC work plan was moved to Q1 FY 2017 when the US and European OEMs meet with both labs at the Global InterOP meeting at Argonne
 - Asia
 - Continued efforts to work with China in an attempt to harmonize PEV interoperability standards; participated in China EV100 Forum; met with MIIT and State Grid
 - Facilitated the Global Alignment Session of the APEC Roadmap for Electric Vehicles; Workshop 1 & 2 in Manila, Sept. 2016

Future Achievements

- Grid Integration
 - Enabling Technologies
 - Demonstrate CIP.io and IoT with the additional components of Smart Energy Plaza Ø2, i.e., EVSE, building systems, solar inverters, stationary battery storage, etc.; includes control algorithms to implement use-cases such as demand charge reduction, distributed energy resource (DER) integration, building islanding, and PEV charge management.
 - Demonstrate alpha prototype SCA in Smart Energy Plaza Ø2 and potentially field testing
 - Demonstrate 5th generation submeters (EUMD Rev 5), commercial submeter prototypes and accessories (e.g., user interface) in Smart Energy Plaza(s)
 - Demonstrate HIL with subset of components/systems in Smart Energy Plaza Ø2

- Testbeds
 - Complete Smart Energy Plaza Ø2 and integrate CIP.io
- Grid Modernization
 - Foundational Tasks
 - GMLC 1.2.2 - Interoperability; support gap analysis and roadmap development
 - GMLC 1.2.3 - Testing Network; technical descriptions of lab capabilities and links to models related to grid integration
 - GMLC 1.4.1 - Standards and Test Procedures for Interconnection and Interoperability; provide liaison to SAE interoperability standards development, identify gaps and opportunities to cooperate with other SDOs/committees to fill gaps in grid interface standards
 - GMLC 1.4.2 - Definitions, Standards and Test Procedures for Grid Services from Devices; develop test fixtures and conduct trial tests with protocols for EVs providing grid services
 - Program-Specific Tasks
 - GM0062 - Vehicle-to-Building Integration Pathway; communication and control use case implementation and testing (focus on behind-the-meter)
 - GM0085 - Systems Research Supporting Standards and Interoperability; coordinate use case implementation and control parameters at the energy service provider interface to define the interactions between grid domains (i.e., behind-the-meter versus public)
- Codes and Standards
 - Continue leadership of SAE J2953 (interoperability) committee
 - Initial publication of J2953/3 DC charging interoperability test cases is planned to be published in 2017.
 - New sections of J2953 are being added to address developments in SAE J2847/4 diagnostic fault identification and messaging.
 - Adaptive load management of AC EVSEs in a local and utility level context are being added to J2953 to respond to industry trends in evolving OCPP/other facility based optimization.
 - Continue leadership of NIST/NCWM Handbook 44-3.41 (commercial dispensing of electricity as a fuel),
 - Support procedure document development and validation (Examination Procedure Outline #30 (EPO30) and NCWM Publication 14 with new sections on primary/secondary examination checklists for National Type Evaluation Program (NTEP) certification of EV charging equipment meeting HB44-3.41
 - Validation testing of EPO30 and Pub14 procedures to support establishing a type evaluation certification that enables the HB44-3.14 requirement to be enforced for commercial transactions involving EV charging.
 - Contribute automotive perspective to IEEE P2030.7 (definition of microgrid controllers), which is expected to be published in late 2016/2017, specifically EV charging as a DER node within a microgrid/nanogrid.
- International Cooperation/Harmonization
 - Europe
 - Interoperability; Potential integration of high power and wireless charging in the scope of Global InterOP and the test facilities of Argonne and JRC, will be addressed in Q1 FY 2017 at the Argonne meeting.
 - Joint paper (ANL and JRC) comparing US and EU PEV test procedures, analysis and results
 - Joint work plan (ANL and JRC interoperability centers) for FY 2017-18
 - Asia
 - Continued discussions regarding implementation of the APEC Roadmap for Electric Vehicles
 - Further efforts to cooperate with China will depend on direction from DOE

V.3.B. Technical Discussion

Background

US and European interoperability centers were established in an agreement between the U.S. Department of Energy (DOE) and the European Commission's Joint Research Centre (JRC-E.C.), signed in November 2011, with the intent of harmonizing EV and battery test procedures as well as EV interoperability. The agreement stipulated the activities listed below; much progress has been made since then and the accomplishments/status of the ANL IOC prior to FY 2016 are shown in parentheses:

- Establish state-of-the-art facilities for development and testing of EV-grid interface technologies
Embedded controls lab and PEV-EVSE integration/test lab were fully operational; various types of EVSE, building systems and a solar system were installed in Smart Energy Plaza 01
- Play an active role in standardization
ANL staff were leading/participating in SAE, IEEE and NIST committees related to charging and communication
- Undertake projects to enhance interoperability
ANL staff had designed/developed proof-of-concept submeters, smart charge adaptor, the common integration platform and test tools to verify compliance with AC connectivity and interoperability standards
- Participate in inter-laboratory 'round-robin' testing
ANL and JRC-E.C. had hosted interoperability 'plugfests' for US and EU automotive and EVSE manufacturers; the plug-in hybrid reference vehicle had been acquired and Level 2 instrumentation was being specified and acquired.

The details of these and other technical accomplishments of the ANL IOC have been reported in the DOE VT Annual Merit Reviews, annual reports, publications and presentations.

Cooperation with the European interoperability center focused on support of the Global InterOP activity; Argonne provided specifics of the SAE AC interoperability requirements, test procedures and test equipment and JRC-E.C. focused on assessing candidate interoperability test equipment supplied by vendors.

Cooperation with Asia focused on next steps with APEC following adoption of the 'APEC EV Roadmap for Electric Vehicles' proposed by the US, which includes establishing an EV Interoperability and Research Center. Discussions over the past couple of years with China regarding joint activities that would facilitate harmonized interoperability standards were not successful.

Introduction

'EV-smart grid interoperability' is (ideally) the ability of any PEV and EVSE to connect and communicate with the infrastructure in a standard manner to enable 'smart' charging (or discharging as the case may be) as an integral element of a managed network of grid-connected devices.

Barriers/challenges to achieving universal interoperability and grid integration include:

- Enabling technologies and open source integration methodologies
 - Open source solutions for integrated communication and control of grid-connected devices
 - Low-cost sensing, communication and control components/integrated systems
 - Test tools to verify interoperability
- Compatible/harmonized standards across mobility, building and utility industries; independent, non-biased technical support for standards definition organizations (SDOs)

The Argonne IOC addresses these issues from a communication/control perspective; developing enabling technologies/methodologies, supporting the development and verification of codes & standards, facilitating harmonization with Europe and Asia, and providing the vehicle perspective in DOE's grid integration and modernization initiatives.

Approach

Grid Integration - Enabling Technologies

Common Integration Platform/IoT

A common integration platform enables communication between and coordinated control of networked devices/systems. The focus of the Argonne IOC is integrated control of EVSE, building systems and distributed energy resources to facilitate smart energy management. The functionality of the CIP, in addition to the hardware and general open source software approach, were described in the FY 2015 annual report; it is now referred to as CIP.io (pronounced sip-e-o).

CIP.io is a combination of open-source tools with specific tasks and purposes. The figure below illustrates the system architecture, which utilizes a global MQTT broker on the wide area network (WAN) bridged to local MQTT brokers on a local area network (LAN). The ability to bridge MQTT brokers allows system administrators to decide what information to keep on the local MQTT broker and what information to share with the global WAN MQTT broker. The global WAN MQTT broker is the gateway to individual building CIP.io platforms and the outside world. This allows other MQTT clients (HIL applications, smart-phone apps, etc.) to interact with the CIP.io platform from the internet via the standardized MQTT protocol. Other services subscribing to the global WAN MQTT broker include a historian database and visualization applications.

A key component of CIP.io is the analytics engine, which processes continuous streams of data in real-time to calculate rolling metrics, aggregate statistics, correlate events, analyze trends, support predictions, etc. The open-source Apache Storm analytics engine with built-in MQTT support is utilized in CIP.io and will be developed further in FY17.

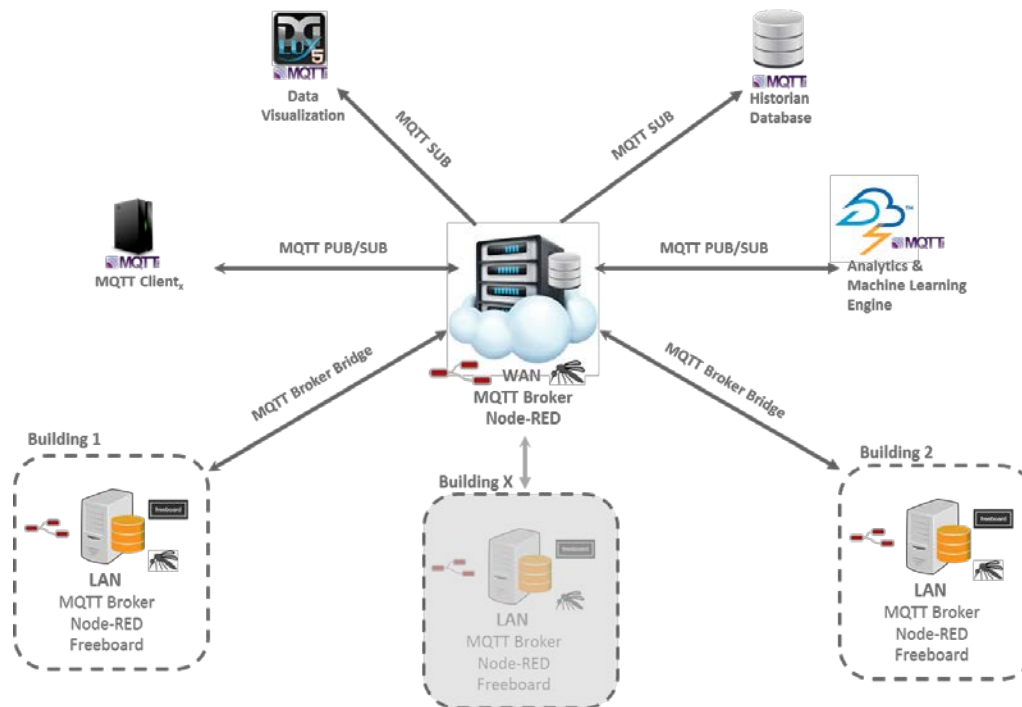


Figure V-9: Common Integration Platform/IoT System Architecture

A system controller is needed to provide local or global monitoring and control of devices and applications. At a local level, a system controller will interface with devices; reading sensors and controlling actuators, converting device protocols to MQTT and, vice-versa, interfacing with visualization applications and storage databases as shown in the following figure. At a global level, a system controller will interface with other web-based systems to aggregate data from diverse web-services.

CIP.io utilizes IBM's open-source Node-RED as a system controller. Node-RED is described as the "visual tool for wiring the Internet of Things". Within the Node-RED environment, nodes are wired together to create flows, these flows perform a specific task similar to the concept of agents in VOLTTRON (ref?). Node-RED allows

browser-based flow editing with real-time debugging and deployment options enabling rapid application development. Node-Red is built on Node.js, taking full advantage of its event-driven, non-blocking model. Node.js' package repository, npm, is the largest ecosystem of open-source libraries in the world. CIP.io utilizes the Node-Red Freeboard node for data visualization. Freeboard is a real-time customizable dashboard, enabling monitoring of devices and visualization of data.

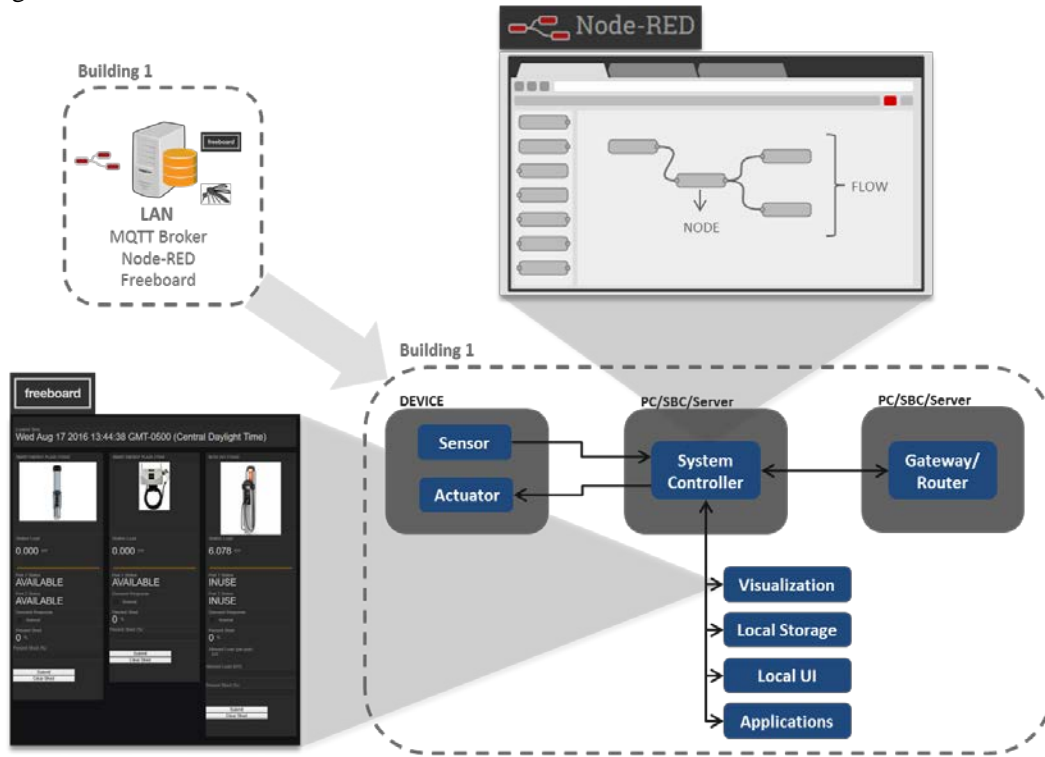


Figure V-10: Architecture for local control and monitoring of subsystems

Within the design of any IoT platform, security considerations are paramount. Every component and interface in CIP.io is a potential attack vector, therefore well-established and widely accepted security mechanisms such as encryption (SSL/TLS), authentication and authorization have been deployed. For example, each node-red web user-interface (UI) utilizes HTTPS for secure communication and authentication. For authentication and authorization, Node-RED users are provided with usernames and passwords with the potential for read/write access configuration. Each MQTT broker in CIP.io utilizes an SSL/TLS connection with authentication and authorization for each device/user. Access control lists are utilized to define what topics each user can publish and subscribe to. Security has been continuously considered and reexamined with continuing efforts focusing on data security, privacy, data integrity, and network security.

In FY16 ANL developed open source Node-Red nodes for CIP.io which includes:

- Nissan Leaf Carwings nodes - for monitoring the Nissan Leaf
- ChargePoint nodes - for monitoring and performing load control of ChargePoint stations
- MODBUS TCP nodes - for communicating with MODBUS TCP devices
- ComEd RRTP nodes - for obtaining Commonwealth Edison (Chicago area utility) Residential Real-Time Pricing (RRTP) information.
- Operating System (OS) nodes - for obtaining cpu system information.

Communication System Platform Architecture Study

As 'smart' networked devices are increasingly integrated into buildings, homes and public infrastructure, the need to monitor and communicate with these devices to enable system control, data analytics and visualization becomes paramount. This effort compared PNNL's VOLTTRON™ platform with ANL's IoT Common Integration Platform (CIP.io) approach; the purpose being to identify similarities and differences between the two platforms, as summarized in the table below.

Table V-2: VOLTTRON and CIP.io Comparison

Feature/Attribute	VOLTTRON	CIP.io
Programming Language	PYTHON	Node.js/Java Script
Message Bus	Information Exchange Bus	MQTT Broker
Message Bus Location	Local (same physical device)	Local or Global
Message Bus Protocol	Publish/Subscribe via ZeroMQ with custom VIP wrapper	Publish/Subscribe via TLS/SSL MQTT
Browser-based Message Bus Client	NO	YES
Applications	Agents	Nodes/Flows
Application Repository Management Interface	GitHub Web-based (VOLTTRON Central)	NPM/GitHub Web-based (Node-Red)
Browser-based Application Editing	NO	YES
Browser-based Application Debugging	NO	YES
Historian	YES	YES
Platform Device Scheduler	YES	NO
Dashboard/Data Visualization	Limited	Yes (Freeboard)
Encryption	YES	YES
Authentication & Authorization	YES	YES
Extensible	YES	YES
Open-source	YES	YES
Scalable	YES	YES
Rapid Application Development	NO	YES

Smart Charge Adaptor

The smart charge adaptor is a handheld, inline device that is connected between any charge station (EVSE) and plug-in electric vehicle (PEV). The SCA converts legacy non-networked AC L1 or L2 charge stations into smart, networked charge stations. The SCA is a plug ‘n play device that locks to the end of an existing SAE J1772 EVSE connector. The SCA enables submetering, access control, billing, charge scheduling, and load control. The SCA has a built in revenue accuracy interval meter, Wi-Fi communication, and the ability

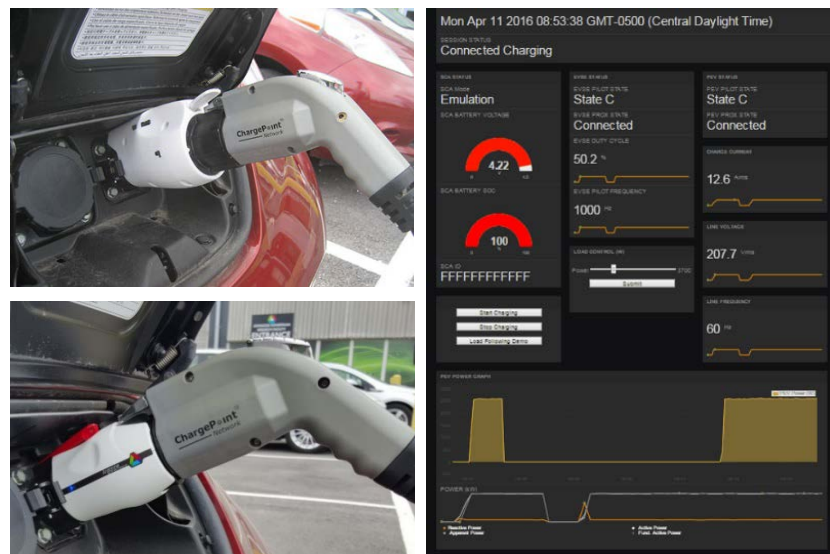


Figure V-11: Proof of Concept Smart Charge Adaptor

to stop, start, increase or decrease any charge session seamlessly. The SCA does not require a licensed electrician to install and is PEV/EVSE agnostic, working with any PEV-EVSE combination with standard connectors. The SCA can also be used with existing networked EVSE to allow choosing network providers.

A proof-of-concept (POC) SCA was manufactured and tested in the Smart Energy Plaza Ø1 (top left photo). Based on the success of this device to meter, monitor and control all EVSE in the plaza, an Alpha industrial design study was commissioned resulting in a mock-up that met design requirements (example screen shot shown on the right above). This design was used as the basis for an Alpha electronic design, shown in the lower left photo, which was finished and tested in Q4 FY 2016. Thirty (30) Alpha prototypes will be manufactured in FY 2017 for testing, validation and conducting pilot programs with partner utilities.

An application for a US patent was filed on November 21, 2014 and published on May 26, 2016 (14/549,758); a PCT application for international coverage was also filed.

Refined Submeters for Commercial Applications

Continuing R&D on lower cost/higher value per function submeters led to the fourth generation (EUMD Rev 4) design in FY 2015. Two iterations of Rev4 boards and enclosures were produced and tested at the start of FY 2016. EUMD Rev4 is based on the low-cost Maxim MAX71315 System-on-Chip metrology IC as well as related power, display, and communication subsystems, mounted in a reconfigurable package format. This flexible packaging is shown at right, configured to fit in the space of standard two-pole circuit breaker in a load center panel board; picking up voltage sensing/logic power from the circuit breaker power terminals. Single internal or multiple external current sensors are used to instrument the required number of loads measured in the panel board. The circuit breaker format (i.e., with no circuit protection functions, only metering) was developed to reduce installation time and interconnection steps. The meter supports an internal compact PCB shunt up to 60A and external Rogowski, DFGM and Hall type current sensors. Output data is provided via MODBUS RTU, along with isolated programmable contacts for switching on/off other controlled devices. Durability testing of the EUMD Rev4 module continued through FY 2016 for ~3000 hours on various real world cycling loads (dehumidifier, air conditioner, EVSE, etc.) without faults. However, due to supplier issues only a few EUMD Rev4 modules were fabricated and only lab testing was accomplished.



Figure V-12: Submeter

Argonne developed communication gateways to enable data from the submeter to MODBUS TCP via Ethernet or Wi-Fi and a GUI was created to display network connected data from the submeter via the gateway. The LabVIEW GUI, Wi-Fi and Ethernet gateways shown below were designed by ANL and implemented/produced under contract by 2G Engineering. The gateways are based on low cost, off-the-shelf Wi-Fi-Ethernet modules and application process for adapting one protocol to another. Devices are ~ 1"x 1.5" x .5"H and can be mounted external to the EUMD, inside the load center panel board live voltage environment.

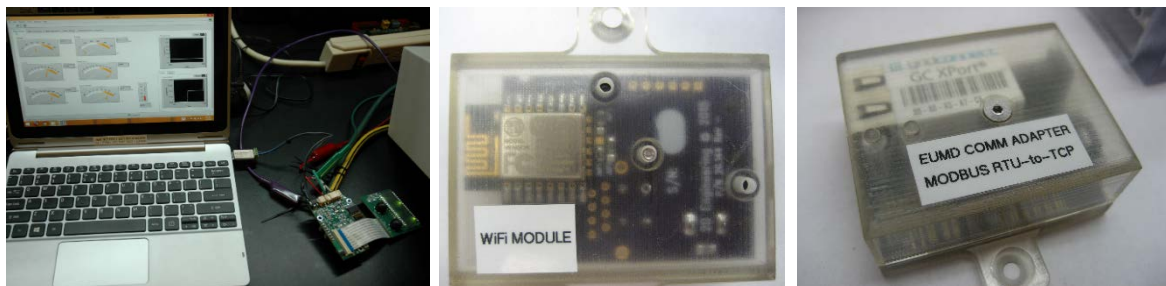


Figure V-13: Communications gateways

Applying the submeter technology to the NCWM/NIST HB44-3.41 standard activity (commercial dispensing of electricity) led to a proof-of-concept, low cost compact EUMD remote display module. Based on off-the-shelf components (e.g., \$5 TFT LCD display and \$10 IP-67 sealed enclosure), shown below, the module can display EV charging/meter information, including quantity of energy dispensed, cost per unit of energy, total transaction cost, state of the charging session, etc., similar to liquid fuel dispensing system displays. The enclosure is weather sealed and user inputs are via capacitive coupled touch pads. The display unit can be powered by the EUMD logic power source as well. The remote display has capabilities for various card reader inputs ranging from Near Field Communication (NFC) from smart phones to standard RFID badge readers.

As mentioned previously, the EUMD Rev4 was designed around the Maxim MAX71315 system on chip metrology IC. In 2016 Maxim sold the Teridian metering technology division to Silergy Inc., discontinued software development support and assured supply of components as Silergy retooled their own version of the MAX71315S. This necessitated the design of EUMD Rev 5 based on the Atmel SAM4C system on chip metrology IC - with far greater computing capabilities and polyphase inputs.

Argonne took advantage of the redesign to incorporate lessons learned from the four previous generations, resulting in a modular approach; separating out functions and employing a stacked configuration (single-three phase) for a more flexible, low cost submeter platform. The EUMD Rev 5 metrology IC board is shown in the figure below; this is the center of the stack, with the AC power/voltage/current sensor components on the (red) lower level board, and multi-input (yellow) metrology expansion board on top (with 3 input plus 16 branch circuits). The 1" monochrome organic light emitting diode (OLED) compact graphic display board (128x64 pixels) with capacitive touch buttons is shown on the right and fits on top of the packaged EUMD Rev5 submeter - only in applications requiring a graphic display/user inputs.

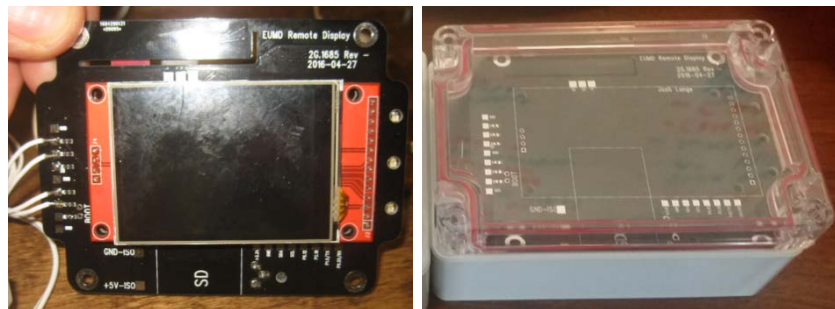


Figure V-14: EUMD Rev 5 metrology IC board

Multi-pin connectors on the top and bottom layer are for external current sensors (DFGM, Rogowski, Hall, etc.), MODBUS data connectors in the center, and 40A 'stake-on' power connectors on the lower board for direct on-board/meter current measurements (i.e. power flows through the meter board). Details are being developed on best practices for installing current sensors in real world installations as well as current sensor lead routing and termination on small pitch heads such as the kind used here



Figure V-15: Submeter data and power connectors

As described in previous reports, the ANL approach to sub-metering is based on a common metrology board (system/stack) capable of AC or DC measurements, which supports multiple current meter types and is configurable to multiple packaging options. The potential of the approach was recognized by the DOE

Building Technologies Office in an award for an FY 2016-17 commercialization project focused on building load submeters. The commercialization process will result in commercially available submeter products that are safety and accuracy certified, as well as open source (cloud based) user/data processing application software that seamlessly passes submeter information to the end user/application.

HB44-3.41 Test Fixture for Commercial Electric Fuel Dispensing

The test tool to measure electric fuel delivery in support of NCWM/NIST Handbook 44, section 3.41 (also called the 'Smart Load DAQ') was refined to include a certified meter data acquisition system and the ANL EUMD Rev 5 submeter. The data acquisition graphic user interface is powered by and communicates over USB port, using MODBUS RTU over USB. This revision also incorporates a MODBUS RTU daisy-chain communication connection to allow up to 128 Smart Load DAQ 20kW AC loads to be controlled by a single host/network connection, emulating up to 128 vehicles (with adequate external logic supply power).

The load current-regulating power converter was redesigned as well to eliminate expensive/bulky DC link electrolytic capacitors by using wide bandgap (SiC) power electronic devices and a switch mode converter topology running at 100 kHz+. The rear panel of the Smart Load DAQ allows for three additional 6kW off-the-shelf air cooled (~\$110) loads as slave devices, giving up to 24kW of AC load, controlled to the nearest watt commanded, in single watt increments.

This load control, MODBUS TCP/RTU command-controller input and certified meter enable use of the Smart Load DAQ as both a compliance testing tool and as a research tool to emulate several EVs charging simultaneously at EV charging stations. Test results can be printed on a metalized Mylar weatherproof label via a portable printer.



Figure V-16: HB44-3.41 Test Fixture

Grid Integration - Testbeds

Smart Energy Plaza Ø1

This network of EVSE, building systems and a solar array was described in the 2015 Annual Report; it was enhanced this year by incorporating the common integration platform (CIP.io), allowing tests of the communication/control system with use cases such as load shedding depending on the availability of solar power or time constraints for charging. This facility is used for development and testing of enabling technologies and PEV-EVSE interoperability testing.

Smart Energy Plaza Ø2

In support of its GREENLAB initiative, Argonne invested in renovating a facility that will substantially enhance the interoperability center's ability to support DOE's vehicle-grid integration and grid modernization objectives. Equipped with additional solar capacity, battery storage, high power charging, a range of AC/DC voltage supplies and isolation switching, the lab will enable studies as part of the lab's electric power grid or as a separate microgrid. Scheduled to be completed in Q1 FY 2017, the facility will be used for grid integration studies, e.g., the control requirements for and the grid impacts of high power DC charging (e.g., with and without battery buffering) or characterization of



Figure V-17: PEV-EVSE interoperability testbed

grid-connected devices to provide grid services (i.e., GMLC tasks), in addition to demonstrating enabling technologies intended for tech transfer.

Grid Modernization - GMLC Foundational Tasks

Interoperability - 1.2.2

The objective of this project is to establish a strategic vision of grid interoperability with implementation illustrations ... intended to provide context and direction to systematically integrate and measure the interoperability of various devices and systems that constitute the electric power grid and related end-use systems. This project looks across all grid technical areas to identify gaps, assess priorities and provide foundational principles relevant for all GMLC efforts requiring interoperability. This includes working with industry to articulate general interoperability requirements, methodology and tools.

Though the multi-lab task was proposed by PNNL in partnership with ANL, LBNL and NREL in FY 2015, the labs were not funded until Q3 FY 2016. The effort has focused on establishing basic principles utilizing the experience of the team members that participate in organizations such as the Smart Grid Interoperability Panel (SGIP), the GridWise Architecture Council (GWAC) as well as communication-related committees of SDOs such as IEEE and SAE.

The industry stakeholder meeting was held in September 2016 and included presentations by task participants regarding the mission, objectives and progress on defining guiding principles and methodologies as well as presentations by industry and association representatives that covered the stakeholders' perspectives and key elements of their approaches to pursuing interoperability. The meeting also included opportunities for industry to evaluate the team's progress and develop recommendations regarding priorities and the role of DOE/GMLC versus industry. An important result was that there are several industry associations that have the experience and willingness to help define strategies for promoting interoperability across the grid. Industry input is critical to the success and continuation of the task; DOE informed the GMLC tasks that FY 2017 funding would depend on Go-No Go decisions to be made in November, 2016.

All GMLC tasks produce quarterly reports, however the team's second report was not complete at the time of submission of this report.

GMLC Testing Network - 1.2.3

The principal goal of this activity is to accelerate grid modernization by (a) enabling access to the comprehensive testing infrastructure of the national laboratory system and (b) creating a repository of models and simulation tools. Since this task began mid-year, the effort has focused on understanding laboratory capabilities, establishing framework documents, assessing methods and tools used by other government activities and gathering industry stakeholder input. This task is supported by all the labs with grid device and systems testing capabilities that support DOE. Argonne's contributions will address testing resources related to PEVs and integration with EVSE, building systems, solar PV and storage as well as links to models/tools associated with embedded controls, control HIL and integrated communication/control systems.

The first industry stakeholder meeting was held in September 2016; the intent was to gain perspective on Testing Network goals, structure, and partnership mechanisms; the testing capabilities information matrix and the Open Library goals and structure. Industry stressed the importance of awareness, industry participation and efficient access to the databases/information. In addition, it was recommended that the team develop a clear strategy to maintain the resources and ensure that information is kept up-to-date.

Standards and Test Procedures for Interconnection and Interoperability - 1.4.1

The project's goal is to help develop and validate interconnection and interoperability standards for existing and new electrical generation, storage, and loads that ensure cross technology compatibility, harmonization of jurisdictional requirements, and ultimately enabling high deployment levels without compromising grid reliability, safety, or security. The objective is to develop an improved cycle of coordination that includes laboratory development and validation as well as working with industry through standards development organizations (SDOs) to accelerate the establishment and revision of standards and test procedures for grid connected devices and systems.

This is a multi-lab effort includes NREL, SNL, LBNL, PNNL, ORNL, INL and ANL, whose role it is to provide expertise on vehicles and grid integration as well as coordination with SAE, IEEE and ISO. The primary effort since the task began mid-year has been a gap analysis for each category of grid-connected devices, e.g., PEVs or solar PV. Lab participants summarized the status of the analysis by category at the first industry stakeholder meeting in September 2016; the task's second quarterly report has not been published at the time of submission of this report.

Definitions, Standards and Test Procedures for Grid Services from Devices - 1.4.2

This project’s goal is to enable and spur the deployment of distributed energy resource (DER) devices with the proven ability to provide the flexibility required for operating a clean and reliable power grid at reasonable cost. The project will define a standard set of grid services, and “drive cycles” that describe the capabilities that DERs must have to provide them. Specifically, the task intends to develop the device characterization protocol, develop and validate a model-based procedure to extrapolate a device’s ability to provide any grid service, utilize the model to project the value of grid services provided by a DER device and provide the validated models for integration into the planning and operational tools used by grid planners and operators so DERs can be valued based on measured performance.

Among the variety of devices and potential services provided, Argonne's has been assigned PEVs and capacity markets, respectively. Obviously, these are not exclusively linked, each lab to define the behavior and a sufficient set of parameters to characterize their assigned device as well as the characteristics of their assigned service; in terms adequate for grid planning. In the next phase of the task, the labs will test the devices to obtain the characterization parameters.

PEVs are essentially batteries with several important operating constraints from the grid perspective. They are the only potential DERs that 'roam', resulting in uncertainty regarding their location(s) and types(s) of grid connectivity over the course of a day. Compared to stationary batteries PEVs are unpredictable, must be considered as part of a fleet and statistically treated to estimate their potential contribution(s) to the grid.

The first industry stakeholder meeting was held in September 2016 and included 'poster sessions' describing the devices and services that could be provided. Argonne presented the conceptual characteristics and uncertainties associated with PEVs, but had not completed the PEV-grid model (in equation form) taking into account those uncertainties.

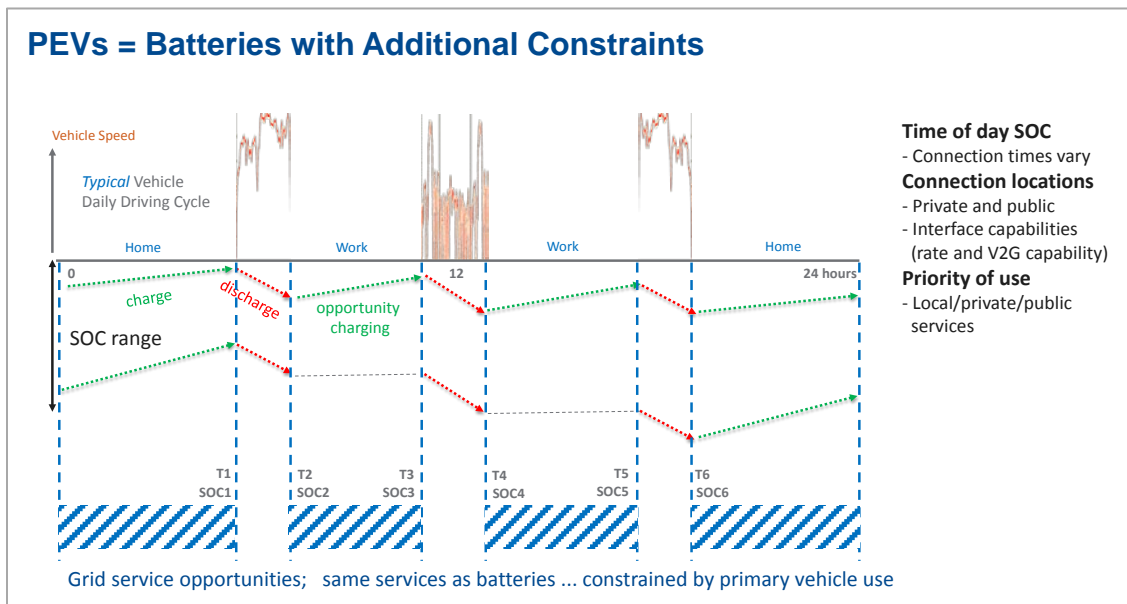


Figure V-18: PEV SOC and drive cycle profile

Grid Modernization - VT Program-Specific Tasks

Vehicle-to-Building Integration Pathway - GM0062

This project's goal is to demonstrate pre-normative methods needed to develop a standardized and interoperable communication pathway and control system architecture between PEVs, EVSE and Building/Campus Energy Management Systems (BEMSs) to enable the integration of clean variable renewable sources with workplace PEV charging infrastructure. The communication and control platform(s) employed will provide access to real-time system information, establish an infrastructure to manage energy consumption behind the meter and potentially participate in energy and/or ancillary services markets.

ANL, INL, LBNL, NREL, and PNNL will develop vehicle charging demonstration use cases, communication requirements, control requirements, communication architecture and testing processes needed to demonstrate coordinated PEV charging under time varying commercial building load conditions that minimize perturbations that could result in demand charges. Since inception of the task mid-year, the focus has been agreement on the initial use cases and communication requirements; the results are documented in a draft report led by Argonne that will be finalized in Q1 FY 2017.

Systems Research Supporting Standards and Interoperability - GM0085

The objective of the task is to understand the degree to which PEVs can provide grid services and mutually benefit the electric utilities, PEV owners, and auto manufacturers. The intent is to perform hardware-in-the-loop (HIL) studies that integrate communication and control system hardware with simulation and analysis activities. The effort will focus on integration of PEV fleets at the electric utility distribution level via a communication layer to provide grid services (i.e., on the grid side of the meter from a building/campus perspective).

Since the project began mid-year, the focus has been the same as that of GM0062, agreement on use cases and communication requirements ... the difference being that this task is focused on the grid side of the meter.

Codes and Standards

Argonne staff continued to provide their expertise and laboratory resources to support committees in several standards definition organizations (SDOs) that address connectivity and communication between plug-in vehicles, the charging infrastructure and the future grid with 'smart' control capabilities. The scope of these committees includes technologies and standards that cross the boundaries of vehicles, buildings and the electric power supply infrastructure. Activities in the past year included:

- Continued as chair of SAE J2953 (interoperability) committee, focusing on DC interoperability
- Continued as technical subcommittee Chair NIST HB44 Commercial Dispensing of Electricity as a Fuel - HB44-3.40 was adopted as tentative code January 1, 2016. California amended the tentative clause to allow their state to enact an HB44-3.40 equipment type evaluation program. ANL edited the draft Publication 14 checklist for NTEP national type approval that is now under review for adoption in 2017. Examination Procedure Outline 30 (EPO30) working document major content/revisions submitted by ANL as an iteration of the work in progress type evaluation and field inspection evaluation process. Pending CEC/CTEP support, field trials of this procedure (using ANL developed corresponding test tools, software and procedures) are expected in early 2017.
- Contributed to SAE committees; SAE J1772 (PEV charging coupler), SAE J2984 (PEV charging power quality), SAE J3068 (heavy duty 480vac coupler), SAE J2847/2 (PEV off-board DC communication), SAE J2847/6 (J2931/6) (wireless charging communication), SAE J2931/7 (cybersecurity of PEV-EVSE-network), SAE J3072-J2836/3-J2847/3 (utility interactive PEV requirements), SAE J2954 (wireless charging).
- Contributed test data and feedback to ANSI C63.30 (wireless charging safety-interoperability EMC field decay measurement procedure development and validation data on ANL wireless charging tests)

- Participated in the inaugural/kickoff meeting of a DC metering standards working group coordinated by the EMerge Alliance to fill a gap in definitions and requirements for revenue accuracy DC metering, and building oriented metered/managed DC loads.
- Coordinated with ISO/IEC/DIN standards committees on AC, DC and wireless charging communication
- Provided the automotive applications and AC/DC submetering perspectives at the bi-monthly P2030.7/P2030.8 (micro-grid controller definition/tests). IEEE P2030.7 is expected to be published in 2016. Joined the initial meeting of IEEE P2030.10 DC Microgrid standard.
- Established a working dialog with the IEC/IEEE P21451 IoT committee on virtual electronic data sheets for sensors/actuators in internet of things/Internet 3.0 context- as applicable to submeter communication and data exchange as a global standard.

International Cooperation

Europe

Efforts to cooperate and harmonize with Europe focused on the industry-led Global InterOP team and Joint Research Center.

Global InterOP - The primary activity of the team was definition of uses cases and interoperability requirements for AC and DC charging to support the German contractor, Scienlab, as they designed and built the prototype interoperability test device (funded by German resources).

Joint Research Center - JRC's new test facility for electric vehicles was launched in the summer of 2015, enabling joint testing to compare EV test procedures and recommend actions to achieve harmonization. A plug-in hybrid reference vehicle was extensively instrumented (described in FY 2016 annual report), tested in Argonne's Advanced Powertrain Research Facility in Q3 FY 2016, shipped to Italy and set up in the VELA-8 dynamometer facility in Q4. Testing is expected to be completed in Q2 FY17 and joint analysis will result in a joint report/publication by ANL and JRC.



Figure V-19: Research center test equipment

At the diplomatic level, the European Commission and DOE expanded cooperation in an agreement on the sidelines of the Clean Energy Ministerial in San Francisco in June 2016; in addition to the interoperability centers, many technologies in DOE's Energy Efficiency and Renewable Energy program were added.

Asia

The effort to establish cooperative programs in Asia has not consumed much resources this year; the budget for the International Cooperation task was eliminated in FY 2016. However, the US-proposed EV Roadmap for APEC (described in last year's report) was accepted and a workshop on implementing the plan was held at the APEC Automotive Dialogue meeting in Manila (Q4 FY 2016). Argonne presented the current status of cooperation with Europe and facilitated two sessions to identify potential areas of global alignment and specific approaches to harmonize charging, communication, regulations and standards.

Results

- Grid Integration
 - Enabling Technologies
 - The Common Integration Platform (CIP.io) and 'Internet of Things' (IoT) approach has successfully demonstrated its utility in integrating PEVs and other grid-connected devices in Smart Energy Plaza Ø1; it will be used to integrate communication and control of the devices in Smart Energy Plaza Ø2 in FY 2017.
 - Argonne's submeter/EUMD designs were recognized with a commercialization award by DOE's Building Technologies Office; focusing on building load management. Development

- will continue in parallel for applications to vehicles, the charging infrastructure and other grid-connected devices.
 - Refinement of the NIST HB44 electric fuel metering system for AC EVSE has led to development of a flexible research tool for vehicle emulation and data acquisition
 - Testbeds
 - Smart Energy Plaza Ø1 is complete with EVSE, simple building systems, solar power and the common integration platform (CIP.io); this capability will be used for acceptance testing of submeters/EUMDs and the alpha prototype SCAs prior to industry/field testing.
 - The construction of Smart Energy Plaza Ø2 will be completed in Q1 2017; integration of CIP.io will be completed in Q2/Q3 FY 2017 enabling grid integration studies that include high power charging, grid storage and microgrid/islanding capabilities for VT and GMLC.
- Grid Modernization
 - GMLC foundational tasks were launched, framework documents were developed, gaps identified in grid-level interoperability, standards and device characterization procedures. This provides the basis for general adoption of principles and the testing program necessary to characterize grid-connected devices and services.
 - VT program-specific tasks produced the use cases and communication requirements that will be the basis for grid system integration and communication/control studies necessary to implement integrated energy management on both sides of the energy service provider's meter.
- Codes and Standards

Chaired and directly supported committees/sub-committees related to sensing, communication and control that impact the technical direction of the grid integration studies as well as design and implementation of enabling technologies.
- International Cooperation/Harmonization
 - Europe
 - Interoperability; development of the use cases and requirements for AC and DC charging provided adequate information to develop the interoperability test device intended for both the US and EU; it will be evaluated at both interoperability centers in FY 2017.
 - PEV testing; The extensive instrumentation and testing at Argonne will enable in depth comparison of test procedures between the US and EC
 - Asia

Acceptance of the APEC Roadmap for Electric Vehicles will allow more specific discussions regarding partners, location(s) and an implementation plan for a cooperative EV Interoperability and Research Center in Asia

Conclusions

Argonne has developed enabling technologies and research facilities to support integration and testing of sensing, communication and control of grid-connected devices; key to accomplishing the objectives of grid integration and modernization as defined by VT and GMLC.

Argonne staff has continued to lead and/or make key contributions to the development and verification of codes and standards for plug-in vehicles and integration with future smart grid functionality.

Argonne is recognized for initiating and leading international cooperation regarding EV interoperability; the recent MoU that expanded the scope of cooperation between DOE and the European Commission is directly related to this success. It is expected to lead to meaningful interactions at the working level that enhance support of related USG initiatives in Europe.

V.3.C. Products**Presentations/Publications/Patents/Copyrights**

1. Bohn, Theodore, "A Real World Technology Testbed for Electric Vehicle Smart Charging Systems and PEV-EVSE Interoperability Evaluation", Paper#1461, IEEE Energy Conversion Conference and Expo, Milwaukee, WI, 22 September 2016
2. Bohn, Theodore, "Microgrid Related Distributed Energy Resource and Automotive Standards" (presentation), M-WERC Microgrids Conference, M-WERC Innovation Center, Milwaukee, WI 13 July 2016
3. Bohn, Theodore, "DC Fast Charger, Wireless Charging, Smart Grid Impacts and Communication Protocols" (presentation), IEEE Transportation Electrification Conference (ITEC), Dearborn, MI, 19 June 2016
4. Bohn, Theodore, "Taking Vehicle-to-Grid (V2G), Battery Storage and Grid-Aware Chargers from Theoretical to Real-World Deployment" (presentation), Electric and Hybrid Electric Vehicle Technology Conference, Novi, MI, 16 October 2015
5. Hardy, Keith, "US/EU EV-Smart Grid Interoperability Centers" (presentation), International Symposium - Towards a Transatlantic E-Mobility Market, Joint Research Centre, Ispra, IT, 28-29 October 2015
6. Hardy, Keith, "EV-Smart Grid Research & Interoperability Activities" (presentation), 2014 DOE Hydrogen Program and Vehicle Technologies Annual Merit Review, Washington, DC, 7 June 2016
7. Hardy, Keith, "Potential Alignment Areas" (presentation), APEC Roadmap for Electric Vehicles Workshop, Manila, Philippines, 20 September 2016
8. Hardy, Keith, "Integrating EVs, Buildings and Energy Infrastructure ... Can We Harmonize Without Global Standards?" (presentation), China EV-100 Forum, Beijing, China, 24 January 2016
9. J. D. Harper, D. Dobrzynski "PEV SMART CHARGE MODULE", Submitted US Patent November 2014, Argonne National Laboratory, 14/549,758.
10. J. D. Harper, D. Dobrzynski "PEV SMART CHARGE MODULE", Submitted International Patent (PCT) November 2015, Argonne National Laboratory, US/061150.
11. J. D. Harper "node-red-contrib-carwings", Copyright 2015, Argonne National Laboratory, SF-15-114.
12. J. D. Harper "node-red-contrib-chargepoint", Copyright 2015, Argonne National Laboratory, SF-15-115.
13. J. D. Harper "node-red-contrib-comed-rrtp", Copyright 2016, Argonne National Laboratory, SF-16-003.
14. J. D. Harper "node-red-contrib-modbustcp", Copyright 2016, Argonne National Laboratory, SF-16-004.
15. J. D. Harper "node-red-contrib-os", Copyright 2016, Argonne National Laboratory, SF-16-005.

VI. Vehicle Systems Efficiency Improvements

AERODYNAMIC DRAG REDUCTION

VI.1. DOE's Effort to Improve Heavy Vehicle Fuel Efficiency through Improved Aerodynamics

Kambiz Salari

Lawrence Livermore National Laboratory
7000 East Avenue, L-090
Livermore, CA 94551
Phone: (925) 424-4635
E-mail: salari1@llnl.gov

Lee Slezak, Manager Vehicle System

Vehicle Technologies Office
U.S. Department of Energy
Phone: (202) 586-2335
E-mail: Lee.Slezak@ee.doe.gov

VI.1.A. Abstract

There are roughly 2.2 million combination trucks on the road today, each traveling an average of 65,000 miles/year and consuming 12,800 gallons of fuel/year for a total of 36 billion gallons of fuel/year. These trucks consume roughly 11-12% of the total United States petroleum usage. At highway speeds, a class 8 tractor-trailer uses over 50% of the usable energy produced by the vehicle engine to overcome aerodynamic drag. To improve the fuel economy of these vehicles Lawrence Livermore National Laboratory (LLNL) has been conducting research in aerodynamics through use of add-on devices and new tractor-trailer shape design. LLNL has demonstrated new drag reduction techniques and concepts for tractor-trailers and tanker-trailers. A new body shape design is proposed for the next generation of highly aerodynamic heavy vehicles with geometry, flow, and thermal integration that radically reduces aerodynamic drag and improves fuel efficiency. This project relies extensively on computational simulations and wind tunnel testing for the development of the new integrated aerodynamic body design. For the selected aero devices and concepts additional track and on-the-road tests are performed. An important part of this effort is to join with industry in getting aerodynamic add-on devices on the road and to provide guidance to industry in design of the next generation of highly integrated heavy vehicles.

In collaboration with National Renewable Energy Laboratory (NREL) fuel saving benefits of platooning heavy vehicles are investigated through use of scaled wind tunnel testing. Results of wind tunnel tests will be validated by NREL conducting full-scale track tests. NREL has established a process for conducting accurate and objective track evaluations of platooning heavy vehicles.

Objectives

- Provide guidance to industry to improve fuel economy of class 8 tractor-trailer through the use of aerodynamics
- Develop innovative aerodynamic concepts for heavy vehicles that are operationally and economically sound
- Demonstrate the potential of new drag-reduction concepts and integrated shapes
- Design the next generation of an integrated highly aerodynamic tractor-trailers and tanker-trailers
- Establish a database of experimental, computational, and conceptual design information
- In collaboration with NEL investigate the potential fuel savings of platooning heavy trucks

- In collaboration with industry to promote the new proposed shape of the next generation of heavy vehicle and getting aerodynamic devices on the road
- On behalf of DOE to expand and coordinate industry participation to achieve significant on-the-road fuel economy improvement

Accomplishments

- Designed the second generation of an integrated tractor-trailer geometry from ground up that radically decreases aerodynamic drag and improves the fuel economy (GSF2)
 - GSF2 tractor design was completed with the aid of wind tunnel testing
 - GSF2 represents a breakthrough in aerodynamic performance
- Conducted 1/8th scale experiments at Army 7'x10' wind tunnel facility at Ames Research Center
- Evaluated the aerodynamic performance of integrated skirt and tail devices
 - Underbody flow investigation
- Developed aerodynamics fairings to improve fuel economy for tanker-trailers
- Compiled wind tunnel test results for the new tractor-trailer shape design GSF2 and modified tanker-trailer conducted at NASA Ames Research Facility operated by Army Research Development and Engineering Command
- Compiled wind tunnel test results for platooning of heavy vehicle with two and three vehicle configurations

VI.1.B. Technical Discussion

Development of the Second Generation of Generic SpeedForm Vehicle Geometry

A baseline geometry (Figure VI-1) was selected and its aerodynamic performance was measured through use of wind tunnel tests at the NASA Ames 7'x10' wind tunnel in collaboration with Navistar and the U.S. Army Research, Development and Engineering Command. The drag coefficient of the model is measured for range of yaw angles from ± 9 degrees, as shown in Figure VI-2. Two unique features of the baseline CD vs. yaw angle curve are that the minimum value of CD always occurs at 0° yaw and CD increases for larger yaw angle.

To improve the aerodynamics of the baseline model, we have developed a generic speedform heavy vehicle geometry. The first generation of generic speedform (GSF1) was tested in the 7'x10' wind tunnel in FY14 (Figure VI-3a). Unlike the baseline model, the CD vs. yaw angle curve for the GSF1 behaves quite differently (Figure VI-2). Not only is the aerodynamic drag less than that of the baseline model, but CD reaches a local maximum at 9 degrees yaw, beyond which it begins to decrease. This behavior is observed for configurations both with and without a trailer boattail. Given these initial results, we subsequently developed a second generation speedform, GSF2 (Figure VI-3b) by making in situ modifications to the clay model during our wind tunnel testing. The resulting GSF2 incorporates a more aggressive teardrop trailer shape, larger radii of curvature along the tractor A-pillars, a more pointed tractor nose, and a smoother hood-windshield transition. With these geometric changes, the CD vs. yaw angle curve decreases in magnitude even further (Figure VI-2), such that CD is 80% less than that of the baseline model at 0° yaw. In addition, a minimum drag coefficient no longer occurs at 0° yaw, as is the case for the baseline and GSF1 models, but rather at the largest yaw angles. And even more interestingly, CD transitions from being positive to negative for yaw angles greater than 17° . This remarkable phenomenon was first highlighted several years ago by Cooper [1], who referred to it as the "sailing effect," which is similar to that of a sailboat. For highly aerodynamic heavy vehicle geometries, such as the GSF2, the vehicle acts as a sail in the crosswind and generates a sizeable force perpendicular to the oncoming flow direction (Figure VI-4). When the vector component of this force in the body-axis direction becomes larger than the aerodynamic drag on the vehicle, a net forward force is generated, resulting in a negative drag coefficient. This "sailing effect" is observed on the GSF2 for configurations both with and without boattails (Figure VI-5). Given these significant improvements in aerodynamic drag, we are continuing to investigate further modifications to the GSF2 geometry and their implications upon the aerodynamic design of next-generation heavy vehicles



Figure VI-1: Baseline heavy vehicle model (1/8th scale) in the NASA Ames 7x10 wind tunnel

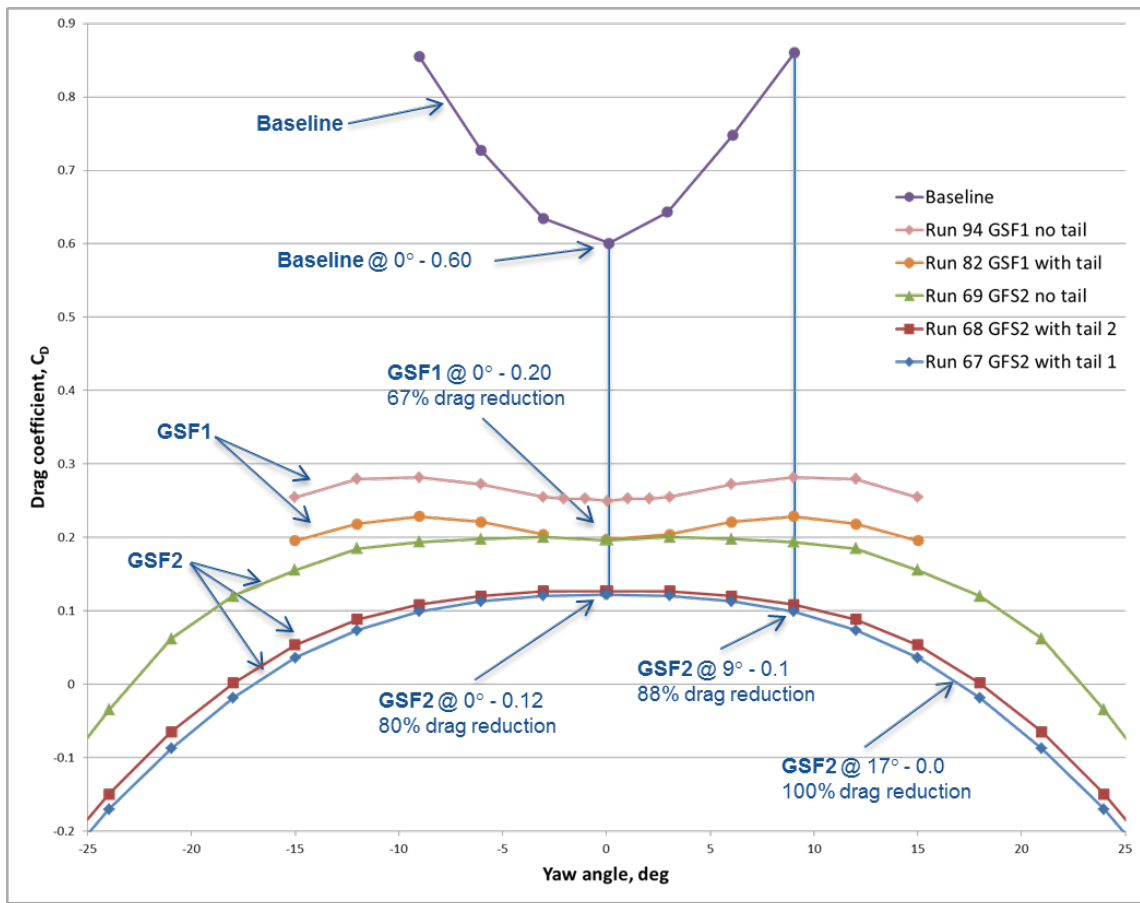


Figure VI-2: Drag coefficient as a function of yaw angle for the 1/8th scale models tested in the NASA Ames 7x10 wind tunnel

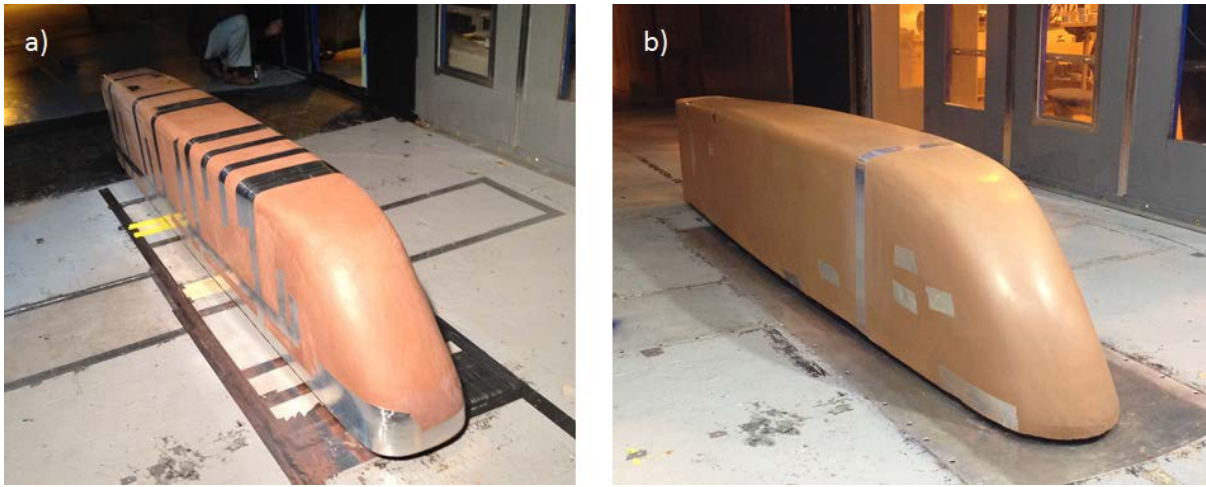


Figure VI-3: One-eighth scale models of the a) GSF1 and b) GSF2 in the NASA Ames 7x10 wind tunnel

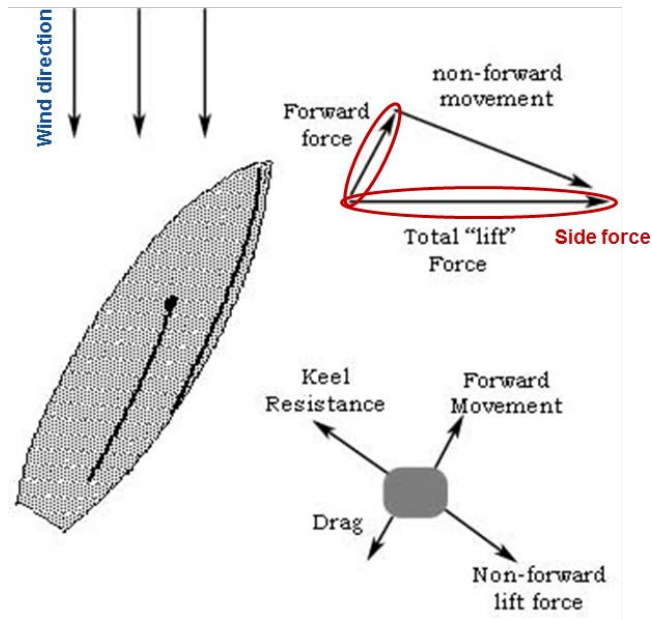


Figure VI-4: Force vector plot of the "sailing effect" exhibited by the GSF2 for large yaw angles

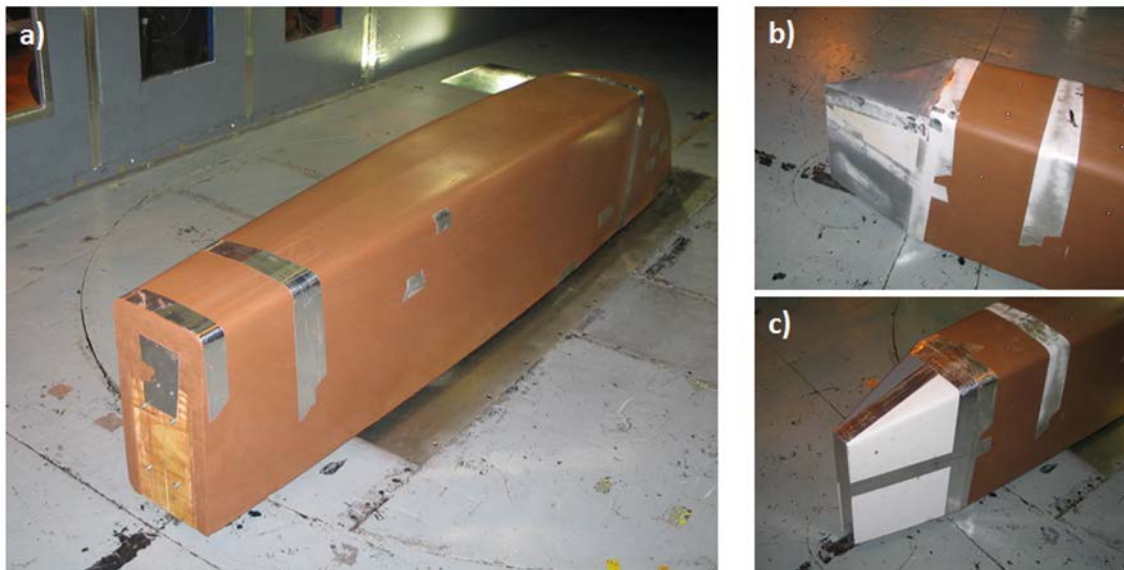


Figure VI-5: a) GSF2 heavy vehicle geometry with boattails b) 1 and c) 2

Flow Diagnostics: Particle Image Velocimetry Data Analysis

To gain a deeper understanding of the flow features in the heavy vehicle wake, an extensive, high-resolution 3D particle image velocimetry (PIV) dataset is obtained for the baseline heavy vehicle with and without a trailer boattail. We utilized a similar PIV approach for both a generic conventional heavy vehicle [2]. The experimental setup (Figure VI-6) for the PIV system is comprised of a horizontal laser sheet formed by two lasers located on each side of the wind tunnel. Two cameras are positioned above the lasers to image the region in the vehicle wake. A theatrical smoke system is used to seed the flow within the wind tunnel, thereby making the laser sheet visible to the cameras. Since the two cameras provide a stereoscopic view of the sheet, all three flow velocity components are acquired. From the PIV data, velocity field data is acquired, highlighting the changes in the wake structure when a trailer boattail is installed (Figure VI-7-Figure VI-8). This data will subsequently be used to computational fluid dynamics (CFD) code validation.

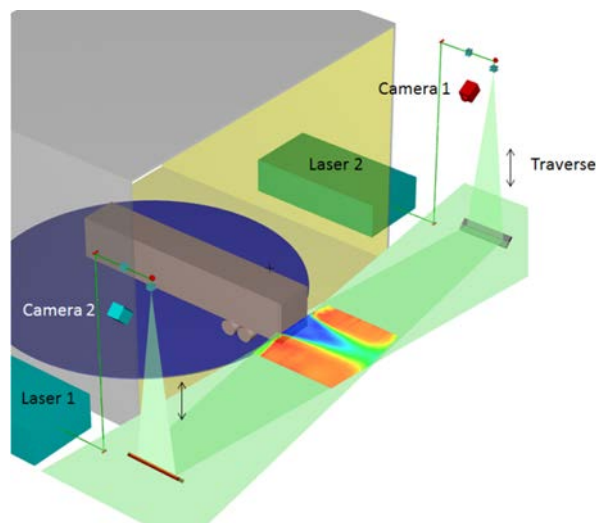


Figure VI-6: Experimental setup for the PIV system in the NASA Ames 7x10 wind tunnel

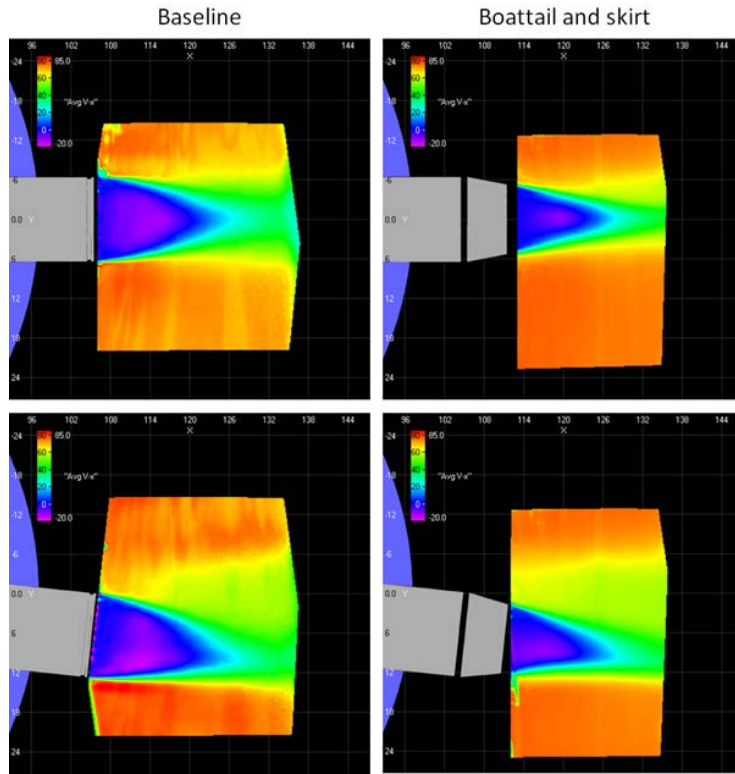


Figure VI-7: Time-averaged velocity magnitude at the mid-height of the trailer at 0 deg (top) and 6 deg (bottom) yaw

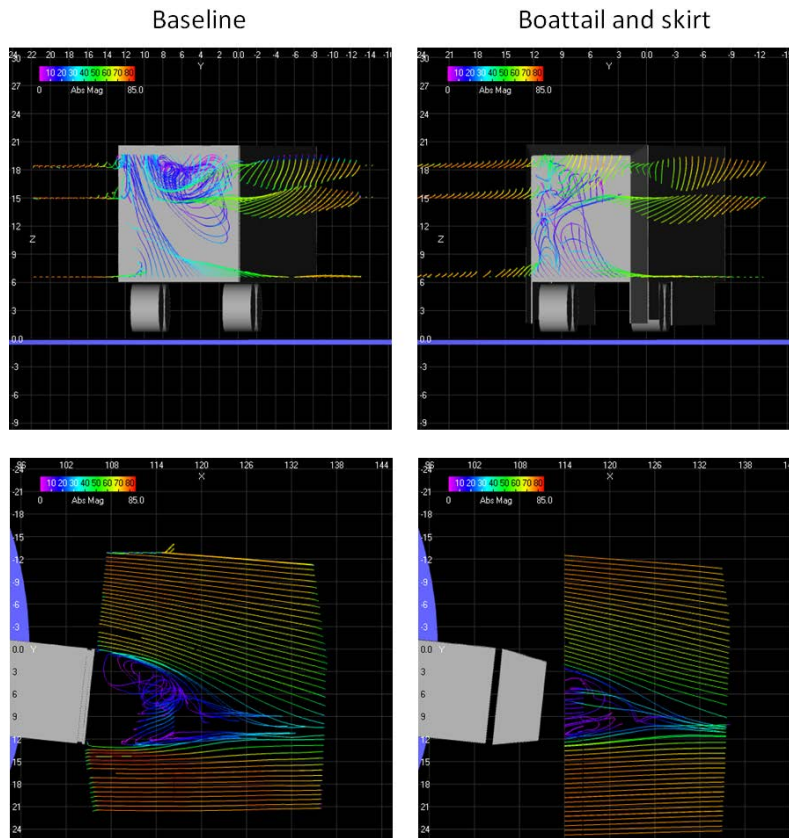


Figure VI-8: Time-averaged velocity streamlines in the trailer wake at 6° yaw

Flow Diagnostics: Thermal Imaging

In addition to PIV, thermal images are taken of the GSF1 and GSF2 using a FLIR SC8240 camera (3-5 μm wavelength sensitivity). With this level of sensitivity, it is possible to correlate very small changes in the model temperature to surface flow patterns. For example, Figure VI-9 shows fingering patterns on the nose of the GSF2 at two different yaw angles. These patterns highlight either defects in the surface geometry or laminar to turbulent transition of the boundary layer flow. Using this information, we can subsequently make modifications to the model surface in order to improve the flow quality and reduce the aerodynamic drag.

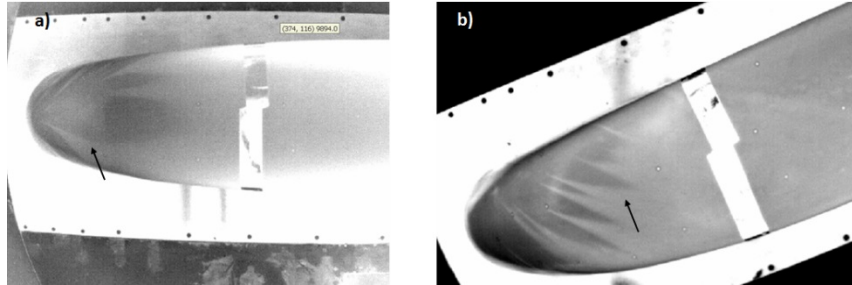


Figure VI-9: Thermal images of the GSF2. The arrows indicate fingering patterns on the model nose at two different yaw angles

Platooning Heavy Vehicles

This project has also been tasked with looking into the aerodynamic benefits of platooning heavy vehicles. Previous studies have shown that a platoon of heavy vehicles results in a decrease in the average drag coefficient across the individual vehicles in the platoon [3-6]. However, the close spacing between the vehicles reduces the amount of cooling flow provided to the radiator of the following vehicle, thus requiring the engine fan to operate. This, in turn, reduces the engine fuel efficiency. To better understand the impact of vehicle spacing upon both the average drag coefficient and the engine cooling flow, a wind tunnel study was conducted at NASA Ames on 1/50th scale heavy vehicle models. The platooning models are mounted on a splitter plate and the aerodynamic drag force on the individual models is measured with an internal load cell (Figure VI-10). The splitter plate positions the platoon above the tunnel floor, thereby reducing the boundary layer thickness in the vicinity of the model platoon. Each vehicle is mounted on a linear bearing that is attached to a load-cell (Figure VI-11). The amount of cooling flow provided to the engine is estimated by means of a pressure port mounted on the grill of each model (Figure VI-12).

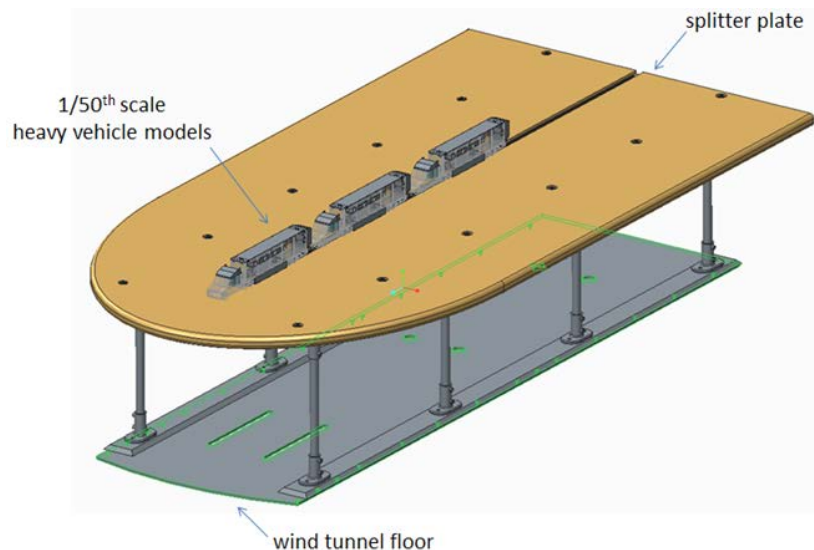


Figure VI-10: Model heavy vehicle platoon (1/50th scale) and splitter plate design

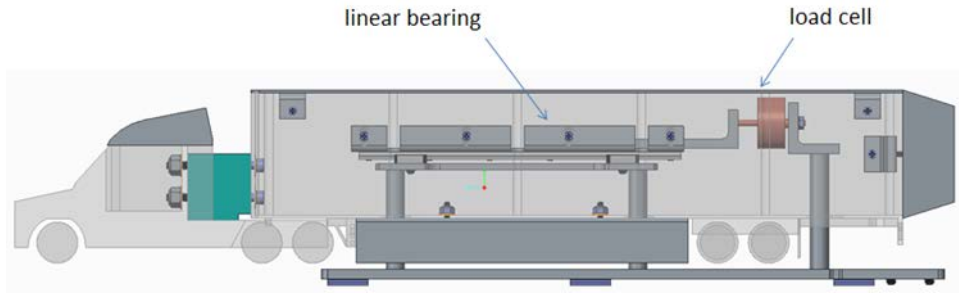


Figure VI-11: Internal details of the 1/50th scale platoon model.

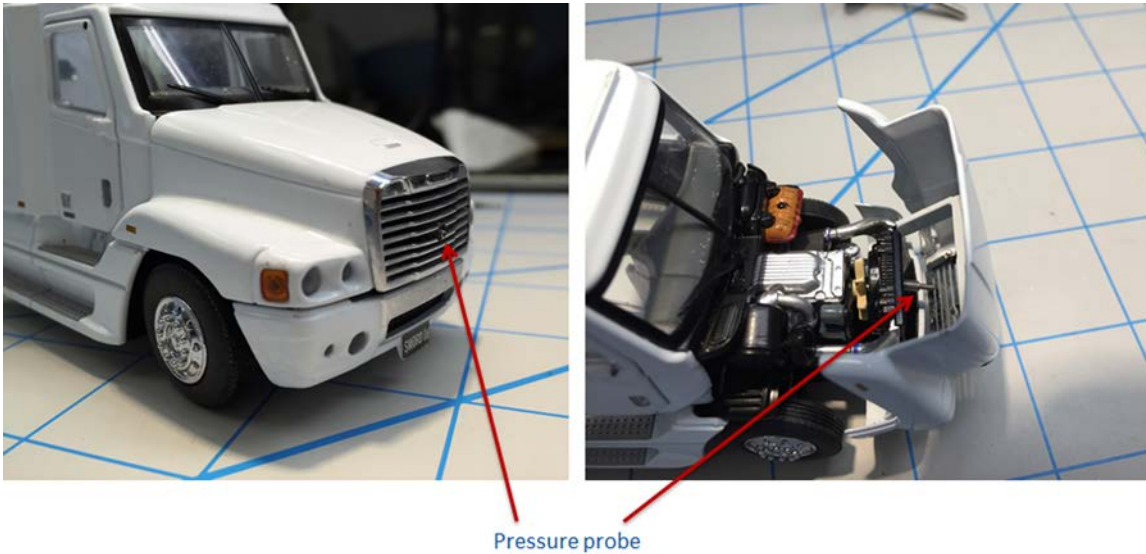


Figure VI-12: Pressure probe installed on the engine grill of the platooning heavy vehicle models.

For the two-vehicle platoon (Figure VI-13), the most remarkable observation is that the wind-averaged drag coefficient of the trailing vehicle does not show a substantial increase as the spacing increases from 20' to 120'. In addition, the pressure coefficient on the trailing tractor grill asymptotes to a value of about 0.65. The three-vehicle platoons both showed similar trends for the cases in which the spacing between the lead and middle vehicles is set to 20' and 30' (Figure VI-13-Figure VI-14). For both cases, the trailing vehicle has the lowest drag at a spacing of 5' (Figure VI-14-Figure VI-15). However, as the spacing between the middle and trailing vehicles is increased, the middle vehicle experiences the lowest drag. In the next wind tunnel test (October 2016), the aerodynamics of these platoons will be investigated for spacings up to 250', thereby allowing us to determine if these trends continue to persist.

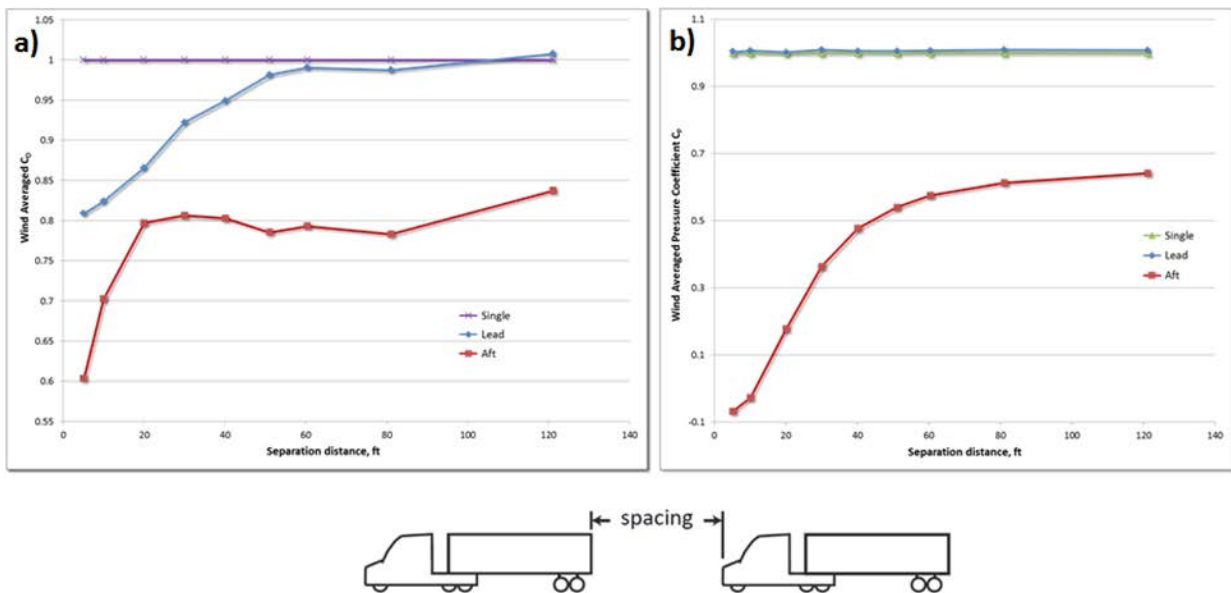


Figure VI-13: Wind-averaged a) drag and b) pressure coefficient as a function of vehicle spacing for the two-vehicle platoon.

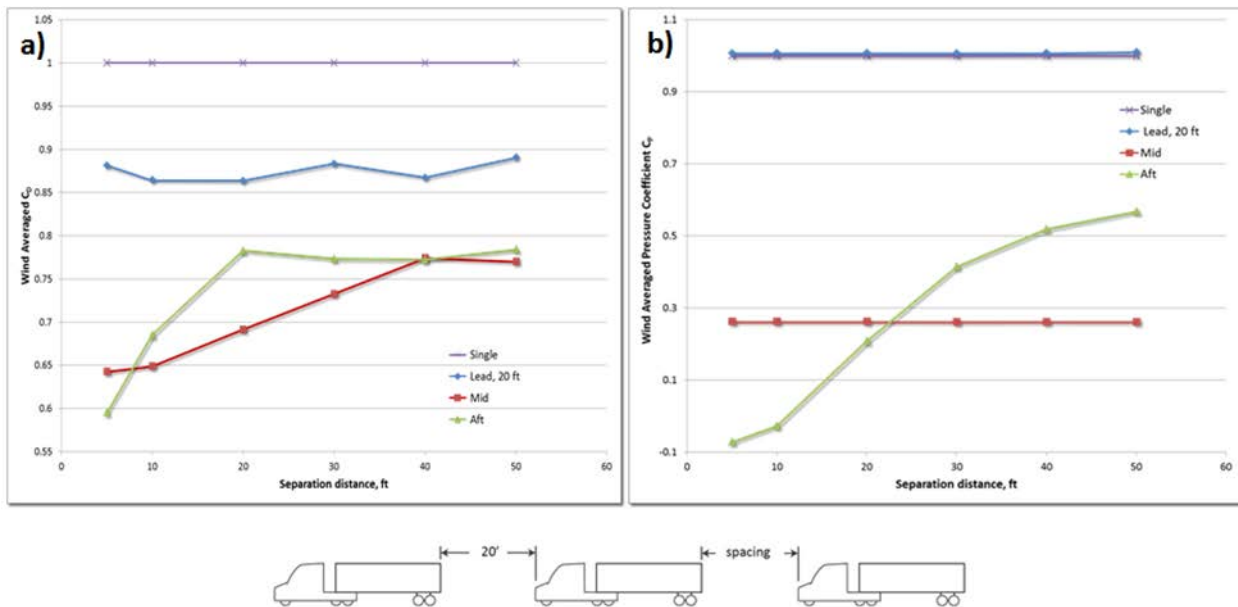


Figure VI-14: Wind-averaged a) drag and b) pressure coefficient as a function of vehicle spacing for the three-vehicle platoon with a lead and middle vehicle spacing of 20'

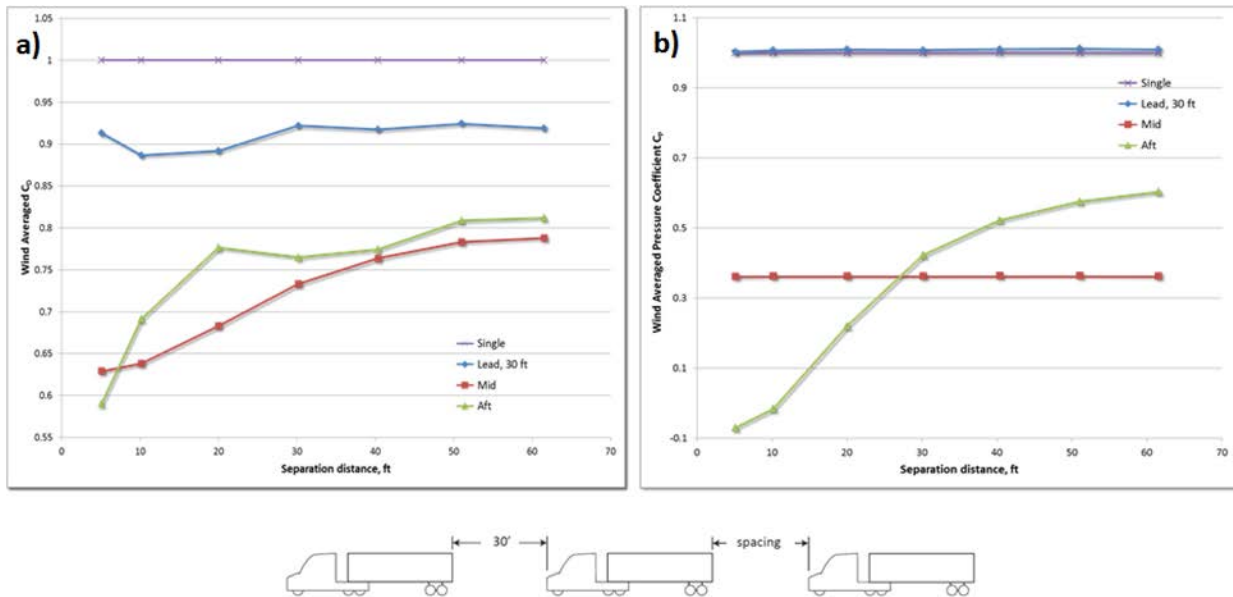


Figure VI-15: Wind-averaged a) drag and b) pressure coefficient as a function of vehicle spacing for the three-vehicle platoon with a lead and middle vehicle spacing of 30'

VI.1.C. References

1. Cooper, K.R. Truck Aerodynamics Reborn—Lessons from the Past. SAE Technical Paper Series 2003-01-3376, 2003.
2. Heineck, J.T., Walker, S.M., Satran, D. The Measurement of Wake and Gap Flows of the Generic Conventional Truck Model (GCM) Using Three-Component PIV. In McCallen, R., Browand, F., Ross, J. (Eds.) The Aerodynamics of Heavy Vehicles: Trucks, Buses, and Trains, Lecture Notes in Applied and Computational Mechanics, Vol. 19, 2004.
3. Lammert M., Duran, A., Diez, J., Burton, K. et al. Effect of Platooning on Fuel Consumption of Class 8 Vehicles over a Range of Speeds, Following Distances, and Mass. SAE Int. J. Commer. Veh. 7(2):2014, doi:10.4271/2014-01-2438.
4. Browand, F., Zabat, M., Tokumaru, P. Aerodynamic Benefits from Close-Following. In Ioannou, P.A. (Ed.) Automated Highway Systems, 1997.
5. Shladover, S.E., et al. Demonstration of Automated Heavy-Duty Vehicles, California PATH Research Report UCB-ITS-PRR-2005-23, 2005.
6. Browand, F., Radovich, C., Boivin, M. Fuel Savings by Means of Flaps Attached to the Base of a Trailer: Field Test Results, SAE Paper 2005-01-1016, 2005.

VI.2. Line Haul Truck Platooning

Kenneth Kelly and Michael Lammert

National Renewable Energy Laboratory
15013 Denver West Parkway, MS 1633
Golden, CO 80401
Phone: (303) 275-4465
E-mail: Kenneth.Kelly@nrel.gov

David Anderson and Lee Slezak

Phone: (202) 287-5688 (David Anderson)
E-mail: David.Anderson@ee.doe.gov
Phone: (202) 586-2335 (Lee Slezak)
E-mail: Lee.Slezak@ee.doe.gov

Start Date: October 1, 2015
End Date: September 30, 2018

VI.2.A. Abstract

Objectives

The primary objective of the test track and fleet evaluation portion of this Vehicle Systems Efficiency Improvements project is to corroborate, at full scale, wind tunnel and computational fluid dynamics (CFD) findings from Lawrence Livermore National Laboratory (LLNL) and evaluate the performance of platooned tractor trailers in real-world conditions. This project provides unbiased heavy-duty (HD) platooning test results and detailed analysis to industry, fleets, government agencies, and the research community. Data, analysis, and reports are shared with DOE, national lab partners, and industry to:

- Help define intelligent usage of platooning technology
- Guide R&D for platooning development.

Due to budget constraints, the planned platooning track testing by Intertek did not occur this year, but NREL was able to partner with Auburn University and others to obtain new track test data that was used to corroborate the LLNL wind tunnel findings, evaluate the performance of platooned tractor trailers in real-world conditions, and provide unbiased heavy-duty platooning test results and detailed analysis to industry, fleets, government agencies, and the research community.

Platooning technology is an early application and supports development of autonomous vehicle technology. Truck platooning is gaining significant attention from industry with public investments in the technology by Volvo, UPS, Nokia, Intel, and Lockheed Martin. However, all the variables impacting possible fuel savings, from following distances and the number of vehicles in platoon to the impact of fleet logistics on the percent of miles that can be platooned, remain unknown. In FY14, the National Renewable Energy Laboratory (NREL) showed that the technology has the potential to reduce fuel use by 3%–6% (tandem average), with analysis indicating a potential opportunity to further optimize system performance.

Accomplishments

- Evaluated data from three independent sets of Society of Automotive Engineers (SAE) J1321 test procedures for full-vehicle fuel consumption testing in comparison to LLNL wind tunnel testing
- Compared Denso CFD analysis to LLNL wind tunnel test results
- Analyzed NOx emissions from 2014 and 2015 SAE J1321 platooning test data sets
- Cooperated with the Volpe National Transportation Center to analyze possible naturalistic "background platooning" effects

- Co-authored platooning poster, titled "Class 8 Tractor Trailer Platooning: Effects, Impacts, and Improvements," with LLNL and presented testing/analysis results and discussed future plans at the Transportation Research Board Automated Vehicle Symposium in July 2016
- Furthered relationship with Auburn University and the Federal Highway Administration by exploring joint track testing options and initializing preliminary planning for joint track testing.

Future Achievements

- Coordinate with LLNL by providing input on experimental design based on vehicle track tests and past wind tunnel results for second round of wind tunnel testing at LLNL, planned for October 2016
- Collaborate with Auburn University to incorporate direct aerodynamic study into track testing (truck-mounted anemometer, pressure transducers, smoke trails, etc.) to confirm LLNL wind tunnel and CFD findings
- Publish technical report on findings to date.

VI.2.B. Technical Discussion

Background

Vehicle automation is a promising petroleum-reduction technology. Platooning systems for heavy-duty line-haul trucks are likely to be an early commercial application of vehicle automation technology. These systems may employ existing technologies such as radar or laser range finders, global positioning system (GPS) equipment, dedicated vehicle-to-vehicle communications, and braking and engine torque authority to enable vehicles to follow safely in close proximity at highway speeds, with the goal of reducing fuel consumption through improved aerodynamics as well as reducing traffic congestion and possibly collisions. Figure VI-16 illustrates how platooning is intended to make two trucks function more like one object in terms of airflow, resulting in reduced turbulence behind the lead truck and reduced fore-body drag on the trailing truck.

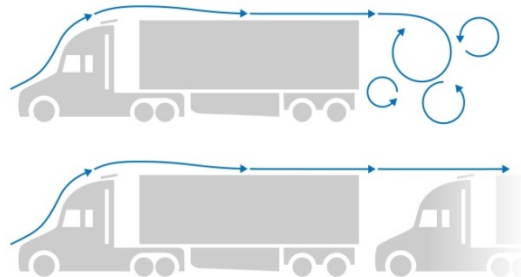


Figure VI-16: Truck platooning air flow

Image: NREL

In FY14, NREL teamed with Intertek and Peloton to evaluate the fuel efficiency of line-haul trucks operated in platooned pairs under controlled track testing. The first round of track testing of the Peloton system was completed in March 2014. The technology showed potential for improving fuel use by 3%–6% (tandem average). Figure VI-17 shows the actual FY14 test vehicles in platoon formation.



Figure VI-17: Trucks in platoon formation during testing

Image: Peloton (NREL 31237)

Introduction

Under this activity, NREL focuses on improving the performance of full-scale platooning of long-haul tractor trailers using both track testing and in-service evaluations in collaboration with LLNL wind tunnel testing and CFD modelling, as called for in DOE Vehicle Technologies Office's "Vehicle Systems Efficiency Improvements" funding (2015 Lab Call - Topic 9D). This activity supports DOE's mission to improve our nation's energy security and support the U.S. economy while providing valuable data and information to DOE research partners. Long-haul commercial vehicles are a critical part of the United States' trade, commerce, and economic growth. The DOE Vehicle Technologies Office capability matrix lists "technology impact on fuel efficiency analysis" as an "enabling capability" provided by NREL.

Approach

NREL has developed a process for conducting accurate and objective track evaluations of tractor-trailer platooning as well as a long-standing method for testing advanced and conventional vehicle technologies in commercial use. The NREL process started with SAE J1321 Type II fuel consumption test procedures modified to meet the requirement of multi-vehicle platooning tests, gravimetric fuel consumption measurement procedures, drivers aid for following speed traces, and 5 Hz engine controller area network (CAN) and vehicle GPS data logging [2].

This DOE-funded research project intends to develop technologies that improve platooning systems' fuel savings through better understanding of the dynamic interactions of the aerodynamics of platooned vehicles in real-world driving conditions. Under the full-scale platooning portion of this project, NREL was to coordinate with Intertek to conduct additional track testing to validate and help guide future LLNL wind tunnel tests on operating envelope parameters and possible aerodynamic devices to improve platooned aerodynamics and/or address the cooling needs of following vehicles. Funding constraints for the testing partner, Intertek, prevented the planned platooning track testing in 2016. However, NREL partnered with Auburn University and others, providing data loggers to obtain additional track test data used to corroborate the LLNL wind tunnel findings. This additional data was also used to further evaluate the performance of platooned tractor trailers in real-world conditions and provide unbiased HD platooning test results. In addition, NREL is leveraging existing published studies and data for meta-analysis to increase understanding of the dynamic interactions between platooning vehicles that impact fuel consumption. This project is intended to answer questions raised from the results from NREL's series of 10 modified SAE Type II J1321 fuel consumption track tests performed in FY14 to document the fuel consumption of two platooned vehicles and a control vehicle at varying steady-state speeds, following distances, and gross vehicle weights [2].

Results

Under the DOE Vehicle Systems Efficiency Improvements project, a collaborative partnership was created between NREL and LLNL to increase understanding of the aerodynamic envelope governing truck platooning and to investigate some of the questions pertaining to close following conditions, long following distances, alignment sensitivity, and three-truck platoons raised from NREL's first round of platooning track tests.

In 2016, NREL conducted an analysis based on five independent platooning studies, including:

- SAE J1321 road testing conducted in 2013 in Utah (North American Council for Freight Efficiency) [1]
- SAE J1321 track testing conducted in 2014 in Uvalde, Texas (NREL) [2]
- SAE J1321 track testing conducted in 2015 in Ohio (Auburn University, Transportation Research Center)
- 1/50th-scale wind tunnel testing conducted in 2015 (LLNL)
- Denso CFD modeling (results presented in 2015 to 21st Century Truck Partnership)

Significant agreement was observed pertaining to the trends and magnitude of fuel savings between track testing and wind tunnel testing as well as from the Denso CFD modeling. Both of NREL's most significant findings from the 2014 test results were corroborated, including:

1. The following vehicle experiences a fuel savings benefit at longer distances than anticipate
2. The following vehicle experiences a reduction in fuel savings at distances closer than 50 ft.

Figure VI-18 shows a comparison of track, road, and wind tunnel tests and the general trend agreement. Figure VI-19 shows the decreased savings for the rear vehicle only.

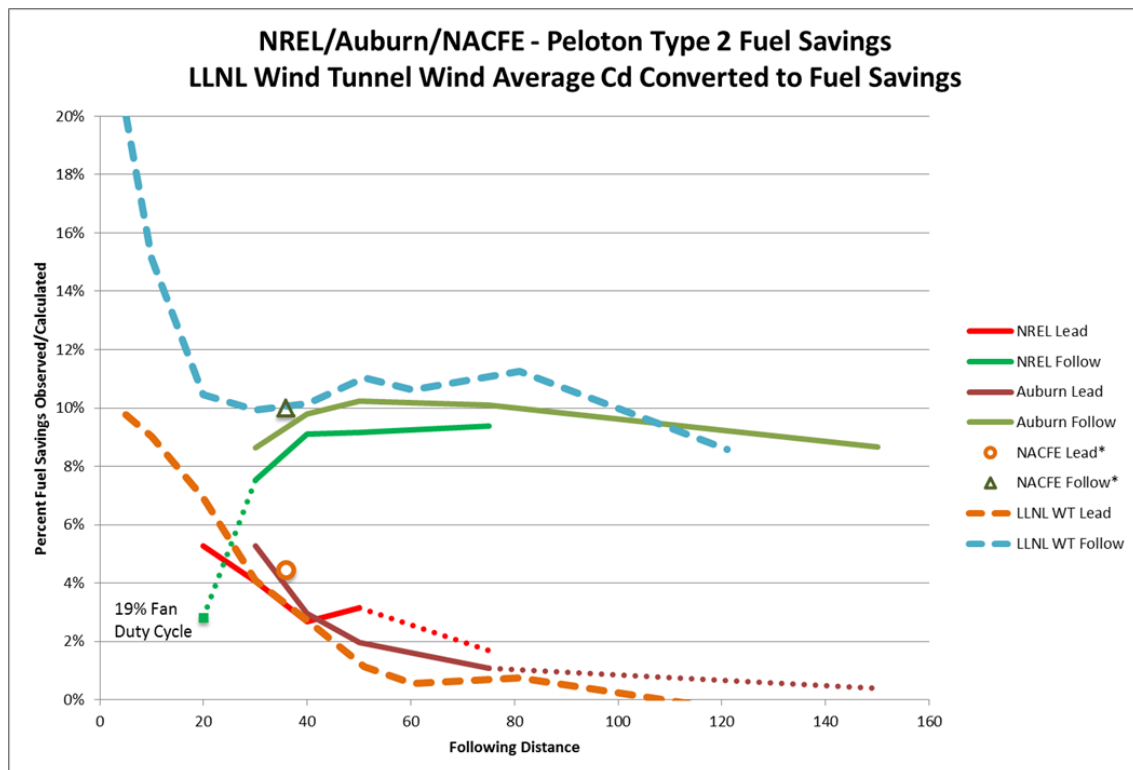


Figure VI-18: Platooning evaluations comparison

Image: NREL

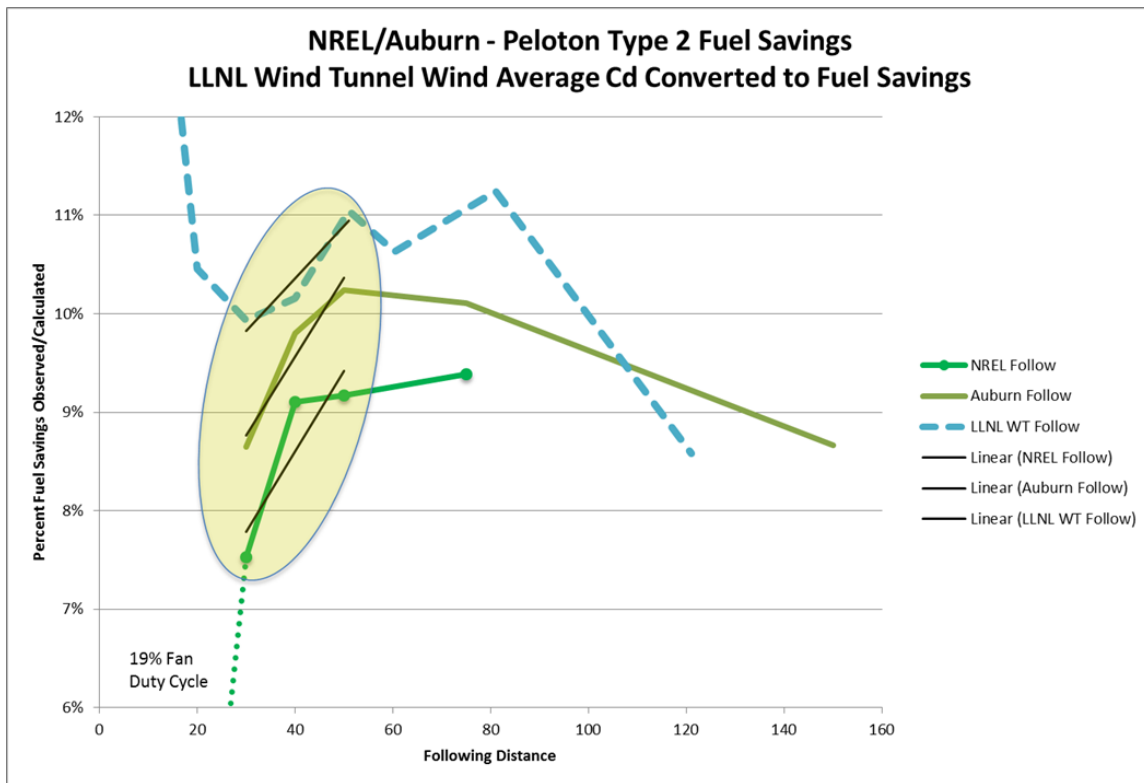


Figure VI-19: Platooning evaluations comparison of savings decrease for rear vehicle from 50' to 30' - Image: NREL

In wind tunnel testing, the wind average stagnation pressure (from flow through radiator-positioned pressure probes) matches well with Denso CFD results of radiator flow during platooning, including the downward bend in fuel savings observed at the 50-foot following distance (see Figure VI-19). The following vehicle experiences a reduction in airflow and pressure at the radiator with a degradation curve similar to the downward trend in fuel savings for the following vehicle (bend in curve at 40–50 feet). Figure VI-20 shows the correlated data from CFD and wind tunnel testing. It is important to note that current testing shows engine cooling packages are adequate at all distances, except at very close following distances. Alternative engine cooling strategies are being developed by industry suppliers such as Denso, while aerodynamic options to feed cooling package are being investigated by NREL/LLNL.

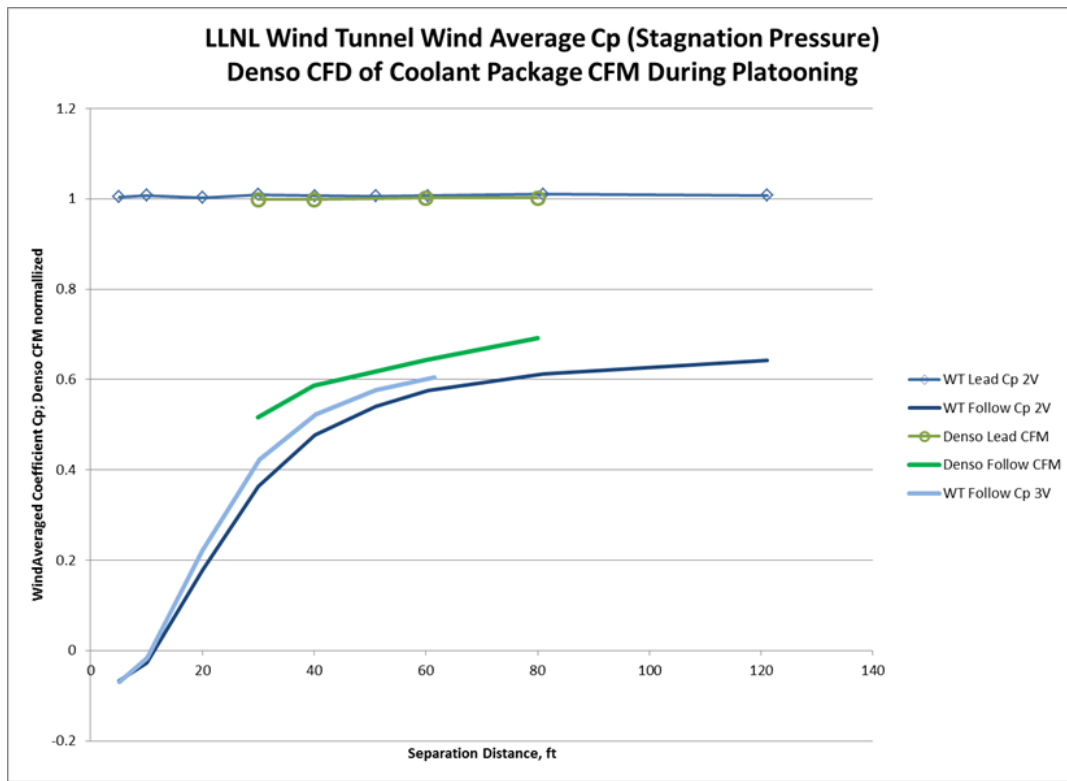


Figure VI-20: Platooning evaluations comparison - Image: NREL

During the 2014 NREL track testing, an increase in NOx emissions for the following vehicle in platoon formation was measured. Engine temperatures (intake air, coolant, and exhaust) and engine map explanations were investigated, but ultimately ruled out as the likely cause. However, NREL showed that the platooning system frequency and amplitude of commanded engine torque correlated with the magnitude of NOx increase. This torque command “dither” rate was discussed with Peloton as a suspected cause of the NOx increase. During the subsequent 2015 testing by Auburn University, NREL installed data-logging devices to observe NOx emissions (and other data) and found:

- Control dither rate was significantly reduced
- Measured raw grams of NOx was lower for the platooned vehicles compared to the baseline vehicles
- Measured brake-specific NOx emissions were lower in the platooned vehicles than in the baseline vehicles at following distances of 50 ft. and 75 ft., while slightly higher at 30 ft. and 40 ft., but greatly reduced from the 2014 test results.

Figure VI-21 shows the increase in total NOx from the 2014 tests and the reduction from the 2015 tests. Figure VI-22 shows the increase in brake-specific NOx from the 2014 tests compared to the results from 2015 testing. Figure VI-23 shows that the torque control dither rate during 2014 testing increased at shorter following distances, which roughly correlates with the increase in brake-specific NOx and the fairly constant and lower dither rates measured during 2015 testing.

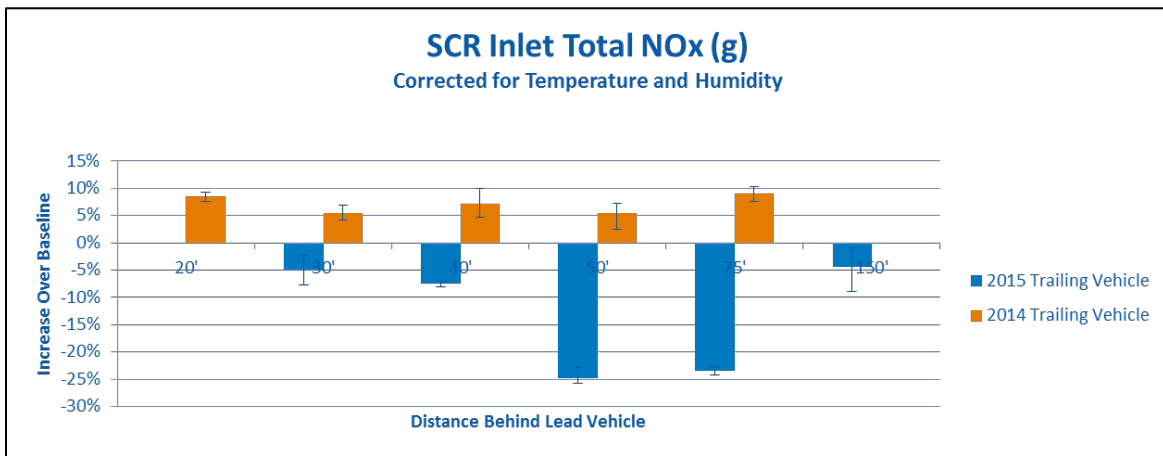


Figure VI-21: Selective Catalytic Reduction (SCR) inlet total NOx comparison

Image: NREL

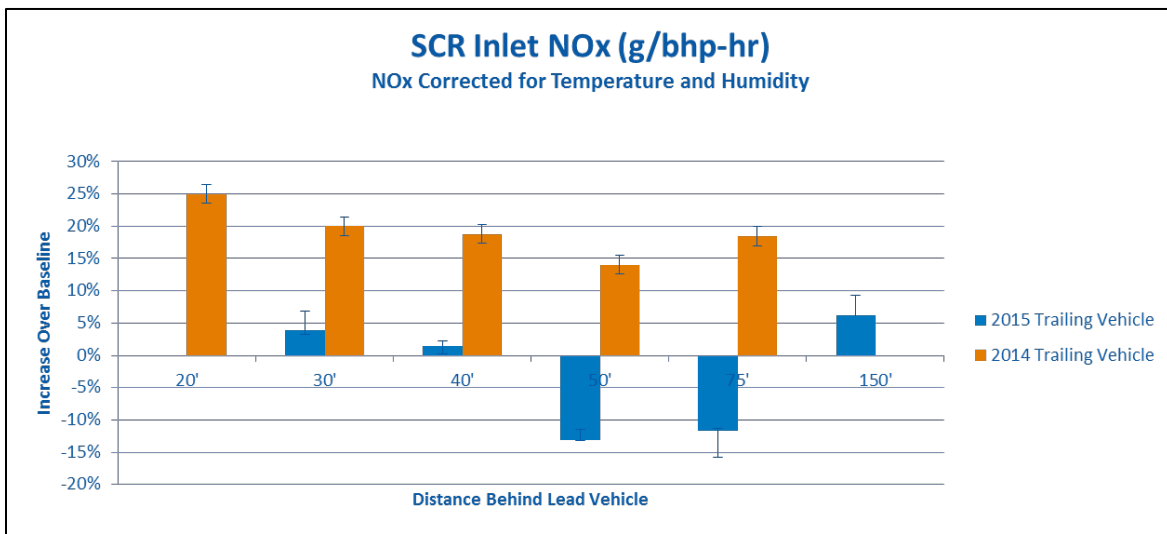


Figure VI-22: SCR inlet brake-specific NOx comparison

Image: NREL

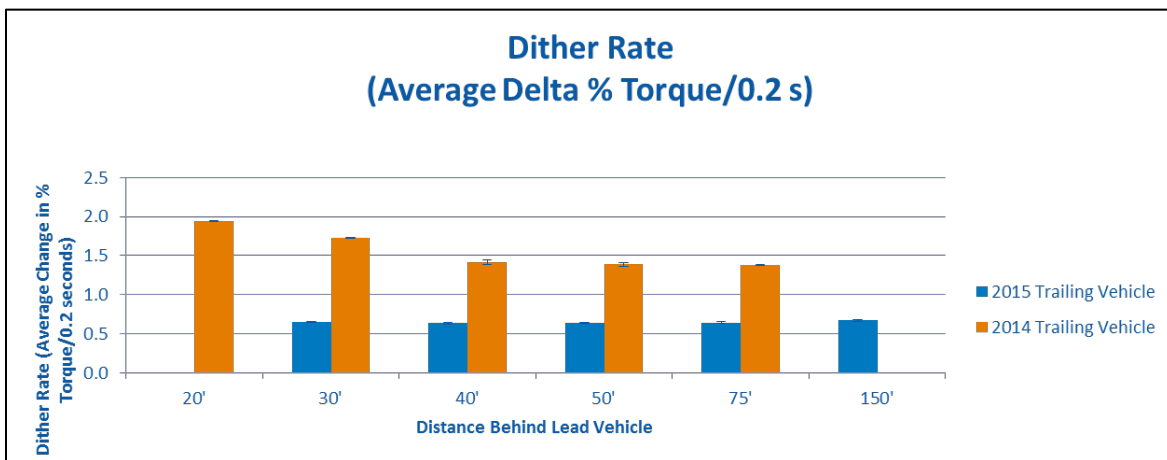


Figure VI-23: Dither rate comparison

Image: NREL

NREL also worked with the Volpe Center to assess data from its 2016 “Naturalistic Study of Truck Following Behavior Final Report” [3] to evaluate the amount of time that truck drivers follow one another at proximities similar to controlled platooning vehicles. The assessment was done to understand if truck drivers are "drafting" behind other trucks and getting platooning savings today without platooning controls technology—this is referred to as "background platooning." The NREL study found that savings from background platooning were insignificant. During lower speed operations, trucks operate in close proximity frequently, but for speeds above 60 mph only 2.2% of driving time showed lead vehicles within 90 meters (295 ft.). Using a degradation curve for savings for the rear vehicle, less than 0.2% background platooning were estimated within this dataset. Figure VI-24 shows following durations in different speed bins compared to average predicted savings for the following vehicle of a platooning pair.

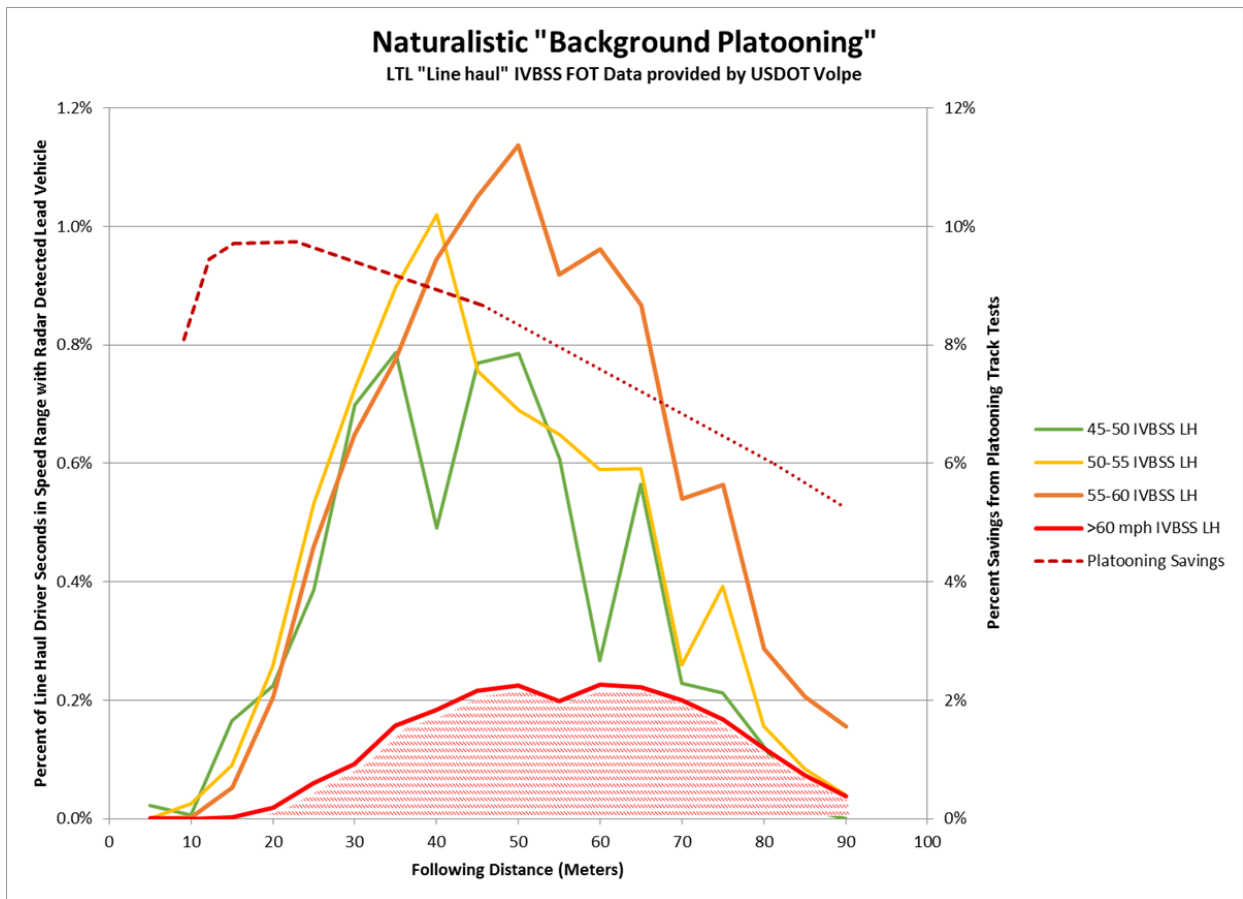


Figure VI-24: Naturalistic "background platooning" - Image: NREL

Conclusions

NREL research to date shows that all platooning scenarios (speeds, following distances, etc.) being considered for near-term technology deployments offer significant opportunities for fuel and emissions savings, but there are still unanswered questions and clear opportunities for greater savings. In the longer term, platooning fuel savings can be significantly enhanced by addressing barriers to closer platoon formation and more vehicles in platoons. Additionally:

- Significant correlation between multiple track studies, wind tunnel testing, and CFD modeling were observed, but there is more to learn regarding close formation and long-distance effects.
- Background platooning is minimal and will not significantly impact realized savings.
- Criteria emissions can be negatively affected by platooning control and must be monitored, but NOx benefits can be realized with proper platooning interaction with the engine.

VI.2.C. Products

Presentations/Publications/Patents

1. M. Lamert, et al., "Class 8 Tractor Trailer Platooning: Effects, Impacts, and Improvements," Automated Vehicle Symposium, July 2016 (<http://www.nrel.gov/docs/fy16osti/66766.pdf>)
2. M. Lammert, et al., "Effect of Platooning on Fuel Consumption of Class 8 Vehicles Over a Range of Speeds, Following Distances, and Mass," SAE 2014 Commercial Vehicle Engineering Congress, October 2014 (<http://www.nrel.gov/docs/fy15osti/62348.pdf>)

VI.2.D. References

1. M. Roeth, "CR England Peloton Technology Platooning Test November 2013," North American Council for Freight Efficiency, December 2013 (<http://nacfe.org/wp-content/uploads/2013/12/CR-England.pdf>)
2. M. Lammert, et al., "Effect of Platooning on Fuel Consumption of Class 8 Vehicles Over a Range of Speeds, Following Distances, and Mass," SAE 2014 Commercial Vehicle Engineering Congress, October 2014 (<http://www.nrel.gov/docs/fy15osti/62348.pdf>)
3. E. Nodine, et al., "Naturalistic Study of Truck Following Behavior Final Report," Volpe National Transportation Systems Center, February 2016 (http://ntl.bts.gov/lib/56000/56800/56891/Truck_Platooning.pdf)

THERMAL

VI.3. Thermal Control of Power Electronics of Electric Vehicles with Small Channel Coolant Boiling

Dileep Singh/Wenhua Yu, Principal Investigators

Argonne National Laboratory
9700 South Cass Avenue
Lemont, IL 60439
Phone: (630) 252-5009; Fax: (630) 252-5568
E-mail: dsingh@anl.gov

Lee Slezak/David Anderson, DOE Program Managers

Vehicle Technologies Office
U.S. Department of Energy
Phone: (202) 586-2335
E-mail: Lee.Slezak@ee.doe.gov

Start Date: October 2013
End Date: September 2016

VI.3.A. Abstract

Objectives

- Explore possibilities of using coolant boiling in cooling of vehicle power electronics.
- Eliminate the hybrid electric vehicle low-temperature cooling system and simplify the cooling system configuration.
- Increase the heat removal capacity and enhance cooling of vehicle power electronics.
- Control the junction temperature of vehicle power electronics and improve the efficiency and lifetime of electronic components.
- Cool high power-density electronics such as wideband-gap semiconductor-based power modules.

Accomplishments

- Developed thermal analysis models of coolant boiling in cooling of vehicle power electronics.
- Developed numerical simulation models of coolant boiling in cooling of vehicle power electronics using the commercial COMSOL Multiphysics software.
- Conducted numerical simulations investigating the effects of various parameters on the boiling cooling system.
 - Thermal conductivity of thermal interface materials.
 - Coolant flow velocity.
 - Fluid inlet temperature.
 - Heat flux of vehicle power electronics.
- Designed, fabricated, and characterized an experimental test system for investigating coolant boiling in cooling of vehicle power electronics.
- Conducted experimental tests for measuring subcooled flow boiling heat transfer coefficients
 - Finned small channels of a real hybrid electric vehicle power electronic cooling module.
 - Top and bottom heating conditions.

- Various coolant flow velocities.

Future Achievements

- Develop predictive boiling heat transfer coefficient correlations based on the experimental data.
- Refine simulation models and results of coolant boiling in cooling of vehicle power electronics.

VI.3.B. Technical Discussion

Background

The current cooling technology for the power electronics in commercial hybrid electric vehicles (HEVs) uses a liquid-cooled heat sink with fins. In order for the fin-structure heat sink to remove the heat from the power electronics, a separate low-temperature radiator and pumping system, in addition to the main engine radiator and pumping system, is required to provide a low coolant inlet temperature. This second radiator and pumping system increases the weight and the cost of the vehicle and decreases the efficiency. This project is aimed to use subcooled or low-vapor quality saturation flow boiling for cooling of vehicle power electronics. It is expected that this cooling technology will enhance cooling of vehicle power electronics, control junction temperatures of vehicle power electronics, and eliminate the second cooling system currently used in hybrid electric vehicles.

Introduction

Various technologies have been proposed to enhance the cooling of the power electronics in HEVs and therefore reduce the system weight and volume of the power electronics and increase the efficiency and the life time of vehicles. These cooling technologies include the single-phase or two-phase jet impingement, the two-phase spray, the immersion pool boiling, and the two-phase saturation boiling. However, all of these previously studied technologies require installation of significant additional hardware to cool the power electronics.

In the present study, with subcooled flow boiling in the cooling channels of power electronics in HEVs, no major additional components are required. The low-temperature radiator and pumping system is replaced with the existing main engine radiator and pumping system, and boiling occurs only in the cooling channels of power electronics and nowhere else in the HEV cooling system. The uniqueness of this technology lies in the use of subcooled flow boiling in addition to liquid convection under controlled conditions in current power electronic cooling channels to improve the cooling capacity without exit vapor from the channels or major additional components in HEVs. These desirable conditions are in contrast to these other cooling technologies.

Approach

As illustrated in Figure VI-25, the subcooled flow boiling system proposed in the present study can be integrated into the main engine cooling system without major additional hardware installation. The conventional engine coolant, a 50/50 ethylene glycol/water (EG/W) mixture, is used for cooling of vehicle power electronics. The coolant flowing out from the radiator is pumped by the main engine coolant pump and divided into two flow paths. One follows the normal engine cooling route, and the other goes into the cooling channels of power electronics. The coolant in the cooling channels absorbs heat from the power electronics through subcooled flow boiling. Then the two coolant flows combine in the flow mixer to form a uniform-temperature fluid. The coolant then enters the radiator to reject the absorbed heat to air. The flow divider and mixer components are considered to be minor additions to an HEV as they may be little more than types of piping tees.

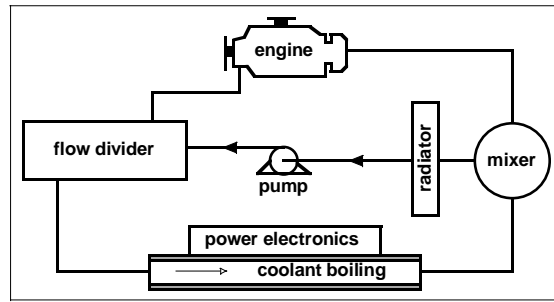


Figure VI-25: Concept of Subcooled Flow Boiling System

Results

The subcooled flow boiling technology for vehicle power electronics cooling has been studied in this project through numerical simulations conducted using the commercial COMSOL Multiphysics software. The effects on coolant subcooled flow boiling of various parameters, including the thermal conductivity of thermal interface materials (TIMs), the coolant flow velocity, the fluid inlet temperature, and the heat flux of vehicle power electronics, were studied. Furthermore, the subcooled flow boiling system was compared to the current single-phase liquid-cooled technology. Results presented subsequently show that coolant subcooled flow boiling in the cooling channels can enhance the cooling for vehicle power electronics and remove the low-temperature radiator and pumping system to simplify the cooling system in HEVs.

Simulation Models and Key Considerations

The vehicle power electronic package studied in the simulations is shown in Figure VI-26. There are two semiconductors on the top, an insulated gate bipolar transistor (IGBT) and a diode. The cooling channels on the bottom are divided by costly fins. A typical power electronics package in a HEV has about a dozen of these semiconductor pairs. This power electronics module was chosen for the simulations of this study because it is used in commercial HEVs. Furthermore, this package allows the cooling on both sides of the semiconductors. Figure VI-27 shows the side view of the configuration of Figure VI-26 identifying each layer of the power electronics and cooling channels, and Table VI-1 gives the materials and dimensions of each layer. The fin structure of the cooling channels for the vehicle power electronic package of Figure VI-26 is enlarged in Figure VI-28. There are 20 channels under each pair of semiconductors.

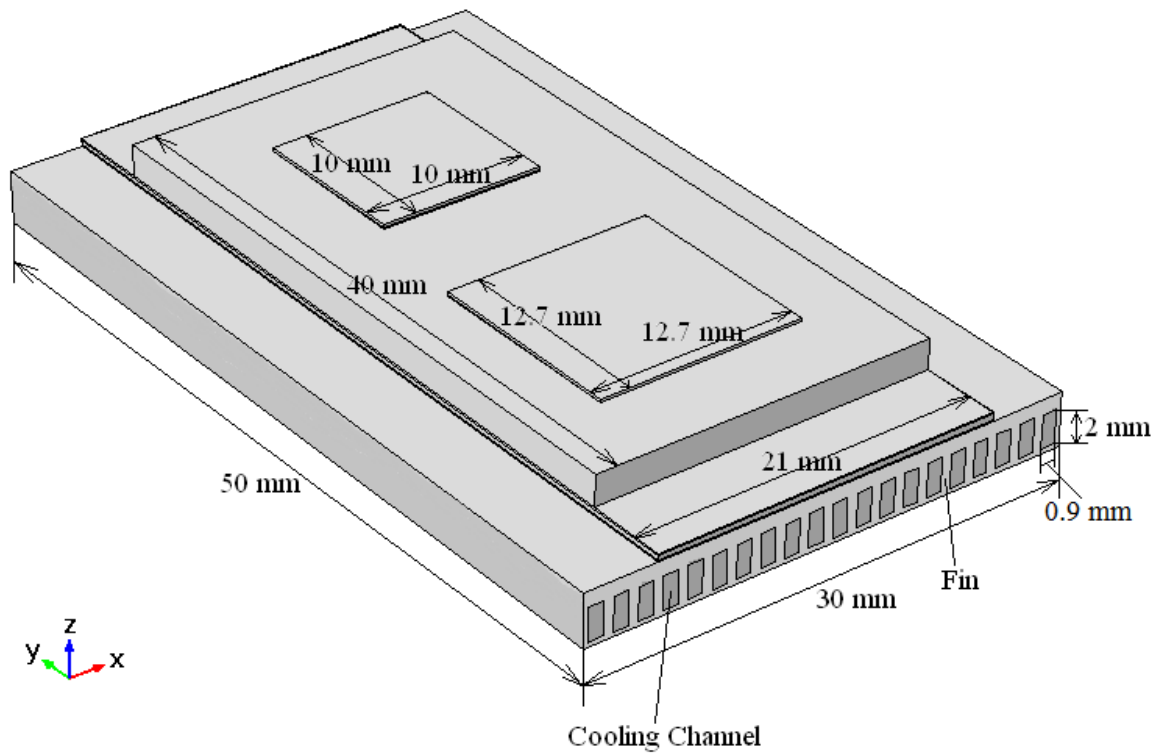


Figure VI-26: Vehicle Power Electronic Package

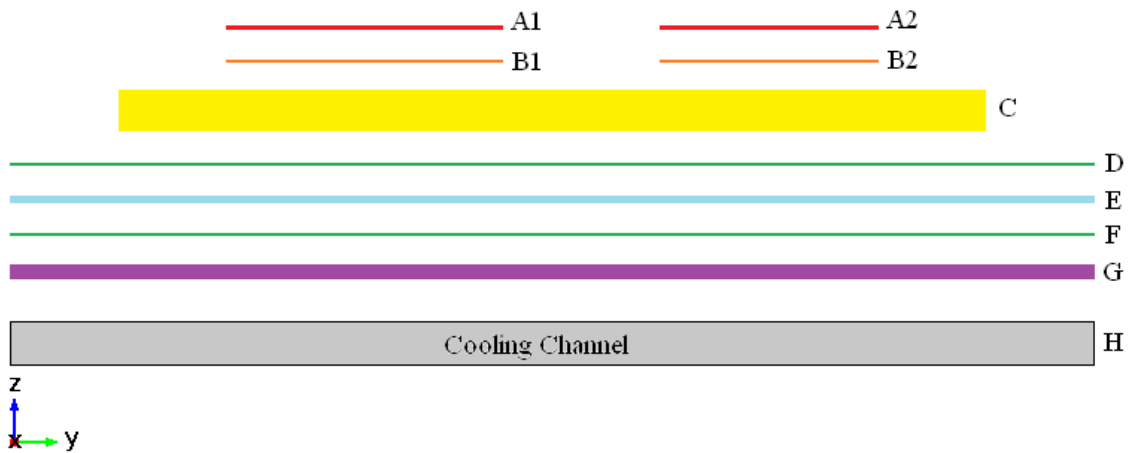


Figure VI-27: Side View of Vehicle Power Electronic Package

Table VI-1: Materials and Dimensions of Each Layer

Index	Material	X (mm)	Y (mm)	Z (mm)
A1	IGBT: Si	12.7	12.7	0.145
A2	Diode: Si	10.0	10.0	0.145
B1	Solder	12.7	12.7	0.076
B2	Solder	10.0	10.0	0.076
C	Heat spreader: Cu	21.0	40.0	1.85

D	TIM: Thermal grease	21.0	50.0	0.1
E	Substrate: SiN	21.0	50.0	0.3
F	TIM: Thermal grease	21.0	50.0	0.1
G	Heat sink: Al	30.0	50.0	0.6
H	Cooling channel	30.0	50.0	2.0

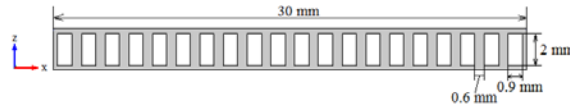


Figure VI-28: Fin Structure

The mesh structure in the numerical model of the configuration of Figure VI-26 is displayed in Figure VI-29. The simulation model consists of 2,007,316 domain elements, 443,403 boundary elements, and 15,374 edge elements. Based on a mesh independence study, these mesh elements are sufficient for the 3-D numerical simulations.

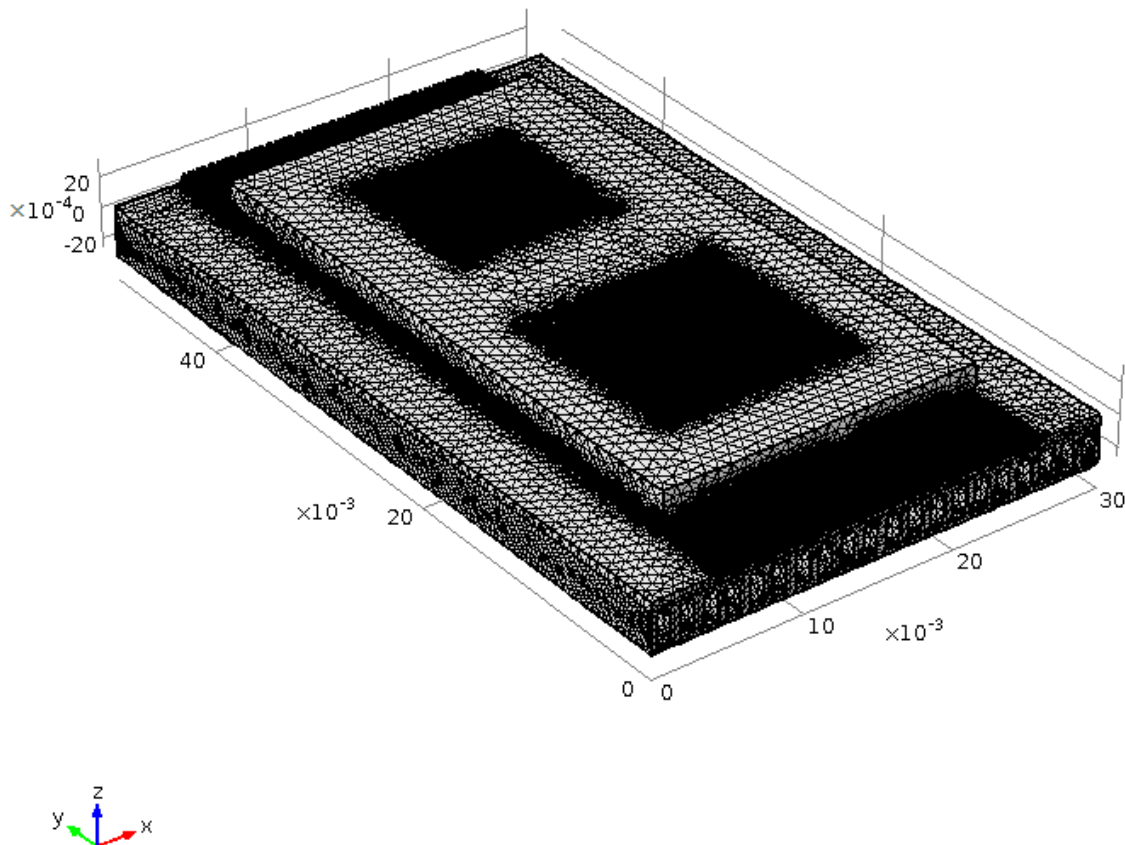


Figure VI-29: Mesh Structure (All Units in Meter)

For the simulation boundary condition of the subcooled flow boiling heat transfer coefficients in the cooling channels, the widely used Shah correlation in the engineering literature was chosen. While the Shah correlation was not developed for subcooled flow boiling of a 50/50 EG/W mixture, the differences between the experimental data from our current PACCAR CRADA project of 50/50 EG/W subcooled flow boiling and the

simulation results based on the Shah correlation are within 10% at various coolant flow velocities, which validates the applicability of the Shah correlation for the simulations.

Other key considerations include: (a) because the subcooled flow boiling system is integrated into the main engine cooling system, the conventional engine coolant, a 50/50 EG/W mixture, is used for cooling of power electronics; (b) the pressure in the cooling channels for power electronics in HEVs is 2 atm. where the saturation point of a 50/50 EG/W mixture is 129°C; (c) in order to eliminate the low-temperature radiator and the associated pumping system, the coolant inlet temperature is assumed to be 105°C; (d) the coolant flow velocity is 0.16 m/s in order to keep the coolant outlet temperature below the saturation point and to generate desired subcooled flow boiling; (e) the coolant outlet temperature is below the saturation point with no net vapor in the rest of the system (outside the power electronics cooling channels); and (f) to have desired subcooled flow boiling, the cooling channel wall temperature is 10-30°C above the saturation point, i.e. a wall superheat of 10-30°C.

TIM Thermal Conductivity Effects

Figure VI-30 shows the junction temperature (the IGBT surface temperature) versus the TIM thermal conductivity for a double-sided cooling system with or without fins for a 100-W/cm² heat flux on the IGBT and diode surfaces, the current commercial heat flux level. The coolant inlet temperature is 105°C. Various TIM thermal conductivities of 1.5 W/mK, 7.5 W/mK, and 15 W/mK were considered. It can be seen from Figure VI-30 that use of subcooled flow boiling in the cooling channels reduces the junction temperature compared to single-phase convective heat transfer. Single-phase cooling at this 105°C coolant inlet temperature cannot keep the junction temperature below 175°C at any TIM thermal conductivities. With a 7.5-W/mK TIM thermal conductivity, the junction temperature is reduced to 175°C without fins in the cooling channel and to 137°C with fins by using subcooled flow boiling as shown in Figure VI-30 and Figure VI-31. At a TIM thermal conductivity of 1.5 W/mK, the junction temperature is still maintained far below the 175°C limit using the subcooled flow boiling system with fins. TIM thermal conductivities higher than 7.5 W/mK do not significantly reduce the junction temperature of the power electronics, as displayed in Figure VI-30, which means that there is little benefit to TIM thermal conductivities above 7.5 W/mK. By using a TIM thermal conductivity of 7.5 W/m K, fins can be eliminated in the double-sided subcooled flow boiling system while maintaining a 175°C junction temperature, which reduces the capital cost and pumping power. Using subcooled flow boiling with fins, the junction temperature can be reduced below 155°C with all TIM thermal conductivities studied, as displayed in Figure VI-30.

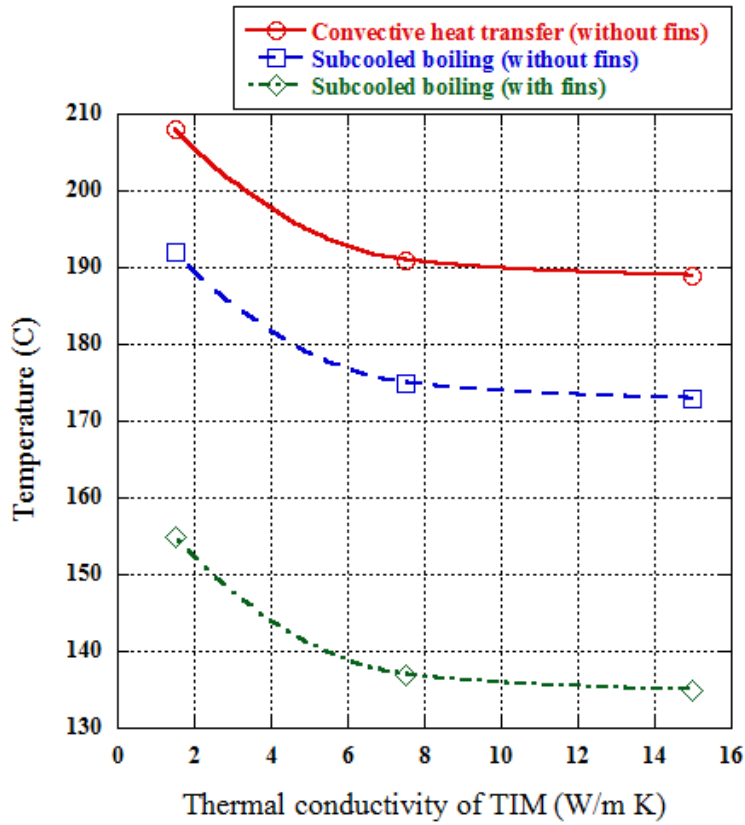


Figure VI-30: TIM Thermal Conductivity Effects

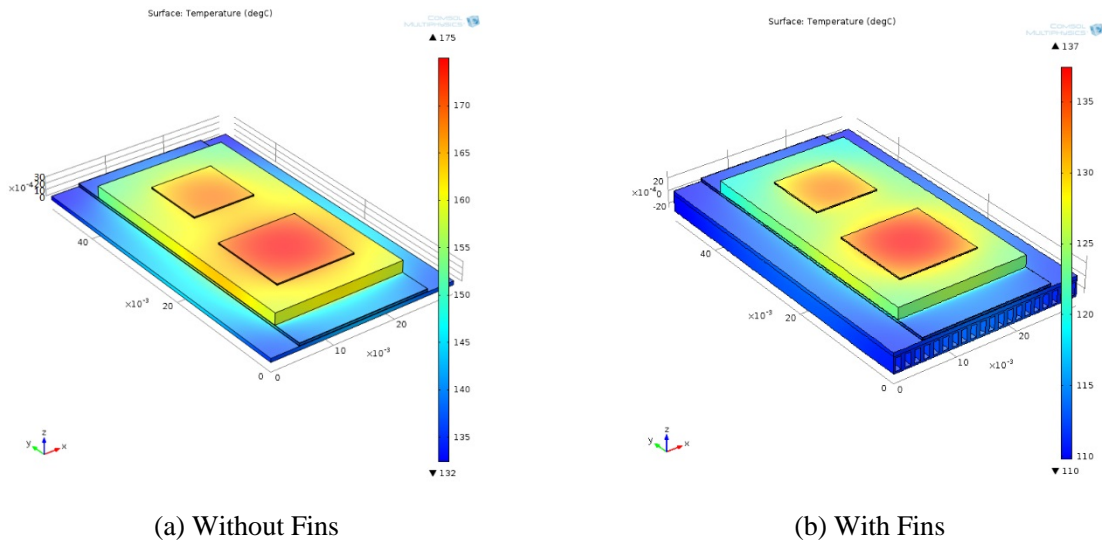


Figure VI-31: Junction Temperatures

Coolant Flow Velocity Effects

Figure VI-32 is a plot of the junction temperature versus the coolant flow velocity. It is for a double-sided cooling system with a 7.5-W/mK TIM thermal conductivity for a 100-W/cm² heat flux on the IGBT and diode surfaces. The coolant flow inlet temperature is 105°C. It is seen that the finned channels combined with subcooled flow boiling can reduce the junction temperature below 140°C for all coolant velocities. Without fins, the junction temperature can be controlled below 175°C when the coolant flow velocity is 0.16 m/s or

higher. It is seen in Figure VI-32 that the coolant flow velocity does not have significant effect on the junction temperature for the subcooled flow boiling system.

Efficient cooling using subcooled flow boiling occurs at low coolant flow velocities, which reduces pressure drops and pumping power requirements. Using fins in the cooling channels, the coolant flow velocity range for subcooled flow boiling is between 0.06 m/s to 0.4 m/s, as shown in Figure VI-32. When the velocity is lower than the lower limit of this range, the coolant outlet temperature would be likely above the saturation point. When the velocity is higher than the higher limit of this range, the cooling channel wall temperature cannot reach 10°C above the saturation point and therefore subcooled flow boiling is unlikely to occur. The subcooled flow boiling pressure drop along the cooling channel predicted based on correlations in the engineering literature is quite small (approximately 1443 Pa), which would result in low pumping power requirements.

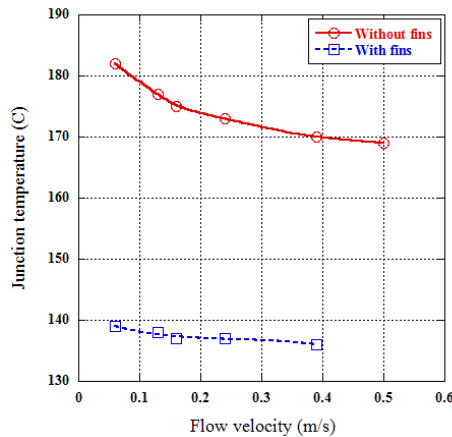


Figure VI-32: Coolant Flow Velocity Effects

Fluid Inlet Temperature Effects

A double-sided cooling system with a 7.5-W/mK TIM thermal conductivity for a 100-W/cm² heat flux on the IGBT and diode surfaces was also considered in the next simulations. Based on the results shown in Figure VI-33, the junction temperature can be controlled below 175°C without fins in the cooling channel and below 150°C with fins when using subcooled flow boiling. Without fins, the subcooled flow boiling dominates the cooling process. High coolant inlet temperatures cause strong subcooled flow boiling due to high subcooled flow boiling heat transfer coefficients caused by low liquid subcooling levels. Therefore, a higher coolant temperature results in a lower junction temperature. With fins in the cooling channels, convective heat transfer is also important. Consequently, a higher coolant temperature results in a higher junction temperature. In order to maintain subcooled flow boiling in the cooling channels, the fluid inlet temperature cannot be below 100°C with fins while the fluid inlet temperature cannot be below 90°C without fins because lower fluid inlet temperatures cause the channel wall temperature to be below the subcooled flow boiling range. Furthermore, according to the simulation results displayed in Figure VI-33, the coolant inlet temperature does not have significant effects on the junction temperature, especially for the non-finned cooling channel.

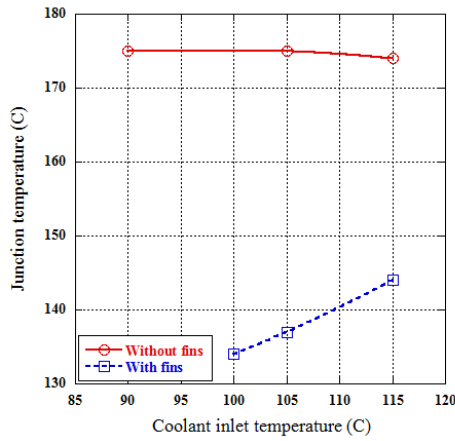


Figure VI-33: Fluid Inlet Temperature Effects

Heat Flux Effects

Figure VI-34 shows the semiconductor junction temperature versus the heat flux from the numerical simulations. The simulations were performed for a single-sided finned cooling system with a coolant inlet temperature of 105°C and a coolant flow velocity of 0.16 m/s. The 7.5-W/mK TIM thermal conductivity was applied. Referring to Figure VI-34, when the heat flux on the IGBT and diode surfaces is small, less than 30 W/cm², a single-phase flow occurs as indicated by the steep slope of the curve. Here, little to no subcooled flow boiling occurs. As the heat flux increases, subcooled flow boiling becomes stronger in the cooling channels and the slope of the curve is reduced in Figure VI-34. The junction temperature increases more gradually with subcooled flow boiling because of the increased heat transfer rates compared to a single-phase flow. Using subcooled flow boiling, the junction temperature can be controlled below 175°C with a heat flux on the IGBT and diode surfaces up to 125 W/cm², as shown in Figure VI-34. For a double-sided cooling system, the heat flux value would be doubled to 250 W/cm². This heat flux is a 25% increase over conventional single-phase cooling of HEV power electronics, and it is accomplished without a low-temperature radiator cooling system.

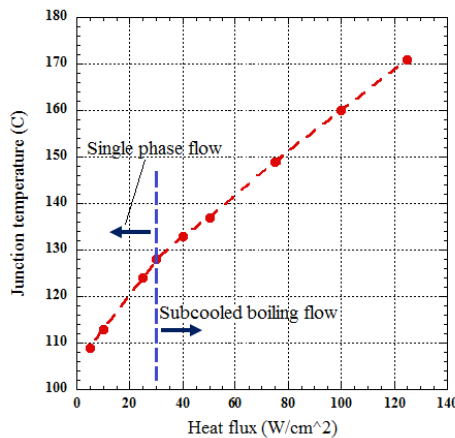


Figure VI-34: Heat Flux Effects

Figure VI-35 shows the temperature profiles through the power electronics for the high heat flux 250 W/cm² application (such as wideband-gap semiconductors) using subcooled flow boiling and convective single-phase cooling. The junction temperature can be maintained below 175°C using subcooled flow boiling combined with fins in a double-sided cooling system with a 7.5-W/mK TIM thermal conductivity, as shown in Figure VI-35(b). Without subcooled flow boiling, the junction temperature would be 200°C, as shown in Figure VI-35(a).

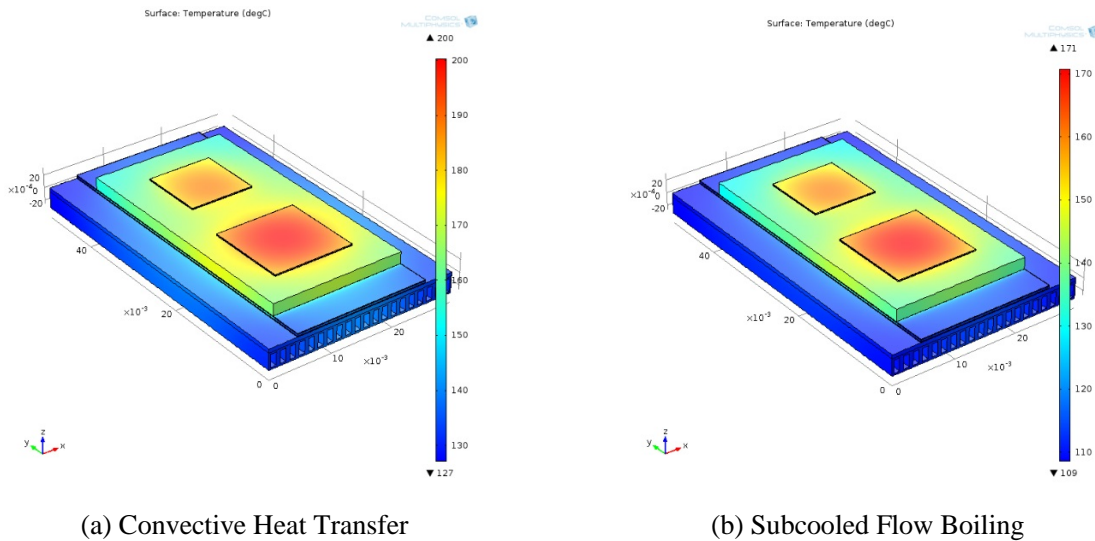


Figure VI-35: High Heat Flux Applications

Comparison of Convection and Subcooled Boiling

The comparison between single-phase convection and subcooled flow boiling for cooling power electronics in HEVs is illustrated in Table VI-2, where SS and DS indicate single-sided and double-sided, respectively. The TIM thermal conductivity is 7.5 W/mK in the simulations. Without fins (as indicated in column 1, Table VI-2), double-sided subcooled flow boiling can control the junction temperature below 175°C. With fins, subcooled flow boiling can increase the cooling rate by 25% (column 2, Table VI-2) compared to convection cooling or reduce the junction temperature (column 3, Table VI-2). By using subcooled flow boiling combined with fins, the double-sided subcooled flow boiling system can cool wideband-gap semiconductors with a heat flux up to 250 W/cm² (column 4, Table VI-2). It should be pointed out that all these are achieved for a coolant inlet temperature of 105°C without the second low-temperature radiator and the associated pumping system.

Table VI-2: Comparison of Convection and Subcooled Boiling

	Subcooled Flow Boiling				Convection	
	105	105	105	105	70	70
Coolant Inlet Temperature (°C)	105	105	105	105	70	70
Total Heat Flux on IGBT and Diode Surfaces (W/cm ²)	100	125	100	250	127	100
Coolant Flow Velocity (m/s)	0.16	0.16	0.16	0.16	0.24	0.24
Fins in the Channel	No	Yes	Yes	Yes	Yes	Yes
Cooling System	DS	SS	SS	DS	DS	SS
Junction Temperature (°C)	175	175	160	175	150	175

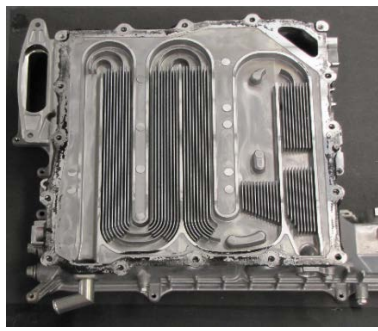
Experimental Test System

Experimental Test Module Design and Fabrication

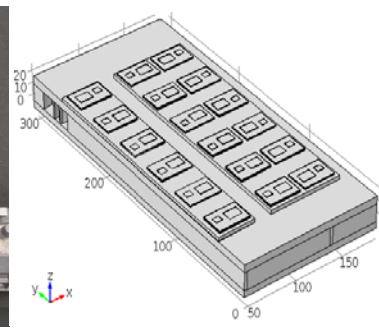
The experimental test module, shown in Figure VI-36, was designed and fabricated to investigate heat transfer characterizations of coolant subcooled boiling in practical power electronic cooling channels of HEVs. The experimental test module is based on the Toyota Prius cold plate as shown in Figure VI-36a of its overview and Figure VI-36b of its channel details. To simulate the heat generated by the power electronic components, a heating wire was affixed to the experimental test module as shown in Figure VI-36d. The material, dimension, and arrangement of the heating wire were carefully chosen to generate uniform heat fluxes similar to the real power electronic cooling system. Thermocouples for measuring the wall temperatures and the in-stream fluid temperatures, a pressure transducer for measuring the system pressure, and a differential pressure transducer for measuring the pressure drop were installed into the experimental test module as shown in Figure VI-36e. The measurements from these sensors are used in the data reduction process to calculate the heat transfer coefficient. As shown in Figure VI-37, the completed experimental test module is attached to a structural frame, which enables the module to be tested on both top-heating and bottom-heating conditions to provide important design information for the double-sided cooling configuration. Through the cooling channel inlet and outlet ports, the experimental test module is connected into an experimental test loop that includes two preheaters for heating the coolant to a desired inlet temperature, a pressure subsystem for setting up the system pressure, and other necessary components such as the flowmeter and the heat exchanger.



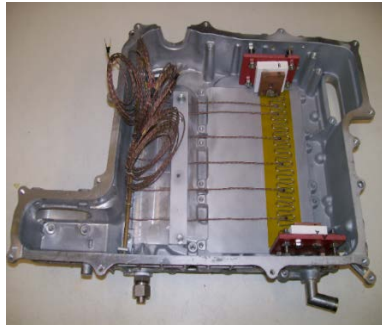
(a) Toyota Prius Cold Plate



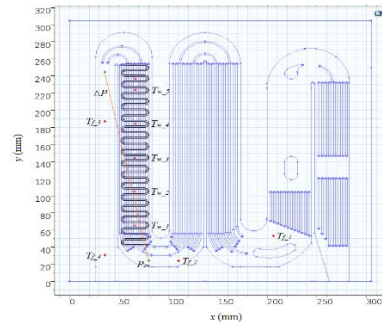
(b) Cooling Channels



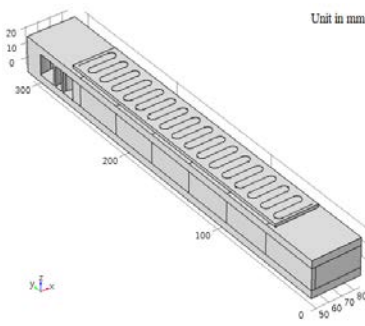
(c) Package Modeling Geometry



(d) Modified Cold Plate



(e) Heating Wire and Sensors



(f) Channel Modeling Geometry

Figure VI-36: Experimental Test Module

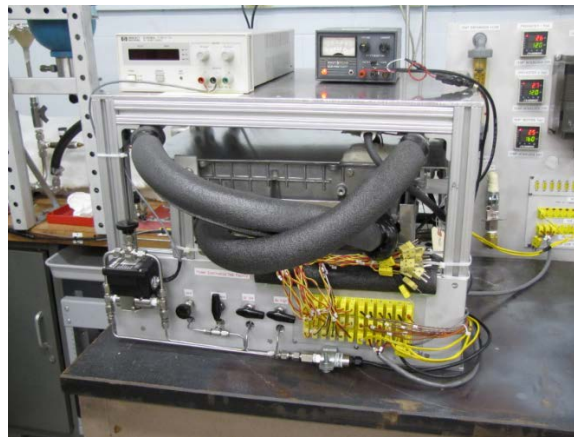


Figure VI-37: Experimental Test Module Overview

Experimental Test Module Characterizations

Two characterizations were performed to the experimental test module. The first is the heat transfer simulations of the cold plate package based on the package modeling geometry shown in Figure VI-36c. Figure VI-38 shows the heat transfer simulation results for single-phase convection. The simulation conditions are: the heat flux of 100 W/cm², the coolant flow velocity of 0.16 m/s, the TIM of 1.5 W/mK, and the coolant inlet temperature of 70°C and 105°C, respectively. It can be seen from Figure VI-38a that for a coolant inlet temperature of 70°C, the junction temperature can be controlled below 175°C. However, when the coolant inlet temperature is increased to 105°C, the junction temperature rises to 183°C as shown in Figure VI-38b. Therefore, the single-phase flow will not work under this condition. Figure VI-39 shows the heat transfer simulation results for subcooled boiling. The simulation conditions are: the coolant flow velocity of 0.16 m/s, the TIM of 1.5 W/mK, the coolant inlet temperature of 105°C, and the heat flux of 100 W/cm² and 114

W/cm², respectively. It can be seen from Figure VI-39 that for a coolant inlet temperature of 105°C, the junction temperature can be controlled below 175°C for both heat flux levels. Therefore, with subcooled boiling, the heat flux of power electronics for this cold plate package can be increased to 114 W/cm² compared to the current technology.

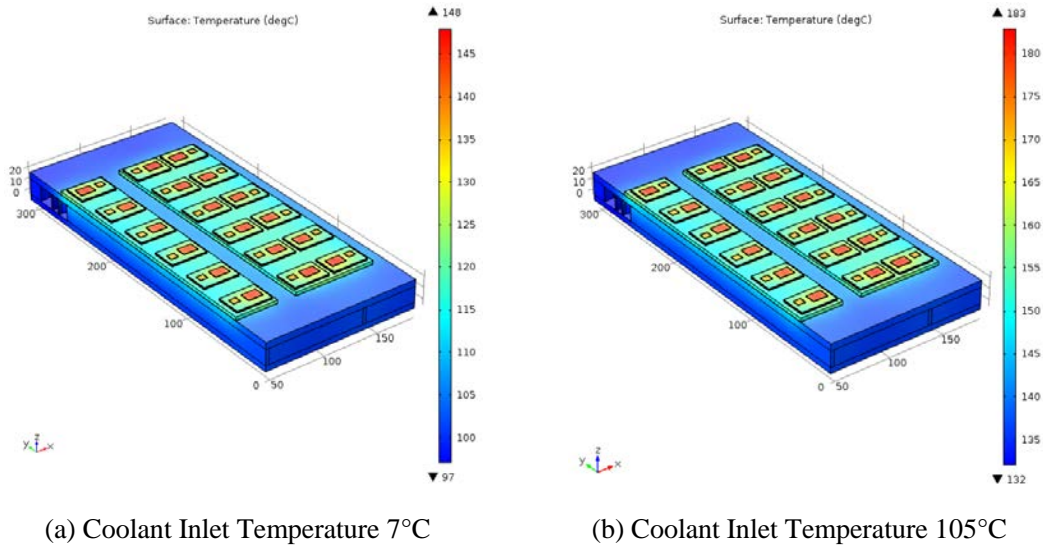


Figure VI-38: Convective Heat Transfer Simulation Results

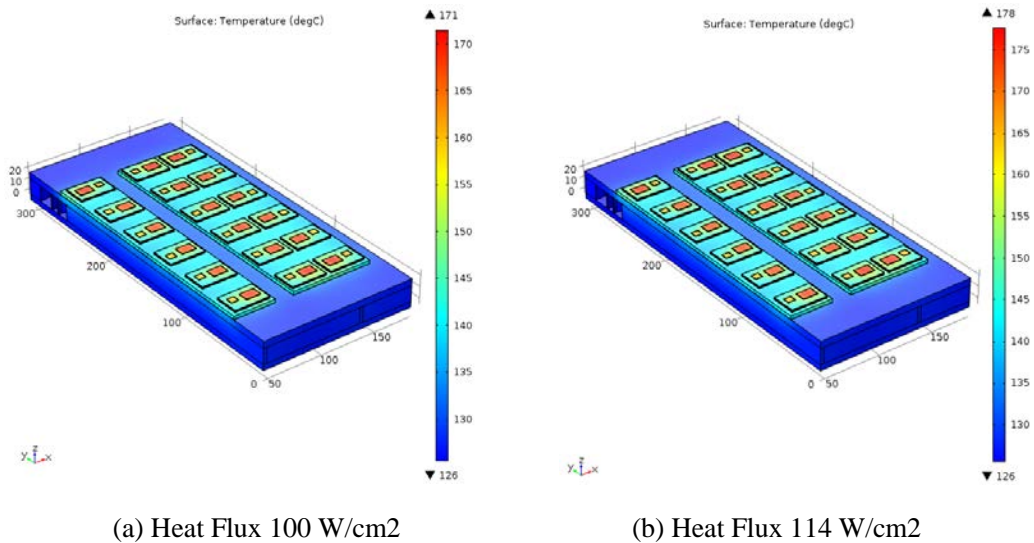


Figure VI-39: Subcooled Boiling Heat Transfer Simulation Results

The second is the heat loss calibrations of the experimental test module. Because of the high thermal conductivity of the module material aluminum, the heat loss is not negligible. Therefore, heat loss tests were conducted by applying certain heating power to the experimental test module to bring its wall temperature to a selected level. The corresponding heat loss or the applied heating power was then correlated as a function of the driving temperature (the difference of the wall temperature and the ambient temperature). It can be seen from Figure VI-40 that the heat loss rate is linearly depending on the driving temperature and is well predicted by the correlation. The heat loss data are incorporated into the data reduction process for single-phase and boiling heat transfer tests.

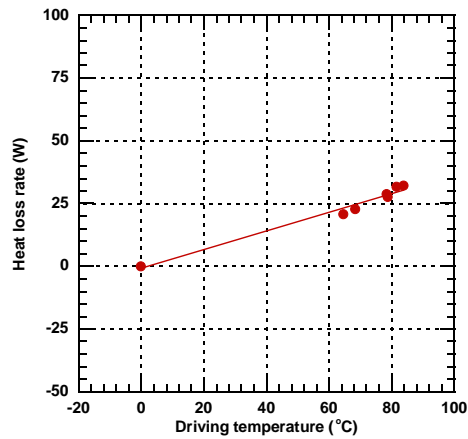


Figure VI-40: Heat Loss Calibration Results

Fin Effects on Subcooled Boiling

The experimental test module has finned multi-channels with the heat input from either the top or the bottom. Therefore, the overall heat transfer is complicated, especially for subcooled boiling heat transfer. During subcooled boiling, the boiling occurs on the inside surface of the heat input base and on certain fin surfaces as shown in Figure VI-41. To account for fin effects, energy balance analyses were conducted and formulae were worked out for calculating the boiling length of the fin surfaces and the boiling heat transfer coefficient. These results are incorporated into the data reduction process for boiling heat transfer tests. Figure VI-42 shows an example from simulations based on the channel modeling geometry in Figure VI-36f under the following conditions: the heat flux of 100 W/cm², the coolant inlet temperature of 105°C, and the coolant flow velocity of 0.16 m/s. It can be seen from Figure VI-42 that the wall temperature slightly increases with the subcooled boiling length of the fins due to the heat transfer improvement and the heat flux reduction from the larger effective area. However, the wall temperature difference is small.

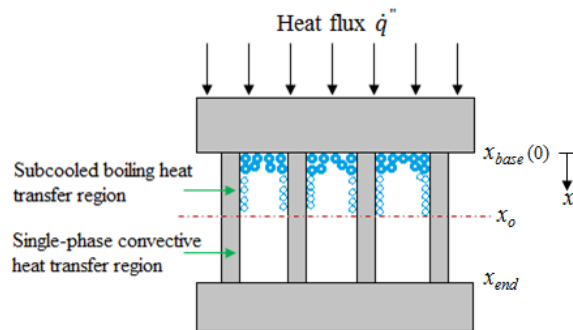


Figure VI-41: Fin Effect on Subcooled Boiling

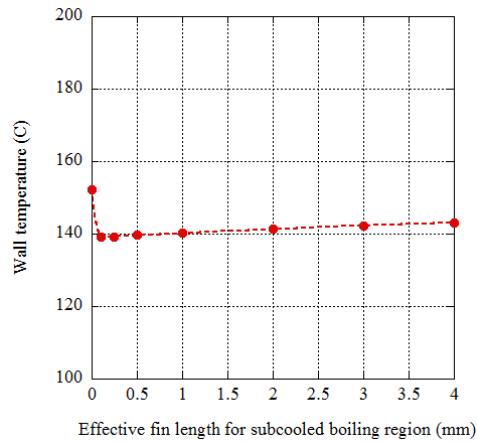


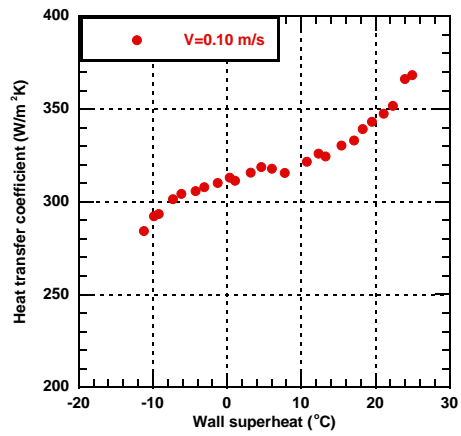
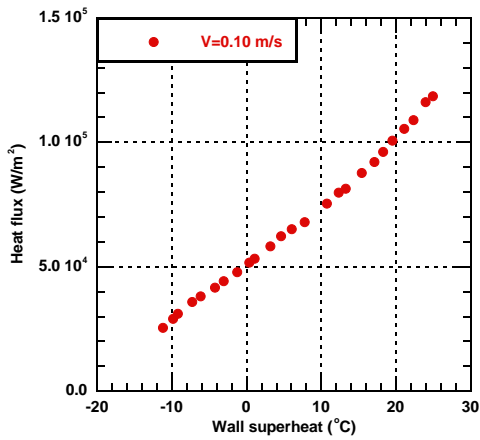
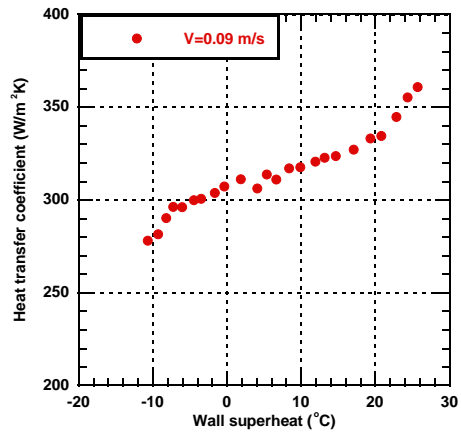
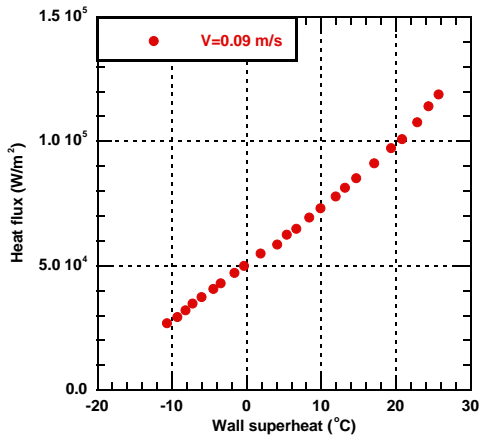
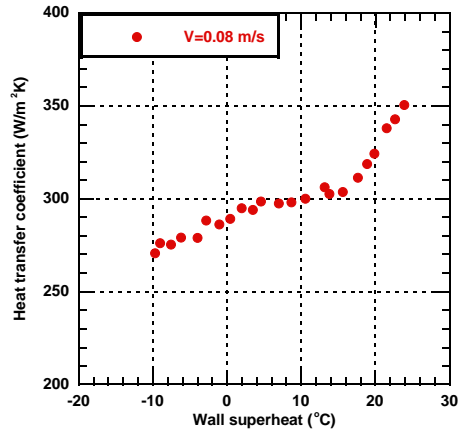
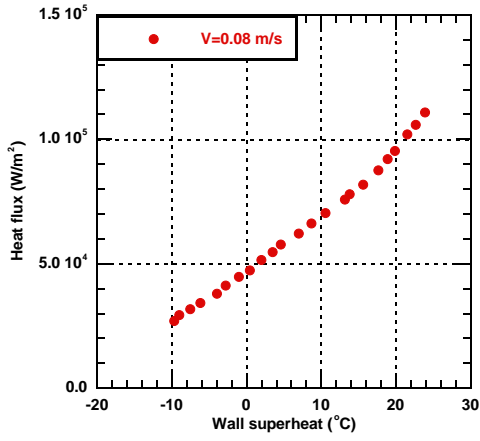
Figure VI-42: Wall Temperature as a Function of Subcooled Boiling Length

Experimental Tests

A series of experimental tests to a 50/50 EG/W mixture was conducted under the following conditions: (a) the fluid inlet temperature of 105°C; (b) the system pressure of 2 atmospheric pressures; (c) the coolant flow velocities of 0.08 m/s, 0.09 m/s, 0.10 m/s, 0.11 m/s, and 0.12 m/s; and (d) the heating methods of top heating and bottom heating. During each set of experimental tests with a constant fluid inlet temperature, a constant system pressure, and a constant coolant flow velocity, the heating power from either the top or the bottom of the test channels was incrementally increased until the wall temperature reached the preset limit. For each heating power incremental step, the outputs from all sensors including the thermocouples, pressure transducer, and flow meter were recorded together with the voltage reading and the current reading. The boiling curves and the heat transfer coefficients were calculated from the experimental data.

Top Heating Condition

The heat fluxes and the heat transfer coefficients are shown in Figure VI-43 as functions of the wall superheat for various coolant flow velocities under the top heating condition. The heat fluxes were calculated on the heating surface. The heat transfer coefficients were calculated on the heating surface with an assumption of the uniform fin effect. It can be seen from Figure VI-43 that (a) both the heat fluxes and the heat transfer coefficients increase with the wall superheat; (b) the overall heat transfer can be divided into three regions of single-phase dominant, transition, and subcooled boiling dominant; (c) in the single-phase dominant region of low wall superheats, the heat transfer coefficients increase fast with the wall superheat; (d) in the transition region of middle wall superheats, the heat transfer coefficients increase slowly with the wall superheat; and (e) in the subcooled boiling dominant region of high wall superheats, the heat transfer coefficients increase fast again with the wall superheat. The transition into the subcooled boiling dominant region can also be seen from slightly different increase slopes of the heat flux plots though it is not as obvious as from the heat transfer coefficient plots. These results indicate that the heat transfer can be improved with subcooled flow boiling in the power electronic cooling module.



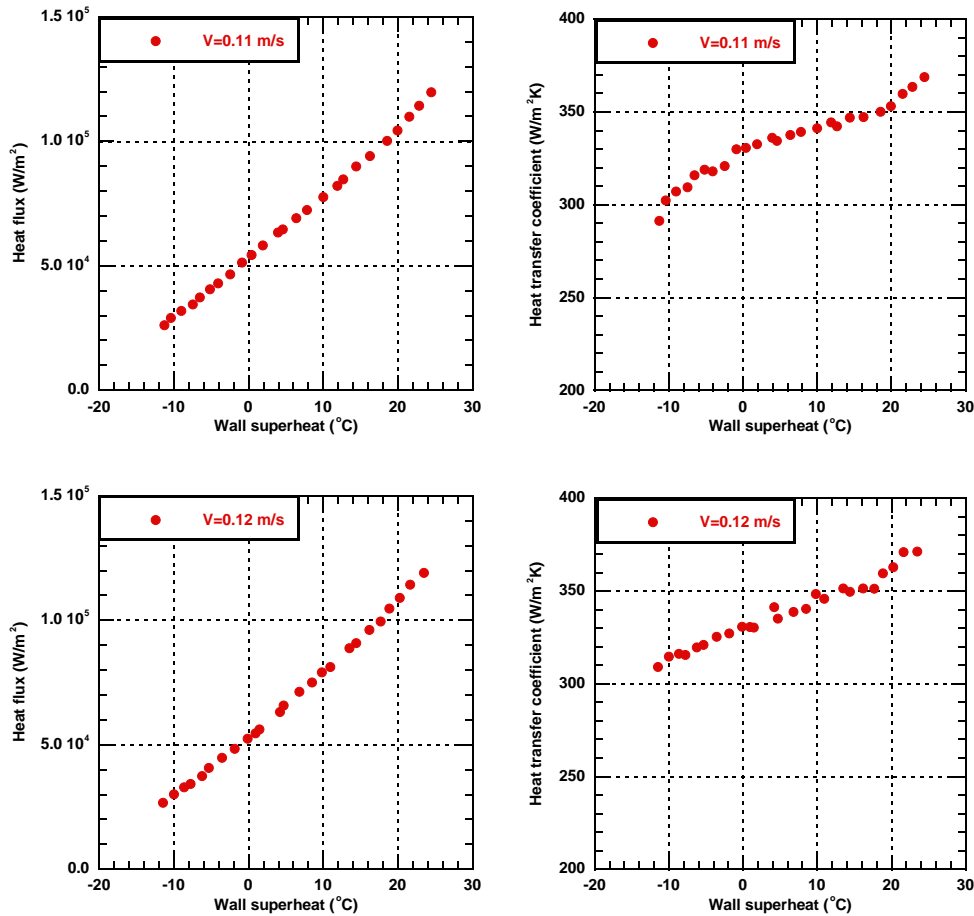
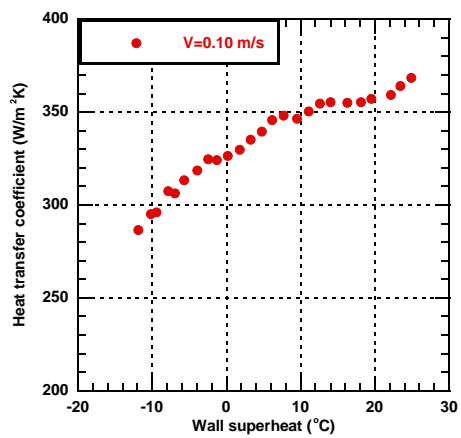
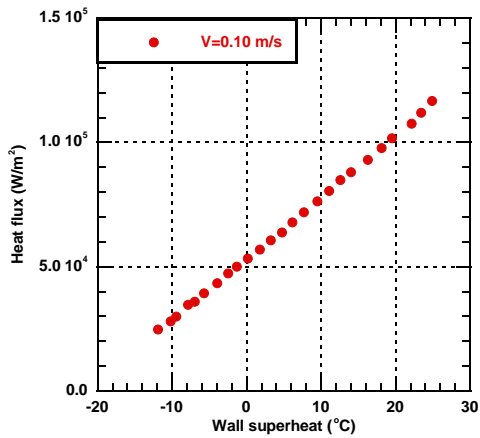
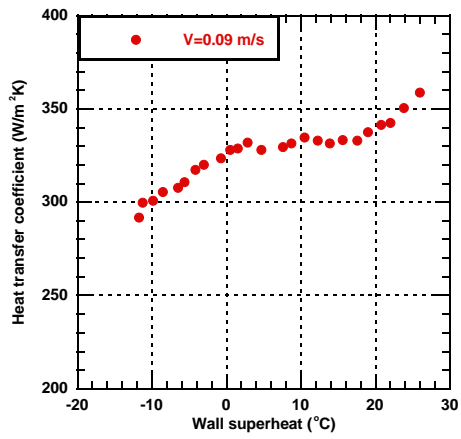
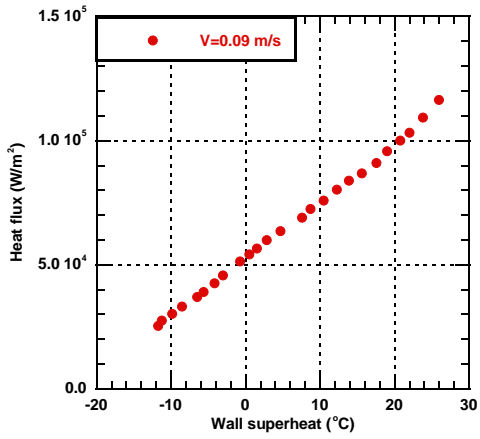
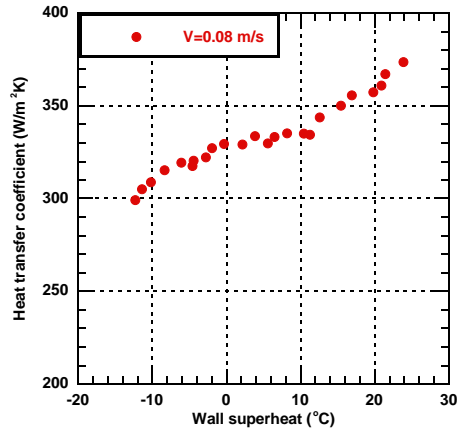
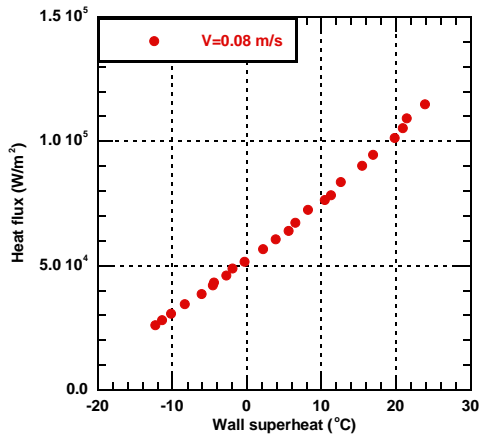


Figure VI-43: Heat Flux and Heat Transfer Coefficient as Functions of Wall Superheat under Top Heating Condition

Bottom Heating Condition

In practical applications of power electronic cooling, the cooling module can be placed on the top of the power electronics or on the bottom of the power electronics. To take the cooling module arrangement condition into consideration, experimental tests were also conducted for the bottom heating condition. Other test conditions for the bottom heating condition were same as those for the top heating condition. The heat fluxes and the heat transfer coefficients of the bottom heating condition were calculated under the same assumptions as those of the top heating condition. The heat fluxes and the heat transfer coefficients are shown in Figure VI-44 as functions of the wall superheat for various coolant flow velocities under the bottom heating condition. It can be seen from Figure VI-44 that the heat fluxes and the heat transfer coefficients of the bottom heating condition are very similar to those of the top heating condition in terms of their increase trends with the wall superheat and their various heat transfer regions. In addition, the heat transfer coefficients of the bottom heating condition are generally higher than those of the top heating condition. This result can be explained by the fact that bubbles generated on the hot surface are easier to move into the colder bulk liquid under the bottom heating condition than under the top heating condition.



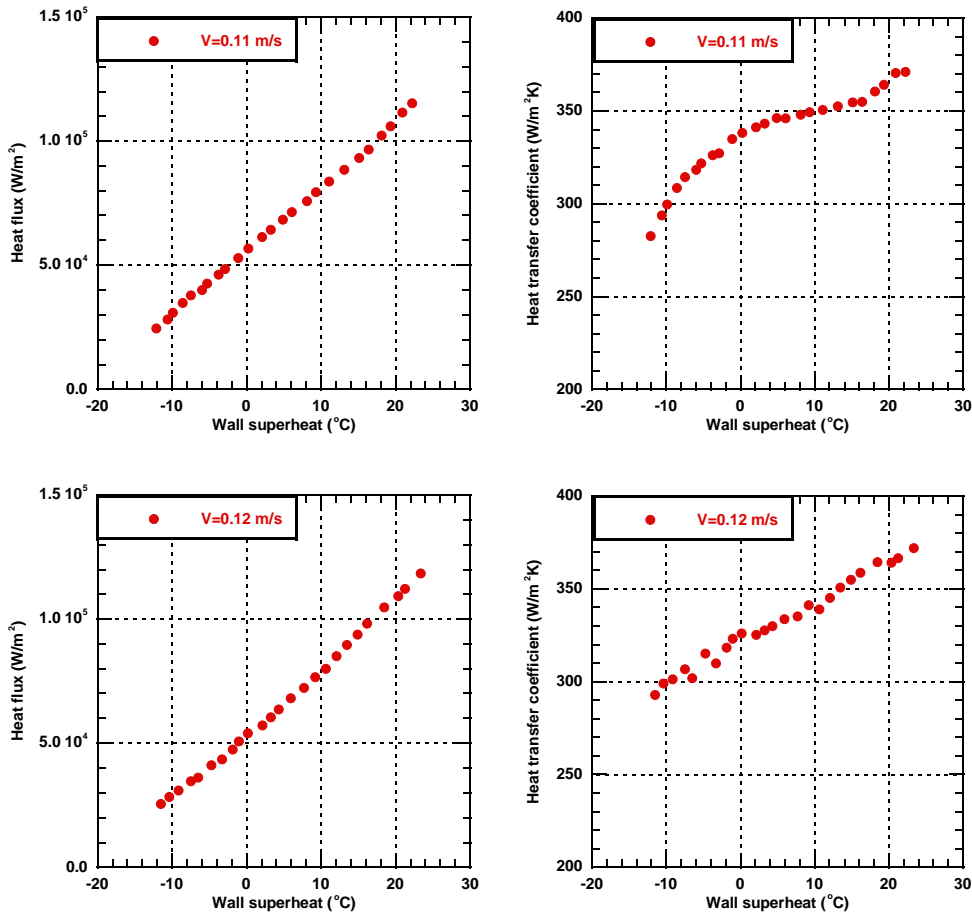


Figure VI-44: Heat Flux and Heat Transfer Coefficient as Functions of Wall Superheat under Bottom Heating Condition

Heat Transfer Coefficient Comparison

The heat transfer coefficients plotted in Figure VI-43 and Figure VI-44 were calculated based on the assumption that a uniform heat transfer on the base surface of heating and on the whole length of the fins. While this is a very reasonable assumption for single-phase heat transfer, the situation for the subcooled flow boiling is more complicated. As shown in Figure VI-41, subcooled boiling only happens on a partial length of the fins. Therefore, once the subcooled boiling dominant region is identified from the experimental data, the heat transfer coefficients should be recalculated according to the fin boiling length for each experimental test. In the present study, the heat transfer coefficient on the boiling portion of the fins was assumed to be an average of the single-phase heat transfer coefficient and the base-surface boiling heat transfer coefficient. The recalculated subcooled boiling heat transfer coefficients on the base surface of heating are shown in Figure VI-45b. As a comparison, the single-phase heat transfer coefficients are also shown in Figure VI-45a. It can be seen from Figure VI-45 that the heat transfer coefficient can be increased by 25%-30% with subcooled flow boiling compared to single-phase heat transfer. It should be pointed out that the experimental tests were conducted on a very smooth aluminum surface with limited nucleation sites. More improvements on heat transfer can be expected with enhanced subcooled flow boiling on an appropriate surface with enough nucleation sites.

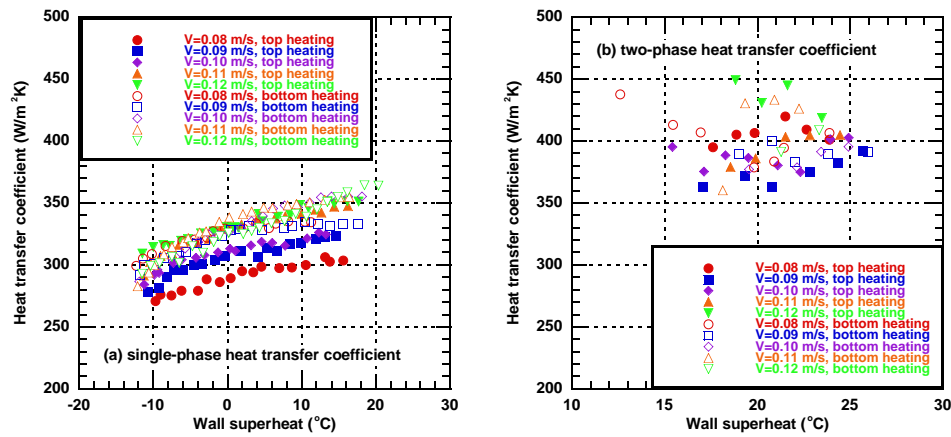


Figure VI-45: Heat Transfer Coefficient Comparison

Conclusions

Use of subcooled flow boiling in the cooling channels to reduce the junction temperature of power electronics in HEVs is a novel cooling technology. Using subcooled flow boiling in the cooling channels can enhance the cooling capacity for vehicle power electronics while the coolant outlet temperature is still below the saturation point. Thus, there is no vapor in the rest of the cooling system. Based on the current numerical simulations, the subcooled flow boiling technology can (a) eliminate the second low-temperature cooling system currently used in HEVs by increasing the coolant inlet temperature to 105°C, thus reducing the weight and cost of HEVs and increasing the efficiency; (b) increase the cooling rate by 25% or reduce the junction temperature compared to convection cooling due to its improved heat transfer; (c) achieve HEV power electronics cooling and junction temperature control at low coolant flow velocities, thus reducing pressure drops and pumping power requirements; and (d) simplify the cooling system of HEV power electronics by integrating it into the main engine cooling system. The subcooled flow boiling system can also be used for cooling of high power-density electronics with a heat flux up to 250 W/cm² and for cooling of all-electric vehicle power electronics.

To investigate heat transfer characterizations of coolant subcooled boiling in practical power electronic cooling channels of HEVs, an experimental test module was designed and fabricated based on the Toyota Prius cold plate. The experimental test module was carefully characterized on heat transfer through numerical simulations and on heat losses through experimental tests. The fin effects on subcooled boiling heat transfer were also considered. These results from calculations and experiments were incorporated into data reduction of single-phase and subcooled boiling heat transfer tests. A series of experimental tests to a 50/50 EG/W mixture was conducted at a 105°C fluid inlet temperature, 2 atmospheric pressures, and various coolant flow velocities under both top heating and bottom heating conditions. The results show that a 25%-30% increase on the heat transfer coefficient is achieved on the tested smooth aluminum surface with limited nucleation sites. More improvements on heat transfer can be expected with enhanced subcooled flow boiling on an appropriate surface with enough nucleation sites.

The future work will focus on (a) developing experimental data-based predictive correlations of the subcooled flow boiling heat transfer coefficients under the application conditions of cooling vehicle power electronics and (b) refining simulation models and results of coolant subcooled flow boiling for cooling of vehicle power electronics based on the experimental heat transfer data.

VI.3.C. Products**Presentations/Publications/Patents**

1. Weihuan Zhao, Wenhua Yu, David M. France, Dileep Singh, Roger K. Smith, Subcooled Boiling Heat Transfer for Thermal Control of Power Electronics in Hybrid Electric Vehicles, SAE 2015 Thermal Management Systems Symposium, September 29-October 1, 2015, Troy, Michigan, USA.
2. Weihuan Zhao, David M. France, Wenhua Yu, Dileep Singh, Subcooled Boiling Heat Transfer for Cooling of Power Electronics in Hybrid Electric Vehicles, ASME Journal of Electronic Packaging 137, July 2015, 031013, DOI: 10.1115/1.4030896.
3. David M. France, Wenhua Yu, Dileep Singh, Weihuan Zhao, System for Cooling Hybrid Vehicle Electronics, Method for Cooling Hybrid Vehicle Electronics, pending U.S. patent application, January 16, 2015.
4. Wenhua Yu, Weihuan Zhao, David M. France, Dileep Singh, Coolant Boiling for Thermal Control of Hybrid Electric Vehicle Power Electronics, SAE 2014 Thermal Management Systems Symposium, September 22-24, 2014, Denver, Colorado, USA.

VI.4. Underhood Thermal Analysis of Tractor-Trailer

T. Sofu, Principal Investigator

Argonne National Laboratory
9700 S. Cass Avenue
Argonne, IL 60439
Phone: (630) 252-4500
E-mail: tsofu@anl.gov

Other Collaborators: Prasad Vegendla

E-mail: svegendla@anl.gov

Lee Slezak, DOE Program Manager

Vehicle Technologies Office
U.S. Department of Energy
Phone: (202) 586-2335
E-mail: Lee.Slezak@ee.doe.gov

Start Date: October 1, 2015

End Date: October 1, 2016

VI.4.A. Abstract

A 3D CFD underhood thermal simulations were performed in two different vehicle platooning configurations; (i) single-lane and (ii) two-lane traffic. The vehicle platooning consists of two identical vehicles, i.e. leading and trailing vehicle. In single-lane, the leading and trailing vehicles separated in longitudinal direction by 30ft, 60ft, 90ft and 150ft. Similarly, the vehicles were separated in two-lane traffic but with a latitude direction of 1.2 m.

In this work, heat exchangers are modeled by two different heat rejection rate models. In the first model, a constant heat rejection rates were considered as similar to no-traffic vehicle condition. In the other model, a varied heat rejection rates were implemented by considering an aerodynamic influence on fuel consumption rates.

In a constant heat rejection rate model, the trailing vehicle thermal performance is significantly dropped in single-lane traffic due to reduced oncoming cold mass air flow velocities from leading vehicle. Also, the similar observations were found in two-lane traffic but at higher vehicle separation distances.

In a varied heat rejection rate model, significant drop in temperature raise was observed in both leading and trailing vehicles when compared to a constant heat rejection rate model in the single-lane and the two-lane traffic conditions. In leading and trailing vehicles, the varied heat rejection rates were obtained from fuel consumption rates.

Apart from the platooning simulations, the fan-shroud optimization performed using Adjoint solver in STAR-CCM+®. In heavy-duty trucks, the cooling package includes heat exchangers, fan-shroud, and fan. The STAR-CCM+® solver was selected and a java macro built to run the primal flow and the Adjoint solutions sequentially in an automated fashion. In this analysis, the primal flow provides flow information (e.g. velocity, temperature and pressure) and the Adjoint solver provides surface morphing details w.r.t. max or min of the specified objective function. In the present work, the fan-shroud surface morphing was performed based on the maximum air mass flow rate through the heat exchanger outlet w.r.t. the spatial positions of the fan-shroud surface. An overall 1.4% increase in cooling air mass flow was observed in the heat exchanger with the optimized/morphed fan-shroud surface. The identified main optimized locations were mainly at the sharp edges of the original manufactured fan-shroud.

Objectives

- Vehicle aerodynamic drag analysis
The aim of this project is to develop a methodology to simulate external aerodynamics of trucks. The main focus of the project is to optimize the fuel consumption.
- Vehicle thermal analysis
The aim of this project is to develop a methodology to simulate underhood thermal performance of trucks. The main focus of the project is to optimize the underhood compartment by modifying fan-shroud and heat exchanger designs, i.e., the CAC and the radiator.

Accomplishments

- Fan-shroud optimization:
- 1.4% raise in cooling air flow was observed with a fan-shroud optimization.
- Vehicle platooning underhood thermal analysis:
- In single- and two-lane leading and trailing vehicle platooning, the significant drop in cold mass flow rates (temperature rise) were observed in cooling package of trailing vehicle due to a big vortex (low velocities) zone between both leading and trailing vehicles.
- At 0 rpm fan speed; 70% lower air mass flow rates (negative performance) observed in trailing vehicle due to low velocity zone from leading vehicle. In single-lane traffic, air flow rates improved with vehicle separation distance.
- At 1400 rpm fan speed; 30% lower air mass flow rates observed in trailing vehicle due to low velocity zone from leading vehicle. In single-lane traffic, air mass flow rates improved with vehicle separation distance.
- In two-lane traffic, at 0 and 1400 rpm, lower air mass flow rates, but negligible compared to single-lane traffic and insignificant to the vehicle separation distance.
- In variable heat rejection, the temperature rise is lower (<4 oC) compared to constant heat rejection (<15 oC) in trailing vehicle [lower amount of heat rejection due to reduced aerodynamic drag and thus leads to lower fuel consumption and lower heat rejection from engine].
- In two-lane traffic and constant heat rejection; the temperature raise is independent to the vehicle separation distance and negligible in variable heat rejection case compared to no-traffic vehicle.

Future Achievements

- Optimization of boat-tail configuration and its influence on aerodynamic drag (e.g. slant angle and plate width)
- Investigation and optimization of road-tunnel influence on aerodynamics of different vehicle configurations in a confined wind obstruction roads
- Identifying the improvements in vehicles for efficient thermal and aerodynamics designs

VI.4.B. Technical Discussion

Background

In automotive and transport industry, aerodynamic thermal improvements are highly desirable in the design of fuel-efficient vehicles. Over the last two decades, continuous efforts to build aerodynamic designs by modifying external vehicle surfaces and through add-on aerodynamic drag reduction devices are growing rapidly. In transport vehicles, external air-flows are heterogeneous and it can have a positive or even negative impact on both aerodynamics and thermal management, depending on the influence of vehicle traffic and vehicle position. Computational Fluid Dynamics (CFD) modeling offers an excellent alternative to experiments in modeling and designing of aerodynamics vehicles. Today's available High Performance

Computing (HPC) allows the building of very robust aerodynamic and thermal fuel-efficient vehicles with minimal amounts of time and cost. This ongoing study is aimed at replacing costly experiments by designing feasible modeling prototypes of the heavy vehicle. CFD is the main tool as mentioned above in designing and optimizing the underhood configuration and the external aerodynamics of the heavy-duty vehicle.

Optimization of medium- and heavy-duty vehicle aerodynamic drag and thermal loads is an important design consideration with significant implications for fuel efficiency. A medium/heavy-duty vehicle's drag-producing components include the mirrors, side extenders, wheels, cabin, and trailer, and also including cooling devices and engine. A component-based analysis helps to identify improvements in aerodynamic drag and cooling performance. Aerodynamic drag optimization lies mostly in redesigning the external surfaces of the above-mentioned vehicle components. On the other hand, vehicle thermal design was focused on the underhood compartment, which comprises the engine, radiator, Charge Air Cooler (CAC), fan-shroud and fan. An efficient cooling system reduces thermal loads and maximizes the use of power because conventional underhood configurations allow conversion of only a fraction of the total fuel energy into mechanical power and the rest is lost through the exhaust system and heat rejection. An ideal temperature distribution in and around the engine allows redesign of a heavy vehicle's underhood configuration and helps to achieve fuel efficiencies through cooling system optimization.

Technical Barriers

- Developing methodology to analyze each phenomena/component separately and its effect on overall full-vehicle performance.
- Model validation with prototypes.
- Scarcity of acceptable-quality heat exchanger performance data and pressure drop.

Technical Targets

- Development of physics-based models and numerical techniques.
- Identification of potential fuel savings in vehicle platooning configurations and improvement of external vehicle surfaces to reduce aerodynamic drag.
- Identification of potential improvements in cooling package thermal efficiency.

Introduction

In the automotive and transport industry, aerodynamic thermal improvements are highly desirable in the design of fuel-efficient vehicles since the expected *global fuel consumption* to grow at a compound annual growth rate (CAGR) of 2.1 percent over the period 2014-2019 [1]. The optimized efficiency in vehicle aerodynamics and thermal management of an engine cooling system and underhood components is highly desirable for achieving durable and fuel-efficient designs that meet today's energy demand [2-5]. CFD analysis offers an inexpensive and fast alternative to experiments. Commercially available CFD simulation software such as STAR-CCM+® can be used to investigate and assess the various factors that affect aerodynamic drag and underhood thermal vehicle performance [3]. Aerodynamic and thermal optimization of vehicles can reduce fuel consumption and vehicle emissions while improving vehicle durability.

On-road highways, vehicle platooning reduces a significant amount of fuel consumption in both leading and trailing vehicles. Most of the recent studies had shown the aerodynamic considerations in vehicle platooning [6-8]. In platooning configurations, lower cold mass air flow rates were observed through the cooling package particularly in trailing vehicles by assuming a constant heat rejection rates for fuel condenser, Charge Air Cooler (CAC) and radiator.

Vegendla et al. [6] had shown the significant aerodynamic drag reduction at lower vehicle separation distance in single-lane traffic. The following observations were also made in their recent work. The aerodynamic drag reduction reduces with an increase of vehicle separation distance in both leading and trailing vehicles. The aerodynamic drag reduction in trailing vehicle was mainly due to the lower air velocities towards the front side of the cabin, which drastically reduces the static pressure at trailing vehicle cabin and thus leads to a lower

aerodynamic drag values when compared to no-traffic vehicle. In two-lane traffic, trailing vehicle aerodynamic drag reduction raise was observed with an increase of vehicle separation distance due to the shedding of low velocity zone from leading to trailing vehicle (vehicles are separated laterally and longitudinally). In leading vehicles, the drop in aerodynamic drag reduction was observed with an increase of vehicle separation distance due to negligible influence of trailing vehicle on leading vehicles.

The objective of this work is to evaluate the thermal performance of on-highway platooning vehicles including fan-shroud optimization in no-traffic vehicle underhood compartment. Underhood thermal performances were modeled by (i) assuming a constant heat rejection rate in both leading and trailing vehicle cooling packages and (ii) variable heat rejection rates were considered to mimic the on-road vehicle platooning conditions based on vehicle fuel consumption rates. It should be noted that the fuel consumption rates varies with an external aerodynamics drag predictions compared to no-traffic vehicle.

In this work, 3D CFD modeling and simulations were performed in STAR-CCM+® commercial tool [1,2,4]. Heat exchanger mass flow rates and thermal numerical results were analyzed for multiple vehicle interactions occurring while the vehicles were under the influence of the on-road traffic that may be impacted by the overall aerodynamic drag of the leading and the trailing vehicles in both single and multiple lanes.

Approach

Aerodynamic drag simulations: 3D isothermal steady-state simulations were conducted using the segregated flow solver in STAR-CCM+. Gas-phase turbulence was modeled using k-ε with standard parameters [9]. Operating and inlet conditions were listed in Table VI-3.

Table VI-3: Operating conditions for aerodynamic drag simulations

Operating Conditions	Values
Velocity Inlet [mph]	55
Temperature Inlet [K]	300
Yaw Angle [deg]	-6, 0 and 6
Outlet Pressure [bar]	1
Computational Domain [m3] [Length x Width x Height]	200x 500 x 100
Number of Hexahedral Cells [millions]	30 to 200
Side Walls	Periodic

Underhood thermal simulations: 3D non-isothermal steady-state simulations were carried out using the segregated flow solver in STAR-CCM+. Gas-phase turbulence was modeled using k- ε with standard parameters. For Fan, the Moving Reference Frame (MRF) is implemented. Operating and inlet conditions were shown in Table VI-3.

In both leading and trailing vehicle heat exchangers, i.e. fuel condenser, CAC and radiator, were modeled using porous body with inertial and viscous resistances as shown in Table VI-8. The heat exchangers and fan locations were described in Figure VI-46. In both vehicles, the fan was operated at constant speed of 1400 rpm. The total heat rejection rates of fuel condenser, CAC and radiator were considered to be 11, 24.25 and 55 kW, respectively.

Table VI-4: Heat exchanger porous body modeling

	Fuel Condenser	CAC	Radiator
Inertial forces [kg/m4]	66	67	330
Viscous forces [kg/m3-s]	66	415	335
Const. heat rejection rate [kW]	11	24.25	55

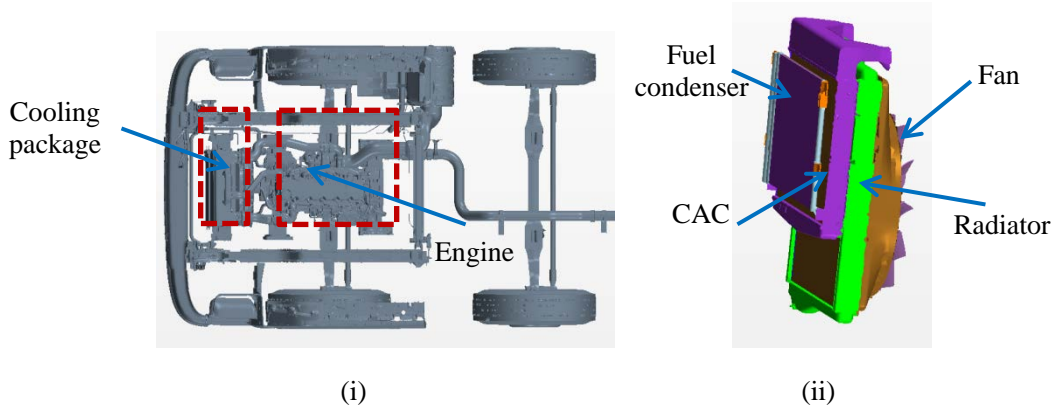


Figure VI-46: Vehicle underhood components; (i) top view and (ii) cooling package

Adjoint simulations for fan-shroud optimization: The optimization process is accomplished using the Adjoint solver and mesh morpher in STAR-CCM+® [10].

First, a well converged primal solution is obtained on a polyhedral mesh. The primal solution is solved steady-state, using a Coupled solver approach and k-epsilon turbulence. Since a steady-state approach is used, actual movement of the fan geometry is not modeled; rather, a Moving Reference Frame approach is used to simulate the effects of the moving geometry. Moreover, the heat transfer in the heat exchangers was not modeled, and compressibility effects were included. The primal solution is driven to convergence by successively increasing the Coupled Solver Courant Number. Convergence is judged by monitors of residuals, which are driven as low as possible, and of mass flow rate through the radiator in front of the fan, which is driven to an asymptotic value.

Using the converged primal solution, a cost function of mass flow rate through the radiator with respect to fan shroud position is solved on pre-defined control points (Figure VI-47i) situated near the fan shroud surface to obtain a solution to the Adjoint equation. The solution to the Adjoint is used to calculate sensitivities of the primal flow to changes in control point position, resulting in a field of Adjoint sensitivity vectors on these points, seen in Figure VI-47ii. These Adjoint sensitivity vectors indicate in which direction movement of the control points, and by extension, the underlying geometry, would increase the mass flow rate, and in which direction movement would decrease the mass flow rate.

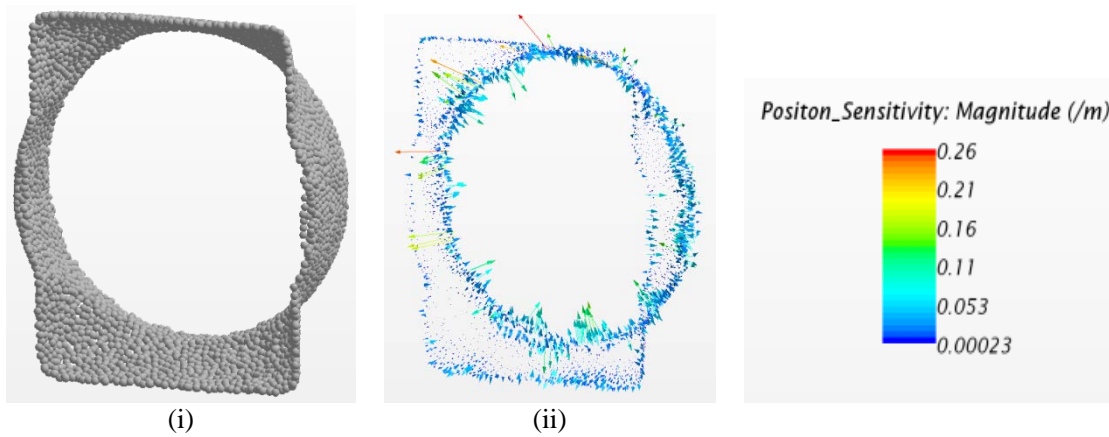


Figure VI-47: Fan-shroud; (i) control points and (ii) Adjoint position sensitivity vectors

These vectors are then scaled using the following definition: $\frac{\text{MaxDisplacement}}{\text{MaxAdjointReport}}$ in order to limit the maximum displacement of the morpher, thus producing a smoother transition to the optimal shape. The scaled sensitivity vector values are then used as displacements for the morpher. The morphing of these control points results in a deformation of the mesh, and ultimately, in the underlying fan shroud geometry. In this work, the ‘MaxDisplacement’ was set at 5 mm and ‘MaxAdjointReport’ was obtained from a report of the maximum ‘Adjoint of Mass Flow w.r.t. Position’.

This process of solving for the primal solution, Adjoint solution, Adjoint sensitivities, and mesh deformation is then repeated multiple times to generate a cumulative displacement of the control points and the shroud geometry in order to increase the mass flow rate through the radiator. Mesh quality metrics, such as cell quality and volume, are reported after each morph of the control points to ensure that the morphing procedure has not degraded the mesh to a point that simulation results would suffer. If the mesh quality falls below a pre-determined value, the driving java macro automatically exports the current morphed geometry, replaces the original CAD model, and re-meshes the domain, resulting in a new, higher quality mesh on the morphed geometry. The process then continues on this new mesh. Automation of this process is accomplished through the use of a java macro in STAR-CCM+®.

Results

Single-lane Traffic

Configuration-1

As shown in Figure VI-48, leading and trailing vehicle separated only in longitudinal direction. The underhood thermal simulations were performed to analyze the cooling package temperatures.

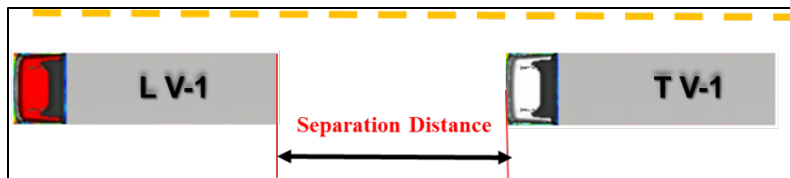


Figure VI-48: Leading Vehicle (LV) and Trailing Vehicle (TV) configuration in single-lane traffic

As shown in Figure VI-49, the Trailing Vehicle (TV) cooling package temperature raise drops with an increase of vehicle separation distance when compared to no-traffic vehicle. This was mainly due to the amount of cold mass air flow rates raises with an increase of the vehicle separation distance [11]. At lower vehicle separation distance of 30 ft., around 20% (equivalent to 25% temperature raise) drop in mass flow rates were observed. This was mainly due to the low velocity vortex region between both leading and trailing vehicles. On the other hand, there was no significant temperature raise in the leading vehicle when compared to no-traffic vehicle

(not shown). It should be noted that the calculated temperatures are averaged of three different yaw angles 0°, -6°, and 6°.

As shown in Figure VI-49, the significant temperature rise was observed in trailing vehicle heat exchangers, i.e., fuel condenser, CAC and radiator. In this model, the constant heat rejection rates were considered for both leading and trailing vehicles as shown in Table VI-4. The raise in temperature was mainly due to the lower oncoming air flow from leading vehicle as described above. As shown in Figure VI-50, the significant hot regions were observed in trailing vehicle when compared to leading vehicle.

In this section, the varied heat rejection rates were obtained from an aerodynamic drag influence on heat rejection rates (heat rejection is proportional to the fuel consumption) as shown in the following equation. It should be noted that, the amount of fuel consumption drop or raise is roughly equal to an half of the amount of aerodynamic drag drop or raise, respectively. For all vehicle platooning configurations, the aerodynamic drag values of leading and trailing vehicles can be found in Vegendla et al. [6,11].

$$\dot{Q} = \dot{Q}_{no-traffic} \left[1.0 - \frac{\left(1.0 - \frac{C_{d,i}}{C_{d,no-traffic}^{yaw=0^\circ}} \right)}{2} \right]$$

where i= 0, 6 and -6°

where, \dot{Q} is heat rejection rates and Cd is vehicle aerodynamic drag coefficient.

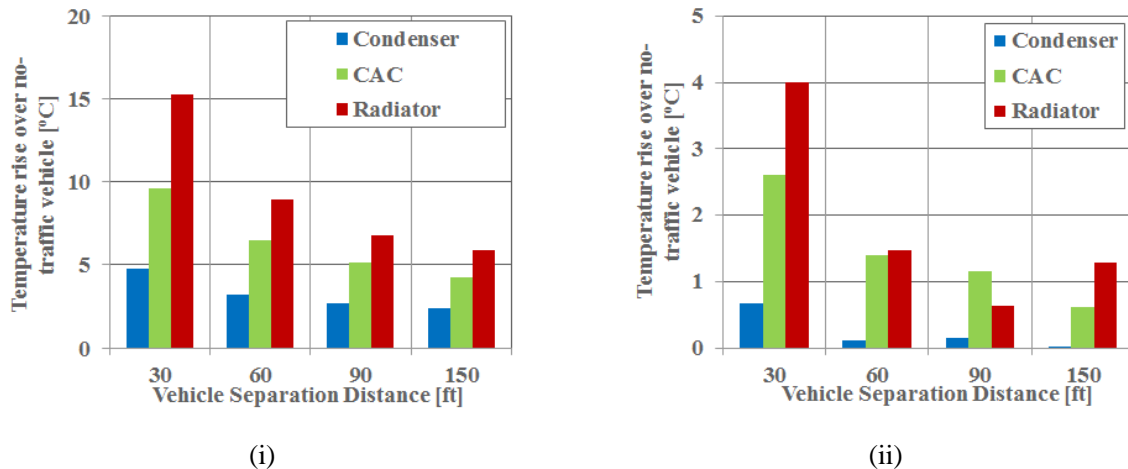


Figure VI-49: Comparison of cooling package temperature in single-lane traffic vehicles at different vehicle separation distances [averaged values of three different yaw angles 0°, -6°, and 6°]; (i) Constant heat rejection rate and (ii) variable heat rejection rate.

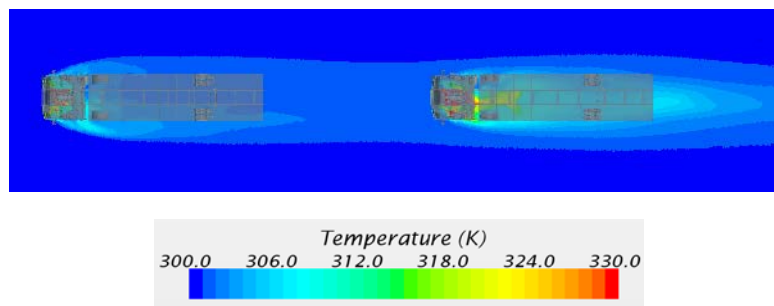


Figure VI-50: Temperature distribution in 0° yaw angle at 30ft vehicle separation distance (constant heat rejection rate)

Multi-lane Traffic

Configuration-2

As shown in Figure VI-51, leading and trailing vehicle separated in longitudinal and latitude directions. The latitude direction was kept at 1.2 m. The underhood thermal simulations were performed to analyze the cooling package temperatures.



Figure VI-51: Leading Vehicle (LV) and Trailing Vehicle (TV) configuration in two-lane traffic

As shown in Figure VI-52i, the raise in temperature was almost independent of the vehicle separation distance in two-lane traffic condition and for constant heat rejection rate simulations. This was mainly due to the average cold mass air flow velocities were almost constant around the trailing vehicle cooling package [11]. The raise in temperature was mainly due to the lower oncoming air flow from the leading vehicle as discussed in Vegendla et al. [11]. In the leading vehicle, no changes were observed in temperatures when compared to no-traffic vehicle (not shown). Also, the similar observations were found in single-lane traffic condition. The small changes in temperatures might be due to the following two reasons; (i) wind flow direction and (ii) higher temperature stream from the leading vehicle. As shown in Figure VI-52, the lower temperature raise was observed when compared to single-lane traffic trailing vehicle (Figure VI-49).

As shown in Figure VI-52ii, the temperature rise drops in trailing vehicle with separation distances compared to constant heat rejection rate (Figure VI-49). In variable heat rejection rate, lower temperatures observed in trailing vehicle than in single-lane for constant heat rejection rate. This is due lower fuel consumption leads to low heat rejection rates, as discussed above. The temperature changes in the fuel condenser were negligible.

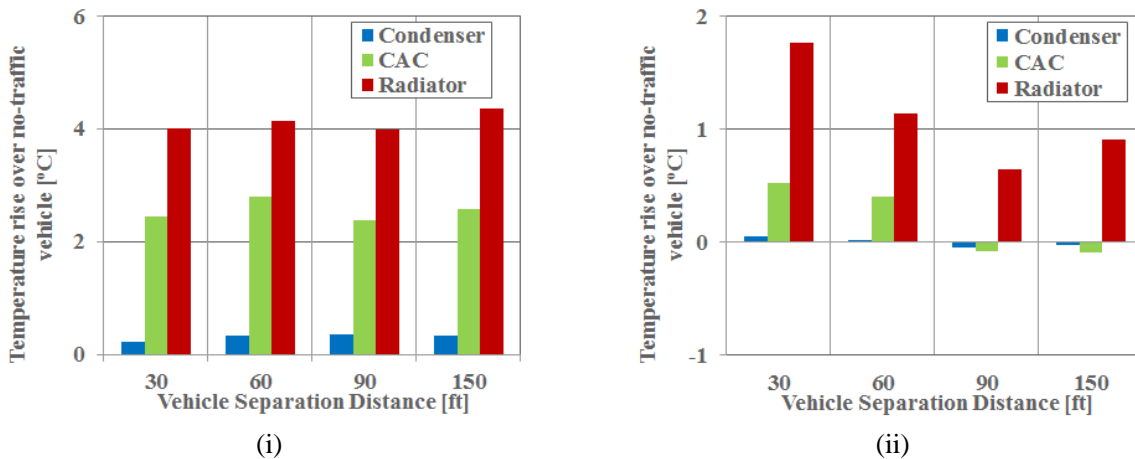


Figure VI-52: Comparison of cooling package temperature in one-way two-lane traffic vehicles at different vehicle separation distances [averaged values of three different yaw angles 0°, -6°, and 6°]; (i) Constant heat rejection rate and (ii) variable heat rejection rate.

As shown in Figure VI-53, temperature fields are similar in both leading and trailing vehicles except few degrees temperature raise in trailing vehicle (Figure VI-52).

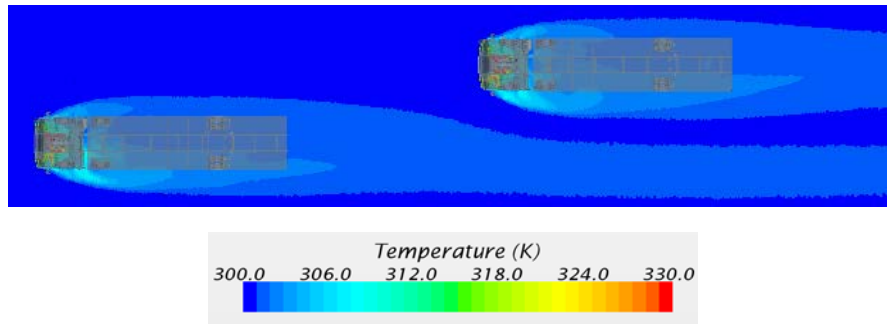


Figure VI-53: Temperature distribution in 0° yaw angle at 30ft vehicle separation distance (constant heat rejection rate)

Fan-shroud Optimization Using Adjoint Solver

In no-traffic vehicle, heat exchangers, i.e. CAC and radiator, were modeled using porous body with inertial and viscous resistances as shown in Table VI-5. The heat exchangers and fan locations were described in Figure VI-54. The operating conditions were specified in the Table VI-6. Additional modeling details can be found in our recent publication [10]. It should be noted that heat transfer in the heat exchangers was not modeled, and compressibility effects were included as described in Approach Section.

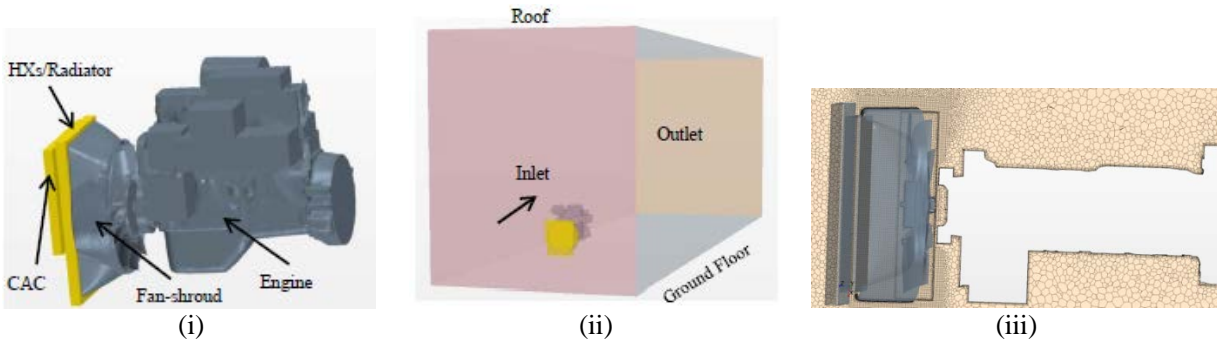


Figure VI-54: Geometry (i) vehicle underhood compartment (ii) computational domain, and (iii) mesh side view

Table VI-5: Heat exchanger porous body modeling

	CAC	Radiator
Inertial forces [kg/m ⁴]	91.67	98.41
Viscous forces [kg/m ³ -s]	-31.43	312.07

Table VI-6: Operating Conditions

Fan speed [rpm]	1400
Inlet velocity [kph]	20
Inlet Temperature [K]	300
Pressure outlet [Pa]	0

Fan-shroud optimization was carried out using the coupled flow solver, Adjoint solver, and mesh morpher in STAR-CCM+® as discussed in Approach section. The optimized solution was based on 20 iterations of primal flows and Adjoints. Mehravaran and Zhang [12] have performed CFD simulations with different shroud

shapes. Contrary, we performed a simulation using the original shroud and optimized its design using the Adjoint solver without any externally modifications of the fan shroud. Note, the fan insertion depth is kept at constant and the only expected fan-shroud changes were in radial direction.

In Figure VI-55, the original shroud surface consists of sharp edges when compared to the morphed/optimized surfaces. The highlighted surface edges show the modified/optimized edges which provide lower pressure loss and higher mass flow rates through the heat exchangers (Figure VI-55(ii)).

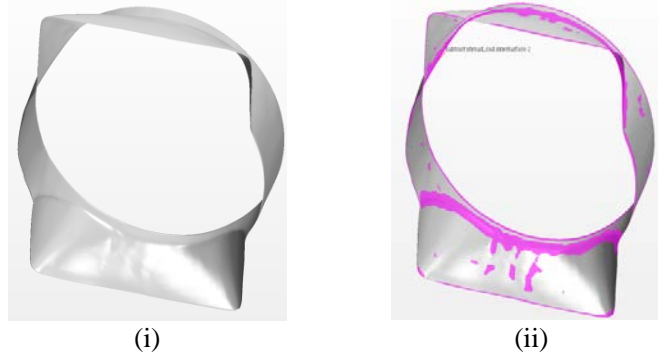


Figure VI-55: Comparison of (i) original and (ii) optimized fan-shroud

As shown in Figure VI-56, the position sensitives are the main determining factor used to optimize the fan-shroud surface. The higher the position magnitude is, the larger the morpher displacement will be on this surface. The position vector direction guides the surface changes towards inner or outer movements of the surface. The significant position sensitivities drop was observed with an increase of adjoint iterations (see 6th and 2nd iteration) and consequently it leads to drop in % of fan-shroud morphing.

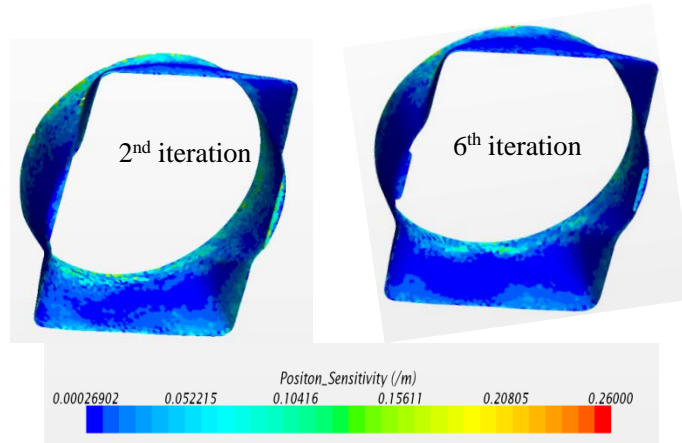


Figure VI-56: Position sensitivity magnitudes at 2nd and 6th iteration [surface optimizes @ higher position sensitivities]

As shown in Table VI-7, a 1.4% increase in air mass flow rate was observed in the heat exchanger (radiator) when compared to original fan-shroud model. To be noted, the simulation residuals are dropped to 10E-8 for flow variables and 10E-10 or lower for Adjoint position sensitivities. In Table VI-7, the simulation data shows that the optimized fan-shroud has a higher cold mass air flow rate compared to the original design. The original fan-shroud has several sharp surfaces, leading to flow separation and a reduced air flow rate through the heat exchangers, as discussed above.

Table VI-7: Heat exchanger cooling air mass outflow rates

Original fan-shroud [kg/s]	3.8
Optimized fan-shroud[kg/s]	3.852 (~1.4%)

Conclusions

A 3D CFD underhood thermal simulations were performed in two different vehicle platooning configurations; (i) single-lane and (ii) two-lane traffic. In this work, heat exchangers were modeled by two different heat rejection rate models. In the first model, a constant heat rejection rates were considered. In the other model, a varied heat rejection rates were implemented by considering an aerodynamic influence on fuel consumption rates.

In trailing vehicle, significant thermal performance drop was observed in both single-lane and two-lane traffic due to lower cold mass air flow rates. A significant temperature raise was observed in the constant heat rejection rate model when compared to the varied heat rejection rate model. On the other hand, the temperature raise was significantly dropped in the varied heat rejection rate model due to an aerodynamic influence on vehicle fuel consumption rates.

In leading vehicle, no changes were observed in the constant heat rejection rate model for both single-lane and two-lane traffic conditions. Contrary, lower temperatures were observed in the varied heat rejection rate model at lower vehicle separation distances due to lower fuel consumption.

Apart from the truck platooning, fan-shroud optimization performed in STAR-CCM+® using Adjoint solver. The flow variables, velocity, pressure and turbulence parameters were solved by using the Coupled Solver. Consequently, the Adjoint solver provides the position sensitivities around the fan-shroud surface w.r.t. heat exchanger outlet air mass flow rates. The fan-shroud surface morphing was carried out using the calculated position sensitivities from the Adjoint solver.

A total 1.4% increase in cold air flow was observed with an optimization of the fan-shroud surface. The improvement gain was mainly due to smoothing of the fan-shroud surface edges, rather than the sharp edges which are present in the original fan-shroud model from the manufacturer. The air flow around the optimized surface edges was much smoother, as they act to reduce pressure losses and ultimately led to a higher mass flow rate through the heat exchanger. Further evaluation is underway to maximize the cooling air mass flow benefit.

VI.4.C. Products

Presentations/Publications/Patents

1. Vegendla, S.N.P., Sofu, T., Saha, R., Kumar, M.M., and Hwang, L.K (2015). 'Investigation on Underhood Thermal Analysis of Truck Platooning' Int. Journal of Commercial Vehicles (submitted).
2. Vegendla, S.N.P., Sofu, T., Saha, R., Kumar, M.M., and Hwang, L.K., D, Steven. (2016). 'Fan-shroud Optimization Using Adjoint Solver', 2016 SAE COMVEC, 2016-01-8070. DOI:10.4271/2016-01-8070.
3. Vegendla, S.N.P., Sofu, T., Saha, R., Kumar, M.M., and Hwang, L.K (2015). 'Aerodynamic drag and Underhood Thermal Analysis of Two Heavy-duty Vehicles'. Int. Journal of Aerodynamics (Accepted).
4. Vegendla, S.N.P., Sofu, T., Saha, R., Kumar, M.M., and Hwang, L.K (2015). 'Aerodynamic Drag Optimization of Medium-duty Delivery Truck'. SAE Int. Journal of Commercial Vehicles (under review).

VI.4.D. References

1. <http://www.prnewswire.com/news-releases/global-fuel-consumption-market-for-transportation-industry-2015-2019-300056696.html>
2. Lee, S. 'Advanced vehicle technology Analysis and Evaluation Activities and Heavy Vehicle Systems Optimization Program'. US DOE APR, 2008.
3. Vegendla, S.N.P., Sofu, T., Lee, S. 'Aerodynamics and Underhood Thermal Analysis of Heavy/Medium Vehicles'. US DOE Annual Report -Vehicle and System Simulation and Testing R&D, 2014, DOE-EE-1165, pp: 345-349.
https://energy.gov/sites/prod/files/2015/08/f25/vehicle_systems_annual_report_080415.pdf

4. Wood, R.M and Bauer, S.X.S. 'Simple and Low-Cost Aerodynamic Drag Reduction Devices for Tractor-Trailer Trucks'. SAE International, 2003-01-3377, 2003.
5. Song, K.S., Kang, S.O., Jun, S.O., Park, H.I., Kee, J.D., Kim, K.H and Lee, D.H. 'Aerodynamic Design Optimization of Rear Body Shapes of a Sedan for Drag Reduction'. International Journal of Automotive Technology, 13(6): 905–914, 2012.
6. Vegendla, P., Sofu, T., Saha, R., Kumar, MM., Hwang,LK. 'Investigation of Aerodynamic Influence on Truck Platooning'. 2015 SAE COMVEC, SAE International technical paper, 2015-01-2895. doi:10.4271/2015-01-2895.
7. Smith, J., Mihelic, R., Gifford, B., Ellis, M. 'Aerodynamic Impact of Tractor-Trailer in Drafting Configuration'. SAE technical paper, 2014, DOI:10.4271/2014-01-2436.
8. Lammert, MP., Duran, A., Diez, J., Burton, K. 'Effect of Platooning on Fuel Consumption of Class 8 Vehicles Over a Range of Speeds, Following Distances, and Mass'. SAE technical paper, 2014, DOI:10.4271/2014-01-2438.
9. STAR-CCM+-v9.06.011, User Guide, 2014.
10. Vegendla, S.N.P., Sofu, T., Saha, R., Kumar, M.M., and Hwang, L.K., D, Steven. (2016). 'Fan-shroud Optimization Using Adjoint Solver'. 2016 SAE COMVEC, 2016-01-8070.
11. Vegendla, S.N.P., Sofu, T., Lee, S. 'Aerodynamics and underhood thermal analysis of Truck Platooning'. US DOE Annual Report -Vehicle systems, 2015, DOE-EE-1304, pp:554-566. <http://energy.gov/sites/prod/files/2016/03/f30/Vehicle%20Systems%202015%20Annual%20Progress%20Report.pdf>
12. Mehravaran, M. and Zhang, Y. 'Optimizing the Geometry of Fan-Shroud Assembly Using CFD'. SAE Technical Paper 2015-01-1336, 2015, doi:10.4271/2015-01-1336.

HYBRIDIZATION

VI.5. Cummins MD&HD Accessory Hybridization CRADA

Dean D. Deter, Principal Investigator, R&D Staff Researcher

Oak Ridge National Laboratory (ORNL)

1 Bethel Valley Road

Oak Ridge, TN 37810

Phone: (865) 576-8620

E-mail: deterdd@ornl.gov

David Anderson, DOE Program Manager

Vehicle Systems

Phone (202) 287-5688

E-mail: David.Anderson@ee.doe.gov

Start Date: July 1, 2013

End Date: January 16, 2016

VI.5.A. Abstract

Objectives:

- Analytically verify novel heavy truck accessory hybridization and electrification approaches, and experimentally validate prototype hardware utilizing the ORNL Vehicle Systems Integration (VSI) Laboratory's component test cell and Cummins' test vehicle.
- Develop and validate medium/heavy duty accessory models by means of data collection on a test vehicle and extraction from Cummins' preexisting models.
- Using the project's generated models and market research, choose and develop an electric or hybrid architecture and controls for one or more accessories depending on fuel consumption reduction and perceived market acceptability.
- Integrate the conventional system and chosen prototype architecture in the component lab for system testing and controls development. This culmination, allows for good comparison of the two systems utilizing the repeatability of the lab environment.
- Add finished system to one of Cummins test vehicles for a proof of concept test.

Accomplishments:

- Typical vehicle level models use a "lumped" mechanical and electrical accessory structure that is not detailed enough to represent dynamic accessory behavior. ORNL has integrated Cummins' accessory models into Autonomie's vehicle architecture to capture these behaviors at a vehicle level.
- Using test vehicle data the power steering model has been validated within the acceptable system assumptions.
- Exercised three different vehicles to determine which vehicle application would have the most impact of fuel consumption: a MD pickup/delivery truck, an HD class 8 bus, and an HD class 8 line haul sleeper cab.
- Validated the class 8 line haul sleeper cab to be accurate within 5% of a chassis tested vehicle.
- Using results from the simulation study as well as data from literature reviews, the CRADA team was able to determine that while line haul sleeper cabs made the smallest impact with hybrid accessories

for driving when compared to MD, P&D, or HD bus, they made the biggest impact when looking into idle mitigation and overnight hotel loads.

- Based on the findings from the literature review and simulation study ORNL proposed and designed a hybrid Auxiliary Power Unit (h-APU) architecture that would allow for hybridization for the air conditioning, electrification of the condenser fans, and energy storage for other electrical hotel loads. This allows for the truck to eliminate or greatly reduce all over night idling by providing hotel loads from a battery pack that utilizes regenerative braking for charging.
- The baseline controls and system architecture have been designed and implemented in Autonomie for further testing and controls development.
- Two possible architectures were chosen and designed for driving the A/C compressor. One is a hybrid system which continues to utilize the existing compressor and the other being a fully electric compressor system.
- Two out of the three lab testing setups have been completed; the conventional and hybrid systems.
- Providing NREL with the proper resources, they have developed a baseline CoolSim Quasi-Transient air conditioning model that can be used with the simulation portion of the system. This will provide a much needed high fidelity model for use in future simulation studies as well as controls development.
- Cummins performed proof of concept testing for the h-APU system, providing validation and better development for all of the work done by simulation and in the component test cell.
- ORNL tested a second compressor architecture that will allow Cummins to make a more educated selection if the prototype system were to be chosen for commercialization.
- Using the data generated in ORNL's VSI Laboratory NREL improved and validate their baseline model to provide even better accuracy for future use in Coolsim and better support should Cummins decide to commercialize.

Future Achievements:

- None, Project Complete

VI.5.B. Technical Discussion

Background

Medium and heavy duty trucks are a growing market and integral part of our society. From the home delivery of goods by medium duty trucks to the freight hauling of heavy duty line haul trucks, they are the main source of material and goods transport. Due to these trends, there is an overwhelming need to quickly address key problems with excess fuel usage and emissions production of these diesel vehicles.

Modern trucks have become much more advanced in terms of engine, aftertreatment, and transmission technologies which greatly reduced both fuel consumption and emissions. Due to these improvements, focus of truck OEMs has shifted to start looking at what other aspects of MD and HD trucks can be impacted by advanced technologies.

Introduction

There are many areas of MD and HD vehicles that can be improved by new technologies and optimized control strategies. Component optimization and idle reduction need to be addressed, this is best done by a two part approach that includes selecting the best component technology, and/or architecture, and optimized controls that are vehicle focused. While this is a common focus in the light duty industry it has been gaining momentum in the MD and HD market as the market gets more competitive and the regulations become more stringent.

When looking into systems optimization and idle reduction technologies, affected vehicle systems must first be considered, and if possible included in the new architecture to get the most benefit out of these new capabilities. Typically, when looking into idle reduction or component optimization for MD/HD, the vehicle's accessories become a prime candidate for electrification or hybridization. While this has already been studied on light duty vehicles (especially on hybrids and electric vehicles) it has not made any head way or market penetration in most MD and HD applications. If hybrids and electric MD and HD vehicles begin to break into the market this would be a necessary step into the ability to make those vehicles successful by allowing for independent, optimized operation separate from the engine.

Approach

ORNL and Cummins began this project by discussing which approach would be most successful in reducing fuel consumption, but also which approach would gain acceptance by the market to enable this technology to penetrate the market more quickly. A two phased approach was selected due to ORNL's test cell capabilities and Cummins market resources and access to a test vehicle for data and proof of concept test.

The first phase is a modeling/simulation/data collection and market study phase that is focused on determining, which accessories would be feasible to hybridized/electrify, what accessories have fuel consumption benefits if hybridized/electrify, the ideal vehicle application which would benefit most from these new technologies, and what architecture on the selected vehicle type would have the most impact on fuel consumption.

Phase one of the project started by collecting all of the data and resources ORNL and Cummins had to begin the modeling and simulation. Cummins was able to supply base models for the four major accessories that the project would be addressing: the engine's cooling fan, the vehicle air conditioning system, the power steering system, and the vehicle's air compressor and air brake system. ORNL opted to use Argonne National Laboratory's Autonomie as the platform for simulation work on a vehicle level.

The first change to model was to switch the Autonomie accessory model structure from a "lumped" accessory structure (Figure VI-57) to a separated accessory structure (Figure VI-58) in order to capture all of the dynamic behaviors of each accessory and how those behaviors change based on vehicle type and drive cycle variability.

Several vehicle types were considered but ultimately class 8 line haul (LH) sleeper cabin trucks were chosen as the projects focus. This vehicle was assessed due to its overwhelming market size and total amount of fuel consumed per year compared to the other two vehicles. Additionally, sleeper cabs spend a large amount of time idling, especially during the driver's overnight hoteling in the warm months of the year. ORNL had access to parameters and data on this vehicle type. The engine and transmission for this vehicle has been tested in ORNL's VSI lab as well as had access to vehicle parameters for a Kenworth T700 to further increase the fidelity of this vehicle model (Figure VI-59).

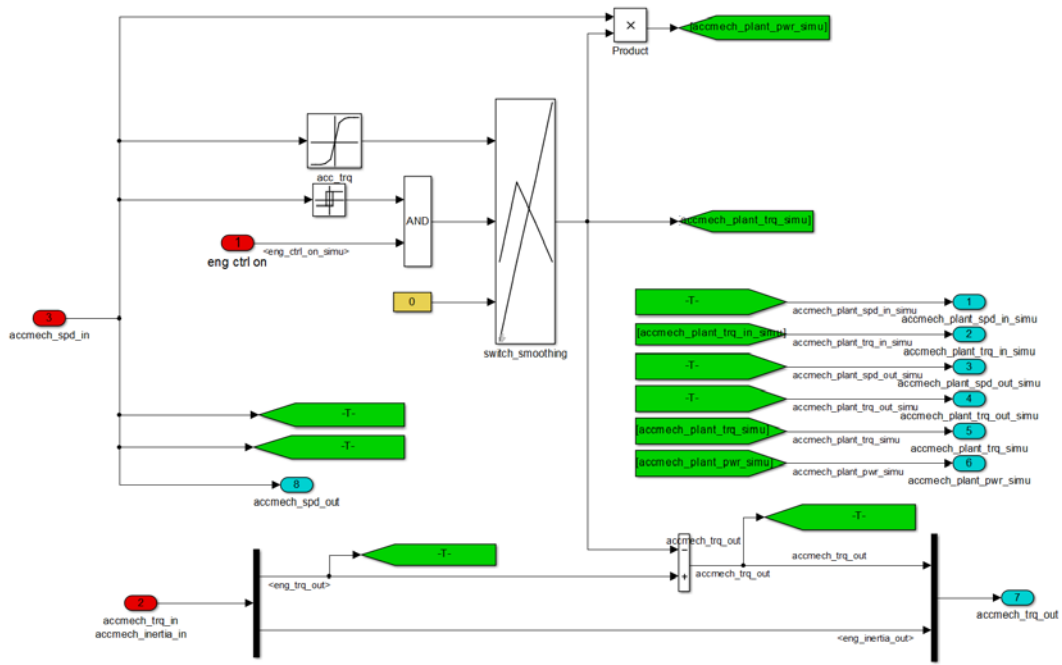


Figure VI-57: Original Autonomie “lumped” mechanical accessory model.

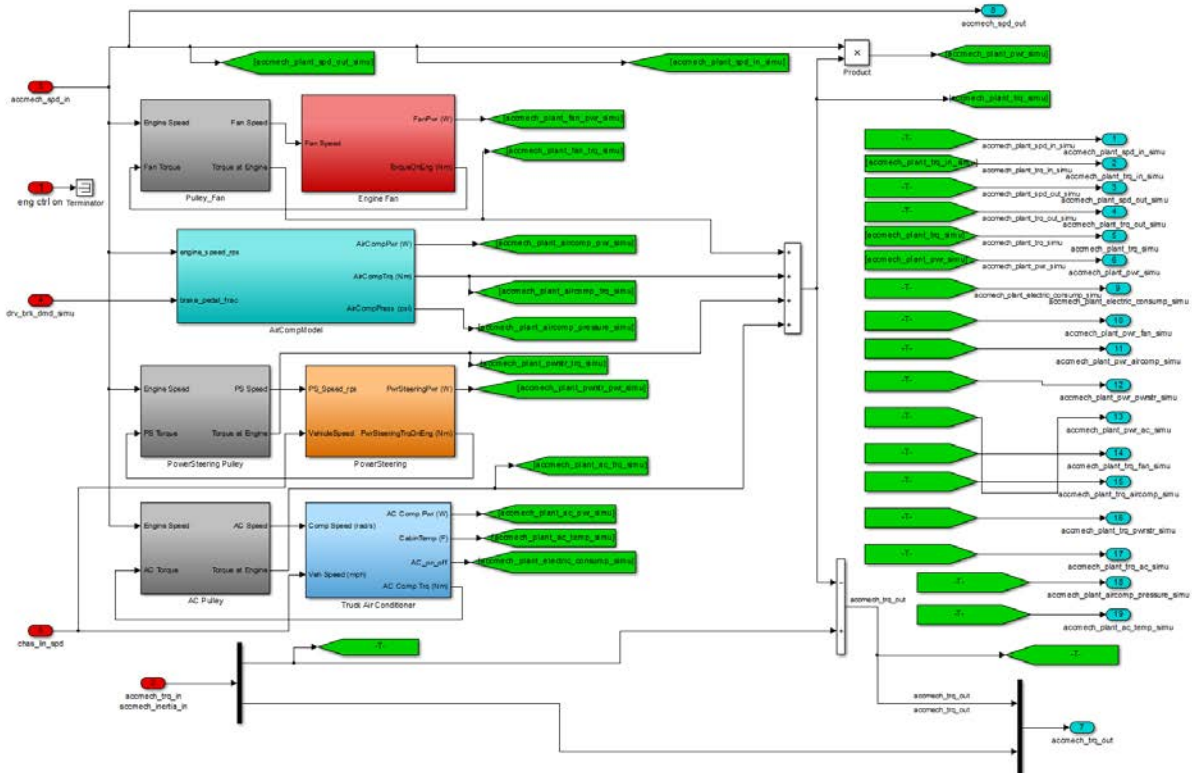


Figure VI-58: Separated accessory models. (cooling fan, air compressor, power steering, air conditioning, and electrical accessories)

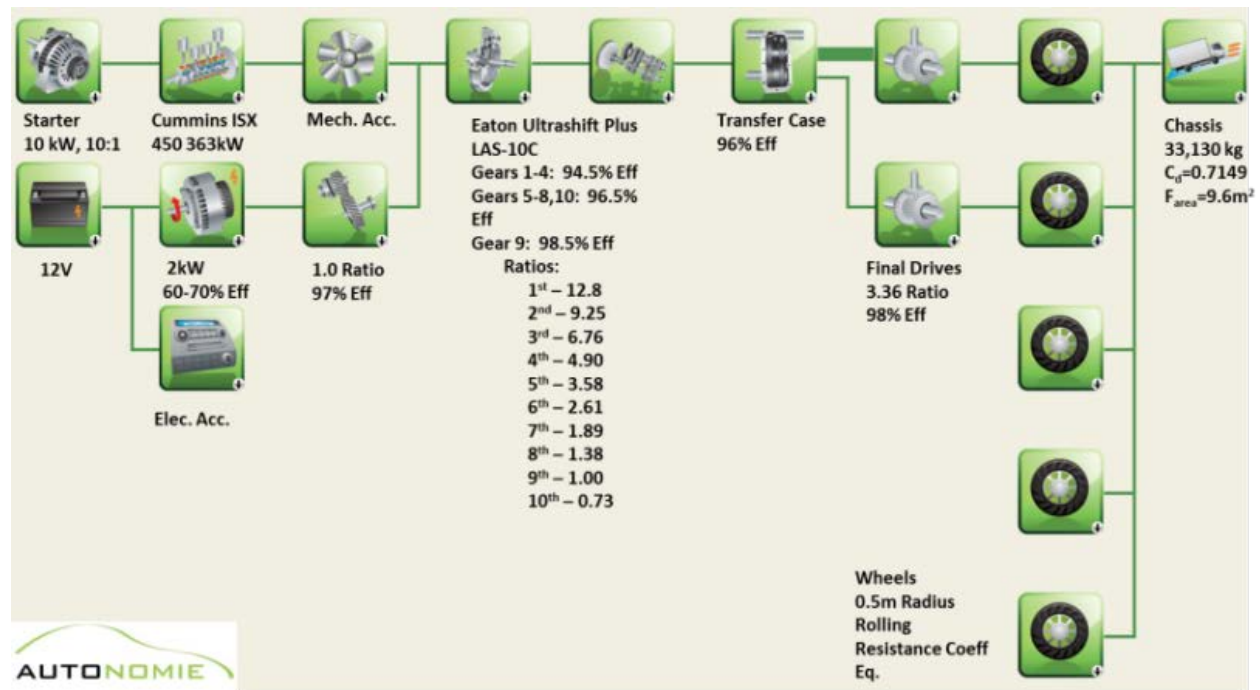


Figure VI-59: HD class 8 line haul sleeper cab based on a chassis tested Kenworth T700.

The second phase of the project is prototype development and component/vehicle testing phase which will be used to: validate the developed component and vehicle models, develop and build a prototype system based on simulation findings, create and test prototype controls in ORNL’s VSI component test cell using HIL practices, and test the finished system in Cummins test vehicle for a final system proof of concept.

In order further develop and validate the accessory and vehicle models, Cummins was able to leverage a test vehicle from another project in order to instrument the accessories and get real world data from most of the accessories. After analyzing the data and making the HVAC system, the main focus of this project the team decided that testing the components of that system in a test cell would both help NREL further develop their CoolSim model, but also allows to more accurately compare the two different compressors chosen for the h-APU architecture. The first setup (Figure VI-60) tested is the conventional setup in the truck with the condenser changed to a remote setup allowing the fan to be electrified.

• Instrumentation

- 1-4: Pressure and Temperature
- 5: Mass Flow of Refrigerant
- 6: Delta Pressure and Temperature
- 7-8: Speed and Airflow from HVAC Boxes

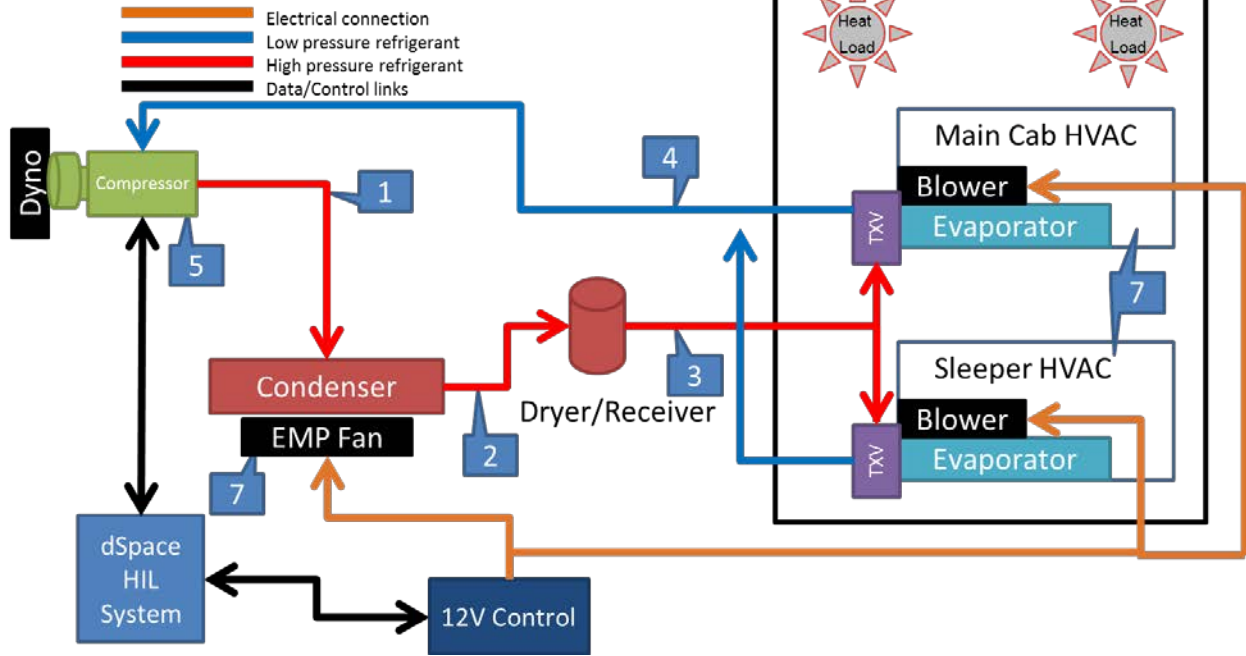


Figure VI-60: First component test cell setup. Conventional sleeper cab setup with electrified condenser fan.

The second setup (Figure VI-61) looks at replacing the conventional A/C compressor with an electrified unit that was supplied by Masterflux. It was essential to achieve the same cooling capacity as the conventional system at certain operating points, so the electric compressor is sized to achieve those selected points. Using two Hioki power analyzers we can characterize both the mechanical and electrical power/efficiency differences between the two systems. This will allow the team to make a choice of which setup best serves the finalized h-APU prototype.

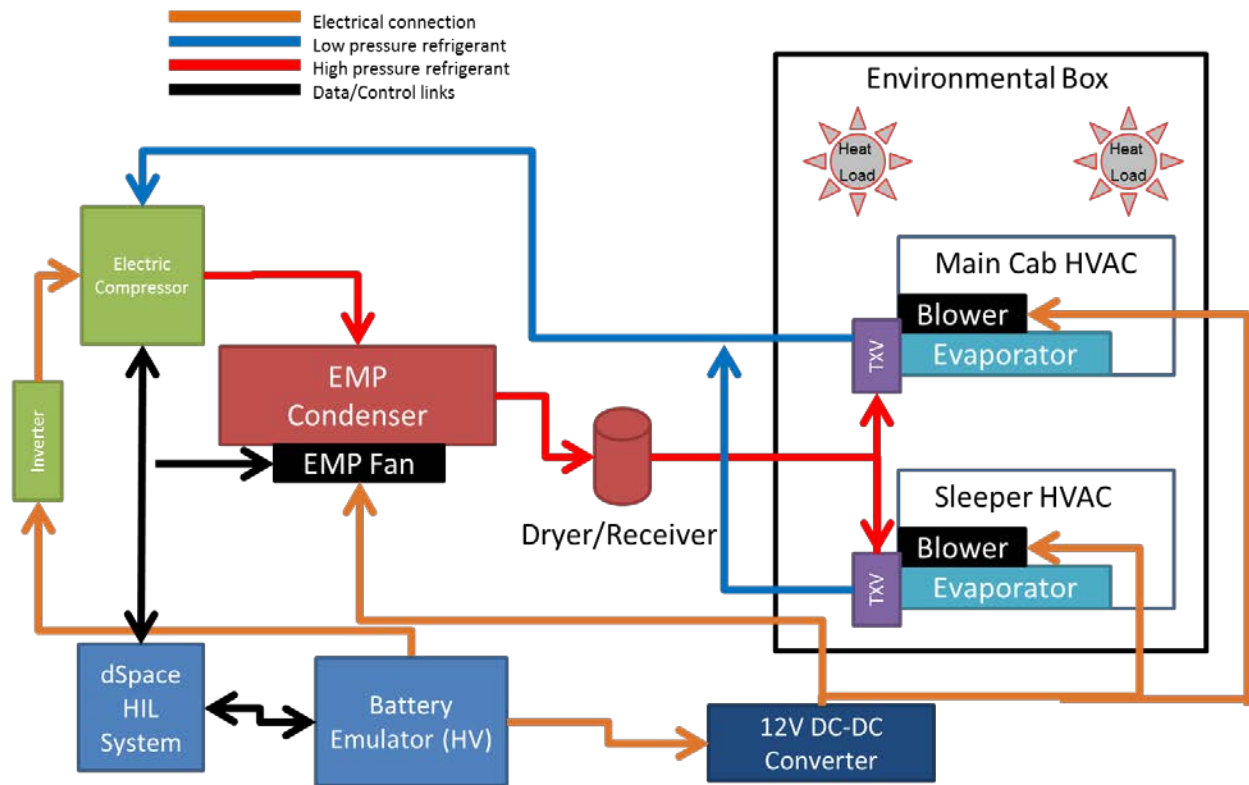


Figure VI-61: Second component test cell setup. Electrified compressor with electrified condenser fan.

While phase two is complete, the specifics of the prototype h-APU architecture, its other components, and results are protected under the CRADA agreement.

Results

The on road portion of the vehicle utilization is only one factor that has to be taken into account when looking at accessory hybridization or electrification. When examining the amount of fuel burned during overnight hoteling in a sleeper cab, researchers found that the amount of fuel consumed was larger than any other application for saving during the on road entitlement studies.

An idling line haul truck consumes between 0.4-0.88 gallons an hour. Required driver rest period is at least 10 hours which translates into 4-9 gallons consumed during idling not including idling that might incur during freight drop-off and pick up, an extended period of time at distribution hubs could also be a factor. Cummins and ORNL have chosen and developed an architecture which allows for idle reduction or elimination during these distribution hub times as well as overnight idling.

Table VI-8: Accessory Fuel Consumption Entitlements for the Cummins Proprietary Cycle (HD class 8 line haul sleeper cabin)

Accessory	Fuel Consumption % Decrease
A/C	0.123
Power Steering	0.438
Brake Air Compressor	0.282
Cooling Fan	0.344

With the A/C and hotel loads being the focus for idle reduction, a full mockup of a typical class 8 sleeper cabs HVAC system was installed into ORNL's VSI Component Laboratory (Figure VI-62). This lab is equipped to be able to control temperature up to 105° F and has an E-Storage emulator that can both supply power to electric test components, but also emulate the types of energy storages that the system may use.



Figure VI-62: ORNL's VSI Component test cell. Open configuration.

Two setups were used to test the different components. One setup with all of the A/C components was open to the ambient air of the test cell and the other used an insulated box to isolate the evaporator boxes from the ambient temperature of the test cell (Figure VI-63). During the first setup we are able to simulate pull down conditions within the truck; this was performed at the temperature set points of 105°F, 90° F, and 75°F. Regarding the second set of tests (using the insulated box) the focus was on finding the maximum cooling capacity of each system setup, and to test temperature regulation controls to find which strategy was the most efficient. In order to test the cooling capacity of the system at different operating points the ambient temperature was set to either 105°F or 90°F and the system is set to maintain 70°F inside the insulated box. A set of fans with known volumetric flows introduces hot ambient air into the box until the system is just able to maintain the desired 70° F, this allows for the calculation of how much heat load is being introduced into the system providing the cooling capacity at that operating point. Once the conventional system with the remote condenser was tested, ORNL then tested the all-electric compressor architecture (as seen in Figure VI-61) using the same method. This allowed Cummins to make well informed decision for a performance vs cost analysis for any possibility of commercialization.

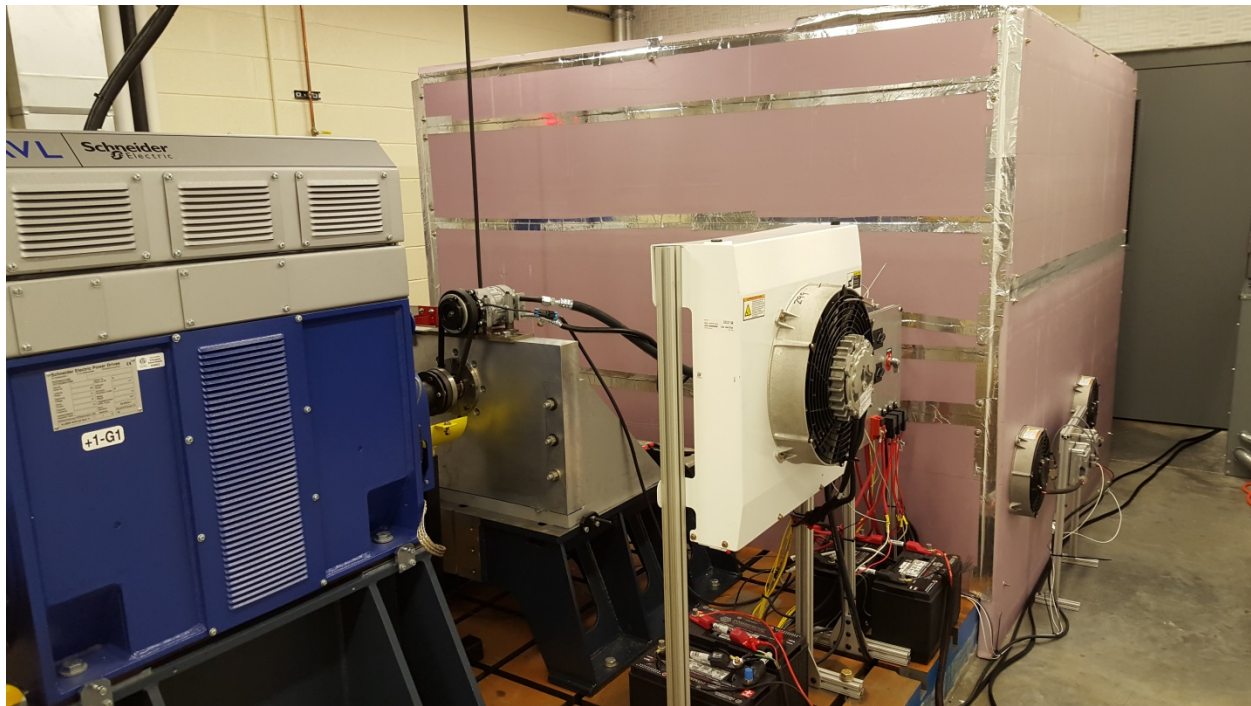


Figure VI-63: ORNL's VSI Component test cell with insulated environmental box.

With the conventional system and remote condenser systems tested ORNL was able to provide NREL with all of the HVAC components geometries, volumes, and other specs to build a baseline system in their CoolSim model. As more data is provided to NREL they will continue to validate and adapt the model to be used in both future simulations as well as providing us an Autonomie compatible model that is to be used in our HIL testing (Figure VI-64). This baseline model being developed with this project will be available for public use once a few proprietary parameters are removed and generic ones take their place. Ultimately the CoolSim model will be an invaluable tool once validated to perform offline simulations of the h-APU system controls on our selected and validated system.

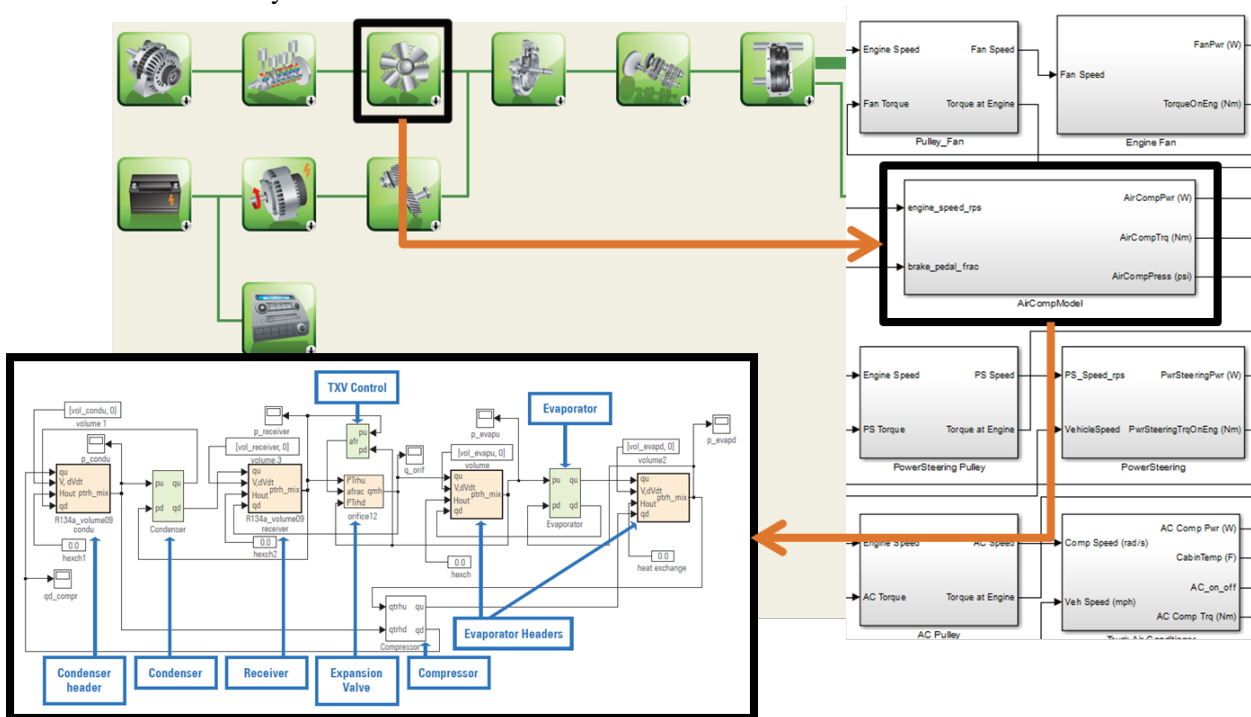


Figure VI-64: NREL's CoolSim model and the structure it will take inside our Autonomie model when validated.

Conclusions

Phase one of the project is completed. As more data from Cummins test vehicle and NREL's CoolSim model becomes available the models will continually be updated to provide more realistic results as well as continue to improve ORNL, NREL and Cummins' model libraries for future projects. Phase one has allowed Cummins and ORNL to create tools to evaluate future accessory technologies as well as discover the current landscape in accessory technologies and idle reduction devices. It has also allowed ORNL and Cummins to settle two possible architectures for use as an overnight anti-idle APU.

Phase two is also complete, but Cummins will continue to explore possibilities for commercialization. ORNL concluded testing on the electric compressor system along with the temperate control strategies, and Cummins has finished integration of the completed h-APU systems into the test truck for the proof of concept demonstration as well as testing. Phase two has also allowed NREL to build a baseline class 8 heavy duty sleeper cab CoolSim model that will be validated and available for public consumption minus a few propriety parameters from this project.

After reviewing the results of the study, Cummins and ORNL determined that a hybrid APU architecture is the best solution for maximized potential in reducing emissions and fuel consumption; this method will either reduce or eliminate the need for idling in HD class 8 trucks. Choosing the hybrid APU architecture best allows the project to address issues of idling for extended periods while accessory loads are still essential, as in overnight hoteling and idling while in queue at distribution hubs. The architecture for this has been chosen and developed based on the findings and testing done on this project, but is protected under the CRADA agreement.

VI.5.C. Products

Presentations/Publications/Patents

1. **Patent Pending:** Dean D. Deter (ORNL), Mahesh M. Kumar, Gary L. Parker, Subbarao Varigonda, Joseph E. Paquette, Benjamin D. Padgett, W. Brent Fields, Praveen C. Mualidhar, Vivek A. Sujan and David E. Smith (ORNL). Apparatus and System for Controlling Power to an Air Conditioning Compressor for a Vehicle, US Patent Application 62/354,364, filed June 24, 2016.

WIRELESS POWER TRANSFER

VI.6. Wireless and Conductive Charger Evaluation

James Francfort, Principal Investigator

Idaho National Laboratory

P.O. Box 1625

Idaho Falls, ID 83415-2209

Phone: (208) 526-6787

E-mail: James.Francfort@inl.gov

Lee Slezak, DOE Program Manager

Vehicle Technologies Office

U.S. Department of Energy

Phone: (202) 586-2335

E-mail: Lee.Slezak@ee.doe.gov

Start Date: October 2013

End Date: Ongoing

VI.6.A. Abstract

Objectives

- Provide the U.S. Department of Energy (DOE) with independent and unbiased benchmark testing results by evaluating emerging technologies developed via DOE and industry investments.
- Benchmark the efficiencies and safety of wireless power transfer (WPT) systems, conductive electric vehicle supply equipment (EVSE), and direct current fast chargers (DCFC).
- Benchmark the cyber security of charging systems
- Benchmark DCFC and Level 2 EVSE compatibility with the new generations of plug-in electric vehicles (PEVs).
- Continue to provide testing results to other DOE programs, national laboratories, industry, and several U.S. drive technical teams that Idaho National Laboratory (INL) staff are members of.

Accomplishments

- Completed vehicle-level testing for the Oak Ridge National Laboratory (ORNL)/Toyota/Evatran wireless charging system. Test results detailed the system efficiency, power quality, electromagnetic field strength around the vehicle, and other performance characteristics.
- Completed testing and evaluation of the ABB DCFC when charging a Nissan Leaf. The test results detailed the efficiency, power quality, and stand-by power loss.

Future Achievements

- Continue identifying WPT, DCFC, and EVSE test partners and obtaining test systems.
- Continue close coordination with the Society of Automotive Engineers J2954 committee.
- Conduct charging compatibility/interoperability testing of DCFC, EVSE, wireless charging systems, and vehicles.

VI.6.B. Technical Discussion

Background

DOE's Advanced Vehicle Testing Activity (AVTA) is part of DOE's Vehicle Technologies Office, which is within DOE's Office of Energy Efficiency and Renewable Energy. AVTA is the only DOE activity tasked by DOE to conduct field evaluations of vehicle technologies and fueling and charging infrastructure that use advanced technology systems and subsystems in light-duty vehicles to reduce petroleum consumption and exhaust emissions.

Most of these advanced technologies include use of electric drive propulsion systems and advanced energy storage systems. However, other vehicle technologies that employ advanced designs, control systems, or other technologies with production potential and significant petroleum reduction potential are also considered viable candidates for testing by AVTA.

Charging infrastructure for PEVs is also a study area of focus, because no singular successful business model has been developed for public charging. In addition, there is much discussion within both the vehicle and charging infrastructure industries about the appropriate level of charging (kW) for the future and where placement of charging infrastructure will occur (e.g., public, workplace, and/or residential). In support of this uncertainty, Idaho National Laboratory (INL) is testing the efficiencies, standby power, unit power during charging, and misalignment (for wireless power transfer) impacts on efficiency and electromagnetic field emissions.

AVTA's light-duty activities are conducted by INL for DOE. INL has responsibility for AVTA's technical execution, direction, management, and reporting, as well as data collection, analysis, and test reporting.

The current AVTA staff has 20+ years of experience testing grid-connected PEVs and PEV charging infrastructure. This experience includes significant use of DCFCs with various battery chemistries since the middle 1990s; this important legacy of experience is still available today. In addition, INL has significant experience performing cyber security testing for various federal agencies that are also being used for this project. During this reporting period, AVTA collected performance and use data from 17,000 Level 2 EVSE from the two largest providers of EVSE and several additional EVSE manufacturers.

Introduction

With the expanding introduction and use of grid-connected PEVs by fleets and individual taxpayers, development of both private and public PEV charging infrastructure (collectively known as conductive EVSE) continues. EVSE currently takes the form of Level 1 (110 Volt) and Level 2 (240 Volt) EVSE, which safely supply alternating current (AC) electricity to the vehicle and the charger that resides on the vehicle. The third type of EVSE is DCFC, which provides DC electricity to the vehicle and the power electronics equipment onboard the vehicle. For DCFCs, the charger is actually located off board the vehicle in the DCFC unit itself. AC Level 1 and 2 EVSE may either be in the form of smart EVSE, with functionalities such as revenue grade electricity meters, bi-directional communication capabilities, and other smart features, or "dumb" EVSE, which only provide electricity with minimal communication and metering capabilities. Regardless whether an EVSE is smart or less than optimally smart, its basic function is to safely transfer AC electricity from the consumers' side of the electric utility meter to a PEV, which has an onboard vehicle battery charger and power electronics. By nature of their design, DCFCs are at least somewhat smart units because they ensure a minimal amount of communication between the DCFC charger and the vehicle's battery control system.

Normally, the term EVSE will refer to AC Levels 1 or 2 and DCFC will be referred to by its acronym. It should be noted that most installed EVSE are AC Level 2 units, which provide significantly shorter charge times than AC Level 1.

Adding to the complexity of charging infrastructure selection and placement is the introduction of wireless charging systems, which transfer power without having the conductive connector of today's EVSE and DCFCs (thus the term WPT). To support introduction of safe and efficient wireless charging systems, DOE and AVTA

are conducting a series of activities to test and benchmark WPT systems. These activities include grants for supporting development of smart EVSE and wireless charging, as well as benchmarking the efficiencies of the different charging options and testing for vehicle-to-charging infrastructure compatibility. The activities discussed here detail the support activities being conducted by INL and some of the benchmarked results.

Approach

INL has created a process for benchmarking wireless charging systems developed with DOE technology funding and with other wireless providers. Testing has been conducted and results from advanced wireless charging system tests will be discussed in the next section. In addition, test procedures were developed and utilized to test a production DCFC, with testing and evaluation results being discussed in the following section.

INL has developed a testing regime for benchmarking AC Level 1 and AC Level 2 conductive EVSE efficiencies; this is being used to quantify grid-to-vehicle energy transfer efficiencies. This work is being leveraged to support benchmarking of DOE Office of Electricity Delivery and Energy Reliability-developed smart grid EVSE.

Much discussion has occurred regarding the efficiency of the emerging wireless charging systems. For this reason, INL tested and provided independent test results from the ORNL/Toyota/Evatran WPT system for FOA-667. INL evaluated this WPT system installed on a Toyota RAV4 Electric to determine system performance characteristics (e.g., efficiency and electromagnetic field strength) and the interaction between the wireless charger and the vehicle.

Testing and evaluation was conducted on an ABB Terra CJ53 DCFC to benchmark the performance and power quality of the charging system when charging a Nissan Leaf. This charging system is one of the few that offer both the CHAdeMO and the J1772 CCS connection protocols.

Results

Wireless Charger Testing

Testing and evaluation was completed on the ORNL/Toyota/Evatran wireless charging system (Figure VI-65) installed on the Toyota RAV4 electric vehicle. Testing was conducted in INL's Electric Vehicle Infrastructure laboratory. The testing evaluated system efficiency, electromagnetic field emissions, power quality at various charge power levels, coil-to-coil misalignment, coil-to-coil gap, input voltage, and output voltage. The vehicle was positioned on non-metallic ramps to elevate it and the wireless charging system to allow space for a coil positioning testing apparatus to be used to accurately misalign the coils of the wireless charger. This is of high importance because coil-to-coil alignment is a significant factor in wireless charging efficiency and electromagnetic field emissions.

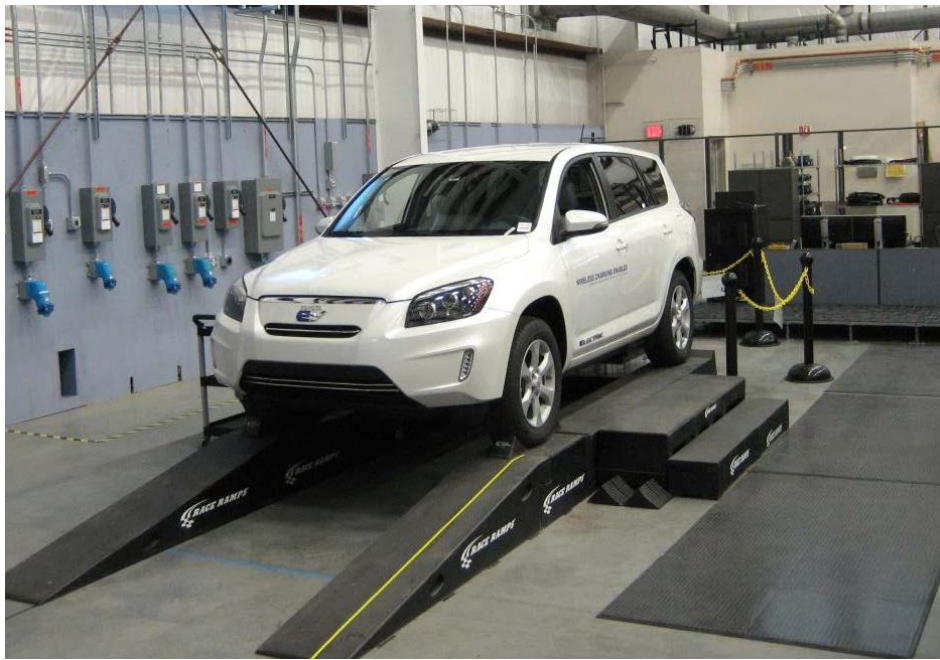


Figure VI-65: Testing conducted on the wireless charging system from the ORNL/Toyota/Evatran wireless charger for FOA-667.

INL

The test results showed the impact of coil-to-coil misalignment and the impact of coil-to-coil gap ground clearance on system efficiency. Figure VI-66 shows that efficiency is best when the coils are aligned and near the designed ground clearance coil gap of 150 mm. As the ground clearance coil gap increases from the 150 mm designed gap, system efficiency decreases. This is due to a decrease in magnetic coupling between the ground-side coil assembly and the vehicle-side coil assembly as the distance between the two increases.

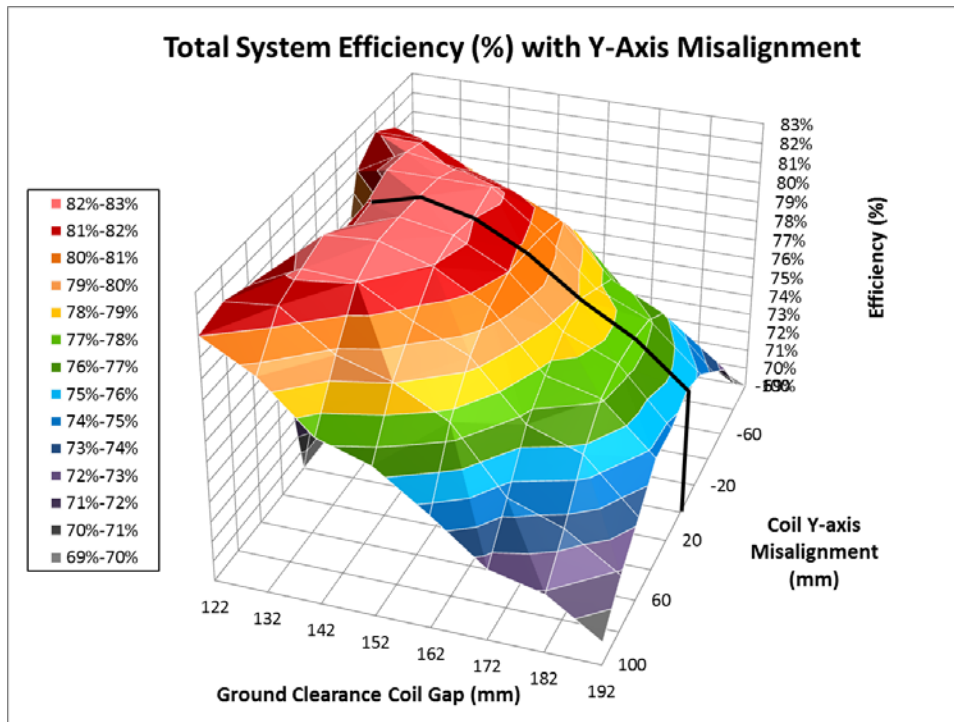


Figure VI-66: Efficiency test results from the ORNL/Toyota/Evatran wireless charger for FOA-667, with respect to coil misalignment and coil gap.

INL

Further testing of the ORNL/Toyota/Evatran wireless charging system showed the symmetrical system efficiency about the central axis of the wireless charger. As seen in Figure VI-67, the highest efficiency occurs when the ground side coil assembly is in alignment with the vehicle side coil assembly. When the two coil assemblies are misaligned, system efficiency decreases. The ORNL/Toyota/Evatran wireless charging system was tested for misalignment up to 100 mm because it was expected that vehicle alignment systems will enable accurate alignment to within 100 mm.

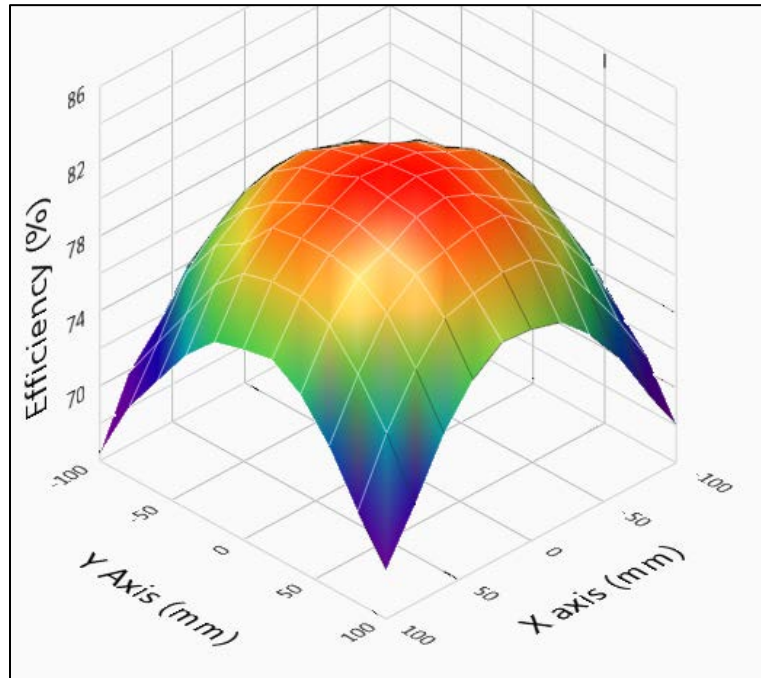


Figure VI-67: System efficiency test results from ORNL/Toyota/Evatran wireless charger for FOA-667 over a wide range of coil misalignment.

INL

Wireless charging systems operate by transferring power via magnetic resonance coupling. This enables efficient wireless charging over wide coil gaps, but also creates stray electromagnetic field emissions. A high level of stray electromagnetic field emissions is undesirable. There are a few industry standards that detail the allowable electromagnetic field strength safe for human public exposure. One of these standards is the International Commission on Non-Ionizing Radiation Protection, version 2010. For public exposure, the magnetic field limit is 21 A/m. Above this limit is undesirable and is considered unsafe. Additionally the electromagnetic field will cause heating in metallic objects if they are in a high-strength electromagnetic field. Therefore, it is crucial to minimize the stray electromagnetic field emissions around the wireless charging system.

The strength of the electromagnetic field around the vehicle perimeter is dependent on the charge power level, the coil-to-coil gap and misalignment, and the design and effectiveness of the wireless charger's design and shielding around the entire system.

Electromagnetic field emissions were measured for the ORNL/Toyota/Evatran wireless charging system using a calibrated electromagnetic field meter in conjunction with a custom built multi-axis positioning device used to move the field meter; this enabled a scan of the area surrounding the vehicle for electromagnetic field strength. As shown in Figure VI-68, the electromagnetic field strength surrounding the rear of the vehicle is highest near the wireless charging system. The brightly colored area is greater than 21 A/m. The highest measured valued was 130 A/m adjacent to the wireless charging system.

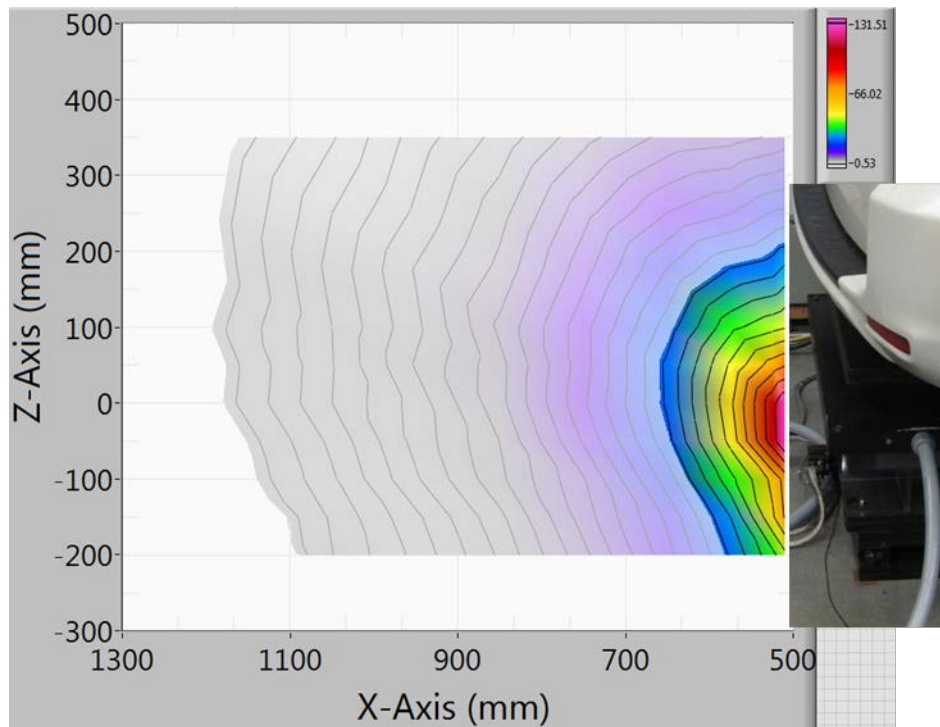


Figure VI-68: Magnetic field results at the rear of the vehicle: ORNL/Toyota/Evatran wireless charger for FOA-667.

INL



Wireless charging testing and evaluation of the ORNL/Toyota/Evatran wireless charging system demonstrates the capabilities of an advanced wireless charging system. In addition, the results identified areas of desired performance improvements to meet industry performance, safety goals, and requirements.

Direct Current Fast Charger Testing

Performance and efficiency testing was completed on the ABB Terra CJ 53 DCFC (Figure VI-66). This testing was conducted while charging a 2015 Nissan Leaf. The DCFC was rated at a 50-kW output power for use by electric vehicles equipped with either the CHAdeMO or Combined Charging System (CCS) connection protocol. The input power requirements for this charge system are 480 VAC, three-phase, with 75-Amp capacity.

These tests evaluated system efficiency, power quality, and stand-by losses when charging a Nissan Leaf. Figure VI-69 shows a photo of the ABB Terra 53 DCFC as installed in INL's Electric Vehicle Infrastructure laboratory.

Figure VI-69: ABB Terra CJ 53 DCFC ready to commence testing.

INL

The ABB DCFC has a user interface touch screen that instructs the driver on the two-step process for charging his/her vehicle. The driver first selects the charger connection protocol (CHAdeMO or CCS) and then plugs in the vehicle and touches the start button on the ABB DCFC. During charging, the ABB display shows battery state of charge and estimated time until charge completion.

For testing of the ABB DCFC, a 2015 Nissan Leaf was discharged to a low state of charge (i.e., less than 5 miles of range). The charging process was then initialized using the CHAdeMO protocol. A laboratory-grade power meter recorded the input and output power of the ABB DCFC during the charge event. The charge event can be described in two phases. The first phase is a constant current mode; this refers to the DC output current to the vehicle. The second phase is a constant voltage mode; this refers to the output voltage to the vehicle

(Figure VI-70). Note that the maximum power is 50-kW input and occurs at the end of the constant current phase. The overall charging event duration is 37 minutes.

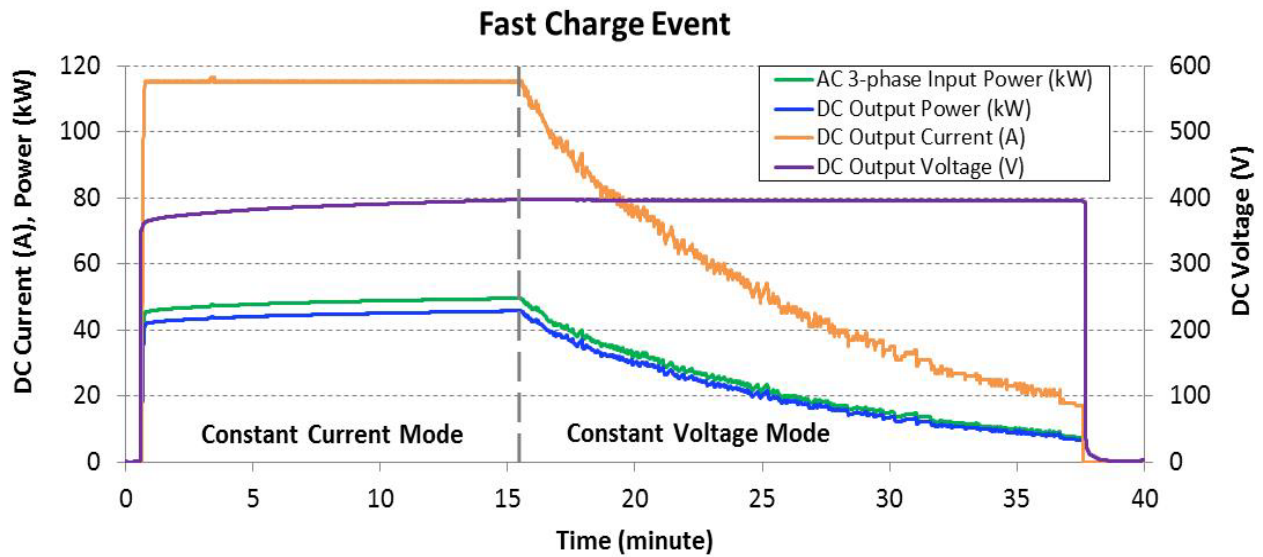


Figure VI-70: Testing and evaluation of the ABB Terra CJ 53 DCFC, showing a constant current and constant voltage mode of operation.

INL

Data collected during the DCFC event shows the calculated efficiency of the ABB DCFC over a wide range of charge power. During the constant current phase, the efficiency was relatively constant at 92.5%; however, during the constant voltage phase and as power decreased, the efficiency varied greatly (Figure VI-71). The cyclical nature of the efficiency indicates the DCFC is likely comprised of five parallel charging stages, each with approximately 10 kW of capability. The stages are used in parallel as necessary to deliver the required total power output. This approach enables higher efficiency at mid-power levels.

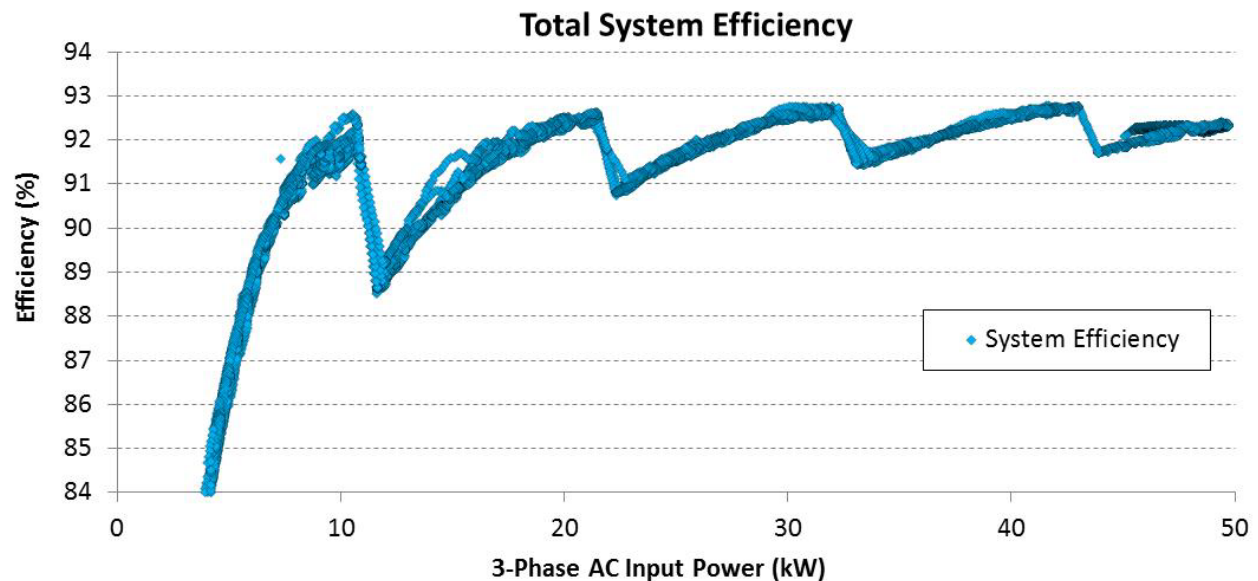


Figure VI-71: Efficiency of the ABB Terra CJ 53 DCFC across a wide range of charge powers.

INL

Conclusions

INL will be testing additional wireless and conductive charging technologies with industry participation during the next 12 months. Industry, DOE, and INL are also conducting research into dynamic vehicle charging technologies that will use WPT technologies for possibly charging vehicles while they are driven on roadways.

Charging infrastructure is important to successful adoption of grid-connected vehicles; therefore, there are multiple key factors to successful integration of vehicles and charging infrastructure. This includes interoperability, safety, test methodology, and efficiency. Therefore, AVTA is working with industry to develop robust testing methodologies for evaluation of wireless and conductive charging systems.

VI.6.C. Products

Presentations/Publications/Patents

1. "INL'S Testing and Evaluation Results: ORNL'S Wireless Charging System for FOA-667," INL/MIS-16-37703, <https://avt.inl.gov/sites/default/files/pdf/presentations/ORNLWPTSAESymposium2016.pdf>, February 2016.
2. "DC Fast Charger Fact Sheet: ABB Terra 53 CJ charging a 2015 Nissan Leaf," INL/MIS-15-34055, <https://avt.inl.gov/sites/default/files/pdf/evse/ABBDCFCFactSheetJune2016.pdf>, June 2016.

GRID MODERNIZATION

VI.7. Vehicle to Building Integration Pathway [GM0062]

Rick Pratt, Principle Investigator

PNNL

P.O. Box 999, K5-17

Richland, WA 99354)

Phone: (509) 375-3820; Fax: (509) 372-4725

E-mail: rmpratt@pnl.gov

Lee Slezak, DOE Program Manager

Vehicle Technologies Office

U.S. Department of Energy

Phone: (202) 586-2335

E-mail: Lee.Slezak@ee.doe.gov

Start Date: April 1, 2016

End Date: September 30, 2018

VI.7.A. Abstract

Objectives

- Finalize development of vehicle charging demonstration Use Cases and the Communication and Control Requirements needed to demonstrate coordinated PEV charging under time varying commercial building load conditions that minimize demand charges.
- Complete an Industry Advisory Board (IAB) review of the GM0062 Use Cases

Accomplishments

- The NREL led GMLC Use Case development task was completed with ANL, INL, LBNL and PNNL each making significant contributions. This team also engaged an Industry Advisory Board to review the use cases and provide feedback. A survey was sent to fourteen OEM, utility, and regulatory entities with over half responding. A follow-up conference call was held to gain additional feedback. Several entities were very excited about the work and eager to receive periodic updates.
- The ANL led GM0062 workplace charging Communication and Control Requirements document development was completed with NREL and PNNL each making significant contributions to the document. The Requirements document will next be reviewed by other GMLC team members and used to develop the Testing Processes document. It also forms the technical basis for the interoperable vehicle charging demonstrations planned at ANL, NREL and PNNL beginning in FY17.

Future Achievements

- Review, evaluate and incorporate industry comments into project plans, use cases and requirements in FY17 Q1. Develop a summary report for the IAB comments.
- Finalize communication architecture and testing processes in FY17 Q1.
- Develop infrastructure needed to demonstrate one standards-compliant, multi-vehicle, workplace charging use case - FY17 Q2.

VI.7.B. Technical Discussion

Background

The DOE Vehicle Technologies Office (VTO) develops and deploys efficient and environmentally friendly highway transportation technologies that will enable America to use less petroleum. These technologies will provide Americans with greater freedom of mobility and energy security, while lowering costs and reducing impacts on the environment.

Electrification of the vehicle fleet can increase the overall energy efficiency of vehicles and decrease the use of petroleum. Transitioning to a light-duty fleet of HEVs and PEVs could reduce U.S. foreign oil dependence by 30-60 percent and greenhouse gas emissions by 30-45 percent, depending on the exact mix of technologies.

The Grid Modernization Laboratory Consortium (GMLC) is a strategic partnership focused on improving the accessibility of the globally-recognized National Lab technical expertise. The GMLC seeks to leverage the key VTO activities including developing interoperability standards and power electronics for PEVs; automotive battery pack design & battery development; and battery status and health monitoring with cross-cutting activities including modeling of high penetration PEV scenarios at bulk-system and distribution system levels; developing new battery and inverter technologies; developing interconnection standards for EVs; developing end-use measurement devices; and gaining stakeholder engagement from industry and regulatory bodies.

This GM0062 VTO project is developing an interoperable, standards-based Vehicle to Building Integration Pathway for Plug-In Electric Vehicle (PEV) charging demonstrations. The project includes hardware and software development to coordinate and manage charging groups of vehicles within the commercial building environment. Efforts will also address power quality challenges associated with PEV charge management in a building environment.

Introduction

The Vehicle to Building Integration Pathway project will develop and demonstrate pre-normative methods needed to develop a standardized and interoperable communication pathway and control system architecture between PEVs, Electric Vehicle Support Equipment (EVSE) and Building/Campus Energy Management Systems (BEMSs) to enable the integration of clean variable renewable resources with workplace PEV charging infrastructure to promote greater PEV adoption. This communications and control platform will provide access to real-time system monitoring information, establish an infrastructure to coordinate intelligent assets, manage energy consumption behind the meter, reduce peak demand charges from vehicle charging, and potentially participate in energy and/or ancillary services markets.

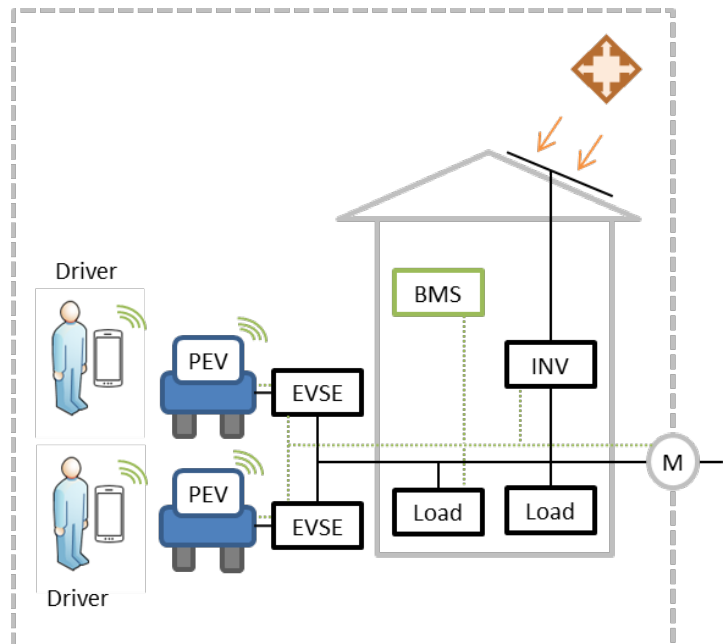


Figure VI-72: Vehicle to Building Integration Pathway (GM0062) Project

Approach

ANL, INL, LBNL, NREL, and PNNL are developing vehicle charging demonstration use cases, communication and control requirements, communication architecture and testing processes needed to demonstrate coordinated PEV charging under time varying commercial building load conditions that minimize demand charges. This effort includes strong collaboration between labs to jointly contribute to three other projects: “Systems Research Supporting Standards and Interoperability” (GM0085), “Modeling and Control Software Tools to Support V2G Integration” (GM0086), and “Diagnostic Security Modules for Electric Vehicle to Building Integration” (GM0163).

After the use cases and the communication and control requirements development milestones are completed; the physical capabilities at ANL, NREL and PNNL will be used to perform use case demonstrations designed to promote PEV adoption through developing standardized, scalable, and interoperable communication pathway and control system architectures that demonstrate workplace PEV charging infrastructure, clean renewables integration, commercial building connectivity, interoperable communications, managed power consumption while maintaining transportation availability, minimize PEV demand charges, and participation in energy / ancillary services markets.

Results

The Use Cases selected for GM0062 were selected after surveying many sources including: Society of Automotive Engineers (SAE) standards (e.g., SAE J-2836/1 use cases, SAE J-2847/1 messages, and SAE J-1772 signaling), ISO/IEC 15118-1 use cases, Open Vehicle Grid Integration Platform (OVGIP) use cases, existing electrical markets, and use cases described in the GM0062 project proposal. Use case descriptions were developed for each, the use case scale determined (e.g., building level, distribution system level, or balancing authority level) and a benefits/justification process was used to down select the use cases for each project (e.g., GM0062, GM0085 or GM0086). For GM0062, these use cases were then divided into four groups based on the control system response time horizon. These time horizon groupings have facilitated the development of control system requirements.

Table VI-9: GM0062 Use Cases

Time Horizon	Use Cases		
Short (10's of Seconds)	Demand Charge Mitigation	Frequency Regulation	Maximize Use and Value of Local Renewables
Medium (10's of Minutes)	RTP (Real-Time Price) Price Control	CPP (Critical Peak Price) Price Control	
Long (10's of Hours)	Demand Response (DR)	Time-Of-Use (TOU) Price Control	Charging Capacity Deferral (Charge Scheduling)
Transactive Control	Transactive Control can use a 5-minute market mechanism where a power goal and electricity price is established and loads negotiate their power demands with the market coordinator based on the load’s price sensitivity. An initial implementation of Transactive Control is a closed-loop form of RTP.		

The Use Cases were reviewed with Lab participants on other GMLC projects. The internal Lab review provided some interesting insights when it was suggested that these use cases economically divide into two major groups - Minimize Bills and Maximize Incentives. The Minimize Bill group includes Demand Charge Mitigation, Maximize Local Renewables, and the RTP, TOU, and CPP use cases. RTP and CPP represent ways of sharing production costs with consumers. The Maximize Incentive group includes Charging Capacity Deferral, Frequency Regulation, and Demand Response. A key question we need to consider in setting up the economic systems around these use cases is to determine who is receiving benefit from the use case service(s).

For example, for Demand Charge reduction and Maximize Local Renewables use cases the building owner is clearly the primary recipient of the value created. This insight suggests that we should consider showing the value created as part of our demonstration output.

The Use Cases selected by the GM0062 team were reviewed by the Industry Advisory Board (IAB) members using a survey. The survey requested each IAB member select two short-term (1-5 year) Use Cases and two longer-term (5-10 year) Use Cases that have the highest priority for their industry. Figure VI-73 shows how IAB prioritized the eight Use Cases selected by the GM0062 team with the responses arranged by Use Case. The demonstrations presented in the GM0062 proposal matched very closely with the Use Cases selected by the IAB.

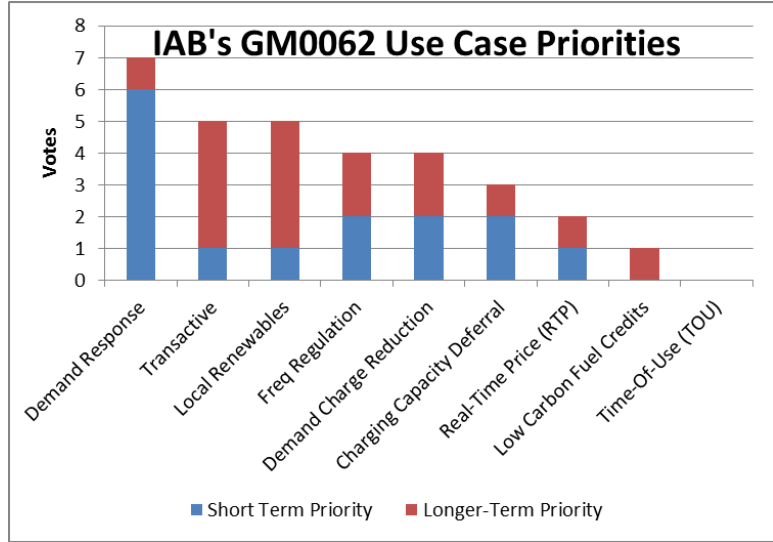


Figure VI-73: Vehicle to Building Integration Pathway Use Case Review Responses

In addition to prioritizing the Use Cases, the IAB members were also asked two additional survey questions regarding the PEV / EVSE communications infrastructure needed for Grid Integration. From a single-family home charging viewpoint, six IAB members answered, "PEVs will be capable of independently communicating with an aggregator no matter where they are located (physically and behind the meter) to bid into a grid resource." Two answered, "PEVs will be capable of communicating only with the EVSE and through the EVSE will be able to bid into a grid resource."

The second question was similar, but with a public/semi-public (including multi-family residential) charging location perspective. One person thought that PEVs will be capable of independently communicating with an aggregator no matter where they are located (physically and behind the meter) to bid into a grid resource; two felt that PEVs will be capable of communicating only with the EVSE and through the EVSE will be able to bid into a grid resource; and four answered that PEVs will be able to choose how they communicate depending on charging location for bidding into a grid resource.

Key IAB comments included: demand charge mitigation and charging capacity deferral have business models that could support these activities today; technology implementation cost is important in the current market especially with unknown financial benefits; the manner PEV drivers receive benefit in workplace charging scenarios needs to be resolved; DR is important since PEVs now use scheduled charging to obtain lower rates, but that won't work once a higher PEV population exists; a telemetry use case should be included; and implementations should maximize use of existing standardized communications (e.g., OpenADR, OCPP, SAE, etc.). Several important reminders were also expressed such as cyber-security and data privacy concerns, minimizing access into electronic vehicle systems, technology implementation challenges associated with vehicle mobility, variability of PEV penetration, and the regional nature of electrical markets.

Conclusions

From the viewpoint of the PI, the multi-lab team assembled for this project has worked very well together and enabled the GM0062, GM0085 and GM0086 projects to all begin achieving an important project goal of improving the accessibility of the globally-recognized National Lab technical expertise while meeting all FY16 goals. This impact was clearly evident by the thought put into the survey questions and project support expressed in the IAB members' use case reviews. The IAB also had a strong message of wanting to stay connected with the project's progress. In addition, the internal Lab use case review provided additional insights not directly available to project team members.

The IAB's Use Case survey results are congruent with the GM0062 team's demonstration plans. The more specific questions on grid integration communications provides valuable insight into the flexibility needed by grid communications interfaces so that control signals can flow either through the EVSE to the PEV or go directly to the PEV. In addition, incorporating economic impacts as well as power/energy affects into demonstrations could more effectively communicate the value of the proposed Vehicle to Building Integration Pathway project.

VI.7.C. Products

Presentations/Publications/Patents

1. Use Cases and Descriptions provided to IAB and IAB Survey responses
2. Draft Project Requirements and Architecture documentation
3. Slides to support VTO Office requests

VI.7.D. References

1. SAE J1772™ - SAE Electric Vehicle and Plug in Hybrid Electric Vehicle Conductive Charge Coupler
2. SAE J2836/1™ - Use Cases for Communication Between Plug-in Vehicles and the Utility Grid
3. SAE J2847/1™ - Communication between Plug-in Vehicles and the Utility Grid

VI.8. Systems Research for Standards and Interoperability [GM0085]

John Smart, Principle Investigator

Idaho National Laboratory
755 University Blvd
Idaho Falls, ID 83415
Phone: (208) 526-5922; Fax: (208) 526-3150
E-mail: John.Smart@inl.gov

Lee Slezak, DOE Program Manager

Vehicle Technologies Office
U.S. Department of Energy
Phone: (202) 586-2335
E-mail: Lee.Slezak@ee.doe.gov

Start Date: May 1, 2016
End Date: Apr 30, 2019

VI.8.A. Abstract

Objectives

- This project will determine the feasibility of plug-in electric vehicles (PEVs) providing grid services and renewable energy integration at the electric utility distribution level without negatively impacting grid stability or the PEV customer experience
- Hardware-in-the-loop (HIL) platforms will be developed at INL and NREL to demonstrate integration of numerous vehicles with distributed energy resources at numerous facilities
- Multiple communications pathways will be emulated and studied to accelerate standards development and understand how to prioritize the needs of the PEV customer, facility, third-party aggregator, and grid operator in multiple use cases

Accomplishments

- Participating national lab researchers have identified and down-selected demonstration use cases and communication pathways to be emulated
- INL has specified requirements for controller development platform integration with INL's DRTS and the procurement process from subcontractor Siemens has started
- INL has completed the vehicle charging characterization of three production PEVs (2013 Ford Fusion Energi, 2016 Chevrolet Volt, 2015 Kia Soul EV)

Future Achievements

- In FY17, development of the HIL environments at INL and NREL will be completed, allowing controller-HIL development with virtual and actual vehicles connected to simulated distribution networks at both laboratories. A study of uncontrolled charging will be conducted as a baseline for FY18 studies of controlled PEV charging to provide specific grid services.
- Additional FY17 tasks required to complete the development of the HIL environments include aggregator model development, communications latency emulation, additional vehicle charging characterization, and vehicle charging system model development

VI.8.B. Technical Discussion

Background

This project is one of a group of projects that will collaboratively demonstrate electric vehicle charging as an integral part of the smart, renewable electricity grid of the future. These projects are being conducted for DOE's Vehicle Technologies Office as part of DOE's Grid Modernization initiative by a team of researchers from six national laboratories: INL, NREL, PNNL, LBNL, ORNL, and ANL. These projects stem from the Multi-Lab EV Smart Grid Integration Requirements Study published in May 2015 [1]. INL is the lead laboratory for this project. Subcontractor Siemens was chosen to provide hardware and technical support.

Introduction

As PEVs increasingly penetrate the marketplace, the integration of PEVs with other distributed energy resources (DERs) and the grid is seen as an opportunity. It has been widely proposed that PEVs can provide valuable grid services, such as load shifting to provide energy storage capacity for wind and solar generation, frequency regulation, and volt/volt-ampere reactive (VAR) support. However, significant technical challenges remain before this vision becomes reality. Prior to broad investment in the technical and business processes required for PEVs to provide grid services, fundamental questions must be answered, such as the following:

- How can PEVs provide grid services to effectively realize anticipated benefits to the grid without negatively impacting the grid or PEV owners?
- What are the standard communications requirements and protocols that need to be put in place to ensure the functionality and interoperability needed to facilitate PEVs providing grid services?
- What measurement and control challenges must be addressed to optimally utilize PEVs as a grid resource?

Approach

The objective of the proposed project is to address the considerable uncertainty regarding the degree to which PEVs can provide grid services and mutually benefit the electric utilities, PEV owners, and auto manufacturers. How can the potential benefits be unlocked without negative unintended consequences?

This project will answer this question by leveraging capabilities of multiple national laboratories with vehicle/grid integration (VGI) to perform HIL studies that integrate communication and control system hardware with simulation and analysis activities. These studies will do the following:

- Study how to effectively incorporate PEVs into the grid as controllable loads
- Perform controller development to verify the viability of controlling PEVs to facilitate renewables integration and other valuable grid services
- Provide an understanding of the impact of using PEVs as DERs on the PEV owner and on distribution network system dynamics, power quality, and stability.

The work will focus on the integration of PEVs at the electric utility distribution level via a communication layer to provide grid services (i.e., on the grid side of the meter from a building/campus perspective). This will be done in the HIL environment to allow the following:

- Verification of open communication standards
- Validation of interface requirements between components of the system developed in GM0062 Vehicle to Building Integration Pathway, with respect to system interactions at the distribution level
- Development of strategies for controlling PEV charging with respect to system dynamics at the distribution level

- Performance of experiments that emulate distribution-level VGI in a variety of scenarios and use cases.

All this will be done using open-source control architectures and communication protocols that adhere to current standards, so that methodologies may be shared and standards can be improved.

This project will develop distribution-level hardware-in-the-loop (HIL) scenarios to emulate a large number of vehicles and other DERs at numerous facilities. The project will be based on dynamic real-time simulation (DRTS), which performs low-level physics modeling of the electrical system.

The platform will develop controls approaches to understand how to prioritize the needs of the PEV customer and the grid in multiple use cases, by the means of a Distribution Management Systems (DMS) and/or 3rd party aggregator. To accomplish this, this project will develop a front-end controller (FEC) to enable coordination of PEV charging with the utility and other entities. The FEC will be built into controller cards that each interface with a single electric vehicle supply equipment (EVSE) unit to control the charging of an individual vehicle. The FEC will determine when to start and end charging and establish the charge power level, based on information received from the vehicle, EVSE, and a coordinating entity behind the meter, such as a DMS or 3rd party aggregator.

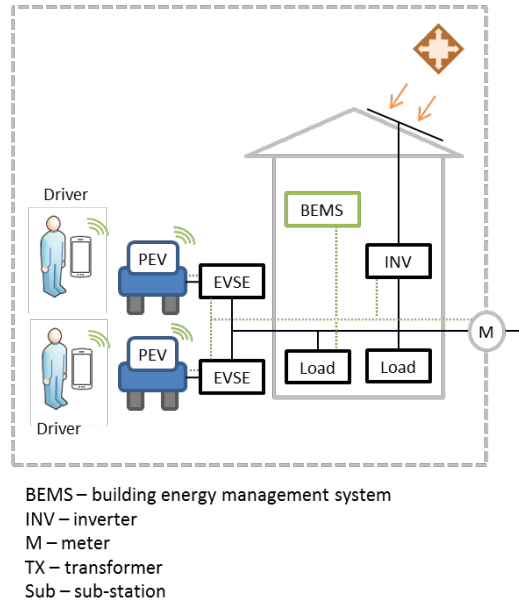
The project will emulate a DMS/3rd party aggregator to generate transactive signals that communicate the grid's needs to FECs. To do this, the project will partner with Siemens to leverage its open-architecture Smart Energy Box (SEB) to implement the FEC and interface with DMS and aggregator models. The SEB is an open-source, vendor-neutral controller development platform and a scalable automation middleware. SEB will enable emulation of distribution management system software and create a bridge between the distribution-level power system simulation running in the DRTS and the FEC cards.

Initially, the FEC will be developed and tested using up to four actual vehicle/EVSE pairs connected to the HIL platform. Then, to simulate a large number of vehicles connected across an entire distribution network (i.e., 1,000 or more), high-fidelity dynamic vehicle charging models will be used. These models will be created by characterizing the actual charging behavior of a variety of production plug-in electric vehicles and EVSE. Dynamic models based on these characterizations will be embedded in the HIL system.

This project will trial multiple communications pathways to accelerate standards development, in coordination with GM0062 Vehicle to Building Integration Pathway. GM0062 will focus on behind-the-meter communication pathways between the vehicle, EVSE, and building energy management system (BEMS). It will integrate production and prototype hardware using multiple protocols and pathways to define functional requirements for and issues with interoperability. This project (GM0085) will focus on communication between the vehicle/EVSE and the grid-side of the meter. Communication between devices will be emulated, such that signals have representative message content and latency. This will allow the study of electrical response and interactions on the distribution level.

Figure VI-74 depicts the elements in GM0085 and GM0062. The scope of each project is depicted by elements inside the dashed-line box.

GM0062 Vehicle to Building Integration Pathway



GM0085 Systems Research Supporting Standards and Interoperability

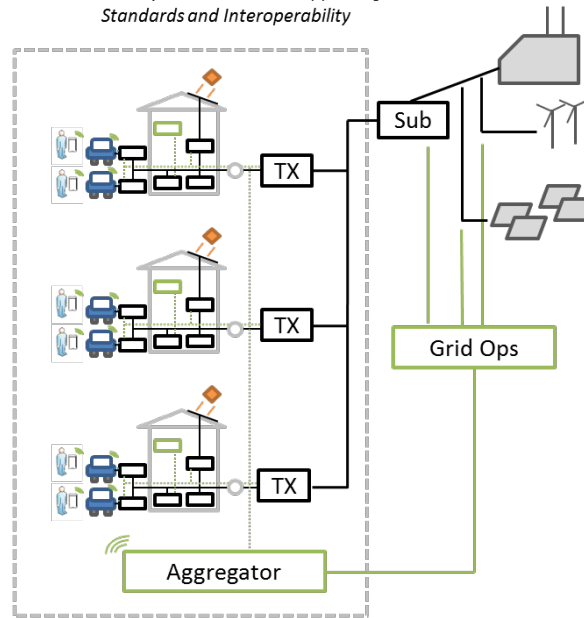


Figure VI-74: Difference in scope of this project with GM0062 Vehicle to Building Integration Pathway.

An advisory group was established for this and other projects to provide feedback on the use cases and other guidance throughout the project. The following organizations are represented in the advisory group: Duke Energy, Eversource Energy, Fiat Chrysler Automobiles, BMW, California Public Utility Commission, Ford Motor Company, NRG Energy, Olivine, University of California San Diego, Nissan North America, Southern California Edison, California ISO, California Energy Commission, MISO Energy

Results

The primary objective for FY16 was to define the set of use cases that the project will study. Use cases were developed in concert with the other vehicle-related Grid Modernization projects (GM0062, GM0086), to coordinate the study of controlled PEV charging on the facility, distribution, and utility levels. The following sections present the use cases that will be studied by this project (GM0085).

1. Distribution Load Management

Uncontrolled charging of PEVs may cause problems on distribution feeders as the number of PEVs increases through time. This use case investigates the extent of the problems that uncontrolled charging might cause on distribution feeders and whether these problems can be mitigated by controlling the charging of PEVs. This use case will focus on three specific areas, each described as follows:

A. Distribution System Capacity Deferral (substation transformers)

For this use case, first we will investigate whether a large increase in uncontrolled PEV charging on a distribution feeder will begin to strain the large substation transformers that supply power to the distribution system. If the uncontrolled PEV charging creates strain on the transformer, then the possibility of reducing transformer loading using controlled PEV charging will then be studied. This will shed light on whether controlled PEV charging can mitigate the potential long-term cost of capacity growth required by uncontrolled charging of PEVs.

B. Distribution Voltage Support

For this use case, we will investigate whether a large increase in uncontrolled PEV charging on a distribution feeder might cause voltage support issues on the distribution feeder. If so, then the possibility of mitigating these issues using controlled PEV charging will then be studied.

C. Phase Imbalance Mitigation

For this use case, we will investigate whether controlled PEV charging can be used to restore phase balance in distribution feeders at times when the phases are severely out of balance.

2. Integrating Distributed Solar Generation

This use case focuses on how controlling the charging of PEVs on a distribution feeder can be used to integrate distributed solar generation that is located on the same feeder. It is advantageous to integrate the variability in solar generation (as close to the source as possible) to improve grid reliability and to maximize the solar generation used (i.e., avoid curtailing the resource). The variability that is mitigated locally at the distribution feeder level will not need to be handled at the utility or balancing authority level. The variability in solar generation consists of both short term variability and daily variability, each described as follows:

A. Short Term Variability

The short term variability in the solar generation consists of minute-by-minute changes in output power and is caused by changing solar intensity on the solar panels, primarily due to clouds. For this use case, we will investigate the degree to which short term variability in solar generation can be mitigated by controlling the PEV charging on the distribution feeder.

B. Daily Variability

The daily variability in the solar generation follows the rising and setting of the sun. Solar generation ramps up in the morning when the sun rises and ramps down in the evening when the sun sets. For high solar penetration levels, this variability can cause very fast ramping and excessive daily load swings in the net feeder load. When feeder loads are aggregated to the utility or balancing authority scale, this net load shape is frequently called the “duck curve.” For this use case, we will investigate the degree to which very fast ramping and excessive daily load swings in the net feeder load can be mitigated by controlling the PEV charging on the distribution feeder. This use case will tie in nicely with the GM0086/VSS183 project and is especially applicable for distribution feeders with distributed solar generation, residential loads, and commercial loads with a lot of work place charging.

3. Demand Response

For some utilities, there are demand response programs that pay participants to respond to automated event signals from the utility. For example, PG&E has a program called Automated Demand Response that pays customers for participation in a program where the utility can actively curtail their demand during the year. Currently in PG&E, there are programs for both HVAC and lighting loads. It is possible that similar programs might be developed for PEV charging in the future.

For this use case, we will simulate the coordination of PEV charging on distribution feeder through an aggregator, using a hypothetical demand response program. We will develop a front-end controller that receives real-time event signals from the simulated aggregator and coordinates the charging of PEVs on the feeder, while ensuring that the PEV owner driving needs are met. Any impacts on the distribution feeder capacity or power quality will be investigated.

Another major emphasis for FY16 was to begin the characterizing production PEV charging system operation to produce the data necessary to develop high-fidelity models of PEVs to be included in controller-HIL studies. Table VI-10 provides a summary of the vehicles to be characterized and status.

Table VI-10: Production PEVs being characterized

Vehicle make/model	Vehicle class	Charge rate	Charge connector protocol	Characterization status
2013 Ford Fusion Energi	PHEV	AC level 2 - 6.6 kW	J1772	Complete
2016 Chevrolet Volt (Gen 2)	PHEV	AC level 2 -3.3 kW	J1772	Complete
2012 Chevrolet Volt (Gen 1)	PHEV	AC level 2 -3.3 kW	J1772	Scheduled for Q1 FY17
2015 Kia Soul EV	BEV	AC level 2 - 6.6 kW DC level 2 - 50 kW	J1772 for AC level 2 CHAdeMO for DC level 2	Complete
2015 Nissan Leaf	BEV	AC level 2 -6.6 kw DC level 2 up to 50 kW	J1772 for AC level 2 CHAdeMO for DC level 2	Scheduled for Q1 FY17
2016 Tesla Model S	BEV	AC level 2 -10 kW DC level 2 - 120 kW	Tesla proprietary protocols for AC level 2 and DC level 2	Scheduled for Q1 FY17

VI.8.C. Products

Presentations/Publications/Patents

1. Use Case Presentation: A description of the use cases defined for this project was distributed to the advisory board, along with a survey instrument that they could use to provide feedback. Eight of the 12 advisory board members provided feedback through this survey. Additionally, a teleconference was conducted with the advisory group to solicit additional feedback. Overall, the advisory group expressed satisfaction with the use cases to be studied. Group members ranked the use cases according to the potential benefit of the results to their organizations. Project researchers will use this information to target additional feedback on specific use cases as they are being studied in the future.

VI.8.D. References

1. Markel, T., A. Meintz, K. Hardy, B. Chen, T. Bohn, J. Smart, D. Scoffield, R. Hovsapian, S. Saxena, J. MacDonald, S Kiliccote, K. Kahl, and R. Pratt, "Multi-Lab EV Smart Grid Integration Requirements Study," National Renewable Energy Laboratory, NREL/TP-5400-63963, May 2015.

VI.9. Modeling and Control Software Tools to Support Vehicle to Grid Integration [GM0086]

Samveg Saxena, Principal Investigator

LBNL, MS90R1121
 One Cyclotron Road, 90-1131
 Berkeley, CA 94720
 Phone: (510) 269-7260
 E-mail: SSaxena@lbl.gov

Lee Slezak, DOE Program Manager

Vehicle Technologies Office
 U.S. Department of Energy
 Phone: (202) 586-2335
 E-mail: Lee.Slezak@ee.doe.gov

Start Date: June 1, 2016
 End Date: May 30, 2019

VI.9.A. Abstract

Objectives

The overall objective defining success for this project is:

Determining the feasibility of VGI by quantifying the potential value, cost, complexity, and risks in different implementations of VGI. Allocating available value among stakeholders and determining pathways for electrification of transportation to enable beneficial grid services such as mitigating renewables intermittency.

In support of this objective, there will be two key outcomes that further define success for the project:

- Developing and releasing the VGISoft co-simulation framework for examining vehicle-grid interactions in any implementation of VGI. VGISoft will enhance GMLC activities by coupling with GMLC foundational models in valuation, design and planning tools, and SETO models to address solar variability.
- Application of VGISoft to address critical knowledge gaps for VGI through targeted case studies that quantify the feasibility of VGI, quantify potential for VGI to provide grid services such as supporting renewables integration, and determine the optimal implementation approaches for VGI.

Fiscal Year (FY) 2016 objectives are:

- Finalized development of case studies and use cases across VTO VGI GMLC projects.
- Structure for VGISoft framework and integrated sub-models: 1) PEV estimation toolkit, and 2) capacity allocation toolkit) completed.

Accomplishments

- Developed the master use case document, together with GM0062 and GM0085 project staff; Finalized development of case studies and use cases across VTO VGI GMLC projects.
- Established the consensus on the structure for the VGISoft model that will be created among all DOE national laboratories. Defined all research topics and technical approaches for this project.
- Completed the structure for VGISoft framework and integrated sub-models: 1) PEV estimation toolkit, and 2) capacity allocation toolkit.

- Proposed a methodology to quantify EV battery degradation from driving and V2G services, considering detailed powertrain model and EV thermal model.
- A journal article which quantifies the magnitude of battery degradation in vehicles from driving and uncontrolled charging compared with driving and offering many different vehicle-grid services has been accepted by Journal of Power Sources.
- Completed research on evaluating EV's capability of enhancing the large-scale integration of renewable energies. An article will be submitted to a high impact journal (Science, Nature, Nature Climate Change, etc.) soon.

Future Achievements

- Create and integrate the three remaining sub-models into VGISoft framework, namely the delivery optimization, resource allocation, and values estimation toolkits.
- Demonstrations, presentation of VGISoft framework to industry advisory panel.
- Create the portfolio optimization method to decide the day-ahead bidding strategy for different grid services based on the aggregate battery model. Publish a journal article on this research topic.
- Create the real-time resource scheduling strategy considering the uncertainties of EV behaviors, real-time price, dispatch signals, etc. Publish a journal article on this research topic.
- Apply VGISoft for targeted use cases on: 1) Quantifying the feasibility (i.e. cost, value, complexity, risk, etc.) for VGI with collections of vehicles offering many available grid services; 2) Development of virtual battery models for integrating capacity from aggregate collections of vehicles into ISO, RTO, and Utility operations; 3) Quantifying the ability for PEVs to mitigate the variability and costs of renewables intermittency at various temporal and spatial scales; 4) Assessing real-time scheduling and control strategies for dispatching capacity from aggregate collections of vehicles (e.g. EDF, LLF, model-predictive, etc.); 5) Determining how value is distributed amongst stakeholders, including drivers, aggregators, utility shareholders and ratepayers, etc.
- Release of VGISoft simulation framework for use by all stakeholders, with accompanying documentation.

VI.9.B. Technical Discussion

Background

A substantial opportunity exists in vehicle-grid integration (VGI) – if 25% of US light-duty vehicles were PHEVs there would be nearly 1,000 GWh of energy storage – an unprecedented scale. This storage is deployed for clean mobility objectives, yet vehicles are parked a majority of the time allowing vehicle batteries to support grid objectives such as renewables integration. From the grid perspective, there is a low capital cost of grid storage using vehicles (capital cost is absorbed for mobility objectives), yet the grid services from vehicles can be used to lower the operating costs for PEV owners. In this manner a synergy exists where storage from clean transportation becomes an enabler for a clean grid, while the value captured by vehicles to support the clean grid further accelerates the deployment of clean vehicles. Furthermore, flexibility in vehicle charging can provide valuable grid support on various temporal and spatial scales of aggregation, from behind-the-meter load management, to distribution systems support, to wholesale market support with ancillary services. Despite this opportunity, it remains unclear whether VGI is feasible in terms of its values, costs, complexity, and risks, and whether it is competitive with other technologies that can offer similar grid services.

Introduction

This project aims to determine the feasibility of VGI by quantifying the potential value, cost, complexity, and risks in different implementations of VGI. Another important goal is to allocate available value among stakeholders and determine pathways for electrification of transportation to enable beneficial grid services such as mitigating renewables intermittency. These project outcomes will occur over a 3-year timeline. The core VGISoft framework will be completed in Years 1 and 2, and applied towards renewables integration and VGI feasibility case studies in Years 2 and 3. Optimal VGI implementation approaches will be explored in Year 3.

The project will be conducted in close coordination with the multi-lab team within VTO's EV Smart Grid Working Group, including LBNL (prime), ANL, INL, NREL, ORNL, and PNNL. The methodologies, case studies, and timeline for this project will be closely coordinated with four other proposals submitted by the EV Smart Grid Working Group (GM0085, GM0150, GM0062, and GM0163).

Development and integration of VGISoft will, where applicable, rely heavily upon leveraging methodologies from complementary software tools developed in prior DOE/national laboratory efforts, including: V2G-Sim, Autonomie, GridLab-D, Blast-V, FastSim, MATSim, Polaris, TUMS, FINDER, ADOPT, VTAG, PEVI, and dSolar. Additionally, the VirGIL and FNCS tools may provide methodologies for enabling integrated co-simulation across several modeling tools.

The multi-lab EV Smart Grid Working Group has established working relationships with several stakeholders for VGI, including OEM automakers, utilities, regulatory agencies, and EV charging station manufacturers. Through these partnerships and working relationships, the tools and results from this project will directly advance VGI. Furthermore, the case studies of this project will be developed in coordination with California's Interagency VGI Working Group. This interagency group oversees the rollout of VGI in a rapidly growing market for PEV deployment and grid integration. It is convened under the California Governor's Office and is comprised of four major State agencies: the California Energy Commission, the California Public Utilities Commission, the California Air Resources Board, and the California Independent System Operator.

Given California's leadership alongside 8 U.S. states that signed an MOU for deployment of 3.3 Million Zero Emissions Vehicles by 2025, the outcomes of this project and established partnerships with the California Interagency VGI working group can provide national benefits to enable the synergistic benefits between clean vehicles and a clean grid through VGI.

Approach

The VGISoft framework that will be created and applied across several case studies is comprised by a collection of toolkits, as shown in Figure VI-75. Several toolkits (especially the PEV estimation toolkit) will leverage prior methodologies and tools created by the DOE national laboratories. A schematic flowchart is provided in Figure VI-76 to show the main structure and approach of this project.

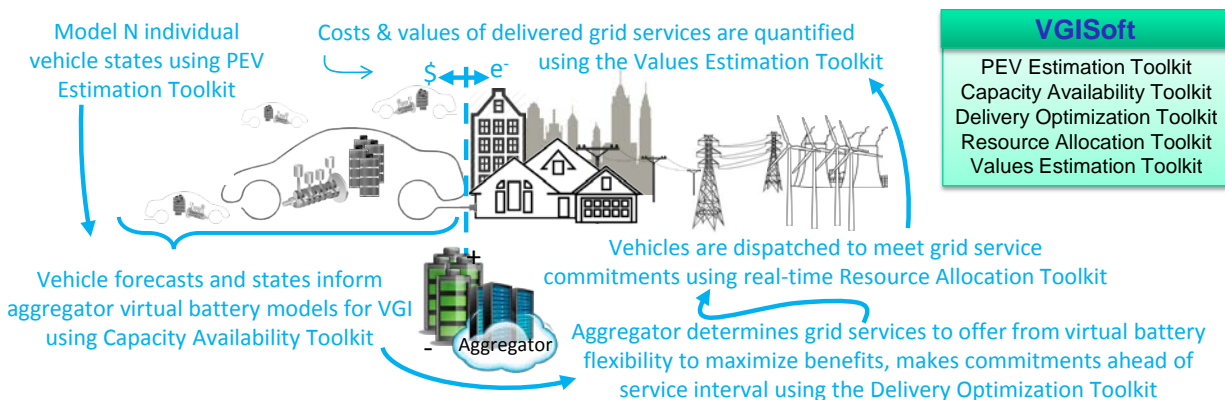


Figure VI-75: Overview of the phenomena considered by each toolkit within VGISoft

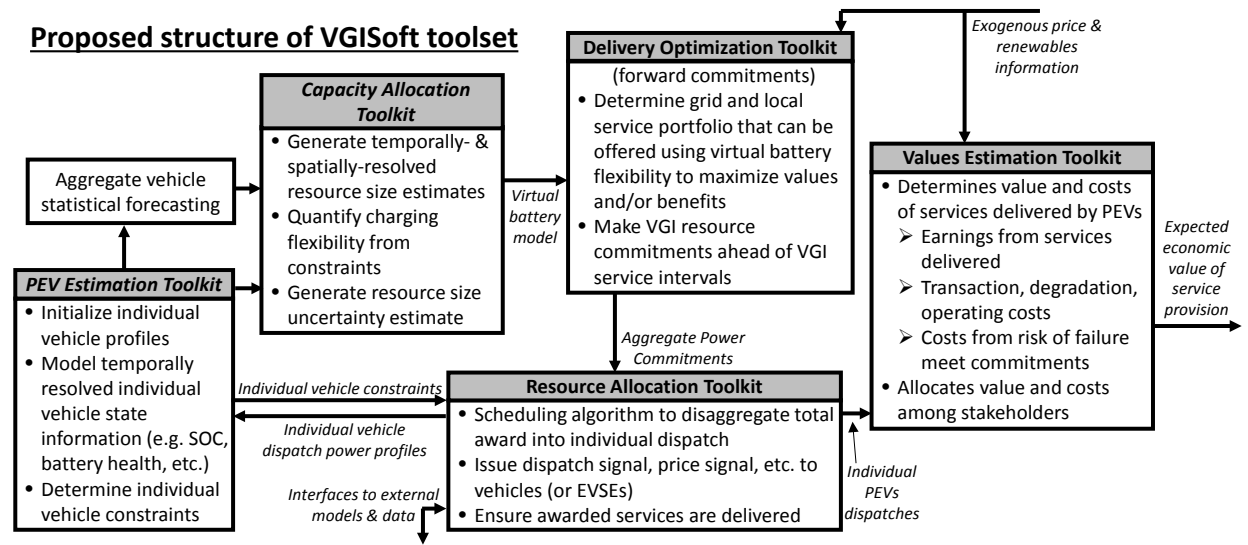


Figure VI-76: Schematic overview of intended functionality and information flow within VGISoft toolkits

Figure VI-76 is articulated as text below:

PEV Estimation Toolkit:

- Initializes individual vehicle profiles
- Model temporally resolved individual vehicle state information (e.g. SOC, battery health, etc.)
- Determine individual vehicle constraints

Prior DOE and other models planned to be leveraged:

- (LBNL) V2G-Sim for its methodology for tracking the state of N vehicles and resolving grid loads under uncontrolled and controlled charging/discharging scenarios, and built-in battery life models.
- (LBNL/ANL) Autonomie powertrain models, where necessary, for energy consumption of vehicles while they are driving (can be initialized and run within V2G-Sim)
- (LBNL/ANL) If necessary, travel demand models, such as MatSim/SmartBay (or Polaris/TUMs), for spatially resolved vehicle travel itineraries. Alternatively, can use data sources such as the National Household Travel Survey for vehicle travel itineraries.
- (NREL) BlastV for battery life models that are calibrated against measurement data.
- (INL) Data insights from vehicle charging datasets

Capacity Allocation Toolkit:

- Generate temporally- and spatially-resolved resource size estimates
- Quantify charging flexibility constraints
- Generate resource size uncertainty estimates

Prior DOE and other models planned to be leveraged (not exhaustive):

- (LBNL) V2G-Sim module for quantifying available flexible capacity for collections of vehicles.
- (ANL) Models for capacity (electricity and ancillary services) assessment from individual and aggregated PEVs.

In order to define the flexible capacity of a fleet of EVs, we use a virtual batter model [1]. All EVs, which are connected to the grid in a specific area, form an aggregate virtual battery. The virtual battery is defined by four parameters: 1) upper bound of the aggregate energy; 1) lower bound of the aggregate energy; 1) upper bound of the aggregate power; 1) lower bound of the aggregate power. The virtual battery model will work as important constraints in the following optimization toolkit.

Delivery Optimization Toolkit (forward commitments):

Determine grid and local service portfolio that can be offered using virtual battery (e.g. aggregated vehicles) flexibility to maximize values and/or benefits

Make VGI resource commitments ahead of VGI service intervals

Prior DOE and other models planned to be leveraged:

Will require application of forward commitments algorithms available in the academic literature, or the creation of new algorithms for forward commitment of vehicles.

In this toolkit, we consider the aggregator's portfolio optimization problem in day-ahead market. The bidding strategy will be optimized for multiple grid services including the bulk energy, frequency regulation, spinning reserve, flexible ramping product and demand response. Through optimization, the aggregator is able to make forward commitments for multiple grid services to maximize its own profits. A risk-averse model can be adapted if the aggregate is exposed to high non-compliance penalties.

Resource Allocation Toolkit:

Scheduling algorithm to disaggregate total award into individual dispatch

Issue dispatch signal, price signal, etc., to vehicles (or EVSEs)

Ensure awarded services are delivered

Prior DOE and other models planned to be leveraged:

(LBNL) V2G-Sim-integrated control algorithms that optimally control vehicle charging/discharging for several grid objectives (e.g. demand response, wholesale-level renewables integration, frequency regulation, etc.)

The forward commitments will be exercised in real time. We need to allocate the aggregate charging/discharging power which is obtained from the optimization toolkit into individual EVs, considering the uncertainties in the real-time market. To be specific, the problem is to decide in real-time: 1) which EVs are to be charged/discharged; 2) the charge/discharge power of each EV. Some classic real-time scheduling methods like EDF, LLF and MPC can be employed to solve this problem.

Values Estimation Toolkit:

Determine value and costs of services delivered by PEVs

Earnings from services delivered

Transactions, degradation, and operating costs

Costs from risks of failure to meet forward commitments

Allocates value and costs among stakeholders

Prior DOE and other models planned to be leveraged:

(NREL) Plexos, and customized NREL static marginal energy cost model (to be developed).

(ANL) Grid economic and reliability models

(PNNL) GridLabD distribution systems models, and values quantification sub-models

Additionally, new frameworks will need to be developed that allow for quantifying values and costs simultaneously captured across multiple temporal and spatial scales

After the real time allocation, we can calculate the earnings for providing different services, also the transaction degradation and operating cost. Penalties will be liquidated by evaluating the deviation between dispatch signal and the real performance. In order to allocate values and costs among different stakeholders, we need to study the business model and market mechanism to maximize the market efficiency, and give all stakeholders enough incentives to participate into VGI.

Results

Our efforts for FY 2016 focus on evaluating the feasibility of VGI and the capability of EVs to enhance the renewable energy integration. One of this year's accomplishments was developing a methodology to quantify EV battery degradation from different grid services. This is the basis for the further investigation on the feasibility of VGI.

Quantifying EV battery degradation:

Vehicle grid integration (VGI) presents a tremendous opportunity to benefit both the electricity grid and the transportation sector, yet concerns about accelerated battery degradation in vehicles that provide grid services remains an obstacle. The lack of a quantitative evaluation method for EV battery degradation amplifies people's anxiety on V2G cost and hinders stakeholders to price V2G services. Therefore, we aimed to quantify the magnitude of battery degradation that is incurred from normal driving and uncontrolled charging of vehicles versus degradation in vehicles that are driving plus offering grid services. In order to comprehensively examine the validity of concerns about battery degradation from VGI, we quantified battery degradation for several different grid services, under various travel and charging itineraries, and at different ambient temperature and solar radiation levels.

We used a semi-empirical model [2] to calculate the capacity losses caused by both cycling and calendar aging for a particular lithium ion chemistry. It takes into account four important experimental parameters including temperature, time, depth of discharge (DOD) and charge/discharge rate. Moreover, this model decouples the capacity loss caused by cycling and calendar aging. Total capacity loss can be calculated by adding them together during any time horizon. Since the temperature is one of the dominant factors in the degradation model, we utilized a car-level lumped capacitance thermal network approach [3] to calculate the battery temperature.

We proposed the simulation flow as shown in Figure VI-77. Given EV itineraries and V2G strategies, V2G-Sim will specify all driving/charging/discharging/idle events and assign a drive cycle to each trip. After setting charging/discharging parameters, all information will be imported into the detailed powertrain model. Then, we can acquire SOC, current, and internal resistance. Values of internal resistance and current will further go to the temperature module where solar radiation and ambient temperature are sourced from historical data. Battery temperature will be used to calculate calendar life loss. Current, SOC and temperature will be used to calculate cycle life. Finally, we can add them together and get the total capacity loss.

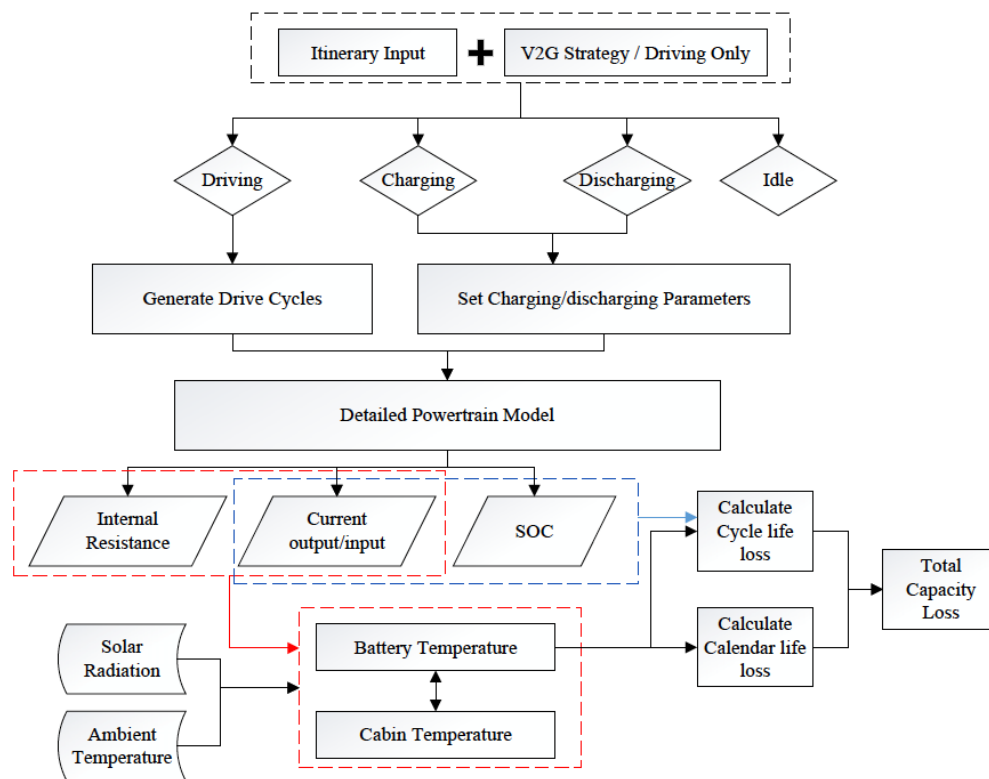


Figure VI-77: The whole framework of quantifying EV battery degradation

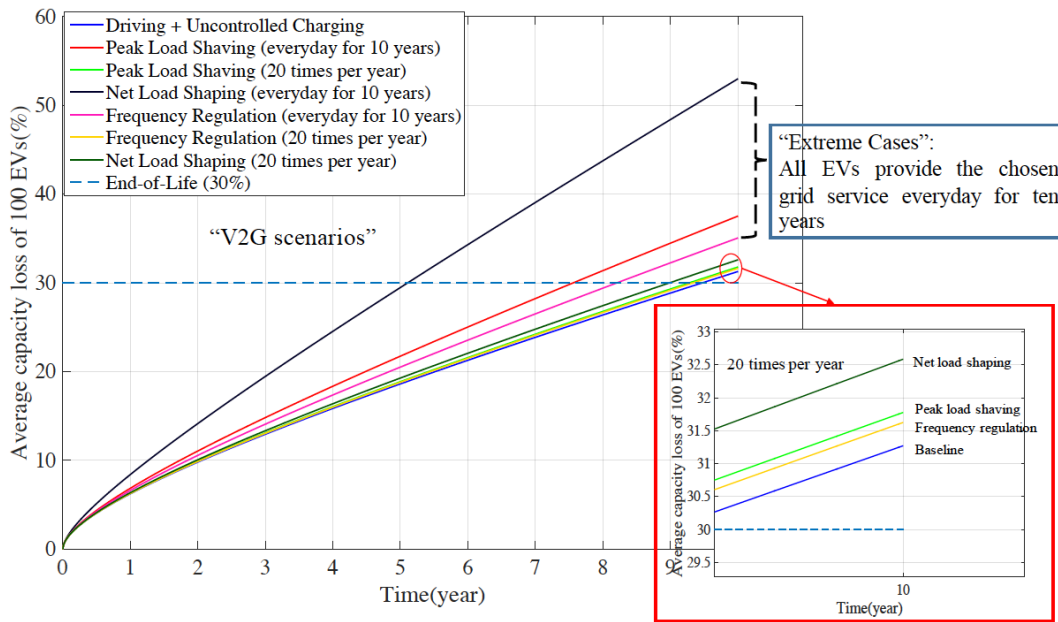


Figure VI-78: Average capacity losses of 100 EVs by performing different V2G services for ten years. In the extreme cases, all EVs provide the chosen grid service every day. The ten-year capacity losses from peak load shaving, frequency regulation and net load shaping increase by 3.62%, 5.6% and 22.6% compared to the base case, respectively. In the more realistic cases, EVs provide V2G services for 20 times per year. The ten-year capacity losses increase by 0.38%, 0.21% and 1.18%, respectively.

We explored the EV battery degradation in four different cases. They are uncontrolled charging, peak load shaving, frequency regulation and net load shaping. In all these cases, we ensured that the grid services offered by each vehicle does not compromise the mobility needs of each driver. The average capacity loss of 100 EVs over 10 years for different grid services are shown in Figure VI-78. V2G service hours for the peak load shaving and frequency regulation are from 7:00pm-9:00pm. For the three extreme cases, each vehicle offers the chosen grid service daily for ten years. The increases in capacity loss from performing the frequency regulation and peak load shaving are 3.62% and 5.60%, compared with the capacity loss in the driving and uncontrolled charging case. In the net load shaping case, because EVs keep charging and discharging almost whole day, the capacity loss is much more than the base case. However, in real cases, the emergency peak load shaving and extreme "duck curve" only happen a couple of times per year. We simulated the cases that 100 EVs provide these services 20 times per year for ten years. The results showed that the V2G services only have minor impacts on the battery degradation. For the peak load shaving, frequency regulation and net load shaping, the 10-year average capacity losses are 0.38%, 0.21% and 1.18% more than that in the base case, respectively. If we assume 30% as the end of life, these grid services will shorten the life time of the battery by 0.25, 0.19, 0.51 years.

Evaluating EVs’ capability to enhance large-scale renewable energy integration:

- In 2015, California increased the Renewables Portfolio Standard (RPS) target from 33 percent by 2020 to 50 percent of renewable energies by 2030. However, several issues will arise by the high penetration of renewable energies:
- Short steep ramps when the ISO must bring on or shut down generation resources to meet an increasing or decreasing electricity demand quickly, over a short period of time;
- Over-generation risk when more electricity is supplied than is needed to satisfy real-time electricity requirements;
- Decrease frequency response when less resources are operating and available to automatically adjust electricity production to maintain grid reliability.

While EVs are necessary to reach the GHG goals, they could serve a dual-purpose by providing storage in the same way as stationary batteries. Clean vehicles can be an enabler for a cleaner grid, in this study we showed the impact of EVs on future power demand curve, and how much stationary storage can be avoided if vehicles are integrated as a grid resource.

We simulated the EV charging power if they charge as soon as they are plugged and until the battery is full (uncontrolled charging). The number of vehicles follows the ZEV mandate [4]. In 2014 we assume the fleet mix of 117,640 PEVs [4] to linearly increase and reach 1.3 millions PEVs in 2025. Each vehicle is associated with an itinerary from the NHTS 2009 California data. One of the main factor to determine the grid consumption of ZEVs depends on the charging infrastructure. In the uncontrolled charging scenario, we considered 2 types of infrastructures, a lower charger (L1) and a higher charger (L2). From 2015 to 2025, charging infrastructures are progressively ramping up to higher power level to reach 70% of L2 and 30% of L1 at home in 2025. The trends of four parameters (minimum load, maximum load, maximum ramping down, maximum ramping up) of the net load with uncontrolled charging demand were forecasted as shown in Figure VI-79.

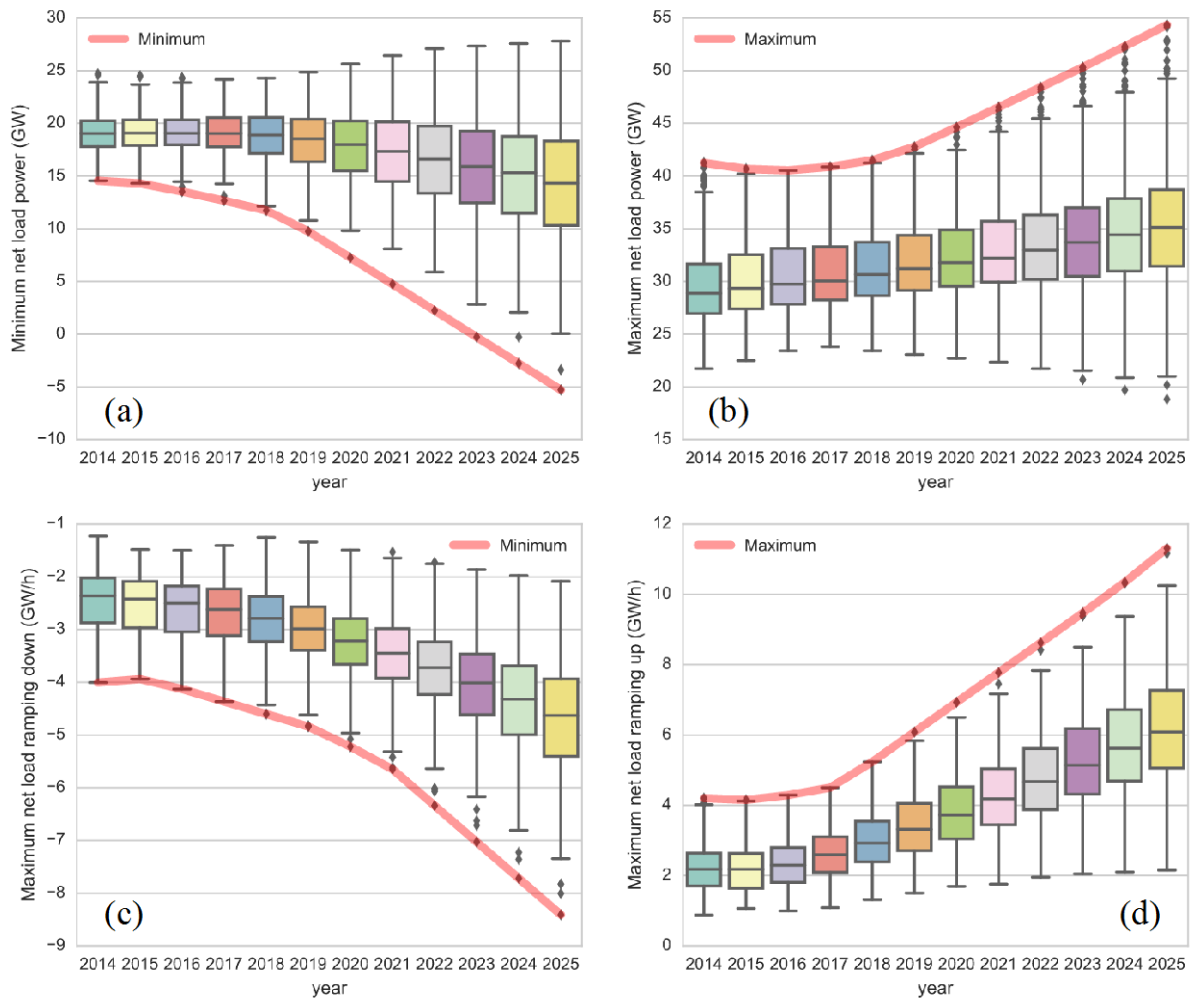


Figure VI-79: Trends of the four parameters of the net load with uncontrolled charging demand on the extreme days: (a) minimum load; (b) maximum load; (c) maximum ramping down; (d) maximum ramping up.

In order to evaluate the capability of EVs to enhance the renewable energy penetration, we investigated two charging controllers separately. The first one is a peak shaving and valley filling algorithm, its goal is to reduce over-generation and extreme peak load. Once EVs arrive at workplaces, they are encouraged to charge when the solar penetration is high. The simulation result showed that in 2025 EVs could potentially fill load valley by 3GW. When the solar generation decreases around 7:00 pm, the controller incentivizes EVs to avoid

charging and even discharge if the charger allows bidirectional power flow. This strategy could reduce the peak power load by 2.7GW as shown in Figure VI-80(b).

The second controller aims at reducing the steep ramps of the net load. The controller coordinates EVs to reduce the abrupt changes on the net load when the solar energy comes online in the morning or stop in the evening. The simulation results in Figure VI-81 shows that r EVs could significantly mitigate both ramping down and up. In 2025, as the solar energy comes online, EVs could reduce the down ramp by 3.5GW/h. In evening, when solar generation stops, PEVs could reduce the up ramp by 3GW/h.

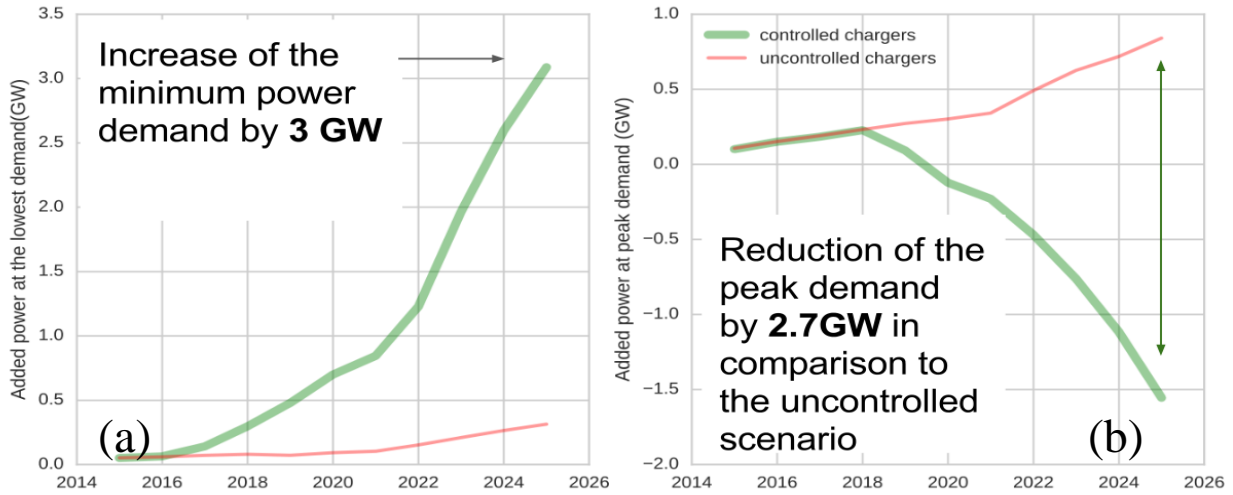


Figure VI-80: The contributions of EVs on (a) filling the load valley and (b) shaving the load peak, on the most extreme days from Year 2015 - 2025.

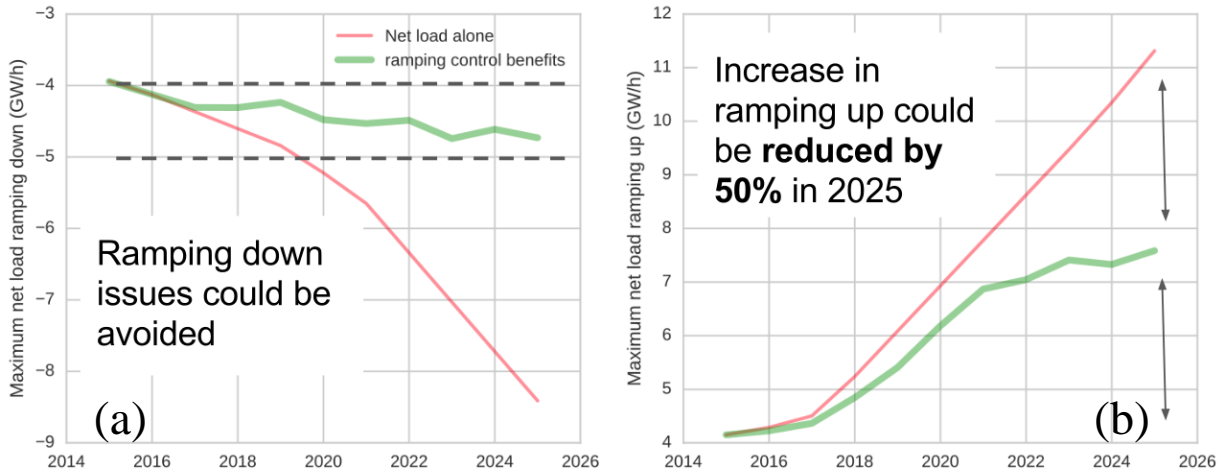


Figure VI-81: The contributions of EVs on mitigating (a) ramping down and (b) ramping up, on the most extreme days from Year 2015 - 2025.

Conclusions

Frequency regulation and peak load shaving at power rates typical for vehicle charging and discharging will not significantly accelerate battery degradation in comparison to the degradation incurred from driving and calendar aging. Even in the "extreme" cases in which we assume all EVs provide grid services from 7:00pm-9:00pm every day for ten years, the capacity losses from frequency regulation and peak load shaving only increase by 3.62% and 5.6%, respectively.

If EVs are only utilized to provide the V2G services occasionally (e.g. in emergency events), which is more realistic, then the impacts on the battery degradation will be minor. The 10-year average capacity losses are 0.38%, 0.21% and 1.18% more than that in the base case, if EVs provide peak load shaving (V2G), frequency regulation (V2G) and net load shaping (V2G) for 20 times per year.

The battery degradation cost of each V2G service is estimated. If we assume the cost of the whole battery pack is \$6000 and the end of life is 30%, battery degradation costs of 2-hour peak load shaping and frequency regulation are \$0.38 and \$0.20, respectively per event. Since the batteries are used for whole day in the net load shaping case, the degradation cost for a day is \$1.18.

We have shown that EV can significantly help the integration of renewable energies in 2025. Controlled charging can mitigate the problems (peak load, over generation, steep up and down ramps) caused by high penetration of renewable energies.

VI.9.C. Products

Presentations/Publications/Patents

1. A presentation entitled "Quantifying EV battery degradation from driving vs. V2G services" was given at IEEE PES General Meeting 2016, in Boston.
2. A publication entitled "Quantifying electric vehicle battery degradation from driving vs. vehicle-to-grid services" has been accepted by Journal of Power Sources. This paper directly advances the research objectives of the project.
3. Release of V2G-Sim toolbox.

VI.9.D. References

1. H. Zhang, Z. Hu, Z. Xu, and Y. Song, "Evaluation of Achievable Vehicle-to-Grid Capacity Using Aggregate PEV Model," IEEE Transactions on Power Systems, 2016
2. J. Wang, et al. "Degradation of lithium ion batteries employing graphite negatives and nickel-cobalt-manganese oxide+ spinel manganese oxide positives: Part 1, aging mechanisms and life estimation." Journal of Power Sources 269 (2014): 937-948.
3. J. Neubauer and E. Wood. "Thru-life impacts of driver aggression, climate, cabin thermal management, and battery thermal management on battery electric vehicle utility." Journal of Power Sources 259 (2014): 262-275.
4. California Energy Commission, "Transportation Energy Demand Forecast, 2016-2026", available online: http://docketpublic.energy.ca.gov/PublicDocuments/15-IEPR-10/TN210539_20160226T101946_Transportation_Energy_Demand_Forecast_20162026.pdf

VI.10. Diagnostic Security Modules for Electric Vehicle to Building Integration [GM0163]

Kenneth Rohde, Principal Investigator

Idaho National Laboratory
 P.O. Box 1625
 Idaho Falls, ID 83415
 Phone: (208) 526-0672
 E-mail: Kenneth.Rohde@inl.gov

Lee Slezak, DOE Program Manager

Vehicle Technologies Office
 U.S. Department of Energy
 Phone: (202) 586-2335
 E-mail: Lee.Slezak@ee.doe.gov

Start Date: May 2016
 End Date: September 2018

VI.10.A. Abstract

Objectives

- Develop a Diagnostic Security Module (DSM) framework for creating an end-to-end security architecture for the integration of a modern Plug-in Electric Vehicle (PEV) with Electric Vehicle Supply Equipment (EVSE) and a Building Energy Management System (BEMS).
- Perform a cyber security investigation of potential vulnerabilities found in commercial AC Level 2 smart charging EVSE.
- Implement a security protocol to exchange cyber health information between PEV, EVSE and BEMS. The protocol can be used to further design and implement emerging standards and protocols such as SEP 2.0, SAE J2931/7.
- Deploy the DSM framework in partner laboratories building environment to demonstrate complete integration of DSM into a large laboratory test environment.
- Perform cyber security testing (red team vs. blue team) of the building environment to examine DSM performance and functionality.
- Deliver the DSM security protocol specification, methods and algorithms to industry for consideration and integration with emerging communication standards.

Accomplishments

- Created a DSM prototype environment in which (4) DSM devices simulate (1) PEV, (2) EVSE stations, and (1) BEMS operator console. The devices communicate using Bluetooth Low-Energy (BLE) and 802.11 WiFi in order to determine which EVSE is in close proximity of a PEV. The EVSE then signals the BEMS that a PEV is ready to connect and charge. A basic communication protocol was created.
- Selected two EVSE vendors based upon the number of EVSE units deployed in the US. This data was retrieved from the DOE Alternative Fuels Data Center. The two selected EVSE vendors are ChargePoint and SemaConnect.
- The University of Louisiana-Lafayette (UL-L) was contracted by INL to provide expertise in Informatics Research. UL-L has identified the professors and students who will be part of this project during FY17. They are currently performing research into known vulnerabilities associated with

EVSE and developing an assessment plan and methodology for use with both the SemaConnect and ChargePoint units. The cyber security assessment of the SemaConnect unit will begin in Q1 FY17 at UL-L.

- The two selected EVSE stations are at INL and being installed and tested in the cyber security lab space. The assessment work will begin in Q1 of FY17 on the ChargePoint by the INL cyber team. When functional testing of the SemaConnect unit is complete, the EVSE will be sent to the UL-L for assessment activities.

Future Achievements

- Integrate DSM hardware with the selected EVSE units and a PEV. The prototype DSM system will integrate with EVSE and EV at minimal effort and cost. The total hardware cost of a DSM for EVSE integration is \$125, and the total cost of a DSM for EV integration is \$175.
- Complete a cyber security assessment of the ChargePoint and SemaConnect EVSE units during Q1 and Q2 FY17. The assessment results will be documented and reported back to the vendors for their consideration. Results of the assessment will be used during FY17 and FY18 testing of the DSM framework.
- Development of cyber security fingerprint and monitoring algorithms for EVSE and PEV. These algorithms, implemented in DSM nodes, will monitor the physical and cyber health of all connected systems and report the status back to the BEMS operator station.
- Finish the development and implementation of the DSM framework in INL lab spaces. Initial functional testing of the DSM framework will complete during FY17 prior to deployment in the Multi-lab EV Smart Grid Working Group environment.

VI.10.B. Technical Discussion

Background

The overall goal of this project is to develop a Diagnostic Security Module (DSM) framework for creating an end-to-end security architecture for the integration of modern Plug-in Electric Vehicle (PEV) with Electric Vehicle Supply Equipment (EVSE) and a Building Energy Management System (BEMS). These devices will create a secure communications channel for the exchange of physical and cyber health information of all of the connected components to a BEMS operator. The DSMs will integrate with a wide range of device types (EVSE, PEVs, etc) and vendors, and provide enhanced awareness of the security state when implementing an integrated building and PEV environment.

The end goal of this project is to provide industry with an example of how a security protocol might be implemented in an integrated Electric Vehicle and Building environment. The intent is to publish the developed protocols, methods and algorithms so that they can be adopted by industry partners and integrated directly into future products. It is not the intent of this research project to create a set of devices that are sold and integrated as third-party products.

Introduction

The integration of smart grid enabled devices, such as EVSE units and PEVs with enhanced communication capabilities poses new risks to the electric grid. The vulnerabilities of the devices and implications of these risks are still not well understood. Given that these new electric vehicles and their chargers are now available to the general public, these devices can be exploited by the cyber security community at large (i.e. hackers) to leverage vulnerabilities for malicious purposes. A theory currently posed by the cyber security community is that a compromised PEV can be used as a mechanism to infect the smart charging stations available to the public. Thus the infected PEV becomes a transport mechanism for malware that specifically targets EVSE stations.

Major activities in this project includes (1) the investigation of potential security vulnerabilities found in commercial AC Level 2 EVSE, (2) the development of the DSMs modules, (3) development of the prototype EVSE BEMS environment, and (4) implementation of a security protocol that can be used to further design and implement future standards and protocols. The later years include the integration of the DSM prototype into the building-level PEV charging environment created by the Multi-lab EV Smart Grid Working Group partners as proposed by GM0062 Vehicle to Building Integration Pathways.

Approach

The DSMs will be designed to provide an additional layer of security by monitoring the devices to which they are connected and reporting any suspicious behavior or abnormal conditions. A safety and security framework will be developed to address the need for a distributed and collaborative intelligent system to monitor and protect a modern automated building. This framework will be distributed as a component of the DSMs located throughout the connected building environment. This will allow for the monitoring and detection of physical and cyber problems that might affect the overall health of the integrated building environment. The development of the DSM modules and communications framework addresses the need for the Vehicle Technologies Office to provide a security framework for the integration of Electric Vehicles and charging equipment into a central monitoring and management station (e.g. BEMS).

The work performed during this project will integrate DSMs with multiple PEVs, a variety of EVSEs (Level 1, Level 2, and DC Fast), and a single BEMS. A new ChargePoint EVSE will be added to the existing equipment located at INL. This additional EVSE, along with other Smart Grid enabled EVSEs located at INL, will provide a variety of equipment for which to test and develop the DSM framework. The ChargePoint EVSE is a new system yet to be evaluated for cyber security issues, so a portion of the first year of development will include an assessment of this device. The other EVSEs at INL have already been assessed as part of a previous DOE project. This prototype environment will allow research and testing of a subset of an integrated building environment with a deep understanding of the potential cyber security issues present in the systems.

The DSM framework will implement a security based protocol for sharing physical and cyber security information of the components to which they are connected. This protocol will be used to further develop standards that are currently being implemented throughout the electric vehicle industry, such as Smart Energy Profile (SEP) 2.0 and SAE J2931/7.

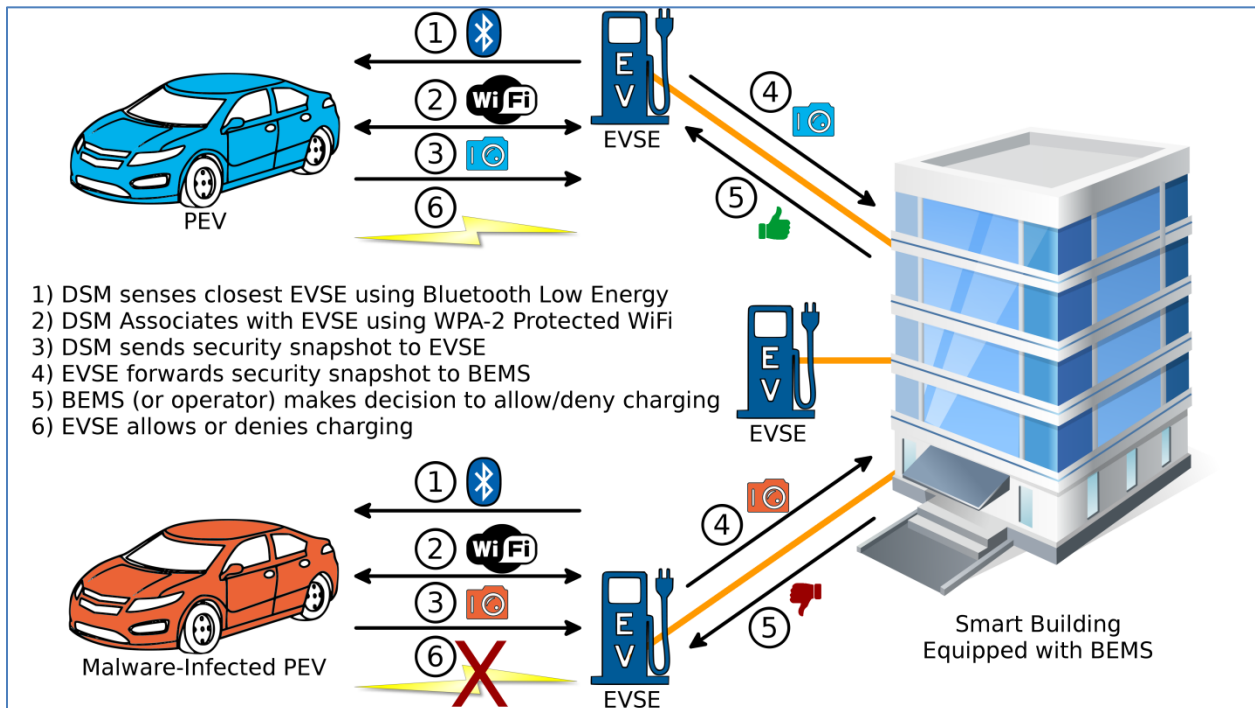


Figure VI-82: DSM Framework and Data Exchange Overview
 INL

Results

DSM Prototype Hardware and Software

The project team studied what available embedded development boards might be suitable as the initial DSM devices. The Raspberry PI 3 was selected, and several devices were procured. A small DSM prototype environment was created in which (4) DSM devices simulate (1) PEV, (2) EVSE stations, and (1) BEMS operator console. The devices communicate using Bluetooth Low-Energy (BLE) and 802.11 WiFi in order to determine which EVSE is in close proximity of a PEV. The EVSE then signals the BEMS that a PEV is ready to connect and charge. A basic communication protocol was created.

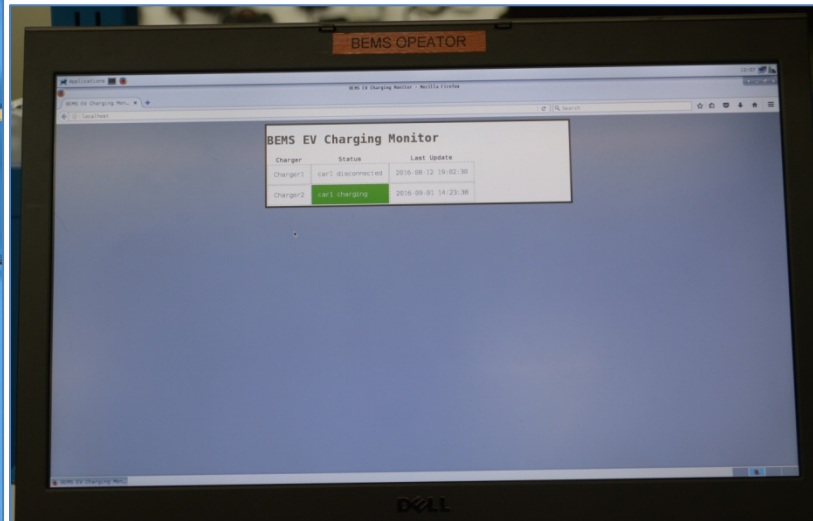
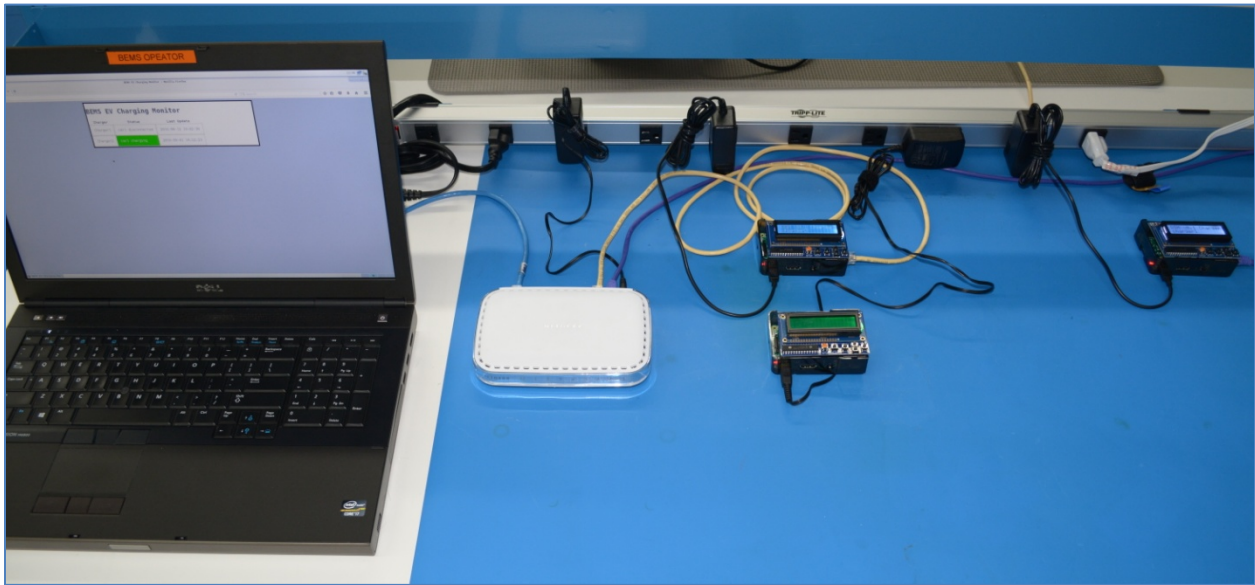


Figure VI-83: The DSM Prototype Hardware and Software - Showing 2 EVSE DSM Nodes (Blue) and a PEV Node (Green) Connected to EVSE #2. The BEMS Displaying the Status of the DSM Framework

INL

Commercial AC Level 2 EVSE Procurement

In addition to the previously received hardware for use as DSM devices, the procurement of a ChargePoint EVSE and a SemaConnect EVSE was completed. Both units are now in the INL cyber security lab space. The ChargePoint unit is installed and commissioned but awaiting final functionality testing. The SemaConnect unit is being assembled for installation.

A PEV is also located in the testing and development lab space and will be integrated with a DSM node. This vehicle will be the initial platform for vehicle testing, but additional PEVs might be used during FY17 development.



Figure VI-84: The Initial DSM Development Lab Space.

INL

The two selected EVSE stations are at INL and being installed and tested in the cyber security lab space. The assessment work will begin in Q1 of FY17 on the ChargePoint by the INL cyber team. When functional testing of the SemaConnect unit is complete, the EVSE will be sent to the University of Louisiana-Lafayette for assessment and development activities.

Conclusions

The GM0163 project is in the early stages of research and development. The current prototypes have provided promising results and raise confidence in integrating DSM nodes with both EVSE and PEV. The next year of research, testing and development will move quickly and determine the effectiveness of the DSM framework.

Early examination by industry partners will aid in guiding the research team to ensure a quality design and useful technology is developed. This advisory board will include members from partner laboratories, utility companies, universities, EVSE vendors, and the automotive sector.

VI.10.C. Products

No products have been developed thus far.

Presentations/Publications/Patents

1. "Diagnostic Security Modules for Electric Vehicle to Building Integration", USCAR GITT Meeting, July 2016

This page is intentionally blank.

U.S. DEPARTMENT OF
ENERGY

Energy Efficiency &
Renewable Energy

For more information, visit: energy.gov/eere

DOE/EE-1517 • October 2017